Diss. ETH No. 23743

Macrocyclic and Acyclic Alleno-Acetylenic Scaffolds with Outstanding Chiroptical Properties and Expansion of the Chemical Space of Electron-Poor Alkenes for the [2+2] Cycloaddition–Retroelectrocyclization (CA–RE) and Related Reactions

A thesis submitted to attain the degree of

DOCTOR OF SCIENCES of ETH ZURICH

(Dr. sc. ETH Zurich)

Presented by

Etienne Donckele

M. Sc. in Chemistry and Chemical Engineering, CPE Lyon, France

Citizen of France

accepted on the recommendation of

Prof. Dr. François Diederich, examiner

Prof. Dr. Jeffrey Bode, co-examiner

Zurich 2016

Dedicated to people who are currently fighting against Cancer

"Become a possibilitarian. No matter how dark things seem to be or actually are, raise your sights and see possibilities – always see them, for they're always there."

Norman Vincent Peale

Acknowledgements

I would like to express my sincere gratitudes to the people who made this thesis a rewarding experience.

First and foremost, I would like to thank *Prof. Dr. François Diederich* for giving me the opportunity to join his group. I am deeply thankful for the freedom to pursue my own research ideas during my PhD. From the first interview to the time of correcting my thesis, he was an inspiring and stimulating mentor as much as an understanding boss.

I thank *Prof. Dr. Jeffrey Bode*, for accepting to be co-examiner of this dissertation.

Many thanks for very fruitful collaborations go to *Prof. Laurent Ruhlmann*, and *Prof. Corinne Boudon* from the University of Strasbourg, France. They carried out a considerable amount of electrochemical measurements of my compounds.

Many thanks go to the team of people who make the Diederich group funtion flawlessly. A very special thanks goes to *Irma Näf* and *Karin Puce-Schmid* for their kindness and for their precious help with any administrative issues. I am also greatful to *Prof. Dr. Carlo Thilgen* for his help with all nomenclature and many scientific discussions. I thank *Dr. Bruno Bernet* for his help in the interpretation of the experimental data, his careful analyses, and corrections.

I would like to thank the staff members at LOC for the high-quality services they provided: *Rolf Hälfinger* for mass spectrometry, the HCI Shop for material support and good mood, *Dr. Nils Trapp* and *Michael Solar* form the Small Molecule Crystallography Center (SMoCC) for their excellent X-ray measurements, which added much value to my research.

A doctorate is a life experience that is not limitied to the sole relationship with your bench but also a perpetual renewal of colleagues and friends. A special thank you belongs to my labmates in G314, *Dr. Aaron D. Finke, Cédric Schaack, Dr. Boris Tchitchanov*, *Elisabeth Schäfer*, *Raoul De Gasparo, Dr. Sophie Müller* and *Dr.*

Yosuke Akae. It was great to work with them. I would also like to thank some particular people in the group, whom I had the pleasure to interact with and made my time in the DCC unforgettable. First of all, thank you *Dr. Tristan A. Reekie* for being not only an outstanding collaborator and an amazing labmate but also a true friend. Many thanks go to *Dr. Ori Gidron*, who helped me a lot with the calculations. It was a pleasure to work with such a talented scientist. I thank my Praktikum partner, *Jovana V. Milić*, as working with her was a wonderful experience, which I appreciated very much. I also thank *Dr. Cagatay Dengiz* for the many profitable discussions and for being an excellent colleague, which turned to a solid friendship. Many thanks go to *Prof. Dr. Pablo Rivera-Fuentes*, *Dr. Manolis D. Tzirakis*, *Dr. Sander Wezenberg,* and especially *Dr. Przemyslaw Gawel* for their valuable discussions, their precious advice and for a smooth introduction to the topic of carbon-rich materials. I would like to thank the french and the german team particularly *Corneluis Gropp*, *Dr. Nicolas Kerisit*, *Geoffrey Schwertz, Dr. David Schweinfurth* and *Dr. Elke Persch* for their friendship and their positive attitude in the group. Thank you also to my swiss colleagues, *Leslie Riwar*, *Maude Giroud* and *Dr. Birgit Lauber* for contributing to the nice atmosphere within the group.

I would like to thank *Dr. Aaron D. Finke*, *Dr. Tristan A. Reekie, Cornelius Gropp* and *Cedric Schaack* for proofreading my dissertation. I am deeply greatful for their critical and careful corrections, which contributed considerably to the quality of this thesis.

During my doctoral studies, I was very fortunate to supervise a very talented student, *Salome Püntener*. I thank her for her commitment and hard work. I wish her all the best for her future.

I would like to express my gratitude to *Dr. Lisa Marcaurelle*, *Dr. Baudouin Gerard,* and *Prof. Dr. Barry M. Trost* for infecting me with their passion and dedication to organic chemistry.

Zürich has been my world for more than three and a half years, but I am truly thankful to my friends from all over the world for being such amazing characters and making me who I am. Thank you to my childhood friends: *Dr. Andréa Bailleuil*, *Thomas Di Franco*, *Patricia Sengel, Benjamin Loyer*, *Florian Nantier,* and *Céline*

Cauchy for seeing me grow up over the years without loosing contact and being very supportive. Thank you to my American friends: *Dr. Mike O'Keefe*, *Dr. Maksim Osipov*, *Dr. Aaron D. Finke*, *Dr. Craig Stivala*, *Huntly Gordon* and *Scott Humphreys* for being so encouraging despite the distance. Last but not least, I had the chance to get to know a lot of fantastic people in Zürich, which made my time in Switzerland an unforgettable experience. Thank you, *Deplhine Uwacu*, *Timoteo Canonica*, *Samuel Thomas, Marco Vario*, *Dr. Clément Dince,* my former flatmate*, Umer Durrani, Toni Hilti*, *Fabien Leisi*, *Stephan Kurmann,* and *Alain Glasson*.

I also thank the Swiss National Science Fundation (SNSF) for a post-doctoral scholarship. I was awarded a 18-months fellowship from the SNSF for a 18-months fellowship to perform my postdoctoral studies at Caltech.

Finally, nothing would have been possible without the love and support from my parents Véronique and Philippe, and my brother *Arnaud* and his family. Growing up, they always emphasized the importance of education and the meaning of life. Their love and care built an exceptional environment that directed me to achieve my goals no matter what and despite the omnipresence of Cancer in my life. This is the reason why this thesis is dedicated to all the people who died and to those who are still fighting against Cancer.

Publications

– Derived from Ph.D. Studies:

[1] **E. J. Donckele**, T. A. Reekie, G. Maneti, S. Püntener, N. Trapp, F. Diederich, *Org. Lett.* **2016**, *18,* 2252–2255. *A Three-Step Synthesis of Tetrasubstituted NH-Pyrroles.*

[2] **E. J. Donckele**, T. A. Reekie, N. Trapp, F. Diederich, *Eur. J. Org. Chem.* **2016**, 7264–7275. *Penta-2,4-dien-1-ones by Formal [3+2] Cycloaddition–Rearrangement of Electron-Deficient Diethyl 2-(Dicyanomethylene)malonate with Alkynes.*

[3] T. A. Reekie, **E. J. Donckele**, L. Ruhlmann, C. Boudon, N. Trapp, F. Diederich, *Eur. J. Org. Chem.* **2015**, 7264–7275. *Ester-Substituted Electron-Poor Alkenes for the Cycloaddition–Retroelectrocyclization (CA–RE) and Related Reactions.*

[4] **E. J**. **Donckele,** A. D. Finke, L. Ruhlmann, C. Boudon, N. Trapp, F. Diederich, *Org. Lett.* **2015**, *17*, 3506–3509. *The [2+2] Cycloaddition–Retroelectrocyclization and [4+2] Hetero-Diels–Alder Reaction of 2-(dicyanomethylene)indan-1,3-dione (DCID) with Electron-Rich Alkynes: Influence of Lewis Acids on Reactivity.*

[5] **E. J. Donckele**, O. Gidron, N. Trapp, F. Diederich, *Chem. Eur. J.* **2014**, *20*, 9558–9566. *Outstanding Chiroptical Properties: A Signature of Enantiomerically Pure Alleno-Acetylenic Macrocycles and Monodisperse Acyclic Oligomers*.

– Derived from Master Studies:

[1] B. M. Trost, **E. J. Donckele**, D. A. Thaisrivongs, M. Osipov, J. T. Masters, *J. Am. Chem. Soc.* **2015**, *137*, 2776–2784. *A New Class of Non-C_2-Symmetric Ligands for Oxidative and Redox-Neutral Palladium-Catalyzed Asymmetric Allylic Alkyation of 1,3-Diketones.*

[2] A. R. Germain, L. C. Carmody, P. P. Nag, B. Morgan, L. VerPlank, C. Fernandez, **E. Donckele,** Y. Feng, J. R. Perez, S. Dandapani, M. Palmer, E. S. Lander, P. B. Gupta, S. L. Schreiber, B. Munoz, B. *Bioorg. Med. Chem. Let.* **2013**, *23*, 1834–1838. *Cinnamides as selective small-molecule inhibitors of a cellular model of breast cancer stem cells*.

[3] B. M. Trost, D. A. Thaisrivongs, **E. J. Donckele,** *Angew. Chem.* **2013**, *125*, 1563–1566; *Angew. Chem. Int. Ed*. **2013**, *52*, 1523–1526. *Palladium-Catalyzed Enantioselective Allylic Alkylations via C–H Activation.*

[4] B. Gerard, M. W. O'Shea, **E. Donckele**, S. Kesavan, L. B. Akella, H. Xu, E. N. Jacobsen, L. A. Marcaurelle, *ACS Comb. Sci.* **2012**, *14*, 621–630. *Application of a Catalytic Povarov Reaction using Chiral Ureas to the Synthesis of Tetrahydroquinoline Library.*

[5] J. T. Lowe, M.D. Lee, L. B. Akella, E. Davoine, **E. J. Donckele**, L. Durak, J. R. Duvall, B. Gerard, E. B. Holson, A. Joliton, S. Kesavan, B. C. Lemercier, H. Liu, J. C. Marié, C. A. Mulrooney, G. Muncipinto, M. W. O'Shea, L. M. Panko, A. Rowley, B. C. Suh, M. Thomas, F. F. Wagner, J. Wei, M. A. Foley, and L. A. Marcaurelle, *J. Org. Chem.* **2012**, *77*, 7187–7211. *Synthesis and Profiling of a Diverse Collection of Azetidine-Based Scaffolds for the Development of CNS-Focused Lead-Like Libraries.*

Patent

[1] A. Germain, B. Munoz, T. A. Lewis, A. Ting, W. Youngsaye, P. P. Nag, C. Dockendorff, C. V. Fernandez, **E. Donckele**, B. Morgan, E. M. Skoda, B.-C Shu. **2013**, WO2013032907 (A1). *Compounds and Methods for the Treatment of Cancer Stem Cells.*

Poster Presentations

– Derived from Ph.D. Studies:

[1] **E. J. Donckele**, T. A. Reekie, L. Ruhlmann, C. Boudon, N. Trapp, F. Diederich (**2016**). *Investigating the Reaction of Ester-Substituted Electron-Poor Alkenes with Alkynes: From Materials to Drug-like Compounds*. . San Diego, USA.

[2] **E. J**. **Donckele,** A. D. Finke, L. Ruhlmann, C. Boudon, N. Trapp, F. Diederich (**2015**). *The [2+2] Cycloaddition–Retroelectrocyclization and [4+2] Hetero-Diels–Alder Reaction of 2-(dicyanomethylene)indan-1,3-dione (DCID) with Electron-Rich Alkynes: Influence of Lewis Acids on Reactivity.* 16th International Symposium on Novel Aromatic Compounds. Madrid, Spain.

[3] **E. J. Donckele**, O. Gidron, N. Trapp, F. Diederich, (**2014**). *Outstanding Chiroptical Properties: A Signature of Enantiomerically Pure Alleno-Acetylenic Macrocycles and Monodisperse Acyclic Oligomers*. Swiss Chemical Society Fall Meeting 2014. Zurich, Switzerland

– Derived from Master Studies:

[1] **E. J. Donckele**, B. Gerard, M. W. O'Shea, S. Kesavan, L. B. Akella, H. Xu, E. N. Jacobsen, and L. A. Marcaurelle, (**2011**). *Application of a catalytic Povarov Reaction using Chiral Ureas to the Synthesis of Tetrahydroquinoline Library.* Gordon Research Seminars, High-Throughput Chemistry and Chemical Biology. New London, USA.

Table of Content

Symbols and Abbreviations

°	degree
Å	Ångström (1 Å = 10^{-10} m)
Ac	acetate
ADA	acceptor–donor–acceptor
Ar	aromatic
br.	broad
Bz	benzoate
CA	cycloaddition
Cal	calories
Calc.	calculated
CC	column chromatography
CCDC	Cambridge crystallography data center
CEE	cyanoethynylethenes
CV	cyclic voltammetry
Cy	cyclohexyl
δ	chemical shift
δr	quinoid character
d	doublet (NMR) or day(s)
D	dimension
D–A	donor–acceptor
DAD	donor–acceptor–donor
DABCO	1,4-diazabicyclo[2.2.2]octane
DCE	1,2-dichloroethane
DCF	6,6-dicyanopentafulvene
DCID	2-(dicyanomethylene)indan-1,3-dione
DCM	dichloromethane
DEA	1,3-diethynylallene
DEE	diethynylethene
DFT	density functional theory
DCNQIs	*N*,*N*'-dicyanoquinone diimides
DMA	*N*,*N*-dimethylamino

DMAP	4-dimethylaminopyridine
DPEphos	(Oxydi-2,1-phenylene)bis(diphenylphosphine)
ε	extinction coefficient (M^{-1} cm^{-1})
E	energy or electrochemical potential
ee	enantiomeric excess
e.g.	exempli gratia
ECD	electron circular dichroism
EDTM	electric transition dipole moment
EPR	electron paramagnetic resonance
equiv	equivalent
Et_2O	diethyl ether
EtOAc	ethyl acetate
e.r.	enantiomeric ratio
ESI	electronspray ionization
eV	electron volt
EWG	electron-withdrawing group
exp.	experimental
Fc	ferrocene
Fc^+	ferricenium
FC	flash column chromatography
g	gram
h	hour(s)
HDA	hetero-Diels–Alder
HMBC	heteronuclear multiple-bond correlation spectroscopy
HOMO	highest occupied molecular orbital
HR	high resolution
HPLC	high performance liquid chromatography
Hz	hertz (s^{-1})
ICT	intramolecular charge-transfer
IR	infrared
J	coupling constant
k	kilo
K	Kelvin

K_a	association constant
λ	wavelength (nm)
LG	leaving group
LiHMDS	lithium bis(trimethylsilyl)amide
LUMO	lowest unoccupied molecular orbital
μ	(10^{-6})
m	meta
M	molarity (mol L^{-1})
MALDI	matrix-assisted laser desorption/ionization
Me	methyl
MeCN	acetonitrile
L	milliliter(s)
MOM	methoxymethyl ether
m.p.	melting point
m/*z*	mass to charge ratio (MS)
MeCN	acetonitrile
MeOH	methanol
min	minute(s)
Mol	mole
MS	mass spectrometry
MTDM	magnetic transition dipole moment
$\tilde{\nu}$	wavelength (cm^{-1})
*n*Bu	*n*-butyl
Ninhydrin	2,2-dihydroxyindane-1,3-dione
NIR	near-infrared
NLO	non-linear optic
NMR	nuclear magnetic resonance
Nu	nucleophile
p	para
Ph	phenyl
ppm	parts per million
q	quartet
RDV	rotating-disk voltammetry

RE	retroelectrocyclization
s	second(s), singlet (NMR), strong (IR)
SM	starting material
t	triplet
TBAF	tetra-*n*-butylammonium fluoride
TCBD	tetracyanobutadiene
TCNE	tetracyanoethene
TCNQ	7,7,8,8-tetracyano-*p*-quinodimethane
TD-DFT	time-dependent density functional theory
TEA	tetraethynylallene
TEE	tetraethynylethene
TFA	trifluoroacetic acid
THF	tetrahydrofuran
TIPS	triisopropylsilyl
TMEDA	*N*,*N*,*N*′,*N*′-tetramethylethane-1,2-diamine
UV/Vis	ultraviolet/visible
V	volt
w	weak

Abstract

Due to the access to three-dimensional structures, the study of chiral allenes has attracted much attention, illuminating their emerging use in pharmaceuticals and catalysis, as well as their potential application in optoelectronic devices. This unique structural motif has also been increasingly investigated as chiral building block in molecular materials and provided access to shape-persistent macrocyclic structures with new topologies and properties. In 2009, we reported the first enantiomerically pure shape-persistent alleno-acetylenic macrocycles with unprecedented chiroptical properties and a few years later, we showed a nonlinear amplification of the Cotton effects of enantiopure acyclic oligomers with increasing oligomeric length. It became mandatory to further validate these chiroptical findings for other, structurally related alleno-acetylenic macrocycles and acyclic oligomers.

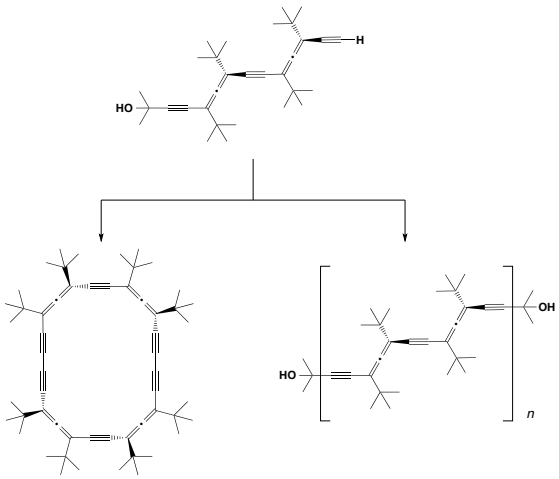

We describe in Chapter 2 a second series of shape-persistent alleno-acetylenic macrocycles and monodisperse acyclic oligomers with conformationally less flexible backbones in enantiomerically pure form by short, high-yielding routes starting from optically active 1,3-diethynylallenes (DEA). The structures of the D_2-symmetric macrocycles were confirmed by X-ray analysis. The macrocycles display remarkably intense chiroptical responses, and strong amplification of chirality is observed in the acyclic oligomeric series. Their preference for helical secondary structures of one handedness was confirmed by X-ray analysis and computational studies. This set of data provides proof that outstanding chiroptical properties are a hallmark of alleno-acetylenic macrocyclic and acyclic oligomeric chromophores. Chapter 2 also describes the isopropanol-substituted DEA derivatives in enantiomerically pure form as well as the tetrameric macrocycles bearing eight lateral acetone protecting groups around the central alleno-

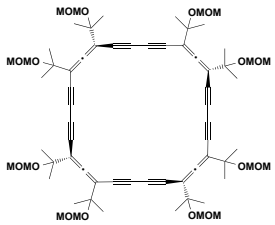

acetylenic all-carbon core. However, the attempt to deprotect the MOM was unsuccessful and no desired product has been observed. Nevertheless, the chiroptical properties of this particular shape persistent alleno-acetylenic macrocycle showed more intense chiroptical properties.

In the aim of designing new push–pull chromophores with significant optoelectronic properties, we have been interested in using the formal [2+2] cycloaddition–retroelectrocyclization (CA–RE) reaction. With this strategy, we could access to a wide range of chromophores in a high-yielding, atom-economic manner with excellent chemo- and regioselectivity. Several electron-deficient acceptors such as tetracyanoethene (TCNE) and 7,7,8,8-tetracyano-*p*-quinodimethane (TCNQ) with activated alkynes have been studied. Nevertheless, few reports of investigating this versatile transformation with different acceptors have been studied.

To address this problem, we introduced 2-(dicyanomethylene)indan-1,3-dione (DCID) as a new electron-poor alkene in a formal CA–RE reaction (Chapter 3). Surprisingly, depending on the reaction conditions, push–pull buta-1,3-dienes are obtained by the CA–RE reaction or tricyclic 4*H*-pyrans by the [4+2] Hetero-Diels–Alder (HDA) reaction. The presence of $LiClO_4$ greatly enhances the formation of the HDA cycloaddition over the CA–RE reaction. The structural and optoelectronic properties of the new chromophores were investigated by X-ray analysis, UV/Vis spctroscopy, electrochemistry, and computational analysis.

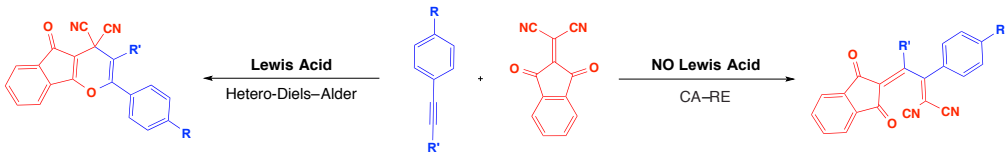

To continue with the reactivity of new electron-poor alkenes, we decided to switch cyano groups to ester moieties on tetrasubstituted electron-deficient alkenes and study the effect on their ability to undergo the CA–RE reaction. Results are described in Chapter 4. The CA–RE reaction was shown to still take place with a single cyano moiety; however, other reactions also occurred, namely a [4+2] HDA

cycloaddition and a [3+2] cycloaddition/rearrangement cascade. Similar to the DCID adducts, the optoelectronic properties of the chromophores were investigated by X-ray analysis, UV/Vis spectroscopy, electrochemistry, and computational analysis. We also describe the possibility of post CA–RE reaction functionalization to ester-substituted butadienes including access to pharmacologically interesting pyrazolopyrans.

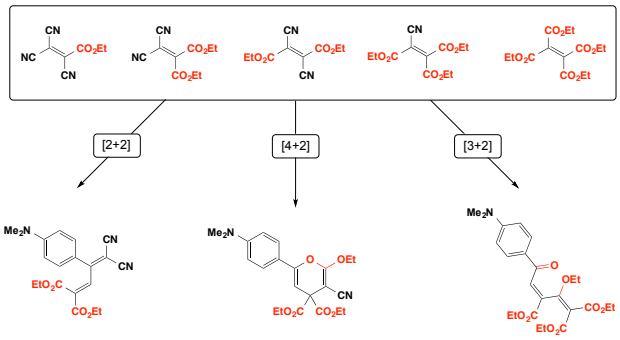

To further explore the products derived from the CA–RE reaction and their potential role in the synthesis of compounds of greater complexity and additional chemical utility, Chapter 5 describes a synthesis of tetra-substituted NH-pyrroles. From readily available starting materials, the CA–RE adducts can be converted to pyrroles in moderate to excellent yields with complete regioselectivity. Penta-2,4-dien-1-ones also undergo a similar transformation providing analogous products and greatly enhancing the substitution of the pyrrole available.

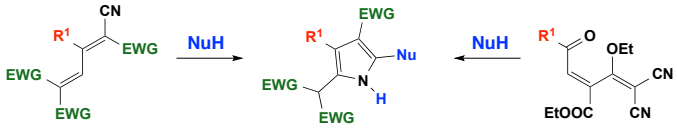

Finally, the last Chapter of the thesis is dedicated to the development of a formal [3+2] cycloaddition/rearrangement cascade reaction between moderately activated to unactivated alkynes and an electron-poor dicyano-diester-substituted alkene to yield a variety of π-conjugated penta-2,4-dien-1-ones. The broad substrate scope (20 examples) and reasonably mild conditions for such a transformation makes this procedure a valuable reaction for the synthesis of dienones.

Résumé

Du fait de sa structure tridimensionnelle, l'étude sur l'allène chirale attire encore aujourd'hui la communauté scientifique. Cela s'explique par une présence émergente dans les composées de type pharmaceutique, dans la catalyse ainsi que dans des applications potentielles aux machines optoélectroniques. Ce motif unique a également été de plus en plus étudié comme composant chiral dans les matériaux et a donné accès à des structures macrocycliques de forme persistante avec de nouvelles topologies et des propriétés interessantes. En 2009, notre groupe de recherche a mis en avant la première synthèse enatiomériquement pure d'un macrocycle allèno-acétylénique avec des propriétés chiroptiques sans précédent. Quelques années plus tard, nous avons montré l'amplification non linéaire des effets Cotton d'oligomères énantiopures et acycliques avec l'augmentation de la longueur oligomérique. Pour confirmer les conclusions sur ces propriétés remarquables, nous avons décidé d'étudier un macrocycle allèno-acétylénique et des oligomères acycliques structurellement apparentées.

C'est pourquoi, le chapitre 2 est consacré à l'étude d'une deuxième série de macrocycles allèno-acétyléniques à forme persistante ainsi que les oligomères acycliques monodisperses enatiomériquement purs composés d'un squelette conformationnellement moins souple. La symétrie D_2 a été confirmée par une analyse aux rayons X. Les nouveaux macrocycles obtenus affichent des réponses chiroptiques intenses et une forte amplification de la chiralité est observée dans la série oligomérique acyclique. La préférence pour des structures secondaires de type hélicoïdales et d'une seule chiralité a été confirmée par analyse aux rayons X et par des études computationnelle. Ce nouvel ensemble de données fournit la preuve que les fortes propriétés chiroptiques sont une caractéristique des macrocycliques et oligomères acycliques alléno-acétyléniques. Le Chapitre 2 décrit également le macrocycle enantiomériquement pur et de forme persistante portant huit groupements protecteurs acétones de manière latérale. Cependant, la tentative de la déprotection du groupement MOM a échoué et aucun

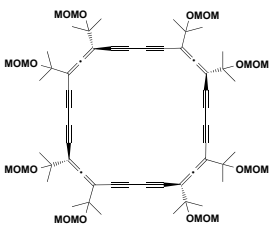

produit désiré n'a été observé. Les propriétés chiroptiques de ce macrocycle ont montré néanmoins des propriétés chiroptiques plus intenses.

Dans l'objectif de développer de nouveaux chromophores push–pull avec des propriétés optoélectroniques intéressantes, nous avons voulu utiliser la réaction [2 + 2] cycloaddition–retroelectrocyclisation (CA–RE) formelle. Avec cette stratégie, nous pouvons avoir accès à une large gamme de chromophores, d'économie d'atome, d'une chimio- et régiosélectivité élevées et avec un excellent rendement. Plusieurs accepteurs d'électrons oléfiniques tels que le tétracyanoéthene (TCNE) et le 7,7,8,8-tétracyano-*p*-quinodiméthane (TCNQ), et leurs réactions avec des alcynes riches en électrons ont été étudiés. Toutefois, peu d'études sur cette transformation avec différents accepteurs ont été reportées.

Pour faire face à cette problématique, nous avons introduit le 2-(dicyanométhylène) indane-1,3-dione (DCID) comme le nouveau alcène pauvre en électron pour la réaction CA–RE (Chapitre 3). Etonnament, en fonction des conditions de la réaction, soit des push–pull buta-1,3-diènes sont obtenus par la réaction de CA–RE ou des 4*H*-pyranes tricycliques par la réaction de hetéro-Diels–Alder. La présence de $LiClO_4$, améliore grandement la formation de la cycloaddition intermoléculaire [4+2] sur la réaction de type CA–RE. Les propriétés structurales et optolélectroniques, l'analyse des rayons X, le spectre UV/Vis, l'électrochimie, et l'analyse computationnelle ont été reportés.

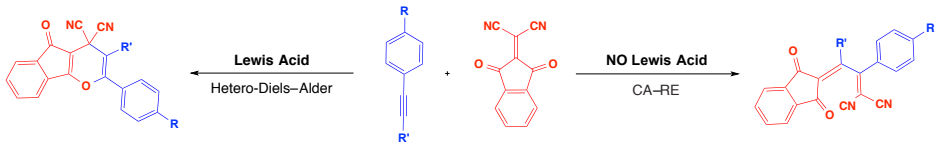

Pour continuer avec la réactivité des nouveaux alcènes, nous avons décidé de changer les groupements cyanos en des groupements esters sur des alcènes tétrasubstitués déficients en électrons afin d'étudier l'effet sur leurs réactivités. Les résultats sont décrits dans le Chapitre 4. La réaction CA–RE a encore lieu avec un seul groupement cyano, mais d'autres réactions sont également observées, à savoir la cycloaddition de Diels–Alder et une cycloaddition de type [3+2] suivie d'un réarrangement. Comme pour les composés issus du DCID, les propriétés

optoélectroniques, rayons X, l'UV/Vis, l'électrochimie et l'analyse computationelle des chromophores ont été étudiées. Nous avons également exposé la possibilité de réaction après la réaction de CA–RE telle que

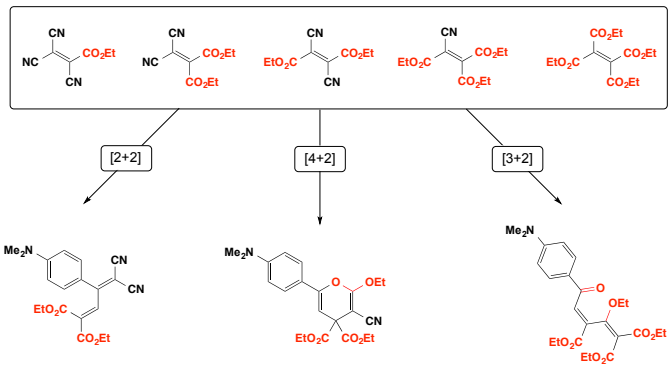

les pyrazolopyrans qui sont des composés pharmacologiquement intéressants.

Pour explorer davantage l'utilité des produits issus de la réaction de CA–RE dans la synthèse de composés de plus grande complexités, le Chapitre 5 décrit une synthèse de pyrroles tétrasubstitués à partir des produits obtenus de l'addition CA–RE avec de bons

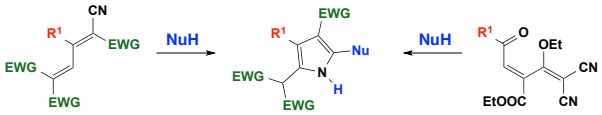

rendements et une excellente régiosélectivité. Les penta-2,4-diène-1-ones peuvent également subir une transformation similaire fournissant des produits analogues, ce qui améliore grandement la diversité en substitution des pyrroles.

Enfin, le dernier Chapitre de la thèse est consacré à la mise au point d'une réaction en cascade ([3+2] cycloaddition/réarrangement) entre des alcynes modérément activés ou inactivés avec un alcène pauvre en électrons pour donner une librairie de differents penta-2,4-diène-1-ones (20 exemples). Les conditions

utilisées et la variété des substrats rendent cette procédure utile pour la synthèse de diénones.

Chapter 1

Introduction

1. Introduction

Apart from being "the element of life" because of its predominance and versatility in living systems, carbon remains the element of choice for the construction of simple functional materials.[1] All-carbon and carbon-rich π-systems have attracted considerable attention in recent years, notably due to their unique electronic properties and their potential use in a number of technologies ranging from molecular wires to solar cells.[2,3]

1.1. Introduction to Alleno-Acetylenes

During the search for new carbon-rich materials, oxidative coupling of small acetylenic building blocks has facilitated the assembly of well-defined molecular architectures extending into one and two dimensions.[4] Such examples include polyynes, 1,2-diethynylethenes (DEEs), and tetraethynylethenes (TEEs) (Figure 1). To expand the chemical space, it was envisioned that acetylenic scaffolding starting from (±)-1,3-diethynylallenes (1,3-DEAs) and 1,1,3,3-tetraethynylallenes (1,1,3,3-TEAs) could provide access to three-dimensional structures.

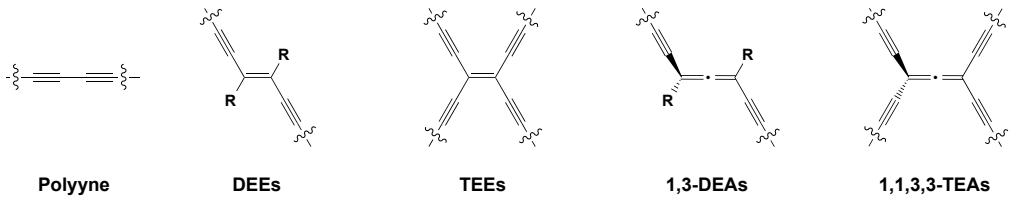

Figure 1. Schematic representations of 1D-, 2D-, and 3D-acetylenic scaffolds.

"Allene" is the name given to hydrocarbons containing two double bonds from one carbon to two others (Figure 2).[5] It was first described by van't Hoff in 1875[6] and confirmed experimentally by Maitland and Mills in 1935.[7] The particularity of this moiety is the presence of an *sp*-hybridized carbon at the central position.[8] It places the outgoing substituents in a perpendicular arrangement, which renders them as ideal building blocks for the construction of three-dimensional acetylenic scaffolds. For this reason, chiral allenes have attracted increasing interest due to the

development of improved synthesis,[9–12] their emerging use in pharmaceuticals[13] and catalysis,[14,15] as well as their potential applications in optoelectronic devices.[16–18]

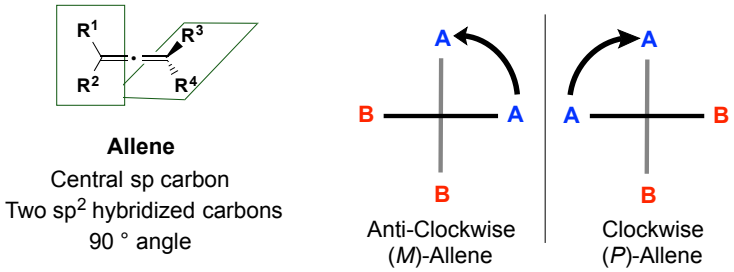

Figure 2. Illustration and configuration of allenes.

1.1.1. Synthesis of Chiral Allenes

In 1887, Barton and von Pechmann reported the first synthesis of an allene by reacting *β*-chloroglutaconic acid (**1**) with potassium hydroxide (Scheme 1).[19] The scarcity of analytical techniques made it very difficult to differentiate **2** from the corresponding alkyne **3** and it was only in 1954 that the Whiting group managed to elucidate the structure of allene **2**.[20]

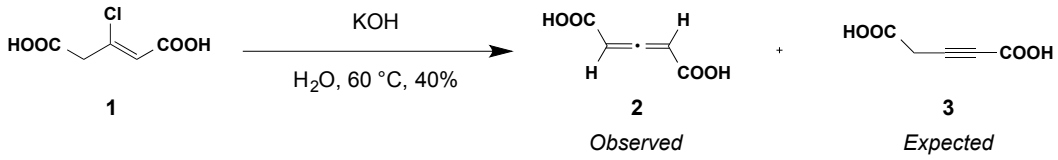

Scheme 1. First synthesis of an allene-containing material. [20]

All main reaction types (addition, elimination, substitution, rearrangement) have been used for the synthesis of allenes.[9–12, 14,15] The 1,2-elimination reaction has proven to be the most commonly used strategy for the construction of C–C bonds. In this subchapter, reported examples of chiral allenes using S_N2' reactions will be reviewed.

In 1935, the first axially chiral allene was synthesized by P. Maitland and M. W. Mills by dehydration of propargyl alcohol derivative **4** in the presence of 10 mol% of *D*-camphorsulfonic acid under reflux to afford (*P*)-(+)-**5** in 73% yield (Scheme 2).[7]

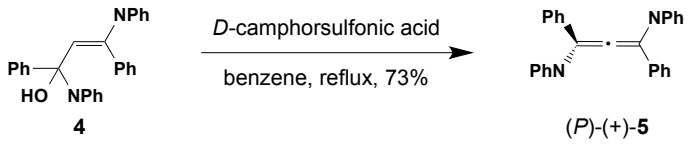

Scheme 2. The first axially chiral allene.[7]

In 1989, Elsevier and coworkers reported the synthesis of chiral dialkylallenes **7** by organocopper(I)-mediated anti-1,3-substitution of **6** (Scheme 3).[21] In all cases described, organocopper(I)-mediated S_N2' reactions **6** proceed with anti stereochemistry with good yield (up to 96%) and excellent stereoselectivity (> 98% *anti*). Subsequent elimination of the leaving group occurs only when the copper and leaving group moieties are antiperiplanar.[22–25]

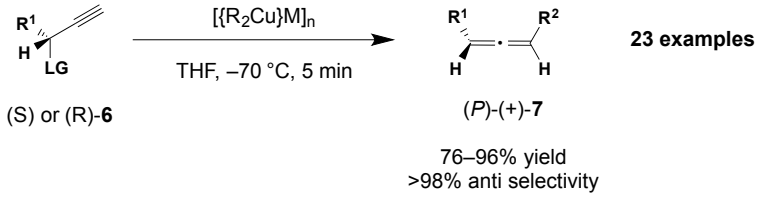

Scheme 3. Synthesis of a chiral allene using organocopper.[22–25] LG = Leaving group.

Palladium can catalyze cross-coupling reactions between propargylic precursors **8** and organometallic species in a S_N2' fashion (Scheme 4).[26,27] The oxidative addition step affords a transient allenylpalladium intermediate **9**, followed by transmetallation to form the corresponding allene **10**. For example, Sarandeses and Sestello reported an S_N2' palladium-catalyzed cross-coupling reaction between triorganoindium derivatives and enantiopure propargylic esters **11** in high *anti*-stereoselectivity providing allenes **12** in good yields and high enantiomeric excess (Scheme 4).[28]

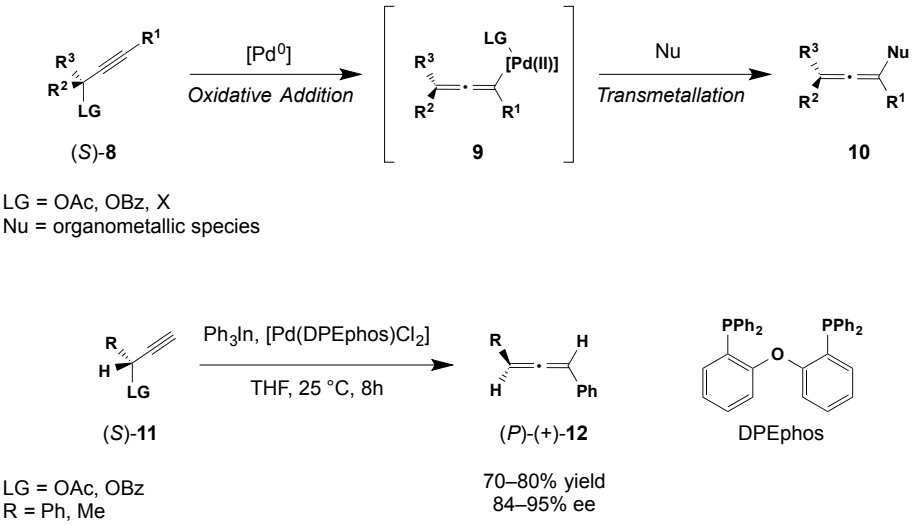

Scheme 4. Palladium-mediated S_N2'-type reaction. [28] LG = leaving group, DPEphos = (Oxydi-2,1-phenylene)bis(diphenylphosphine)

In 2008, the Schwartz reagent $Cp_2Zr(H)Cl$ was used for the S_N2'-type reaction between optically active propargylic alcohols **13** and ethylmagnesium or ethylzinc reagents to yield disubstituted allenes **14** (Scheme 5).[29]

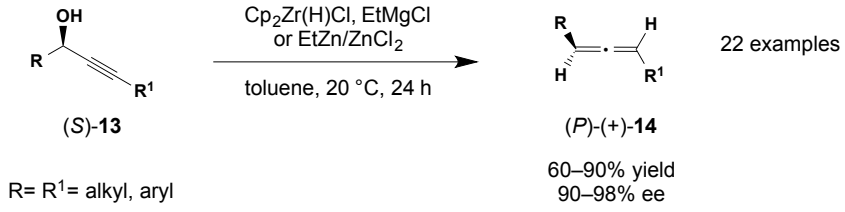

Scheme 5. Enantioselective synthesis of allenes **14**.[29]

To access chiral allenes, most strategies to date have been founded on the chirality transfer from enantioenriched propargyl derivatives. Later, Knochel and coworkers reported the use of propargyl dichlorides **15** as prochiral substrates for the synthesis of allene **16** (Scheme 6).[30] However, in both studies, stoichiometric amounts of copper salts were employed, and no example of an asymmetric version has been reported. Stimulated by these studies, Alexakis and coworkers intended to combine these two approaches, namely the use of prochiral substrates in this reaction under catalytic conditions.[31] Trisubstituted chloroallenes **16** have been obtained in good yields and high selectivities.

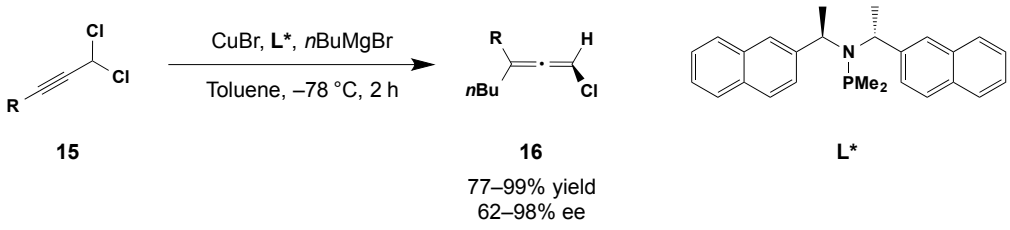

Scheme 6. Enantioselective synthesis of allenes **16**.[31]

The diversity of methods presented in this subchapter reveals the richness of allene chemistry. In the following subchapters, the focus moves to the use of allenes in their potential application in molecular materials.

1.1.2. Development of DEAs as Chiral Building Blocks

One of the most attractive features of DEAs is their chirality. Efforts towards the resolution of (±)-DEA **17** by HPLC (Scheme 8) were unsuccessful for several years,[32,33] so a stereoselective synthesis was pursued to obtain enantiopure DEAs.[34,35] An optically pure bispropargylic precursor was used to investigate the enantioselectivity of the palladium-mediated S_N2'-type reaction. In 2007, our group established the synthesis of bispropargylic esters (*R*)-(+)-**18** and (*S*)-(–)-**18** (Scheme 8).[34] First, addition of 2,2-dimethylbutyne to pivaloyl chloride (**19**) gave the propargylic ketone **20** in 95% yield (Scheme 7). Ketone **20** was then converted into the corresponding alcohol (±)-**21** by addition of lithium trimethylsilylacetylide. Bispropargylic alcohol (±)-**22** was obtained by deprotection of alkyne (±)-**21** using K_2CO_3, which was finally treated with enantiopure (*S,R*)-camphanic acid to give a bispropargylic camphanic ester **23** as a mixture of diastereoisomers (*R,S,R*)-**23** and (*S,S,R*)-**23**. These diastereoisomers were separated by fractional crystallization from CH_2Cl_2/cyclohexane. The camphanic appendages were removed from (*R,S,R*)-**23** with 1 M NaOH to give enantiopure (*R*)-(–)-**24** in 94% yield. The corresponding enantiopure tertiary alcohol **24** was treated with *n*-BuLi and triisopropylsilyl chloride to give (*S*)-(–)-**25** in moderate yield (60%). Finally, enantiopure (*S*)-(–)-**25** was converted into (*S*)-(–)-**18** using LiHMDS and pentafluorobenzoyl chloride in 80% yield. (*R*)-(+)-**18** was obtained in a similar manner starting from (*S,S,R*)-**23**.

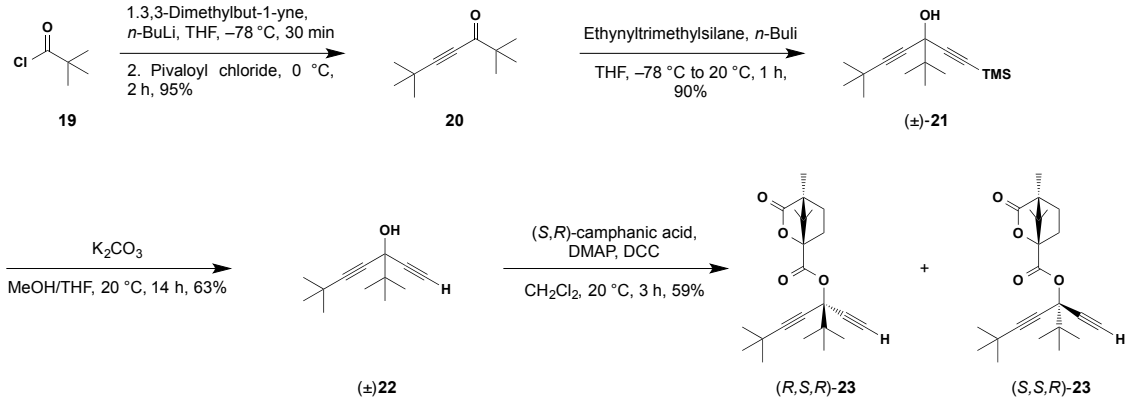

Scheme 7. Synthesis of **23**.[34] DMAP = 4-Dimethylaminopyridine; DCC = *N,N′*-Dicyclohexylcarbodiimide.

Enantiomerically enriched DEA (*M*)-(–)-**26** was obtained in 69% yield with an enantiomeric ratio (e.r.) of 96:4 by a palladium-mediated S_N2'-type reaction using the optically pure bispropargylic ester (*S*)-(–)-**18** (Scheme 8). Si(*i*Pr)$_3$ group removal from (*M*)-(–)-**26** gave DEA (*M*)-(–)-**17**, which can be resolved with an e.r. of 100:0 using HPLC and the CSP Chiralpak IA® (enantiomer (*P*)-(+)-**17** was obtained in an equivalent manner).[35]

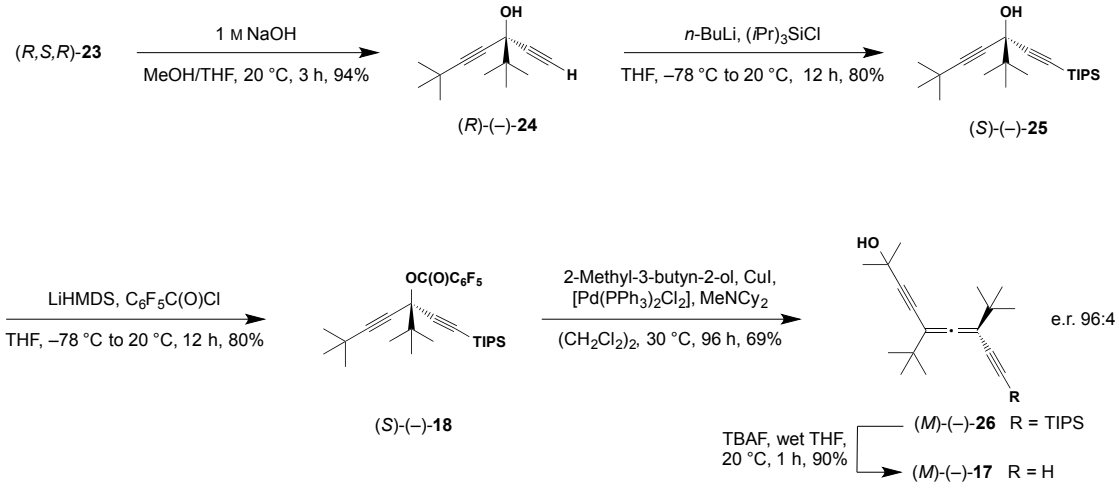

Scheme 8. Enantioselective synthesis of DEA **17**. [34] Cy = Cyclohexyl; LiHMDS = Lithium bis(trimethylsilyl)amide; TBAF = Tetra-*n*-butylammonium fluoride

Since 2008, the CSP Chiralpak IA® was also used to perform preparative separations of the racemate (±)-**17**.[35] This method is more convenient than the enantioselective route because both enantiomeric building blocks are obtained in enantiomerically pure form, and less synthetic operations are involved.

The availability of stable, enantiopure DEA building blocks (*P*)-(+)-**17** and (*M*)-(–)-**17** was the starting point of many projects in our group.

1.1.3. DEAs for the Construction of Alleno-Acetylenic Macrocycles

The Diederich group has previously succeeded in the preparation of various 1,3-DEAs.[32–36] Apart from allowing for the construction of a three-dimensional acetylenic network, one additional advantage brought about by the allene moiety is their inherent chirality, which they exhibit when they are suitably substituted, thus opening the door to chiral three-dimensional advanced materials.[12,37] It should also be noted that numerous achiral and chiral allenes with different substitution patterns have been reported in the literature.[12,36–38] Several types of allenes with unusual topologies and properties are still in their relative infancy. Among these are 1,3-DEAs and their macrocyclic and oligomeric analogues, which represent a new class of compounds with promising reactivity and chiroptical properties.[36]

Macrocyclic cyclophanes bearing acetylene bridges have attracted the curiosity of organic chemists for the determination of the relationship between molecular structure and physical properties.[39–43] Allenophanes, allenic macrocycles incorporating aromatic rings in the backbones, are conformationally rigid and shape-persistent structures and can exhibit molecular functions such as aggregation behavior, host-guest complexation, and unique electronic properties.[44–49] The first synthesis of allenophane **27** was described in 1999 by Thorand, Vögtle, and Krause (Figure 3).[50] Allenophane **27** was synthesized over 16 steps in 5% overall yield and obtained as a complex mixture of stereoisomers. Attempts to separate these compounds by HPLC failed due to their poor solubility. It was only in 2005 that Clay and Fallis reported the first optically active allenophane $(P)_2$-(–)-**28**.[51] Intense Cotton effects ($\Delta\varepsilon$ = +90 M^{-1} cm^{-1} at 260 nm and $\Delta\varepsilon$ = –100 M^{-1} cm^{-1} at 240 nm) were observed from the electronic circular dichroism (ECD) spectrum. Three years later, the Fallis group reported *meta*-allenophanes $(P)_3$-(–)-**29** and $(P)_4$-(–)-**30**.[52] The Cotton effects of $(P)_3$-(–)-**29** and $(P)_4$-(–)-**30** are surprisingly weaker than that of $(P)_2$-(–)-**28** ($\Delta\varepsilon$ = +20 M^{-1} cm^{-1} and $\Delta\varepsilon$ = +5 M^{-1} cm^{-1} at 260 nm for $(P)_3$-(–)-**29** and $(P)_4$-(–)-**30**, respectively) and these allenophanes were shown to be very unstable.

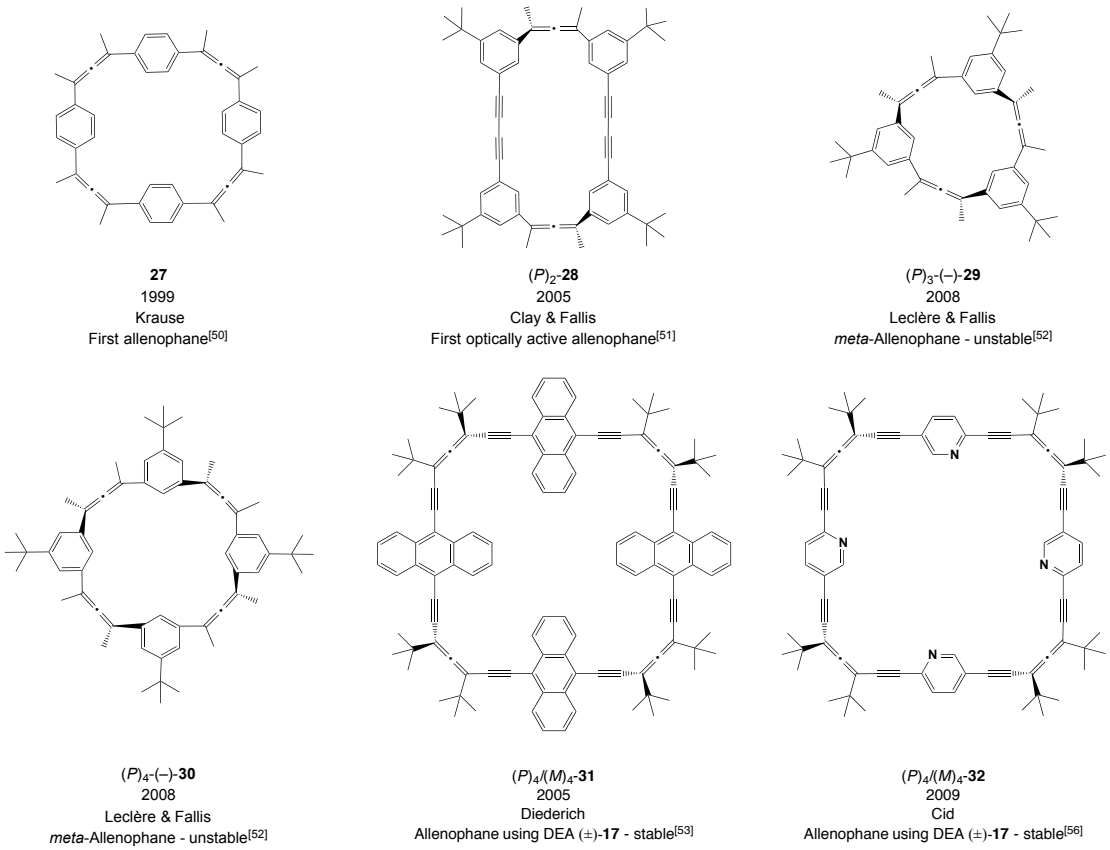

Figure 3. Selected Allenophanes.

DEA (±)-**17** has been used for the synthesis of fairly stable anthracenophanes $(P)_4$-(–)-**31** and $(M)_4$-(+)-**31**.[53] All diastereoisomers were identified and separated by HPLC. However, the racemates could not be resolved. It has been shown that allene moieties racemize under daylight due to the anthracene moieties acting as intramolecular photosensitizer leading to photoracemization of allenes.[54,55]

Cid and coworkers reported the synthesis of chiral allenophanes $(P)_4$-(–)-**32** and $(M)_4$-(+)-**32** incorporating four pyridine-2,5-diyl spacers in the backbone (Figure 4).[56] All diastereoisomers were separated by HPLC techniques, and their structures assigned by their symmetry using ^{13}C NMR spectroscopy.

In 2005, our group reported the first shape-persistent alleno-acetylenic macrocycle (SPAAM) without aromatic rings in the backbone (Figure 4). Compound **33** was prepared as a mixture of seven stereoisomers, starting from racemic (±)-**17**.[53] HPLC techniques enabled the separation of all diastereoisomers, including two racemates and three achiral stereoisomers. Unfortunately, only one

chiral diastereoisomer could be assigned by NMR spectroscopy, and the other chiral stereoisomer could not be identified. In addition, the racemates could not be resolved.

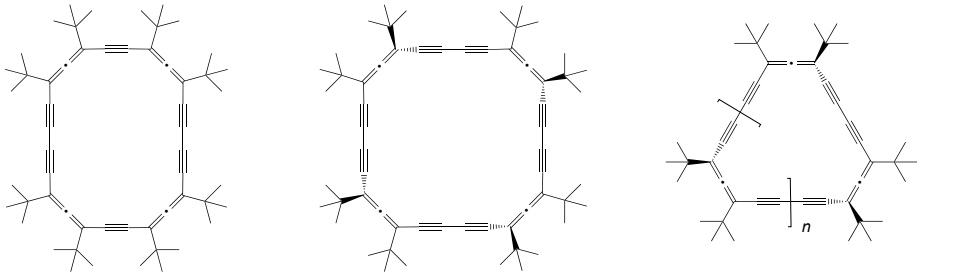

33
2005
First SPAAM
Mixture of diastereoisomers[53]

$(P)_4$-(–)-**34**
2008
First enantiopure SPAAM
Outstanding chiroptical properties[57]

$(P)_n$-(–)-**35**
2011
n = 1,3,4
Monodisperse alleno-acetylenic macrocycles[59]

Figure 4. SPAAMs **33**–**35**.

It is only in 2009 that our group synthesized the enantiomerically pure alleno-acetylenic macrocycles $(P)_4$-(–)-**34** and $(M)_4$-(+)-**34**.[57] They exhibit exceptionally intense Cotton effects, surpassing those of helicenes and fullerenes and reaching $\Delta\varepsilon$ values up to 790 $M^{-1}cm^{-1}$ (in *n*-hexane at 25 °C) as a result of a unique combination of geometric and electronic properties.[58] These promising results demonstrate that the synthesis of new macrocycles, starting from enantiomerically pure DEAs as well as the investigation of their reactivity and properties, are crucial to the developement of new molecular materials.

In 2011, a series of enantiopure, monodisperse alleno-acetylenic macrocycles $(P)_4$-(–)-**35** and $(M)_4$-(+)-**35** were synthesized (Figure 4).[59] Larger oligomers did not lead to stronger chiroptical properties and it was shown that the symmetry of the molecular structure has a strong impact on the intensity of ECD signals. We noticed that D_n symmetries optimized the angle between the electric transition dipole moment (ETDM) and the magnetic transition dipole moment (MTDM), contributing to stronger Cotton effects.

Our current efforts in this field have focused on the lateral functionalization of DEAs with the aim of triggering self-association of the corresponding macrocycles into chiral columnar super-structures with amplified chiroptical properties. We demonstrated that phenol-substituted macrocycles **36** form hydrogen-bonded pillared arrays in the solid state (Figure 5).[60,61] Intra- or intermolecular linkage may

be promoted *via* non-covalent interactions (*e.g.* hydrogen-bonding, metal coordination). Aggregation was also observed in solution at NMR concentration, but at lower concentration (UV, CD range) the compound was found to exist as a monomer.

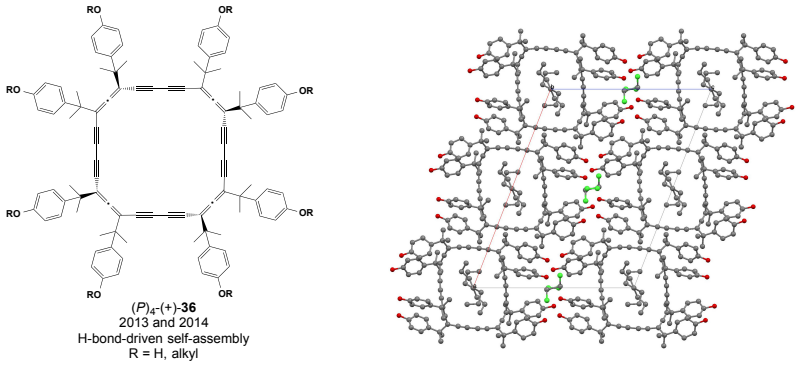

Figure 5. Packing of $(P)_4$-(–)-**36** in the solid state. R = H. Hydrogen atoms are omitted for clarity. Color code: green = Cl, red = O, grey = C.[60]

In MeCN, both macrocycles show intense Cotton effects centred at 257 nm ($\Delta\varepsilon$ = ± 415 M^{-1} cm^{-1}, **34**) and 254 nm ($\Delta\varepsilon$ = ± 375 M^{-1} cm^{-1}, **36**) (Figure 6). ECD spectra of monomer **37** and dimer **38** are shown in Figure 6 for comparison with SPAMMs **34** and **36**. While these values remain very large, they are reduced with respect to the tetrameric macrocycle peripherally decorated by eight *tert*-butyl groups. This reduced intensity of the Cotton effects correlates with a reduction in the molar extinction coefficients, presumably induced by the phenolic substituents, which also increase the conformational flexibility of the macrocycle.

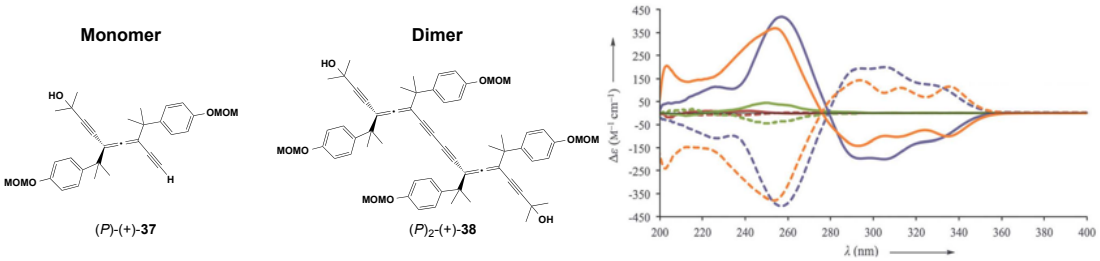

Figure 6. ECD spectra of $(P)_4$-(–)-**34**, (purple line), $(P)_4$-(–)-**36** (orange line), (*P*)-(+)-**37** (red line), $(P)_2$-(+)-**38** (green line), $(M)_4$-(+)-**36**, (dashed purple line), $(M)_4$-(–)-**37** (dashed orange line), (*M*)-(–)-**37** (dashed red line), and $(M)_2$-(–)-**38** (dashed green line). Measured in MeCN at 25 °C.[60]

Recently, Cid and coworkers reported the use of $(P)_4$-(–)-**39** as a molecular host by exploiting halogen-bonding interactions (Figure 7).[62] A chiral bidentate inclusion complex has been formed by halogen-bond interaction between the pyridyl moieties of a pyridoallenoacetylenic host and octafluorodiiodobutane. X-ray crystallography demonstrated that the guest adopts a chiral conformation inside the molecular channels formed by stacking of the host units. Applicability of these new complexes may involve the design of new chiral switches and sensors as well as the preparation of chiral chromatographic layers[63] for the resolution of racemic halogenated compounds.[64]

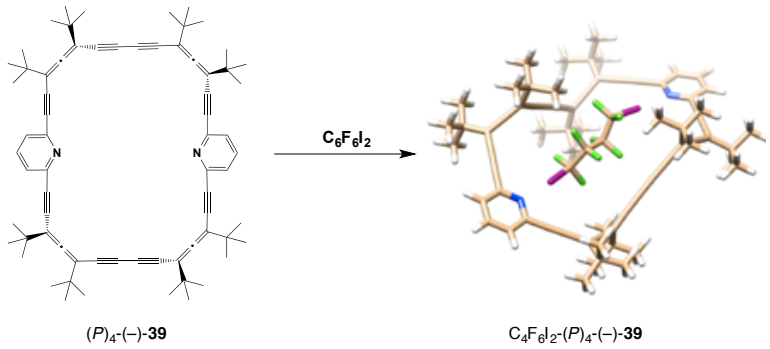

Figure 7. Halogen-bonded shape-persistent chiral alleno-acetylenic inclusion complex. X-Ray structure of $C_4F_6I_2$-$(P)_4$-(–)-**39**.[62]

Lately, Cid, Alonso-Gómez and coworkers reported a covalent organic helical cage with remarkable chiroptical properties (Figure 8).[65] Covalent dimerization of a tripodal fragment $(P)_3$-(+)-**40** including DEAs forms the molecular twisted prism $(P_2)_3$-(+)-**41**. A 10-fold amplification of the Cotton effects of $(P_2)_3$-(+)-**41** compared to its isolated building blocks is described. A selective inclusion complex formation with ferrocenium ions was confirmed and quantified using HR-ESI-MS and NMR spectroscopy.

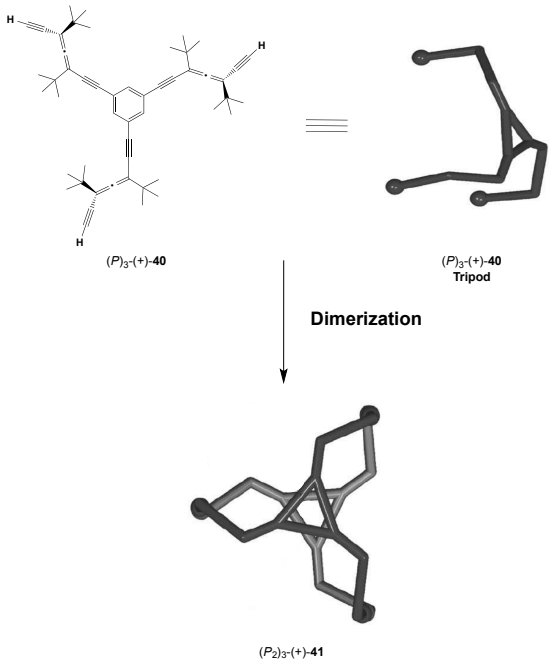

Figure 8. Molecular twisted prism $(P_2)_3$-(+)-**41**.[65]

1.1.4. DEAs for the Construction of Alleno-Acetylenic Oligomers

The development of novel monodisperse oligomers that adopt well-defined conformations in solution ("foldamers"), analogous to the folded state of nucleic acids or proteins,[66,67] attracts attention due their potential applications in sensing, optics and electronics. Chiral oligomers can fold into single-handed helices as a consequence of chiral induction,[68–70] and their chiroptical properties can be significantly increased by conformational rigidity. Oligomers and polymers containing allenes in the main chain are extremely rare due to their participation in many polymerization processes, especially those involving insertion of transition metals[71] and living coordination polymerization.[72]

In 2002, the first synthesis of a conjugated allene polymer was reported by Kijima.[73] Polymer **42** was synthesized as a mixture of stereoisomers *via* a nickel-mediated polymerization process (Figure 9). This polymer has good solubility and processability, but low average molecular weight (5000 g mol^{-1}) and broad polydispersity. The polymer exhibits strong blue fluorescence upon irradiation with UV light. Moreover, a shift in absorption, from λ_{max} = 310 nm to λ_{max} = 700 nm, has been observed upon protonation with trifluoroacetic acid (TFA). This phenomenon

could possibly be explained by the formation of an allylic carbocation, leading to a fully conjugated backbone.

A similar polymer **43** was synthesized by Hiroki and Kijima (Figure 10).[74] This copolymer also revealed good solubility and processability as well as strong blue fluorescence when irradiated with UV light. The quantum yield was close to 1.0, which is a consequence of the suppression of excimeric radiative processes by the twisted (helical) conformation of **43**. Unfortunately, **43** was obtained as a mixture of stereoisomers and consequently, the chiroptical properties could not be determined.

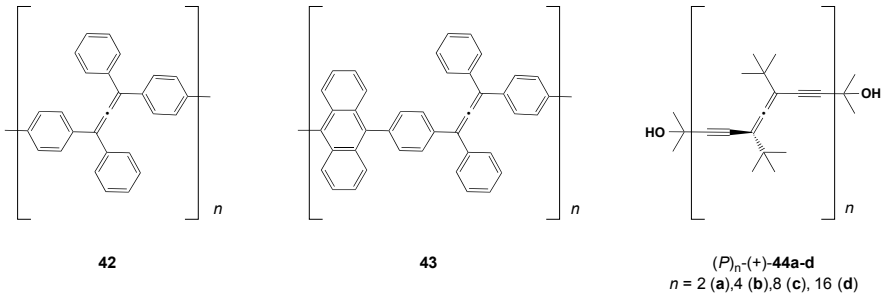

42 **43** $(P)_n$-(+)-**44a-d**
n = 2 (**a**),4 (**b**),8 (**c**), 16 (**d**)

Figure 10. Acyclic oligomers **42** and **43** and enantiopure acyclic alleno-acetylenic oligomers $(P)_n$-**44a-d**.[73–75]

In 2007, our group reported the oligomerization of a racemic DEA.[75] Monodisperse oligomers were obtained as complex mixtures of stereoisomers after gel permeation chromatography (GPC). It is only in 2010 that our group reported enatiomerically pure alleno-acetylenic oligomers $(P)_n/(M)_n$-**44a-d** from optically pure DEA (Figures 10 and 11).[74] These novel acyclic oligomers exhibit chiroptical properties that are among the most intense reported to date. The ECD intensity increases remarkably from the monomer ($\Delta\varepsilon$ = ±9 $M^{-1}cm^{-1}$at λ = 225 nm) to the octamer ($\Delta\varepsilon$ = ±825 $M^{-1}cm^{-1}$at λ = 265 nm) and reaches exceptionally high values ($\Delta\varepsilon$ = ±1360 $M^{-1}cm^{-1}$, λ = 266 nm) for the hexadecamer (Figure 11). The intensity of the Cotton effect of the hexadecamer **44d** at shorter wavelength (λ = 212 nm), is even up to $\Delta\varepsilon$ = ±1690 $M^{-1}cm^{-1}$. The ECD spectra are nearly independent of solvent polarity, from *n*-hexane to MeOH. The non-linear amplification of these chiroptical responses suggests the existence of a conformational preference preserved along the backbone of all oligomers. Based on chiroptical properties and calculations, oligomers bearing (*P*)-(+)-DEAs exist predominantly as an ensemble of right-handed

helical conformations with the torsion angle across the butadiyne axes ranging predominantly from 0° to 45°.

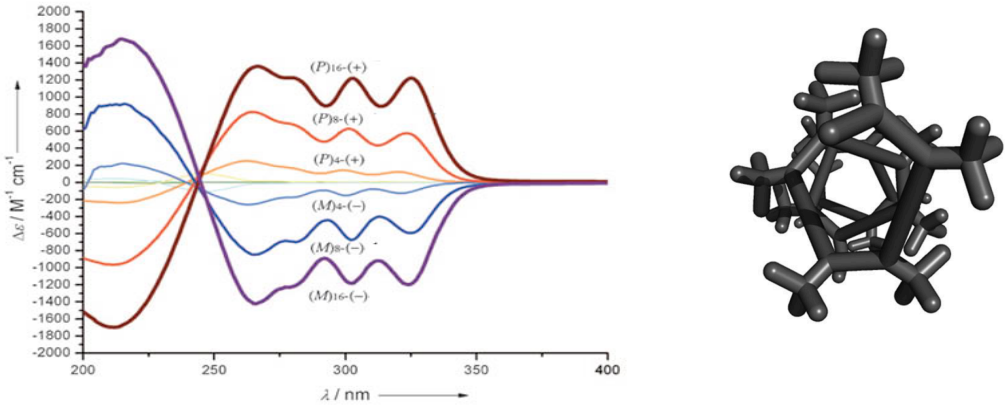

Figure 11. Right: CD spectra of alleno-acetylenic oligomers $(P)_n/(M)_n$-**44a-d** in *n*-hexane at 25 °C. Left: view along the helical axis of the proposed conformer at $\theta = 0°$.[75]

In an attempt to stabilize the helical secondary structure of oligomeric alleno-acetylenes by bridging and thus, increase their exceptional chiroptical responses, we studied the cyclization of dimeric alleno-acetylenes starting from (*P*)-(+)-**45** (Figure 12).[76] Rigidification of the chiral dimer was attempted by oxidative Hay coupling to form a macrocyclic cyclohexadeca-1,3,9,11-tetrayne $(P)_2$-(+)-**46** with two vinylidene substituents. Unfortunately, no enhancement of the chiroptical properties was observed.

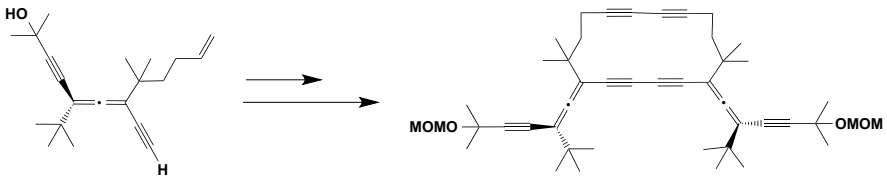

(*P*)-(+)-**45** $(P)_2$-(+)-**46**

Figure 12. Stapling of helical alleno-acetylene oligomers.[76]

1.1.5. Lateral Functionalization of DEA

In 2011, our group investigated the use of DEAs as push–pull chromophores for the formation of chromophoric advanced materials with great molecular complexity (Scheme 9).[77] By adding *N*,*N*-dimethylanilino residues onto the lateral alkyne chain,

DEAs (±)-**47**–**49** become electron-rich and upon addition of 1,1,2,2-tetracyanoethene (TCNE) or 7,7,8,8-tetracyano-*p*-quinodimethane (TCNQ), a cascade reaction occurs. Alleno-acetylene (±)-**47** undergoes a 4π electrocyclization to form cyclobutene (±)-**50** in 60% yield. Compound (±)-**48** reacts through an allenyl-Cope rearrangement to yield [4]dendralene **51** in 90% yield. Lastly, tetrahydroindene (±)-**52** is obtained from (±)-**49** *via* a [4+2] Diels–Ader reaction in excellent yield.

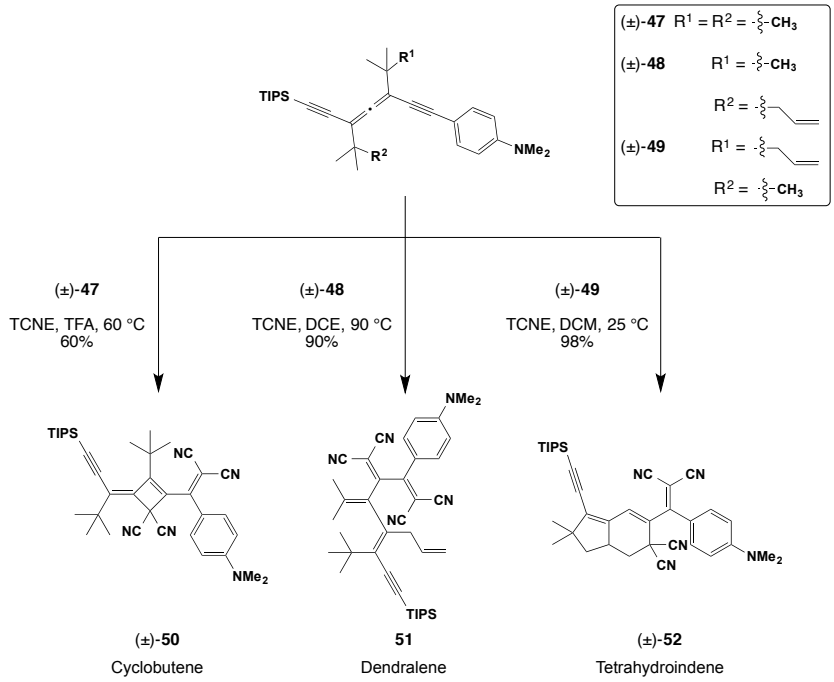

Scheme 9. Cascade pericyclic reactions of alleno-acetylenes.[77]

Axially chiral alleno-acetylenes, modified with lateral aryl groups can be used as an efficient chiral dopant for producing cholesteric liquid crystals (Figure 13).[78] It has been shown that allene derivatives (*P*)-(+)-**53a-d** and (*P*)-(+)-**54a-b** are effective inducers of cholesteric phases, comparable to widely applied biaryl-based dopants.

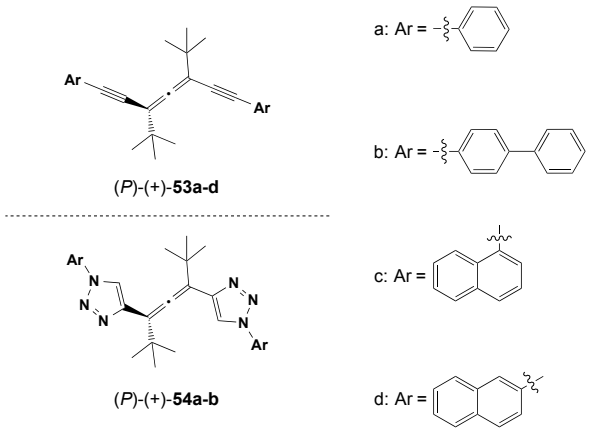

Figure 13. DEA derivatives for cholesteric liquid crystal line phase inducers.[78]

The attachment of C_{60} on the terminal alkyne (*P*)-(+)-**17** was reported for the preparation of enantiopure dumbbell-type dimeric fullerenes $(P)_2$-(+)-**55a**,**b** (Figure 14).[79] Optically pure alleno-acetylenes can be used as stable, non-racemizable addends for the construction of chiral fullerene derivatives with intense chiroptical response. ECD spectra not only featured alleno-acetylene-based Cotton effects, but also revealed chiral induction from the optically active allene moiety into the C_{60} chromophores.

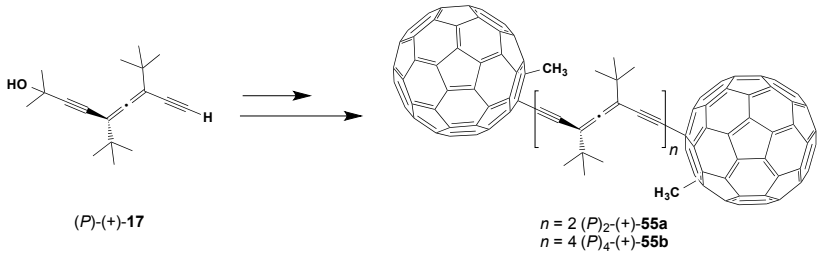

Figure 14. Alleno-acetylenic scaffolding for the construction of axially chiral C_{60} dimers.[79]

In 2014, our group became interested in transferring the molecular properties of alleno-acetylenes to supramolecular assemblies.[80] DEAs have been used to construct enantiopure triple-stranded Zn^{II}-helicates from ligands (*P*)-(+)-**56** and (*M*)-(–)-**56** bearing a helical cage ("helicage") for the encapsulation and detection of small organic molecules (Figure 15). The formation of this cavity in (*Δ*,*Δ*)-$(P)_3$-**57** resulted from a combination of the lean alleno-acetylenic moieties and the all-carbon backbone, which provided guest-binding space in the triple helicate. High affinity

towards 1,4-dioxane as guest was observed at ppm levels in aqueous solution (K_a = 1800 M^{-1} in D_2O/CD_3OD 1:1 or D_2O/CD_3OD 19:1).

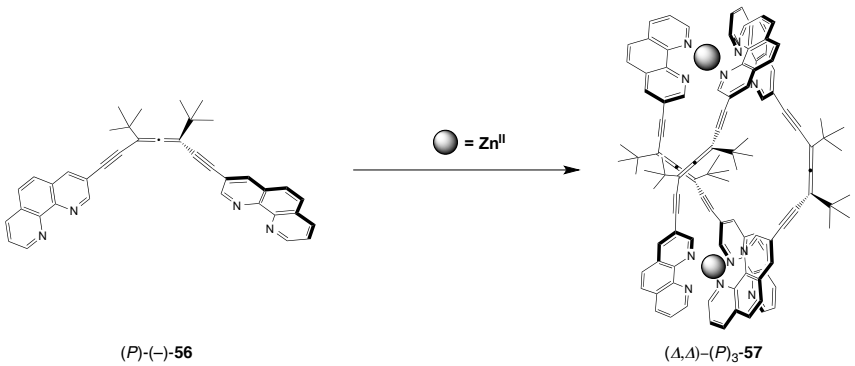

Figure 15. From alleno-acetylenes to supramolecular assemblies.[80]

In the aim of exploring further topologies formed by this scaffold, we reported the highly selective catenation of the homochiral alleno-acetylenic strands (*P*)-(+)-**56** and $(P)_2$-**58** and their corresponding enantiomers upon addition of silver(I) salts to form dinuclear (Δ_2)-(P_2)-**59** and trinuclear double helicates (Δ_3)-(P_4)-**60**, respectively (Figure 16).[80,81] When the solvent polarity is increased, the dinuclear and trinuclear helicates interlock to yield [2]catenane (Δ_4)-(P_2)-**61** and the unprecedented bis[2]catenane (Δ_6)-(P_8)-**62**, bearing 14 chirality elements. Highly selective narcissistic self-sorting is demonstrated for a racemic mixture, consisting of both the short and the long ligand.

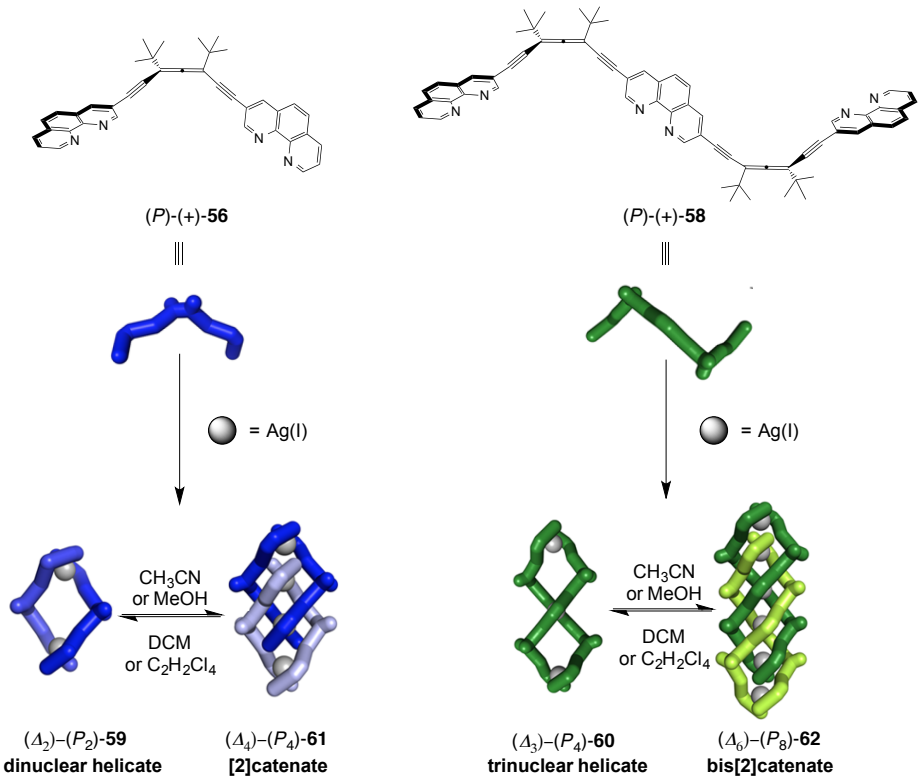

Figure 16. From alleno-acetylenes to supramolecular assemblies.[81]

1.2. Introduction to the [2+2] Cycloaddition–Retroelectrocyclization Reaction.

Over the past decades, molecules containing electron donors and electron acceptors separated by a π-conjugated spacer have been intensively studied.[82–95] One of the main goals is the fine-tuning of the gap between the highest occupied molecular orbital (HOMO) and lowest unoccupied molecular orbitals (LUMO) (HOMO–LUMO gap).[82,96] These chromophores often exhibit intramolecular charge-transfer (ICT) and can be used as functional materials for electronic and optical applications.[96–103] In addition, chromophores that show intense ICT continuously receive much attention as active non-linear optical (NLO) materials.[82–95,104]

Advanced organic materials used in electronic and optoelectronic applications are generally employed in the form of thin films.[105] Monitoring the morphology is therefore crucial for the properties. Planar chromophores tend to crystallize readily, and aggregation usually has a deleterious effect upon the optical properties.[96]

In this sense, non-planar push–pull chromophores offer several advantages over planar systems, including improved solubility and sublimability, and formation of regular amorphous films.[96,102, 106] In the case of NLO materials, the symmetry of the solid-state packing is crucial as well. In this regard, the development of new push–pull chromophores attracts increasing interest to the scientific community.

Over the past 12 years, our group has made important contributions to this field with the discovery of novel non-planar push–pull chromophores for organic materials with interesting optoelectronic properties.

With the aim of developing new push–pull chromophores, we have been interested in using a click-chemistry type reaction of electron-donating alkynes with electron-withdrawing alkenes.[107] This strategy allowed us to have access to a variety of chromophores in high-yielding, atom-economic reactions with excellent chemo- and regioselectivity. Several electron-deficient electron acceptors such as tetracyanoethene (TCNE), 7,7,8,8-tetracyano-*p*-quinodimethane (TCNQ) and others were investigated and described in the following subsections.

1.2.1. [2+2] Cycloaddition–Retroelectrocyclization Mechanism

The CA–RE reaction was reported for the first time in 1981 by Bruce and coworkers from an electron-rich ruthenium acetylide complex and tetracyanoethylene (TCNE) to yield a 1,1,4,4-tetracyanobuta-1,3-diene.[108] Further investigations into this transformation revealed a broader applicability to organic electron-donor-activated alkynes.[101,102,109–113] This cascade reaction starts with an initial formal [2+2] intermolecular cycloaddtion between an electron-rich alkyne **63** and an electron-poor alkene, such as TCNE (**64**) to afford cyclobutene intermediate **65**, which then undergoes spontaneous retroelectrocyclization to give the corresponding donor-substituted tetracyanobutadiene (TCBD) **66** (Scheme 10).[101,102] The CA–RE transformation has the advantage to occur under mild conditions and without any catalyst.

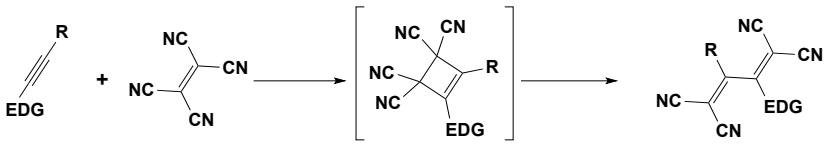

63 64 65 66

Scheme 10. General representation of the CA–RE reaction between TCNE and electron-rich alkynes. EDG = electron-donating group.

The non-planar push–pull chromophores derived from the CA–RE reaction exhibit interesting properties, such as tunable intramolecular charge-transfer bands expanding into the near-infrared (NIR), large third-order optical nonlinearities, high two-photon absorption cross-sections, thermal and environmental stability up to 300 °C, and in many cases sublimability, as will be described in the following subchapters.

1.2.2. Cycloaddition–Retroelectrocyclization with TCNE

In 2005, our group reported a new class of organic donor–acceptor molecules with large third-order NLO properties.[114] Figure 17 shows selected examples of donor-substituted TCBDs (**67** and **68**) obtained from the CA–RE transformation of TCNE and different DMA-donor alkyne derivatives.[114] They feature intense intramolecular charge-transfer bands, substantial quinoid character in the donor rings, and reversible electrochemical reductions as well as oxidations. The low energy of the CT bands and the low electrochemical HOMO–LUMO gaps demonstrate substantial π-conjugative effects despite the overall nonplanarity. The compounds are thermally stable and can be sublimed without any decomposition, which opens perspectives for device construction. Compound **68** has found application in optical silicon-organic hybrid slot waveguides for all-optical high-speed signal processing.[106,114–116]

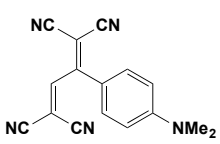

67

λ_{max} = 570 nm
$E_{ox,\,1}$ = +0.86 V
$E_{red,\,1}$ = –0.69 V

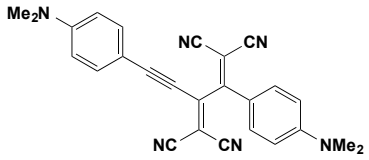

68 (DDMEBT)

λ_{max} = 526 nm
$E_{ox,\,1}$ = +0.72 V
$E_{red,\,1}$ = –0.89 V

Figure 17. Donor-substituted TCBDs and their optoelectronic properties. Electrochemical data observed by CV at a scan rate of v = 0.1 V s^{-1} and rotating disk voltammetry (RDV) in CH_2Cl_2 + 0.1 M Bu_4NPF_6. All potentials are given versus ferrocene, used as internal standard reference.[106,114–116]

Resulting from our preliminary studies showing the efficiency of the CA–RE reaction, our group prepared a variety of more sophisticated push–pull chromophores with significant redox properties (Figure 18). Chromophore **69** displays six reversible $1e^-$ reductions on the strongly electron-accepting TCBD units.[117] Additionally, electrochemistry results confirmed that the donor units behave as independent redox centers. Systems **70** and **71** were designed and synthesized based on multiple TCNE additions to the corresponding activated systems.[118] In total, six TCBDs exhibit six well-separated $1e^-$ reduction steps followed by one $6e^-$ reduction in dendimeric-type branched **70**, whereas system **71** displays two reversible $12e^-$ reduction steps in a very narrow potential range. Similar to **69**, donor units behave as independent systems and oxidize in a $12e^-$ transfer step.

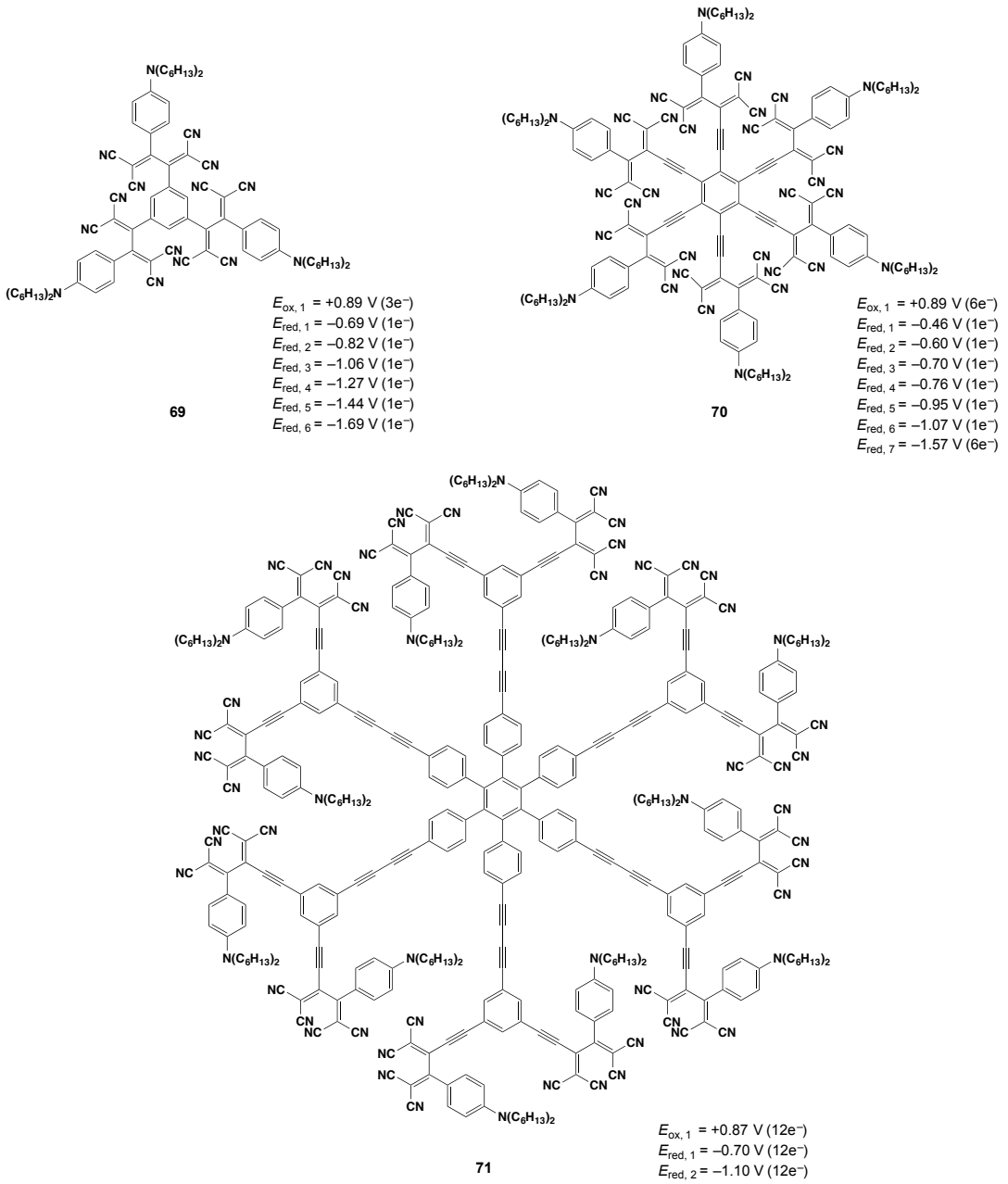

Figure 18. Multivalent charge-transfer chromophores.[117,118]

In 2009, chiral *N*-phenyldinaphthazepine-capped TCBDs were synthesized from enantiopure 1,1'-bi(2,2'-naphtol) (BINOL) and anilines derivatives (Figure 19).[119] With their elongated shape and the rigidity of the donor part of the molecule, these chromophores were investigated as potential cholesteric liquid-crystal inducers and displayed very high helical twisting power (HTP) values β. Although a low β value (+27 μm^{-1}) was observed for (*S,S*)-**72**, in the case of (*S,S*)-**73**, it reached up to +132 μm^{-1}. Only a couple of dopants have been reported exhibiting such a high value (Figure 19).

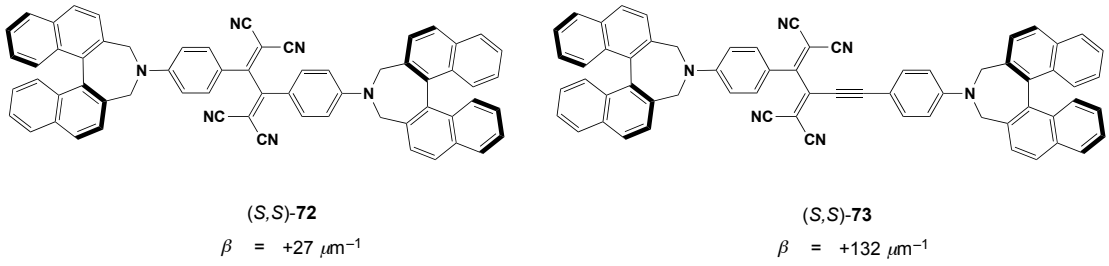

Figure 19. Helical twisting power of (*S,S*)-**72** and (*S,S*)-**73**.[119]

A systematic study on donor–acceptor-substituted polyyne chromophores has been reported (Figure 20).[120] The design of the compounds was inspired by DDMEBT **68**. This study offered a clear explanation for the influence of the lengh of the alkyne spacer on the third-order NLO properties of the chromophores **74**.

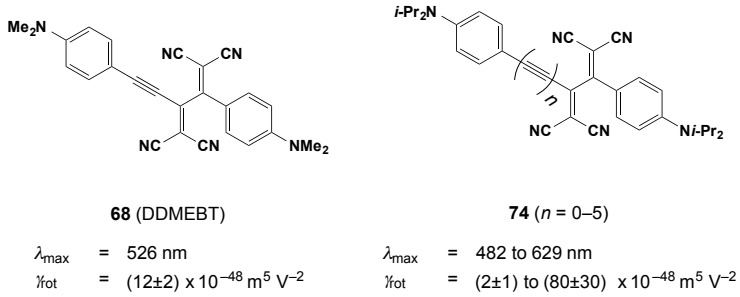

Figure 20. Influence of spacer length on third-order NLO properties.[120]

The CA–RE reaction can give access in an efficient way to new photoactive multicomponent systems.[121,122] The conjugates comprise a Zn^{II} porphyrin as electron donor, which is connected with different spacers such as phenylene–ethynylene–phenylene derivatives to anilino-substituted multicyanobutadiene analogues such as in dyad **75** (Figure 21).[122] The optoelectronic properties were assessed by electrochemical, spectroelectrochemical, and steady-state fluorescence spectroscopic studies.

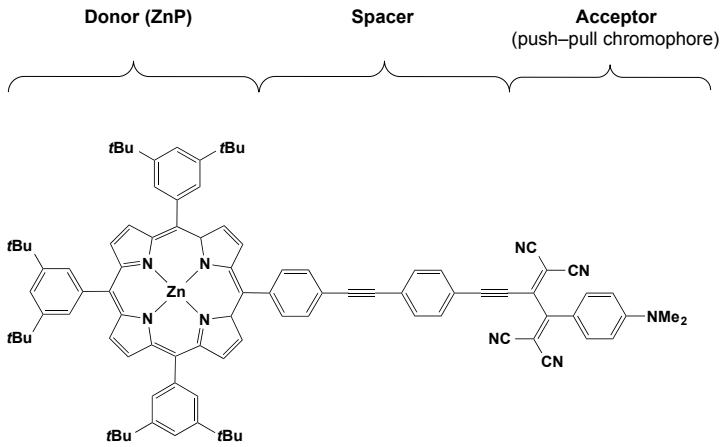

75

Figure 21. Molecular dyad **75**.[121]

A comparison of acyclic and cyclic strained donor-substituted alkynes also showed interesting results. The thermal [2+2] CA–RE reaction of TCNE with strained, electron-rich cyclooctyne **76** was studied in detail (Scheme 11).[123] The impact of ring strain on the reaction kinetics was investigated for the formation of **77** *via* intermediate **78**. The reaction rates of cycloaddition for cyclic, donor-substituted alkynes are up to 5500 times greater than those of unstrained systems.

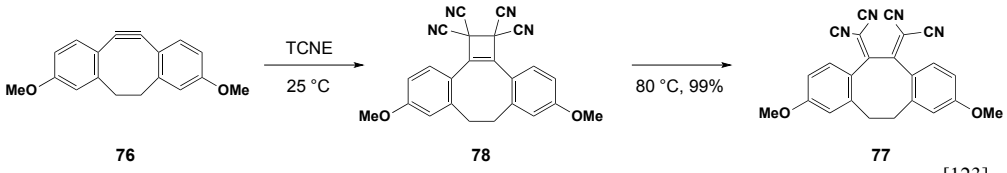

76 78 77

Scheme 11. CA–RE reactions of TCNE with strained, electron-rich alkynes.[123]

Lastly, the synthesis of multivalent, Janus-dendrimer-type donor–acceptor (D–A) system **79** is described (Figure 22).[124] The key steps of the multistep approach were the Sonogashira cross-coupling of two different dendrons and the regioselective, formal [2+2] CA–RE reaction of the coupling product with excess of TCNE. The existence of a mixture of rotamers in the Janus-dendrimer-type system was shown through ^{1}H and ^{13}C NMR analysis and was supported by a series of control experiments. The strong ferrocenyl electron donors in one hemisphere are not in electronic communication with the strong electron acceptors in the second: the extended π-system with several *meta* connectivities behaves similar to a σ-bonded

bridge preventing intramolecular charge transfer from the ferrocene donor hemisphere to the TCBD acceptor hemisphere.

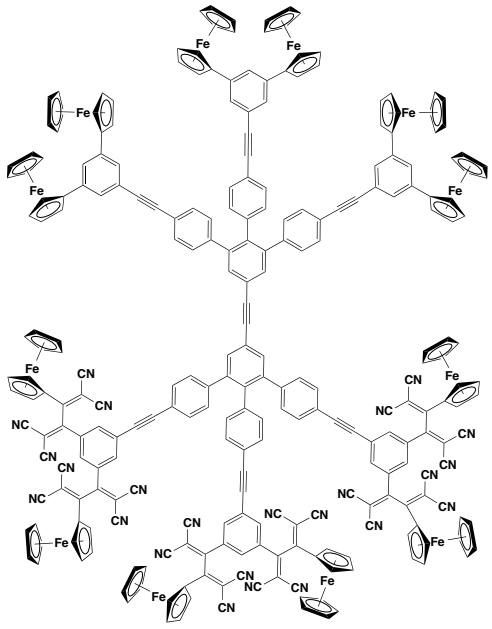

79

Figure 22. Janus-dendrimer-type system **79**.[124]

In 2015, our group reported the preparation of cyano-substituted diaryltetracenes through a reaction cascade involving the CA–RE reaction of TCNE to the central bond of the tetraaryl[3]cumulene **80**, electrocyclization to **81** and formal elimination of cyanogen to afford tetracenes **82** (Scheme 12).[125] In a short time, this method has attracted much interest due to significant applications of the tetracene products in molecular sensing and singlet exciton fission studies.[125,126]

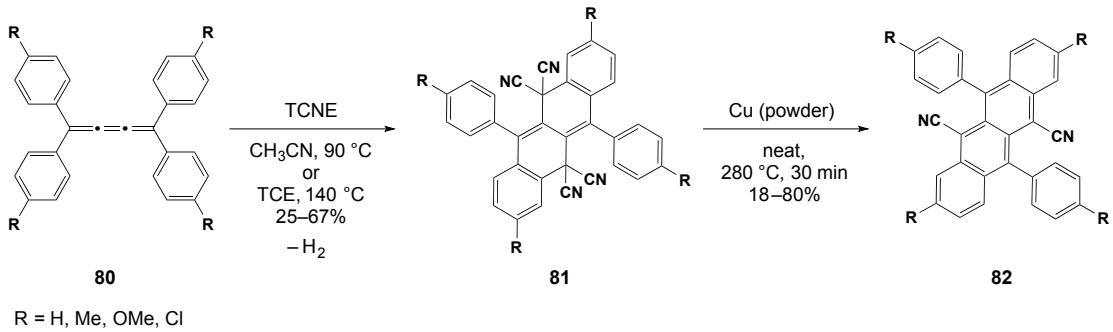

80 81 82

R = H, Me, OMe, Cl

Scheme 12. Synthesis of cyano-substituted diaryltetracenes **82**.[125]

1.2.3. Cycloaddition–Retroelectrocyclization with TCNQ

In parallel to the study of the CA–RE reaction of TCNE with electron-rich substrates, our group explored 7,7,8,8-tetracyano-*p*-quinodimethane (TCNQ) (**83**) as an electron-poor component for the discovery of new push–pull chromophores (Scheme 13).[127–129]

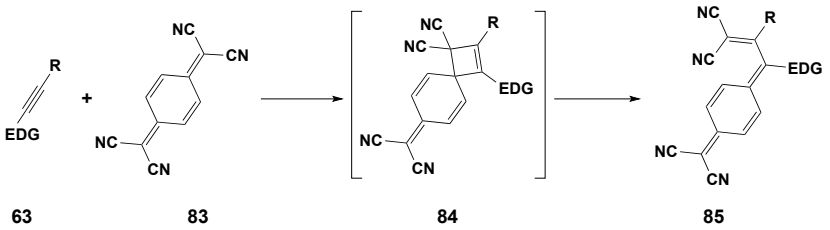

Scheme 13. General representation of the regioselective CA–RE reaction between TCNQ and electron-rich alkynes.

As in the reaction with TCNE, the CA–RE reaction begins with initial formal [2+2] cycloaddition between TCNQ **83** and activated alkyne **63** affording cyclobutene intermediate **84**, which then forms **85** after retroelectrocyclization. The use of TCNQ was first reported in 1972 by Hagihara and coworkers.[130]

Reactions between organometallic Pt(II) alkynyls and TCNQ were described but they could not propose appropriate structures for the obtained products. Later, structure elucidation by X-ray analysis of one of these products revealed the formation of CA–RE adducts.[131] Astonishingly, CA–RE reactions of TCNQ remained untouched for quite some time in constrast to reactions of TCNE. In 2007, our group synthesized chromophores, such as **86**–**89** (Figure 23) from the CA–RE reactions of TCNQ with electron-rich alkynes.[127,128]

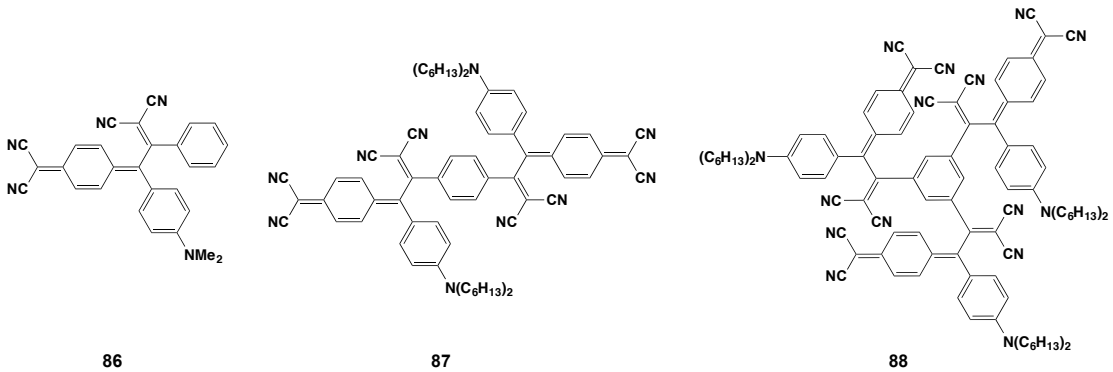

Figure 23. Selected expanded 7,7,8,8-tetracyanoquinodimethanes.[127,128]

Further investigations on expanded TCNQ as acceptor demonstrate that these chromophores could also be employed as organic super electron-acceptors.[129] Scheme 13 describes the reaction of expanded 7,7,8,8-tetracyanoquinodimethane **89** with decamethylferrocene, a strong donor. Single crystal X-ray analysis unambiguously confirmed that the initially obtained intermolecular charge-transfer (ICT) salt **90** forms **91** in the solid state upon σ-dimerization.

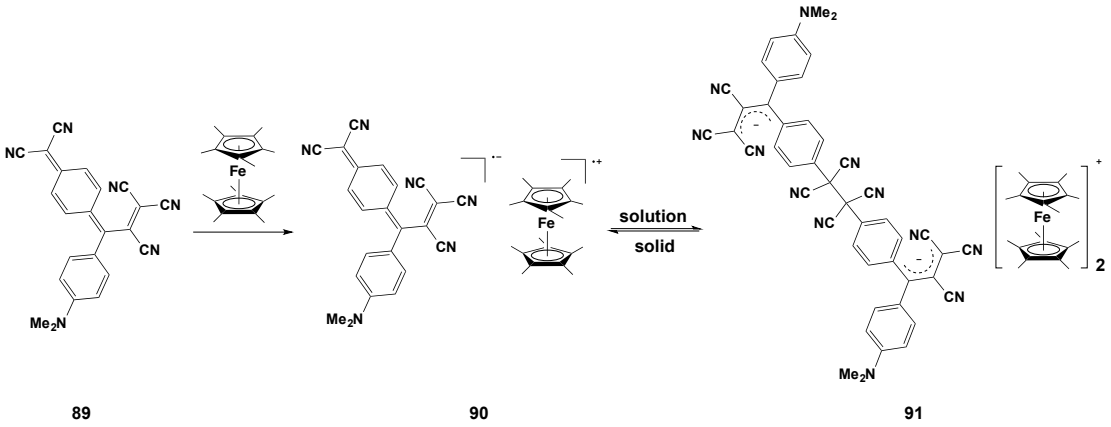

89 90 91

Scheme 13. Reactivity of strong electron acceptor **89** with decamethylferrocene.[129]

Encouraged by these preliminary results, stronger electron acceptors were prepared by CA–RE of F_4-TCNQ with different cyano-, dicyanovinyl-, and tricyanovinyl-substituted *N*,*N*-dialkylanilinoalkyne (DAA-alkynes) (Figure 24).[129] The resulting push–pull chromophores **92**–**94** display intense ICT interactions with end absorptions reaching into the near infrared (IR) region.

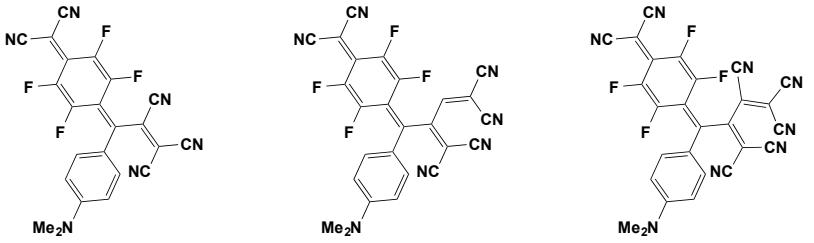

92 93 94

Figure 24. Strong electron acceptors from CA–RE of F_4-TCNQ with corresponding cyano-, and cyanovinyl-substituted DAA-alkynes.[129]

1.2.4. Cycloaddition–Retroelectrocyclization with DCNQI

Less electron-poor *N,N'*-dicyanoquinone diimide (DCNQI)[132] (**95**) could also be employed for the CA–RE reaction yielding a new class of cyanoimine-based, donor–acceptor chromophores, such as **96** and **97** (Scheme 14).[133] The products of CA–RE reactions with DCNQI exhibit strong solvatochromism and third-order polarizabilities in addition to their intense ICT transitions.

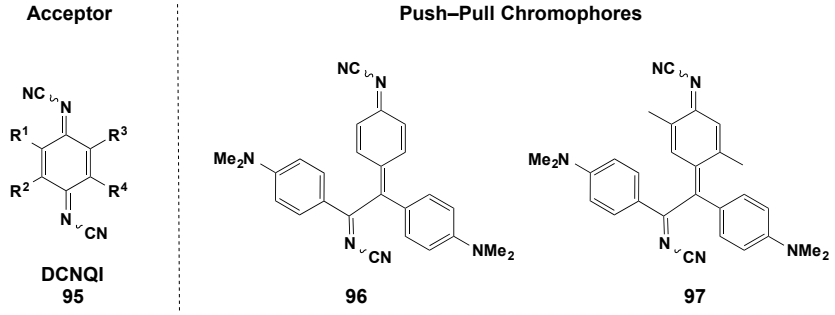

Scheme 14. Synthesis of DCNQI CA–RE Adducts **96** and **97**.[133]

1.2.5. Cycloaddition–Retroelectrocyclization with Dicyanofulvenes

Since 2011, we turned our attention to investigating the use of dicyanofulvenes (DCFs) as acceptors in CA–RE reactions.[134–137] A formal 1,5-elimination of HCN followed by an intramolecular cyclization of an *E*/*Z* mixture of pentacyano-hexatriene **98** gave push–pull DCF **99** in 80% yield (Scheme 15).[134,135] The optoelectronic properties of **9** are remarkable. An ICT band at around 782 nm was observed with an extinction coefficient of 27500 M^{-1} cm^{-1}.

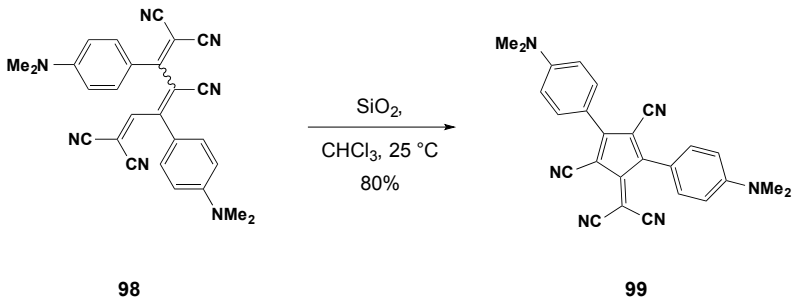

Scheme 15. Synthesis of push–pull DCF **99**.[134]

Phenylated and alkynylated DCFs **100** and **101** were designed. Starting from **102**, DCF adducts **103** and **104** were obtained in good yield and showed opposite regioselectivity (Scheme 16).[136] This is the first report describing the substituent-dependent regioselectivity in CA–RE chemistry.

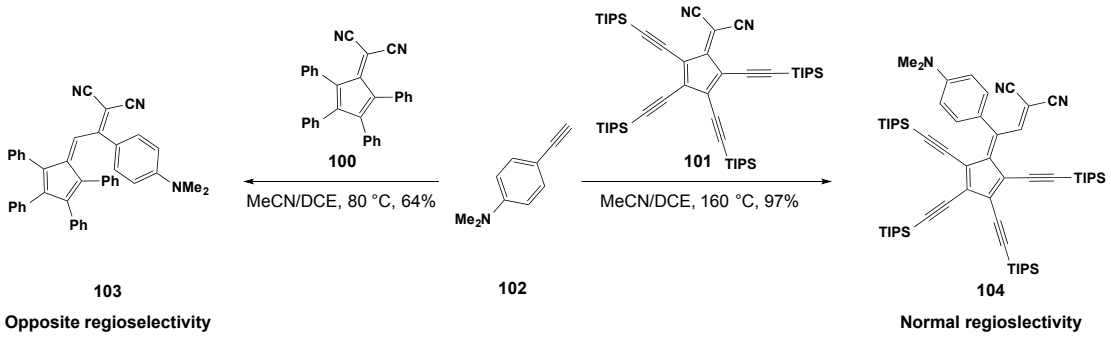

Scheme 16. CA–RE reaction with DCFs.[136]

1.3. Thesis Outline

The first goal of the thesis is to provide testimony that exceptional chiroptical responses are an intrinsic property of shape-persistent macrocyclic and acyclic alleno-acetylenic oligomers with conformational preferences for secondary helical structures of one handedness.

In Chapter 2, the synthesis of a second series of shape-persistent alleno–acetylenic macrocycles and new acyclic alleno-acetylenic oligomers with more rigidified all-carbon backbones in enantiomerically pure form is discussed. Structures and optoelectronic properties are explored by comprehensive studies including X-ray analysis, ECD and UV/Vis spectroscopy, as well as computational calculations. In continuation of exploring lateral functionalization of SPAAMs for the improvement of the chiroptical response and introducing new properties, an attempt towards the synthesis of alcohol-substituted SPAAMs is described.

Push–pull chromophores have long been valuable targets for scientists due to their remarkable optoelectronic properties. Up to now, common acceptor units, such as TCNE and TCNQ, were used to construct sophisticated non-planar push–pull systems. To further expand the chemical space of electron-poor alkenes for the CA–RE reaction, cycloaddition reactions of 2-(dicyanomethylene)indan-1,3-dione

(DCID) to electron-rich alkynes are described in Chapter 3. The structures of the new set of chromophores and their optoelectronic properties are explored by a comprehensive study including X-ray analysis, UV/Vis spectroscopy, electrochemistry and computational studies.

In Chapter 4, the reactivity of new tetrasubstituted electron-deficient alkenes with ester moieties is investigated. The CA–RE reaction still takes place with a single cyano moiety, however other reactions also occur, namely a HDA cycloaddition and a [3+2] cycloaddition/rearrangement cascade. Similar to the DCID adducts, the optoelectronic properties of the chromophores were investigated by X-ray analysis, UV/Vis spectroscopy, electrochemistry and computational analysis. We also described the possibility of post CA–RE reaction functionalization to ester-substituted butadienes including access to pharmacologically interesting scaffolds.

To further explore the role of products derived from the CA–RE reaction in the synthesis of compounds of greater complexity and additional chemical utility, Chapter 5 is dedicated to the synthesis of NH-pyrroles from CA–RE adducts.

Finally, the last Chapter highlights the development of a formal [3+2] cycloaddition/rearrangement cascade reaction between moderately activated to non-activated alkynes and electron-poor dicyano-diester-substituted alkenes to yield a variety of π-conjugated penta-2,4-dien-1-ones.

Chapter 2

Design, Synthesis, and Reactivity of Novel Enantiopure Alleno-Acetylenic Scaffolds

2. Design, Synthesis, and Reactivity of Novel Enantiopure Alleno-Acetylenic Scaffolds

The time-dependent density functional theory theoretical calculation (TD-DFT), and the conformational analysis of the dimeric model were performed by Dr. Ori Gidron. The crystal structures were solved by Dr. Nils Trapp. The results of this Chapter have been the subject of a publication.[137]

2.1. Introduction

The significantly growing interest of chiral allenes is driven by its applications in asymmetric catalysis, chiral sensing, and optoelectronic devices.[10–19] Allenes have also been considered important chiral building blocks in molecular materials and have offered access to shape-persistent macrocyclic structures with new properties and topologies.[58–60] Stable enantiopure DEAs such as (*P*)-(+)-**17** were investigated as building blocks for the construction of optically active, shape-persistent alleno-acetylenic macrocycles. In 2009, our group described the first enantiopure SPAAM $(P)_4$-(–)-**34** and its $(M)_4$-enantiomer, which revealed outstanding chiroptical properties (Scheme 17).[59] Unexpectedly, large chiral amplification and record high Cotton effects were also measured for conformationally highly flexible acyclic alleno-acetylenic oligomers. We postulated that the origin of such nonlinear amplification of chirality could be explained by the preference for a helical secondary structure of one handedness.

2.2. Outstanding Chiroptical Properties: a Hallmark of Shape-Persistent Macrocyclic and Acyclic Alleno-Acetylenic Oligomers

In order to validate this hypothesis, we decided to prepare an earlier reported chiral SPAAM, which at that time had only been isolated as a complex mixture of diastereoisomers with unresolved racemates.[53] In parallel, we also set out to synthesize the corresponding acyclic oligomers. In the new derivatives $(P)_4$-(–)-**33a** and $(P)_{2n}$-(+)-**105a-c** (n = 1 (**a**), 2 (**b**), 4 (**c**)), the all-carbon backbone is conformationally rigidified by introducing alternating –C≡C– and –C≡C–C≡C–

fragments connecting the allene moieties, instead of the all-buta-1,3-diynediyl linkers in $(P)_4$-(–)-**34** and $(P)_n$-(+)-**44a-d** (Scheme 17).

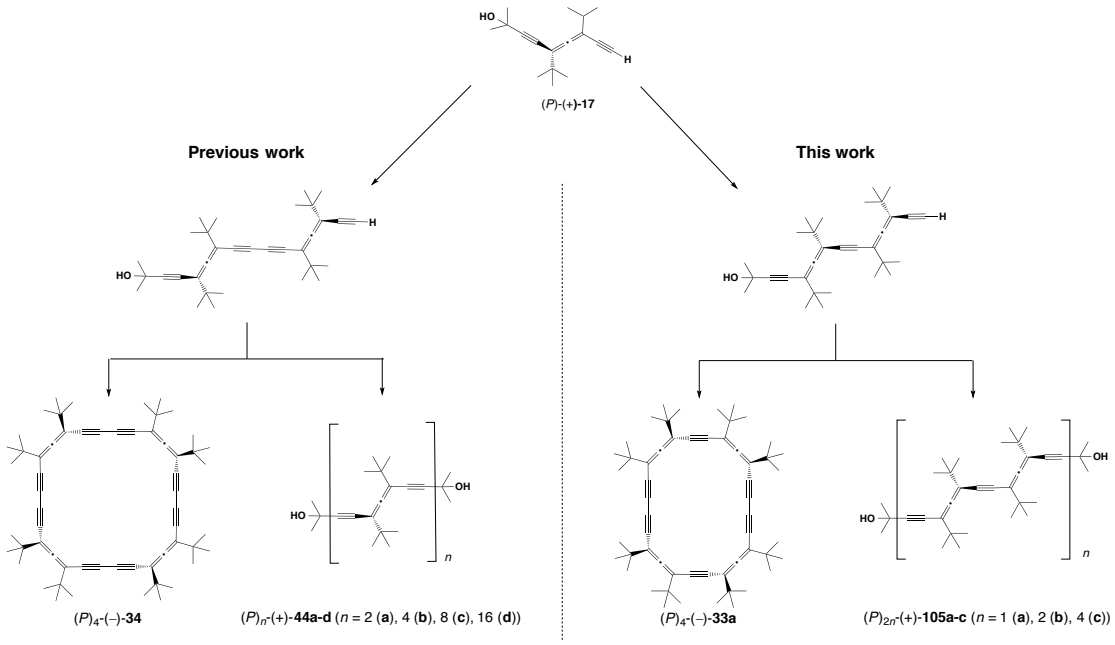

Scheme 17. The previously reported series (left)[34,57] and the new series (right) of macrocyclic and acyclic alleno-acetylenic oligomers. Only compounds with *P*-configured allene moieties are shown.

2.2.1. Synthesis of SPAAM 33

Macrocycle (±)-**33** has already been synthesized starting from a racemic 1,3-DEA building block (Scheme 17).[53] It was obtained together with a second pair of enantiomers and three achiral diastereoisomers. The three achiral stereoisomers and the two pairs of enantiomers could be separated by chromatography. At the time, optically active 1,3-DEA precursors were not available. Therefore, the racemic mixtures could not be optically resolved. The relative configuration could only be assigned for the C_1-symmetric racemate (*M*,*P*,*P*,*P*)/(*P*,*M*,*M*,*M*)-**33b**, which displayed eight diagnostic *tert*-butyl resonances in the ^{1}H NMR spectrum. With enantiomerically pure (*P*)-(+)-**17** and (*M*)-(–)-**17** available in multigram quantities and in enantiomeric purity greater than 99.9%,[59] we reinvestigated the preparation and isolation of $(P)_4$-(–)-**33a** and its six stereoisomers. Their four-step high-yielding synthesis, isolation, and configurational assignment were then reported.

The synthesis of $(P)_4$-(–)-**33a** and acyclic oligomers $(P)_{2n}$-(+)-**105a-c** are shown in Schemes 18 and 19. The mixture of dimeric diastereoisomers $(P)_2$-(+)-**106a**/(*P,M*)-(+)-**106b** is obtained from enantiomerically pure (*P*)-(+)-**17** and (±)-**18** in a *syn*-S_N2'-type Pd-catalyzed cross-coupling reaction in 70% yield (Scheme 18). Si(*i*Pr)$_3$ group deprotection gave $(P)_2$-(+)-**107a** and (*P,M*)-(+)-**107b**, which could be further separated by chiral HPLC (CSP Chiralpak® IA, *n*-hexane/*i*PrOH 99.6:0.4). Acyclic dimeric allene $(P)_2$-(+)-**105a** was synthesized in three steps starting from $(P)_2$-(+)-**107a.** First, the hydroxy group of $(P)_2$-(+)-**107a** was protected with a methoxymethyl (MOM) to give $(P)_2$-(+)-**108**. The terminal alkyne of $(P)_2$-(+)-**108** was then protected with acetone in the presence of catalytic *t*-Bu-P_4 (ca. 30 mol%),[138] followed directly by MOM-deprotection under acidic conditions to form $(P)_2$-(+)-**105a** in 72% yield over two steps. Acetone protection of the terminal alkyne does not proceed in the presence of the free alcohol.

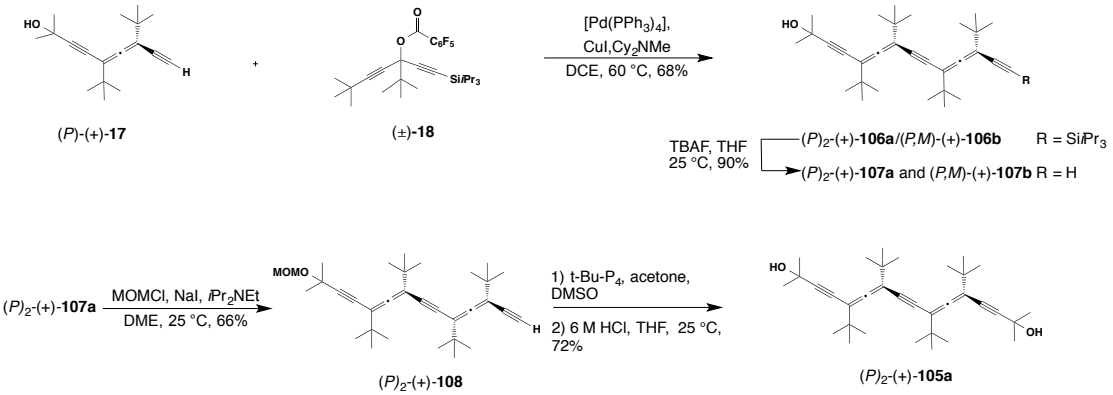

Scheme 18. Synthesis of all-(*P*)-configured alleno-acetylenic macrocycles and acyclic oligomers. Cy_2NMe = *N,N*-Dicyclohexylmethylamine; TBAF = Tetra-*n*-butylammonium fluoride.

SPAAM $(P)_4$-(–)-**33a** was synthesized in a one-pot dimerization–cyclization reaction under Eglinton-Galbraith conditions of compound $(P)_2$-(+)-**109**, obtained by deprotection of $(P)_2$-(+)-**106a** (Scheme 19). To favor cyclization, a solution of $(P)_2$-(+)-**109** in pyridine was added slowly to the solution of $CuCl/CuCl_2$ in pyridine over a period of 20 h. Under these conditions, $(P)_4$-(–)-**33a** was obtained in 75% yield. SPAAM $(P)_4$-(–)-**33a** and its enantiomer can also be obtained *via* a different pathway. Monoprotected $(P)_2$-(+)-**107a** was dimerized by Pd-catalyzed oxidative homocoupling using air as oxidant and TMEDA as base to obtain acyclic tetrameric

allene $(P)_4$-(+)-**105b** quantitatively.[139] Treatment of $(P)_4$-(+)-**105b** with a large excess of KOH (100 equiv) in toluene at 90 °C gave fully deprotected $(P)_4$-(+)-**110a**, which underwent cyclization under Eglinton-Galbraith conditions to give $(P)_4$-(–)-**33a** in 75% yield. Removal of only one of the alkyne protecting groups in $(P)_4$-(+)-**105b** using 5 equiv of KOH[140] provided monodeprotected $(P)_4$-(+)-**110b** (86% yield) besides fully deprotected $(P)_4$-(+)-**110a** (82% yield) using an excess of KOH (100 equiv). Pd-catalyzed homocoupling of $(P)_4$-(+)-**110a** provided the acylic octameric allene $(P)_8$-(+)-**105c**. The same transformations were also applied to the preparation of the all-(*M*)-configured macrocycle and acyclic oligomers, starting from enantiomerically pure (*M*)-(–)-**17**.

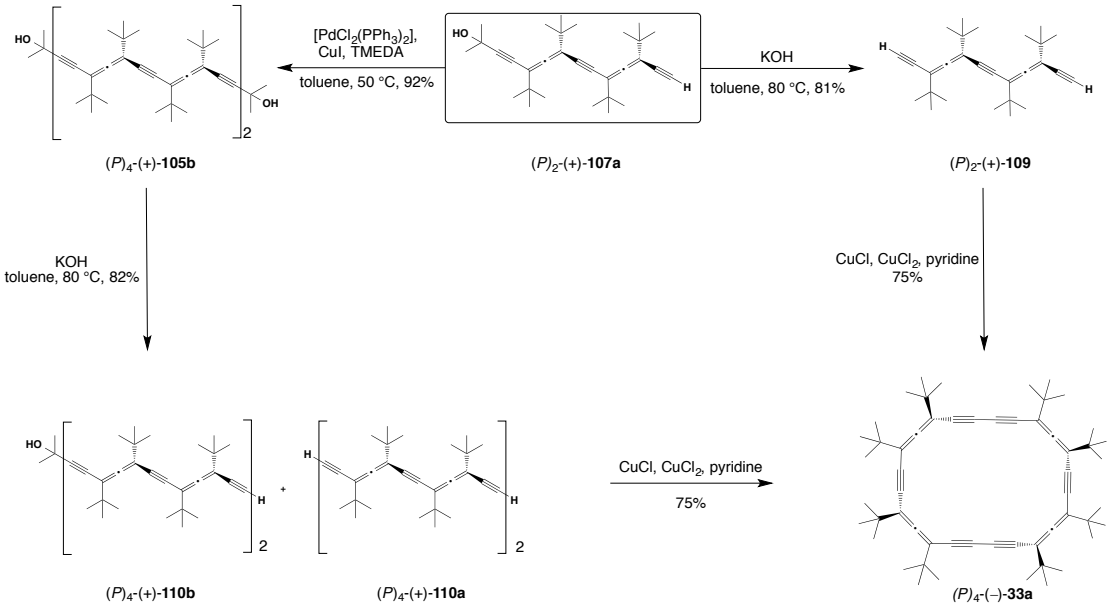

Scheme 19. Synthesis of all-(*P*)-configured alleno-acetylenic macrocycle and acyclic oligomers. TMEDA = *N,N,N',N'*-Tetramethylethane-1,2-diamine.

We also prepared and isolated the other five stereoisomers of $(P)_4$-(–)-**33a** and $(M)_4$-(+)-**33a**, namely the enantiomers of the second racemate and the three achiral stereoisomers, in pure form. In contrast to earlier work,[53] their structures and absolute configurations could all be assigned. We ensured that the same mixture of stereoisomers was formed as reported earlier, when starting from racemic (±)-**17** and (±)-**18**, following the synthetic route depicted in Scheme 20.

Scheme 20. Synthesis of the three achiral oligomers and the second pair of enantiomers of **33**, starting from optically active, dimeric allene precursors.

Macrocyclization of a mixture of stereoisomers of tetrameric allene $(P)_4$-(–)-**109** provided five products in a 1:1:4:1:1 ratio, as shown by analytical HPLC (Kromasil 100 Si, 5μm, *n*-hexane, 1 mL/min), thereby confirming the earlier results (Figure 25A). Subsequently, we started from optically active precursors and obtained, after chiral HPLC separation (Kromasil 100 Si, *n*-hexane) of the formed mixture, all five stereoisomers in pure form: achiral C_{2h}-symmetric (*M,M,P,P*)-**33b**, C_{2v}-symmetric (*P,M,P,M*)-**33d**, and C_{2h}-symmetric (*M,P,P,M*)-**33e** as well as the two C_1-symmetric enantiomers (*P,M,M,M*)-(+)-**33c** and (*M,P,P,P*)-(–)-**33c** (Figure 25B). This enabled us to assign the individual fractions eluted by HPLC to the different stereoisomers (Figure 25C).

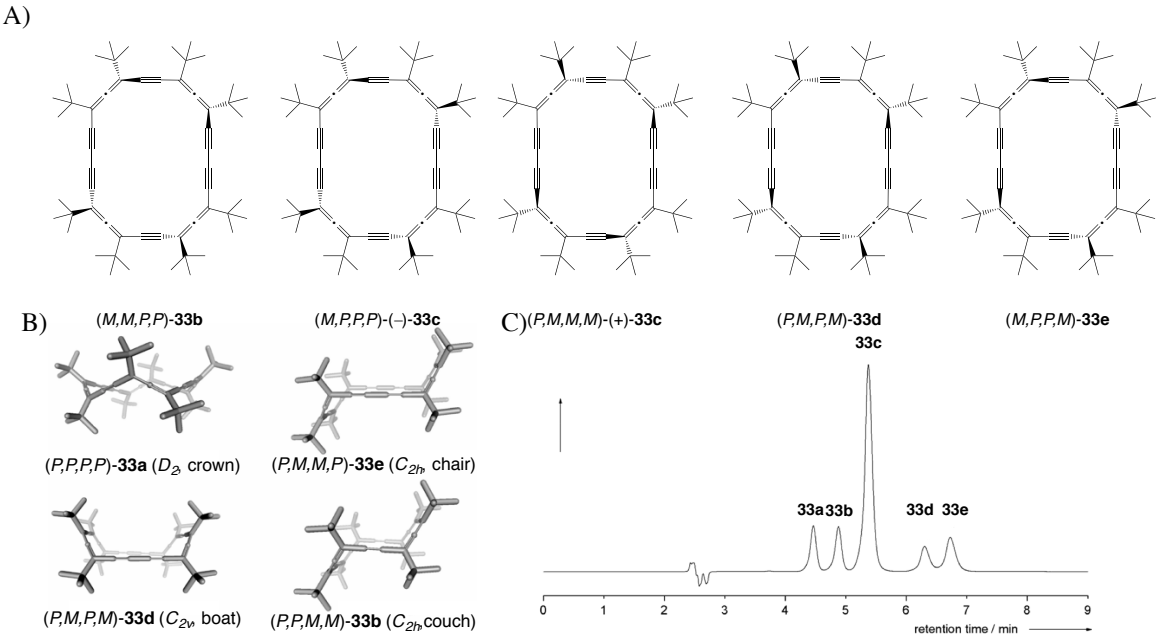

Figure 25. A) Representation of SPAAMs **33b-e**. B) Conformation and symmetry of SPAMMs **33a**,**b**,**e**,**d**. C) Analytical HPLC trace for the separation of macrocycles **33** in this work. Conditions: Kromasil 100 Si, 5 μm, *n*-hexane, 1 mL/min.

2.2.2. Solid-State Structures

Both the acyclic oligomers and the macrocycles are stable in the presence of moisture for weeks at ambient atmosphere. They do not undergo photoisomerization under daylight.[58,75] The structure of $(P)_4$-(–)-**33a** was confirmed by X-ray diffraction studies. Single crystals, suitable for X-ray analysis, were obtained by slow evaporation of a mixture of *n*-hexane/$CHCl_3$ 9:1 at low temperature (Figure 26). The macrocycle crystallized in the monoclinic space group $P2_1$ and shows D_2 symmetry. It exists in a crown conformation, similarly to the previously reported $(P)_4$-(–)-**34**. The X-ray structure was also solved for the acyclic tetrameric allene $(P)_4$-(+)-**109** using crystals obtained by slow evaporation of *n*-hexane/$CHCl_3$ 9:1. This crystal was mounted at low temperature and crystallized in the monoclinic space group $P2_1$. The alleno-acetylenic backbone of the oligomer clearly adopts a secondary helical structure with right-handed helicity in the solid state. Such a helical secondary structure with preferred handedness of the alleno-diacetylenic backbone had previously been suggested for solutions of $(P)_n$-(+)-**105a-d**, based on the nonlinear increase of the Cotton effects in the ECD spectra with increasing oligomer length.[75]

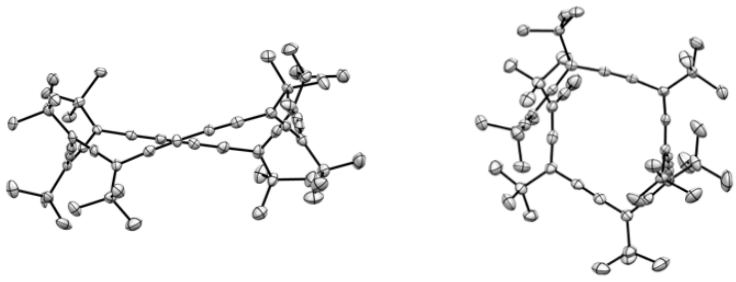

Figure 26. Left side: side view on X-ray structure of isomer of $(P)_4$-(–)-**33a**. Right side: X-ray structure of tetrameric allene $(P)_4$-(+)-**109**. Hydrogen atoms are omitted for clarity. T = 100 K. Thermal ellipsoids shown at the 50% probability level.

2.2.3. Chiroptical Properties

ECD spectroscopy was employed to probe the chiroptical properties of the enantiopure macrocycles (Figure 27). In *n*-hexane, the ECD spectra of $(P)_4$-(–)-**33a** and $(M)_4$-(+)-**33a** showed outstandingly intense Cotton effects at 243 nm

($\Delta\varepsilon$ = ±657 $M^{-1}\,cm^{-1}$) and at 280 nm ($\Delta\varepsilon$ = ±742 $M^{-1}\,cm^{-1}$). It is interesting to compare $(P)_4$-(–)-**33a** and the corresponding $(P)_4$-(–)-**34**.[57,58] For the higher-energy transition located around 250 nm, $\Delta\varepsilon$ is slightly lower, by ca. 80 $M^{-1}\,cm^{-1}$ in the spectrum of $(P)_4$-(–)-**33a**, while for the lower-energy transition (around 280 nm), which is controlled by the magnetic dipole moment (see below), $\Delta\varepsilon$ is larger by a factor of ca. 2.5 for $(P)_4$-(–)-**33a**, compared to $(P)_4$-(–)-**34**. This is remarkable as the absorption spectrum of $(P)_4$-(–)-**33a** and $(P)_4$-(–)-**34** show electronic absorptions of nearly identical intensity above 260 nm. Additionally, the vibrational fine structure of the buta-1,3-diyne-1,4-diyl fragments[75] is reduced in intensity and appearance in the ECD trace of $(P)_4$-(–)-**33a** is due to the reduced number of such units.

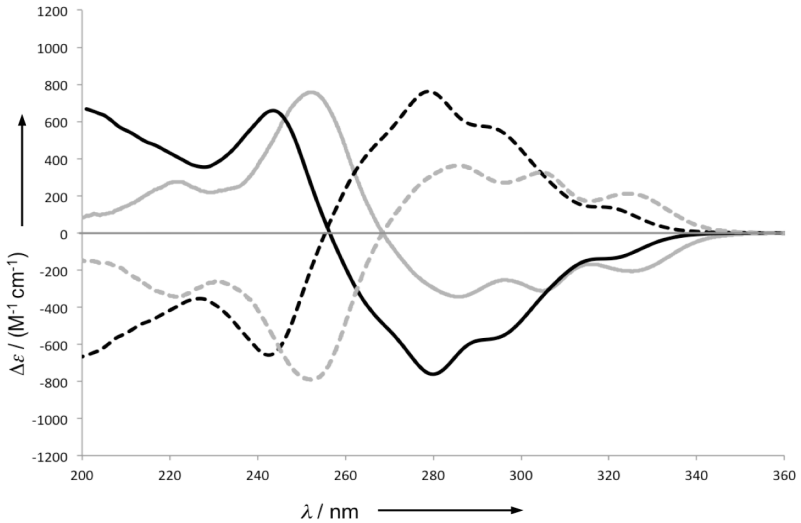

Figure 27. ECD spectra of $(P)_4$-(–)-**33a** (black line), $(P)_4$-(–)-**34** (grey line), $(M)_4$-(+)-**33a** (dashed black line) and $(M)_4$-(+)-**34** (dashed grey line), measured in *n*-hexane. T = 298 K.

Figure 28 shows a comparison of *g*-factor plots for $(P)_4$-(–)-**33a** and $(P)_4$-(–)-**34**. The *g*-factor is the ratio between the molar electronic circular dichroism $\Delta\varepsilon$ and the molar extinction coefficient ε ($g = \Delta\varepsilon / \varepsilon$),[140,141] and *g*-factor plots enable estimation of the relative contributions of electric (ETDM) and magnetic (MTDM) transition dipole moments to the Cotton effects. The *g*-factor values in the region between 270 nm and 350 nm are significantly higher for the new SPAAM, clearly suggesting stronger contributions from the magnetic transition dipole moments. This also may explain the larger Cotton effects in this region.

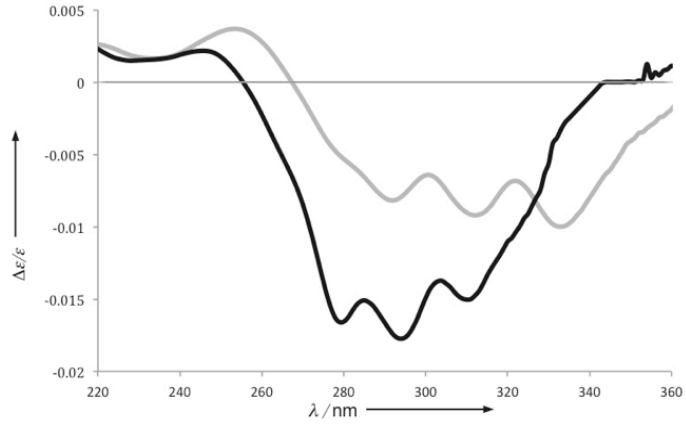

Figure 28. g-Factor plots for $(P)_4$-(–)-**33a** (black line) and $(P)_4$-(–)-**34** (grey line). T = 298 K.

The ECD and *g*-factor traces for the second pair of enantiomers, twisted C_1-symmetric (*P,M,M,M*)-(+)-**33c** and (*M,P,P,P*)-(–)-**33c** are shown in Figures 29 and 30, respectively. Both the Cotton effects and the *g*-factor values are strongly reduced compared to those in the spectra of the D_2-symmetric enantiomers $(P)_4$-(–)-**33a**/$(M)_4$-(+)-**33a**. This decrease in chiroptical response had also been observed in the first series of SPAAMs[57] and had been mainly explained by a reduction in symmetry.[59]

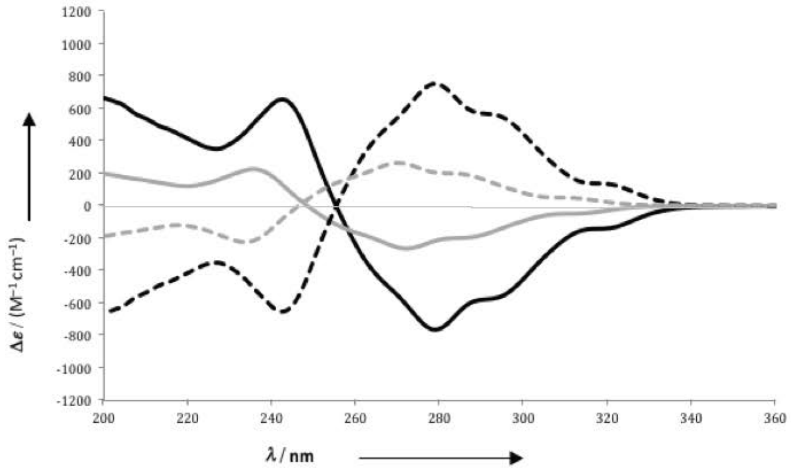

Figure 29. CD spectra of $(M)_4$-(+)-**33a** (dashed black line), $(P)_4$-(–)-**33a** (solid black line), (*P,M,M,M*)-(+)-**33c** (dashed grey line), and (*M,P,P,P*)-(–)-**33c** (solid grey line) measured in *n*-hexane. T = 298 K.

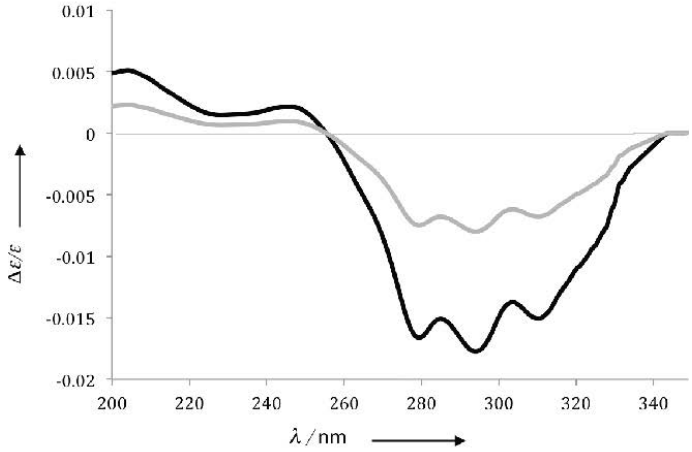

Figure 30. g-factor plot of $(P)_4$-(–)-**33a** (black line) and (*M*,*P*,*P*,*P*)-(–)-**33c** (grey line) measured in *n*-hexane. $T = 298$ K.

For the series of acyclic oligomers $(P)_{2n}$-(+)-**105a-c**, the CD intensity ($\Delta\varepsilon$ in M^{-1} cm^{-1}) increases remarkably from dimeric allene $(P)_2$-(+)-**105a** ($\Delta\varepsilon = +50$, $\lambda = 225$ nm) to tetrameric allene $(P)_4$-(+)-**105b** ($\Delta\varepsilon = +225$, $\lambda = 225$ nm) and reaches exceptionally high values of up to $\Delta\varepsilon = \pm 946$ at $\lambda = 285$ nm for the octameric allene $(P)_8$-(+)-**105c** (Figure 31). A similar nonlinear enhancement of the chiroptical responses had previously been observed for the oligomeric series $(P)_{2n}$-(+)-**105a-c**. In both cases, the amplification of chirality can be explained by the conformational preference for a secondary helical structure with right handedness. Octameric allene $(P)_8$-(+)-**105c** shows very similar Cotton effects to those previously reported for $(P)_8$-(+)-**44c**.[75]

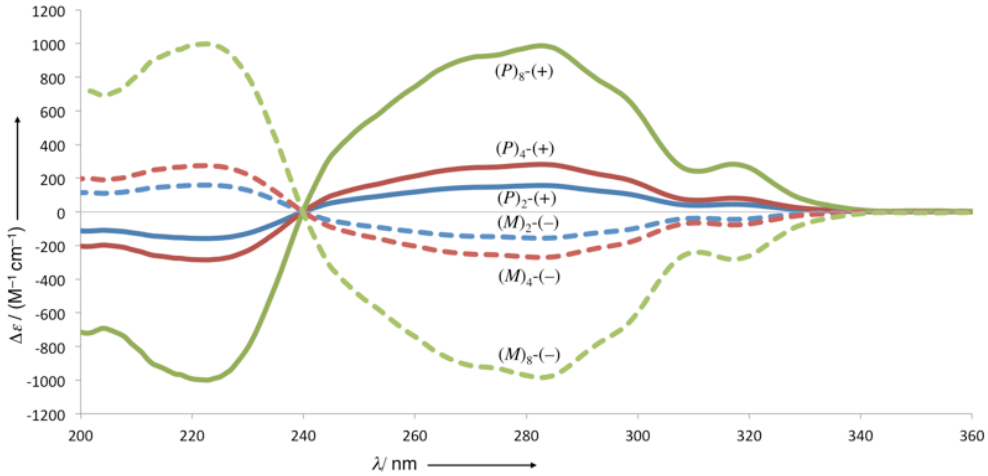

Figure 31. ECD spectra of the alleno-acetylenic oligomers $(P)_{2n}$-(+)-**105a-c** and $(M)_{2n}$-(–)-**105a-c** in *n*-hexane. $T = 298$ K.

2.2.4. TD-DFT Calculations.

TD-DFT calculations were performed on macrocycle $(P)_4$-(–)-**33a** in order to gain further understanding of the origin of its chiroptical properties. The X-ray structure of $(P)_4$-(–)-**33a** was optimized at the B3LYP(CPCM(*n*-hexane))/6-31G(d) level, followed by single point calculation at the TD-CAM-B3LYP(CPCM (*n*-hexane))/6-31G(d) level. [142–146] The calculated CD spectra provide an excellent reproduction of the main ECD features (Figure 32A). Three major transitions (denoted as S1, S2 and S3) are responsible for the CD spectra. Unlike the spectra previously calculated for $(P)_4$-(–)-**34**,[57] the S2 transition in $(P)_4$-(–)-**33a** is not degenerate, which stems from the lower symmetry of the macrocycle (D_2 *vs.* D_4).

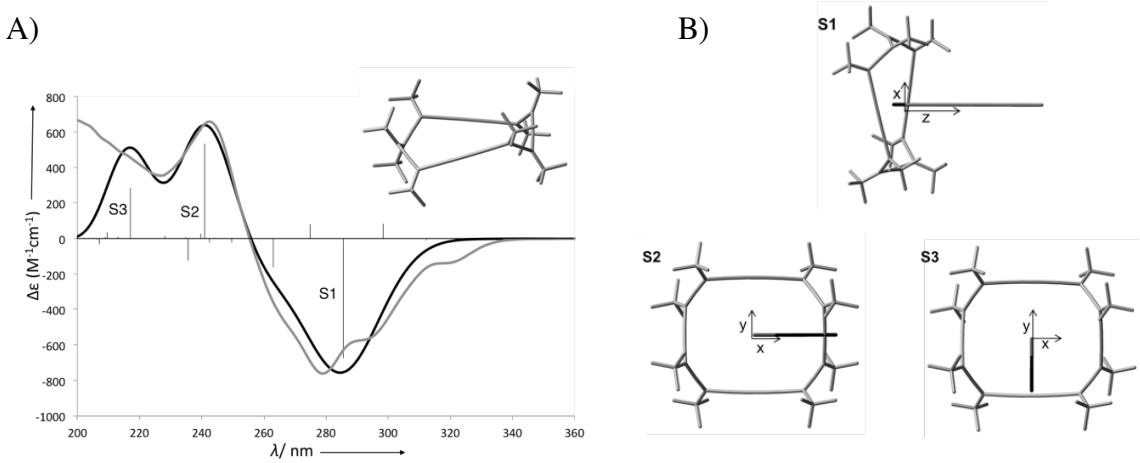

Figure 32. A) Experimental (grey line) and calculated (black line) ECD spectra of enantiopure $(P)_4$-(–)-**33a** (rotational strength in black bars). Geometry optimized at the B3LYP(CPCM(*n*-hexane))/6-31G(d). TD-DFT was performed at the TD-CAM-B3LYP(CPCM(*n*-hexane))/6-31G(d) level. B) Schematic representation of MTDM (grey line) and ETDM (black line) of transitions S1, S2, and S3 for $(P)_4$-(–)-**33a** at the TD-CAM-B3LYP(CPCM(*n*-hexane))/6-31G(d) level of theory.

The strong Cotton effect of $(P)_4$-(–)-**33a** indicates that the rotational strength, which is proportional to the product of the ETDM and the magnetic transition dipole moment (MTDM),[57,58] is very large. To gain insight into the origin of this effect, the ETDM and MTDM for the prominent electronic transitions are visualized in Figure 32B. For the lower-energy transition (S1), the MTDM and ETDM are parallel to each other and anti-parallel to the *z* axis (C_2-symmetry axis), giving rise to a negative transition. The extraordinarily large MTDM for transition S1 is the major contributor

to the intense Cotton effect while the ETDM is very small, which means that the transition S1 is electrically weak, but magnetically allowed and similarly strong to $(P)_4$-(–)-**34**.[58] Accordingly, the *g*-factor of the transition S1 is large, as observed experimentally. The EDTM of transitions S2 and S3 is relatively strong while the MTDM is relatively small. While the character of transition S1 is similar for both $(P)_4$-(–)-**33a** and $(P)_4$-(–)-**34**, the nature of the higher-energy transitions is different. The S2 transition for $(P)_4$-(–)-**34** is degenerate, stemming from its D_4 symmetry, with components in both the *x* and *y* directions. In contrast, for $(P)_4$-(–)-**33a** two transitions are observed: S2, for which both ETDM and MTDM are parallel to the *x* axis, and S3 for which both ETDM and MTDM are anti-parallel to the *y* axis.[57] This results from the presence of two different spacers, buta-1,3-diyne-1,4-diyl and ethyne-1,2-diyl, oriented on the *x* and *y* axes, respectively.

2.2.5. Conformational Study of the Dimeric Model

Rotational energies around the acetylenic bond were calculated for model dimers $(M)_2$-(–)-**109**, $(P)_2$-(+)-**109** and $(P)_2$-(+)-**111** at the SCS-MP2/cc-PVTZ level of theory (Figure 33).[147] As can be observed in Figure 34 and 35, there is correlation between the axial chirality of the allene and the helicity of the dimer. For the $(P)_2$-(+)-**111** dimer, positive θ values were lower in energy compared with the corresponding negative values, indicating a preference for right hand helicity (positive θ), while the opposite is true for the (*M,M*)-**109** dimer. For all cases, the local minima are observed for $\theta = 0^{\circ}$ while the global minima are at $\theta = 180^{\circ}$.

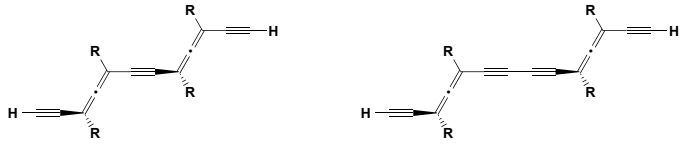

Figure 33. Representation of dimeric allenes for calculation.

While the same trend is observed for calculated $(P)_2$-(+)-**112**, containing two acetylenes, the rotational energy is 3 times lower than $(P)_2$-(+)-**111**, indicating a more flexible structure (Figure 34). The greater distance between the chiral allenic moieties can account for this difference. We note that, while the difference in energy between

the two helicities is small (ca. 0.1 kcal/mol), the energy difference is expected to increase linearly with increasing oligomer length, providing a more defined secondary structure for longer oligomers, and explaining the nonlinear increase in Cotton effect with increasing length.

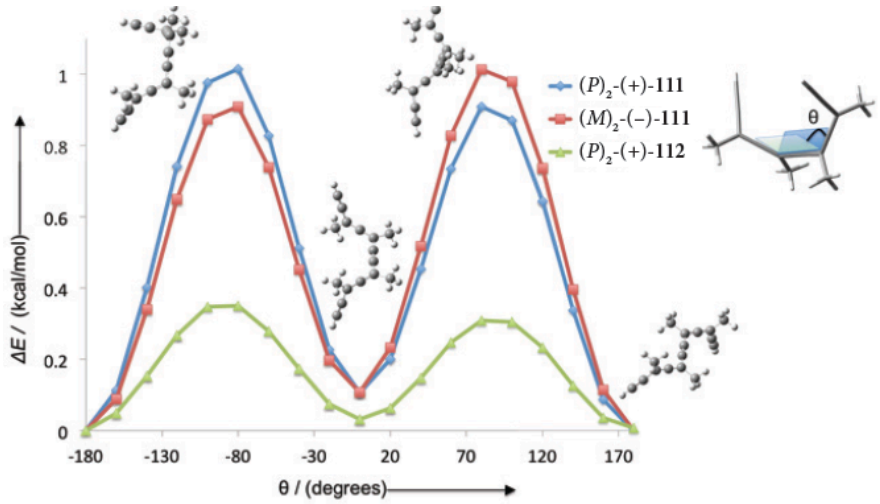

Figure 34. Calculated (SCS-MP2/cc-pVTZ) rotational energy around the acetylenic bond for $(P)_2$-(+)-**111**, $(M)_2$-(–)-**111**, and $(P)_2$-(+)-**112**, with representative structures of $(P)_2$-(+)-**111**.

To test the validity of the use of model dimers (*M,M*)-**111**, $(P)_2$-(+)-**111** and $(P)_2$-(+)-**112**, the rotational barrier was also calculated for dimers containing *tert*-butyl groups (*M,M*)-**109**, $(P)_2$-(+)-**109** and $(P)_2$-(+)-**113** (Figure 35).

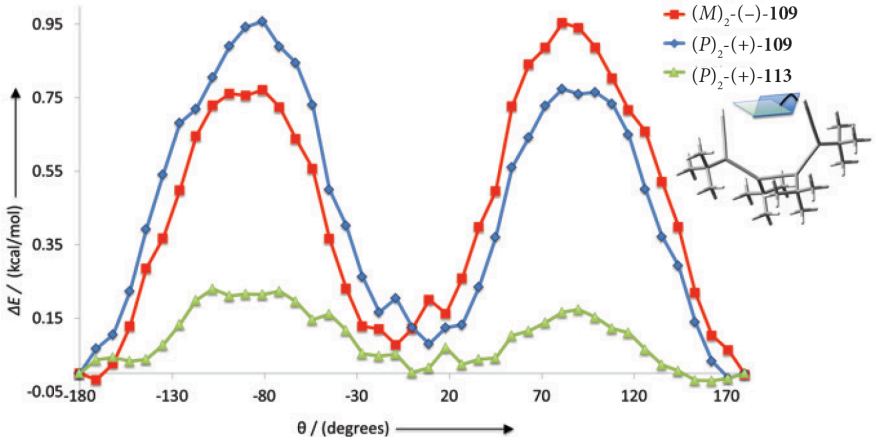

Figure 35. Calculated (B3LYP-D3/cc-pVTZ) rotational energy around the acetylenic bond for $(P)_2$-**109**, $(M)_2$-**109**, and $(P)_2$-**113**.

We have used the B3LYP-D3/cc-pVTZ[91] level of theory (applying Grimme's D3 dispersion correction to B3LYP) since calculations at the SCS-MP2/cc-pVTZ level were too costly for molecules of such size. Similar correlation between the axial chirality of the allene and the helicity of the dimer as described above was also observed in this case. Furthermore, despite the addition of the bulkier *tert*-butyl groups, the rotational barrier remains around 1 kcal/mol. We note however, that the difference between the two helicities is slightly larger (ca. 0.18 kcal/mol *vs.* 0.1 kcal/mol). Nevertheless, such a small difference might be with in the error range of this level of theory.

Overall, calculations show helical preference for the secondary structure, which is directly affected by the chirality of the allenes, and in addition the removal of one acetylene bond should stabilize the preferred helical secondary structure. Importantly, this is the first time such screw-sense dependence is verified computationally for alleno-acetylenic scaffolds.

2.3. Lateral Functionalization of Chiral Alleno-Acetylenes

2.3.1. Introduction

Macrocycles and oligomers of the *tert*-butyl-substituted DEAs were found to have exceptional chiroptical properties. Our current efforts in this field have focused on the lateral functionalization of DEAs with the aim of triggering self-association of the corresponding macrocycles into chiral columnar super-structures with amplified chiroptical properties.

The major objectives of the current section are:

(i) the synthesis and enantiomeric resolution of chiral 1,3-DEAs possessing lateral functional groups (tertiary alcohol),

(ii) the oligomerization and macrocyclization of these new 1,3-DEA building blocks, and

(iii) the enhancement of chiral properties *via* hydrogen bonding.

2.3.2. Lateral Alcohol Functionalization

Recently, we demonstrated that phenol-substituted macrocycles **36** form hydrogen-bonded pillared arrays in the solid state (see Section 1.1).[60,61] Intermolecular linkage may be promoted via non-covalent interactions (*e.g.* hydrogen-bonding, metal coordination). Aggregation was also observed in solution at NMR concentration, but at lower concentration (UV, CD range concentration) the compound was found to exist as the monomer.

Alcohol-substituted DEAs may be synthesized from α-hydroxy acids (Scheme 21). Previously, Dr. Nicolas Marion attempted this using trimethylsilyl (TMS) and triethylsilyl (TES) protecting groups. Unfortunately, the synthesis failed in the ethynyltriisopropylsilane addition to the ynone, which is most probably due to instability of the protecting group towards the basic reaction conditions. Therefore, we have selected the more inert MOM (methoxymethyl ether) group as an alternative protecting group and this successfully afforded allene (±)-**114** in an overall yield of 23% starting from the commercially available ethyl 2-hydroxy-2-methylpropionate (**115**), (Scheme 21). This yield is comparable to the one obtained when using *tert*-butyl substituents.

The relatively low yield of intermediate **116**, formed by MOM-protection of **115** is due to its volatility and some polymer formation. When THF was used as the solvent instead of diethyl ether, part of the product evaporated upon concentration of the solution (in case of evaporation of Et_2O: $T \leq 35$ ºC, $p \leq 0.55$ bar). Polymer formation, resulting from intermolecular attack of the alkoxide on the ester carbonyl group, could be reduced by adding MOM chloride shortly after deprotonation and by keeping the solution well cooled to 0 °C. Compound **116** was easily converted into the Weinreb amide **117**, which was reacted with 3-(methoxymethoxy)-3-methylbut-1-yne to afford ynone **118**. After ethynyltriisopropylsilane addition, (±)-**119** was obtained in 96% yield. Introduction of the pentafluorobenzoyl leaving group led to formation of (±)-**120** in 81% yield, and (±)-**120** was coupled with commercially available 2-methylbut-3-yn-2-ol to yield (±)-**121**. Allene (±)-**114** was obtained after TIPS deprotection in quantitative yield.

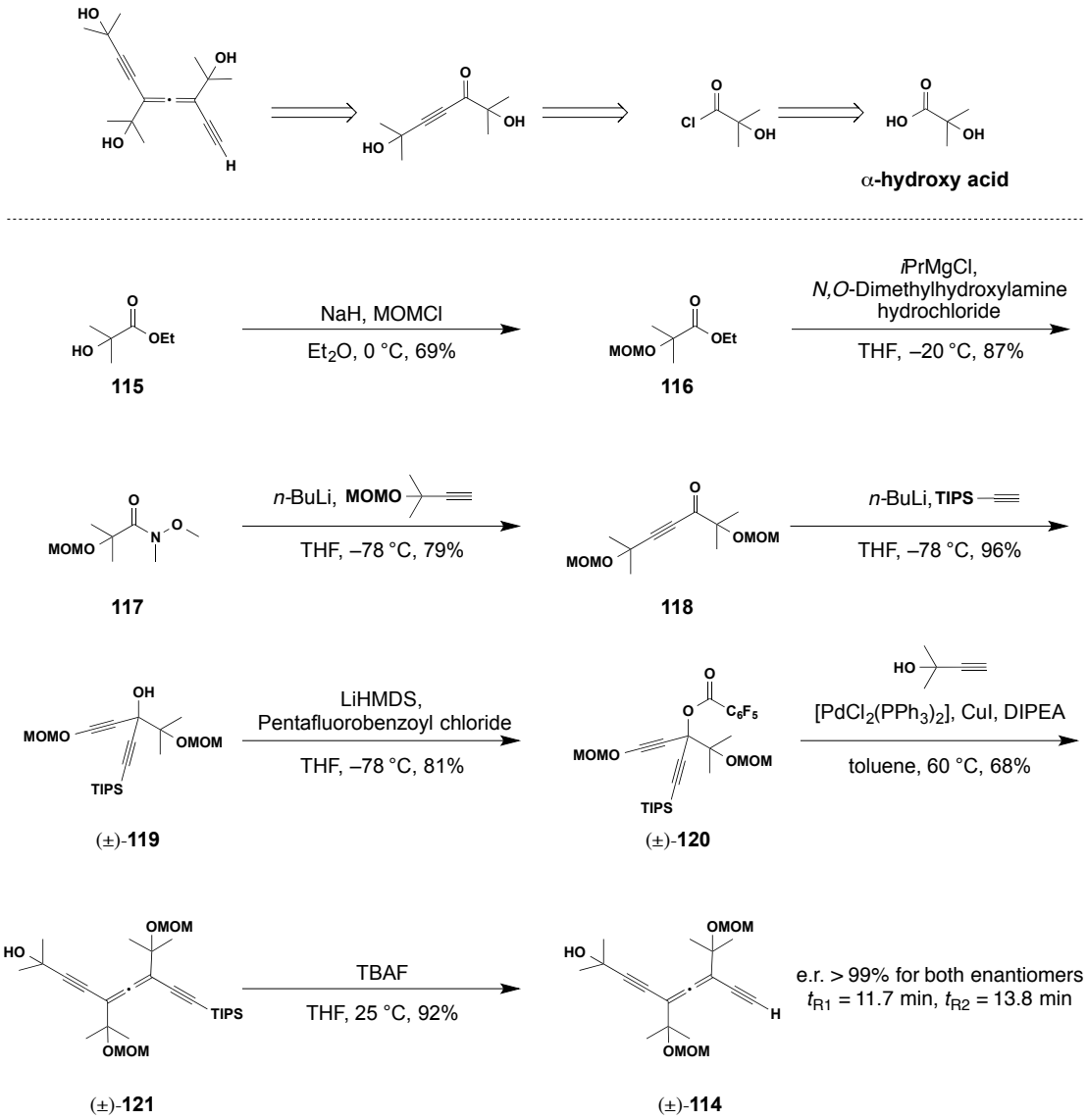

Scheme 21. Synthesis of MOM-protected alcohol-substituted DEA (±)-**114**. DIPEA = *N*,*N*-Diisopropylethylamine; LiHMDS = Lithium bis(trimethylsilyl)amide.

Enantiomers of (±)-**114** were resolved by HPLC on a chiral stationary phase (Chiralpack® IA). After much effort, a satisfactory resolution method was developed and the two enantiomers were separated by preparative HPLC on a chiral stationary phase (Chiralpak IA, *n*-hexane/*i*PrOH 98:2). In order to prepare alcohol-substituted macrocycles and oligomers *via* acetylenic homo-coupling, (*P*)-(+)-**114** was dimerized to obtain $(P)_2$-(+)-**122** (Scheme 22) in 89% yield. Removal of the isopropyl alcohol protecting group with sodium hydroxide afforded both monodeprotected $(P)_2$-(+)-**123** and fully deprotected $(P)_2$-(+)-**124** which can be applied in oligomerization and macrocyclization, respectively.

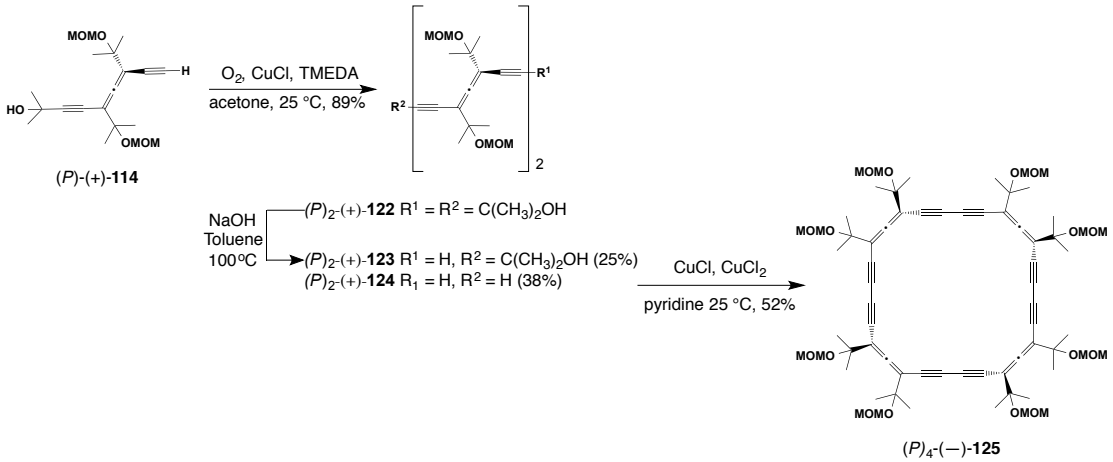

Scheme 22. Synthesis of macrocycle $(P)_4$-(–)-**125**.

SPAAM $(P)_4$-(–)-**125** was synthesized in a one-pot dimerization-cyclization reaction under Eglinton–Galbraith conditions of compound $(P)_2$-(+)-**124** (Scheme 22). To favor cyclization, a solution of $(P)_2$-(+)-**124** in pyridine was added slowly to the solution of CuCl/$CuCl_2$ in pyridine over a period of 20 h. Under these conditions, $(P)_4$-(–)-**125** was obtained in 52 % yield. The last step is the MOM deprotection. However, this step gave mainly decomposition of the starting material and no desired product $(P)_4$-(–)-**126** was observed upon exploring a variety of conditions (Table 1).

ECD spectroscopy was finally employed to probe the chiroptical properties of the enantiopure macrocycle $(P)_4$-(–)-**125** (Figure 36). In *n*-hexane, macrocycle $(P)_4$-(–)-**125** showed remarkable Cotton effects centred at 257 nm ($\Delta\varepsilon = \pm 880$ M^{-1} cm^{-1}). These very large values are higher than those of the tetrameric macrocycle peripherally garnered by eight phenols ($\Delta\varepsilon = \pm 375$ M^{-1} cm^{-1})[60] or of the *tert*-butyl-garnered macrocycle $(P)_4$-(–)-**125** ($\Delta\varepsilon = \pm 790$ M^{-1} cm^{-1} in *n*-hexane).[57]

Table 1. Conditions for MOM deprotection.

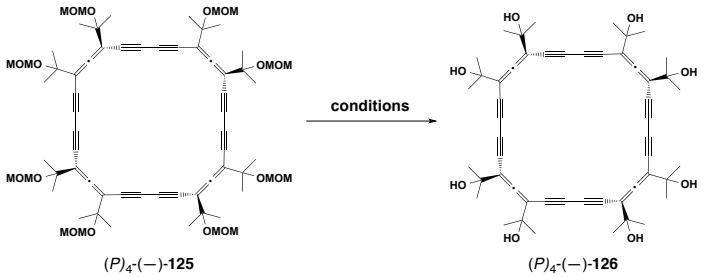

entry	conditions	Solvent	T °C	observations
1	6 M HCl	THF/MeOH	20 °C to reflux	20 °C No reaction Reflux decomposition
2	TFA	CH_2Cl_2	20 °C	SM + decomposition
3	BF_3•OEt_2	PhSH	20 °C	Decomposition
4	Me_2BBr	CH_2Cl_2	–78 °C to 20°C	Only SM
5	$LiBF_4$	MeCN/H_2O	25 °C	Decomposition

SM: Starting material

The reduced intensity of the Cotton effects of SPAAM $(P)_4$-(–)-**36** correlates with a reduction in the molar extinction coefficients, presumably induced by the phenolic substituents, which also increase the conformational flexibility of the macrocycle which is not the case for the MOM-protected SPAAM $(P)_4$-(–)-**125**.

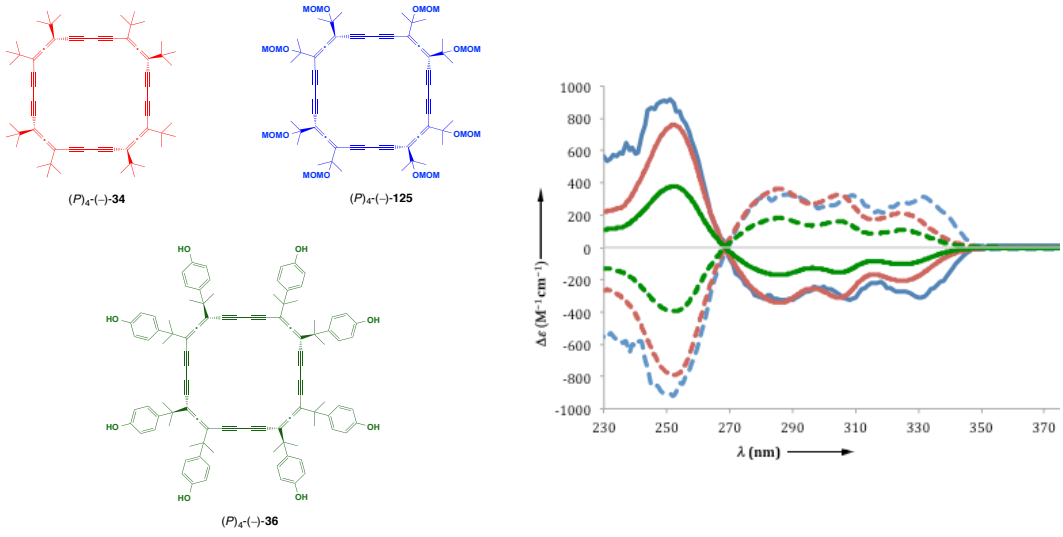

Figure 36. ECD spectra of tetrameric macrocycles (**34**, **36**, and **125**) measured in *n*-hexane at 25 °C. ECD spectra of $(P)_4$-(–)-**34** (red line), $(P)_4$-(–)-**36** (gren line), $(P)_4$-(–)-**124** (blue line), $(M)_4$-(+)-**33a** (dashed red line), $(M)_4$-(+)-**36** (dashed green line), $(M)_4$-(+)-**125** (dashed blue line) measured in *n*-hexane. T = 298 K.

2.4. Conclusion and Outlook

In the first Chapter, a second series of shape-persistent alleno-acetylenic macrocycles (SPAAMs) and new acyclic alleno-acetylenic oligomers with more rigidified all-carbon backbones were prepared in enantiomerically pure form. The D_2-symmetric macrocycle $(P)_4$-(–)-**33a** was characterized by X-ray crystallographic analysis, featuring a rigid crown conformation. The chiroptical responses of SPAAMs $(P)_4$-(–)-**33a** and $(M)_4$-(+)-**33a** are outstanding, with very large Cotton effects despite lower symmetry and fewer buta-1,3-diynediyl chromophore units, when compared to the systems in the earlier first series. TD-DFT calculations indicate a very strong contribution from the MTDM for the lower-energy transition, while the higher-energy transition is mostly dominated by the EDTM. This observation is in agreement with the experimental *g*-factor plots. A second C_1-symmetric pair of enantiomers, (*P,M,M,M*)-(+)-**33c** and (*M,P,P,P*)-(–)-**33c** gives much less intense Cotton effects as a result of the reduction in symmetry from D_n to C_n.

A nonlinear increase in the intensity of the Cotton effects with increasing oligomeric length was observed for the new series of acyclic alleno-acetylenic oligomers, which was explained with the preference for a helical secondary structure of one handedness. Structural support for this proposal is provided by the X-ray structure of the enantiopure tetrameric allene $(P)_4$-(+)-**109**, which displays a right-handed helical conformation in the solid state. Computational studies are in agreement with this observation and also confirm the reduced flexibility of the new oligomers as a result of exchanging the all-buta-1,3-diynediyl spacers between allene moieties in the previous series by alternating –C≡C– and –C≡C–C≡C– spacers. Most importantly, the results reported here provide testimony that exceptional chiroptical responses are a hallmark of shape-persistent macrocyclic and acyclic alleno-acetylenic oligomers with conformational preferences for secondary helical structures.

In the second subchapter, we prepared the MOM-protected DEA derivatives (*P*)-(+)- and (*M*)-(–)-**114** in enantiomerically pure form and further reacted to afford the tetrameric macrocycles $(P)_4$-(–)-**125** and $(M)_4$-(+)-**125** bearing eight lateral MOM-protected alcohol groups around the central alleno-acetylenic all-carbon core.

However, all attempts to deprotect the MOM group were unsuccessful and no desired product was observed. The chiroptical properties of SPAAMs $(P)_4$-(–)-**125** and $(M)_4$-(+)-**125** showed remarkable chiroptical properties.

Chapter 3

The Influence of Lewis Acid on the Reactivity between DCID and Electron-Rich Alkynes

3. The Influence of Lewis Acid on the Reactivity between DCID and Electron-Rich Alkynes

The crystal structures were solved by Dr. Nils Trapp and Dr. Aaron D. Finke. Electrochemical measurements were performed by Dr. Laurent Ruhlmann and Dr. Corinne Boudon at the University of Strasbourg. The results of this Chapter are the subject of a recent publication.[148]

3.1. Introduction

As described previously (cf. see Section 1.2), the formal CA–RE reaction has been a versatile and robust method for the construction of push–pull chromophores and compounds obtained from this transformation have been used for their potential applications in optoelectronic devices. To further expand the chemical space for functional materials, we became interested in novel acceptor units beyond commonly used electron-deficient alkene motifs, such as TCNE and TCNQ. We became interested in DCID (**127**) as an acceptor for the formation of new push–pull chromophores (Scheme 23). DCID was first described in the literature in 1968,[149] but has received little attention as an electron acceptor due to its facile rearrangement to 2,3-dicyano-1,4-naphthoquinone (**128**) upon reduction.[150] DCID can be prepared in good yield as yellow, air-stable crystals by reacting ninhydrin (**129**) and malononitrile in water.[149]

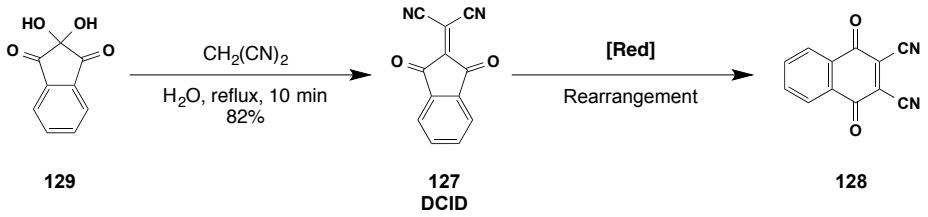

129 **127 DCID** **128**

Scheme 23. DCID synthesis. [Red] = reduction.

3.2. Preliminary Results

First, the CA–RE reaction of **127** with 1.0 equivalent of *N*,*N*-dimethylanilinoacetylene (DMA-acetylene) **102** afforded **130** (85% yield) as the major product and oligoene (*E*)-**131** as a minor product (10% yield) (Scheme 24). By mixing 2.1 equiv of **102** with 1 equiv of DCID in $CHCl_3$, (*E*)-**131** was obtained in 83% yield. In coherence with our previous work, only the (*E*)-isomer of **131** was observed.[151]

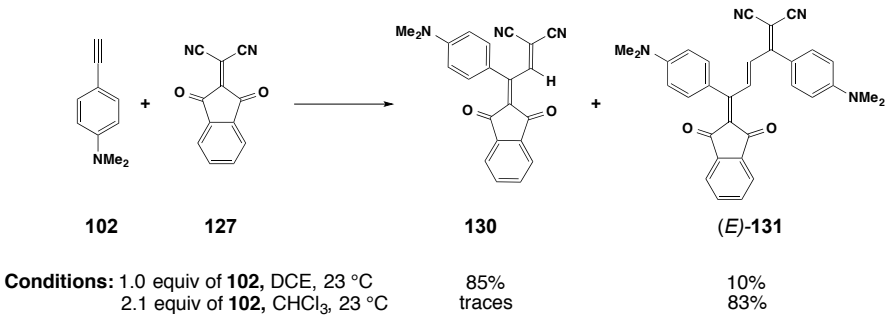

Scheme 24. CA–RE reaction of **102** with **127**.

Surprisingly, oligoene formation was suppressed when DCID and the bis-DMA-acetylene **132** were used and the expected CA–RE adduct **133a** was observed as the major product (90% yield), along with the unexpected, fused 4*H*-pyran **133b** (10% yield). Compound **133b** is obtained from an inverse electron demand Hetero-Diels–Alder (HDA) reaction (Scheme 25).[152–154] The presence of 4*H*-pyran derivatives in natural products and biologically active compounds[155–157] as well as in optoelectronics,[158–160] sparked our interest in controlling the selectivity of this transformation to bias the formation of 4*H*-pyran **133b**.[161–166]

In 1994, Hall and coworkers reported the influence of Lewis acids on the cycloaddition of cyano- and carbomethoxy-substituted olefins with donor-substituted alkenes.[167] In the absence of $LiClO_4$ or $ZnCl_2$, the [4+2] HDA pathway to yield 3,4-dihydro-2*H*-pyrans was favored, whereas Lewis acids promoted the [2+2] cycloaddition pathway. A similar selectivity is observed when 4-vinylanisole **134** is added to DCID (Scheme 25), yielding cyclobutane (±)-**135a** and dihydropyran (±)-**135b**.

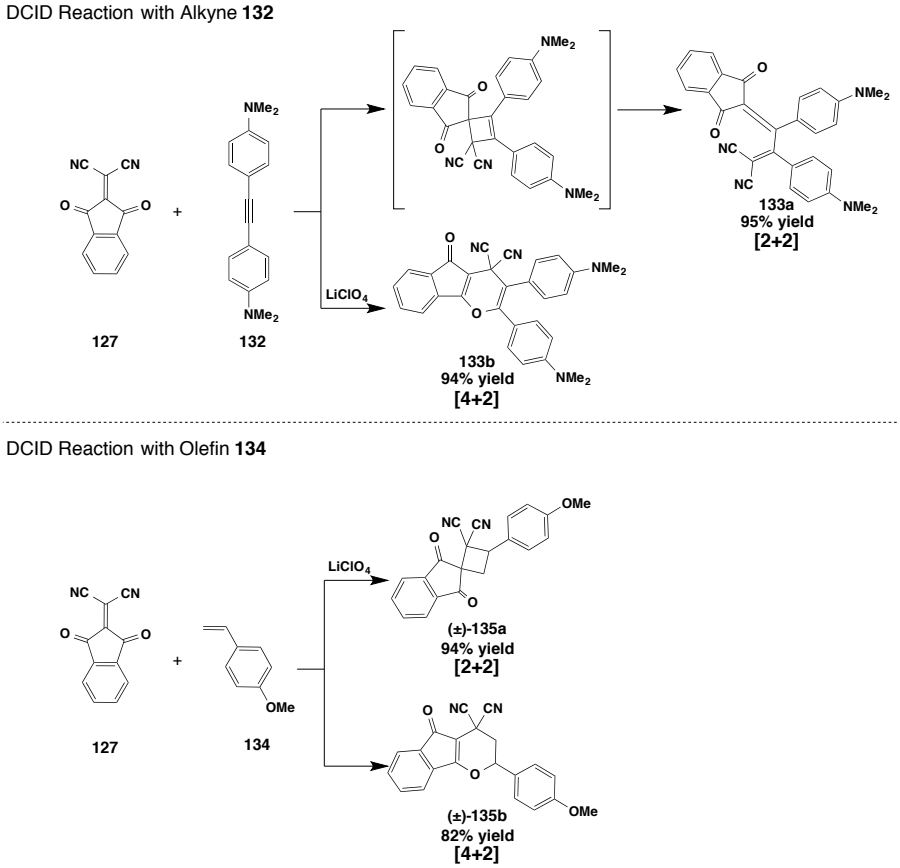

Scheme 25. Differences in the reactivity of electron-donating olefins and alkynes with DCID.

Surprisingly, Lewis acids have the opposite effect on DCID reactivity with electron-rich alkynes. Indeed, addition of 1.0 equiv of different Lewis acids activates the enone moiety of DCID for the HDA reaction (Scheme 25).

3.3. Mechanistic Studies

The putative mechanistic pathway for the reaction of DCID with 4-vinylanisole **134** is shown in Scheme 26.[167] When a Lewis acid is added to the reaction, the zwitterionic tetramethylene is formed. The corresponding Lewis acid-complexed intermediate can exist as either the gauche or trans conformer. The [2+2] cycloaddition occurs through the gauche conformer. Nonpolar solvents favor the gauche conformer due to Columbic interactions between the ionic ends, so that it easily undergoes ring-closure. This reaction is stereoselective with a preference to pathway a, which we ascribe to steric interactions between the DCID moiety and the anisole.

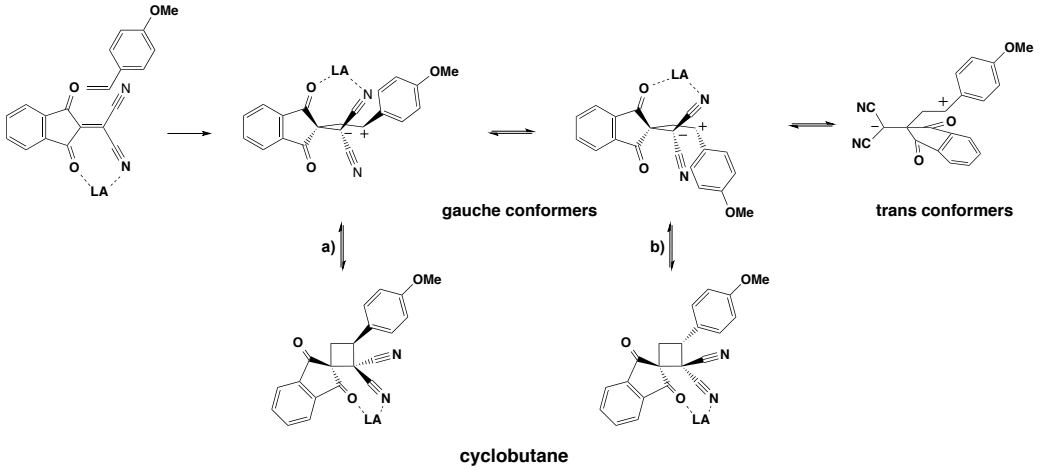

Scheme 26. Mechanism for the [2+2] cycloaddition of DCID with 4-vinylanisole **134**.

Mild Lewis acids, such as $ZnCl_2$ and $LiClO_4$, have the opposite effect on DCID reactivity with donor-substituted alkynes. In this particular case, Lewis acids promote reaction *via* the [4+2] pathway over the [2+2] pathway (Scheme 27). This can be justified by a different mechanistic pathway.[167] In the absence of a Lewis acid, 1,2-addition of the electron-rich alkyne to DCID is followed by a ring closure to form the cyclobutene intermediate. The corresponding intermediate then undergoes a retroelectrocyclization to yield the desired CA–RE product. Addition of Lewis acid activates the enone moiety of DCID to favor the Michael addition. Furthermore, the presence of Lewis acid results in a larger electron disparity between the reactants, as well as making the lone pair on the oxygen more electronegative. The corresponding oxygen is nucleophilic enough to attack the allene to yield 3,4-dihydro-2*H*-pyran derivatives.

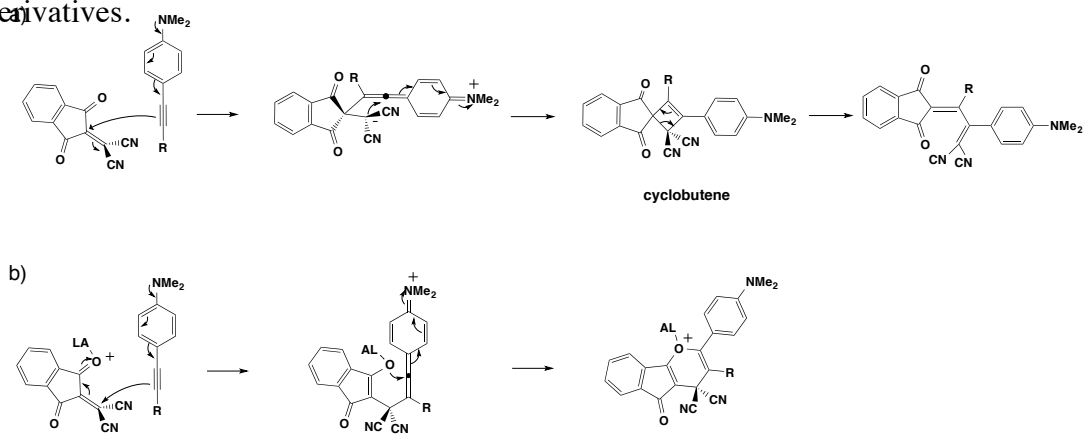

Scheme 27. Putative mechanisms for the two transformations of DCID with a donor-substituted alkyne: a) formal [2+2] CA–RE reaction; b) Lewis acid-promoted [4+2] HDA reaction.

3.4. Optimization of the Reaction

After an intensive screening (Table 2), the use of $LiClO_4$ in the presence of a mixed-solvent system at 80 °C gave the best selectivity (**133a**:**133b** = 5:95) towards the formation of the 4*H*-pyran adduct **133b**.

Table 2. Selected results for the chemoselectivity in the reaction of DCID with bis-DMA-acetylene.[a]

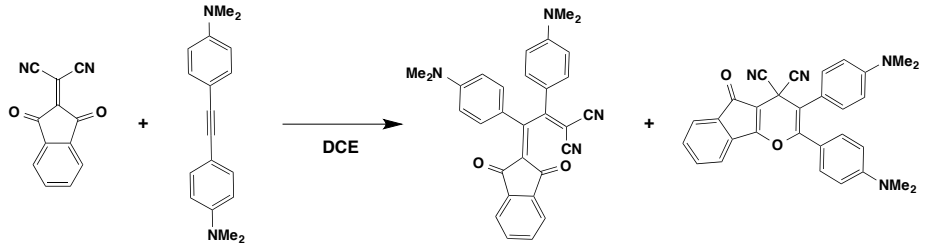

127 **132** **133a** [2+2] CA–RE **133b** [4+2] hetero-D-A

entry	additives	solvent	ratio[a]	yield(%) 113a	Yield(%) 113b
1	-	DCM	75:25	75	25
2	-	MeCN	85:15	82	14
3	-	DCE	90:10	90	10
4	$TiCl_4$	DCE	28:72	27	70
5	$AlCl_3$	DCE	34:66	32	63
6	BF_3•Et_2O	DCE	35:65	33	61
7	$ZnCl_2$	DCE	20:80	19	76
8	$LiClO_4$	DCE	14:86	14	86
9	$LiClO_4$	DCE	10:90[b]	10	90
10[b]	$LiClO_4$	DCE/MeCN(98:2)	5:95[b]	5	95

a) All reactions were conducted using 1.0 equiv of **127**, 1.05 equiv of **132**, and 1.0 equiv of additive on 0.15 mmol scale at 0.1 M concentration, 3 h at 25 °C. Ratios and yields determined by ^{1}H NMR using dibromomethane as the internal standard. b) Reaction conducted at 80 °C.

3.5. Scope of the Reaction

With optimized conditions in hand, we evaluated the scope of the reaction with a series of different donor-substituted alkynes **132–148** (Table 3).

Table 3. CA–RE and HDA reaction of DCID with various donor-substituted alkynes.[a]

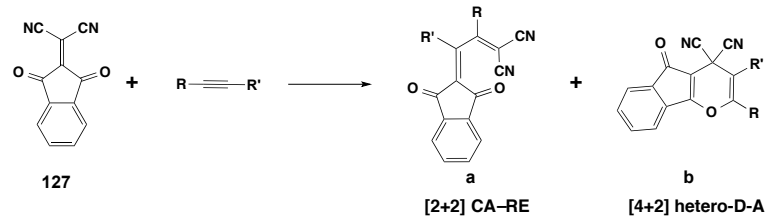

127 a [2+2] CA–RE b [4+2] hetero-D-A

entry	donor	product	Condition A			Condition B		
			ratio	yield(%) a	yield(%) b	ratio	yield(%) a	Yied(%) b
1	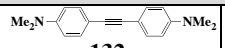 **132**	**133a/133b**	95:5	95	5	5:95	5	94
2	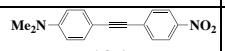 **136**	**149a/149b**	85:15	65	11	5:95	5	85
3	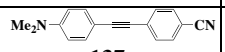 **137**	**150a/150b**	80:20	76	18	13:87	13	87
4	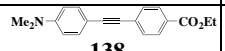 **138**	**151a/151b**	95:5	95	5	10:90	9	91
5	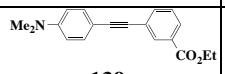 **139**	**152a/152b**	94:6	70	4	5:95	3	66
6	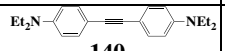 **140**	**153a/153b**	94:6	94	6	5:95	4	80
7	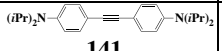 **141**	**154a/154b**	94:6	85	5	4:96	4	81
8	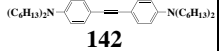 **142**	**155a/155b**	94:6	89	6	4:96	4	91
9	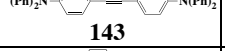 **143**	**156a/156b**	90/10	63	7	8:92	6	59
10	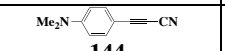 **144**	**157a/157b**	98/2	83	2	10:90	8	74
11	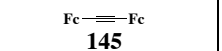 **145**	–	–	–	–	–	–	–[b]
12	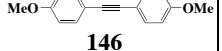 **146**	–	–	–	–	–	–	–[b]
13	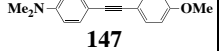 **147**	–	–	–	–	–	–	–[c]
14	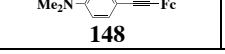 **148**	–	–	–	–	–	–	–[c]

a) Condition A: 1.05 equiv of alkyne and 1.0 equiv of **127** at 0.15 mmol scale in 0.1 M MeCN for 3 h at 25 °C. Condition B: 1.05 equiv of alkyne, 1.0 equiv of **1**, and 1.0 equiv of $LiClO_4$ on 0.15 mmol scale in 0.1 M DCE/MeCN 98:2 at 80 °C for 2 h. Fc = ferrocenyl. Ratios determined by yields of isolated compounds. b) No reaction. c) Regioisomers observed.

In general, good to excellent yields and chemoselectivities were obtained starting from anilino-substituted alkynes. The CA–RE transformation was consistently favored in the absence of a Lewis acid, providing buta-1,3-dienes **133a, 149a–157a**, while addition of $LiClO_4$ afforded 4*H*-pyrans **133b, 149b–157b** with excellent selectivity. However, the use of alkynes with less activating donor

substitutents, such as OMe[152] (alkyne **146**) or ferrocenyl[124] (alkyne **147**), led to no reaction and transformation of DCID with asymmetric alkynes **147** and **148** gave mixtures of regioisomers that were inseparable by chromatography and recrystallization.

3.6. X-ray Structures of Adducts

The majority of the products obtained from CA–RE or HDA reactions were characterized by X-ray crystallographic analysis. Examples for the proof of the regioselectivity of the desired adducts are shown in Figure 37. All obtained crystal structures are described in the appendix.

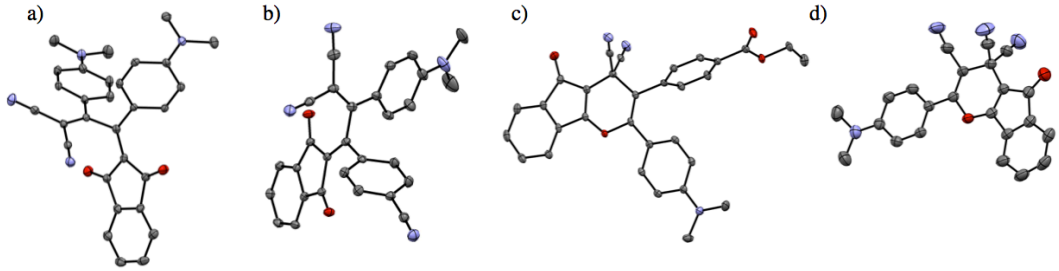

Figure 37. ORTEP representation of the molecular structures of CA–RE adducts **133a** (a) and **150a** (b) and HDA adducts **151b** (c) and **157b** (d). Thermal ellipsoids are shown at the 50% probability level. Hydrogen atoms not shown. T = 100 K.

3.7. UV/Vis

UV/Vis spectra of CA–RE and HDA products, recorded in CH_2Cl_2 at 25 °C are shown in Figures 38 and 39. The CA–RE products display intense ICT bands with λ_{max} values in the range of 450–545 nm (ε = 22500 to 49000 M^{-1} cm^{-1}) whereas the ICT bands of the HDA adduct are hypsochromically shifted and less intense ($\lambda_{max} \approx$ 290–487 nm, ε =10000–26000 M^{-1} cm^{-1}).

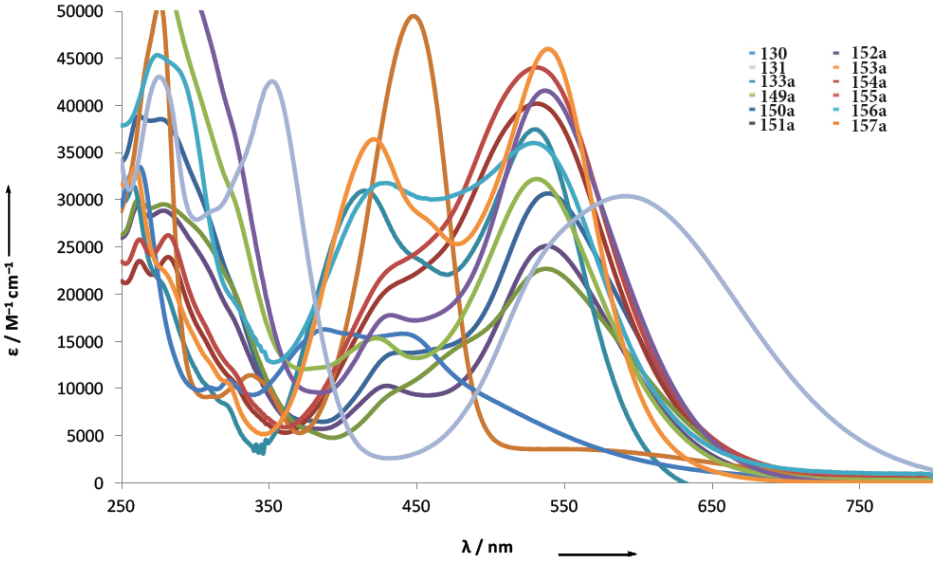

Figure 38. UV/Vis absorption spectra of [2+2] adducts at 298 K .

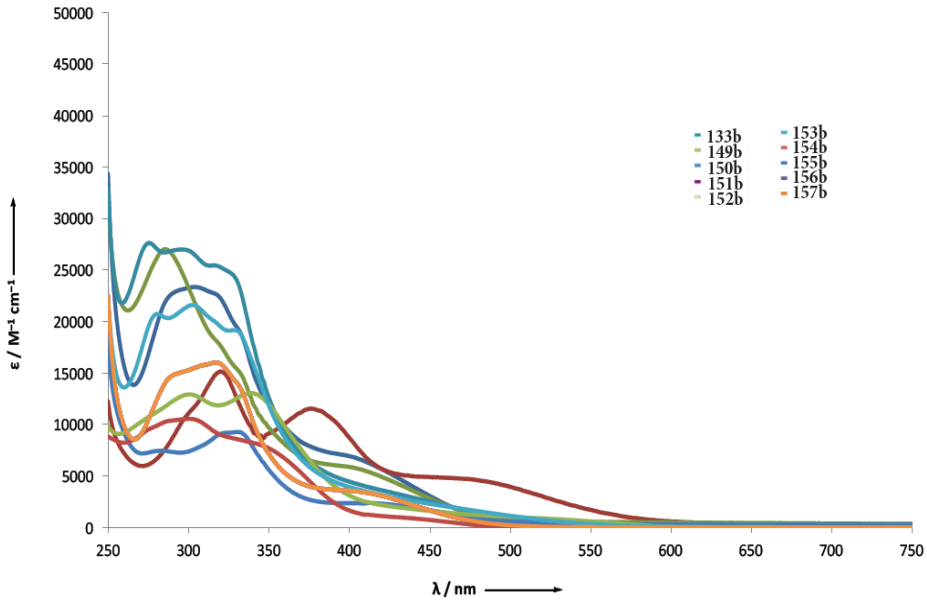

Figure 39. UV/Vis absorption spectra of [4+2] adducts at 298 K.

Both CA–RE and HDA products feature positive solvatochronism providing proof of intramolecular CT interaction (Figures 40 and 41).

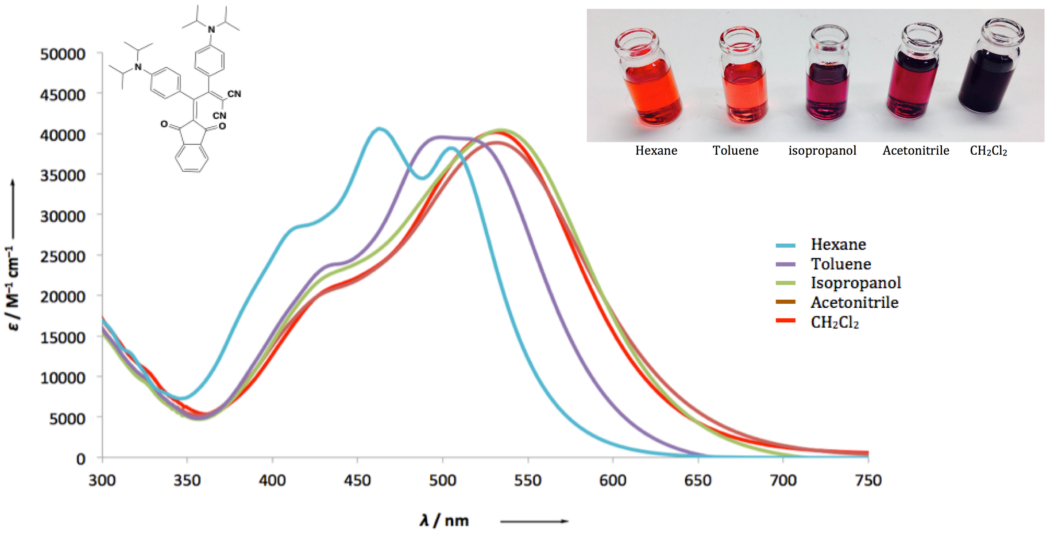

Figur

The ICT nature of these bands was confirmed by protonation with TFA, leading to attenuation of the band, followed by neutralization with triethylamine, which reconstituted the initial transition. Compounds **154a** and **154b** are shown in Figures 41 and 42, respectively, as an example. Other examples are shown in the appendix.

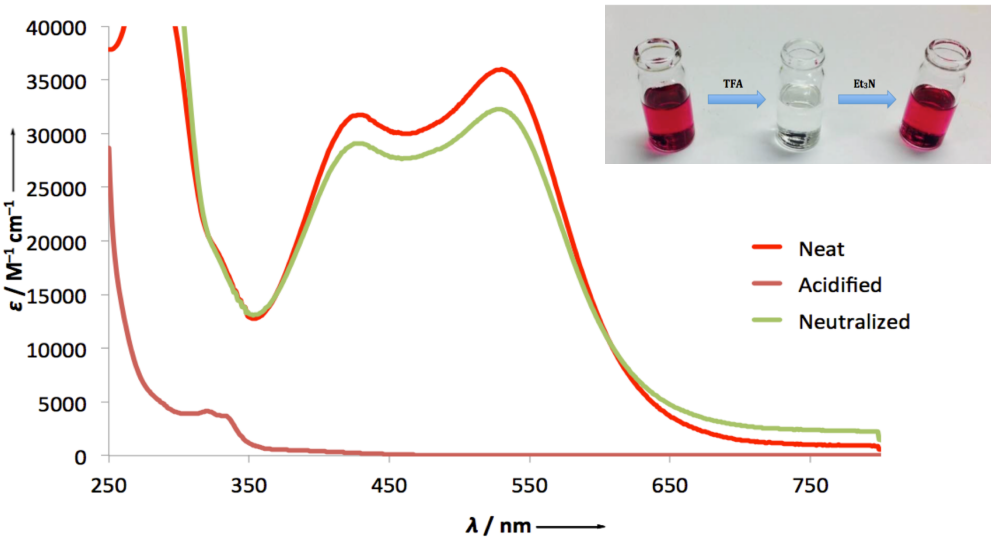

Figure 41. UV/Vis absorption spectra of **154a** in CH_2Cl_2 at 298 K recorded in CH_2Cl_2 (neat), after acidification with TFA, and after neutralization with Et_3N.

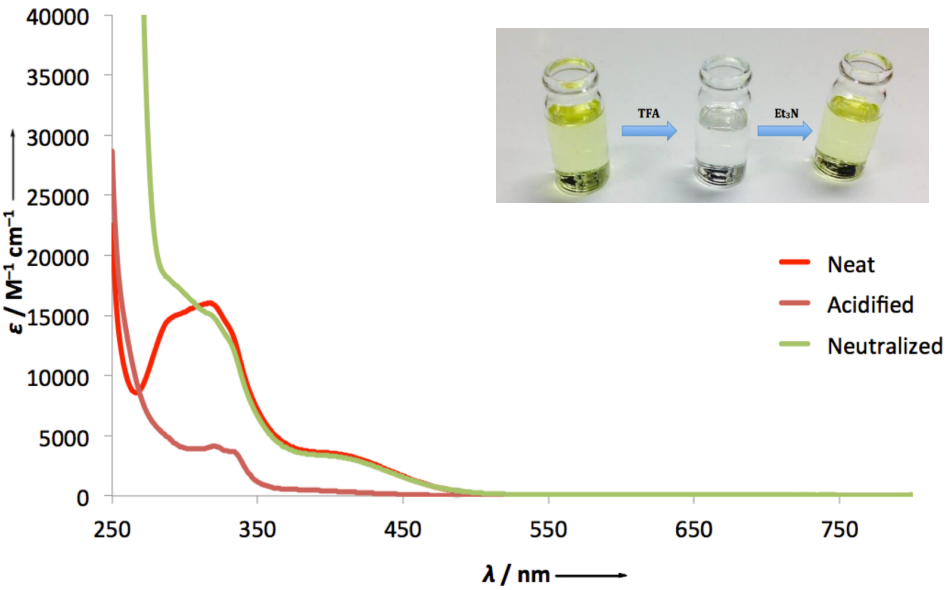

Figure 42. UV/Vis absorption spectra of **154b** in CH_2Cl_2 at 298 K recorded in CH_2Cl_2 (neat), after acidification with TFA, and after neutralization with Et_3N.

3.8. Electrochemistry

The redox properties of all the compounds were studied by cyclic voltammetry (CV) and rotating-disk voltammetry (RDV). Electrochemical data observed by CV at a scan rate of v = 0.1 V s^{-1} and rotating disk voltammetry (RDV) in CH_2Cl_2 + 0.1 M Bu_4NPF_6. All potentials are given versus ferrocene, used as internal standard reference. Compounds commonly exhibit one or two, usually reversible oxidation waves corresponding to the oxidation of the anilino moieties (Table 4). At least two, mostly reversible reduction waves can be observed, corresponding to the electron transfer to the extended DCID acceptor in the CA–RE products and the tricyclic acceptor moiety in the HDA products. The reduction of the CA–RE products is more facile, with $E^{o}_{red,1}$ occurring between –0.53 and –1.17 V, than the reduction of the HDA adducts, with $E^{o}_{red,1}$ occurring between –0.84 and –1.50 V. On the other hand, the HDA adducts ($E^{o}_{ox,1}$ between +0.34 and +0.78 V) are easier to oxidize than the

CA–RE products ($E^{o}_{ox,1}$ between +0.63 and +0.88 V, Table 4). Both CA–RE and HDA products feature positive solvatochronism.

From the CV data (Tables 4 and 5), we calculated a HOMO–LUMO energy gap of 1.80 eV and 1.84 eV for **153a** and **153b**, respectively, in agreement with the optical gaps obtained from the lowest-energy absorption maximum or the end-absorption in the UV/Vis spectra. For compound **153a**, two successive reversible mono-electronic oxidations of the DAA moieties occur at +0.63 V and +0.80 V respectively, while they are oxidized at +0.39 V and +0.46 V, respectively, in case of **153b**, showing that the alkylanilino moieties in **153a** are harder to oxidize, by 240 mV and 340 mV, respectively, than in **153b** (Figure 42). Additionally, the oxidation potential of the compounds with DAA moieties depends on the type of substituent on the phenyl ring: more donor-substitution leads to more facile oxidation.

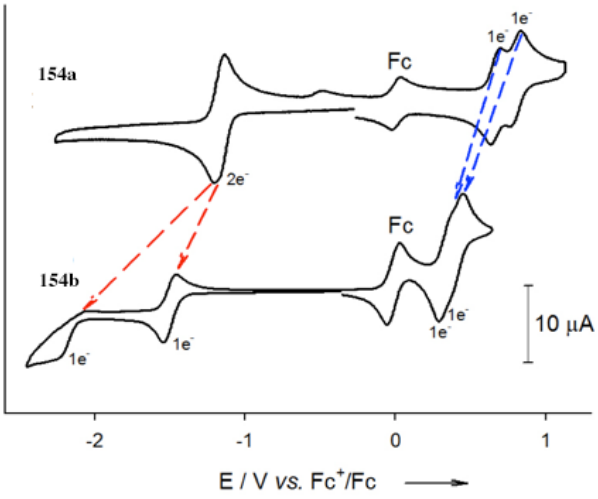

Figure 42. Cyclic voltammograms of **153a** and **153b** in CH_2Cl_2 + 0.1 M nBu_4NPF_6 in the presence of ferrocene on a glassy carbon working electrode at a scan rate of 0.1 V s^{-1}.

Table 4. Electrochemical data observed by CV at a scan rate of v = 0.1 V s^{-1} and rotating disk voltammetry (RDV) in CH_2Cl_2 + 0.1 M Bu_4NPF_6. All potentials are given versus ferrocene, used as internal standard reference.

entry	CV			RDV	
	$E°$ [a] V/$_{Fc+/Fc}$	ΔEp [b] mV	Ep [c] V/$_{Fc+/Fc}$	$E_{1/2}$ V/$_{Fc+/Fc}$	Slope (mV) [d]
130			+0.79	+0.78 (1e$^-$)	60
	–0.83	100		–0.86 (1e$^-$)	60
	–1.05	100		–1.10	80
131	+0.70	58		+0.73 (2e$^-$)	60
	–0.80	77		–0.79 (2e$^-$)	65
	–1.00	30		–0.81 (1e$^-$)	80
	–1.12	51		–1.13 (1e$^-$)	80
133a			+0.87	+0.88 (1e$^-$)	60
	+0.66	60		+0.67 (1e$^-$)	60
	–1.01	100		–0.99 (2e$^-$)	80
	–1.69	80		–1.71 (1e$^-$)	110
	–1.95	100	-2.38	–1.94	-
133b	+0.42	90		+0.44 (2e$^-$)	60
	–1.50	90		–1.51 (1e$^-$)	70
			-2.29	–2.30 (1e$^-$)	90
149a	+0.83	69		+0.82 (1e$^-$)	70
	–0.84	111		–0.88 (2e$^-$)	80
	–1.78	69		–1.85 (1e$^-$)	55
149b	+0.74	60		+0.74 (1e$^-$)	60
	–0.85	75		–0.84 (1e$^-$)	60
	–0.95	75		–0.95 (1e$^-$)	60
	–1.69	75		–1.67 (1e$^-$)	80
150a	+0.75	95		+0.76 (1e$^-$)	70
	–0.89	84		–0.91 (1e$^-$)	60
	–0.99	99		–1.06 (1e$^-$)	60
150b	+0.65	75		+0.67 (1e$^-$)	60
			-1.45	–1.43 (1e$^-$)	60
	–2.09	150		–2.19	60
151a	+0.74	70		+0.74 (1e$^-$)	75
	–0.92	108		–0.93 (2e$^-$)	75
151b	+0.62	80		+0.64 (1e$^-$)	60
	–1.43	110		–1.45 (1e$^-$)	75
152a	+0.75	54		+0.72 (1e$^-$)	65
	–0.93	106		–0.99 (2e$^-$)	75
152b	+0.64	60		+0.65(1e$^-$)	60
			-1.41[e]	–1.42 (1e$^-$)	60
			-2.12	–2.13 (1e$^-$)	70
163a	+0.80	80		+0.78 (1e$^-$)	55
	+0.63	69		+0.63 (1e$^-$)	55
	–1.17	49	-1.17	–1.19 (2e$^-$)	80
153b	+0.46	71		+0.45 (2e$^-$)	70
	+0.39	92		+0.37 (1e$^-$)	70
	–1.45	79		–1.52 (1e$^-$)	70
			-2.20	–2.24 (1e$^-$)	85
154a	+0.73	72		+0.78 (1e$^-$)	55
	+0.63	88		+0.65 (1e$^-$)	55
	–0.92	95		-0.96 (1e$^-$)	55
	–1.01	63		-1.06 (1e$^-$)	80
154b	+0.49	74		+0.51 (1e$^-$)	60
	+0.34	47		+0.36 (1e$^-$)	60
	–1.42	61		–1.41 (1e$^-$)	70
			-2.12	–2.10 (1e$^-$)	70
155a	+0.80	45		+0.77 (1e$^-$)	90
	+0.66	43		+0.64 (1e$^-$)	60
			-1.17	–1.13 (2e$^-$)	60
155b	+0.42	60		+0.45 (1e$^-$)	60
	+0.34	60		+0.34 (1e$^-$)	60
	–1.49	75		–1.48 (1e$^-$)	75
			-2.25	–2.22 (1e$^-$)	75
156a	+0.71	180		+0.71 (2e$^-$)	80
	–1.04	130		–1.06 (2e$^-$)	80
156b	+0.68	60		+0.62 (1e$^-$)	60
	+0.60	60		+0.67 (1e$^-$)	60
	–1.45	70	-2.16	–1.60 (1e$^-$)	160
157a	+0.88	83		+0.92 (1e$^-$)	65
	–0.55	70		–0.56 (1e$^-$)	55
	–0.73	59		–0.73 (1e$^-$)	65
157b	+0.78	80		+0.75 (1e$^-$)	60
	–0.85	110		–0.83 (2e$^-$)	75

a) $E^o = (E_{pc} + E_{pa})/2$, where E_{pc} and E_{pa} correspond to the cathodic and anodic peak potentials, respectively. b) $\Delta E_p = E_{pa} - E_{pc}$. c) E_p = irreversible peak potential. d) Logarithmic analysis of the wave obtained by plotting E versus $\log[I/(I_{lim}-I)]$. e) Peak at –1.41 V became reversible for v > 0.5 V/s.

Table 5. Electrochemical, and optical data for derivatives **130**, **131**, **133**a, **133b** and **149–157a,b.**

Comp.	Electrochemical[a]					
	E_{1ox}[c] [V]	E_{1red} [V]	E_{HOMO} [eV]	E_{LUMO} [eV]	E_{gap} [eV]	$\lambda_{max\ calc}$ [nm]
130	+0.79[c]	–0.83[b]	–5.59	–3.97	1.62	765
131	+0.67[b]	–0.43[b]	–5.47	–4.37	1.01	1228
133a	+0.66[b]	–1.01[b]	–5.46	–3.79	1.67	743
133b	+0.42[b]	–1.50[b]	–5.22	–3.30	1.92	646
149a	+0.83[b]	–0.84[b]	–5.63	–3.96	1.67	743
149b	+0.74[b]	–0.85[b]	–5.54	–3.95	1.59	780
150a	+0.75[b]	–0.89[b]	–5.55	–3.91	1.64	756
150b	+0.65[b]	–1.45[c]	–5.45	–3.35	2.10	590
151a	+0.74[b]	–0.92[b]	–5.54	–3.88	1.66	747
151b	+0.62[b]	–1.43[b]	–5.42	–3.37	2.05	605
152a	+0.75[b]	–0.93[b]	–5.55	–3.87	1.68	738
152b	+0.64[b]	–1.41[c]	–5.54	–3.39	2.15	577
153a	+0.63[b]	–1.17[b]	–5.43	–3.63	1.80	689
153b	+0.39[b]	–1.45[b]	–5.19	–3.35.	1.84	674
154a	+0.63[b]	–0.92[b]	–5.43	–3.88	1.55	800
154b	+0.34[b]	–1.42[b]	–5.14	–3.38	1.76	705
155a	+0.66[b]	–1.17[c]	–5.46	–3.63	1.83	678
155b	+0.34[b]	–1.49[b]	–5.14	–3.31	1.83	678
156a	+0.71[b]	–1.04[b]	–5.51	–3.76	1.75	709
156b	+0.60[b]	–1.45[b]	–5.40	–3.35	2.05	605
157a	+0.88[b]	–0.55[b]	–5.68	–4.25	1.43	867
157b	+0.78[b]	–0.85[b]	–5.58	–3.95	1.63	761

a) Electrochemical data obtained at a scan rate of 0.1 V s^{-1} in CH_2Cl_2 containing 0.1 M nBu_4NPF_6 on a glassy carbon-working electrode. All potentials are given versus the Fc^+/Fc couple used as internal standard. HOMO and LUMO energy levels in eV were approximated from the reversible half-potential reduction waves or the irreversible first reduction wave using the equation, HOMO = –(4.80 + E_{1ox}), LUMO = –(4.80 + E_{1red}),[168,169] E_{gap} = LUMO–HOMO. $\lambda_{max\ calc.}$ is the calculated

Furthermore, one reversible $2e^-$ reduction step or two successive one-electron reduction steps are detected, corresponding to the reduction of the acceptor moieties, namely the extended DCID obtained in the case of the CA–RE reaction or the tricyclic pyran scaffold in the case of the HDA reaction. For instance, for compound **153a** obtained from the CA–RE reaction, one reversible and bi-electronic reduction is measured at –1.17 V while **153b** shows two successive and monoelectronic reductions at –1.45 V and –2.20 V, the second reduction being irreversible. It can be noted that the tricyclic pyran scaffold is always more difficult to be reduced than the extended DCID (Figure 42) and is reduced generally in two separate steps, separated by 750 mV in the case of **153b**.

3.9. TD-DFT Calculations

The vertical optical transitions of the optimized structures of **130**, **131**, **133a**, **133b** **149a–157a** and **133b**, **149b–157b** were calculated by TD-DFT using the software package Gaussian 09.[147] In most cases, the computed transition energies are slightly larger than the experimental values (Figures 43 and 44),

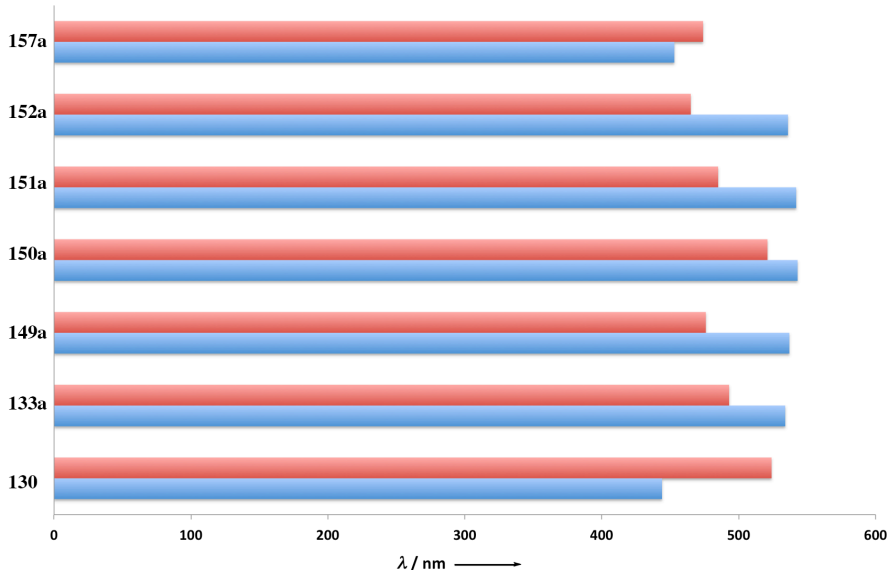

Figure 43. Comparison of experimental (blue bars, λ_{exp}) and calculated (red bars, λ_{calc}) low-energy transitions of the CA–RE products.

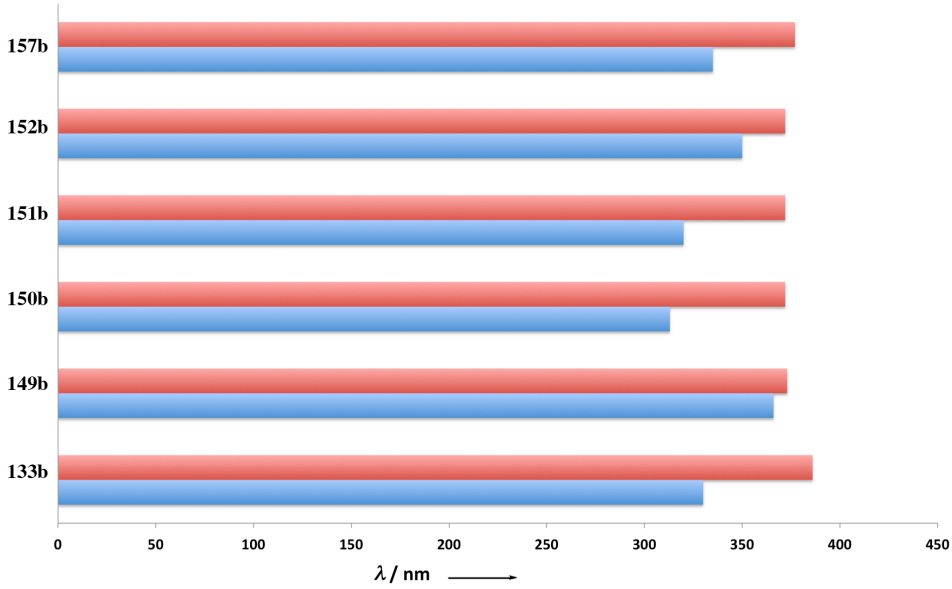

Figure 44. Comparison of experimental (blue bars, λ_{exp}) and calculated (red bars, λ_{calc}) low-energy transitions of the HDA products.

Differences between computed excitation energies and experimental absorption maxima are in the range of 0.12–0.43 eV for **133a**, **149a–157a** and in the range of 0.07–0.63 eV for **133b**, **149b–157b**, well within the expected range for anilino-cyano-type push–pull chromophores.

The lowest-energy band in CA–RE products **133a**, **149a–157a** involves mostly ITC from the HOMO, localized on the terminal anilino donor to the LUMO of the acceptor moiety. In contrast, the calculation of the HDA adducts **133b**, **149b–157b** shows that the lowest energy band ($S_0 \rightarrow S_1$ band) consists majorly of a HOMO–1→LUMO transition. An electronic absorption band involving an allowed HOMO→LUMO transition occurs at higher energy, and proximity in energy of HOMO–1 and HOMO would lead to near overlap of the both transitions, which is consistent with the observed absorption spectra of HDA adducts **133b**, **149b–157b**.

3.10. Conclusion

To accomplish the previously stated goal of extending acceptor units in formal [2+2] CA–RE reactions, reactivity of DCID with electron-rich anilinoalkynes was investigated. Depending on the reaction conditions, push–pull buta-1,3-dienes are obtained by the CA–RE reaction or tricyclic 4*H*-pyrans by the [4+2] HDA reaction. The presence of Lewis acids, such as $LiClO_4$, greatly enhances the formation of the HDA cycloaddition over the CA–RE reaction. This is opposite to the effect of the Lewis acids on cycloadditions with electron-rich olefins. Optoelectronic applications of the new push–pull chromophores and the rapid construction of complex 4*H*-pyran derivatives will be further investigated.

Chapter 4

Ester-Subtituted Electron-Poor Alkenes for CA–RE and Post-Functionalization

4. Ester-Subtituted Electron-Poor Alkenes for CA–RE and Post-Functionalization

The results of this paragraph have been obtained in collaboration with Dr. Tristan A. Reekie. Dr. Laurent Ruhlmann and Dr. Corinne Boudon carried out electrochemistry measurements at the University of Strasbourg. The crystal structures were solved by Dr. Nils Trapp. The results of this Chapter are the subject of a recent publication.[171]

4.1. Introduction

We wanted to continue extending acceptor units in formal [2+2] CA–RE reactions investigating the CA–RE reaction by using new types of acceptors. A particular focus lies on whether the reaction could be achieved without any cyano groups present on the acceptor and to determine if they were essential for the reaction to proceed. We decided to choose the ester functionality due to its ability to be more easily derivatized following the CA–RE reaction while still providing electron-withdrawing capabilities analogous to the cyano moiety. The Hammett parameters (σ_p) of CN and ethyl ester moieties are reported to be 0.66 and 0.45, respectively,[172] therefore a drop in reactivity should be observed by exchanging cyano groups in the starting alkene for ester groups.[172] Previous reports, such as the utilization of DCID in Chapter 3, have shown that these types of electron deficient olefins can react with electron-rich double bonds affording compounds derived either from [4+2] or [2+2] cycloaddition reactions.[148] A comprehensive study into the stepwise replacement of cyano moieties with ethyl esters was therefore undertaken to explore the CA–RE reaction.

4.2. Synthesis

The monoester-substituted alkene **158** was subjected to a reaction with alkyne **102** to afford three different products **159**–**161** (Scheme 28). Intriguingly, isomer **159** containing an ester closer to the activating group was observed in 13% yield. This is in contrast to usual observations, where the better electron-withdrawing groups are located closer to the DAA-activating group. The less sterically demanding cyano moiety is facing towards the aromatic ring. Compounds **160** and **161** are *E*/*Z* isomers

and are the favored products based on yields of 52% and 32%, respectively. The geometries of products **159–161** are demonstrated by X-ray analysis (Figure 45).

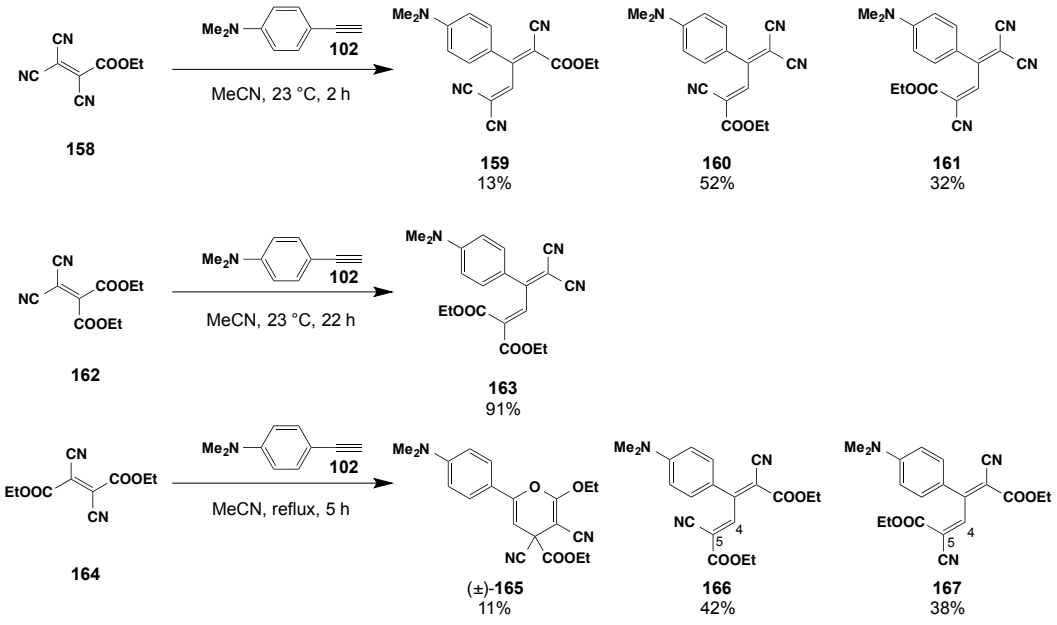

Scheme 28. Reaction of alkyne **102** with monoester cyanoalkene **158** and diester cyanoalkenes **162**, and **164**.

Diester **162** undergoes the CA–RE reaction to form only **163** in 91% yield. Reaction times at 25 °C are slower requiring 22 h to reach completion. When the isomeric diester **164** was used for the reaction, three products (±)-**165, 166** and **167** were obtained. Compound (±)-**165**, which arises from a HDA reaction, was isolated in 11% yield. Despite the potential of four isomeric products arising from the CA–RE reaction, only compounds **166** and **167** were observed, those being the C4–C5 *E*/*Z* isomers. This is most likely due to the steric demands forcing the ester moiety away from the aromatic ring, allowing only the *E* isomer for the second double bond.

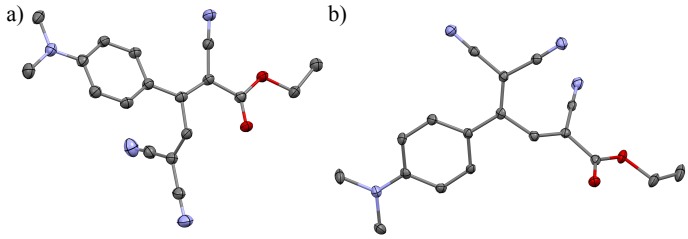

Figure 45. ORTEP plots of a) **159** and b) **160**, H-atoms omitted for clarity. Atomic displacement parameters at 100 K are drawn at 50% probability level.

When triester **168** was engaged in the reaction, increased temperatures (82 °C) were necessary for the reaction to proceed in a timely fashion (5 h) (Scheme 29). Three compounds were also isolated from the reaction including compound **169**, arising from a HDA reaction in 21% yield, and compound **170** from the CA–RE reaction in 63% yield.

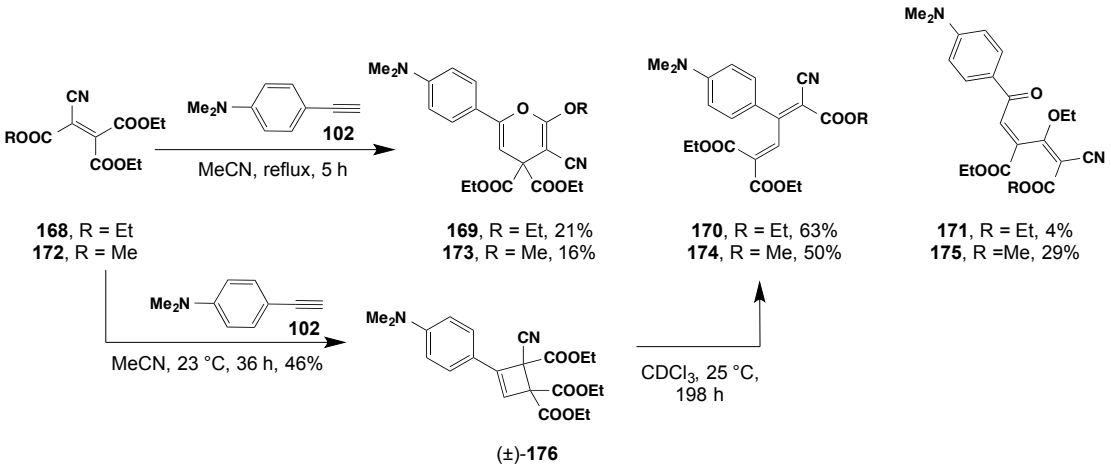

Scheme 29. Reaction of alkyne **102** with triester cyanoalkenes **168** and **172**.

Both structures were confirmed by X-ray analysis, which again showed for compound **170** that the cyano moiety, and not the ester, points towards the aromatic ring (Figure 46a). A third product, pentadienone **171** was also isolated and its structure confirmed by X-ray analysis (Figure 46c). Yields of this product could be improved from 4% to 66% by using cyclohexane as solvent (**169** and **170** were in this case isolated in 2% and 26% yield, respectively). Analysis of the quinoid character (δr) of **169–171** provided values of 0.028, 0.028 and 0.037 Å, respectively. Bond length alternation (BLA) in the DMA rings is a good indication for the efficiency of the charge-transfer from the donor to the acceptor moieties, which can be expressed by the δr of the ring. For comparison, the δr value is 0 in benzene whereas for quinoid rings the values are in the range of 0.08–0.10 Å. The highest BLA is observed for pentadienone **171**.

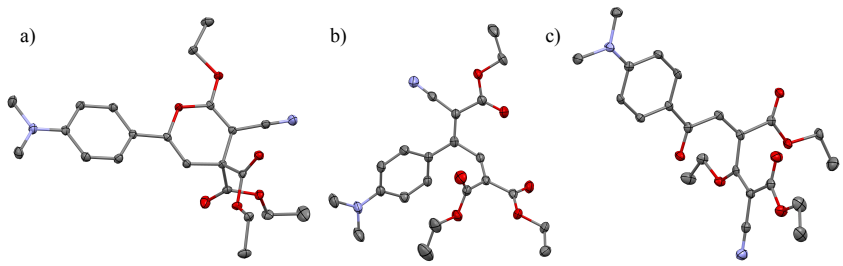

Figure 46. ORTEP plots of a) **169**, b) **170**, and c) **171**. H-atoms omitted for clarity. Atomic displacement parameters at 100 K are drawn at 50% probability level.

Further studies were undertaken in order to reach a better insight into the mechanism by which pentadienone **171** was formed. Performing the reaction with methanol as the solvent, or with methyl cyanoacetate or malononitrile as additives resulted in the same products with no incorporation of solvent or additives, which suggests a concerted mechanism. The addition of $LiClO_4$ as a Lewis acid did not change the selectivity of the reaction compared with DCID as acceptor.[148] When the mono-methylated triester **172** was also subjected to the reaction then analogous products **173–175** were obtained. Alkene **168** was reacted with alkyne **102** at 23 °C, which led to the isolation of cyclobutene (±)-**176** in addition to compounds **169–171** in 15%, 9% and 28% yield, respectively.

Retroelectrocyclization was monitored by ^{1}H NMR to rule out the possibility that **176** results from a cyclobutene rearrangement. Over a period of 198 h at 25 °C, ^{1}H NMR monitoring showed quantitative conversion of cyclobutene (±)-**176** into **170**, with no other product observed (Figure 47).

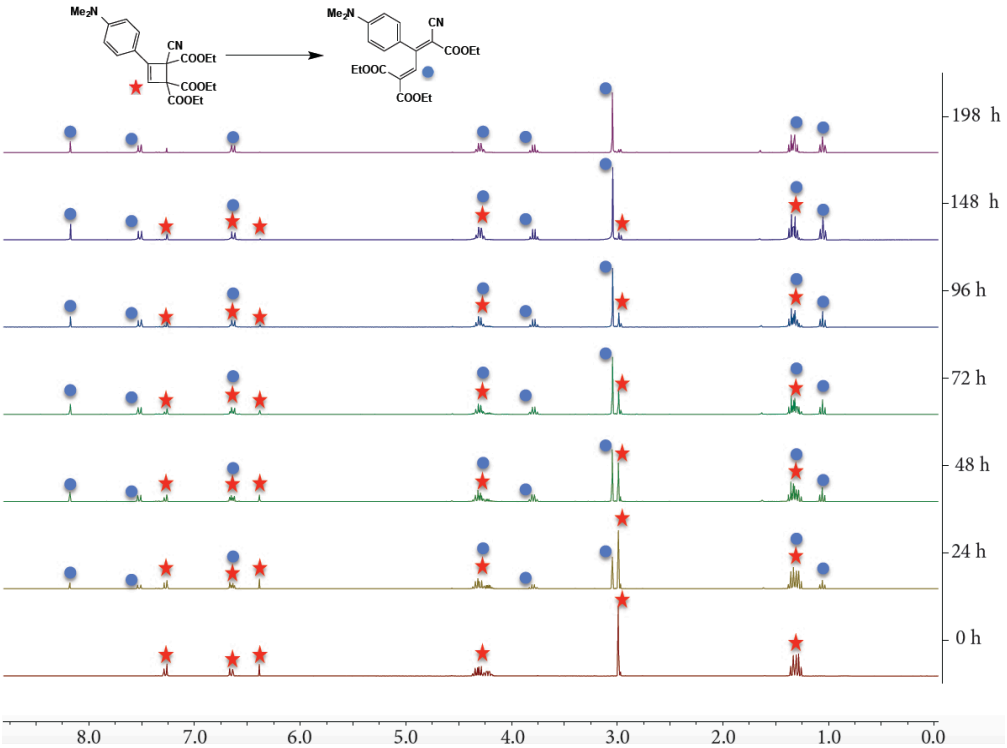

Figure 47. Selected ^{1}H NMR spectra of compound (±)-**176** in $CDCl_3$ solution as it undergoes retroelectrocyclization to compound **170** over time (h) at 298 K (300 MHz).

A first-order rate constant of 4.957 x 10^{-6} s^{-1} at 298 K for the conversion of (±)-**176** into **170** was calculated from the combined ^{1}H NMR spectroscopic data from the slope of the linear plot of ln[(±)**176**] versus time (Figure 48).

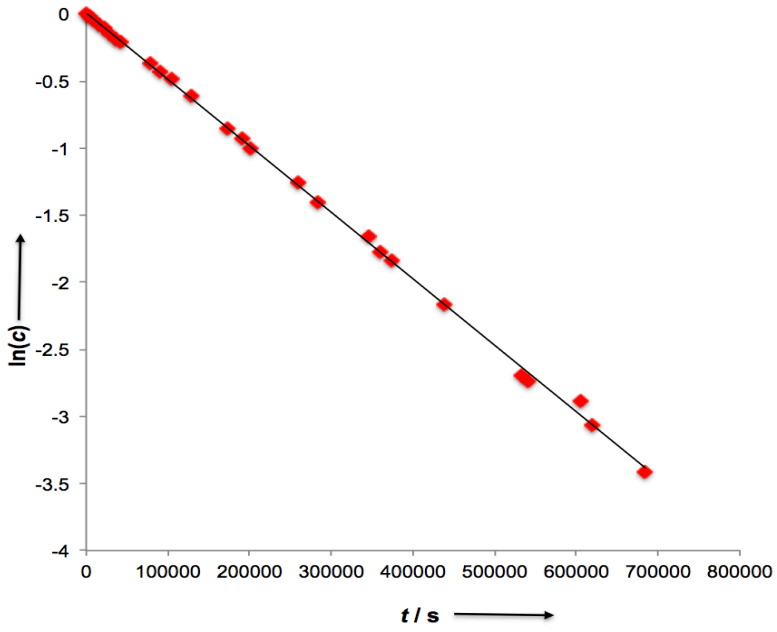

Figure 48. Plot and fit of ln[(±)-**176**] vs. time at 298 K for the retroelectrocyclization.

The combined experimental results led to the following mechanistic proposal (Scheme 30) for the formation of penta-2,4-dien-1-ones **171** and **175**. The first step most likely involves the carbonyl oxygen atom and the olefinic carbon atom of alkene **168** engaging in a [3+2] cycloaddition with the alkyne **102** to yield the zwitterionic intermediate **177**. The two adjacent oxygen atoms provide stabilization of the positive charge while the negative charge can be delocalized over the cyano and ethyl carboxylate moieties. Intramolecular cyclopropanation of 1,3-dipole **177** affords the second intermediate **178**. Rather than cyclizing to form cyclobutene (±)-**176** or pyran **169**, an intramolecular [3+2] cycloaddition reaction occurs to give the oxabicyclo[3.1.0]hexene intermediate **178**. The concluding step of the mechanism involves a Claisen-type rearrangement with cyclopropane ring opening of **178** to give the isolated product **171**. This ring opening of oxabicyclo[3.1.0]hexene is not without precedent, however previous reports showed that high temperatures (160 °C or greater) were necessary for the reaction to occur.[173,174] The lower temperatures employed in this case can be explained by the substituents present on the cyclopropane ring. As previously reported, cyclopropylfuran **179a** (R = H) requires temperatures of 250 °C (conventional heating) or 400 °C (flash vacuum pyrolysis) to rearrange to the aldehyde **180a**.[173,174] When an electron-withdrawing substituent is connected to the cyclopropane, as in **179b** (R = COOMe), the same rearrangement can happen at 160 °C (neat) to yield **180b**.[173,174] The electron-withdrawing groups at C5 and at C6 of **178** most likely lower the energy required for ring-opening of the bicycle, allowing for product **171** to be isolated at room temperature.

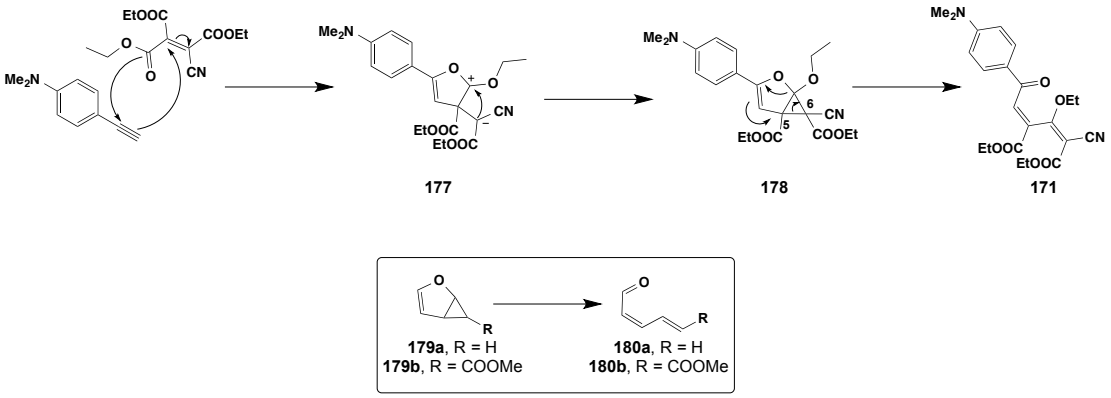

Scheme 30. Proposed mechanism for the formation of **171**.

Tetraester **181** was also subjected to reaction with alkyne **102**, however elevated temperatures of 200 °C were required for any reaction to proceed (Scheme 31). This resulted in significant decomposition and compounds **182** arising from HDA was isolated in 3% yield. Unexpectedly, the product **183** expected from a CA–RE reaction was not observed and **184** from [3+2] cycloaddition was obtained in low yield. However, by substituting two of the ethyl esters with $–CH_2CN$ moieties to give the more reactive alkene **185**, the CA–RE reaction with DMA-substituted alkyne **102** occured at 82 °C over 36 h. This reaction led to three distinct products **186–188** arising from [4+2], [2+2], and [3+2] cycloadditions, respectively. When the $–CH_2CF_3$ alkene analogue **189** was employed, the analogous compounds **190–192** were observed. The change in alkene reactivity can be justified by a comparison of the Hammett parameters (σ_p) of the CH_2CH_3, CH_2CN and CH_2CF_3 groups, which equals –0.15, 0.18, and 0.09, respectively.[172]

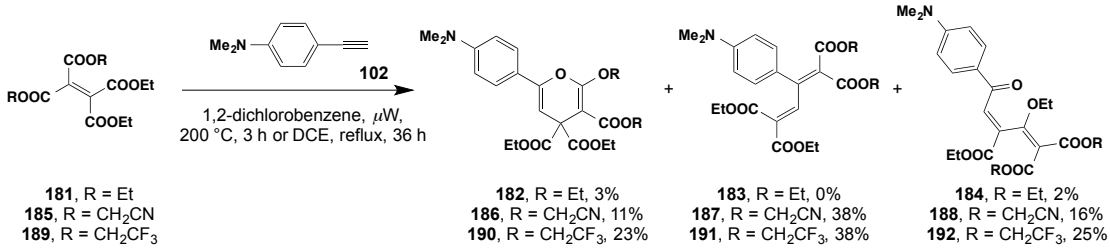

181, R = Et
185, R = CH_2CN
189, R = CH_2CF_3

182, R = Et, 3%
186, R = CH_2CN, 11%
190, R = CH_2CF_3, 23%

183, R = Et, 0%
187, R = CH_2CN, 38%
191, R = CH_2CF_3, 38%

184, R = Et, 2%
188, R = CH_2CN, 16%
192, R = CH_2CF_3, 25%

Scheme 31. Reaction of alkyne **102** with tetraester alkenes **181**, **185**, and **189**.

We tested the ester-substituted alkenes **162** and **164** in transformations with other activated alkynes (Scheme 32). Bis-DMA-substituted alkyne **132** reacting with alkene **164** gave both [4+2] and [2+2] cycloaddition products (±)-**193** and **194** in 16% and 70% yield, respectively. The presence of Lewis acids combined with a screening of solvents from acetonitrile to 1,2-dichloroethane did not significantly change the chemoselectivity. With alkene **162**, the doubly activated alkyne **132** affords the CA–RE product **195**, besides very minor amounts of **196**, resulting from [3+2] cycloaddition/rearrangement. Lewis acids also did not influence the reaction selectivity for the two ester-substituted alkenes **162** and **164**. When the unsymmetrical phenyl-substituted alkyne **197** was reacted with alkene **162**, only product **198**, formed by the CA–RE reaction is observed in excellent yield (95%). Similarly, ethynylferrocene (**199**) underwent a facile CA–RE reaction with **162** to afford product **200** in 78% yield.

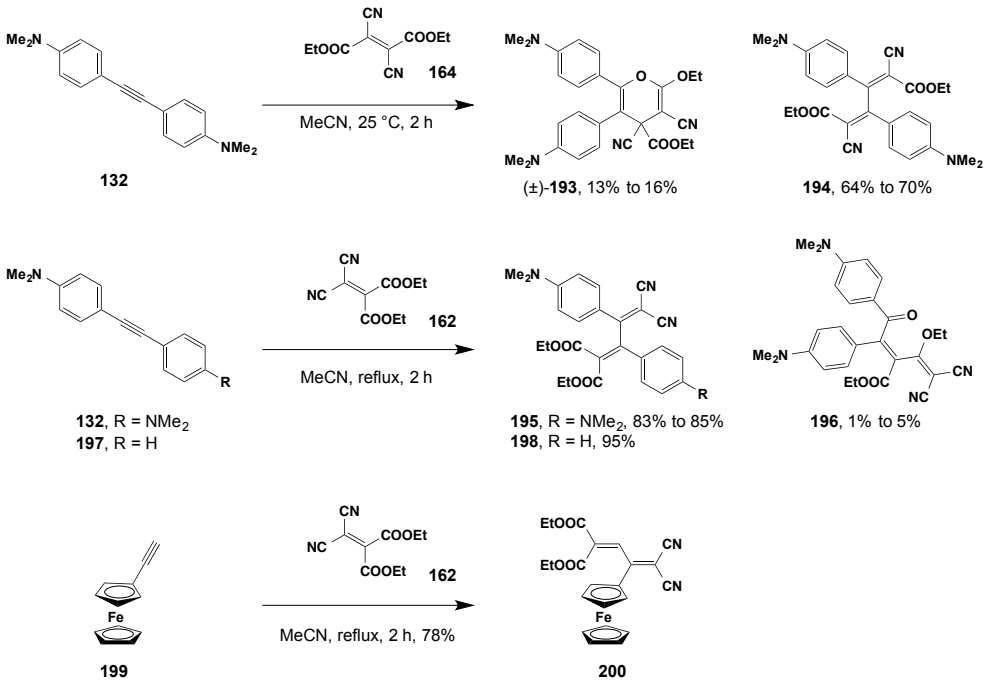

Scheme 32. Reaction of activated alkynes **132**, **198**, and **199** with alkenes **162** and **164**.

4.3. Post-functionalization of CA–RE adducts

With a new series of products derived from the CA–RE reaction in hand and based on our previous work,[175] we turned our attention to exploring some post-reaction functionalization reactions (Scheme 33). 4-Ethynylaniline (**201**) was reacted with alkene **162** to yield the desired CA–RE product **202** (X = NH_2) in 72% yield. The free aniline moiety allowed for reduction to the phenyl analogue **203** (X = H) or oxidation to the nitro analogue **204** (X = NO_2) in 42% and 75% yield, respectively. Diazonium chemistry allowed for the conversion to the iodo derivative **205**, which could then be subjected to Suzuki or Sonogashira cross-couplings to afford compounds **206** and **207** correspondingly. In addition, the incorporation of the newly activated alkyne in compound **207** allowed for a second CA–RE reaction with TCNE or TCNQ to afford **208** and **209**, respectively.

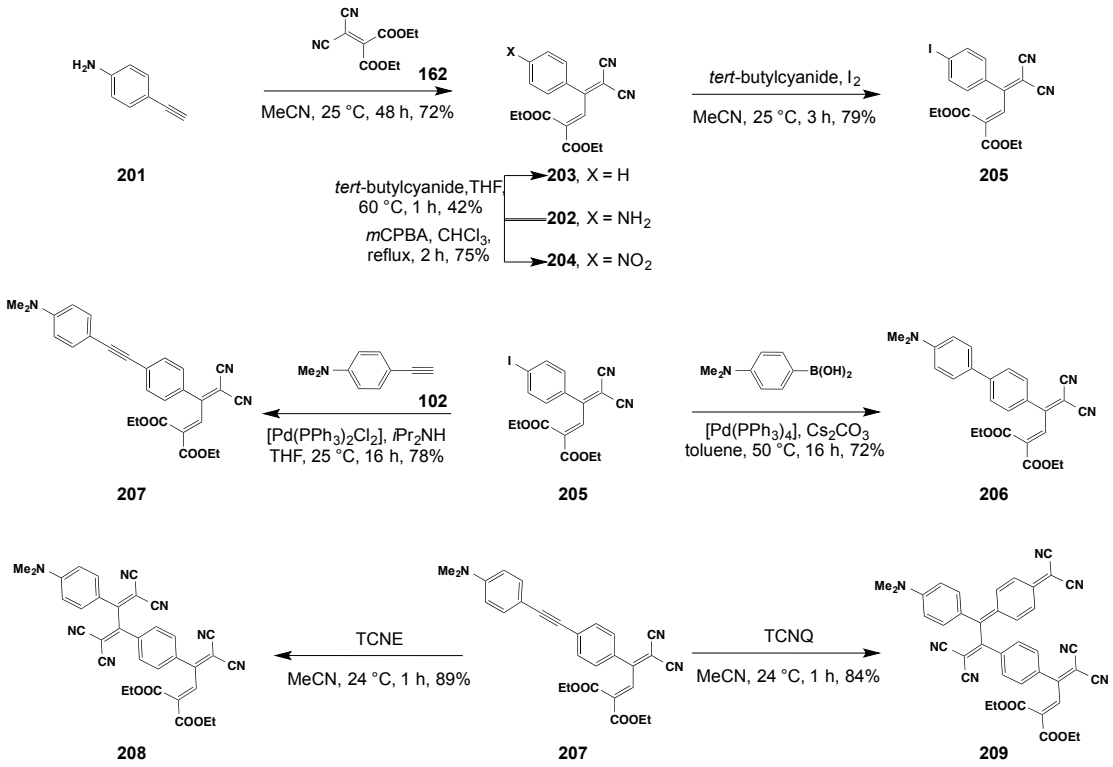

Scheme 33. Post-CA–RE reaction functionalization.

Taking advantage of the presence of the ester moieties in compound **163**, additional post-CA–RE functionalization was investigated (Scheme 34). Transesterification with MeOH gave compound **210** in 69% yield. However, all attempts to hydrolyze either the ethyl- or methyl ester to the corresponding acid were unsuccessful.

We have recently reported the pharmaceutical potential of pyrazolopyrans derived from the reaction of olefinic malononitriles with pyrazolones such as **211**.[176] Pyralzolopyran derivatives have been identified as potent inhibitors of plasmodial serine hydroxymethyltransferase (SHMT) for the treatment of Malaria.[176–178] The olefinic malononitriles in that report resulted from a condensation between malononitrile and a carbonyl moiety and not from a CA–RE reaction. Therefore, we wished to expand the application of the CA–RE reaction by converting one of the products to a pharmaceutically useful compound (Scheme 34). To reach this goal, compound **163** was reacted with pyrazolone **212** selectively at the dicyano-substituted double bond to form **211** exclusively in 38% yield.

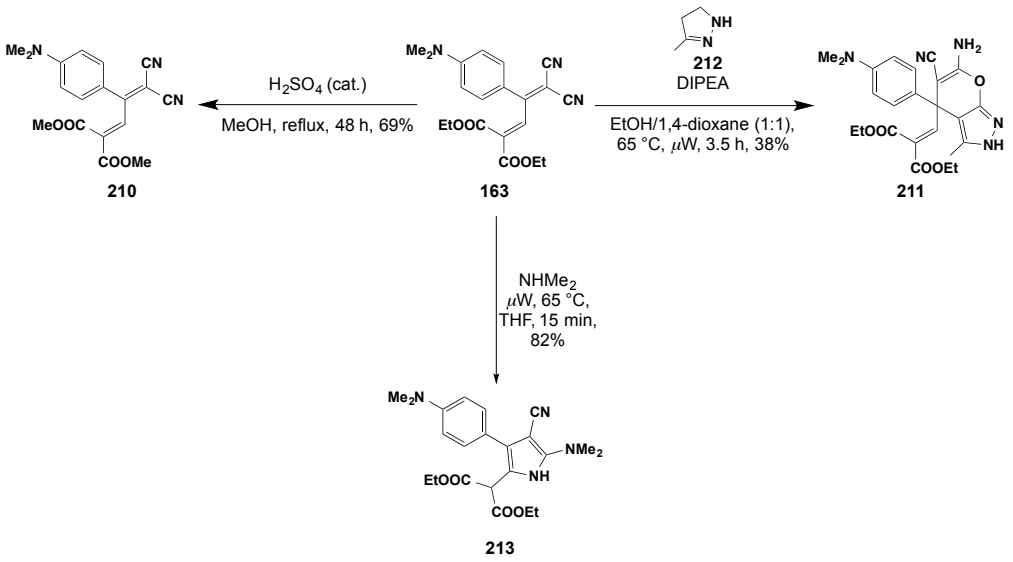

Scheme 34. Post-CA–RE reaction functionalization of **163**.

The regioselectivity of the reaction could be demonstrated by ^{13}C NMR spectra where the two carbonyl signals can be observed at 167.50 and 166.76 ppm while only a single nitrile carbon signal is observed at 112.31 ppm. This assignment is supported by the ^{1}H NMR spectra where the pyrazole NH signal is clearly distinguished at 8.94 ppm while the NH_2 signal appears at 5.29 ppm. This is the first time that such a structure has been obtained from post-CA–RE modification, highlighting the prospective for these products to be employed to construct molecules of greater complexity.

Pyrroles can also be synthesized from the corresponding CA–RE adduct **163** by using secondary amines. Pyrroles with multiple ring substituents are an important class of heterocycles. Of particular interest is the 2-aminopyrrole functionality, which, despite the synthetic challenges associated with its synthesis,[179,180] is present in a number of bioactive structures.[181,182] Pyrrole **213** can be obtained from **163** in 82%. An extensive study of the synthesis of tetrasubstituted NH-pyrroles will be given in Chapter 5.

4.4. UV/Vis

UV/Vis spectra of the new series of push–pull chromophores were recorded. Figure 47 shows selected examples of CA–RE adducts. A hypsochromic shift (464 to 448 nm) was observed when varying from three to two cyano groups (compound **160** and **167**) (Figure 49). However, roughly the same values were obtained for compounds **167** and **170** (448 and 449 nm) despite having two and one cyano groups, respectively.

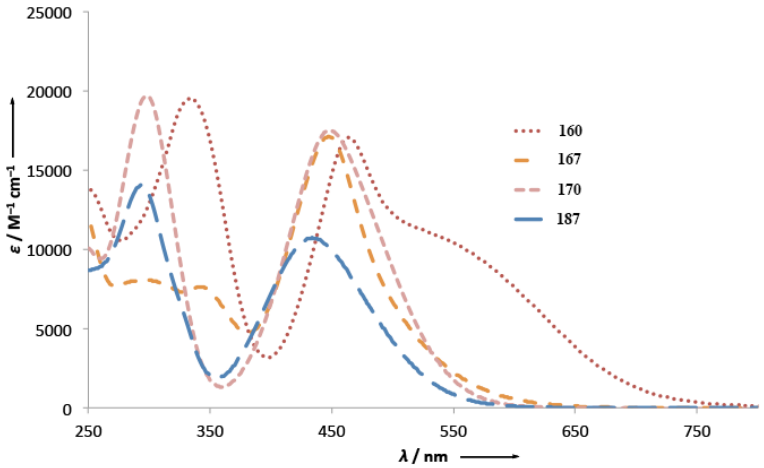

Figure 49. UV/Vis spectra in $CHCl_3$ at 298 K showing the changes upon substituting cyano by ester groups in the buta-1,3-dienes **160**, **167**, **170**, and **187** obtained from the CA–RE reaction.

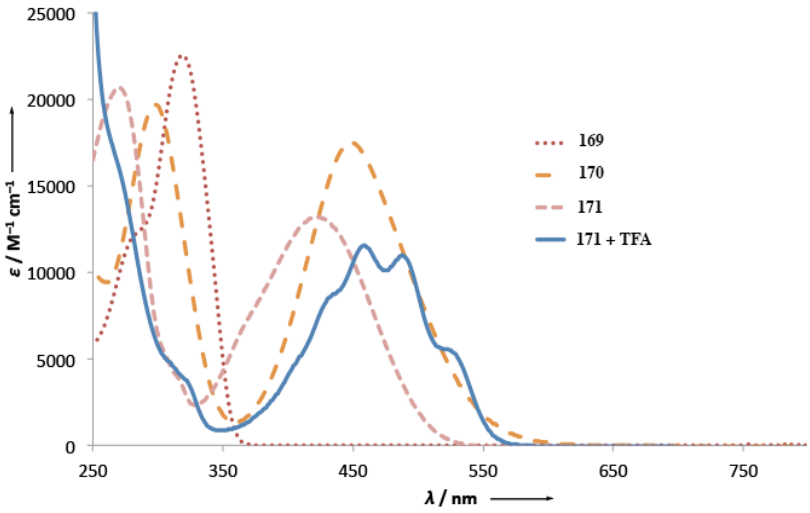

Figure 50. UV/Vis spectra in $CHCl_3$ at 298 K showing the three products 4*H*-pyran **169**, buta-1,3-diene **170**, and pentadienone **171**. Also shown is the unusual absorption band obtained upon addition of TFA to a solution of pentadienone **171**.

The optical properties of compounds derived from the CA–RE reaction are consequently more dependent on the identity of the groups of the butadiene more proximate to the donor than being a sum of the parts. The CA–RE adduct **163**, which has two cyano groups on the alkene more proximate to the donor, has an absorption maximum at 455 nm, which confirms the previous results. Tetraester **187** shows both a hypsochromic shift (434 nm) and a reduction in extinction coefficient highlighting the role of the cyano group for the decent optical properties for this particular family of compounds.

Figure 50 shows the comparison of the UV/Vis spectra of the three compounds obtained from the reaction between **168** and DMA-substituted alkyne **102**. The CA–RE adduct **170** has the longest wavelength of absorption at 449 nm while pentadienone **171** has an absorption at 423 nm with a reduced extinction coefficient. The HDA product **169** has a single absorption at 319 nm, which is consistent with its reduced linear π-conjugation. In contrast, protonation of compound **171** (and the other DMA-substituted pentadienones derived from the [3+2] cycloaddition) generated a bathochromically shifted absorption band with vibrational fine structure, with neutralization regenerating the original spectrum. The identity of the protonated species is still under investigation.

4.5. TD-DFT Calculations

The vertical transition energies were calculated by TD-DFT at the CAM-B3LYP/6-31G(d) level of theory, with the PCM solvation model in $CHCl_3$ using the Gaussian 09 software package.[147] The theoretical results show good agreement with the experimental values obtained and are within the expected error range for anilino-cyano type push–pull chromophores (Figures 51–54).

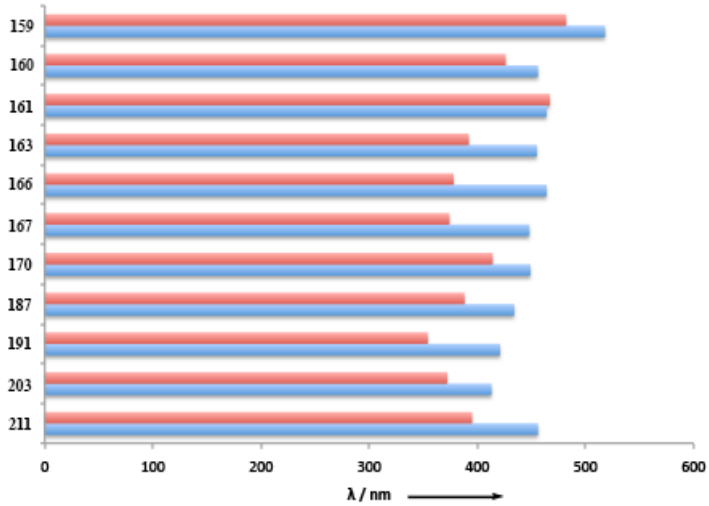

Figure 51. Comparison of experimental (red bars, λ_{exp}) and calculated (blue bars, λ_{calc}) low-energy transitions of CA–RE derived products.

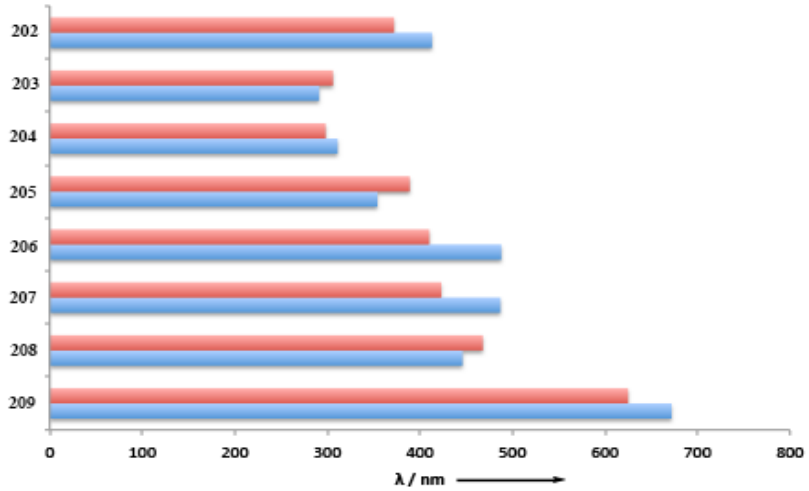

Figure 52. Comparison of experimental (red bars, λ_{exp}) and calculated (blue bars, λ_{calc}) low-energy transitions of post-functionalized CA–RE compounds.

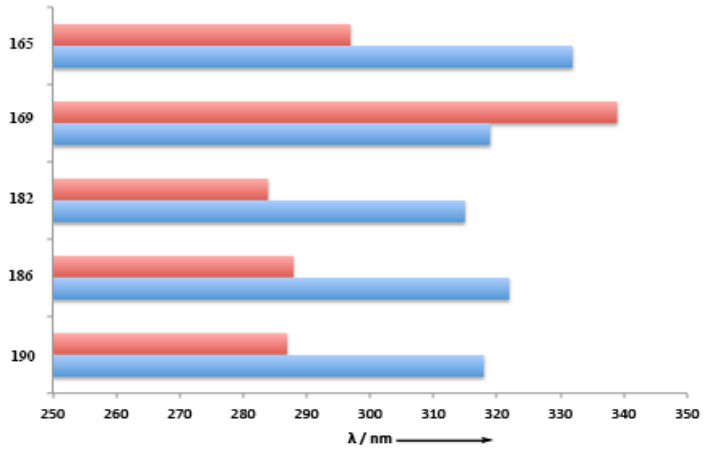

Figure 53. Comparison of experimental (red bars, λ_{exp}) and calculated (blue bars, λ_{calc}) low-energy transitions of HDA addcuts.

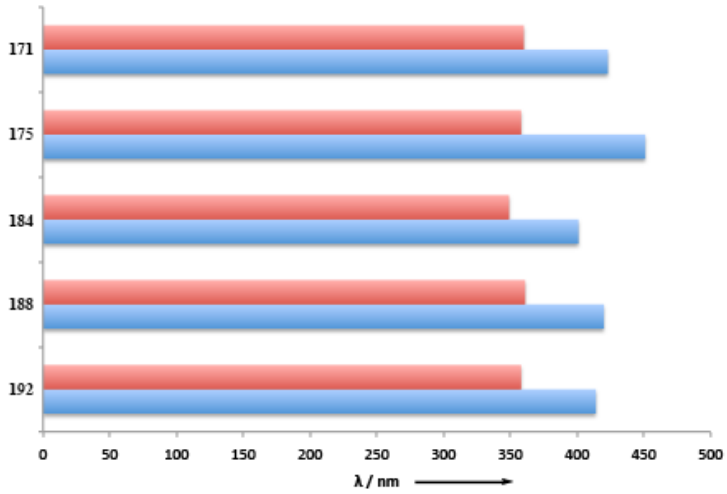

Figure 54. Comparison of experimental (red bars, λ_{exp}) and calculated (blue bars, λ_{calc}) low-energy transitions of [3+2] products.

4.6. Electrochemistry

The redox properties of all compounds were studied by CV and rotating-disk voltammetry (RDV). All electrochemical measurements were carried out in CH_2Cl_2 containing nBu$_4$NPF$_6$ (0.1 M) in a classical three-electrode cell, with potentials given *vs*. the ferrocenium/ferrocene (Fc^+/Fc) couple, and are uncorrected for ohmic drop. The values for selected compounds are shown in Table 6.

Oxidation occurs at the DMA moiety with values varying from +0.66 to +0.86 V for the CA–RE and the [3+2] adducts, regardless of the number of ester groups present. Compounds **203–205**, which do not contain DMA moieties, show a different initial oxidation value. Compounds that result from the HDA reaction, such as **169**, lack an observable reduction peak; they display a slightly lower value for the oxidation potential (**169**: E^o_{ox} = +0.53 V) due to the absence of an electron-withdrawing group in linear π-conjugation with the DMA moiety.

The first reduction potentials of the buta-1,3-dienes from the CA–RE reaction are dependent on the number of cyano moieties present, but not on their location. The comparison of values for compounds **67**, **160, 166,** and **167** revealed a decrease of around 0.18 V in the first reduction potential for every cyano group substituted by an ester moiety. Despite the different locations of the ester moieties in the isomeric

monoesters **159–161**, the values are quite similar (around E^{o}_{1} = –0.86 V). Comparable values are also shown for the diester isomers **163**, **166**, and **167**. The second reduction potentials across all compounds derived from the CA–RE reaction are within a similar range (–1.26 to –1.33 V) regardless of the number of cyano moieties present. However, a significant difference is observed for diesters **187** and **191** with CH_2CN and CH_2CF_3 moieties, respectively. Their first reduction potential is in a similar range to the one of monocyano-triethyl ester **170**.

Table 6. Cyclic voltammetry and rotating disk voltammetry data recorded in CH_2Cl_2 with 0.1 M nBu$_4$NPF$_6$, against the Fc^+/Fc couple.

entry	CV			RDV	
	$E°$ [a] V/$_{Fc+/Fc}$	ΔEp [b] mV	Ep[c] V/$_{Fc+/Fc}$	$E_{1/2}$ V/$_{Fc+/Fc}$	Slope (mV) [d]
67[114]	+0.86	80		+0.87 (1e$^-$)	70
	–0.69	80		–0.70 (1e$^-$)	70
	–1.26	90		–1.38 (1e$^-$)	140
159	+0.80	75		+0.81 (1e$^-$)	75
	–0.85	100		–0.91 (1e$^-$)	80
	–1.26	100		–1.40 (1e$^-$)	80
160	+0.83	78		+0.84 (1e$^-$)	65
	–0.85	92		–0.89 (1e$^-$)	75
	–1.29	89		–1.36 (1e$^-$)	75
161	+0.82	97		+0.82 (1e$^-$)	65
	–0.88	158		–0.97 (1e$^-$)	65
	–1.27	87		–1.33 (1e$^-$)	65
163	+0.80	97		+0.80 (1e$^-$)	60
	–1.12	80		–1.15 (1e$^-$)	60
	–1.36	80		–1.43 (1e$^-$)	60
166	+0.75	68		+0.76 (1e$^-$)	80
	–1.03	78		–1.03 (1e$^-$)	90
	–1.29	92		–1.35 (1e$^-$)	130
167	+0.73	119		+0.71 (1e$^-$)	80
	–1.08	180		–1.10 (1e$^-$)	80
	–1.31	101		–1.27 (1e$^-$)	100
169	+0.53	130		+0.56 (1e$^-$)	79
170	+0.71	104		+0.74 (1e$^-$)	80
	–1.24	63		–1.34 (1e$^-$)	100
	–1.33	73		–1.44 (1e$^-$)	100
171	+0.80	100		+0.84 (1e$^-$)	65
			–1.51	–1.53 (2e$^-$)	120
187	+0.66	92		+0.66 (1e$^-$)	65
	–1.26	120		–1.32 (2e$^-$)	110
191	+0.66	70		+0.69 (1e$^-$)	60
	–1.34	170		–1.44 (2e$^-$)	130
203	–0.99	106		–0.95 (1e$^-$)	70
	–1.33	109		–1.29	70
204	–0.86	128		–0.80 (1e$^-$)	80
	–1.21	150		–1.17 (1e$^-$)	80
	–1.81	135		–1.80 (1e$^-$)	100
205	–0.96	70		–0.95 (1e$^-$)	60
	–1.29	81		–1.29	70
208	+0.93	66		+0.87 (1e$^-$)	60
	–0.77	80		–0.72 (1e$^-$)	70
	–0.99	70		–0.94 (1e$^-$)	55
	–1.28	84		–1.25 (1e$^-$)	55
	–1.46	108		[e]	
209			+0.46	+0.45 (1e$^-$)	50
	–0.60	71		–0.58 (1e$^-$)	60
	–0.73	75		–0.73 (1e$^-$)	70
	–1.11	60		–1.11 (1e$^-$)	70
	–1.37	129		–1.33 (1e$^-$)	70

Scan rate, ν = 0.1 V s^{-1}. a) E^{o} = (E_{pc} + E_{pa})/2, where E_{pc} and E_{pa} correspond to the cathodic and anodic peak potentials, respectively. b) $\Delta E_p = E_{pa} - E_{pc}$. c) E_p = irreversible peak potential. d) Logarithmic analysis of the wave obtained by plotting E versus log[I/(I_{lim}–I)]; I_{lim} is the limiting current and I the current. e) Not observed.

The first reduction potentials of the buta-1,3-dienes from the CA–RE reaction are dependent on the number of cyano moieties present, but not on their location. The comparison of values for compounds **67**, **160, 166,** and **167** revealed a decrease of around 0.18 V in the first reduction potential for every cyano group substituted by an ester moiety. Despite the different locations of the ester moieties in the isomeric monoesters **159–161**, the values are quite similar (around E^{o}_{1} = –0.86 V). Comparable values are also shown for the diester isomers **163**, **166**, and **167**. The second reduction potentials across all compounds derived from the CA–RE reaction are within a similar range (–1.26 to –1.33 V) regardless of the number of cyano moieties present. However, a significant difference is observed for diesters **187** and **191** with CH_2CN and CH_2CF_3 moieties, respectively. Their first reduction potential is in a similar range to the one of monocyano-triethyl ester **170**.

The first reduction potentials of compounds derived from the [3+2] cycloaddition/rearrangement are much more negative than those of the corresponding CA–RE products (for example –1.51 ($2e^-$) *vs*. –1.24 V ($1e^-$) for **171** and **170**, respectively) and are non-reversible. A second reduction potential is not observed for these compounds but rather the first reduction is a two-electron process.

Compounds **208** and **209** formed by two CA–RE reactions undertake four reduction steps. The first two reductions are shifted and comparable to those of compounds derived from the CA–RE reaction of DMA-acetylenes with TCNE (compound **90**)[114] or TCNQ.[127] The reduction potentials for the third and fourth reductions are comparable to the first and second reduction potentials of dicyano-diester **163**. The oxidation potential remains consistent between all compounds with the DMA moiety regardless of the number and type of acceptor units, in accordance with earlier studies.[175]

4.7. Conclusion

In summary, to continue investigating the reactivity of electron-poor alkenes, we decided to replace cyano groups with ester moieties on tetrasubstituted electron-deficient alkenes and study the effect on their ability to undergo the CA–RE reaction. The CA–RE reaction was shown to still take place with a single cyano moiety, however other reactions also occurred, namely a [4+2] HDA cycloaddition

and a novel reaction with a proposed [3+2] cycloaddition and subsequent rearrangement mechanism. The all ethyl ester analogue was generally not reactive enough to engage in the CA–RE reaction but adding a CN or CF_3 substituent to the alkyl chain of the ester could increase its reactivity. We also described the possibility of post-CA–RE reaction functionalization with ester-substituted butadienes, including the access to pharmacologically interesting pyrazolopyrans.

Chapter 5

A Short Synthesis of NH-pyrroles

5. A Short Synthesis of NH-pyrroles

The results of this Chapter were obtained in collaboration with Dr. Tristan A. Reekie. This project was also partially done by two semester project students: Salome Püntener and Giorgio Manenti. Dr. Nils Trapp resolved single crystal X-ray structures. The results of this Chapter are the subject of a recent publication.[183]

5.1. Introduction

With the short and easy preparation of CA–RE compounds in large quantities starting from electron-deficient, mono- and diester-substituted alkenes **158**, **162**, and **164** (see Chapter 4) and based on their ability to act as good electrophiles, we decided to further investigate post-functionalization to construct molecules of greater complexity and broader utility. When buta-1,3-diene **163** was added to dimethylamine, a tetrasubstituted NH-pyrrole **213** was obtained in 82% yield (Scheme 35).

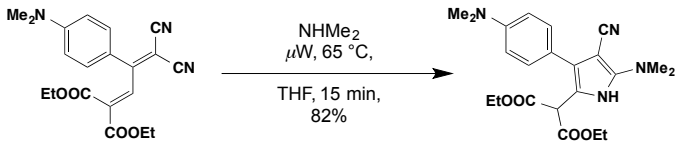

163 **213**

Scheme 35. Preliminary result for the formation of NH-pyrrole with a secondary amine.

The pyrrole framework is an important structural motif found in many biologically active natural products as well as pharmaceutically active agents.[178–182,184,185] Members of this ubiquitous class of heterocyclic compounds exhibit a variety of pharmacological properties including antibacterial, antiviral, anti-inflammatory, anticancer, and antioxidant activity.[186–197] Consequently, there is significant interest in the development of efficient methods for the synthesis of pyrrole derivatives bearing diverse substitution patterns. There are several classical methods for the synthesis of pyrroles, including the Knorr,[191] Paal–Knorr,[192] and Hantzsch methodology.[193] Although these methods have proven effective for the preparation of pyrrole derivatives, they involve multistep in-flask (batch) syntheses that limit the scope and efficiency or do not provide the regioselectivity required for

polysubstituted pyrroles. Attempts to circumvent these problems have focused on multicomponent reactions[194–196] and metal-catalyzed routes,[197–202] among others.[203–206]

5.2. Optimization and Scope of the Reaction

Optimization of the reaction conditions for the formation of **213** from **163** with dimethylamine revealed that a variety of solvents gave similar yields, and scant difference when the reaction is done under microwave irradiation or conventional heating. The preferred conditions include microwave irradiation at 65 °C for 15 min in THF (Table 7).

Table 7. Optimization of the reaction.[a]

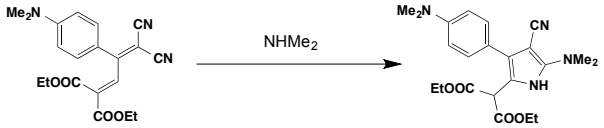

entry	163 solvent	213 yield(%)
1	EtOH	67
2	1,4-dioxane	78
3	$CHCl_3$	75
4	DCE	78
5	MeCN	59
6	DMF	36
7	Toluene	75
8	THF	81
9	THF (conventional heating)	78

a) All reactions were conducted using 1.0 equiv of **163**, and 1.05 equiv of base on 0.15 mmol scale at 0.1 M concentration, 15 min at 65 °C.

With optimized conditions in hand, we investigated pyrrole formation with various nucleophiles (Scheme 36). Secondary amines provided the corresponding NH-pyrroles **213–216** in good yields (67–82%). When dihexylamine was used to the reaction, 1 h of microwave irradiation was necessary for the reaction to reach completion. With NH_3 in isopropanol (2.0 M), the 2-NH_2-substituted pyrrole **217** was obtained in the moderate yield of 53%. Conducting the reaction with cyclopentylamine, *N*-cyclopentylpyrrole **218** was obtained in 81% yield. Other primary amines afforded the *N*-substituted pyrroles **219** and **220** in 69% and 73% yield, respectively. In these particular cases, the *N*-atom of the entering nucleophile becomes the pyrrole ring nitrogen.

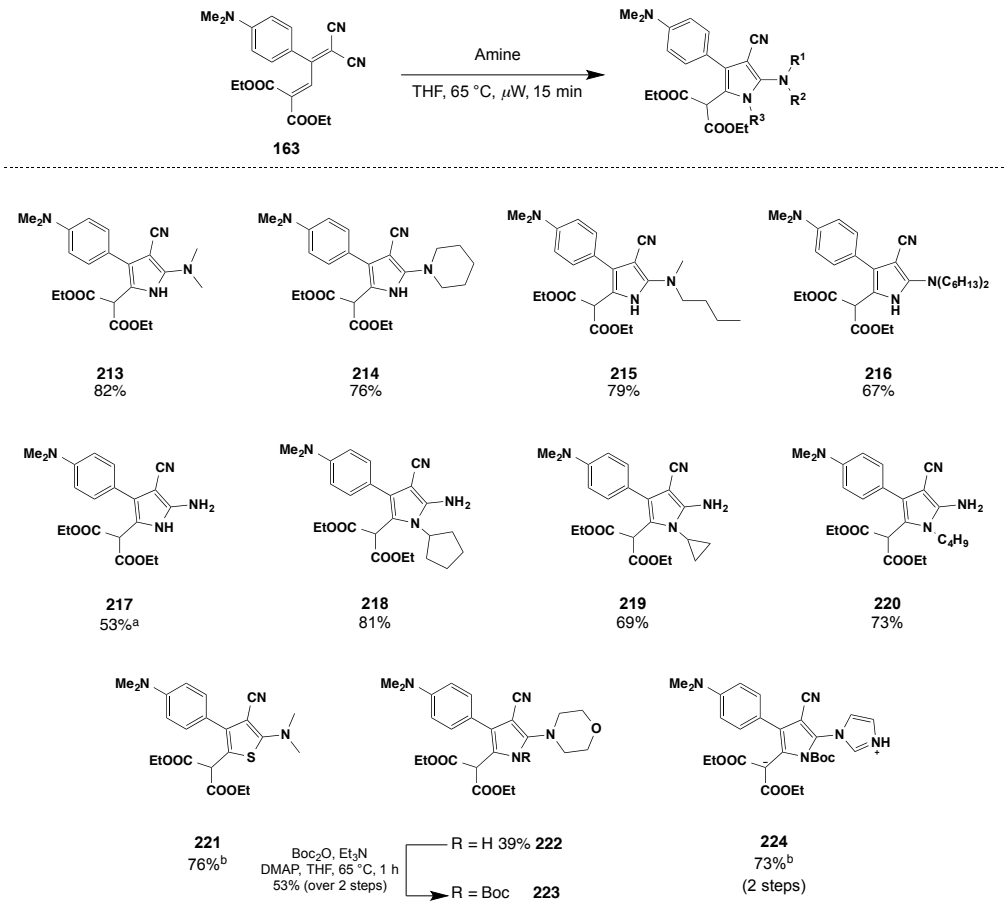

a)1 h of heating was required. b) Addition of 1.0 equiv of DABCO and 20 min of conventional heating was required. c) Protection with Boc_2O was required immediately following pyrrole formation.

Scheme 36. Scope of the reaction with different amines.

When $Na_2S{\cdot}9H_2O$ was used in the presence of 1,4-diazabicyclo[2.2.2]octane (DABCO), the 2-aminothiophene **221** was isolated in 76% yield. However, when S_8 was used as the source of sulfur, under standard Gewald-type conditions,[207,208] higher amounts of decomposition were observed and **221** was isolated in 29% yield. Morpholine gave the unstable product **222**, immediate protection with di-*tert*-butyl dicarbonate (Boc_2O) allowed for the isolation of the Boc-protected derivative **223** in improved yield (53%) over 2 steps. Imidazole attack required immediate Boc-protection to give **224** as a stable product. This product exists as a zwitterion as evidenced in the ^{1}H NMR spectrum through the N–H peak at 7.54 ppm and its lack of a malonate C–H, with the corresponding carbon seen at 96.23 ppm in the ^{13}C NMR spectrum. The generality of our synthetic protocol was further evaluated with other nucleophiles (Scheme 37). Dinucleophilic piperazine afforded the dipyrrole species **225** in moderate yield of 54%. The carbon-based nucleophile dimethyl malonate also underwent the reaction to provide the corresponding pyrrole **226** in 62% yield.

All attempts at pyrrole formation with an oxygen nucleophile (such as EtOH, EtO–) failed, however. Also, the transformation did not occur with phospine-based nucleophiles.

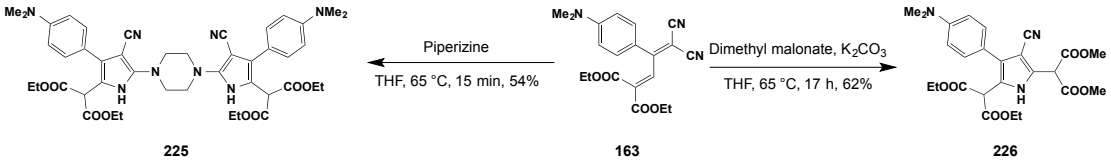

Scheme 37. Synthesis of pyrroles using different nucleophiles

To broaden the scope of the pyrrole formation, we turned our attention to investigate different aromatic substitution (Scheme 38). Compound **227** containing a free aniline moiety is isolated in 81% yield. Similarly, tetrasubstituted pyrroles **228–231** are obtained in high yields (66 to 94%) from easily accessible CA–RE adducts.

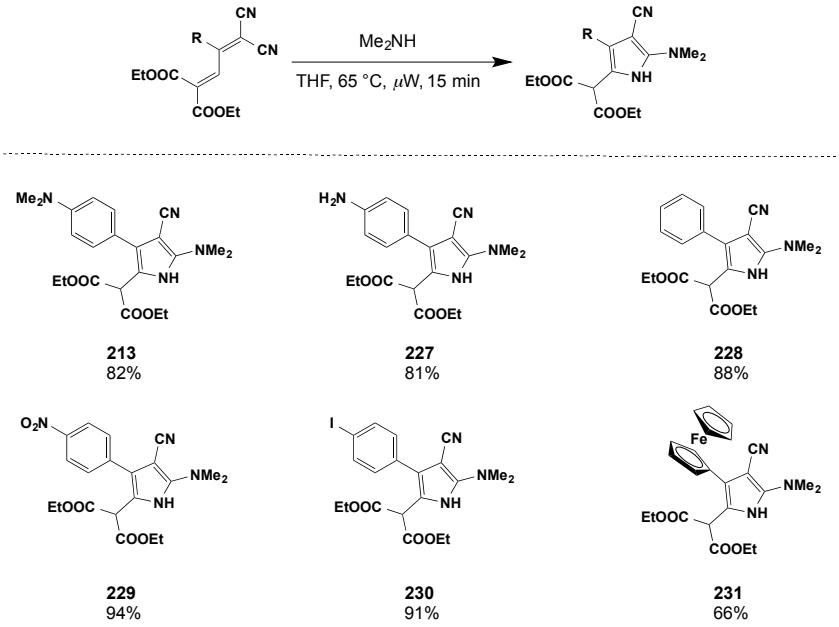

Scheme 38. Synthesis of pyrroles with various aromatic substituents.

We next explored the influence of ester *vs*. cyano substitution on pyrrole formation using dimethylamine as nucleophile (Scheme 39) and differently substituted buta-1,3-dienes previously reported (see Chapter 4).[171] In line with previous observations,[175] the tetracyano derivative **90** (R^1–R^3 = CN) underwent immediate decomposition upon exposure to dimethylamine with no isolable product formation. The monoester compounds **160** (R^1 and R^2 = CN, R^3 = COOEt) and **161** (R^1 and R^3 = CN, R^2 =

COOEt) both underwent pyrrole formation to give (±)-**232**, which was isolated as the racemate. The triester derivative **170** (R^1 and R^3 = COOEt) was also easily transformed into pyrrole **233** in 73% yield. Similar conversion of **210** (R^1 = CN, R^2 and R^3 = COOMe) into pyrrole **234** was also observed.

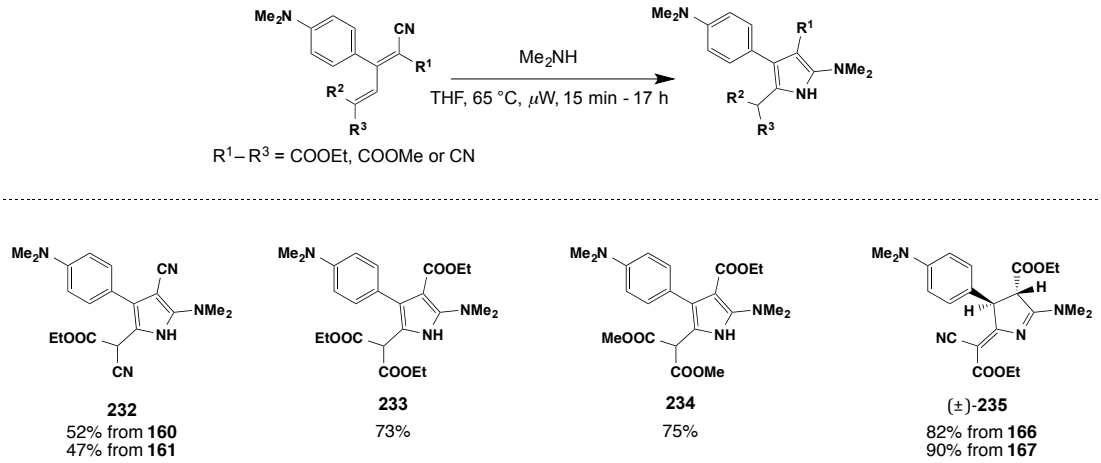

Scheme 39. Synthesis of pyrroles from different buta-1,3-dienes.

When the configurational isomers **166** and **167** were reacted with dimethylamine, the same product (±)-**235** was obtained in high yield. The structure was identified through interpretation of 1D and 2D NMR spectra. There are two aliphatic CH signals at 5.15/55.3 and 3.72/59.3 ppm in the ^{1}H and ^{13}C NMR spectra, respectively, which show a weak vicinal coupling. From the two-dimensional HMBC study, they have cross peaks with the quaternary carbon (128.4 ppm) of the dimethylanilino (DMA) ring and the same C=O (168.0 ppm). The other C=O and CN carbons show no HMBC signals. The DMA and CO_2Et substituents are *trans* leading to a torsion angle of 120° for the two aliphatic hydrogens, agreeing well with the small coupling (J = 1.5 Hz). The two non-anilino NMe moieties appear as separate singlets at 3.10 and 3.42 ppm, providing evidence for the conjugation of the NMe_2 group with the imine double bond. Combining these elements suggests the structure assigned to (±)-**235**. The reason for the formation of this different product is currently unknown.

Penta-2,4-dien-1-ones from electron-deficient alkenes and non-activated alkynes, which will be described in detail in Chapter 6, can also be transformed into tetrasubstituted NH-pyrroles (Scheme 40). Tetrasubstituted NH-pyrroles **236** and **237**

were obtained in 68% and 75% yield, respectively. Additionally, we were able to show the transformation, in which an aliphatic substituent was included at the 3-position of pyrrole **237**. Structural confirmation was obtained under the same conditions to give **228** already obtained from the buta-1,3-diene reaction. Spectral and structural data confirmed the identity of **228** obtained from the two different starting materials. The 2-aminothiophene **238** could also be obtained using $Na_2S{\cdot}9H_2O$ and DABCO in 71% yield.

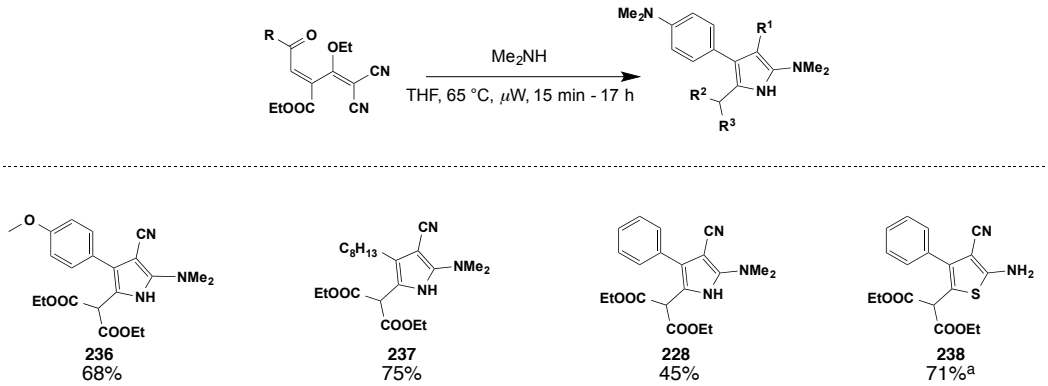

a) Addition of 1.0 equiv of DABCO and 20 min of conventional heating was required.

Scheme 40. Synthesis of pyrroles from penta-2,4-dien-1-ones.

5.3. Post-Functionalization of Pyrroles

Next, we conducted preliminary studies on how these pyrroles could be further employed (Scheme 41). Krapcho decarboxylation[209] of **213** occurred under standard conditions without the need for N–H protection, affording the decarboxylated product **239** in 82% yield. Cyclization of **213** with 1,2-dibromoethane gave the aryl-appended bicyclic structure **240** in high yield. Sonogashira cross-coupling of aryl iodide **219** led to **241** in 52% yield, without the need for a protecting group.

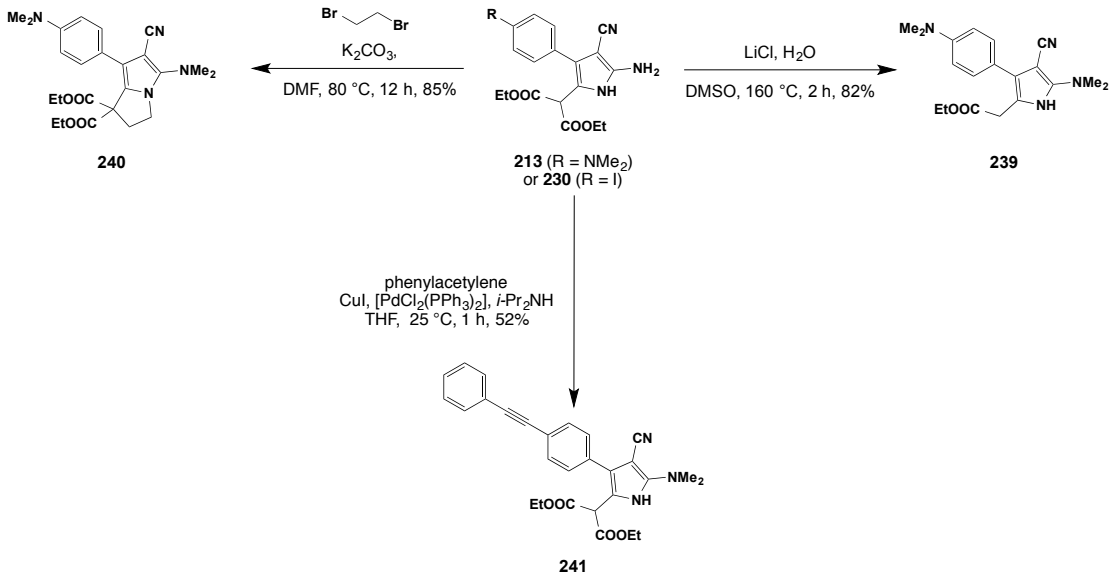

Scheme 41. Further functionalization of the obtained pyrroles.

5.4. Mechanism

The mechanisms suggested for the formation of pyrroles from the CA–RE adduct are shown in Scheme 42. The first step is the attack of the nucleophile onto the carbon of the nitrile. It is shown here attacking the nitrile less closed to the aryl group however attack at either nitrile would lead to the same product. But since the same transformation also occurs in the formation of **233**, where only one nitrile is present and close to the aryl ring, indicates that this nitrile group can also react. Proton transfer from the amine then results in intermediate **242**. Subsequent intramolecular 1,4-addition of the nitrogen and proton transfer leads to intermediate **243**. Tautomerization affords the observed product **213**.

A similar mechanism occurs when primary amines are used as the nucleophile (Scheme 42). The first step also involves the attack of the nucleophile onto the carbon of the nitrile to yield intermediate **244**. This is where the mechanism deviates as the intramolecular nucleophilic attack now occurs from the amine rather than the imine to give **245**. Subsequent tautomerization leads the corresponding pyrroles **218**–**220**.

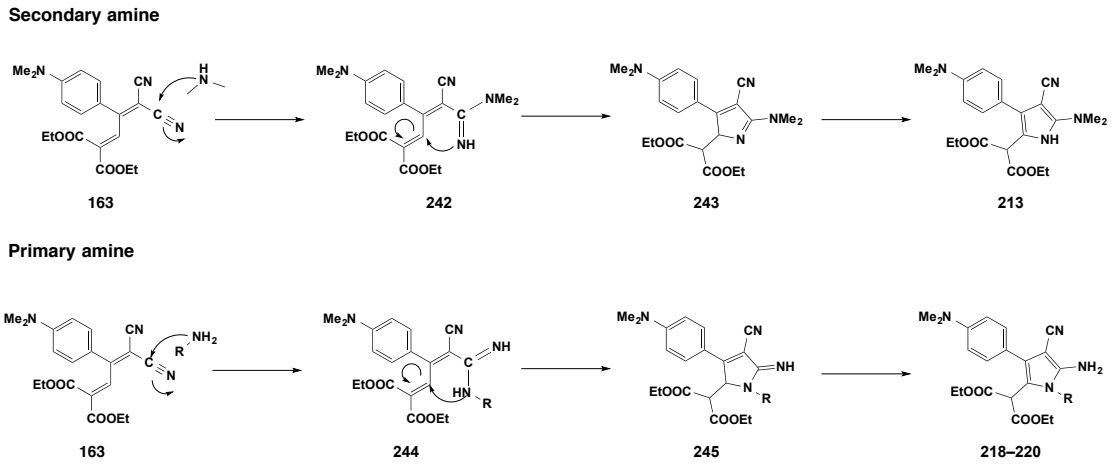

Scheme 42. Proposed mechanism for pyrrole formation.

In Scheme 43, we propose a mechanism for how the penta-2,4-dien-1-ones react with amines to give buta-1,3-dienes, which subsequently undergo the pyrrole-forming transformation. This could happen by nucleophilic attack onto the carbonyl group of penta-2,4-dien-1-ones by the nucleophilic amine, with subsequent intramolecular 1,4-addition and proton transfer to afford the furan **246**. Malononitrile shift and ester formation could lead to intermediate **247** which can then eject the initiating amine in a β-elimination affording the buta-1,3-dienes **228**, **236**–**238**.

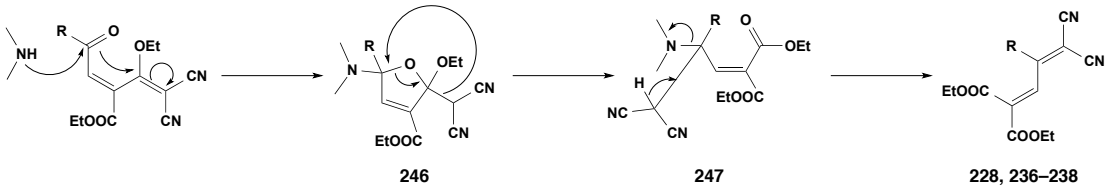

Scheme 43. Proposed mechanism for pyrrole formation from penta-2,4-dien-1-ones.

5.5. X-ray

Pyrroles **213**, **221**, **227** and **229** were obtained as crystalline solids by slow evaporation of *n*-hexane/ethyl acetate solution at 25 °C (Figure 55). Besides the structural confirmation, the crystal structures allowed for further analysis of the pyrroles. Determination of the quinoid character (δr) of the aniline rings in **213**, **221**, and **227** and the nitroaryl ring in **229** gave values of 0.010, 0.016, 0.013, and 0.005 Å, respectively (Table 8). For comparison, the δr value is 0 Å in benzene, 0.042 Å in the

starting material **163**, whereas for quinoid rings the values are in the range of 0.08–0.10 Å.[172] This low quinoid character and the corresponding low BLA suggest that little π-conjugation occurs between the aryl rings and the pyrrole moiety.

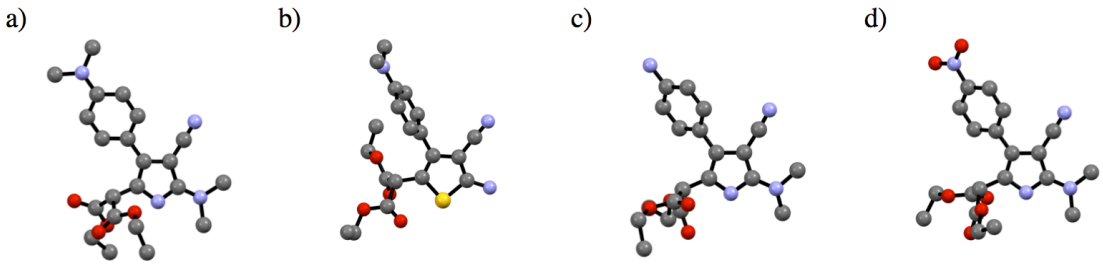

Figure 55. X-ray strutures of pyrroles **213** (a), **221** (b), **227** (c), and **229** (d).

The bond lengths of the 2-amino–to–heterocycle bond where calculated at 1.364(2) Å for **213**, 1.356(4) Å for **221**, 1.379(2) Å for **227**, and 1.365(2) Å for **229**, suggesting these bonds have greater double bond character. In fact, these lengths were similar to bonds within the pyrrole/thiophene rings signifying some delocalization.

Table 8. Average bond distances [Å] used to calculate the quinoid character, δr [Å], of DMA rings.

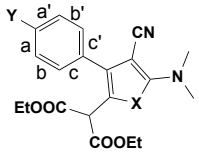

X = NH or S
Y = NMe_2, NH_2 or NO_2

entry	compound	average a [Å]	average b [Å]	average c [Å]	δr [Å]
1	**213**	1.401	1.385	1.399	0.010
2	**221**	1.406	1.385	1.396	0.016
3	**227**	1.396	1.385	1.400	0.013
4	**229**	1.383	1.385	1.397	0.005

Quinoid character: δr = (((a + a')/2 – (b + b')/2) + ((c + c')/2 – (b + b')/2))/2). For benzene, δr = 0 Å; for fully quinoid rings, δr = 0.08–0.10 Å.

5.6. Oxidation of Pyrroles

Some of the pyrrole products started to decompose, particularly when in solution and exposed to air. We investigated these processes in more detail (Scheme 44). When morpholine-substituted pyrrole **222** was left in dichloromethane solution open to air, it underwent an oxidation process to give azafulvene **248**. More interestingly, the oxidation product of **213** underwent further hydrolysis to afford the purple-colored, push–pull-substituted 2-azacyclopentadienone **249**.

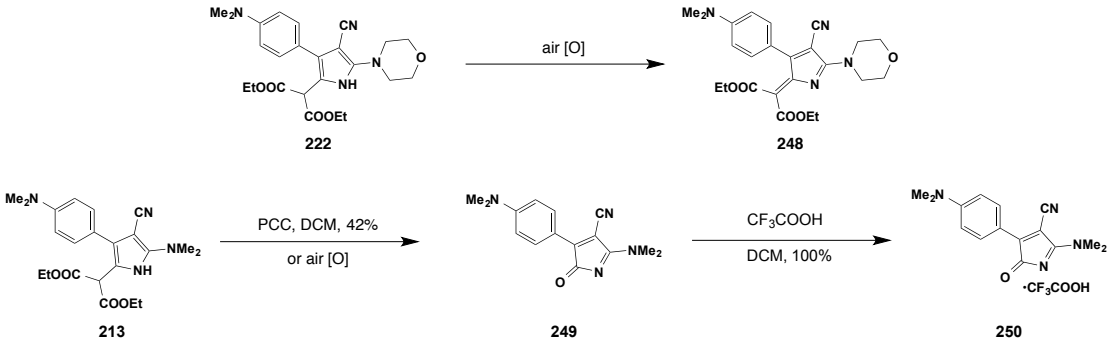

Scheme 44. Oxidation of pyrroles

5.7. UV/Vis

The UV/Vis spectrum of pyrrolidine **219** displays a strong longest-wavelength band at λ_{max} = 545 nm (ε = 18700 M^{-1} cm^{-1}) and a second band with vibrational fine structure around 400 nm (Figure 56). These absorptions vary considerably from those of pyrrole **213** which shows a single higher-energy band at λ_{max} = 280 nm (ε = 19800 M^{-1} cm^{-1}). When **249** was treated wih TFA, it underwent a color change from purple to blue (Figure 56, inset). The color change was revealed in the UV/Vis spectrum with a bathochromic shift of the longest-wavelength band to two maxima at 638 and 599 nm and an approximate doubling of the extinction coefficient to 40500 and 32500 M^{-1} cm^{-1}, respectively. These observations resulted from the result of a reversible protonation. Re-neutralization with triethylamine regenerated the original purple color and UV/Vis spectrum of **249**. Compound **250** could be isolated as a blue solid, however the site of protonation could not yet be identified (Scheme 46).

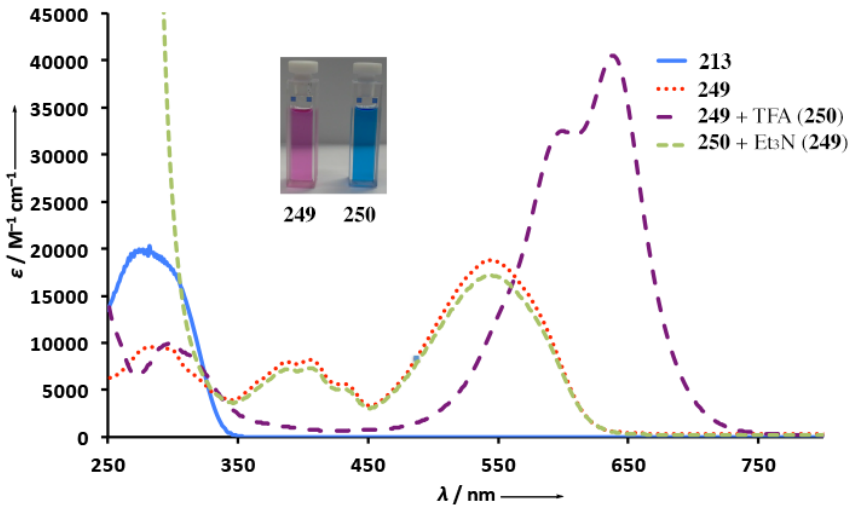

Figure 56. UV/Vis spectra of compounds **213**, **249**, **250** following treatment with TFA affording **250**, and following re-neutralization with Et_3N fully regenerating **249**. Inset: actual color of compounds **249** and **250.**

5.8. Conclusion

In summary, to further explore the role products derived from the CA–RE reaction in the synthesis of more complex systems through post-reaction functionalization, we describe a simple three-step synthesis of tetra-substituted NH-pyrroles from readily available starting materials (22 examples). Variation of substituents can be achieved by altering the starting material, which is easily accessible from the CA–RE reaction, or by using a different reacting nucleophile. Air oxidation of the pyrroles led to highly colored products, which showed interesting reversible color changes upon protonation with TFA.

Chapter 6

π-Conjugated Dienones by Formal [3+2] Cycloaddition / Rearrangement of Electron-Poor Alkenes with Alkynes

6. π-Conjugated Dienones by Formal [3+2] Cycloaddition / Rearrangement of Electron-Poor Alkenes with Alkynes

The crystal structures were solved by Dr. Nils Trapp. Some compounds have been prepared by Dr. Tristan A. Reekie. The results of this paragraph are the subject of a recent publication.[210]

6.1. Introduction

Reactions with alkynes have been widely studied by our group and others (see Section 1.2), with a focus on those that are electronically activated, particularly DMA-substituted alkyne **102**. In Chapters 4 and 5, we emphasized the replacement of cyano groups on TCNE with ester moieties to afford tetrasubstituted electron-deficient alkenes for the study of the CA–RE reaction.[171,183] In addition to the expected products from the CA–RE and the HDA reaction, a third product was observed, namely π-conjugated dienones, when the tri- or tetraester-substituted alkenes **168** and **181** were used.[171] We proposed that these products arosed from a formal [3+2] cycloaddition and subsequent rearrangement.

[3+2] Cycloaddition reactions, or reactions that may be formally named as such, have been featured fairly frequently in the strategies being added to the chemical lexicon.[211–217] The [3+2] cycloaddition is usually engaged using 1,3-dipoles,[211] such as ozonolysis,[212] and Huisgen dipolar cycloadditions[213] commonly employed in click chemistry,[117] for the formation of triazoles from azides and alkynes,[214] isoxazolines from nitrile oxides and alkenes,[215] and pyrrolidines from azomethine ylides.[216,217] Such methods are attractive because they satisfy a desirable ambition of modern synthesis, that of atom economy[218] and this is the reason why we decided to expand the synthetic utility of this method by turning our attention to poorly donor-activated or unactivated alkynes.

6.2. Optimization of the Reaction

We initiated our studies with phenylacetylene (**251**) and electron-deficient alkene **162** to explore the feasibility of such a transformation (Table 9). Pleasingly, when less activated alkyne **251** reacts with **162**, only **252** is obtained without any CA–RE and HDA adducts being observed.

Encouraged by this initial result, we evaluated the effect of solvent, temperature, and additives[148] on the reactivity (Table 9), DCE was identified as the most suitable solvent (entries 1-3). Increasing the temperature significantly enhanced the formation of [3+2] adduct **252** from 30% to 65% (entries 3-5), whereas the addition of Lewis acids had no significant effect on the reaction (entries 6,7).

Table 9. Selected optimization studies.[a]

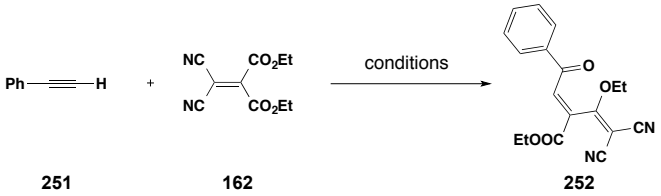

251 **162** **252**

entry	addititve	solvent	Temperature	Yield (%)
1	–	DCM	25 °C	12
2	–	MeCN	25 °C	22
3	–	DCE	25 °C	30
4	–	DCE	50 °C	42
5	–	DCE	reflux	65
6	$TiCl_4$	DCE	reflux	62
7	$LiClO_4$	DCE	reflux	63

[a]All reactions were performed with 1.0 equiv of **251**, 1.0 equiv of alkene **162** at 0.15 mmol (0.1 M concentration) in DCE, 56 h. Yield determined by ^1H NMR using dibromomethane as the internal standard.

6.3. Scope of the Reaction

We subsequently investigated whether this [3+2] cycloaddition/rearrangement cascade is a general process for dicyano-diester-substituted alkene **162** (Scheme 45). When TCNE was employed for the reaction, only the CA–RE product **253** was observed with a poor yield of less than 10%. Only traces of **254** were obtained when

tricyano-monoester-substituted alkene **158** was used. No reaction was observed for alkenes **168**, **164** and **181**. The fact that they could not engage in the [3+2] cycloaddition suggests the importance of balancing alkene and alkyne reactivity for this reaction to proceed.

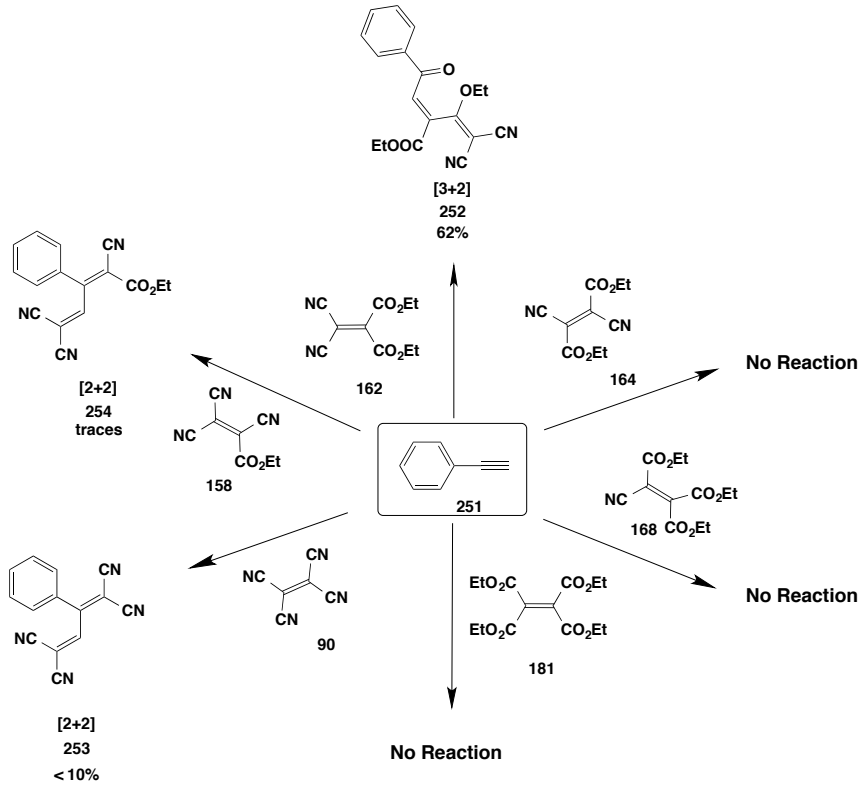

Scheme 45. Different reactivities of electron-rich alkenes.

With optimized conditions in hand, a wide range of substituted alkynes were prepared and subjected to the reaction (Scheme 46 and 47). The π-conjugated dienones resulting from the formal [3+2] cycloaddition/rearrangement cascade were formed as the only isolable products.

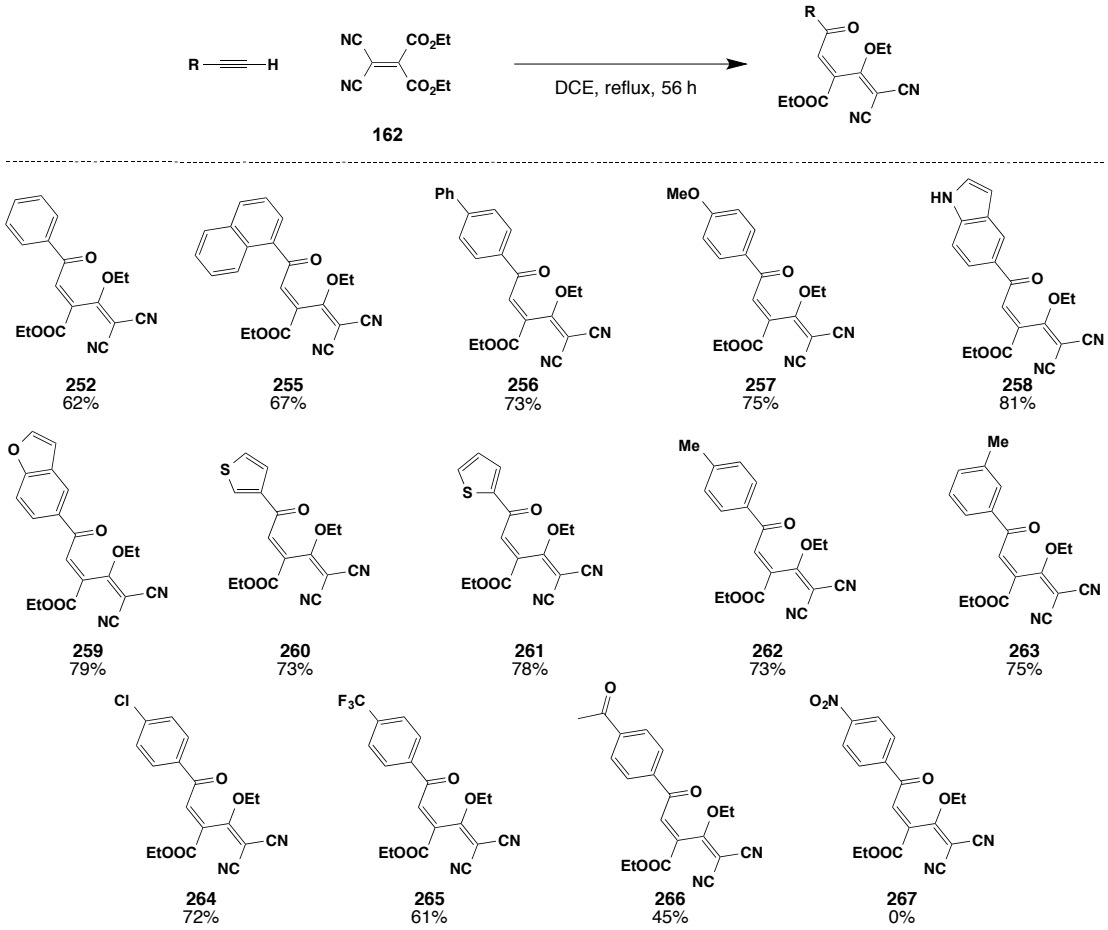

Scheme 46. Scope of the reaction with different arylated alkynes.

In general, moderate to excellent yields were obtained. 1-Ethynylnaphthalene gave compound **255** in 67% yield whereas 4-ethynyl-1,1'-biphenyl analogue yielded compound **256** in 73% yield. Yields were higher (73–81%) when mildly electron-rich substituents were present on the aromatic ring. Intriguingly, when an anisole-substituted alkyne was used, only product **257** arising from [3+2] cycloaddition was obtained in 75% yield, despite this alkyne undergoing a CA–RE reaction with TCNE.[127] Other moderately electron-rich substrates are also tolerated and **258** and **259** were obtained in similar yields. Diverse electron-rich aromatic systems are well tolerated, providing products such as 3-substituted thiophene **260** and 2-substituted thiophene **261** derivatives in 73% and 78%, respectively. Performing the reaction with *p*-ethynyltoluene gave **262** in 73% yield, while the *meta* analogue provided **263** in 75% yield. The *para*-chloro and the *para*-trifluoromethyl starting materials gave **264** and **265** in 72% and 61% yield,

respectively. In a demonstration of the versatility of the reaction conditions, the electron-poor 4-acetylphenyl alkyne gave the [3+2] adduct **266** in moderate yield (45%). However, the attempt of obtaining the corresponding nitro derivative **267** failed, probably because of its strong electron-withdrawing character.

The application of the [3+2] cycloaddition could be extended further, showing that the reaction is not limited to terminal or aryl-substituted alkynes. For instance, ynamides with electron-withdrawing protecting groups have previously been shown to be activated enough to engage in the CA–RE reaction (Scheme 47).[219] In this circumstance, the terminal ynamide only undergoes [3+2] cycloaddition to afford **268** in 84% yield with no CA–RE product observed. In comparison, (*S*)-4-benzyl-3-ethynyloxazolidin-2-one afforded product (*R*)-**269** in 84% yield. Thiolated alkyne derivatives also underwent the [3+2] transformation to give **270** in 75% yield.

We were also pleased to see similar reactivity with alkyl substituents, delivering **271** in 71% (Scheme 47). The octyl analog **272** performed moderately well to generate dienone **272** in 49% yield. Interestingly, bis-substituted alkynes gave **273** and **274** in comparable yields and only one regioisomer was observed.

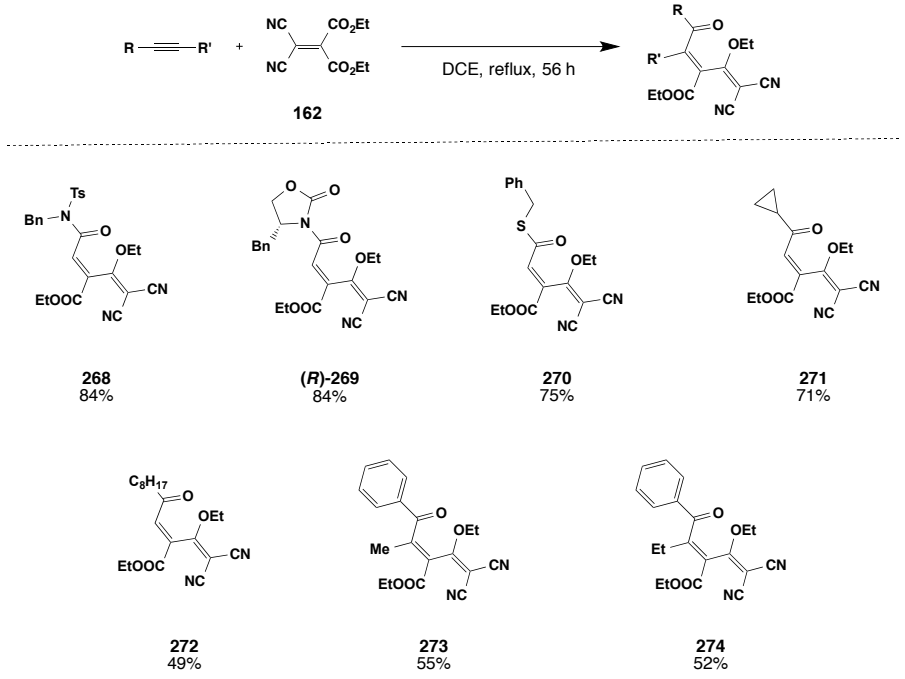

Scheme 47. Scope of the reaction with different arylated alkynes.

6.4. X-ray

Some of the new products described herein were characterized by X-ray crystallographic analysis, providing proof for the obtained structures. Figure 57 shows the crystal structures of **255**, **258, 262**, and **268**. The alkyl derivatives **271–274** were isolated as oils.

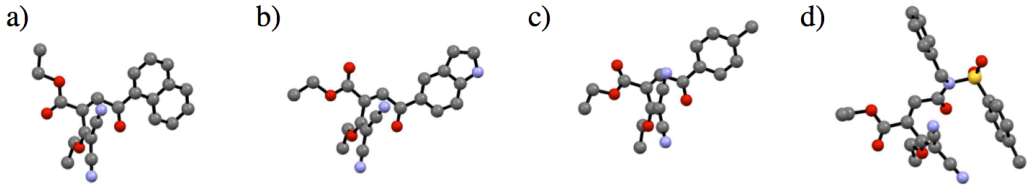

Figure 57. X-ray structures of selected penta-2,4-dien-1-ones **255** (a), **258** (b), **262** (d), and **268** (d).

6.5. Mechanistic Studies

For the reactions of DMA-acetylene (**102**) with olefins **168**, shown in Scheme 48,[171] we proposed a mechanism starting with the nucleophilic attack of the activated alkyne on the electrophilic alkene, leading to a zwitterionic intermediate **177**, in which the cationic charge is favorably stabilized as an oxocarbenium ion. This intermediate is identical to the one formed in the first step of the CA–RE reaction. We proposed that it would subsequently cyclize to a cyclopropane-fused dihydrofuran **178**, which rearranges to the dienone product **171**.

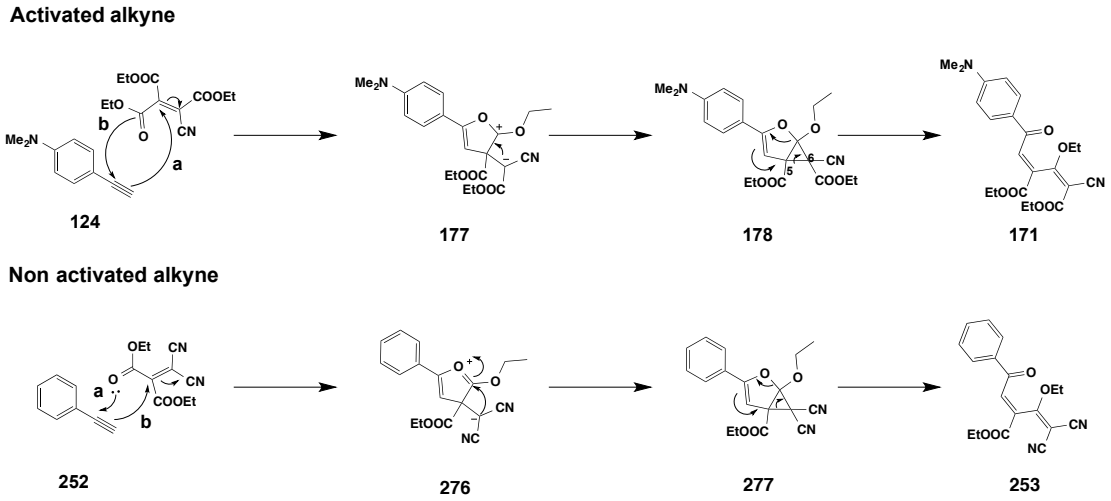

Scheme 48. Putative mechanisms.

In the case of unactivated alkynes reported in this Chapter, a nucleophilic attack is less feasible as the initial zwitterionic intermediate would not benefit from the iminium-ion-type stabilization. Therefore, we propose another mechanism, shown in Scheme 50, to afford product **253** from phenylacetylene (**252**) with alkene **162**. The first step presumably implicates the first the attack of the carbonyl oxygen atom (a) and subsequently the ring closure at the β-carbon atom (b) of the dicyanovinyl moiety in **154**, engaging in a [3+2] cycloaddition with alkyne **236** to lead to the corresponding zwitterionic intermediate **276**. Then, intramolecular cyclopropanation affords the second intermediate **277**, which intersects with the original mechanism proposed for the transformation of DMA-acetylene. The electron-deficient character of the cyclopropane most likely lowers the energy required to induce this transformation allowing for the observed products to be isolated.

6.6. Conclusion

In summary, we reported the a formal [3+2] cycloaddition/rearrangement cascade reaction between moderately activated to unactivated alkynes and electron-poor dicyano-diester-substituted alkene **162** to yield a variety of π-conjugated penta-2,4-dien-1-ones. This atom-economic process was obtained in moderate to excellent yields (20 examples) without the presence of a catalyst. The broad substrate scope and reasonably mild conditions for such a transformation make this procedure a

valuable reaction for the synthesis of dienones. We are currently investigating post-reaction functionalizations for the synthesis of more complex systems.

Chapter 7

Conclusion and Outlook

7. Conclusion and Outlook

The primary goal of this dissertation was to provide testimony that outstanding chiroptical properties are a signature of enantiomerically pure alleno-acetylenic macrocycles and monodisperse acyclic oligomers. To validate this statement, the synthesis of a second series of shape-persistent alleno-acetylenic macrocycles (SPAAMs) and new acyclic alleno-acetylenic oligomers with more rigidified all-carbon backbones in enantiomerically pure form were reported in Chapter 2. The D_2-symmetric macrocycle $(P)_4$-(–)-**33a** was characterized by X-ray crystallographic analysis, featuring a rigid crown conformation. The chiroptical responses of SPAAMs $(P)_4$-(–)-**33a** and $(M)_4$-(+)-**33a** are remarkable, with very large Cotton effects despite lower symmetry and fewer buta-1,3-diynediyl chromophore units, when compared to the systems in the earlier first series. TD-DFT calculations indicate a very strong contribution from the MTDM for the lower-energy transition, while the higher-energy transition is mostly dominated by the EDTM. This observation is in agreement with the experimental *g*-factor plots. A second C_1-symmetric pair of enantiomers, (*P,M,M,M*)-(+)-**33c** and (*M,P,P,P*)-(–)-**33c** gives much less intense Cotton effects, as a result of the reduction in symmetry from D_n to C_n.

Futhermore, a nonlinear amplification in the intensity of the Cotton effects with increasing oligomeric length was observed for the new series of acyclic alleno-acetylenic oligomers, which was explained with the preference for a helical secondary structure of one handedness. Structural support for this proposal is provided by the X-ray structure of the enantiopure tetrameric allene $(P)_4$-(+)-**108**, which displays a right-handed helical conformation in the solid state. Computational studies are in agreement with this observation and also confirm the reduced flexibility of the new oligomers as a result of exchanging the all-buta-1,3-diynediyl spacers between allene moieties in the previous series by alternating –C≡C– and –C≡C–C≡C– spacers.

We also prepared the MOM-protected DEA derivatives (*P*)-(+)- and (*M*)-(–)-**114** in enantiomerically pure form and further reacted to afford them the tetrameric macrocycles $(P)_4$-(–)-**125** and $(M)_4$-(+)-**125** bearing eight lateral

MOM-protected alcohol groups around the central alleno-acetylenic all-carbon core. However, all attempts to deprotect the MOM group were unsuccessful and no desired product was observed. The ECD spectra of SPAAMs $(P)_4$-(–)-**125** and $(M)_4$-(+)-**125** showed remarkably intense Cotton effects.

Besides lateral functionalization, we have presented different conditions for acetylene functionalization in DEAs. Arylated allenes have been successfully applied as chiral dopants for producing cholesteric liquid crystals.[78] Importantly, some arylated DEAs undergo photo-racemization upon standing of a solution (1×10^{-5} M) in daylight and the underlying principles of this racemization process are still under investigation.

We set out to reverse this process upon chiral substrate binding to an alcohol-substituted DMA-functionalized DEA (photochirogenesis). Although chiral diamines bind, and different diastereoisomers could clearly be distinguished in the ^{1}H NMR spectrum, daylight irradiation did not lead to favored formation of one of the DEA enantiomers. However, at lower concentrations, this approach might be successful, although stronger substrate binding is required. The diol moiety could, for example, be converted into a crown ether, which is able to bind chiral ammonium cations (Figure 58).[220] This binding is much stronger than the diamine/diol interaction. DMA-substituents could also be replaced by naphthalenes, leading to a more stable product; this substituent can also be introduced via the one-step Sonogashira cross-coupling/acetylene alcohol deprotection.

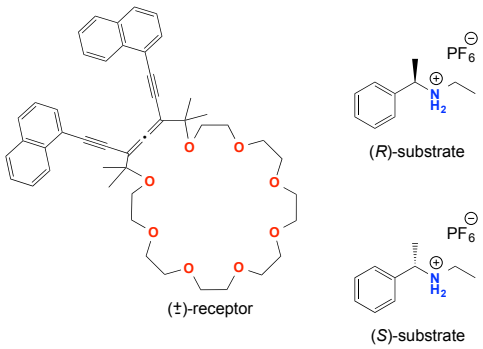

Figure 58. Crown-ether based DEA able to bind chiral ammonium cations.

Lastly, (*M*)-(–)-DEA could be made and modified with donor–acceptor–donor (DAD) uracil and acceptor–donor–acceptor (ADA) diacetamide hydrogen-bonding motifs. The monomer may give cyclic structures (Figure 59).

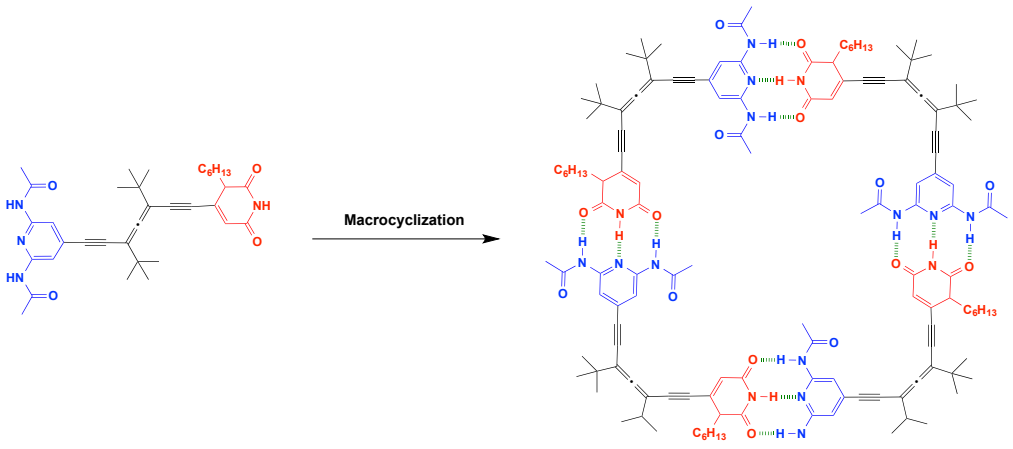

Figure 59. DEA dimer and tetramer capable of hydrogen-bonding.

To accomplish the secondary objective of this dissertation, namely, of expanding the chemical space of electron acceptor units in a formal [2+2] CA–RE reaction, the reactivity of DCID with electron-rich anilinoalkynes was investigated in Chapter 3. It was initially expected that DCID would also undergo CA–RE reactions, but the results were surprising. Not only CA–RE adducts but also tricyclic 4*H*-pyrans from the [4+2] HDA reaction were obtained and their formation could easily be controlled by altering the reaction conditions. The presence of Lewis acids, such as $LiClO_4$, greatly enhances the formation of the HDA cycloaddition over the CA–RE reaction. This is opposite to the effect of Lewis acids on cycloadditions with electron-rich olefins. Optoelectronic applications of the new push–pull chromophores and the rapid construction of complex 4*H*-pyran derivatives will be further investigated.

Inspired by these initial results on the reactivity of new electron-poor alkenes, we decided to replace cyano groups with ester moieties on tetrasubstituted electron-deficient alkenes and study the effect on their ability to undergo the CA–RE reaction. The CA–RE reaction still takes place with a single cyano moiety, however other reactions also occurred, namely a [4+2] HDA cycloaddition and a novel reaction with a proposed [3+2] cycloaddition and subsequent rearrangement mechanism.

The all-ethyl ester analogue was generally not reactive enough to engage in the CA–RE reaction but its reactivity could be increased by adding CN or CF_3 to the alkyl chain of the ester. We also described the possibility of post-CA–RE reaction functionalization to ester-substituted butadienes, including the access to pharmacologically interesting pyrazolopyrans.

To further explore the role of products derived from the CA–RE reaction in the synthesis of more complex systems through post-reaction functionalization, we described in Chapter 5 a three-step synthesis of tetra-substituted NH-pyrroles from readily available starting materials (22 examples). Variation of substituents can be achieved by altering the starting material, which is easily accessible from the CA–RE reaction, or by using a different reacting nucleophile.

Finally, Chapter 6 was dedicated to the development a formal [3+2] cycloaddition/rearrangement cascade reaction between moderately activated to unactivated alkynes and electron-poor dicyano-diester-substituted alkene **162** to yield a variety of π-conjugated penta-2,4-dien-1-ones. This atom-economic process was obtained in moderate to excellent yields (20 examples) without the presence of a catalyst. The broad substrate scope and reasonably mild conditions for such a transformation make this procedure a valuable reaction for the synthesis of dienones. We are currently investigating post-reaction functionalizations for the synthesis of more complex systems.

With the short and easy preparation of CA–RE compounds in large quantities starting from electron-deficient, mono- and diester-substituted alkenes based on their ability to act as good electrophiles, we could further investigate post-functionalization to construct molecules of greater complexity and broader utility with the use of 1,3-dipole molecules such as diazoalkanes, azomethine ylides or nitrile oxides, for example (Figure 60). They are normally used in 1,3-dipolar cycloaddition reactions to form 5-membered heterocycles[221], but in this case they could give new reactivities towards more complex systems.

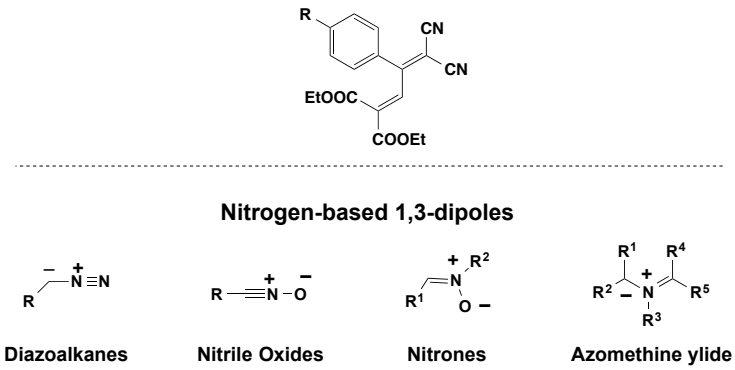

Figure 60. Further post-functionalization of CA–RE adducts for the construction of molecules of greater complexity.

As shown in Chapters 4–6, electron-deficient alkene **162** proned to be an interesting compound for the formation of CA–RE products and π-conjugated penta-2,4-dien-1-ones and can be easily prepared in large quantities. To further expand the chemical space for the construction of molecules of greater complexity, a variety of substituted ketones could be prepared and subjected to the reaction conditions. Preliminary synthetic attempts resulted in the formation of 2-amino-4*H*-pyran-3-carbonitrile derivatives and the structure of which was confirmed by X-ray analysis (Scheme 49).

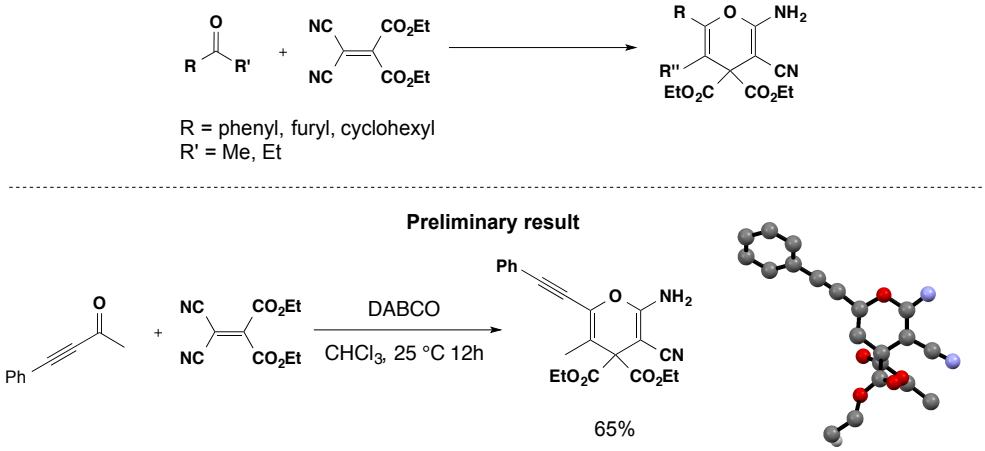

Scheme 49. Synthesis of 2-amino-4*H*-pyran-3-carbonitriles.

As described in Chapter 2, 4*H*-pyran derivatives are an important class of heterocycles, especially when featuring multiple ring-substitutions. They are found in natural products and biologically active compounds[155–157] as well as in

optoelectronics.[158–160] More specifically, 2-amino-4*H*-pyran-3-carbonitriles, which, despite the synthetic challenge associated with their synthesis, are used as pharmacophores of antitubercular agents[222,223]. This methodology could be a valuable reaction for the synthesis of 2-amino-4*H*-pyran-3-carbonitriles and needs to be further investigated.

Tetrasubstituted pyridines could also be easily accessible in 2 steps starting from 2-amino-4*H*-pyran-3-carbonitrile (Scheme 50). As for 4*H*-pyran, the pyridine motif is present in many biologically active molecules, and widespread in both agrochemicals and pharmaceuticals.[224,225] Due to the broad synthetic and medicinal application of these molecules there has been much effort directed toward their synthesis.[226–228] Despite these advances, highly functionalized pyridines synthesized from easily accessible starting materials and in the absence of a catalyst still remains a key focus within the synthetic community.

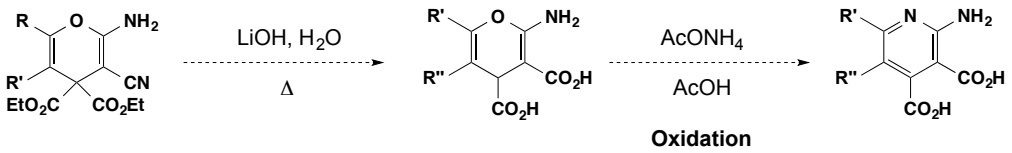

Scheme 50. Pyridine synthesis.

Chapter 8

Experimental Part

8. Supporting Information

8.1. Materials

Reagents (ABCR, Acros, Aldrich, Fluka, and TCI) were purchased as reagent grade and used without further purification. **Solvents** for flash column chromatography (FC), plug filtrations, and extraction were of technical grade and distilled before use. **Dry solvents** for reactions were purified by a solvent drying system (LC Technology Solutions Inc. SP-105) under nitrogen atmosphere (H_2O content < 10 ppm as determined by Karl-Fischer titration). All other solvents were purchased in p.a. quality. For all aqueous solutions, deionized water was used. **Reactions** with exclusion of air or water were performed in oven-dried glassware and under an Ar or N_2 atmosphere. **Flash column chromatography** (FC) was carried out using silica gel (particle size: 40–63 μm, 230–400 mesh ASTM; Fluka). **Analytical thin layer chromatography** (TLC) was performed on aluminum sheets or glass plates coated with silica gel 60 F_{254} (Merck); visualization with a UV lamp (254 nm). **Evaporation in vacuo** was performed at 45–60 °C and 900–10 mbar. **Reported yields** refer to spectroscopically and chromatographically pure compounds that were dried under high vacuum (10^{-2} mbar) before analytical characterization. **Nomenclature** follows the suggestions proposed by the computer program ACD Name by ACD Labs. The atoms were labeled arbitrarily, if necessary. **High-performance liquid chromatography (HPLC)** was run on a Merck-Hitachi LaChrom D-Line system equipped with a D-7000 Interface, an L-7100 pump, and an L-7400 UV-detector.

8.2. Physical Characterization

^{1}H and ^{13}C nuclear magnetic resonance (NMR) spectra were recorded on Varian Gemini 300, Varian Mercury 300, Bruker ARX 300, Bruker DRX 400, and Bruker AV 400 spectrometers at 300 MHz or 400 MHz (^{1}H) and 75 MHz or 100 MHz (^{13}C), respectively. Chemical shifts (δ) are reported in ppm downfield from tetramethylsilane using the residual deuterated solvent signals as an internal reference. For ^{1}H NMR, coupling constants J are given in Hz and the resonance multiplicity is

described as s (singlet), d (doublet), t (triplet), q (quartet), quint. (quintet), sext. (sextet), sept. (septet), m (multiplet), and br. (broad). All spectra were recorded at 25 °C. **UV/Vis spectra** were recorded on a Varian Cary-500 Scan spectrophotometer. The spectra were measured in a quartz cuvette (1 cm) at 25 °C. The absorption wavelengths are reported in nm with the extinction coefficient ε ($L\,mol^{-1}\,cm^{-1}$) in brackets. **Infrared (IR) spectra** were recorded on a Perkin-Elmer 1600 FT-IR spectrometer (ATR, Golden Gate) and are reported in wavenumbers $\tilde{\nu}$ (cm^{-1}) with band intensities indicated as s (strong), m (medium), w (weak), very weak (vw), br. (broad), and sh (shoulder). **Mass spectrometry (MS) and high-resolution mass spectrometry (HR-MS)** were performed by the MS-service of the Laboratory for Organic Chemistry at the ETH Zurich on a Waters Micromass AutoSpec-Ultima spectrometer (EI), on a Bruker maXis spectrometer (ESI), or on a Varian IonSpec FT-ICR spectrometer (MALDI). For MALDI measurements, the matrix was 2-[(2*E*)-3-(4-tert-butylphenyl)-2-methylprop-2-enylidene]malononitrile (DCTB) or 3-hydroxypyridine-2-carboxylic acid (3-HPA). Masses are reported in *m*/*z* units for the molecular ion M^+, or $[M + H]^+$, $[M + Na]^+$ or $[M + K]^+$ with the corresponding intensities in %. **Electrochemical measurements** were carried out in CH_2Cl_2 containing 0.1 M Bu_4NPF_6 in a classical three-electrode cell by cyclic voltammetry (CV) and rotating-disk voltammetry (RDV). The working electrode was a glassy carbon disk (3 mm in diameter), the auxiliary electrode a Pt wire, and the pseudo reference electrode a Pt wire. The cell was connected to an Autolab PGSTAT30 potentiostat (Eco Chemie, Holland) driven by a GPSE software running on a personal computer. All potentials are given *vs*. Fc^+/Fc used as internal reference and are uncorrected from Ohmic drop.

8.3. General Procedures

General Procedure A (GPA): Removal of One Hydroxyisopropyl Protecting Group: Pulverized KOH (5 equiv.) was placed in a Schlenk tube and dried with a heat gun under vacuum (0.1 Torr). The tube was then filled with nitrogen. A solution of enantiopure diprotected alleno-acetylenic oligomer (1 equiv.) in dry toluene (3 mL) under nitrogen atmosphere was transferred to the Schlenk tube. The tube was placed in an oil bath preheated to 80 °C. The mixture was stirred for 3h, when LC/MS showed a 1:1 mixture of starting material and monoprotected product. The mixture

was allowed to cool to 20 °C, diluted with *n*-hexane, and washed with a saturated aqueous NH_4Cl solution (10 mL). The organic phase was dried over Na_2SO_4, and was evaporated. The monoprotected product was separated from the starting material by Flash chromatography (FC; *n*-hexane/EtOAc 9:1).

General Procedure B (GPB): Removal of Two Hydroxyisopropyl Protecting Group: Pulverized KOH (100 equiv) was placed in a Schlenk tube and dried with a heat gun under vacuum (0.1 Torr). The tube was then filled with nitrogen. A solution of enantiopure diprotected alleno-acetylenic oligomer (1 equiv) in dry toluene (3 mL) under nitrogen atmosphere was transferred to the Schlenk tube. The tube was placed in an oil bath preheated to 80 °C. The mixture was stirred for 3h. The mixture was allowed to cool to 20 °C, diluted with hexanes, and washed with a saturated aqueous NH_4Cl solution (10 mL). The organic phase was dried over Na_2SO_4 and evaporated. The monoprotected product was separated from the starting material by FC (SiO_2; *n*-hexane/EtOAc 95:5). The starting material recovered from the column was treated as described above with pulverized KOH (170 equiv.) until LC/MS analysis showed no starting material.

General Procedure C (GPC): Oxidative Homo-coupling of Terminal Alkynes: The monoprotected alkyne or a mixture of alkynes (1.0 equiv) was dissolved in toluene (2 mL) under air atmosphere. Catalytic amounts of $[Pd(PPh_3)_2Cl_2]$ (0.1 equiv), CuI (0.1 equiv) and TMEDA (1.0 equiv) were added to the solution. The mixture was heated to 50 °C and stirred for 24 h. Evaporation and FC (SiO_2; *n*-hexane/EtOAc 9:1) gave the coupled product. The procedure was identical for enantiomers and diastereoisomers.

General Procedure D (GPD): Eglington-Galbraith Macrocyclization: A solution of CuCl (200 equiv) and $CuCl_2$ (20 equiv) in dry pyridine (10^{-4} mol/L) was degassed by bubbling argon for 60 min. A solution of the terminal alkyne or a mixture of alkynes (1 equiv) in dry, degassed pyridine (10 mL) was added over a period of 20 h. The mixture was stirred for an additional 3 h, and pyridine was evaporated. A solution of the remaining solid in saturated aqueous NH_4Cl solution (20 mL) was extracted with pentane. The organic phase was dried over Na_2SO_4 and evaporated to dryness. The residue was purified by FC (SiO_2; cyclohexane).

General Procedure E (GPE): DCID (1.0 equiv) was added to a solution of donor (1.05 equiv) in DCE and stirred at 25 °C for 3 h. Evaporation of the solvent in vacuo and FC (SiO_2; *n*-hexane/EtOAc 8:2) gave a mixture of [4+2] and [2+2] cycloaddition products.

General Procedure F (GPF): DCID (1.0 equiv) and $LiClO_4$ (1.0 equiv) were added to a solution of donor (1.05 equiv) in DCE/MeCN 98:2 at 80 °C for 2 h. Evaporation of the solvent in vacuo and FC (SiO_2; *n*-hexane/EtOAc 8:2) give a mixture of products from [4+2] HDA cycloaddition and [2+2] CA–RE.

General Procedure G (GPG): A solution of pyrrole precursor (1.0 equiv) and nucleophile (2.0 equiv) in THF (0.1 M solution) were combined in a microwave vial, heated at 65 °C with microwave irradiation for 15 min, and evaporated.

General Procedure H (GPH): A solution of pyrrole precursor (1.0 equiv) and nucleophile (2.0 equiv) in THF (0.1 M solution) were conventionally heated to 65 °C for the time period given and evaporated.

8.4. Synthetic Procedures

$(P)_4$-(–)-1,3,6,8,13,15,18,20-Octa-*tert*-butylcyclotetracosa-1,2,6,7,13,14,18,19-octaen-4,9,11,16,21,23-hexayne ($(P)_4$-(–)-33a)

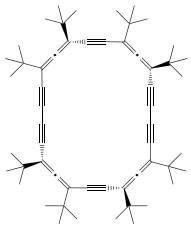

A solution of CuCl (211 mg, 2.13 mmol) and $CuCl_2$ (28.7 mg, 0.213 mmol) in dry pyridine (10^{-4} mol/L) was degassed by bubbling argon through for 60 min. Tetrameric allene $(P)_4$-(+)-**108** (8 mg, 0.01 mmol) in dry, degassed pyridine (10 mL) was added over a period of 20 h. The mixture was stirred for an additional 3 h, and pyridine was evaporated. The remaining solid in saturated aqueous NH_4Cl solution

(20 mL) was extracted with pentane. The organic phase was dried over Na_2SO_4 and evaporated to dryness. Flash chromatography (FC; cyclohexane) gave $(P)_4$-(−)-**33a** as a white solid (5 mg, 75 %). R_f = 0.73 (SiO_2; *n*-hexane); m.p. > 200 °C; $[\alpha]_D^{20}$ = –650° (*c* = 1.0 in $CHCl_3$); ^{1}H NMR (400 MHz, C_6D_6): δ 1.11 (s, 36 H; 4 *t*Bu); 1.14 ppm (s, 36 H; 4 *t*Bu); ^{13}C NMR (C_6D_6, 100 MHz): δ 28.63 (4 C*Me*$_3$), 28.82 (4 C*Me*$_3$), 35.18 (4 *C*Me$_3$), 35.33 (4 *C*Me$_3$), 75.54 (C(10, 11, 22, 23)), 78.29 (C(9, 12, 21, 24)), 86.49 (C(4, 5, 16, 17)), 103.27 (C(1, 8, 13, 20)), 104.56 (C(3, 15)), 214.49 ppm (C(6, 18)); IR (ATR): $\tilde{\nu}$ = 2964 (m), 2903 (s), 2867 (m), 1459 (m), 1393 (w), 1363 (w), 1222 (m), 1077 (s) cm^{-1}; UV/Vis (*n*-hexane): λ_{max} (ε) = 321 (10000), 303 (26500), 285 (42600), 240 (331000), 227 nm (237000 M^{-1} cm^{-1}); HR-MALDI-MS: *m/z* (%): 744.5627 (100, $[M]^+$, calcd for $C_{56}H_{72}^+$: 744.5629). The enantiomer $(M)_4$-(+)-**33a** was obtained by the same protocol: $[\alpha]_D^{20}$ = +651° (*c* = 1.0 in $CHCl_3$).

(*P,P,M,M*)-1,3,6,8,13,15,18,20-Octa-*tert*butylcyclotetracosa1,2,6,7,13,14,18,19-octaen-4,9,11,16,21,23-hexayne (33b).[51]

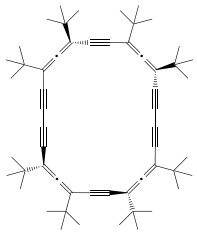

The monoprotected alkynes $(P)_2$-(+)-**106a** (10 mg, 0.023 mmol) and $(M)_2$-(−)-**106a** (10 mg, 0.023 mmol) were dissolved in toluene (2 mL) in air. Catalytic amounts of $[Pd(PPh_3)_2Cl_2]$ (1.6 mg, 0.0023 mmol) and CuI (0.4 mg, 0.0023 mmol) were added to the solution along with TMEDA (3.4 μL, 0.023mmol). The mixture was placed in an oil bath preheated to 50 °C and stirred for 24 h. The solvent was evaporated, the remaining solid diluted in toluene, and KOH (219 mg, 3.91 mmol) added. The mixture was heated to 50 °C for 6 h. The mixture was allowed to cool to 20 °C, diluted with hexanes, and washed with a saturated aqueous NH_4Cl solution (15 mL). The organic phase was dried over Na_2SO_4 and the solvent evaporated. The mixture of deprotected tetra-allenes ((*P,P,M,M*), $(P)_4$, and $(M)_4$) was treated with CuCl (455 mg, 4.6 mmol) and $CuCl_2$ (61.8mg, 0.46 mmol) according to GPD to give a mixture of $(M)_4$-(+)-**33a**, $(P)_4$-(–)-**33a**, and (*P,P,M,M*)-**33b** (1:1) as a

white solid (12.8 mg, 75 %); m.p > 200 °C. The racemate and the achiral stereoisomer were separated by analytical HPLC (Kromasil 100 Si, 5 μm, hexanes, 1 mL/min). Spectroscopic properties were identical to those previously reported for (*P*,*P*,*M*,*M*)-**33b**.[51]

***(P,M,M,M)*-(+)-1,3,6,8,13,15,18,20-Octa-*tert*-butylcyclotetracosa-1,2,6,7,13,14,18, 19-octaen-4,9,11,16,21,23-hexayne ((*P,M,M,M*)-(+)-33c)**[51]

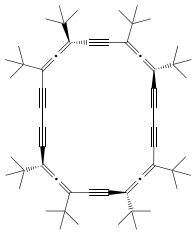

The monoprotected alkynes (*P*,*M*)-(+)-**106b** (10 mg, 0.023 mmol) and $(M)_2$-(−)-**106a** (10 mg, 0.023 mmol) were dissolved in toluene (2 mL) in air. Catalytic amounts of $[Pd(PPh_3)_2Cl_2]$ (1.6 mg, 0.0023 mmol) and CuI (0.4 mg, 0.0023 mmol) were added to the solution along with TMEDA (3.4 μL, 0.023mmol). The mixture was placed in an oil bath preheated to 50 °C and stirred for 24 h. The solvent was evaporated, the remaining solid was diluted in toluene, and KOH (219 mg, 3.91 mmol) was added. The mixture was heated to 50 °C for 6 h. The mixture was allowed to cool to 20 °C, diluted with hexanes, and washed with a saturated aqueous NH_4Cl solution (15 mL). The organic phase was dried over Na_2SO_4 and the solvent evaporated. The mixture of deprotected tetra-allenes ((*P*,*M*,*M*,*M*), (*P*,*M*,*M*,*P*), and $(M)_4$) was treated with CuCl (455 mg, 4.6 mmol) and $CuCl_2$ (61.8mg, 0.46 mmol) according to GPD to give (*P*,*M*,*M*,*M*)-(+)-**33c,** (*P*,*M*,*M*,*P*)-**33e**, and $(M)_4$-(+)-**33a** (2:1:1 mixture) as a white solid (12.8 mg, 75 %); m.p > 200 °C. The three stereoisomers were separated by analytical HPLC (Kromasil 100 Si, 5 μm, *n*-hexane, 1 mL/min). Spectroscopic properties for (*P,M,M,M*)-(+)-**33c** were identical to those previously reported.[51] $[\alpha]_D^{20}$ = +480° (*c* = 0.01 in $CHCl_3$) for (*P,M,M,M*)-(+)-**33c** and $[\alpha]_D^{20}$ = −477° (*c* = 0.008 in $CHCl_3$) for (*M,P,P,P*)-(−)-**33c**.

***(P,M,P,M)*-1,3,6,8,13,15,18,20-Octa-*tert*-butylcyclotetracosa-1,2,6,7,13,14,18,19-octaen-4,9,11,16,21,23-hexayne (33d)**[51]

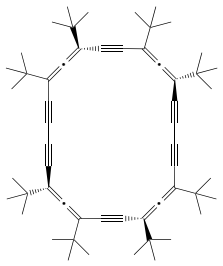

The monoprotected alkynes (*P,M*)-(+)-**106b** (10 mg, 0.023 mmol) and (*M,P*)-(−)-**106b** (10 mg, 0.023 mmol) were dissolved in toluene (2 mL) in air. Catalytic amounts of $[Pd(PPh_3)_2Cl_2]$ (1.6 mg, 0.0023 mmol) and CuI (0.4 mg, 0.0023 mmol) were added to the solution along with TMEDA (3.4 μL, 0.023mmol). The mixture was placed in an oil bath preheated to 50 °C and stirred for 24 h. The solvent was evaporated, the remaining solid diluted in toluene, and KOH (219 mg, 3.91 mmol) added. The mixture was heated to 50 °C for 6 h. The mixture was allowed to cool to 20 °C, diluted with hexanes, and washed with a saturated aqueous NH_4Cl solution (15 mL). The organic phase was dried over Na_2SO_4 and the solvent evaporated. The mixture of deprotected tetra-allenes ((*P,M,P,M*) and (*P,M,M,P*)/(*M,P,P,M*)) was treated with CuCl (455 mg, 4.6 mmol) and $CuCl_2$ (61.8mg, 0.46 mmol) according to GPD to give a mixture of (*P,M,P,M*)-**33d** and (*M,P,P,M*)-**33e** as a white solid (12.8 mg, 75 %); m.p > 200 °C. The achiral macrocycles were separated by analytical HPLC (Kromasil 100 Si, 5 μm, hexanes, 1 mL/min). Spectroscopic properties for (*P,M,P,M*)-**33d** were identical to those previously reported.[51]

(*P*,*M*,*M*,*P*)-1,3,6,8,13,15,18,20-Octa-*tert*-butylcyclotetracosa-1,2,6,7,13,14,18,19-octaen-4,9,11,16,21,23-hexayne ((*P*,*M*,*M*,*P*)-33e) [51]

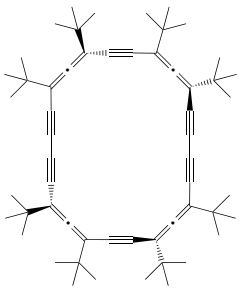

The monoprotected alkyne (*P*,*M*)-(+)-**106b** (10 mg, 0.023 mmol) was dissolved in toluene (2 mL) in air. Catalytic amounts of $[Pd(PPh_3)_2Cl_2]$ (1.6 mg, 0.0023 mmol) and CuI (0.4 mg, 0.0023 mmol) were added to the solution along with TMEDA (3.4 μL, 0.023mmol). The mixture was placed in an oil bath preheated to 50 °C and stirred for 24 h. The solvent was evaporated, the remaining solid dissolved in toluene, and KOH (219 mg, 3.91 mmol) added. The mixture was heated to 50 °C for 6 h. The mixture was allowed to cool to 20 °C, diluted with hexanes, and washed with a saturated aqueous NH_4Cl solution (15 mL). The organic phase was dried over Na_2SO_4 and the solvent evaporated. The deprotected (*P*,*M*,*M*,*P*)-tetra-allene was treated with CuCl (455 mg, 4.6 mmol) and $CuCl_2$ (61.8mg, 0.46 mmol) according to GPD to give (*P*,*M*,*M*,*P*)-**65e** as a white solid (12.8 mg, 75 %); m.p > 200 °C. Spectroscopic properties for (*P*,*M*,*M*,*P*)-**65e** were identical to those previously reported.[52]

$(P)_2$-(+)-5,7,10,12-Tetra-*tert*-butyl-2,15-dimethylhexadeca-5,6,10,11-tetraen-3,8,13-triyne-2,15-diol ($(P)_2$-(+)-105a)

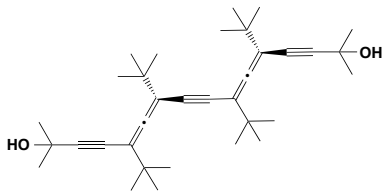

A solution of dimeric allene $(P)_2$-(+)-**105a** (50 mg, 0.105 mmol) in Me_2SO (1.1 ml) was treated with acetone (0.660 mL, 0.525 mmol) and dropwise with 1 M *t*-Bu-P4 base in hexane (30 μL). The mixture was stirred for 3 h at 25 °C, diluted with a saturated NH_4Cl, and extracted with $CHCl_3$ (3 x 15 mL). The organic layer was dried over $MgSO_4$ and the solvent removed under reduced pressure. The

remaining solid was diluted in THF (1.1 mL) and treated with 6 M HCl (0.1 mL). The mixture was stirred at 25 °C for 2 h, then treated with a saturated NH_4Cl solution (5 mL) and extracted with Et_2O (3 x 15 mL). The combined organic phases were dried over $MgSO_4$ and evaporated. FC (*n*-hexane/EtOAc 8:2) gave $(P)_2$-(+)-**105a** (37 mg, 72%) as a white solid. R_f = 0.30, (SiO_2; *n*-hexane/EtOAc 8:2); m.p. 75 °C; $[\alpha]_D^{20}$ = +300° (*c* = 1.0 in $CHCl_3$); ^{1}H NMR (400 MHz, CD_2Cl_2): δ 3 s, 18 H; 2 *t*Bu), 1.16 (s, 18 H, 2 *t*Bu), 1.53 (s, 12 H; 2 C*Me*$_2$OH), 2.00 and 2.02 ppm (br, 2 H; OH); ^{13}C NMR (101 MHz, CD_2Cl_2): δ = 28.63 (C*Me*$_3$), 28.76 (C*Me*$_3$), 31.29 (C*Me*$_2$OH), 35.45 (*C*Me$_3$), 35.59 (*C*Me$_3$), 65.48 (C(2,15)), 75.32 (C(4,13)), 86.29 (C(8,9)), 97.59 (C(3,14)), 102.74 (C(5,12)), 103.81 (C(7,10)), 210.76 ppm (C(6,11)); IR (ATR): $\tilde{\nu}$ = 3350 (w), 2951 (m, sh), 2226 (w), 2144 (w), 1928 (very w), 1450 (m), 1363 (s), 1151(w), 964 (m) cm^{-1}; UV/Vis (*n*-hexane): λ_{max} (ε) = 315 (2915), 301 (9500), 284 (14000), 240 (110600), 225 nm (74700 M^{-1} cm^{-1}). HR-MALDI-MS: *m/z* (%): 513.3701 (100, $[M + Na]^+$, calcd for $C_{34}H_{50}NaO_2^+$: 513.3703). The enantiomer $(M)_2$-(–)-**105a** was obtained by the same protocol: $[\alpha]_D^{20}$ = –301° (*c* = 1.0 in $CHCl_3$).

$(P)_4$-(+)-5,7,10,12,17,19,22,24-Octa-*tert*-butyl-2,27-dimethyloctacosa-5,6,10,11, 17,18,22,23-octaen-3,8,13,15,20,25-hexayne-2,27-diol ($(P)_4$-(+)-105b)

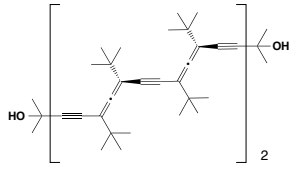

Enantiopure $(P)_2$-(+)-**107a** (80 mg, 0.18 mmol), dissolved in toluene (2 mL) under air, was treated with $[Pd(PPh_3)_2Cl_2]$ (14 mg, 0.02 mmol), CuI (4 mg, 0.02 mmol), and *N,N,N',N'*-tetramethylethylenediamine (TMEDA; 28 μL, 0.18 mmol). The mixture was stirred at 50 °C for 2 h, evaporated, and FC (*n*-hexane/EtOAc 9:1) gave $(P)_2$-(+)-**105b** as a white solid (70 mg, 92 %). R_f = 0.30 (SiO_2; *n*-hexane/EtOAc 8:2); m.p. 212 °C; $[\alpha]_D^{20}$ = +994° (*c* = 1.0 in $CHCl_3$); ^{1}H NMR (400 MHz, $CDCl_3$): δ s, 18 H; 2 *t*Bu), 1.13 (s, 18 H, 2 *t*Bu), 1.14 (s, 18 H; 2 *t*Bu), 1.15 (s, 18 H; 2 *t*Bu), 1.56 (s, 12 H; 2 C*Me*$_2$OH), 2.25 ppm (br, 2 H; OH); ^{13}C NMR (101 MHz, $CDCl_3$): δ 28.95 (2 C*Me*$_3$), 29,00 (2 C*Me*$_3$), 29.03 (2 C*Me*$_3$), 29.06 (2 C*Me*$_3$), 31.52 (C*Me*$_2$OH), 35.52 (2 *C*Me$_3$), 35.66 (2 *C*Me$_3$), 35.86 (2 *C*Me$_3$), 35.89 (2 *C*Me$_3$), 65.73 (C(2, 27)), 75.43 (C(4, 25)), 75.97 (C(14, 15)), 76.95 (C(13, 16)), 85.63

(C(8, 21)), 87.12 (C(9, 20)), 96.99 (C(3, 26)), 102.37 (C(5, 24)), 102.61 (C(7, 22)), 103.63 (C(10, 19)), 104.68 (C(12, 17)), 211.01 (C(6, 23)), 213.46 ppm (C(11, 18)); IR (ATR): $\tilde{\nu}$ = 2949 (s), 2918 (m, sh), 2864 (w, sh), 2351 (very w), 2347 (very w, sh), 1912 (very w), 1453 (m), 1445(m, sh), 1373 (s), 1213 (m), 10632(m), 948 (m), 664 (m) cm^{-1}; UV/Vis (*n*-hexane): λ_{max} (ε) = 315 (10700), 301 (29300), 284 (44000), 240 (333100), 225 nm (225100 $M^{-1}\,cm^{-1}$). HR-MALDI-MS: *m/z* (%): 862.6624 (100, $[M]^+$, calcd for $C_{62}H_{86}O_2^+$: 862.6628). The enantiomer $(M)_4$-(–)-**63b** was obtained by the same protocol: $[a]_D^{20}$ = –995° (*c* = 1.0 in $CHCl_3$).

$(P)_8$-(+)-5,7,10,12,17,19,22,24,29,31,34,36,41,43,46,48-Hexadeca-*tert*-butyl-2,51-dimethylhexadecacosa-5,6,10,11,17,18,22,23,29,30,34,35,41,42,46,47-hexadecaen-3,8,13,15,20,25,27,32,37,39,44,49-dodecayne-2,51-diol ($(P)_8$-(+)-105c)

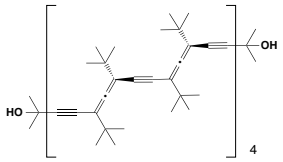

$(P)_4$-(+)-**110b** (10 mg, 0.012 mmol), dissolved in toluene (2 mL) under air, was treated with $[Pd(PPh_3)_2Cl_2]$ (10 mg, 0.02 mmol), CuI (4 mg, 0.02 mmol), and *N,N,N',N'*-tetramethylethylenediamine (TMEDA; 28 μL, 0.18 mmol). The mixture was stirred at 50 °C for 2 h, evaporated, and FC (*n*-hexane/EtOAc 9:1) gave $(P)_8$-(+)-**105c** as a white solid (8.5 mg, 85 %). R_f = 0.21; (*n*-hexane/EtOAc 8:2); m.p. 250 °C; $[\alpha]_D^{20}$ = + 3231° (*c* = 1.0 in $CHCl_3$); ^{1}H NMR (400 MHz, $CDCl_3$): δ = 1.12–1.15 (m, 144 H; 16 *t*Bu), 1.56 (s, 12H; 2 C*Me*$_2$OH), 1.97 and 1.98 ppm (br, 2 H; 2 OH); ^{13}C NMR (101 MHz, $CDCl_3$): δ = 28.95 (2 C*Me*$_3$), 29.02 (4 C*Me*$_3$), 29.03 (4 C*Me*$_3$), 29.07 (6 C*Me*$_3$), 31.51 and 31.52 (C*Me*$_2$OH), 35.52 (2 *C*Me$_3$), 35.67 (2 *C*Me$_3$), 35.87 (2 *C*Me$_3$), 35.90 (10 *C*Me$_3$), 65.75 (C(2, 51)), 75.41 (C(4, 49)), 76.01 (C(14, 15, 26, 27, 38, 39)), 77.20 (C(13, 16, 25, 28, 37, 40), 85.64 (C(8, 21, 33, 45)), 86.45 (C(9, 44)), 87.11 (C(20, 32)), 96.95 (C(3, 50)), 102.36 (C(5, 48)), 102.62 (C(7, 46)), 102.69 (C(10, 22, 31, 43)), 103.64 (C(19, 34)), 104.59 (C(12, 17, 36, 41)), 104.67 (C(24, 29)), 211.02 (C(6, 18, 35, 47)), 213.49 ppm (C(11, 23, 30, 42)); IR (ATR): $\tilde{\nu}$ = 2949 (s), 2918 (m, sh), 2864 (w, sh), 2351 (very w), 2347 (very w, sh), 1912 (very w), 1736 (very w), 1453 (m), 1445(m, sh), 1373 (s), 1213 (m), 10632(m), 948 (m), 664 (m) cm^{-1}; UV/Vis (*n*-hexane): λ_{max} (ε) = 320 (22600), 301 (61500), 284

(92600), 240 (699500), 225 nm (472800 $M^{-1}\,cm^{-1}$); HR-MALDI-MS: *m/z* (%): 1607.2264 (100, $[M]^+$, calcd for $C_{59}H_{80}O^+$: 1607.2262). The enantiomer $(M)_8$-(–)-**105c** was obtained by the same protocol: $[\alpha]_D^{20} = -3229°$ (*c* = 1.0 in $CHCl_3$).

$(P)_2$-(+)- and (*P,M*)-(+)-5,7,10,12-Tetra-*tert*-butyl-2-methyl-14-(triisopropylsilyl) tetra deca-5,6,10,11-tetraen-3,8,13-triyn-2-ol ($(P)_2$-(+)-106a and (*P,M*)-(+)-106b

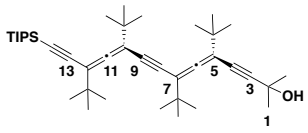

A solution of (*P*)-(+)-**17** (1.01 g, 3.91 mmol), pentafluorobenzoic ester (±)-**18** (2.97 g, 5.47 mmol), and Cy_2NMe (2.0 mL) in $(CH_2Cl)_2$ (30 mL) was degassed with Ar. A second flask with $[Pd(PPh_3)_4]$ (445 mg, 0.385 mmol) and CuI (75 mg, 0.39 mmol) was evacuated and filled with Ar. $(CH_2Cl)_2$ (5 mL) and Cy_2NMe (3 mL) were added, and the suspension was degassed with Ar. The suspension was transferred *via* syringe to the first solution. The flask was rinsed with Cy_2NMe (3 mL) and quickly degassed. The brown-red solution was heated to 60 °C for 3.5 h. The mixture was then concentrated to ca. 10 mL and filtered through SiO_2 (cyclohexane/CH_2Cl_2 1:1). After concentrating, the dark oil was diluted with cyclohexane and the solution washed twice with saturated aqueous NH_4Cl solution (70 ml) and 1 M HCl (20 mL). The organic phase was dried over $MgSO_4$ and evaporated. Column chromatography (CC) of the brown oil residue (SiO_2; cyclohexane/CH_2Cl_2 1:0→1:1→1:2) gave a 1:1 mixture of $(P)_2$-**106a**/(*P,M*)-**106b** as a yellowish liquid. R_f = 0.40 (*n*-hexane); ^{1}H NMR (400 MHz, $CDCl_3$): δ 1.08 (*s*, 21 H; *t*Bu), 1.119 and 1.123 (*s*, 9 H; *t*Bu), 1.13-1.15 (*m*, 27 H; 3 *t*Bu), 1.56 (*s*, 6 H; C*Me*$_2$OH), 1.957 and 1.962 ppm (*s*, 1 H; OH); ^{13}C NMR (101 MHz, $CDCl_3$): δ 11.38 (Si*C*HMe$_2$), 18.67 (SiCH*Me*$_2$), 28.95 (2 C*Me*$_3$), 29.02 (C*Me*$_3$), 29.05 (C*Me*$_3$), 29.07 (C*Me*$_3$), 31.52 (C*Me*$_2$OH), 35.29 (*C*Me$_3$), 35.53 (*C*Me$_3$), 35.71(*C*Me$_3$), 35.75 (*C*Me$_3$), 65.75 (C(2)), 76.07 (C(4)), 86.15 and 86.21 (C(8)), 86.50 and 86.53 (C(9)), 93.82 (*C*≡C–Si), 93.84 (*C*≡C–Si), 96.89 (C(3)), 96.91 (C(3)), 100.56 (C≡*C*–Si), 100.58 (C≡*C*–Si), 102.25 (C(5)), 103.41 and 103.45 (C(7)), 103.47 and 103.49 (C(10)), 103.82 and 103.87 (C(12)), 210.92 and 210.94 (C(6)), 212.13 and 212.17 ppm (C(11)); IR (ATR): $\tilde{\nu}$ = 3330 (m), 2961 (s),

2236 (w), 1938 (very w), 1459 (m), 1361 (s), 1165, 956 (m) cm^{-1}; HR-MALDI-MS: *m/z* (%): 589.4798 (100, $[M + H]^+$, calcd for $C_{40}H_{65}OSi^+$: 589.4799).

$(M)_2$-(–)- and (*M,P*)-(–)-5,7,10,12-Tetra-*tert*-butyl-2-methyl-14-(triisopropylsilyl)tetra deca-5,6,10,11-tetraen-3,8,13-triyn-2-ol ($(M)_2$-(–)-106a and (*M,P*)-(–)-106b

A solution of (*M*)-(–)-**17** (1.01 g, 3.91 mmol), pentafluorobenzoic ester (±)-**18** (2.97 g, 5.47 mmol), and Cy_2NMe (2.0 mL) in $(CH_2Cl)_2$ (30 mL) was degassed with Ar. A second flask with $[Pd(PPh_3)_4]$ (445 mg, 0.385 mmol) and CuI (75 mg, 0.39 mmol) was evacuated and filled with Ar. $(CH_2Cl)_2$ (5 mL) and Cy_2NMe (3 mL) were added, and the suspension was degassed with Ar. The suspension was transferred *via* syringe to the first solution. The flask was rinsed with Cy_2NMe (3 mL) and quickly degassed. The brown-red solution was heated to 60 °C for 3.5 h. The mixture was then concentrated to ca. 10 mL and filtered through SiO_2 (cyclohexane/CH_2Cl_2 1:1). After concentrating, the dark oil was diluted with cyclohexane and the solution washed twice with saturated aqueous NH_4Cl solution (70 ml) and 1 M HCl (20 mL). The organic phase was dried over $MgSO_4$ and evaporated. CC of the brown oil residue (SiO_2; cyclohexane/CH_2Cl_2 1:0→1:1→1:2) gave a 1:1 mixture of $(M)_2$-(–)-**106a** and (*P,M*)-(–)-**106b** as a yellowish liquid. R_f = 0.40 (*n*-hexane).

$(P)_2$-(+)- and (*P,M*)-(+)-5,7,10,12-Tetra-*tert*-butyl-2-methyltetradeca-5,6,10,11-tetraen-3,8,13-triyn-2-ol ($(P)_2$-(+)- 107a and (*P,M*)-(+)-107b)

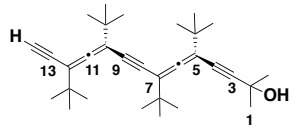

A 1:1 mixture of $(P)_2$-(+)-**106a** and (*P,M*)-(+)-**106b** (290 mg, 0.49 mmol) in THF (5 mL) was treated with 1 M nBu_4NF in THF (0.5 mL) at 0 °C and stirred for 1 h. The mixture was diluted with Et_2O, and washed with a saturated aqueous NH_4Cl solution (10 mL). The organic phase was dried over Na_2SO_4 and evaporated. FC (*n*-hexane/EtOAc 9:1) yielded a mixture of $(P)_2$-(+)-**107a** and (*P,M*)-(+)-**107b** (63 mg, 90%) as a yellow oil. *R*f = 0.20 (*n*-hexane).

Diastereoisomers $(P)_2$-(+)-**107a** and (*P*,*M*)-(+)-**107b** were separated by preparative HPLC using the CSP Chiralpak® IA (Diacel Chemical Industries Ltd.). Elution was performed with a mixture of *n*-hexane/*i*PrOH 99.6:0.4 at a flow of 18 mL/min. Under these conditions, a sample of $(P)_2$-(+)-**107a**/(*P*,*M*)-(+)-**107b** (20 mg dissolved in 2 mL of *n*-hexane) was resolved into diastereoisomers:

$(P)_2$-(+)-**107a**: t_R = 8.1 min, d.r. > 99:1, $[\alpha]_D^{20}$ = +275° (c = 1.0 in $CHCl_3$).
(*P*,*M*)-(+)-**107b**: t_R = 8.9 min, d.r. > 99:1, $[\alpha]_D^{20}$ = +84° (c = 1.0 in $CHCl_3$).

Data of $(P)_2$-(+)-**107a** : ^{1}H NMR (400 MHz, $CDCl_3$): δ H; *t*Bu), 1.13 (s, 9 H; *t*Bu), 1.15 (s, 18 H; 3 *t*Bu), 1.56 (s, 6 H; C*Me*$_2$OH), 1.97 (s, 1 H; OH), 2.99 ppm (s, 1 H; C≡C–H); ^{13}C NMR (101 MHz, $CDCl_3$): δ 28.85 (C*Me*$_3$), 28.95 (C*Me*$_3$), 29.01 (C*Me*$_3$), 29.03 (C*Me*$_3$), 31.52 and 31.53 (C*Me*$_2$OH), 35.25 (*C*Me$_3$), 35.52 (*C*Me$_3$), 35.68 (*C*Me$_3$), 35.72 (*C*Me$_3$), 65.75 (C(2)), 76.01 (C(4)), 77.74 (C(13)), 80.14 (C(14)), 85.94 (C(8)), 86.69 (C(9)), 96.96 (C(3)), 101.96 (C(5)), 102.33 (C(7)), 103.67 (C(10)), 104.24 (C(12)), 210.97 (C(6)), 211.82 ppm (C(11)); IR (ATR): $\tilde{\nu}$ = 3325 (w), 3312 (w, sh), 2950 (s), 2925 (s, sh), 2865 (m, sh), 2382 (w), 2370 (w, sh), 1549 (m), 1479 (m, sh), 1393 (w), 1362 (m), 1243 (w, sh), 1222 (w), 849 (very w), 724 (very w), 631 (m) cm^{-1}; UV/Vis (*n*-hexane): λ_{max} (ε) = 315 (3500), 301 (9700), 284 (14700), 240 (111000), 225 nm (225100 M^{-1} cm^{-1}); HR-MALDI-MS: *m*/*z* (%): 455.3284 (100, $[M + Na]^+$, calcd for $C_{31}H_{44}NaO^+$: 455.3284).

Data of (*P*,*M*)-(+)-**107b**: ^{1}H NMR (400 MHz, $CDCl_3$): δ 1.11 (s, 9 H; *t*Bu), 1.138 (s, 9 H; *t*Bu), 1.144 (s, 9 H; *t*Bu), 1.15 (s, 9 H; *t*Bu), 1.56 (s, 6 H; C*Me*$_2$OH); 1.96 (s, 1 H; OH), 2.99 ppm (s, 1 H; C≡C–H); ^{13}C NMR (101 MHz, $CDCl_3$): δ 28.83 (C*Me*$_3$), 28.94 (C*Me*$_3$), 29.02 (C*Me*$_3$), 29.04 (C*Me*$_3$), 31.51 (C*Me*$_2$OH), 35.24 (*C*Me$_3$), 35.50 (*C*Me$_3$), 35.63 (*C*Me$_3$), 35.66 (*C*Me$_3$), 65.74 (C(2)), 76.01 (C(4)), 77.74 (C(13)), 80.14 (C(14)), 85.98 (C(8)), 86.75 (C(9)), 96.95 (C(3)), 101.93 (C(5)), 102.27 (C(7)), 103.73 (C(10)), 104.31 (C(12)), 211.04 (C(6)), 211.87 ppm (C(11)); IR (ATR): $\tilde{\nu}$ = 3325 (w), 3312 (w, sh), 2950 (s), 2925 (s, sh), 2865 (m, sh), 2382 (w), 2370 (w, sh), 1549 (m), 1479 (m, sh), 1393 (w), 1362 (m), 1243 (w, sh), 1222 (w), 849 (very w), 724 (very w), 631 (m) cm^{-1}; HR-MALDI-MS: *m*/*z* (%): 455.3284 (100, $[M + Na]^+$, calcd for $C_{31}H_{44}NaO^+$: 455.3284).

(M)$_2$-(−)- and (M,P)-(−)-5,7,10,12-Tetra-*tert*-butyl-2-methyltetradeca-5,6,10,11-tetraen-3,8,13-triyn-2-ol (M)$_2$-(−)-107a and (M,P)-(−)-107b)

A 1:1 mixture of (M)$_2$-(−)-**106a** and (M,P)-(−)-**106b** (290 mg, 0.49 mmol) in THF (5 mL) was treated with 1 M nBu$_4$NF in THF (0.5 mL) at 0 °C and stirred for 1 h. The mixture was diluted with Et_2O and washed with a saturated aqueous NH_4Cl solution (10 mL). The organic phase was dried over Na_2SO_4 and evaporated. FC (SiO_2; n-hexane/EtOAc 9:1) yielded a mixture of (M)$_2$-(−)-**107a** and (M,P)-(−)-**107b** (63 mg, 90%) as a yellow oil. R_f = 0.20 (n-hexane).

(M)$_2$-(−)-**107a**: $[\alpha]_D^{20}$ = −276° (c =1.0 in $CHCl_3$), t_R = 8.2 min, d.r. > 99:1.
(M,P)-(−)-**107b**: $[\alpha]_D^{20}$ = −82° (c =1.0 in $CHCl_3$), t_R = 9.0 min, d.r. > 99:1.

(P)$_2$-(+)-3,8,10-Tri-*tert*-butyl-5-isopropyl-13-(methoxymethoxy)-13-methyltetradeca-3,4,8,9-tetraen-1,6,11-triyne ((P)$_2$-(+)-108)

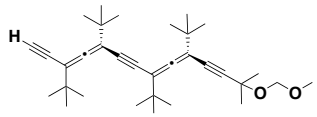

A solution of alcohol (P)$_2$-(+)-**107a** (85 mg, 0.196 mmol) in DME (0.2 mL) was treated with NaI (118 mg, 0.786 mmol), iPr$_2$NEt (190 μL, 1.08 mmol), and dropwise with MOMCl (75 μL, 0.983 mmol). The mixture was stirred for 16 h at 25 °C, diluted with a saturated Na_2CO_3 solution, and extracted with CH_2Cl_2 (3 x 20 mL). The combined organic phases were washed with brine, dried with $MgSO_4$, and the solvents were evaporated. FC (n-hexane/EtOAc 9:1) gave (P)$_2$-(+)-**108** (61 mg, 66%) as a yellowish oil. R_f = 0.64 (SiO_2; n-hexane/EtOAc 9:1). $[\alpha]_D^{20}$ = +283° (c = 0.1 in $CHCl_3$); ^{1}H NMR (400 MHz, CD_2Cl_2): δ =1.13 (s, 9 H; tBu), 1.15 (s, 18 H; tBu), 1.16 (s, 9 H; tBu), 1.53 (s, 6 H; CMe_2OH), 3.07 (s, 1 H; C≡C–H), 3.55 (s, 3 H; OMe), 4.87 ppm (s, 2 H; OCH_2O); ^{13}C NMR (101 MHz, CD_2Cl_2) δ = 28.53 (CMe_3), 28.65 (CMe_3), 28.74 (CMe_3), 28.76 (CMe_3), 29.92 and 29.97 (CMe_2O), 35.14 (CMe$_3$), 35.44 (CMe$_3$), 35.59 (CMe$_3$), 35.62 (CMe$_3$), 55.18 (OMe), 71.36 (C(2)), 77.28 (C(4)), 77.98 (C(13)), 80.37 (C(14)), 85.95 (C(8)), 86.59 (C(9)), 93.09 (OCH_2O), 94.68 (C(3)), 102.30 (C(5)), 102.75 (C(7)), 103.72 (C(10)), 104.26 (C(12)), 210.95 (C(6)), 211.71 ppm (C(11)); IR (ATR): $\tilde{\nu}$ = 3300 (w), 3290

(w), 2960 (s), 2918 (s, sh), 2865 (m, sh), 2382 (w), 2370 (w, sh), 1549 (m), 1479 (m, sh), 1393 (w), 1362 (m), 1243 (w, sh), 1222 (w), 1088 (m), 1033 (s), 1001 (m), 911 (very w), 724 (very w) cm^{-1}; HR-MALDI-MS: *m/z* (%): 499.3549 (100, $[M + Na]^+$, calcd for $C_{33}H_{48}NaO_2^+$: 499.3547). The enantiomer $(M)_2$-(–)-**108** was obtained by the same protocol: $[\alpha]_D^{20} = -284°$ (*c* = 1.0 in $CHCl_3$).

$(P)_2$-(+)-3,5,8,10-Tetra-*tert*-butyldodeca-3,4,8,9-tetraen-1,6,11-triyne($(P)_2$-(+)-109)

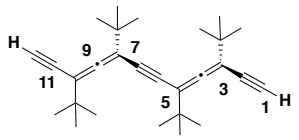

Enantiopure $(P)_2$-(+)-**107a** (10 mg, 0.023 mmol) was treated according to GPA to give $(P)_2$-(+)-**109** (8.9 mg, 81%) as a white solid. R_f = 0.62 (*n*-hexane/EtOAc 95:5); m.p. 70 °C; $[\alpha]_D^{20}$ = + 294° (*c* = 1.0 in $CHCl_3$); ^{1}H NMR (400 MHz, $CDCl_3$): δ = 1.15 (s, 36 H; 4 *t*Bu), 2.99 ppm (s, 2 H; C≡C–H); ^{13}C NMR: δ = 28.83 (2 CMe_3), 28.98 (2 CMe_3), 35.24 (2 *C*Me$_3$), 35.69 (2 *C*Me$_3$), 77.71 (C(2, 11)), 80.14 (C(1, 12), 86.29 (C(6, 7)), 101.98 (C(3, 10)), 104.18 (C(5, 8)), 211.82 ppm (C(4, 9)); IR (ATR): $\tilde{\nu}$ = 3300 (w), 2931 (s), 2365 (w), 2343 (w, sh), 2158 (m), 1715 (m), 1061 (w), 660 (s) cm^{-1}; UV/Vis (*n*-hexane): λ_{max} (ε) = 315 (2800), 301 (9300), 284 (13500), 240 (110100), 225 nm (74200 M^{-1} cm^{-1}); HR-MALDI-MS: *m/z* (%): 375.3046 (100, $[M + H]^+$, calcd for $C_{28}H_{39}^+$: 375.3046). The enantiomer $(M)_2$-(–)-**109** was obtained by the same protocol: $[\alpha]_D^{20} = -293°$ (*c* = 1.0 in $CHCl_3$).

***P*)$_4$-(+)-3,5,8,10,15,17,20,22-Octa-*tert*-butyltetracosa-3,4,8,9,15,16,20,21-octaen-1,6,11,13,18,23-hexayne ($(P)_4$-(+)-110a)**

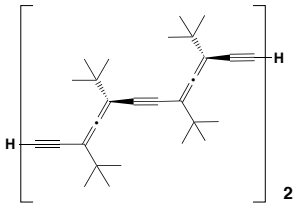

Enantiopure $(P)_4$-(+)–**105b** (10 mg, 0.011 mmol) was treated according to GPB to give $(P)_4$-(+)-**110a** (9 mg, 82%) as a white solid. R_f = 0.73 (*n*-hexane/EtOAc 95:5); m.p. 175 °C; $[\alpha]_D^{20}$ = +1029° (*c* = 1.0 in $CHCl_3$); ^{1}H NMR (400 MHz, $CDCl_3$):

δ = 1.14 (br, 72 H; 8 *t*Bu), 2.99 ppm (s, 2 H; 2 C≡C–H); ^{13}C NMR (101 MHz, $CDCl_3$): δ 28.85 (2 C*Me*$_3$), 29.01 (4 C*Me*$_3$), 29.07 (2 C*Me*$_3$), 35.28 (2 *C*Me$_3$), 35.71 (2 *C*Me$_3$), 35.89 (4 *C*Me$_3$), 75.42 (C(12, 13)), 77.22 (C(11, 14)), 77.72 (C(2, 23)), 80.16 (C(1, 24)), 86.01 (C(6, 19)), 86.73 (C(7, 18)), 102.03 (C(3, 22)), 102.66 (C(5, 20)), 104,16 (C(8, 17)), 104.63 (C(10, 15)), 211.88 (C(4, 21)), 213.47 ppm (C(9, 16)); IR (ATR): $\tilde{\nu}$ = 3298 (w), 2921 (s), 2347 (w), 2339 (w, sh), 2152 (m), 1715 (m), 1061(w), 668 (s) cm^{-1}; UV/Vis (*n*-hexane): λ_{max} (ε) = 315 (10100), 301 (29000), 284 (43600), 240 (332900), 225 nm (224500 M^{-1} cm^{-1}); HR-MALDI-MS: *m/z* (%): 746.5784 (100, [M]$^+$, calcd for $C_{56}H_{74}^+$: 746.5791). The enantiomer (M)$_4$-(–)-**110a** was obtained by the same protocol: $[\alpha]_D^{20}$ = –1029° (*c* = 1.0 in $CHCl_3$).

(*P*)$_4$-(+)-5,7,10,12,17,19,22,24-Octa-*tert*-butyl-2-methylhexacosa-5,6,10,11,17,18, 22,23-octaen-3,8,13,15,20,25-hexayn-2-ol ((*P*)$_4$-(+)-110b)

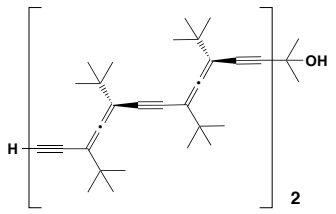

Enantiopure (*P*)$_4$-(+)–**105b** (10 mg, 0.011 mmol) was treated according to GPA to give (*P*,*P*,*P*,*P*)-(+)-**110b** (9 mg, 86%) as a white solid. R_f = 0.42 (*n*-hexane/EtOAc 95:5); m.p. 108 °C; $[\alpha]_D^{20}$ = +994°; ^{1}H NMR (400 MHz, $CDCl_3$): δ – *m*, 72 H; *t*Bu), 1.55 (s, 12 H; C*Me*$_2$OH), 1.96 (s, 1 H; OH), 2.99 ppm (s, 2H; C≡C–H); ^{13}C NMR (101 MHz, $CDCl_3$): δ 28.85 (C*Me*$_3$), 28,96 (C*Me*$_3$), 29.01 (3 C*Me*$_3$), 29.04 (C*Me*$_3$), 29.07 (C*Me*$_3$), 31.53 (C*Me*$_2$OH), 35.28 (2 *C*Me$_3$), 35.53 (2 *C*Me$_3$), 35.68 (2 *C*Me$_3$), 35.89 (2 *C*Me$_3$), 65.76 (C(2)), 75.43 (C(14, 15)), 76.02 (C(4)) 77.22 (C(13, 16)), 77.72 (C(25)), 80.17 (C(26)), 85.66 and 86.01 (C(8, 21)), 86.73 and 87.12 (C(9, 20)), 96.95 (C(3)), 102.03 (C(24)), 102.37 (C(22)), 102.62 and 102.66 (C(12, 17)), 103.65 (C(7)), 104.16 (C(5)), 104.63 and 104.68 (C(10, 19)), 211.03 (C(11, 18)), 213.47 ppm (C(6, 23)); IR (ATR): $\tilde{\nu}$ = 3325 (w), 2949 (s), 2918 (m, sh), 2864 (w, sh), 2351 (very w), 2347 (very w, sh), 1912 (very w), 1736 (very w), 1453 (m), 1445(m, sh), 1373 (s), 1213 (m), 10632(m), 948 (m), 664 (m) cm^{-1}; UV/Vis (*n*-hexane): λ_{max} (ε) = 315 (10500), 301 (29100), 284 (43900), 240 (332900), 225 nm (225100 M^{-1} cm^{-1}); HR-MALDI-MS: *m/z* (%): 804.6210 (100,

[M]$^+$, calcd for $C_{59}H_{80}O^+$: 804.6209). The enantiomer $(M)_4$-(–)-**110b** was obtained by the same protocol: $[\alpha]_D^{20} = -993°$ (c = 1.0 in $CHCl_3$).

(±)-5,7-Bis[2-(methoxymethoxy)propan-2-yl]-2-methylnona-5,6-dien-3,8-diyn-2-ol [(±)-114]

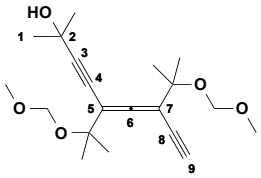

Tetra-*n*-butylammonium fluoride (1M in THF, 0.55 mL, 0.55 mmol) was slowly added to (±)-**121** (277 mg, 0.55 mmol) in THF (10 mL). After 2 h of stirring, the solution was concentrated. FC (SiO_2; cyclohexane/EtOAc 3:2) gave (±)-**114** (177 mg, 92%) as an amber oil. R_f = 0.56 (SiO_2; cyclohexane/EtOAc 1:1). ^{1}H NMR (400 MHz, $CDCl_3$): δ =1.41–1.46 (m, 12H; $C(CH_3)_2OMOM$), 1.54 (s, 6H; $C(CH_3)_2OH$), 2.22 (s, 1 H; OH), 3.07 (s, 1H; C≡CH) 3.39 (s, 6H; OCH_3), 4.72 (2× s, 2 H; OCH_2O), 4.74 (s, 2 H; OCH_2O). ^{13}C NMR (100 MHz, $CDCl_3$): δ = 26.8, 26.9, 27.1, 27.3 ($C(CH_3)_2OMOM$), 31.5 (C1), 55.7 (2×, OCH_3), 65.7 (C2), 73.9 (C8), 75.8 (C4), 77.3, 77.4 ($C(CH_3)_2OMOM$), 82.1 (C9), 92.4 (2×, OCH_2O), 99.2 (C3), 99.8 (C7), 100.8 (C5), 214.3 (C6) ppm. IR (ATR): $\tilde{\nu}$ (br. w), 3284 (br. w), 2982 (m), 2935 (w, sh), 1463 (br. w), 1382 (w, sh), 1365 (m), 1228 (br. m), 1144 (s), 1086 (m), 1029 (s), 994 (m), 961 (m), 921 (m), 829 (w), 755 (w), 699 (w), 662 (w) cm^{-1}. HR-ESI-MS: m/z (%): 373.1981 (18, [M + Na]$^+$, calcd for $C_{20}H_{30}NaO_5^+$: 373.1985), 274.1879 (11), 273.1849 (56, [M – OMOM – OH + H]$^+$, calcd for $C_{18}H_{25}O_2^+$: 273.1849), 260.1729 (18), 259.1691 (100, [M – OMOM – OMe + H]$^+$, calcd for $C_{17}H_{23}O_2^+$: 259.1693).

Enantiomers (*P*)-(+)-**114** and (*M*)-(–)-**114** were resolved by preparative HPLC using the chiral stationary phase Chiralpack® IA (Diacel Chemical Industries Ltd.). Aliquots of 2 mL of a solution of (±)-**15** in hexanes (8.3 mg/mL) were injected and eluted with hexanes/iPrOH 98:2 at a flow rate of 18 mL min^{-1}.

(*P*)-(+)-**114**: t_R = 11.7 min; e.r. > 99:1 $[\alpha]_D^{20} = +71°$ (c = 1.0 in CH_3CN).

(*M*)-(–)-**115**: t_R = 13.8 min; e.r. >99.1 $[\alpha]_D^{20} = -71°$ (c = 1.0 in CH_3CN).

Ethyl 2-(methoxymethoxy)-2-methylpropanoate (116)[229]

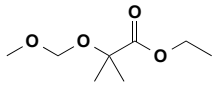

Under a N_2 atmosphere, ethyl 2-hydroxy-2-methylpropanoate (**115**) (4.49 g, 34.0 mmol) dissolved in 10 mL Et_2O was added dropwise over 10 min. to a dispersion of sodium hydride (60% w/w in mineral oil, 1.50 g, 37.5 mmol) in 25 mL Et_2O cooled at 0 ºC. The mixture was stirred for 5 min., after which MOM chloride (2.60 mL, 34.0 mmol) was added dropwise over 5 min. After stirring for 1.5 h at rt. the mixture was treated with 20 mL H_2O and the aqueous layer was extracted with Et_2O (3×, 30 mL). The combined organic phases were dried over $MgSO_4$ and evaporated. FC (SiO_2; pentane/Et_2O 8:1) afforded **116** (4.12 g, 69%) as a colorless volatile liquid. R_f = 0.41 (SiO_2; pentane/Et_2O 9:1). Spectroscopy properties of **1165** were identical to those previously reported.[229]

***N*-Methoxy-2-(methoxymethoxy)-*N*,2-dimethylpropanamide (117)**[230]

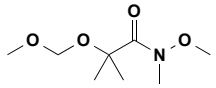

Under a N_2 atmosphere, *N,O*-dimethylhydroxylamine hydrochloride (3.13 g, 32.1 mmol) was added to a stirred solution of **116** (3.77 g, 21.4 mmol) in THF (40 mL). Whilst cooled at –20 ºC, isopropylmagnesium chloride (2 M in THF, 32 mL, 64 mmol) was added dropwise over 15 min. The solution was stirred for an additional 45 min. maintaining the temperature below –10 ºC. The mixture was treated with a saturated aqueous NH_4Cl solution (20 mL) and extracted with Et_2O (3×, 35 mL). The combined organic phases were dried over $MgSO_4$ and evaporated. FC (SiO_2; CH_2Cl_2/Et_2O 9:1) gave **117** (3.57 g, 87%) as a colorless volatile liquid. R_f = 0.42 (SiO_2; CH_2Cl_2/Et_2O 9:1 Spectroscopy properties of **117** were identical to those previously reported.[230]

5,5,9,9-Tetramethyl-2,4,10,12-tetraoxatridec-7-yn-6-one (118)

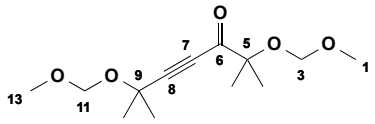

Under a N_2 atmosphere, n-butyllithium (1.6 M in hexanes, 6.3 mL, 10.1 mmol) was added dropwise to 3-(methoxymethoxy)-3-methylbut-1-yne (1.29 g, 10.1 mmol) in THF (25 mL) at –78 ºC. The solution was stirred for 15 min. at –78 ºC and then for 15 min. at rt., after which **117** (1.75 g, 9.15 mmol) in THF (5 mL) was added dropwise at –78 ºC. The solution was further stirred for 16 h upon which the temperature was allowed to increase to rt. The solution was treated with a saturated aqueous NH_4Cl solution (25 mL) and the aqueous layer was extracted with Et_2O (3×, 30 mL). The combined organic phases were dried over $MgSO_4$ and evaporated. FC (SiO_2; pentane/Et_2O 4:1) afforded **118** (1.87 g, 79%) as a colorless volatile liquid. R_f = 0.41 (SiO_2; pentane/Et_2O 4:1); ^{1}H NMR (400 MHz, $CDCl_3$): δ = 1.44 (s, 6 H; C5$(CH_3)_2$), 1.58 (s, 6 H; C9$(CH_3)_2$), 3.40 (s, 3 H; OC1H_3), 3.41 (s, 3 H; OC13H_3), 4.72 (s, 2H; OC3H_2O), 4.90 (s, 2H; OC11H_2O); ^{13}C NMR (100 MHz, $CDCl_3$): δ = 23.7 (C5(CH_3)$_2$), 29.5 (C9(CH_3)$_2$), 55.8, (C1) 56.2 (C13), 70.8 (C9), 81.6 (C5), 81.8 (C7), 92.8 (C3), 93.5 (C11), 96.3 (C8), 190.1 (C6) ppm; IR (ATR): ν = 2988 (w), 2936 (w), 2824 (w, sh), 2216 (w), 1682 (m), 1464 (w), 1380 (w), 1364 (w), 1268 (w), 1236 (w), 1213 (w), 1144 (s), 1086 (s), 1026 (s), 1000 (m, sh), 921 (s), 741 (m) cm^{-1}; HR-ESI-MS: m/z (%): 198.1202 (11), 197.1166 (100, [*M* – OMOM]$^+$, calcd for $C_{11}H_{18}O_3^+$: 197.1172).

(±)-5,5,9,9-Tetramethyl-6-[(triisopropylsilyl)ethynyl]-2,4,10,12-tetraoxatridec-7-yn-6-ol [(±)-119]

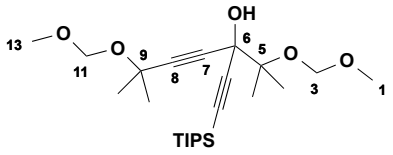

Under a N_2 atmosphere, n-butyllithium (1.6 M in hexanes, 4.5 mL, 7.2 mmol) was added dropwise to ethynyltriisopropylsilane (1.6 mL, 7.2 mmol) in THF (25 mL) at –78 ºC. The solution was stirred for 15 min. at –78 ºC and then for 15 min. at rt., after which **118** (1.68 g, 6.50 mmol) dissolved in THF (5 mL) was added dropwise at

–78 ºC. The solution was further stirred for 16 h upon which the temperature was allowed to increase to r.t. The solution was treated with a saturated aqueous NH_4Cl solution (25 mL), and the aqueous layer was extracted with Et_2O (3 x 30 mL). The combined organic phases were dried over $MgSO_4$ and evaporated. FC (SiO_2; pentane/Et_2O 4:1) afforded (±)-**119** (2.75 g, 96%) as a colorless oil. R_f = 0.39 (SiO_2; cyclohexane/EtOAc 4:1); ^{1}H NMR (400 MHz, $CDCl_3$): δ = 1.08 (s, 21 H; TIPS), 1.48 (s, 3 H; C5(CH_3)), 1.50 (s, 3H; C5(CH_3)), 1.51 (s, 6 H; C9(CH_3)$_2$), 3.37 (s, 3 H; OC1H_3), 3.45 (s, 3H; OC13H_3), 4.25 (s, 1H; OH), 4.78 (s, 2H; OC3H_2O), 4.89 (s, 2 H; OC11H_2O); ^{13}C NMR (100 MHz, $CDCl_3$): δ = 11.4 (Si*C*H(CH_3)$_2$), 18.7 (SiCH(*C*H_3)$_2$), 22.0, 22.6 (C5*C*H_3), 27.1, 30.0 (C9(*C*H_3)$_2$), 55.6 (C1), 55.9 (C13), 70.8 (C6-*C*≡C-TIPS), 71.0 (C9), 82.4 (C5), 84.1 (C7), 85.8 (2×, C8, C6-C≡*C*-TIPS), 91.6 (C3), 93.4 (C11), 106.1 (C6) ppm; IR (ATR): ν = 3378 (br. w), 2942 (m), 2892 (w, sh), 2866 (m), 1463 (m), 1380 (m), 1363 (m), 1252 (m), 1144 (s), 1090 (s), 1069 (s), 1029 (s), 999 (m, sh), 920 (m), 882 (m), 800 (w), 749 (w), 705 (w), 674 (m), 659 (w, sh) cm^{-1}; HR-ESI-MS: m/z (%): 463.2853 (5, [*M* + Na]$^+$, calcd for $C_{24}H_{44}NaO_5Si^+$: 463.2850), 393.2824 (9, [*M*–OMe–OH + H]$^+$, calcd for $C_{23}H_{41}O_3Si^+$: 393.2819), 365.2734 (6), 364.2740 (28), 363.2712 (100, [*M* – OMOM – OH + H]$^+$, calcd for $C_{22}H_{39}O_2Si^+$: 363.2714).

(±)-5,5,9,9-Tetramethyl-6-[(triisopropylsilyl)ethynyl]-2,4,10,12-tetraoxatridec-7-yn-6-yl 2,3,4,5,6-pentafluorobenzoate [(±)-120]

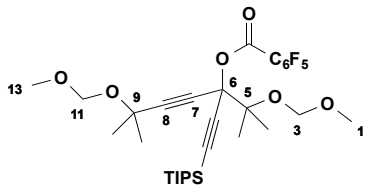

Under a N_2 atmosphere, lithium bis(trimethylsilyl)amide (1M in THF, 6.9 mL, 6.9 mmol) was added dropwise to (±)-**119** (2.75 g, mmol) in THF (40 mL) at –78 ºC. The solution was stirred for 15 min. at –78 ºC and then for 15 min. at r.t., after which 2,3,4,5,6-pentafluorobenzoyl chloride (0.95 mL, 6.9 mmol) was added at –78 ºC. The solution was further stirred for 16 h upon which the temperature was allowed to increase to r.t. The solution was treated with a saturated aqueous NH_4Cl solution (25 mL), and the aqueous layer was extracted with Et_2O (3×, 30 mL). The

aqueous layer was extracted with Et_2O (3×, 30 mL), and the combined organic phases were dried over $MgSO_4$ and evaporated. FC (SiO_2; pentane/Et_2O 9:1) afforded (±)-**120** (3.19 g, 81%) as a colorless oil. R_f = 0.43 (SiO_2; pentane/Et_2O 9:1). ^{1}H NMR (400 MHz, $CDCl_3$): δ = 1.08 (s, 21 H; TIPS), 1.52 (s, 6 H; C5(CH_3)), 1.56 (s, 6H; C9(CH_3)$_2$), 3.38 (s, 3 H; OC1H_3), 3.38 (s, 3 H; OC13H_3), 4.83 (s, 2H; OC3H_2O), 4.90 (2× s, 2H; OC11H_2O). ^{13}C NMR (100 MHz, $CDCl_3$): δ = 11.3 (Si*C*H(CH_3)$_2$), 18.6 (SiCH(*C*H_3)$_2$), 22.0, 22.3 (C5*C*H_3), 29.8 (C9(*C*H_3)$_2$), 55.4 (C1), 55.7 (C13), 70.9 (C9), 76.6 (C6-*C*≡C–TIPS), 79.9 (C7), 80.9 (C5), 89.1 (C8), 89.8 (C6-C≡*C*–TIPS), 91.9 (C3), 93.5 (C11), 101.0 (C6), 108.6 (*C*-C=O), 136.6, 139.1, 142.0, 144.2, 146.9 (CF), 155.7 (C=O) ppm. IR (ATR): $\tilde{\nu}$ = 2944 (m), 2893 (w, sh), 2867 (m), 1757 (m), 1652 (w), 1522 (m, sh), 1505 (s), 1464 (m), 1422 (w, sh), 1382 (w), 1366 (w), 1327 (m), 1259 (w, sh), 1213 (s), 1142 (s), 1091 (m), 1065 (m, sh), 1031 (s), 999 (s), 968 (m, sh), 941 (w, sh), 919 (m), 882 (m), 804 (m), 727 (m), 709 (w, sh), 695 (w, sh), 676 (m), 660 (w, sh) cm^{-1}. HR-ESI-MS: m/z (%): 364.2738 (30), 363.2714 (100 [*M* – $COOC_6F_5$ – OMOM + H]$^+$, calcd for $C_{22}H_{39}O_2Si^+$: 363.2714.

(±)-5,7-Bis[2-(methoxymethoxy)propan-2-yl]-2-methyl-9-(triisopropylsilyl)nona-5,6-dien-3,8-diyn-2-ol [(±)-121]

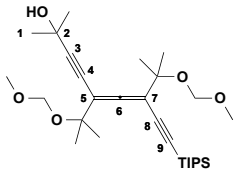

Under a N_2 atmosphere, bis(triphenylphosphine)palladium(II) dichloride (56 mg, 10 mol%), copper(I) iodide (15 mg, 10 mol%), *N*,*N*-diisopropylethylamine (0.27 mL, 1.6 mmol) and 2-methylbut-3-yn-2-ol (0.16 mL, 1.6 mmol) were added consecutively to (±)-**120** (0.51 g, 0.80 mmol) in degassed toluene (20 mL). After stirring for 16 h at 60 ºC, the solution was treated with a saturated aqueous NH_4Cl solution (10 mL). The aqueous layer was extracted with Et_2O (3×, 25 mL), and the combined organic phases were dried over $MgSO_4$ and evaporated. FC (SiO_2; cyclohexane/EtOAc 3:1) afforded (±)-**121** (0.28 g, 69%) as an amber oil. R_f = 0.32 (SiO_2; cyclohexane/EtOAc 3:1); ^{1}H NMR (400 MHz, $CDCl_3$): δ = 1.08 (s, 21 H; TIPS), 1.37–1.50 (m, 12H; C(CH_3)$_2$OMOM), 1.55 (s, 6H; C(CH_3)$_2$OH), 2.25 (s, 1H;

OH), 3.38 (2× s, 6 H; OCH_3), 4.67-4.79 (m, 4 H; OCH_2O); ^{13}C NMR (100 MHz, $CDCl_3$): δ = 11.5 (Si*C*H(CH_3)$_2$), 18.8 (SiCH(*C*H_3)$_2$), 26.9 (2×), 27.3, 27.5 (C(*C*H_3)$_2$OMOM), 31.5 (C1), 55.6, 55.8 (OCH_3), 65.8 (C2), 74.3 (C8), 77.4 (2×, *C*(CH_3)$_2$OMOM), 92.4, 92.5 (OCH_2O), 96.7 (C9), 98.2 (C4), 98.7 (C3), 100.0 (C7), 101.1 (C5), 214.6 (C6) ppm; IR (ATR): $\tilde{\nu}$ (br. w), 2941 (m), 2866 (m), 2143 (w), 1463 (m), 1381 (m), 1364 (m), 1229 (br. m), 1144 (s), 1087 (m), 1031 (s), 994 (m), 961 (w), 920 (m), 882 (m), 810 (w), 758 (w), 728 (m), 676 (m) cm^{-1}; HR-ESI-MS: m/z (%): 525.3793 (18), 524.3758 (45, $[M + NH_4]^+$, calcd for $C_{29}H_{54}NO_5Si^+$: 524.3766), 416.3055 (33), 415.3024 (100, $[M - OMOM - OMe + H]^+$, calcd for $C_{26}H_{43}O_2Si^+$: 415.3027).

(6*M*,13*M*)-(–)-5,7,12,14-Tetrakis[2-(methoxymethoxy)propan-2-yl]-2,17-dimethyloctadeca-5,6,12,13-tetraen-3,8,10,15-tetrayne-2,17-diol [(*M*,*M*)-(–)-122]

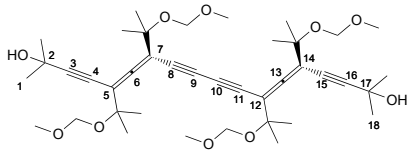

Tetramethylethylenediamine (7.0 mL, 47 mmol) was added to copper(I) chloride (1.20 g, 12.1 mmol) in acetone (40 mL). The solution was stirred for 30 min, filtered and added to (*M*)-(–)-**114** (120 mg, 0.34 mmol) in acetone (10 mL). The resulting mixture was purged with air, stirred for 2 h, filtered over Celite, and the solvent was evaporated. FC (SiO_2; cyclohexane/EtOAc 7:3) afforded (*M*,*M*)-(–)-**122** (109 mg, 91%) as an amber oil. R_f = 0.49 (SiO_2; cyclohexane/EtOAc 7:3), $[\alpha]_D^{20}$ = – 268° (*c* = 1.0 in CH_3CN); ^1H NMR (400 MHz, $CDCl_3$): δ = 1.43-1.46 (m, 24H; C(CH_3)$_2$OMOM), 1.54 (s, 12H; C(C*H*$_3$)$_2$OH), 2.19 (br. s, 2H; OH), 3.39 (2× s, 12H; OCH_3), 4.69–4.74 (m, 8H; OCH_2O); ^{13}C NMR (100 MHz, $CDCl_3$): δ = 26.7, 27.0, 27.3, 27.4 (C(*C*H_3)$_2$OMOM), 31.4 (C1, C18), 55.7 (2×, OCH_3), 65.7 (C2, C17), 73.7 (C9, C10), 74.2 (C8, C11), 77.4, 77.7 (*C*(CH_3)$_2$OMOM), 78.2 (C4, C15), 92.4 (2×, OCH_2O), 99.7 (C3, C16), 100.3 (C7, C12), 101.5 (C5, C14), 215.7 (C6, C13) ppm; IR (ATR): $\tilde{\nu}$ 3433 (br. w), 2982 (m), 2934 (w, sh), 1463 (w), 1382 (m), 1365 (m), 1231 (br. m), 1144 (s), 1086 (m), 1030 (s), 995 (m), 961 (w), 921 (m), 809 (br. w), 752 (w) cm^{-1}; HR-ESI-MS: m/z (%): 718.4428 (15), 717.4401 (53), 716.4372

(100, $[M + NH_4]^+$, calcd for $C_{40}H_{62}NO_{10}^+$: 716.4368). Enantiomer (*P*,*P*)-(–)-**122** was prepared identically, starting from (*P*) -(+)-**15**; $[\alpha]_D^{20}$ = + 268° (*c* = 1.0 in CH_3CN).

(6*M*,13*M*)-(–)-5,7,12,14-Tetrakis[2-(methoxymethoxy)propan-2-yl]-2-methylhexadeca-5,6,12,13-tetraen-3,8,10,15-tetrayn-2-ol [(*M*,*M*)-(–)-123]

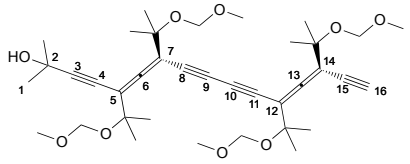

(7*M*,14*M*)-(–)-6,15-diethynyl-8,13-bis[2-(methoxymethoxy)propan-2-yl]-5,5,16,16-tetramethyl-2,4,17,19-tetraoxaicosa-6,7,13,14-tetraen-9,11-diyne [(*M*,*M*)-(–)-124]

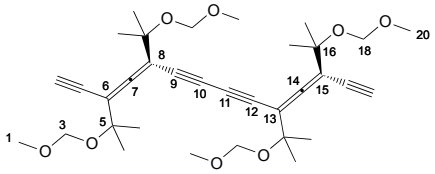

Under a N_2 atmosphere, (*M*,*M*)-(–)-**114** (96 mg, 0.14 mmol) in toluene (5 mL) was added to sodium hydroxide powder (33 mg, 0.83 mmol). The solution was heated under reflux for 3 h, after which TLC analysis indicated full consumption of the starting material. The solution was diluted with brine (5 mL) and extracted with Et_2O (3 × 10 mL). The combined extracts were dried over $MgSO_4$ and evaporated. FC (SiO_2; cyclohexane/EtOAc 7:3) afforded (*M*,*M*)-(–)-**123** (18 mg, 20%) and (*M*,*M*)-(–)-**124** (46 mg, 57%) as amber oils.

Data for (*M*,*M*)-(–)-**123**: R_f = 0.49 (SiO_2; cyclohexane/EtOAc 7:3), $[\alpha]_D^{20}$ = –180° (*c* = 1.0 in CH_3CN). ^1H NMR (400 MHz, $CDCl_3$): δ = 1.42-1.44 (m, 24 H; $C(CH_3)_2$), 3.10 (s, 2 H; C≡CH), 3.39 (2× s, 12 H; OCH_3), 4.71-4.76 (m, 8H; OCH_2O). ^{13}C NMR (100 MHz, $CDCl_3$): 26.6, 26.9, 27.3, 27.4 ($C(CH_3)_2OMOM$), 55.7 (OCH_3), 73.9, 75.2 (C9-C12), 77.4, 77.7 ($C(CH_3)_2OMOM$), 78.4 (*C*≡CH), 82.9 (C≡*C*H), 92.4 (2×, OCH_2O), 100.9, 101.1 (C6, C8, C13, C15), 216.2 (C7, C14) ppm. IR (ATR): $\tilde{\nu}$ 3288 (br. w), 2983 (m), 2934 (m, sh), 1929 (w), 1463 (m), 1382 (m), 1365 (m), 1228 (m), 1200 (m), 1142 (s), 1085 (m), 1025 (s), 994 (s), 919 (m),

807 (br. w), 734 (w), 708 (w), 660 (w) cm^{-1}. HR-ESI-MS: m/z (%): 601.3567 (39), 600.3531 (100, $[M + NH_4]^+$, calcd for $C_{34}H_{50}NO_8^+$: 600.3531).

Enantiomers (*P*,*P*)-(+)-**123** were prepared identically, starting from (*P*,*P*)-(+)-**114**; $[\alpha]_D^{20} = + 179°$ (*c* = 1.0 in CH_3CN).

Data for (*M*,*M*)-(–)-**124**: R_f = 0.21 (SiO_2; cyclohexane/EtOAc 7:3), $[\alpha]_D^{20} = - 210°$ (*c* = 1.0 in CH_3CN); ^1H NMR (400 MHz, $CDCl_3$): δ = 1.45-1.46 (m, 24H; $C(CH_3)_2OMOM$), 1.54 (s, 12H; $C(CH_3)_2OH$), 2.21 (s, 1H; OH), 3.10 (s, 1H; C≡CH), 3.39 (s, 12H; OCH_3), 4.6-4.76 (m, 8H; OCH_2O). ^{13}C NMR (100 MHz, $CDCl_3$): δ = 26.7 (2×), 26.9, 27.0, 27.3, 27.4 (2×) ($C(CH_3)_2OMOM$), 31.4 (C1), 55.7 (2×, OCH_3), 65.7 (C3), 73.6, 73.8, 74.3, 75.2 (C8-C11), 77.4 (2×), 77.7 (2×) ($C(CH_3)_2OMOM$), 78.2, 78.5 (C4, C15), 82.9 (C16), 92.4 (2×, OCH_2O), 99.8 (C2), 100.3, 100.9, 101.0, 101.5 (C5, C7, C12, C14), 215.7, 216.2 (C6, C13) ppm. IR (ATR): $\tilde{\nu}$ 3440 (br. w), 3286 (br. w), 2982 (m), 2934 (m, sh), 1463 (br. m), 1382 (m), 1365 (m), 1230 (br. m), 1144 (s), 1086 (m), 1030 (s), 995 (m), 961 (w), 921 (m), 808 (w), 724 (w), 660 (w) cm^{-1}. HR-ESI-MS: m/z (%): 660.4011 (11), 659.3979 (39), 658.3942 (100, $[M + NH_4]^+$, calcd for $C_{37}H_{56}NO_9^+$: 658.3950).

Enantiomers (*P*,*P*)-(+)-**124** were prepared identically, starting from (*P*,*P*)-(+)-**114**; $[\alpha]_D^{20} = + 210°$ (*c* = 1.0 in CH_3CN).

(2*P*,9*P*,16*P*,23*O*)-1,3,8,10,15,17,22,24-octakis(2-(methoxymethoxy)propan-2-yl)cyclo octacosa-1,2,8,9,15,16,22,23-octaen-4,6,11,13,18,20,25,27-octayne [(*P*,*P*,*P*,*P*)-(+)-125].

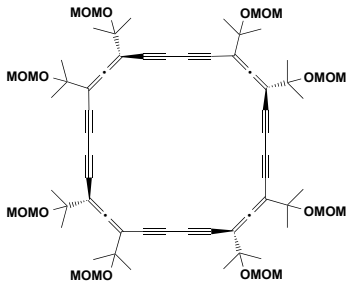

A solution of CuCl (211 mg, 2.13 mmol) and $CuCl_2$ (28.7 mg, 0.213 mmol) in dry pyridine (10^{-4} mol/L) was degassed by bubbling argon through for 60 min. Tetrameric allene *(P)*$_4$-(+)-**124** (10 mg, 0.01 mmol) in dry, degassed pyridine (10 mL) was added over a period of 20 h. The mixture was stirred for an additional 3 h, and

pyridine was evaporated. The remaining solid in saturated aqueous NH_4Cl solution (20 mL) was extracted with pentane. The organic phase was dried over Na_2SO_4 and evaporated to dryness. Flash chromatography (FC; cyclohexane) gave $(P)_4$-(−)-**125** as a white solid (5 mg, 52 %). R_f = 0.52 (SiO_2; *n*-hexane); m.p. > 200 °C; $[\alpha]_D^{20}$ = –729° (*c* = 1.0 in $CHCl_3$); ^{1}H NMR (400 MHz, CD_2Cl_2): δ 1.43 (s, 48 H; OCH_3); 3.36 (s, 24 H; OCH_3), 4.67-4.72 ppm (m, 16H, OCH_2O); ^{13}C NMR (CD_2Cl_2, 101 MHz): δ 26.50, 26.93, 55.36, 73.98, 74.09, 74.28, 77.13, 78.39, 92.20, 101.54, 218.49 ppm. IR (ATR): $\tilde{\nu}$ = 2964 (m), 2903 (s), 2867 (m), 1459 (m), 1393 (w), 1363 (w), 1222 (m), 1077 (s) cm^{-1}; UV/Vis (*n*-hexane): λ_{max} (ε) = 321 (10000), 303 (26500), 285 (42600), 240 (331000), 227 nm (237000 M^{-1} cm^{-1}); HR-MALDI-MS: *m/z* (%): 1180.6556 (10), 1179.6483 (39), 1178.6613 (100, $[M + NH_4]^+$, calcd for $C_{68}H_{92}NO_{16}^+$: 1178.6611).

The enantiomer $(M)_4$-(+)-**84** was obtained by the same protocol: $[\alpha]_D^{20}$ = +730° (*c* = 1.0 in $CHCl_3$).

2-(1,3-Dioxo-1*H*-inden-2(3*H*)-ylidene)malononitrile (DCID, 127)[149]

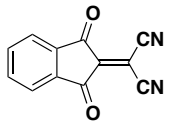

A mechanically stirred solution of ninhydrin (32.0 g, 0.18 mol) in hot water (800 mL) was treated with a solution of malononitrile (32.0 g, 0.48 mol) in hot water (500 mL). A yellow precipitate formed quickly. The mixture was kept at reflux for 5 min and cooled to room temperature. The product was filtered off, dried in the air, and crystallized from acetonitrile to yield compound **127** (26.0 g, 70%) as shining yellow plates. Analytical data of **127** matched those of the literature.[149]

(*E*)-2-{1,4-Bis[4-(Dimethylamino)phenyl]-4-[1,3-dioxo-1*H*-inden-2(3*H*)-ylidene)but-2-en-1-ylidene}malononitrile (130) and **2-{2-[4-(Dimethylamino) phenyl]-2-[1,3-dioxo-1*H*-inden-2(3*H*)-ylidene]ethylidene}malononitrile (131)**

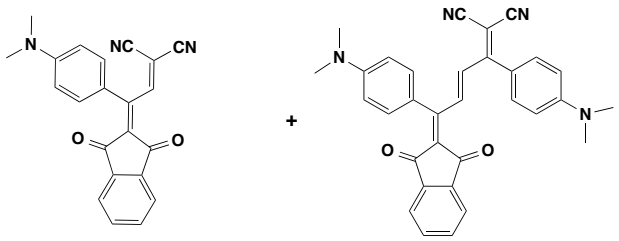

2-(1,3-Dioxo-1*H*-inden-2(3*H*)-ylidene)malononitrile (68 mg, 0.33 mmol) was added to a solution of 4-ethynyl-*N*,*N*-dimethylaniline (50 mg, 0.34 mmol) in $(CH_2Cl)_2$. The mixture was stirred for 30 min at 25 °C. Evaporation and FC (SiO_2; *n*-hexane/EtOAc 8/2) afforded two fractions, A and B. Concentration of fraction A (R_f = 0.50, (SiO_2; *n*-hexane/EtOAc 6:4)) gave **130** (99 mg, 85%) as a blue solid and B (R_f = 0.30, (SiO_2; *n*-hexane/EtOAc 6:4)) gave **131** (16 mg, 10%) as a red metallic solid, respectively.

Data of **130**: m.p > 200 °C; ^{1}H NMR (400 MHz, CD_2Cl_2): δ 3.09 6 H; NMe_2), 6.71 (d, J = 8 Hz, 2 H), 7.74 (m, J = 8 Hz, 3 H), 7.89-7.92 (m, 2 H), 7.97–8.00 (m, 1 H), 8.06–8.09 ppm (m, 1 H); ^{13}C NMR (101 MHz, CD_2Cl_2): 39.86, 75.02, 111.35, 114.38, 114.81, 118.93, 123.84, 123.88, 131.41, 136.33, 136.37, 136.44, 136.81, 137.19, 141.20, 142.47, 153.82, 163.73, 186.39, 186.86 ppm; IR (ATR): $\tilde{\nu}$ = 3049 (m), 2918 (w), 2898(w), 2215 (s), 1736 (m), 1701 (s), 1601 (s), 1489 (s), 1436 (m), 1376 (s), 1205 (s), 1173 (s), 977 (m), 943 (m), 818 (s), 739 cm^{-1} (s); UV/Vis (CH_2Cl_2): λ_{max} (ε) = 444 (15000), 391 (15800), 326 (11000), 309 nm (10000 M^{-1} cm^{-1}); HR-MALDI-MS: *m/z* (%): 354.1166 (100, [*M* + H]$^+$, calcd for $C_{22}H_{16}N_3O_2^+$: 354.1164).

Data of **131**: m.p > 200 °C; ^{1}H NMR (400 MHz, CD_2Cl_2): δ 3.21 12 H; NMe_2), 6.81 (d, J = 4 Hz, 4 H), 7.51 (d, J = 8 Hz, 4 H), 7.83 (d, J = 12 Hz, 2 H), 7.91–7.96 (m, 2 H), 8.85 ppm (s, 2 H); ^{13}C NMR (101 MHz, CD_2Cl_2): δ 30.26, 40.62, 94.90, 110.90, 111.49, 113.60, 121.67, 123.12, 123.44, 125.50, 135.82, 140.89, 142.93, 149.98, 154.52, 166.35, 187.60, 191.64 ppm; IR

(ATR): $\tilde{\nu}$ = 3050 (m), 2922 (w), 2890 (w), 2213 (s), 1736 (m), 1698 (s), 1599 (s), 1488 (s), 1436 (m), 1378 (s), 1208 (s), 1170 (s), 976 (m), 944 (m), 818 (s), 735 cm^{-1} (s); UV/Vis (CH_2Cl_2): λ_{max} (ε) = 596 (30400), 356 (43065), 279 nm (42600 M^{-1} cm^{-1}); HR-MALDI-MS: *m*/*z* (%): 499.2128 (100, [*M* + H]$^+$, calcd for $C_{32}H_{27}N_4O_2^+$: 498.2129).

4,4'-Ethynylenebis(*N*,*N*-dimethylaniline) (132)[136]

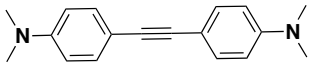

A solution of (trimethylsilyl)diazomethane (3.72 mL of a 2.0 M solution in Et_2O, 7.45 mmol) in Et_2O (50 mL) was cooled to 0 °C. *n*-BuLi (4.65 mL of a 1.6 M solution in *n*-hexane, 7.45 mmol) was added dropwise and stirred for an additional 1 h at 0 °C. A solution of Michler's ketone (1.0 g, 3.73 mmol) in THF (20 mL) was added to this solution. The resulting mixture was warmed to room temperature, stirred for 2 h, quenched with saturated NH_4Cl solution (100 mL), and the aqueous layer extracted with dichloromethane (3 x 50 mL). The combined organic layers were dried over Na_2SO_4 and the solvent removed to give **132** (0.852 g, 86%) as a yellow solid. Analytical data of **132** matched those of the literature.[136]

2-{1,2-Bis[4-(dimethylamino)phenyl]-3,3-diisocyanoallylidene}-1*H*-indene-1,3(2*H*)-dione (133a) and **2,3-Bis[4-(Dimethylamino)phenyl]-5-oxoindeno[1,2-*b*]pyran-4,4(5*H*)-dicarbonitrile (133b)**

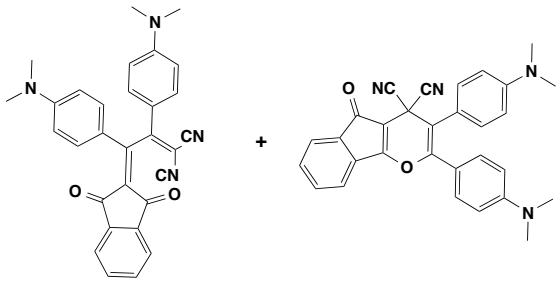

4,4'-Ethynylenebis(*N*,*N*-dimethylaniline) (42 mg, 0.16 mmol) was treated according to GPE. Evaporation of the solvent in vacuo and FC (SiO_2; *n*-hexane:EtOAc 8/2) afforded two fractions, A and B. Concentration of fraction A (R_f = 0.29, (SiO_2; *n*-hexane/EtOAc 8:2)) gave **133a** (50 mg, 95 %) as a red

metallic solid and B (R_f = 0.38, (SiO_2; *n*-hexane/EtOAc 8:2)) gave **133b** (2.6 mg, 5%) as a red solid.

Data of **133a:** m.p > 200 °C; ^{1}H NMR (400 MHz, CD_2Cl_2): δ 3.03 6 H; NMe_2), 3.12 6 H; NMe_2), 6.63 (d, J = 8 Hz, 2 H), 6.71 (d, J = 8 Hz, 2 H), 7.67 (d, J = 8 Hz, 2 H), 7.73-7.79 (m, 5 H), 7.89–7.91 ppm (m, 1 H); ^{13}C NMR (101 MHz, CD_2Cl_2): 40.30, 40.46, 75.24, 111.20, 111.67, 115.13, 116.09, 120.89, 121.25, 122.86, 123.20, 124.17, 132.67, 135.27, 135.32, 135.98, 140.63, 142.17, 153.93, 154.38, 157.04, 173.23, 188.31, 189.52 ppm; IR (ATR): $\tilde{\nu}$ = 3028 (w), 2916 (m), 2890 (m), 2213 (s), 1675 (s), 1597 (s), 1476 (s), 1432 (m), 1317 (s), 1232 (s), 1067 (m), 1008 (m), 986 (m), 943 (m), 817 (s), 735 cm^{-1} (s); UV/Vis (CH_2Cl_2): λ_{max} (ε) = 534 (37100), 454 (23400), 394 (30600), 324 (7700), 260 nm (30900 M^{-1} cm^{-1}); HR-MALDI-MS: *m/z* (%) 473.1972 (100, [M + H]$^+$, calcd for $C_{30}H_{25}N_4O_2^+$: 473.1972).

Data of **133b:** m.p > 200 °C; ^{1}H NMR (400 MHz, CD_2Cl_2): δ 2.96 6 H; NMe_2), 2.99 6 H; NMe_2), 6.54 (d, J =12 Hz, 2 H), 6.72 (d, J = 8 Hz, 2 H), 7.24 (d, J = 12 Hz, 2 H), 7.31 (d, J = 8 Hz, 2 H), 7.48–7.51 (m, 1 H), 7.52–7.55 (m, 2 H), 7.64-7.66 ppm (m, 1 H); ^{13}C NMR (101 MHz, CD_2Cl_2): δ 27.49, 40.32, 40.47, 98.86, 104.54, 111.35, 112.67, 113.60, 118.97, 120.72, 121.37, 123.29, 130.83, 132.07, 132.30, 132.71, 133.71, 135.45, 150.53, 151.27, 151.51, 170.06, 188.74 ppm; IR (ATR): $\tilde{\nu}$ = 3074 (w), 2918 (m), 2890 (m), 2282 (s), 1670 (s), 1599 (s), 1476 (s), 1433 (m), 1316 (s), 1232 (s), 1168 (s), 1067 (m), 1017 (m), 987 (m), 944 (m), 817 (s), 735 cm^{-1} (s); UV/Vis (CH_2Cl_2): λ_{max} (ε) = 330 (24000), 307 (26000), 279 nm (27300 M^{-1} cm^{-1}); HR-MALDI-MS: *m/z* (%): 473.1973 (100, [M + H]$^+$, calcd for $C_{30}H_{25}N_4O_2^+$: 473.1972).

4,4'-Ethynylenebis(*N*,*N*-dimethylaniline) (42 mg, 0.16 mmol) was treated according to GPF. Evaporation of the solvent in vacuo and FC (SiO_2; *n*-hexane:EtOAc 8/2) afforded two fractions, A and B. Concentration of fraction A gave **133a** (3 mg, 5 %) as a black metallic solid and fraction B gave **133b** (47 mg, 94 %).

(±)-4-(4-Methoxyphenyl)-1',3'-dioxo-1',3'-dihydrospiro[cyclobutane-1,2'-indene]-2,2-dicarbonitrile ((±)-135a) and **(±)-2-(4-Methoxyphenyl)-5-oxo-2,3-dihydroindeno[1,2-*b*]pyran-4,4(5*H*)-dicarbonitrile ((±)-135b)**

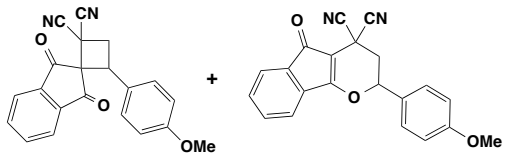

2-(1,3-Dioxo-1*H*-inden-2(3*H*)-ylidene)malononitrile (68 mg, 0.33 mmol) was added to a solution of 4-methoxystyrene (45 μL, 0.34 mmol) in $(CH_2Cl)_2$. The mixture was stirred for 3 h at 25 °C. Evaporation and FC (SiO_2; *n*-hexane/EtOAc 6/4) afforded two fractions, A and B. Concentration of fraction A (R_f = 0.50, (SiO_2; *n*-hexane/EtOAc 5:5)) gave (±)-**135a** (11 mg, 10%) as a white/yellow solid and B (R_f = 0.30, (SiO_2; *n*-hexane/EtOAc 5:5)) gave (±)-**135b** (92 mg, 82%) as a yellow solid, respectively.

Data of **(±)-135a:** m.p = 165 °C; ^{1}H NMR (400 MHz, CD_2Cl_2): δ 2.64 dd *J* = 12, 12 Hz, 1 H), 3.20 t *J* = 12 Hz, 1 H), 3.85 (s, 3 H), 4.81 (dd, *J* = 12, 12 Hz, 1 H), 7.02 (d, *J* = 8 Hz, 2 H), 7.42 ppm (d, *J* = 8 Hz, 2 H), 7.98–8.03 (m, 2 H), 8.08–8.11 ppm (m, 1 H), 8.13–8.17 ppm (m, 1 H); ^{13}C NMR (101 MHz, CD_2Cl_2): 29.49, 39.38, 45.32, 51.32, 55.35, 110.38, 112.66, 114.36, 124.27, 124.40, 125.98, 129.16, 137.21, 137.49, 140.77, 141.53, 160.52, 192.63, 195.62 ppm; IR (ATR): $\tilde{\nu}$ = 3021 (w), 3008 (w) 2914 (m), 2881 (m), 2190 (s), 1691 (s), 1571 (s), 1491 (s), 1402(m), 1321 (s), 1218 (s), 1071 (m), 1002 (m), 979 (m), 949 (m), 832 (s), 735 cm^{-1}; HR-MALDI-MS: *m/z* (%): 343.1077 (100, $[M + H]^+$, calcd for $C_{21}H_{15}N_2O_3^+$: 343.1077).

Data of **(±)-135b:** m.p = 167 °C; ^{1}H NMR (400 MHz, CD_2Cl_2): δ 2.77 dd *J* = 12, 12 Hz, 1 H), 3.00 dd *J* = 12, 12 Hz, 1 H), 3.86 (s, 3 H), 5.50 (dd, *J* = 12, 12 Hz, 1 H), 7.03 (d, *J* = 8 Hz, 2 H), 7.33-7.35 (m, 1 H), 7.43 ppm (d, *J* = 8 Hz, 2 H), 7.47–7.50 (m, 2 H), 7.58–7.60 ppm (m, 1 H); ^{13}C NMR (101 MHz, CD_2Cl_2): 26.16, 39.15, 56.01, 79.60, 98.15, 113.43, 114.63, 115.10, 120.64, 122.87, 127.49, 128.86, 132.81, 133.52, 135.95, 161.58, 176.71, 188.04 ppm; IR

(ATR): $\tilde{\nu}$ = 3024 (w), 3003 (w) 2911 (m), 2886 (m), 2210 (s), 1671 (s), 1578 (s), 1481 (s), 1414 (m), 1326 (s), 1214 (s), 1081 (m), 1000 (m), 977 (m), 949 (m), 832 (s), 735 cm^{-1}; HR-MALDI-MS: *m/z* (%): 343.1078 (100, $[M + H]^+$, calcd for $C_{21}H_{15}N_2O_3^+$: 344.1077).

2-(1,3-Dioxo-1*H*-inden-2(3*H*)-ylidene)malononitrile (68 mg, 0.33 mmol) was added to a solution of 4-methoxystyrene (45 µL, 0.34 mmol) and $LiClO_4$ (34 mg, 0.33 mmol) in $(CH_2Cl)_2$/MeCN 98/2 according to GPF. The mixture was stirred for 3 h at 25 °C. Evaporation and FC (SiO_2; *n*-hexane/EtOAc 6/4) afforded two fractions, A and B. Concentration of fraction A (R_f= 0.50, (SiO_2; *n*-hexane/EtOAc 5:5)) gave (±)-**135a** (106 mg, 94%) as a white/yellow solid.

_N,N_-Dimethyl-4-[(4-nitrophenyl)ethynyl]aniline (136)[231]

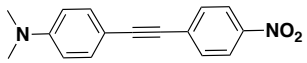

1-Iodo-4-nitrobenzene (248 mg, 1.0 mmol), 4-ethynyl-*N*,*N*-dimethylaniline (145 mg, 1.0 mmol), dichlorobis(triphenylphosphine)palladium(II) (79 mg, 10 µmol), and copper(I) iodide (19 mg, 10 µmol) were added into degassed triethylamine (8 mL). The mixture was stirred for 12 h at 60 °C under nitrogen atmosphere. After filtration, the solvent was removed under reduced pressure. FC (*n*-hexane/EtOAc 92:8) gave **136** (180 mg, 68%). Analytical data of **136** matched those of the literature.[231]

4-{[4-(Dimethylamino)phenyl]ethynyl}benzonitrile (137)[136]

4-Iodo-*N*,*N*-dimethylaniline (200 mg, 0.81 mmol), 4-ethynylbenzonitrile (103 mg, 0.81 mmol), dichlorobis(triphenylphosphine)palladium(II) (6.4 mg, 8.1 µmol), and copper(I) iodide (1.5 mg, 8.1 µmol) were added into degassed triethylamine (8 mL). The mixture was stirred for 12 h at 60 °C under nitrogen atmosphere. After filtration, the solvent was removed under reduced pressure. FC (*n*-hexane/EtOAc 95:5) gave **137** (149 mg, 71%). Analytical data of **137** matched those of the literature.[136]

Ethyl 4-{[4-(Dimethylamino)phenyl]ethynyl}benzoate (138)

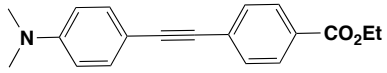

Ethyl 4-iodobenzoate (275 mg, 1.0 mmol), 4-ethynyl-*N*,*N*-dimethylaniline (145 mg, 1.0 mmol), dichlorobis(triphenylphosphine)palladium(II) (79 mg, 10 μmol), and copper(I) iodide (19 mg, 10 μmol) were added into degassed triethylamine (8 mL). The mixture was stirred for 12 h at 60 °C under nitrogen atmosphere. After filtration, the solvent was removed under reduced pressure. FC (*n*-hexane/EtOAc 95:5) gave **138** (228 mg, 79%) as a white solid. $R_f = 0.65$ (SiO_2; *n*-hexane/EtOAc 9:1); m.p > 200 °C; ^{1}H NMR (400 MHz, CD_2Cl_2): δ 1.40 (t, J = 6.9 Hz, 3 H), 2.99 (s, 6 H; NMe_2), 4.38 (q, J = 7.1 Hz, 2 H), 6.66 (d, J = 12 Hz, 2 H), 7.42 (d, J = 12 Hz, 2 H), 7.53 (d, J = 8 Hz, 2 H), 7.99 ppm (d, J = 8 Hz, 2 H); ^{13}C NMR (101 MHz, CD_2Cl_2): δ 14.50, 40.32, 61.16, 87.21, 94.19, 109.45, 111.92, 129.05, 129.56, 131.14, 133.09, 150.53, 166.41 ppm; IR (ATR): $\tilde{\nu}$ = 3050 (m), 2993 (m), 2907 (m), 2207 (s), 2100 (w), 1702 (s), 1594 (s), 1523 (s), 1443 (m), 1271 (s), 1137 (m), 1095 (m), 1025 (s), 815 (s), 771 (s) cm^{-1}; HR-MALDI-MS: *m*/*z* (%): 316.1309 (100, $[M + Na]^+$, calcd for $C_{19}H_{19}NNaO_2^+$: 316.1308).

Ethyl 3-{[4-(Dimethylamino)phenyl]ethynyl}benzoate (139)

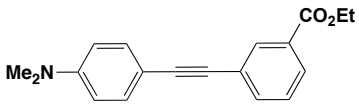

Ethyl 3-iodobenzoate (275 mg, 1.0 mmol), 4-ethynyl-*N*,*N*-dimethylaniline (145 mg, 1.0 mmol), dichlorobis(triphenylphosphine) palladium(II) (79 mg, 10 μmol), and copper(I) iodide (19 mg, 10 μmol) were added into a degassed solution of triethylamine (8 mL). The mixture was stirred for 12 h at 60 °C under a nitrogen atmosphere. After filtration, the solvent was removed under reduced pressure. FC (*n*-hexane/EtOAc 95:5) gave **139** (266 mg, 91%) as a white solid. $R_f = 0.66$

(SiO_2; *n*-hexane/EtOAc 9:1); m.p > 200 °C; ^{1}H NMR (400 MHz, CD_2Cl_2): δ 1.39 (t, J = 6.9 Hz, 3 H), 3.01 (s, 6 H; NMe_2), 4.37 (q, J = 7.1 Hz, 2 H), 6.68 (d, J = 12 Hz, 2 H), 7.39–7.44 (m, 3 H), 7.66 (d, J = 12 Hz, 1 H), 7.94 (d, J =12 Hz, 1 H), 8.14 (s, 1 H); ^{13}C NMR (101 MHz, CD_2Cl_2): δ 14.66, 40.51, 61.70, 86.86, 92.14, 109.71, 112.31, 125.11, 128.81, 129.00, 131.49, 132.59, 133.24, 135.60, 151.03, 166.41; IR (ATR): $\tilde{\nu}$ = 3050 (m), 2993 (m), 2907 (m), 2207 (s), 2100 (w), 1702 (s), 1594 (s), 1523 (s), 1443 (m), 1271 (s), 1137 (m), 1095 (m), 1025 (s), 815 (s), 771 (s) cm^{-1}; HR-MALDI-MS: *m/z* (%): 316.1309 (100, $[M + Na]^+$, calcd for $C_{19}H_{19}NNaO_2^+$: 316.1308).

4,4'-Ethynylenebis(*N*,*N*-diethylaniline) (140)[232]

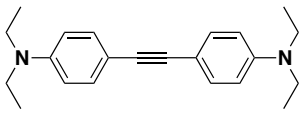

N,*N*-Diethyl-4-iodoaniline (275 mg, 1.0 mmol), *N*,*N*-diethyl-4-ethynylaniline (173 mg, 1.0 mmol), copper(I) iodide (19 mg, 0.01 mmol), and dichlorobis(triphenylphosphine)palladium(II) (39 mg, 0.05 mol) were added into degassed piperidine (8 mL). The mixture was stirred for 8 h at 60 °C under a nitrogen atmosphere. After filtration, the solvent was removed under reduced pressure. FC (*n*-hexane/EtOAc 95:5) gave **140** (230 mg, 72%). Analytical data of **140** matched those of the literature.[232]

4,4'-Ethynylenebis(*N*,*N*-diisopropylaniline) (141)[120]

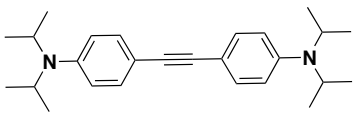

4-Iodo-*N*,*N*-diisopropylaniline (255 mg, 1.0 mmol), 4-ethynyl-*N*,*N*-dimethylaniline (201 mg, 1.0 mmol), copper(I) iodide (19 mg, 0.01 mmol), and dichlorobis(triphenylphosphine) palladium(II) (39 mg, 0.05 mol) were added into degassed piperidine (8 mL). The mixture was stirred for 8 h at 60 °C under a nitrogen atmosphere. After filtration, the solvent was removed under reduced pressure. FC (*n*-hexane/EtOAc 95:5) gave **141** (218 mg, 58%). Analytical data of **141** matched those of the literature.[120]

4,4'-Ethynylenebis(*N*,*N*-dihexylaniline) (142)[233]

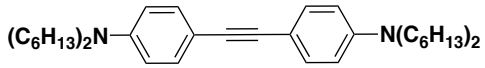

N,*N*-Dihexyl-4-iodoaniline (387 mg, 1.0 mmol), 4-ethynyl-*N*,*N*-dihexylaniline (201 mg, 1.0 mmol), copper(I) iodide (19 mg, 0.01 mmol), and dichlorobis(triphenylphosphine) palladium(II) (39 mg, 0.05 mol) were added into degassed piperidine (8 mL). The mixture was stirred for 8 h at 60 °C under a nitrogen atmosphere. After filtration, the solvent was removed under reduced pressure. FC (*n*-hexane/EtOAc 95:5) gave **142** (435 mg, 80%). Analytical data of **142** matched those of the literature.[233]

4,4'-Etynylenebis(*N*,*N*-diphenylaniline) (143)

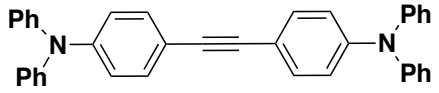

4-Iodo-*N*,*N*-diphenylaniline (185 mg, 0.5 mmol), 4-ethynyl-*N*,*N*-diphenylaniline (134 mg, 0.5 mmol), copper(I) iodide (10 mg, 0.005 mmol), and dichlorobis(triphenylphosphine) palladium(II) (20 mg, 0.03 mmol) were added into degassed piperidine (8 mL). The mixture was stirred for 8 h at 60 °C under a nitrogen atmosphere. After filtration, the solvent was removed under reduced pressure. FC (*n*-hexane/EtOAc 95:5) gave **143** (143 mg, 56%) as a white/yellow solid. R_f = 0.70 (SiO_2; *n*-hexane/EtOAc 9:1); m.p > 200 °C; ^{1}H NMR (400 MHz, CD_2Cl_2): δ 6.93 (d, J = 8 Hz, 2 H), 6.97 (d, J = 12 Hz, 2 H), 7.05–7.12 (m, 12 H), 7.27–7.35 ppm (m, 12 H); ^{13}C NMR (101 MHz, CD_2Cl_2): δ 88.66, 116.32, 121.25, 122.21, 123.53, 124.03, 124.96, 125.42, 129.35, 129.46, 132.21, 133.32, 146.83, 147.21, 147.71 ppm; IR (ATR): $\tilde{\nu}$ = 3050 (m), 2993 (m), 2907 (m), 2207 (s), 2100 (w), 1702 (s), 1594 (s), 1523 (s), 1443 (m), 1271 (s), 1137 (m), 1095 (m), 1025 (s), 815 (s), 771 (s) cm^{-1}; HR-MALDI-MS: *m/z* (%): 513.2325 (100, $[M + H]^+$, calcd for $C_{38}H_{29}N_2^+$: 513.2325).

3-(4-(Dimethylamino)phenyl)propiolonitrile (144)[128]

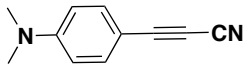

Oven-dried $MgSO_4$ and 2M NH_3 in *i*-PrOH (5.7 mL, 11.4 mmol) were added to a solution of 3-(4-(*N,N*-dimethylamino)phenyl)prop-2-yn-1-ol (500 mg, 2.85 mmol) in THF (25 mL). Subsequently, MnO_2 (2.47 g, 28.5 mmol) was added and the solution stirred at 20 °C for 3 h. The mixture was filtered through a pad of Celite and evaporated to dryness. The crude product was re-dissolved in a 1:1 mixture of CH_2Cl_2 and n-pentane and filtered through a plug of SiO_2. After removal of the solvent, the solid was dissolved in a minimal amount of CH_2Cl_2. *n*-Heptane was added until precipitation started. Crystallization at 0 °C afforded **144** (268 mg, 56%) as an off white solid. Analytical data of **144** matched those of the literature.[128]

2-{2-[4-(Dimethylamino)phenyl]-2-[1,3-dioxo-1*H*-inden-2(3*H*)-ylidene]-1-(4-nitrophenyl)ethylidene}malononitrile (149a) and **2-[4-(Dimethylamino)phenyl]-3-(4-nitrophenyl)-5-oxoindeno[1,2-*b*]pyran-4,4(5*H*)-dicarbonitrile (149b)**

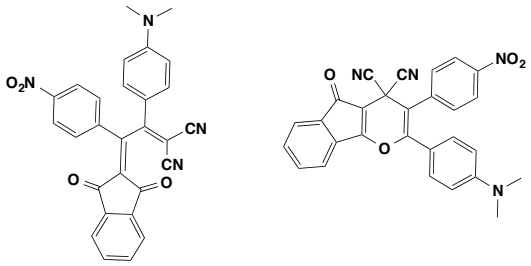

N,N-Dimethyl-4-[(4-nitrophenyl)ethynyl]aniline (43 mg, 0.16 mmol) was treated according to GPE. Evaporation of the solvent in vacuo and FC (SiO_2, *n*-hexane:EtOAc 8/2) afforded two fractions, A and B. Concentration of fraction A (R_f = 0.29, (SiO_2; *n*-hexane/EtOAc 7:3) gave **149a** (46 mg, 65%) as a black metallic solid and fraction B (R_f = 0.32, (SiO_2; *n*-hexane/EtOAc 7:3) gave **149b** (5.7 mg, 11%) as an orange solid.

Data of **149a**: m.p > 200 °C; ^{1}H NMR (400 MHz, $CDCl_3$): δ 3.18 (s, 6 H; NMe_2), 6.75 (d, J = 8 Hz, 2 H), 7.68 (d, J = 8 Hz, 2 H), 7.72–7.79 (m, 3 H), 7.89–7.94

(m, 3 H), 8.24 ppm (d, J = 12 Hz, 2 H); ^{13}C NMR (101 MHz, $CDCl_3$): δ 40.05, 74.31, 111.84, 114.47, 114.54, 117.90, 123.33, 123.98, 131.04, 131.89, 132.04, 136.44, 138.95, 141.03, 142.03, 149.01, 151.69, 153.82, 168.51, 186.37, 187.04 ppm; IR (ATR): $\tilde{\nu}$ = 3009 (w), 2917 (m), 2849 (m), 2216 (s), 1695 (s), 1601 (s), 1497 (s), 1444 (m), 1381 (m), 1334 (s), 1322 (s), 1260 (m), 1189 (s), 1160 (s), 1067 (m), 1019 (m), 983 (s), 944 (m), 826 (s), 735 cm^{-1} (s); UV/Vis (CH_2Cl_2): λ_{max} (ε) = 537 (22600), 477 (14200), 427 (8720), 323 (19200), 281 (29200), 263 nm (29900 M^{-1} cm^{-1}); HR-MALDI-MS: m/z (%): 475.1400 (100, $[M + H]^+$, calcd for $C_{28}H_{19}N_4O_4^+$: 475.1401).

Data of **149b**: m.p > 200 °C; ^{1}H NMR (400 MHz, $CDCl_3$): δ 3.11 (s, 6 H, NMe_2), 6.68 (d, J = 12 Hz, 2 H), 7.63 (d, J = 8 Hz, 2 H), 7.80 (d, J = 12 Hz, 2 H), 7.88-7.91 (m, 2 H) 7.91–7.97 (m, 2 H), 8.25 ppm (d, J = 8 Hz, 2 H); ^{13}C NMR (101 MHz, $CDCl_3$): δ 29.71, 40.21, 87.89, 111.45, 112.33, 119.46, 122.73, 123.15, 123.24, 123.86, 130.89, 135.09, 135.32, 135.60, 139.67, 139.87, 141.90, 149.30, 153.04, 154.30, 173.93, 187.33 ppm; IR (ATR): $\tilde{\nu}$ = 3009 (w), 2926 (m), 2894 (m), 2216 (s), 1709 (m), 1695 (m), 1601 (s), 1523 (s), 1444 (m), 1381 (s), 1333 (s), 1307 (s), 1207 (s), 1175 (m), 1189 (m), 1175 (s), 1008 (m), 977 (s), 944 (m), 852 (s), 735 cm^{-1} (s); UV/Vis (CH_2Cl_2): λ_{max} (ε) = 402 (5400), 332 (15700), 319 (17900), 291 nm (26300 M^{-1} cm^{-1}); HR-MALDI-MS: m/z (%): 475.1399 (100, $[M + H]^+$, calcd for $C_{28}H_{19}N_4O_4^+$: 475.1401).

N,*N*-Dimethyl-4-[(4-nitrophenyl)ethynyl]aniline (43 mg, 0.16 mmol) was treated according to GPF. Evaporation of the solvent in vacuo and FC (SiO_2; *n*-hexane:EtOAc 8/2) afforded two fractions, A and B. Concentration of fraction A gave **149a** (3 mg, 5%) and fraction B gave **149b** (54 mg, 85%).

2-{1-(4-Cyanophenyl)-2-[4-(dimethylamino)phenyl]-2-[1,3-dioxo-1*H*-inden-2(3*H*)-ylidene]ethylidene}malononitrile (150a) and **3-(4-Cyanophenyl)-2-[4-(dimethylamino)phenyl]-5-oxoindeno[1,2-*b*]pyran-4,4(5*H*)-dicarbonitrile (150b)**

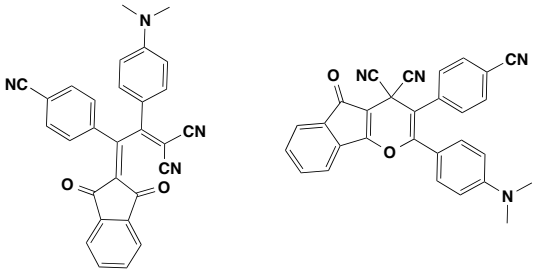

4-{[4-(Dimethylamino)phenyl]ethynyl}benzonitrile (39 mg, 0.16 mmol) was treated according to GPE. Evaporation of the solvent in vacuo and FC (SiO_2; *n*-hexane:EtOAc 8/2) afforded two fractions, A and B. Concentration of fraction A (R_f = 0.3, (SiO_2; *n*-hexane/EtOAc 8:2)) gave **150a** (46 mg, 76%) as a black metallic solid and fraction B (R_f = 0.41, (SiO_2; *n*-hexane/EtOAc 8:2)) gave **150b** (11 mg, 19 %) as a red solid.

Data of **150a:** m.p > 200 °C; ^{1}H NMR (400 MHz, CD_2Cl_2): δ s, 6 H; NMe_2), 6.77 (d, J = 8 Hz, 2 H), 7.64–7.76 (m, 7 H), 7.84–7.89 ppm (m, 3 H); ^{13}C NMR (101 MHz, CD_2Cl_2): δ 40.05, 87.41, 111.23, 111.98, 112.53, 115.50, 117.65, 119.22, 122.49, 122.89, 123.40, 130.31, 132.41, 135.01, 135.24, 135.55, 138.12, 139.72, 141.88, 153.01, 154.29, 174.21, 187.20, 189.41 ppm; IR (ATR): $\tilde{\nu}$ = 3009 (w), 2917 (m), 2849 (m), 2229 (s), 1672 (s), 1595 (s), 1496 (s), 1434 (m), 1402 (s), 1371 (m), 1322 (s), 1193 (s), 1164 (s), 1074 (m), 1017 (m), 989 (s), 944 (m), 822 (s), 740 cm^{-1} (s); UV/Vis (CH_2Cl_2): $\lambda_{max}(\varepsilon)$ = 543 (30500), 436 (13800), 325 (20300), 283 (37800), 262 nm (38900 M^{-1} cm^{-1}); HR-MALDI-MS: *m/z* (%): 455.1503 (100, $[M + H]^+$, calcd for $C_{29}H_{19}N_4O_2^+$: 455.1503).

Data of **150b**: m.p > 200 °C; ^{1}H NMR (400 MHz, CD_2Cl_2): δ 2.96 (s, 6 H, NMe_2), 6.52 (d, J = 8 Hz, 2 H), 6.73 (d, J = 8 Hz, 2 H), 7.49–7.73 ppm (m, 8 H); ^{13}C NMR (101 MHz, CD_2Cl_2): δ 30.25, 40.27, 98.64, 102.33, 111.46, 113.00, 113.64, 117.09, 118.71, 120.95, 123.59, 131.14, 132.06, 132.44, 133.01, 133.50, 135.12, 139.84, 152.10, 152.76, 169.98, 188.26 ppm; IR (ATR): $\tilde{\nu}$ = 3009 (w), 2920 (m), 2851 (m), 2230 (s), 1709 (m), 1659 (m), 1596 (s), 1523 (s), 1456 (m), 1402 (s), 1347

(m), 1307 (s), 1203 (s), 1162 (m), 1067 (m), 1008 (m), 977 (s), 944 (m), 820 (s), 715 cm^{-1} (s); UV/Vis (CH_2Cl_2): λ_{max} (ε) = 399 (6780), 331 (18500), 308 nm (23200 M^{-1} cm^{-1}); HR-MALDI-MS: *m/z* (%): 455.1503 (100, $[M + H]^+$, calcd for $C_{29}H_{19}N_4O_2^+$: 455.1503).

4-{[4-(Dimethylamino)phenyl]ethynyl}benzonitrile (39 mg, 0.16 mmol) was treated according to GPF. Evaporation of the solvent in vacuo and FC (SiO_2; *n*-hexane:EtOAc 8/2) afforded two fractions, A and B. Concentration of fraction A gave **150a** (8 mg, 13%) as a black metallic solid and fraction B gave **150b** (53 mg, 87%).

Ethyl 4-{1,1-Dicyano-3-[4-(dimethylamino)phenyl]-3-[1,3-dioxo-1*H*-inden-2(3*H*)-ylidene] prop-1-en-2-yl}benzoate (151a) and **Ethyl 4-{4,4-Dicyano-2-[4-(dimethylamino)phenyl]-5-oxo-4,5-dihydroindeno[1,2-*b*]pyran-3-yl}benzoate (151b)**

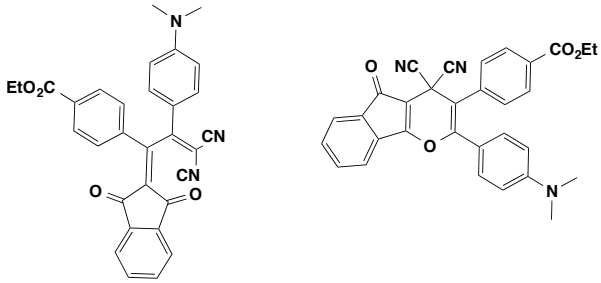

Ethyl 4-{[4-(dimethylamino)phenyl]ethynyl}benzoate (47 mg, 0.16 mmol) was treated according to GPE. Evaporation of the solvent in vacuo and FC (SiO_2; *n*-hexane:EtOAc 8/2) afforded two fractions, A and B. Concentration of fraction A (R_f = 0.37, (SiO_2; *n*-hexane/EtOAc 8:2)) gave **151a** (67 mg, 95%) as a purple metallic solid and fraction B (R_f = 0.45, (SiO_2; *n*-hexane/EtOAc 8:2)) gave **151b** (3.5 mg, 5%) as an orange/red solid.

Data of **151a**: m.p > 200 °C; ^{1}H NMR (400 MHz, CD_2Cl_2): δ 1.35 (t, *J* = 6.9 Hz, 3 H), 3.17 (s, 6 H), 4.34 (q, *J* = 6.9 Hz, 2 H), 6.75 (d, *J* = 12 Hz, 2 H), 7.66 (d, *J* = 12 Hz, 2 H), 7.72–7.80 (m, 3 H), 7.83 (d, *J* = 8 Hz, 2 H), 7.89–7.91 (m, 1 H), 8.06 ppm (d, *J* = 8 Hz, 2 H); ^{13}C NMR (101 MHz, CD_2Cl_2): δ 14.00, 40.01, 61.47, 86.43, 111.05, 112.26, 112.85, 119.51, 122.47, 122.82, 123.51, 129.58, 129.80, 133.73, 134.92, 135.10, 135.53, 137.92, 139.81, 153.79, 154.16, 165.12, 175.07,

187.30, 189.31 ppm; IR (ATR): $\tilde{\nu}$ = 3009 (w), 2981 (m), 2922 (m), 2229 (s), 1715 (s), 1668 (s), 1608 (s), 1480 (s), 1401 (s), 1434 (s), 1321 (s), 1272 (s), 1192 (s), 1173(s), 1156 (s), 1105 (s), 1019 (m), 995 (s), 944 (m), 818 (m), 740 cm^{-1} (s); UV/Vis (CH_2Cl_2): λ_{max} (ε) = 542 (25000), 352 (18500), 284 (28500), 261 nm (29340 M^{-1} cm^{-1}); HR-MALDI-MS: *m/z* (%): 502.1761 (100, $[M + H]^+$, calcd for $C_{31}H_{24}N_3O_4^+$: 502.1761).

Data of **151b**: m.p > 200 °C; ^{1}H NMR (400 MHz, CD_2Cl_2): δ 1.39 (t, J = 6.9 Hz, 3 H), 2.95 (s, 6 H, NMe_2) 4.37 (q, J = 7.1 Hz, 2 H), 6.51 (d, J = 12 Hz, 2 H), 7.17 (d, J = 12 Hz, 2 H), 7.50–7.57 (m, 3 H), 7.59 (d, J = 8 Hz, 2 H), 7.66–7.68 (m, 1 H), 8.07 ppm (d, J = 8 Hz, 2 H); ^{13}C NMR (101 MHz, CD_2Cl_2): δ 14.65, 33.23, 40.29, 61.79, 98.77, 103.16, 111.43, 113.11, 117.69, 120.89, 123.51, 130.71, 131.08, 131.67, 131.81, 132.13, 132.93, 133.88, 135.23, 139.41, 151.91, 152.11, 166.26, 170.04, 188.39 ppm; IR (ATR): $\tilde{\nu}$ = 3009 (w), 2981 (m), 2922 (m), 2300 (s), 1711 (s), 1665 (s), 1600 (s), 1528 (s), 1455 (m), 1401 (s), 1377 (m), 1317 (s), 1278 (s), 1260 (s), 1180 (s), 1160 (s), 1067 (m), 1019 (m), 983 (s), 944 (m), 819 (s), 715 cm^{-1} (s); UV/Vis (CH_2Cl_2): λ_{max} (ε) = 407 (32300), 323 (15500), 291 nm (14900 M^{-1} cm^{-1}); HR-MALDI-MS: *m/z* (%): 502.1760 (100, $[M + H]^+$, calcd for $C_{31}H_{24}N_3O_4^+$: 502.1761).

Ethyl 4-{[4-(dimethylamino)phenyl]ethynyl}benzoate (47 mg, 0.16 mmol) was treated according to GPF. Evaporation of the solvent in vacuo and FC (SiO_2; *n*-hexane/EtOAc 8:2) afforded two fractions, A and B. Concentration of fraction A gave **151a** (6.4 mg, 9%) and fraction B gave **151b** (58 mg, 81%).

Ethyl 3-{1,1-Dicyano-3-[4-(dimethylamino)phenyl]-3-[1,3-dioxo-1*H*-inden-2(3*H*)-ylidene]prop-1-en-2-yl}benzoate (152a) and **Ethyl 3-{4,4-Dicyano-2-[4-(dimethylamino)phenyl]-5-oxo-4,5-dihydroindeno[1,2-*b*]pyran-3-yl}benzoate (152b)**

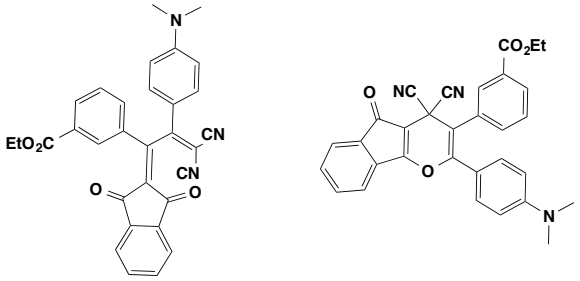

Ethyl 3-{[4-(dimethylamino)phenyl]ethynyl}benzoate (47 mg, 0.16 mmol) was treated according to GPF. Evaporation of the solvent in vacuo and FC (SiO_2; *n*-hexane/EtOAc 8:2) afforded two fractions, A and B. Concentration of fraction A (R_f = 0.37, (SiO_2; *n*-hexane/EtOAc 8:2)) gave **152a** (57 mg, 70%) as a purple metallic solid and fraction B (R_f = 0.45, (SiO_2; *n*-hexane/EtOAc 8:2)) gave **152b** (3.0 mg, 4%) as an orange/red solid.

Data of **152a**: m.p > 200 °C; ^{1}H NMR (400 MHz, CD_2Cl_2): δ 1.35 (t, J = 6.9 Hz, 3 H), 3.17 (s, 6 H), 4.34 (q, J = 7.1 Hz, 2 H), 6.75 (d, J =12 Hz, 2 H), 7.66 (d, J =12 Hz, 2 H), 7.72–7.80 (m, 3 H), 7.83 (d, J = 8 Hz, 2 H), 7.89–7.91 (m, 1 H), 8.06 ppm (d, J = 8 Hz, 2 H); ^{13}C NMR (101 MHz, CD_2Cl_2): δ 14.00, 40.01, 61.47, 86.43, 111.05, 112.26, 112.85, 119.51, 122.47, 122.82, 123.51, 129.58, 129.80, 133.73, 134.92, 135.10, 135.53, 137.92, 139.81, 153.79, 154.16, 165.12, 175.07, 187.30, 189.31 ppm; IR (ATR): $\tilde{\nu}$ = 3009 (w), 2981 (m), 2922 (m), 2229 (s), 1715 (s), 1668 (s), 1608 (s), 1480 (s), 1401 (s), 1434 (s), 1321 (s), 1272 (s), 1192 (s), 11173(s), 1156 (s), 1105 (s), 1019 (m), 995 (s), 944 (m), 818 (m), 740 cm^{-1} (s); UV/Vis (CH_2Cl_2): λ_{max} (ε) = 537 (32000), 425 (15100), 381 (12400), 325 nm (27200 M^{-1} cm^{-1}); HR-MALDI-MS: *m/z* (%): 502.1761 (100, [M + H]$^+$, calcd for $C_{31}H_{24}N_3O_4^+$: 502.1761).

Data of **152b**: m.p > 200 °C; ^{1}H NMR (400 MHz, CD_2Cl_2): δ 1.39 (t, J = 6.9 Hz, 3 H), 2.95 (s, 6 H, NMe_2) 4.37 (q, J = 7.1 Hz, 2 H), 6.51 (d, J =12 Hz, 2 H), 7.17 (d, J =12 Hz, 2 H), 7.50–7.57 (m, 3 H), 7.59 (d, J = 8 Hz, 2 H), 7.66–7.68 (m, 1 H), 8.07 ppm (d, J = 8 Hz, 2 H); ^{13}C NMR (101 MHz, CD_2Cl_2): δ 14.07, 29.69,

40.31, 61.32, 78.23, 111.30, 113.00, 113.47, 124.31, 127.55 131.64, 132.68, 132.20, 134.86, 135.26, 135.95, 153.23, 155.66, 163.02, 165.64, 183.93, 190.53 ppm; IR (ATR): $\tilde{\nu}$ = 3009 (w), 2981 (m), 2922 (m), 2300 (s), 1711 (s), 1665 (s), 1600 (s), 1528 (s), 1455 (m), 1401 (s), 1377 (m), 1317 (s), 1278 (s), 1260 (s), 1180 (s), 1160 (s), 1067 (m), 1019 (m), 983 (s), 944 (m), 819 (s), 715 cm^{-1} (s); UV/Vis (CH_2Cl_2): λ_{max} (ε) = 451 (760), 350 (8000), 264 nm (9600 M^{-1} cm^{-1}); HR-MALDI-MS: *m/z* (%): 502.1760 (100, $[M + H]^+$, calcd for $C_{31}H_{24}N_3O_4^+$: 502.1761).

Ethyl 3-{[4-(dimethylamino)phenyl]ethynyl}benzoate (47 mg, 0.16 mmol) was treated according to GPF. Evaporation of the solvent in vacuo and FC (SiO_2, *n*-hexane:EtOAc 8/2) afforded two fractions, A and B. Concentration of fraction A gave **152a** (2 mg, 3%) and fraction B gave **152b** (49 mg, 66%).

2-{1,2-Bis[4-(diethylamino)phenyl]-3,3-dicyanoallylidene}-1*H*-indene-1,3(2*H*)-dione (153a) and **2,3-Bis[4-(diethylamino)phenyl]-5-oxoindeno[1,2-*b*]pyran-4,4(5*H*)-dicarbonitrile (153b)**

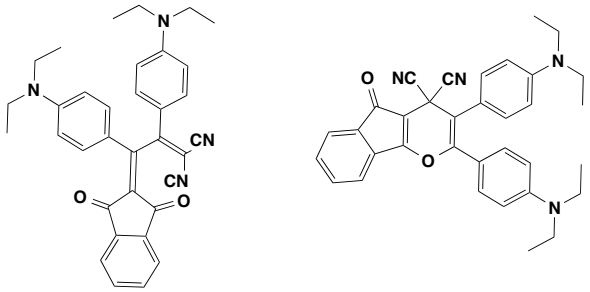

4,4'-Ethynylenebis(*N*,*N*-diisopropylaniline) (51 mg, 0.16 mmol) was treated according to GPE. Evaporation of the solvent in vacuo and FC (SiO_2; *n*-hexane/EtOAc 8:2) afforded two fractions, A and B. Concentration of fraction A (R_f = 0.34, (SiO_2; *n*-hexane/EtOAc 7:3)) gave **153a** (79 mg, 94%) as a dark metallic liquid and fraction B (R_f = 0.42, (SiO_2; *n*-hexane/EtOAc 7:3)) gave **153b** (4.7 mg, 6%) as an orange dark liquid.

Data of **153a**: ^{1}H NMR (400 MHz, CD_2Cl_2): δ 1.22 (t, *J* = 4 Hz, 6 H), 1.29 (t, *J* = 4 Hz, 6 H), 3.47 (q, *J* = 8 Hz, 4 H), 3.53 (q, *J* = 8 Hz, 4 H), 6.67 (d, *J* = 8 Hz, 2 H), 6.77 (d, *J* = 8 Hz, 2 H), 7.70 (d, *J* = 8 Hz, 2 H), 7.75–7.85 (m, 5 H), 7.91–7.96 ppm (m, 1 H); ^{13}C NMR (101 MHz, $CDCl_3$): δ 12.81, 12.86, 26.14, 44.77, 44.80, 98.88, 104.11, 110.76, 112.08, 113.69, 118.12, 120.42, 120.68, 123.26, 131.05,

132.27, 132.67, 133.68, 135.50, 148.84, 149.08, 150.33, 170.06, 188.78 ppm; IR (ATR): $\tilde{\nu}$ = 3028 (w), 2916 (m), 2890 (m), 2213 (s), 1675 (s), 1597 (s), 1476 (s), 1432 (m), 1317 (s), 1232 (s), 1067 (m), 1008 (m), 986 (m), 943 (m), 817 (s), 735 cm^{-1} (s); UV/Vis (CH_2Cl_2): λ_{max} (ε)= 543 (45600), 459 (27600), 425 (36000), 326 (9510), 284 (21500), 262 nm (33500 M^{-1} cm^{-1}); HR-MALDI-MS: 529.2596 (100, [*M* + H]$^+$, calcd for $C_{34}H_{33}N_4O_2^+$: 529.2598).

Data of **153b**: ^{1}H NMR (400 MHz, CD_2Cl_2): δ 1.16–1.24 (m, 12 H), 3.36–3.45 (m, 8 H), 6.55 (d, *J* = 8 Hz, 2 H), 6.72 (d, *J* = 8 Hz, 2 H), 7.26 (d, *J* = 8 Hz, 2 H), 7.32 (d, *J* = 8 Hz, 2 H), 7.51–7.60 (m, 3 H), 7.66–7.71 (m, 1 H); ^{13}C NMR (101 MHz, CD_2Cl_2): δ 12.81, 12.86, 34.08, 44.77, 44.80, 98.87, 104.10, 110.76, 112.07, 113.69, 118.11, 120.42, 120.68, 123.26, 131.05, 132.27, 132.34, 132.67, 133.68, 135.49, 148.83, 149.07, 150.32, 170.05, 188.77 ppm; IR (ATR): $\tilde{\nu}$ = 3009 (w), 2926 (m), 2894 (m), 2216 (s), 1710 (m), 1695 (m), 1601 (s), 1523 (s), 1444 (m), 1381 (s), 1333 (s), 1307 (s), 1207 (s), 1175 (m), 1189 (m), 1175 (s), 1008 (m), 977 (s), 944 (m), 852 (s), 735 cm^{-1} (s); UV/Vis (CH_2Cl_2): λ_{max} (ε) = 334 (18400), 306 (21600), 284 nm (20500 M^{-1} cm^{-1}); HR-MALDI-MS: *m/z* (%): 529.2599 (100, [*M* + H]$^+$, calcd for $C_{34}H_{33}N_4O_2^+$: 529.2598).

4,4'-Ethynylenebis(*N*,*N*-diisopropylaniline) (51 mg, 0.16 mmol) was treated according to GPF. Evaporation of the solvent in vacuo and FC (SiO_2; *n*-hexane/EtOAc 8:2) afforded two fractions, A and B. Concentration of fraction A gave **153a** (3 mg, 4%) as a black metallic solid and concentration of fraction B gave **153b** (63 mg, 80%).

2-{1,2-Bis[4-(diisopropylamino)phenyl]-2-[1,3-dioxo-1*H*-inden-2(3*H*)-ylidene] ethylidene}malononitrile (154a) and **2,3-Bis[4-(diisopropylamino)phenyl]-5-oxoindeno[1,2-*b*]pyran-4,4(5*H*)- dicarbonitrile (154b)**

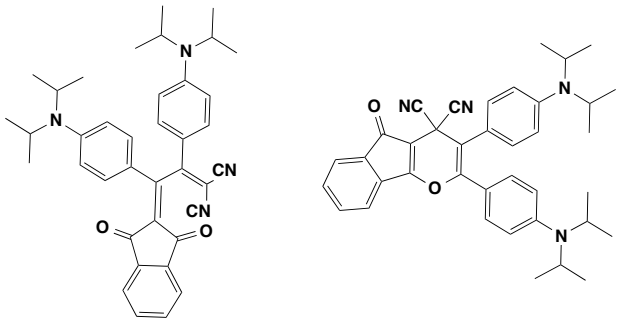

4,4'-Ethynylenebis(*N*,*N*-diisopropylaniline) (60 mg, 0.16 mmol) was treated according to GPE. Evaporation of the solvent in vacuo and FC (SiO_2; *n*-hexane/EtOAc 8:2) afforded two fractions, A and B. Concentration of fraction A (R_f = 0.34, (SiO_2; *n*-hexane/EtOAc 7:3)) gave **154a** (74 mg, 85%) as a dark metallic liquid and B (R_f = 0.42, (SiO_2; *n*-hexane/EtOAc 7:3)) gave **154b** (4.7 mg, 5%) as an orange dark liquid.

Data of **154a**: ^{1}H NMR (400 MHz, CD_2Cl_2): δ 1.30 (d, J = 8 Hz, 12 H), 1.39 (d, J = 8 Hz, 12 H), 3.96 (sept., J = 8 Hz 2 H), 4.12 (sept., J = 8 Hz, 2 H), 6.77 (d, J = 8 Hz, 2 H), 6.90 (d, J = 8 Hz, 2 H), 7.36 (d, J = 8 Hz, 2 H), 7.73 (d, J = 8 Hz, 2 H), 7.76–7.79 (m, 2 H), 7.86–7.92 ppm (m, 2 H); ^{13}C NMR (101 MHz, $CDCl_3$): δ 20.53, 47.77, 48.20, 86.72, 89.35, 105.30, 112.60, 113.47, 114.69, 118.90, 120.50, 122.44, 122.48, 122.63, 134.74, 134.79, 134.95, 140.26, 141.69, 151.07, 151.72, 152.78, 157.38, 187.88, 189.15 ppm; IR (ATR): $\tilde{\nu}$ = 3010 (w), 2969 (m), 2931 (m), 2136 (s), 1672 (m), 1594 (s), 1523 (s), 1480 (s), 1421 (m), 1330 (m), 1297 (s), 1198 (s), 1034 (m), 1008 (m), 976 (m), 943 (m), 819 (m), 735 cm^{-1} (m); UV/Vis (CH_2Cl_2): $\lambda_{max}(\varepsilon)$ = 537 (39900), 439 (21300), 325 (11600), 285 (24600), 265 nm (24600 M^{-1} cm^{-1}); HR-MALDI-MS: *m*/*z* (%): 585.3224 (100, [M + H]$^+$, calcd for $C_{38}H_{41}N_4O_2^+$: 585.3224).

Data of **154b**: ^{1}H NMR (400 MHz, CD_2Cl_2): δ 1.30 (d, J = 8 Hz, 12 H), 1.35 (d, J = 8 Hz, 12 H), 3.90 (sept., J = 8 Hz, 2 H), 4.01 (sept,. J = 8 Hz, 2 H), 6.81 (d, J = 8 Hz, 2 H), 6.92 (d, J = 8 Hz, 2 H), 7.35 (d, J = 8 Hz, 2 H), 7.49–7.56 (m, 3 H), 7.65–7.67 (m, 1 H), 8.01 ppm (d, J = 8 Hz, 2 H); ^{13}C NMR (101 MHz, CD_2Cl_2): δ

20.68, 20.76, 22.65, 47.45, 47.52, 81.63, 88.48, 97.26, 101.44, 108.02, 112.82, 114.02, 115.36, 116.74, 120.21, 122.86, 128.95, 131.60, 132.24, 133.22, 134.67, 149.03, 150.40, 153.03, 168.79, 187.90 ppm; IR (ATR): $\tilde{\nu}$ = 3010 (w), 2969 (m), 2931 (m), 2185 (s), 1716 (m), 1658 (m), 1596 (s), 1508 (s), 1401 (m), 1330 (s), 1292 (s), 1067 (m), 1008 (m), 986 (m), 943 (m), 817 (s), 735 cm^{-1} (s); UV/Vis (CH_2Cl_2): λ_{max} (ε) = 363 (4650), 329 (10600), 324 (13200), 284 nm (10300 M^{-1} cm^{-1}); HR-MALDI-MS: *m/z* (%): 585.3225 (100, [*M* + H]$^+$, calcd for $C_{38}H_{41}N_4O_2^+$: 585.3224).

4,4'-Ethynylenebis(*N*,*N*-diisopropylaniline) (60 mg, 0.16 mmol)) was treated according to GPF. Evaporation of the solvent in vacuo and FC (SiO_2; *n*-hexane/EtOAc 8:2) afforded two fractions, A and B. Concentration of fraction A gave **154a** (3.7 mg, 4%) as a black metallic solid and fraction B gave **154b** (71 mg, 81%).

2-{1,2-Bis[4-(dihexylamino)phenyl]-3,3-dicyanoallylidene}-1*H*-indene-1,3(2*H*)-dione (155a) and **2,3-Bis[4-(dihexylamino)phenyl]-5-oxoindeno[1,2-*b*]pyran-4,4(5*H*)-dicarbonitrile (155b)**

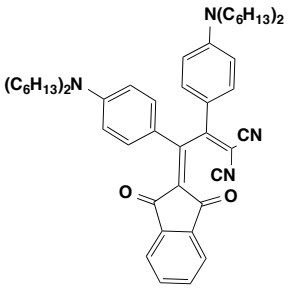

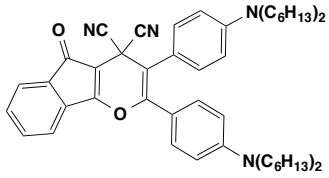

4,4'-Ethynylenebis(*N*,*N*-dihexylaniline) (87 mg, 0.16 mmol) was treated according to GPE. Evaporation of the solvent in vacuo and FC (SiO_2; *n*-hexane/EtOAc 8:2) afforded two fractions, A and B. Concentration of fraction A (R_f = 0.41, (SiO_2; *n*-hexane/EtOAc 7:3)) gave **155a** (100 mg, 89%) as a dark metallic liquid and fraction B (R_f = 0.49, (SiO_2; *n*-hexane/EtOAc 7:3)) gave **155b** (6.4 mg, 6%) as an orange dark liquid.

Data of **155a**: ^{1}H NMR (400 MHz, $CDCl_3$): δ 0.88–0.95 (m, 12 H), 1.32-1.45 (m, 24 H), 1.58–1.69 (m, 8 H), 3.31–3.45 (m, 8 H), 6.61 (d, *J* = 12 Hz, 2 H), 6.69 (d, *J* =12 Hz, 2 H), 7.73–7.82 (m, 5 H), 7.88–7.95 ppm (m, 1 H); ^{13}C NMR (101

MHz, CD_2Cl_2): δ 14.36, 23.18, 23.22, 27.18, 27.25, 27.70, 27.82, 32.17, 51.70, 51.93, 74.20, 111.24, 111.62, 115.41, 116.38, 120.72, 122.82, 123.11, 132.96, 135.17, 136.43, 140.70, 142.21, 152.38, 152.91, 156.94, 172.74, 188.56, 189.63 ppm; IR (ATR): $\tilde{\nu}$ = 3029 (w), 2916 (m), 2890 (m), 2213 (s), 1675 (s), 1599 (s), 1476 (s), 1432 (m), 1317 (s), 1232 (s), 1067 (m), 1010 (m), 986 (m), 943 (m), 817 (s), 735 cm^{-1} (s); UV/Vis (CH_2Cl_2): $\lambda_{max}(\varepsilon)$ = 537 (44000), 436 (23000), 327 (11000), 286 (26000), 265 nm (25000 M^{-1} cm^{-1}); HR-MALDI-MS: *m/z* (%): 753.5102 (100, $[M + H]^+$, calcd for $C_{50}H_{65}N_4O_2^+$: 753.5102).

Data of **155b**: ^1H NMR (400 MHz, CD_2Cl_2): δ 0.89–0.93 (m, 12 H), 1.31–1.35 (m, 24 H), 1.52–1.61 (m, 8 H), 3.23–3.31 (m, 8 H), 6.46 (d, *J* = 12 Hz, 2 H), 6.65 (d, *J* = 8 Hz, 2 H), 7.21 (d, *J* = 8 Hz, 2 H), 7.27 (d, *J* = 8 Hz, 2 H), 7.47–7.56 (m, 3 H), 7.64–7.66 ppm (m, 1 H); ^{13}C NMR (101 MHz, CD_2Cl_2): δ 14.38, 23.25, 27.28, 27.66, 32.26, 32.29, 51.36, 51.45, 98.88, 104.04, 110.83, 112.06, 113.72, 117.99, 120.24, 120.67, 123.26, 130.96, 132.17, 132.35, 132.67, 133.68, 135.51, 149.22, 149.48, 150.28, 170.05, 188.77 ppm; IR (ATR): $\tilde{\nu}$ = 3005 (w), 2969 (m), 2931 (m), 2191 (s), 1711 (m), 1658 (m), 1596 (s), 1508 (s), 1401 (m), 1330 (s), 1292 (s), 1067 (m), 1008 (m), 986 (m), 943 (m), 859 (s), 778 cm^{-1} (s); UV/Vis (CH_2Cl_2): λ_{max} (ε) = 363 (2200), 329 (9000), 324 (9200), 284 nm (7400 M^{-1} cm^{-1}); HR-MALDI-MS: *m/z* (%): 753.5101 (100, $[M + H]^+$, calcd for $C_{50}H_{65}N_4O_2^+$: 753.5102).

4,4'-Ethynylenebis(*N*,*N*-dihexylaniline) (87 mg, 0.16 mmol) was treated according to GPF. Evaporation of the solvent in vacuo and FC (SiO_2; *n*-hexane/EtOAc 8:2) afforded two fractions, A and B. Concentration of fraction A gave **155a** (4.5 mg, 4%) as a black metallic solid and B gave **155b** (102 mg, 91%).

2-{1,2-Bis[4-(diphenylamino)phenyl]-3,3-diisocyanoallylidene}-1*H*-indene-1,3(2*H*)-dione (156a) and **2,3-Bis[4-(diphenylamino)phenyl]-5-oxoindeno[1,2-*b*]pyran-4,4(5*H*)-dicarbonitrile (156b)**

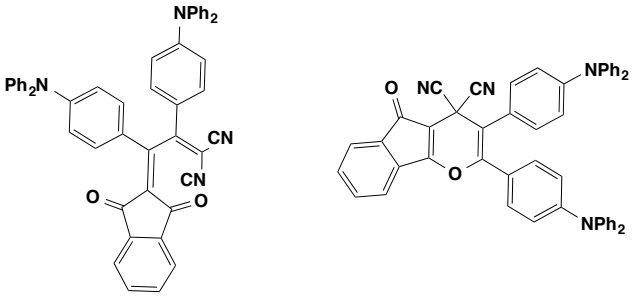

4,4'-Ethynylenebis(*N*,*N*-diphenylaniline) (82 mg, 0.16 mmol) was treated according to GPE. Evaporation of the solvent in vacuo and FC (SiO_2; *n*-hexane/EtOAc 8:2) afforded two fractions, A and B. Concentration of fraction A (R_f = 0.71, (SiO_2; *n*-hexane/EtOAc 7:3)) gave **156a** (68 mg, 63%) as a dark metallic liquid and fraction B (R_f = 0.8, (SiO_2; *n*-hexane/EtOAc 7:3)) gave **157b** (7.5 mg, 7%) as an orange dark liquid.

Data of **157a**: ^{1}H NMR (400 MHz, $CDCl_3$): δ 6.89 (d, J = 12 Hz, 2 H), 6.95 (d, J = 8 Hz, 2 H), 7.20–7.31 (m, 12 H), 7.37–7.46 (m, 8 H), 7.55 (d, J =12 Hz, 2 H), 7.72 (d, J =8 Hz, 2 H), 7.83–7.85 (m, 2 H), 7.89–7.91 (1 H, m), 7.95–7.98 (1 H, m); ^{13}C NMR (101 MHz, CD_2Cl_2): δ 78.53, 114.41, 115.13, 117.94, 118.48, 123.37, 123.66, 124.20, 124.67, 126.31, 126.37, 127.32, 127.40, 130.37, 132.06, 134.71, 135.85, 135.93, 140.83, 142.44, 145.92, 146.11, 146.48, 152.92, 155.45, 172.68, 187.83, 189.27 ppm; IR (ATR): $\tilde{\nu}$ = 3009 (w), 2917 (m), 2849 (m), 2229 (s), 1672 (s), 1595 (s), 1496 (s), 1434 (m), 1402 (s), 1371 (m), 1322 (s), 1193 (s), 1164 (s), 1074 (m), 1017 (m), 989 (s), 944 (m), 822 (s), 740 cm^{-1} (s); UV/Vis (CH_2Cl_2): $\lambda_{max}(\varepsilon)$ = 536 (35900), 473 (30300), 429 (31700), 330 nm (17900 M^{-1} cm^{-1}); HR-MALDI-MS: *m/z* (%): 721.2597 (100, $[M + H]^+$, calcd for $C_{50}H_{33}N_4O_2^+$: 721.2598).

Data of **157b**: ^{1}H NMR (400 MHz, CD_2Cl_2): δ 6.89 (d, J = 8 Hz, 2 H), 7.03 (d, J = 8 Hz, 2 H), 7.08–7.16 (m, 12 H), 7.21 (d, J = 8 Hz, 2 H), 7.28–7.35 (m, 10 H),

7.47–7.49 (m, 1 H), 7.53–7.55 (m, 2 H), 7.66–7.68 ppm (m, 1 H); ^{13}C NMR (101 MHz, CD_2Cl_2): δ 33.55, 98.87, 105.86, 113.22, 120.43, 120.81, 122.64, 123.46, 123.98, 124.35, 124.90, 125.76, 126.22, 126.56, 130.00, 130.11, 130.75, 132.12, 132.32, 132.87, 133.85, 135.22, 169.93, 188.51 ppm; IR (ATR): $\tilde{\nu}$ = 3009 (w), 2926 (m), 2894 (m), 2216 (s), 1709 (m), 1695 (m), 1601 (s), 1523 (s), 1444 (m), 1381 (s), 1333 (s), 1307 (s), 1207 (s), 1175 (m), 1189 (m), 1175 (s), 1008 (m), 977 (s), 944 (m), 852 (s), 735 cm^{-1} (s); UV/Vis (CH_2Cl_2): λ_{max} (ε) = 409 (31800), 330 (13000), 321 (15800), 289 nm (14700 M^{-1} cm^{-1}); HR-MALDI-MS: *m/z* (%): 721.2598 (100, [*M* + H]$^+$, calcd for $C_{50}H_{33}N_4O_2^+$: 721.2598).

4,4'-Ethynylenebis(*N*,*N*-diphenylaniline) (82 mg, 0.16 mmol) was treated according to GPF. Evaporation of the solvent in vacuo and FC (SiO_2; *n*-hexane/EtOAc 8:2) afforded two fractions, A and B. Concentration of fraction A gave **157a** (6.4 mg, 6%) as a black metallic solid and fraction B gave **157b** (63.7 mg, 59%).

2-{[4-(Dimethylamino)phenyl][1,3-dioxo-1*H*-inden-2(3*H*)-ylidene]methyl}-3,3-dicyanoacrylonitrile (157a) and **2-[4-(Dimethylamino)phenyl]-5-oxoindeno[1,2-*b*]pyran-3,4,4(5*H*)-tricarbonitrile (157b)**

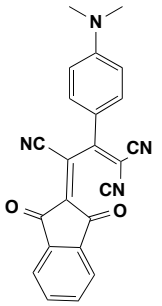

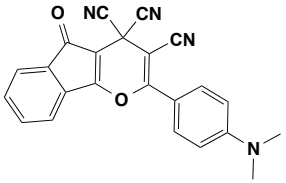

3-[4-(Dimethylamino)phenyl]propiolonitrile (27 mg, 0.16 mmol) was treated according to GPE. Evaporation of the solvent in vacuo and FC (SiO_2; *n*-hexane/EtOAc 5:5) afforded two fractions, A and B. Concentration of fraction A (R_f = 0.4, (SiO_2; *n*-hexane/EtOAc 5:5)) gave **157a** (47 mg, 83%) as a green solid and fraction B (R_f = 0.6, (SiO_2; *n*-hexane/EtOAc 5:5)) afforded the [2+2] compound **157b** (1 mg, 2%) as a green solid.

Data of **157a**: m.p > 200 °C; ^{1}H NMR (400 MHz, $CDCl_3$): δ 3.14 (s, 6 H;

NMe_2), 6.70 (d, J = 12 Hz, 2 H), 7.79 (d, J = 8 Hz, 2 H), 7.92–8.03 (m, 3 H), 8.16 (d, J= 8 Hz, 2 H); ^{13}C NMR (101 MHz, CD_2Cl_2): δ 40.13, 111.92, 112.64, 113.63, 114.08, 117.38, 118.85, 124.80, 131.97, 137.39, 13.53, 141.70, 141.95, 143.12, 154.28, 158.80, 183.17, 184.20 ppm; IR (ATR): $\tilde{\nu}$ = 3009 (w), 2981 (m), 2922 (m), 2300 (s), 1711 (s), 1665 (s), 1600 (s), 1528 (s), 1455 (m), 1401 (s), 1377 (m), 1317 (s), 1278 (s), 1260 (s), 1180 (s), 1160 (s), 1067 (m), 1019 (m), 983 (s), 944 (m), 819 (s), 715 cm^{-1} (s); UV/Vis (CH_2Cl_2): λ_{max} (ε) = 453 (48400), 314 (13200), 278 nm (50000 M^{-1} cm^{-1}); HR-MALDI-MS: m/z (%): 379.1191 (100, [M + H]$^+$, calcd for $C_{23}H_{15}N_4O_2^+$: 379.1190).

Data of **157b**: ^{1}H NMR (400 MHz, $CDCl_3$): δ 6.70 (d, J = 12 Hz, 2 H), 7.88-7.97 (m, 5 H), 8.06-8.08 ppm (m, 1 H); ^{13}C NMR (101 MHz, CD_2Cl_2): 31.71, 40.45, 72.38, 111.85, 115.30, 116.47, 118.83, 124.44, 124.61, 132.16, 133.40, 137.31, 142.04, 142.34, 146.48, 154.70, 164.49, 165.90, 186.98 ppm; IR (ATR): 3009 (w), 2989 (m), 2922 (m), 2220 (s), 1705 (s), 1630 (s), 1590 (s), 1460 (s), 1395 (s), 1377 (m), 1299 (s), 1278 (s), 1263 (s), 1180 (s), 1156 (s), 1062 (m), 1024 (m), 989 (s), 938 (m), 849 (s), 735 cm^{-1} (s); UV/Vis (CH_2Cl_2): λ_{max} (ε) = 417 (3250), 326 (15300), 291 nm (14900 M^{-1} cm^{-1}); HR-MALDI-MS: m/z (%): 379.1190 (100, [M + H]$^+$, calcd for $C_{23}H_{15}N_4O_2^+$: 379.1190).

3-[4-(Dimethylamino)phenyl]propiolonitrile (27 mg, 0.16 mmol) was treated according to GPF. Evaporation of the solvent in vacuo and FC (SiO_2; n-hexane/EtOAc 5:5) afforded two fractions, A and B. Concentration of fraction A afforded the [2+2] compound **157a** (4.6 mg, 8%) and concentration of fraction B afforded the [4+2] compound **157b** (42mg, 74%) as a green solid.

Reaction of DCID with Alkynes 147 and 148

Alkyne **147** (40 mg, 0.16 mmol) was treated according to GPE. Evaporation of the solvent in vacuo gave 4 inseparable regioisomers (52 mg, 75%). All attempts to separate the regioisomers either by chromatography or recrystallization were unsuccessful. HR-MALDI-MS: m/z (%): 460.1658 (100, [M + H]$^+$, calcd for $C_{29}H_{22}N_3O_3^+$: 460.1656).

Alkyne **148** (52 mg, 0.16 mmol) was treated according to GPE. Evaporation of the solvent in vacuo gave 4 inseparable regioisomers (73 mg, 85%). All attempts to separate the regioisomers either by chromatography or recrystallization were unsuccessful. HR-MALDI-MS: *m/z* (%): 537.1211 (100, $[M + H]^+$, calcd for $C_{32}H_{24}FeN_3O_2^+$: 538.1212).

Ethyl 2,3,3-Tricyanoacrylate (158)[234]

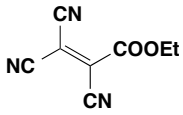

Procedure modified from one previously reported.[234] A stirred solution of TCNE (6.0 g, 46.7 mmol) in dry THF (30 mL) was heated to 70 °C and treated with ethyl cyanoacetate (904 μL, 8.5 mmol) and pyridine (100 μL, 1.24 mmol). The mixture was heated at reflux for 16 h, cooled to 25 °C, and diluted with $CHCl_3$ (50 mL) and pentane (100 mL). The mixture was allowed to stand for 1 h before being filtered, and the filtrate washed with water (3 x 100 mL). The organic phase was dried ($MgSO_4$), filtered, and concentrated under reduced pressure until a precipitate started to form. The mixture was filtered, and the filtrate treated with heptane (50 mL) before being concentrated under reduced pressure. When a precipitate started to form, the solution was cooled to 0 °C and the white solid that formed collected and recrystallized from chloroform/pentane 1:9 to afford compound **158** (179 mg, 12%) as a white solid. Analytical data of **158** matched those of the literature.[234]

(*E*)-Ethyl 2,5,5-tricyano-3-[4-(dimethylamino)phenyl]penta-2,4-dienoate (159), **(*E*)-Ethyl 2,5,5-tricyano-4-[4-(dimethylamino)phenyl]penta-2,4-dienoate (160)** and **(*Z*)-Ethyl 2,5,5-tricyano-4-[4-(dimethylamino)phenyl]penta-2,4-dienoate (161)**

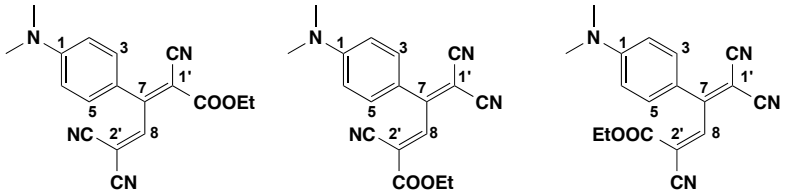

A solution of alkyne **158** (50 mg, 0.344 mmol) in MeCN (3.4 mL) was treated with alkene **102** (60 mg, 0.344 mmol) and stirred for 2 h at 25 °C. Evaporation and

flash column chromatography (SiO_2; EtOAc/cyclohexane 1:4 v/v) afforded two fractions, A and B. Evaporation of fraction A afforded *E*-**159** (14 mg, 13%) as a red solid. Evaporation of fraction B afforded a red solid that was dissolved in warm 2-propanol/cyclohexane (1:9). The precipitate was filtered off to give *Z*-**161** (35 mg, 32%) as a red solid. The filtrate was evaporated give *E*-**160** (57 mg, 52%) as a red solid.

Data *E*-**159**: R_f = 0.50 (SiO_2; EtOAc/cyclohexane 3:7); m.p. 118–121 °C; ^{1}H NMR (400 MHz, $CDCl_3$): δ = 1.39 (t, J = 7.1 Hz, 3 H; CH_3), 3.12 (s, 6 H, $N(CH_3)_2$), 4.34 (q, J = 7.1 Hz, 2 H; OCH_2), 6.73 (d, J = 9.2 Hz, 2 H; H–C(2,6)), 7.50 (d, J = 9.2 Hz, 2 H; H–C(3,5)), 8.55 ppm (s, 1 H; H–C(8)); ^{13}C NMR (100 MHz, $CDCl_3$): δ = 14.28 (1 C, H_3C), 40.19 (2 C, $N(CH_3)_2$), 63.11 (1 C, OCH_2), 92.79 (1 C, C(1')), 100.04 (1 C, C(2')), 109.87 (1 C, CN), 111.94 (2 C, HC(2,6)), 112.47 (1 C, CN), 116.78 (1 C, CN), 120.76 (1 C, C(4)), 132.72 (2 C, HC(3,5)), 153.78 (1 C, C(1)), 157.77 (1 C, C(7)), 162.50 (1 C, HC(8)), 163.10 ppm (1 C, COOEt); IR (ATR): $\tilde{\nu}$ = 2921 (w), 2213 (w), 1702 (m), 1604 (s), 1497 (s), 1439 (m), 1366 (m), 1331 (m), 1252 (s), 1202 (s), 1171 (m), 1155 (m), 1101 (s), 1017 (m), 943 (m), 853 (w), 822 (s), 796 (w), 765 (w), 745 (w), 711 (w), 692 (w), 642 (w), 612 cm^{-1} (w); UV/Vis ($CHCl_3$): λ_{max} (ε) = 518 (7930), 486 (7740), 339 (13100 $M^{-1}cm^{-1}$); HR-MALDI-MS (3-HPA) *m/z* (%): 343.1165 (96, $[M + Na]^+$), 321.1346 (73, $[M + H]^+$), 320.1268, (100, $[M]^+$, calcd for $C_{18}H_{16}N_4O_2$: 320.1268).

Data of *E*-**160**: R_f = 0.20 (SiO_2; CH_2Cl_2); m.p. 118–119 °C; ^{1}H NMR (400 MHz, $CDCl_3$): δ = 1.40 (t, J = 7.1 Hz, 3 H; CH_3), 3.14 (s, 6 H, $N(CH_3)_2$), 4.41 (q, J = 7.1 Hz, 2 H; OCH_2), 6.72 (d, J = 9.2 Hz, 2 H; H–C(2,6)), 7.57 (d, J = 9.2 Hz, 2 H; H–C(3,5)), 8.33 ppm (s, 1 H; H–C(8)); ^{13}C NMR (100 MHz, $CDCl_3$): δ = 14.15 (1 C, H_3C), 40.23 (2 C, $N(CH_3)_2$), 64.01 (1 C, OCH_2), 77.63 (1 C, C(1')), 111.88 (1 C, C(2')), 111.95 (2 C, HC(2,6)), 113.58 (1 C, CN), 114.33 (1 C, CN), 117.21 (1 C, CN), 118.65 (1 C, C(4)), 132.25 (2 C, HC(3,5)), 151.34 (1 C, HC(8)), 154.30 (1 C, C(1)), 159.93 (1 C, COOEt), 161.44 ppm (1 C, C(7)); IR (ATR): $\tilde{\nu}$ = 3027 (w), 2924 (w), 2218 (m), 1732 (m), 1600 (s), 1538 (w), 1496 (s), 1443 (m), 1412 (w), 1384 (s), 1350 (s), 1316 (m), 1293 (s), 1252 (s), 1212 (s), 1168 (s), 1069 (m), 1011 (w), 994 (w), 943 (m), 870 (w), 844 (w), 825 (s), 800 (w), 770 (w), 761 (w), 742 (w), 724 (w), 660 (w), 613 (w), 631 cm^{-1} (w); UV/Vis ($CHCl_3$): λ_{max} (ε) = 500 (12200), 464 (17000), 334

(19500 $M^{-1}cm^{-1}$); HR-MALDI-MS (3-HPA) *m/z* (%): 343.1167 (96, $[M + Na]^+$), 321.1347 (73, $[M + H]^+$), 320.1268, (100, $[M]^+$, calcd for $C_{18}H_{16}N_4O_2$: 320.1268).

Data of *Z*-**161**: R_f = 0.17 (SiO_2; CH_2Cl_2); m.p. 109–110 °C (decomp.); ^1H NMR (400 MHz, $CDCl_3$): δ = 1.27 (t, *J* = 7.1 Hz, 3 H; CH_3), 3.13 (s, 6 H, $N(CH_3)_2$), 4.21 (q, *J* = 7.1 Hz, 2 H; OCH_2), 6.69 (d, *J* = 9.3 Hz, 2 H; H–C(2,6)), 7.65 (s, 1 H; H–C(8)), 7.67 ppm (d, *J* = 9.3 Hz, 2 H; H–C(3,5)); ^{13}C NMR (100 MHz, $CDCl_3$): δ = 13.96 (1 C, H_3C), 40.21 (2 C, $N(CH_3)_2$), 63.66 (1 C, OCH_2), 74.25 (1 C, C(1')), 111.78 (2 C, HC(2,6)), 113.91 (1 C, CN), 114.24 (1 C, CN), 114.39 (1 C, C(2')), 115.69 (1 C, CN), 117.88 (1 C, C(4)), 131.57 (2 C, HC(3,5)), 150.93 (1 C, HC(8)), 154.06 (1 C, C(1)), 158.89 (1 C, COOEt), 162.57 ppm (1 C, C(7)); IR (ATR): $\tilde{\nu}$ = 2939 (w), 2212 (m), 1735 (m), 1601 (s), 1538 (w), 1488 (s), 1439 (m), 1382 (s), 1344 (s), 1328 (m), 1295 (m), 1230 (m), 1211 (s), 1189 (m), 1170 (s), 1122 (w), 1079 (w), 1016 (w), 941 (w), 883 (w), 851 (w), 831 (m), 799 (w), 778 (w), 754 (w), 739 (w), 711 cm^{-1} (w); UV/Vis ($CHCl_3$): λ_{max} (ε) = 456 (17500), 359 (5290 $M^{-1}cm^{-1}$); HR-MALDI-MS (3-HPA) *m/z* (%): 343.1166 (36, $[M + Na]^+$), 321.1347 (42, $[M + H]^+$), 320.1268, (100, $[M]^+$, calcd for $C_{18}H_{16}N_4O_2$: 320.1268).

Diethyl 2-(Dicyanomethylene)malonate (162)[235]

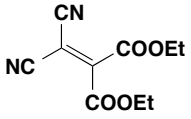

Procedure modified from one previously reported.[235] A solution of diethyl 2-oxomalonate (4.69 g, 26.9 mmol) and malononitrile (1.78 g, 26.9 mmol) in toluene (27 mL) was treated with acetic acid (286 µL, 5.0 mmol) and β-alanine (72 mg, 0.12 mmol) and heated at reflux under Dean-Stark conditions for 24 h. Evaporation and flash column chromatography (SiO_2; EtOAc/cyclohexane 3:7) gave **162** (4.54 g, 76%) as a clear colorless oil. Analytical data of **162** matched those of the literature.[235]

Diethyl 2-{3,3-Dicyano-2-[4-(dimethylamino)phenyl]allylidene}malonate (163)

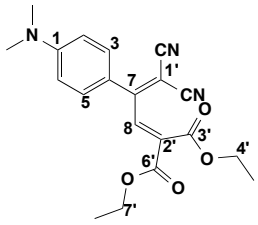

A solution of alkyne **102** (65 mg, 0.450 mmol) in MeCN (4.5 mL) was treated with alkene **162** (100 mg, 0.450 mmol) and stirred for 22 h at 25 °C. Evaporation and flash column chromatography (SiO_2; EtOAc/cyclohexane 3:7 v/v) gave **163** (150 mg, 91%) as a red solid. R_f = 0.30 (SiO_2; EtOAc/cyclohexane 3:7); m.p. 100–101 °C; ^{1}H NMR (400 MHz, $CDCl_3$): δ = 1.10 (t, J = 7.1 Hz, 3 H; $H_3C(5')$), 1.34 (t, J = 7.1 Hz, 3 H; $H_3C(8')$), 3.09 (s, 6 H, $N(CH_3)_2$), 3.88 (q, J = 7.1 Hz, 2 H; $H_2C(4')$), 4.33 (q, J = 7.1 Hz, 2 H; $H_2C(7')$), 6.65 (d, J = 9.2 Hz, 2 H; H–C(2,6)), 7.57 (d, J = 9.2 Hz, 2 H; H–C(3,5)), 7.74 ppm (s, 1 H; H–C(8)); ^{13}C NMR (100 MHz, $CDCl_3$): δ = 13.84 (1 C, $H_3C(5')$), 14.14 (1 C, $H_3C(8')$), 40.14 (2 C, $N(CH_3)_2$), 62.09 (1 C, $H_2C(4')$), 62.68 (1 C, $H_2C(7')$), 76.87 (1 C, C(1')), 111.32 (2 C, HC(2,6)), 113.81 (1 C, CN), 114.68 (1 C, CN), 119.06 (1 C, C(4)), 132.22 (2 C, HC(3,5)), 136.40 (1 C, C(2')), 139.34 (1 C, HC(8)), 153.77 (1 C, C(1)), 162.50 (1 C, C(6')), 163.09 (1 C, C(3')), 165.05 ppm (1 C, C(7)); IR (ATR): $\tilde{\nu}$ = 2984 (w), 2216 (w), 1725 (m), 1603 (m), 1541 (w), 1497 (m), 1439 (w), 1377 (m), 1345 (w), 1294 (w), 1253 (m), 1209 (m), 1174 (w), 1065 (w), 1016 (w), 945 (w), 861 (w), 819 cm^{-1} (w); UV/Vis ($CHCl_3$): λ_{max} (ε) = 455 (19600), 305 (15100 $M^{-1}cm^{-1}$); HR-MALDI-MS (3-HPA) m/z (%): 390.1424 (100, $[M + Na]^+$), 368.1605 (4, $[M + H]^+$), 367.1527, (29, $[M]^+$, calcd for $C_{20}H_{21}N_3O_4$: 367.1527).

Diethyl 2,3-Dicyanofumarate (164)[236]

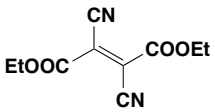

Procedure modified from one previously reported.[236] Ethyl cyanoacetate (11.3 g, 100 mmol) and thionyl chloride (12.3 mL, 170 mmol) were heated at reflux for 3 h, then cooled to 24 °C and stirred for 16 h. The solid that formed was collected

and washed with cold ethanol before being recrystallized from warm ethanol. The crystals were collected and dried under reduced pressure to give **164** (12.9 g, 58%) as white crsytals. Analytical data of **164** matched those of the literature.[236]

Ethyl 3,4-dicyano-6-[4-(dimethylamino)phenyl]-2-ethoxy-4*H*-pyran-4-carboxylate (165), **(2*E*,4*E*)-Diethyl 2,5-dicyano-3-[4-(dimethylamino)phenyl]hexa-2,4-dienedioate (166)** and **(2*E*,4*E*)-Diethyl 2,5-dicyano-3-[4-(dimethylamino)phenyl]hexa-2,4-dienedioate (167)**

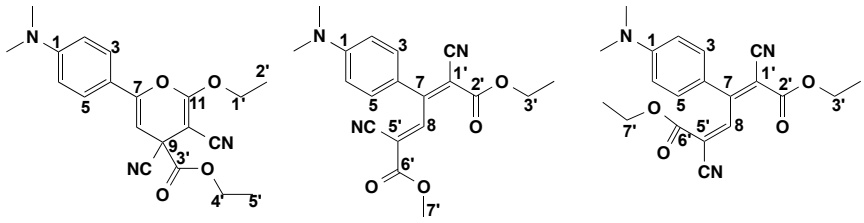

A solution of alkyne **164** (65 mg, 0.450 mmol) in MeCN (4.5 mL) was treated with alkene **164** (100 mg, 0.450 mmol) and stirred for 22 h at 25 °C. Evaporation and flash column chromatography (SiO_2; EtOAc/cyclohexane 1:4 v/v) gave a single fraction that consisted of three compounds. Crystallization from cyclohexane and collection of the solid afforded (±)-**165** (18 mg, 11%) as yellow crystals. The solvent remaining from crystallization was concentrated to give a solid that was then crystallized from 2-propanol and cyclohexane to give **166** (69 mg, 42%) as a red solid. The filtrate was evaporated and subjected to flash column chromatography (SiO_2; EtOAc/cyclohexane 1:9 → :7 v/v gradient elution) to give **167** (63 mg, 38%) as a red solid.

Data of **165**: R_f = 0.25 (SiO_2; EtOAc/cyclohexane 3:7); m.p. 137–138 °C; ^{1}H NMR (400 MHz, $CDCl_3$): δ = 1.42 (t, J = 7.1 Hz, 3 H; $H_3C(5')$), 1.50 (t, J = 7.1 Hz, 3 H; $H_3C(2')$), 3.05 (s, 6 H, $N(CH_3)_2$), 4.40 (qd, J = 7.1, 1.2 Hz, 2 H; $H_2C(4')$), 4.50 (qd, J = 7.1, 0.8 Hz, 2 H; $H_2C(1')$), 5.46 (s, 1 H; H–C(8)), 6.71 (d, J = 9.0 Hz, 2 H; H–C(2,6)), 7.41 ppm (d, J = 9.2 Hz, 2 H; H–C(3,5)); ^{13}C NMR (100 MHz, $CDCl_3$): δ = 14.14 (1 C, $H_3C(5')$), 14.91 (1 C, $H_3C(2')$), 40.23 (2 C, $N(CH_3)_2$), 44.90 (1 C, C(9)), 60.60 (1 C, C(10)), 64.45 (1 C, $H_2C(4')$), 66.51 (1 C, $H_2C(1')$), 90.04 (1 C, HC(8)), 111.76 (2 C, HC(2,6)), 114.8 (1 C, CN), 116.60 (1 C, CN), 116.98 (1 C, C(4)), 126.34 (2 C, HC(3,5)), 150.36 (1 C, C(7)), 151.96 (1 C, C(1)), 163.48 (1 C, C(11)), 165.89 ppm (1 C, C(3')); IR (ATR): $\tilde{\nu}$ = 2984 (w), 2913 (w), 2207 (w), 1737 (s), 1680 (s),

1607 (s), 1531 (m), 1445 (w), 1412 (w), 1370 (m), 1346 (w), 1323 (w), 1285 (s), 1243 (2), 1201 (s), 1176 (m), 1119 (w), 1096 (w), 1071 (w), 1046 (m), 1027 (m), 1009 (m), 948 (w), 854 (w), 815 (m), 791 (w), 774 (w), 759 (w), 745 (w), 697 (w), 684 (w), 643 (w), 623 cm^{-1} (w); UV/Vis ($CHCl_3$): λ_{max} (ε) = 332 (20300 $M^{-1}cm^{-1}$); HR-MALDI-MS (3-HPA) *m/z* (%): 390.1421 (76, $[M + Na]^+$), 368.1604 (73, $[M + H]^+$, calcd for $C_{20}H_{22}N_3O_4$: 368.1605).

Data of **166**: R_f = 0.25 (SiO_2; EtOAc/cyclohexane 3:7); m.p. 155–156 °C; ^1H NMR (400 MHz, $CDCl_3$): δ = 1.37(5) (overlapping t, J = 7.1 Hz, 3 H; $H_3C(4'$ or $8')$), 1.37(9) (overlapping t, J = 7.1 Hz, 3 H; $H_3C(4'$ or $8')$), 3.10 (s, 6 H, $N(CH_3)_2$), 4.31 (q, J = 7.1 Hz, 2 H; $H_2C(3')$), 4.38 (q, J = 7.1 Hz, 2 H; $H_2C(7')$), 6.71 (d, J = 9.2 Hz, 2 H; H–C(2,6)), 7.54 (d, J = 9.2 Hz, 2 H; H–C(3,5)), 8.79 ppm (s, 1 H; H–C(8)); ^{13}C NMR (100 MHz, $CDCl_3$): δ = 14.22 (1 C, $H_3C(4'$ or $8')$), 14.31 (1 C, $H_3C(4'$ or $8')$), 40.13 (2 C, $N(CH_3)_2$), 62.72 (1 C, $H_2C(3')$), 63.33 (1 C, $H_2C(7')$), 99.75 (1 C, C(1')), 111.67 (2 C, HC(2,6)), 112.52 (1 C, CN), 112.62 (1 C, CN), 117.26 (1 C, C(5')), 121.48 (1 C, C(4)), 132.63 (2 C, HC(3,5)), 153.50 (1 C, C(1)), 157.26 (1 C, HC(8)), 160.18 (1 C, C(7)), 160.95 (1 C, C(6')), 163.13 ppm (1 C, C(2')); IR (ATR): $\tilde{\nu}$ = 3068 (w), 2922 (w), 2217 (w), 1730 (m), 1703 (m), 1681 (w), 1598 (s), 1537 (w), 1502 (m), 1441 (m), 1382 (m), 1366 (m), 1323 (m), 1297 (m), 1259 (s), 1201 (s), 1176 (m), 1109 (s), 1072 (m), 1009 (m), 964 (w), 945 (m), 870 (w), 842 (w), 824 (m), 802 (m), 786 (m), 760 (m), 720 (m), 649 (w), 622 cm^{-1} (w); UV/Vis ($CHCl_3$): λ_{max} (ε) = 464 (6630), 327 (13500 $M^{-1}cm^{-1}$); HR-MALDI-MS (3-HPA) *m/z* (%): 390.1424 (73, $[M + Na]^+$), 368.1605 (100, $[M + H]^+$), 367.1527, (62, $[M]^+$, calcd for $C_{20}H_{21}N_3O_4$: 367.1527).

Data of **167**: R_f = 0.25 (SiO_2; EtOAc/cyclohexane 3:7); m.p. 107–111 °C; ^1H NMR (400 MHz, $CDCl_3$): δ = 1.16 (t, J = 7.1 Hz, 3 H; $H_3C(4')$), 1.36 (t, J = 7.1 Hz, 3 H; $H_3C(8')$), 3.07 (s, 6 H, $N(CH_3)_2$), 4.06 (q, J = 7.1 Hz, 2 H; $H_2C(3')$), 4.30 (q, J = 7.1 Hz, 2 H; $H_2C(7')$), 6.66 (d, J = 9.2 Hz, 2 H; H–C(2,6)), 7.59 (d, J = 9.2 Hz, 2 H; H–C(3,5)), 8.08 ppm (s, 1 H; H–C(8)); ^{13}C NMR (100 MHz, $CDCl_3$): δ = 13.95 (1 C, $H_3C(4')$), 14.29 (1 C, $H_3C(8')$), 40.11 (2 C, $N(CH_3)_2$), 62.57 (1 C, $H_2C(7')$), 62.79 (1 C, $H_2C(3')$), 97.68 (1 C, C(1')), 109.75 (1 C, CN), 111.32 (2 C, HC(2,6)), 115.32 (1 C, C(5')), 117.13 (1 C, CN), 120.54 (1 C, C(4)), 131.78 (2 C, HC(3,5)), 153.07 (1 C, C(1)), 157.08 (1 C, HC(8)), 159.92 (1 C, C(2')), 161.43 (1 C, C(7)), 163.27 ppm (1 C, C(6')); IR (ATR): $\tilde{\nu}$ = 2984 (w), 2216 (w), 1732 (m), 1708 (m), 1603 (s), 1514 (s), 1443 (w), 1368 (m), 1326 (m), 1255 (s), 1226 (s), 1204 (s), 1172 (w), 1109 (s), 1018

(w), 946 (w), 852 (w), 822 (w), 778 (w), 748 (w), 711 cm^{-1} (w); UV/Vis ($CHCl_3$): λ_{max} (ε) = 448 (17100) 343 (7600 $M^{-1}cm^{-1}$); HR-MALDI-MS (3-HPA) *m/z* (%): 390.1424 (70, $[M + Na]^+$), 368.1605 (100, $[M + H]^+$), 367.1527, (62, $[M]^+$, calcd for $C_{20}H_{21}N_3O_4$: 367.1527).

Triethyl 2-Cyanoethene-1,1,2-tricarboxylate (168)

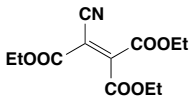

A solution of diethyl 2-oxomalonate (1.0 g, 5.74 mmol) and ethyl cyanoacetate (433 mg, 3.83 mmol) in toluene (4 mL) was treated with acetic acid (164 µL, 2.87 mmol) and β-alanine (41 mg, 0.46 mmol) and heated at reflux under Dean-Stark conditions for 24 h. Evaporation and flash column chromatography (SiO_2; EtOAc/cyclohexane 3:7) gave **168** (536 mg, 52%) as a clear colorless oil. R_f = 0.50 (SiO_2; EtOAc/cyclohexane 3:7); ^{1}H NMR (400 MHz, $CDCl_3$): δ = 1.36 (m, 9 H; H_3C), 4.37 ppm (m, 6 H; OCH_2); ^{13}C NMR (100 MHz, $CDCl_3$): δ = 13.89 (1 C, H_3C), 13.91 (1 C, H_3C), 13.96 (1 C, H_3C), 63.23 (1 C, H_2C), 63.96 (1 C, H_2C), 64.23 (1 C, H_2C), 112.04 (1 C, CN), 114.82 (1 C, C(2)), 147.27 (1 C, $(EtO_2C)_2C$), 159.25 (1 C, CO), 159.91 (1 C, CO), 161.99 ppm (1 C, CO); IR (ATR): $\tilde{\nu}$ = 2987 (w), 1739 (s), 1468 (w), 1447 (w), 1393 (w), 1369 (w), 1231 (s), 1143(m), 1096 (w), 1049 (w), 1018 (m), 855 (w), 750 (w), 641 cm^{-1} (w); HR-ESI-MS *m/z* (%): 287.1235 (100, $[M + NH_4]^+$, calcd for $C_{12}H_{19}N_2O_6$: 287.1238).

Diethyl 3-Cyano-6-[4-(dimethylamino)phenyl]-2-ethoxy-4*H*-pyran-4,4-dicarboxylate (169), **(*E*)-Triethyl 4-cyano-3-[4-(dimethylamino)phenyl]buta-1,3-diene-1,1,4-tricarboxylate (170)** and **(*E*)-Triethyl 4-cyano-3-[4-(dimethylamino)phenyl]buta-1,3-diene-1,1,4-tricarboxylate (171)**

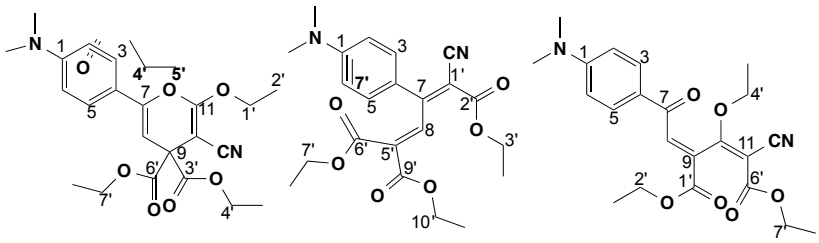

A solution of alkyne **102** (50 mg, 0.344 mmol) in MeCN (3.4 mL) was treated with alkene **168** (60 mg, 0.344 mmol) and stirred for 5 h at reflux. Evaporation and

flash column chromatography (SiO_2; EtOAc/cyclohexane 1:4 v/v) afforded two fractions, A and B. Evaporation of fraction A gave a red solid that was dissolved in warm cyclohexane and the solid that formed collected to give **169** (29 mg, 21%) as a yellow solid. The filtrate was concentrated under reduced pressure to afford compound **170** (87 mg, 63%) as a red solid. Evaporation of fraction B afforded compound **171** (6 mg, 4%) as yellow crystals.

Data for compound **169**: R_f = 0.30 (SiO_2; EtOAc/cyclohexane 3:7); m.p. 154–155 °C; ^{1}H NMR (400 MHz, $CDCl_3$): δ = 1.32 (t, J = 7.1 Hz, 6 H; H_3C(5',8')), 1.45 (t, J = 7.1 Hz, 3 H; H_3C(2')), 3.00 (s, 6 H, $N(CH_3)_2$), 4.29 (overlapping q, J = 7.1 Hz, 2 H; H_2C(4' or 7')), 4.30 (overlapping q, J = 7.1 Hz, 2 H; H_2C(4' or 7')), 4.42 (q, J = 7.1 Hz, 2 H; H_2C(1')), 5.58 (s, 1 H, H–C(8)), 6.68 (d, J = 9.0 Hz, 2 H; H–C(2,6)), 7.41 ppm (d, J = 9.0 Hz, 2 H; H–C(3,5)); ^{13}C NMR (100 MHz, $CDCl_3$): δ = 14.16 (2 C, H_3C(5',8')), 14.97 (1 C, H_3C(2')), 40.32 (2 C, $N(CH_3)_2$), 54.75 (1 C, C(10)), 61.79 (1 C, C(9)), 62.75 (2 C, H_2C(4',7')), 65.85 (1 C, H_2C(1')), 93.36 (1 C, HC(8)), 111.78 (2 C, HC(2,6)), 116.52 (1 C, CN), 118.55 (1 C, C(4)), 126.14 (2 C, HC(3,5)), 148.67 (1 C, C(7)), 151.49 (1 C, C(1)), 163.53 (1 C, C(11)), 168.81 ppm (2 C, C(3',6')); IR (ATR): $\tilde{\nu}$ = 2982 (w), 2906 (w), 2211 (m), 1754 (m), 1725 (s), 1686 (s), 1608 (s), 1530 (m), 1474 (w), 1443 (w), 1401 (w), 1374 (m), 1341 (w), 1322 (w), 1285 (m), 1251 (s), 1198 (s), 1160 (m), 1122 (w), 1074 (w), 1028 (s), 982 (w), 950 (w), 890 (w), 865 (w), 851 (w), 812 (s), 758 (w), 727 (w), 716 (w), 683 (w), 653 (w), 639 (w), 623 cm^{-1} (w); UV/Vis ($CHCl_3$): λ_{max} (ε) = 319 (22500 M^{-1}cm^{-1}); HR-MALDI-MS (3-HPA) m/z (%): 437.1682 (100, $[M + Na]^+$), 415.1864 (33, $[M + H]^+$, calcd for $C_{22}H_{27}N_2O_6$: 415.1864).

Data for compound **170**: R_f = 0.30 (SiO_2; EtOAc/cyclohexane 3:7); m.p. 85 °C; ^{1}H NMR (400 MHz, $CDCl_3$): δ = 1.05 (t, J = 7.1 Hz, 3 H; H_3C(4')), 1.31 (overlapping t, J = 7.1 Hz, 3 H; H_3C(8' or 11')), 1.34 (overlapping t, J = 7.1 Hz, 3 H; H_3C(8' or 11')), 3.04 (s, 6 H, $N(CH_3)_2$), 3.79 (q, J = 7.1 Hz, 2 H; H_2C(3')), 4.32 (overlapping q, J = 7.1, Hz, 2 H; H_2C(7' or 10')), 4.33 (overlapping q, J = 7.1, Hz, 2 H; H_2C(7' or 10')), 6.63 (d, J = 9.2 Hz, 2 H; H–C(2,6)), 7.51 (d, J = 9.2 Hz, 2 H; H–C(3,5)), 8.16 ppm (s, 1 H; H–C(8)); ^{13}C NMR (100 MHz, $CDCl_3$): δ = 13.80 (1 C, H_3C(4')), 14.16 (1 C, H_3C(8' or 11')), 14.23 (1 C, H_3C(8' or 11')), 40.04 (2 C, $N(CH_3)_2$), 61.56 (1 C, H_2C(3')), 62.08 (1 C, H_2C(7' or 10')), 62.21 (1 C, H_2C(7' or 10')), 99.41 (1 C, C(1')), 111.01 (2 C, HC(2,6)), 117.64 (1 C, CN), 121.46 (1 C, C(4)),

131.50 (1 C, C(5')), 132.50 (2 C, HC(3,5)), 144.31 (1 C, HC(8)), 152.94 (1 C, C(1)), 162.91 (1 C, C(6' or 9')), 162.95 (1 C, C(6' or 9')), 163.25 (1 C, C(7)), 163.92 ppm (1 C, C(2')); IR (ATR): $\tilde{\nu}$ = 2989 (w), 2211 (w), 1717 (m), 1703 (m), 1631 (w), 1602 (m), 1542 (w), 1508 (m), 1464 (w), 1441 (w), 1377 (w), 1365 (w), 1322 (w), 1243 (s), 1207 (s), 1135 (m), 1106 (m), 1096 (m), 1066 (m), 1021 (m), 943 (w), 890 (w), 860 (w), 835 (w), 820 (w), 797 (w), 764 (s), 749 (s), 709 (w), 670 (w), 643 (w), 620 cm^{-1} (w); UV/Vis ($CHCl_3$): λ_{max} (ε) = 449 (17500), 298 (19700 $M^{-1}cm^{-1}$); HR-MALDI-MS (3-HPA) *m/z* (%): 437.1683 (100, $[M + Na]^+$), 415.1868 (23, $[M + H]^+$), 414.1788 (60, $[M]^+$, calcd for $C_{22}H_{26}N_2O_6$: 414.1785).

Data for compound **171**: R_f = 0.15 (SiO_2; EtOAc/cyclohexane 3:7); m.p. 143–145 °C; ^{1}H NMR (400 MHz, $CDCl_3$): δ = 1.20 (t, *J* = 7.1 Hz, 3 H; $H_3C(8')$), 1.32 (t, *J* = 7.1 Hz, 3 H; $H_3C(5')$), 1.39 (t, *J* = 7.1 Hz, 3 H; $H_3C(3')$), 3.10 (s, 6 H, $N(CH_3)_2$), 4.08 (q, *J* = 7.1 Hz, 2 H; $H_2C(7')$), 4.33 (m, 4 H, $H_2C(2',4')$), 6.65 (d, *J* = 9.2 Hz, 2 H; H–C(2,6)), 7.88 (d, *J* = 9.2 Hz, 2 H; H–C(3,5)), 8.10 ppm (s, 1 H; H–C(8)); ^{13}C NMR (100 MHz, $CDCl_3$): δ = 14.21 (1 C, $H_3C(5'$ or $8')$), 14.24 (1 C, $H_3C(5'$ or $8')$), 14.89 (1 C, $H_3C(3')$), 40.19 (2 C, $N(CH_3)_2$), 61.29 (1 C, $H_2C(7')$), 62.60 (1 C, $H_2C(2')$), 67.95 (1 C, $H_2C(4')$), 86.32 (1 C, C(11)), 111.07 (2 C, HC(2,6)), 114.74 (1 C, CN), 124.27 (1 C, C(4)), 131.66 (2 C, HC(3,5)), 133.77 (1 C, C(9)), 136.69 (1 C, HC(8)), 154.40 (1 C, C(1)), 162.96 (1 C, C(1')), 163.54 (1 C, C(6')), 178.56 (1 C, C(10)), 185.37 ppm (1 C, C(7)); IR (ATR): $\tilde{\nu}$ = 2986 (w), 2217 (w), 1722 (s), 1651 (w), 1616 (w), 1562 (s), 1541 (m), 1480 (w), 1441 (w), 1416 (w), 1396 (w), 1378 (m), 1318 (w), 1275 (s), 1260 (s), 1195 (m), 1169 (m), 1128 (m), 1105 (s), 1088 (s), 1034 (m), 1012 (m), 941 (w), 917 (w), 895 (w), 882 (w), 855 (w), 833 (m), 800 (w), 764 (s), 749 (s), 711 (w), 680 (w), 631 (w), 610 cm^{-1} (w); UV/Vis ($CHCl_3$): λ_{max} (ε) = 423 (13200), 271 (20700 $M^{-1}cm^{-1}$); HR-MALDI-MS (3-HPA) *m/z* (%): 437.1683 (100, $[M + Na]^+$), 415.1865 (13, $[M + H]^+$, calcd for $C_{22}H_{27}N_2O_6$: 415.1864).

1,1-Diethyl 2-Methyl 2-Cyanoethene-1,1,2-tricarboxylate (172)

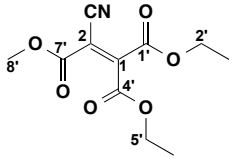

A solution of diethyl 2-oxomalonate (1.0 g, 5.74 mmol) and methyl cyanoacetate (379 mg, 3.83 mmol) in toluene (4 mL) was treated with acetic acid (164 μL, 2.87 mmol) and β-alanine (41 mg, 0.46 mmol) and heated at reflux under Dean-Stark conditions for 24 h. Evaporation and flash column chromatography (SiO_2; EtOAc/cyclohexane 3:7) gave **172** (469 mg, 48%) as a clear colorless oil. R_f = 0.33 (SiO_2; EtOAc/cyclohexane 3:7); ^{1}H NMR (400 MHz, $CDCl_3$): δ = 1.36 (t, J = 7.1 Hz, 3 H; H_3C(3' or 6')), 1.37 (t, J = 7.1 Hz, 3 H; H_3C(3' or 6')), 3.92 (s, 3 H; H_3C(8'), 4.40 ppm (overlapping q, J = 7.1 Hz, 4 H; H_3C(2',5')); ^{13}C NMR (100 MHz, $CDCl_3$): δ = 13.89 (1 C, H_3C(3' or 6')), 13.93 (1 C, H_3C(3' or 6')), 54.47 (1 C, H_3C(8'), 63.32 (1 C, H_3C(2' or 5')), 64.02 (1 C, H_3C(2' or 5')), 112.01 (1 C, CN), 114.27 (1 C, C(2)), 147.63 (1 C, C(1)), 159.77 (1 C, C(7')), 159.82 (1 C, H_3C(1' or 4')), 161.92 ppm (1 C, H_3C(2' or 5')); IR (ATR): $\tilde{\nu}$ = 2986 (w), 1834 (w), 1736 (s), 1438 (w), 1392 (w), 1370 (w), 1240 (s), 1174 (w), 1133 (m), 1095 (w), 1048 (m), 1024 (m), 906 (w), 859 (w), 833 (w), 768 (w), 650 cm^{-1} (w); HR-ESI-MS m/z (%): 273.1080 (100, $[M + NH_4]^+$, calcd for $C_{11}H_{17}N_2O_6$: 273.10814).

Diethyl 3-cyano-6-[4-(dimethylamino)phenyl]-2-methoxy-4*H*-pyran-4,4-dicarboxylate (173), **(*E*)-1,1-Diethyl 4-methyl 4-cyano-3-[4-(dimethylamino)phenyl]buta-1,3-diene-1,1,4-tricarboxylate (174)** and **(2*E*,4*E*)-5-Ethyl 1-methyl 2-cyano-4{2-[4-(dimethylamino)phenyl]-2-oxoethylidene}-3-ethoxypent-2-enedioate (175)**

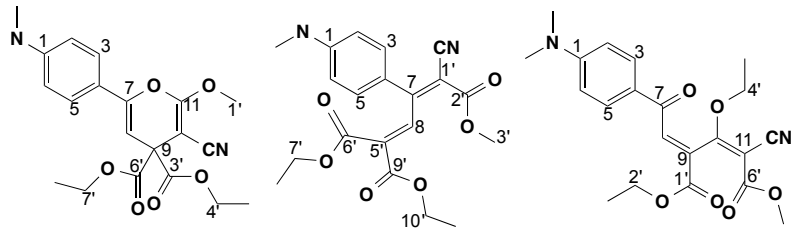

A solution of alkyne **102** (57 mg, 0.391 mmol) in MeCN (3.4 mL) was treated with alkene **172** (100 mg, 0.391 mmol) and stirred for 5 h at reflux. Evaporation and flash column chromatography (SiO_2; EtOAc/cyclohexane 1:4 v/v) afforded two fractions, A and B. Evaporation of fraction A gave a red oil that consisted of **173** and **174** (103 mg, 66%) in a 1:3 ratio. Attempted separation through crystallization or

additional chromatography was unsuccessful. Evaporation of fraction B afforded **175** (45 mg, 29%) as yellow crystals.

Data for the 1:3 mixture of compounds **173** and **174**: R_f = 0.61 (SiO_2; EtOAc/cyclohexane 1:1); ^{1}H NMR (400 MHz, $CDCl_3$): δ = 1.05 (t, J = 7.1 Hz, 3 H; H_3C(b7')), 1.29–1.33 (complex m, 5 H; H_3C(a4',a7',b10')), 2.99 (s, 2 H, aN(CH_3)$_2$), 3.04 (s, 6 H, bN(CH_3)$_2$), 3.78 (q, J = 7.1 Hz, 2 H; H_2C(b6')), 3.84 (s, 3 H; H_3C(b3')), 4.02 (s, 1 H; H_3C(a1')), 4.26–4.33 (complex m, 3.33 H; H_2C(b9',a3',a6')), 5.58 (s, 0.33 H, H–C(a8)), 6.63 (d, J = 9.2 Hz, 2 H; H–C(b2,b6)), 6.67 (d, J = 9.0 Hz, 0.66 H; H–C(a2,a6)), 7.41 (d, J = 9.0 Hz, 2 H; H–C(a3,a5)), 7.52 (d, J = 9.2 Hz, 2 H; H–C(b3,b5)), 8.16 ppm (s, 1 H; H–C(b8)); ^{13}C NMR (100 MHz, $CDCl_3$): δ = 13.78 (1 C, H_3C(b7'), 14.08 (2 C, H_3C(a4',a7')), 14.15 (1 C, H_3C(b10')), 40.03 (2 C, bN(CH_3)$_2$), 40.23 (2 C, aN(CH_3)$_2$), 52.97 (1 C, H_3C(b3')), 54.65 (1 C, C(a10)), 56.00 (1 C, H_3C(a1')), 61.32 (1 C, C(a10)), 61.57 (1 C, H_2C(b6')), 62.10 (1 C, H_2C(b9')), 62.70 (2 C, H_2C(a3',a6')), 93.33 (1 C, HC(a8)), 98.54 (1 C, C(b1')), 111.00 (2 C, HC(b2,b6)), 111.70 (2 C, HC(a2,a6)), 116.30 (1 C, aCN), 117.72 (1 C, bCN), 118.30 (1 C, C(a4)), 121.37 (1 C, C(b4)), 126.08 (2 C, HC(a3,a5)), 131.68 (1 C, C(b4')), 132.57 (2 C, HC(b3,b5)), 144.25 (1 C, HC(b8)), 148.56 (1 C, C(a7)), 151.45 (1 C, C(a1)), 153.02 (1 C, C(b1)), 163.21 (1 C, C(b2')), 163.35 (1 C, C(b7)), 163.40 (1 C, C(b8')), 163.66 (1 C, C(a11)), 163.88 (1 C, C(b5')), 168.66 ppm (2 C, C(a2',a5')); IR (ATR): $\tilde{\nu}$ = 2983 (w), 2215 (w), 1716 (s), 1684 (w), 1603 (s), 1514 (m), 1436 (w), 1370 (m), 1325 (w), 1243 (s), 1198 (s), 1116 (s), 1063 (s), 1037 (m), 944 (w), 904 (w), 860 (w), 818 (m), 764 (w), 712 (w), 674 (w), 623 cm^{-1} (w); UV/Vis ($CHCl_3$): λ_{max} (ε) = 451 (15800), 304 (21900 M^{-1}cm^{-1}); HR-MALDI-MS (3-HPA) *m/z* (%): 423.1527 (9, [M + Na]$^+$), 401.1709 (13, [M + H]$^+$), 400.1628 ([M]$^+$, calcd for $C_{21}H_{24}N_2O_6$: 400.1629).

Data for **175**: R_f = 0.14 (SiO_2; EtOAc/cyclohexane 3:7); m.p. 153–154 °C; ^{1}H NMR (400 MHz, $CDCl_3$): δ = 1.32 (t, J = 7.1 Hz, 3 H; H_3C(3' or 5')), 1.39 (t, J = 7.1 Hz, 3 H; H_3C(3' or 5')), 3.09 (s, 6 H, N(CH_3)$_2$), 3.63 (s, 3 H; H_3C(7')), 4.20–4.33 (complex m, 4 H; H_2C(2',4')), 6.65 (d, J = 9.1 Hz, 2 H; H–C(2,6)), 7.87 (d, J = 9.1 Hz, 2 H; H–C(3,5)), 8.10 ppm (s, 1 H; H–C(8)); ^{13}C NMR (100 MHz, $CDCl_3$): δ = 14.20 (1 C, H_3C(3' or 5')), 14.83 (1 C, (1 C, H_3C(3' or 5')), 40.16 (2 C, N(CH_3)$_2$), 52.15 (1 C, H_3C(7')), 62.60 (1 C, H_2C(2' or 4')), 67.98 (1 C, H_2C(2' or 4')), 85.79 (1 C, C(11)), 111.04 (2 C, HC(2,6)), 114.70 (1 C, CN), 124.19 (1 C, C(4)), 131.64 (2 C, HC(3,5)),

133.29 (1 C, C(9)), 136.64 (1 C, HC(8)), 154.39 (1 C, C(1)), 162.86 (1 C, C(1')), 163.96 (1 C, C(6')), 178.94 (1 C, C(10)), 185.18 ppm (1 C, C(7)); IR (ATR): $\tilde{\nu}$ = 2990 (w), 2219 (w), 1714 (m), 1646 (w), 1619 (w), 1567 (m), 1546 (w), 1477 (w), 1438 (w), 1415 (w), 1397 (w), 1379 (w), 1369 (w), 1319 (w), 1275 (s), 1262 (s), 1242 (w), 1186 (m), 1164 (w), 1123 (m), 1090 (m), 1016 (w), 941 (w), 918 (w), 868 (w), 833 (w), 805 (w), 764 (s), 750 (s), 718 (w), 662 (w), 632 cm^{-1} (w); UV/Vis ($CHCl_3$): λ_{max} (ε) = 451 (15800), 304 (21900 $M^{-1}cm^{-1}$); HR-MALDI-MS (3-HPA) *m/z* (%): 423.1527 (10, $[M + Na]^+$), 401.1708 (13, $[M + H]^+$), 400.1628 ($[M]^+$, calcd for $C_{21}H_{24}N_2O_6$: 400.1629).

Triethyl 2-cyano-3-(4-(dimethylamino)phenyl)cyclobut-3-ene-1,1,2-tricarboxylate (176)

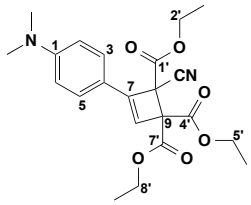

A solution of alkyne **102** (50 mg, 0.344 mmol) in $(CH_2Cl)_2$ (3.4 mL) was treated with alkene **168** (60 mg, 0.344 mmol) and stirred for 36 h at 23 °C. Evaporation and flash column chromatography (SiO_2; EtOAc/cyclohexane 1:4 v/v) afforded three fractions, A, B and C. Fractions A and B were further purified as detailed immediately above to afford compounds **169** (17 mg, 15%), **170** (10 mg, 9%) and **171** (31 mg, 28%). Evaporation of fraction C gave cyclobutene (±)-**176** (51 mg, 46%) as a pale yellow oil. Cyclobutene (±)-**176** slowly underwent retroelectrocyclization to afford compound **170**. R_f = 0.32 (SiO_2; EtOAc/cyclohexane 3:7); ^{1}H NMR (300 MHz, $CDCl_3$): δ = 1.26–1.36 (complex m, 9 H; $H_3C(3',6',9')$), 2.99 (s, 6 H, $N(CH_3)_2$), 4.18–4.37 (complex m, 6 H; $H_2C(2',5',8')$), 6.39 (s, 1 H; H–C(8)), 6.65 (d, *J* = 9.2 Hz, 2 H; H–C(2,6)), 7.27 ppm (d, *J* = 9.2 Hz, 2 H; H–C(3,5)); ^{13}C NMR (75 MHz, $CDCl_3$): δ = 14.02 (1 C, $H_3C(3',6'$ or $9')$), 14.08 (1 C, $H_3C(3',6'$ or 9')), 14.12 (1 C, $H_3C(3',6'$ or 9')), 40.25 (2 C, $N(CH_3)_2$), 52.57 (1 C, C(10)), 62.41 (1 C, C(9)), 62.43 (1 C, $H_2C(2',5'$ or $8')$), 63.29 (1 C, $H_2C(2',5'$ or $8')$), 63.64 (1 C, $H_2C(2',5'$ or $8')$), 111.83 (2 C, HC(2,6)), 115.10 (1 C, CN), 116.93 (1 C, C(4)), 122.31 (1 C, HC(8)), 126.76 (2 C, HC(3,5)), 144.97 (1 C, C(7)), 151.43 (1 C, C(1)), 164.86 (1 C, C(1',4' or 7')), 166.11 (1 C, C(1',4' or 7')), 166.40 ppm (1 C, C(1',4' or 7')); IR

(ATR): $\tilde{\nu}$ = 2984 (w), 2346 (w), 1739 (s), 1631 (w), 1606 (m), 1522 (m), 1445 (w), 1366 (w), 1295 (w), 1216 (s), 1196 (s), 1171 (w), 1138 (w), 1097 (m), 1201 (m), 944 (w), 913 (w), 855 (w), 816 (m), 729 (w), 647 (w), 625 cm^{-1} (w); HR-MALDI-MS (DCTB) *m*/*z* (%): 437.1683 (1, $[M + Na]^+$), 414.1784 (13, $[M]^+$, calcd for $C_{22}H_{26}N_2O_6$: 414.1785).

Diethyl 3-cyano-6-(4-(dimethylamino)phenyl)-2-ethoxy-4*H*-pyran-4,4-dicarboxylate (182) and **(*E*)-3-ethyl 1,1-bis(2,2,2-trifluoroethyl) 5-(4-(dimethylamino)phenyl)-2-ethoxy-5-oxopenta-1,3-diene-1,1,3-tricarboxylate (184)**

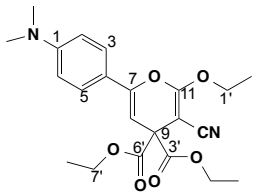

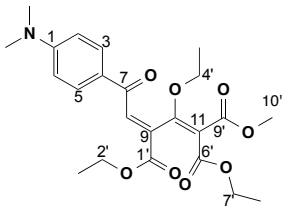

A solution of alkyne **102** (145 mg, 1.0 mmol) in 1,2-dichlorobenzene (2 mL) was treated with alkene **181** (316 mg, 1.0 mmol) and heated with microwave irradiation for 3 h at 200 °C. Flash column chromatography (SiO_2; CH_2Cl_2/EtOAc/cyclohexane 0:0:1→ v/v gradient elution) afforded two fractions, A and B. Evaporation of fraction A afforded **182** (13 mg, 3%) as an orange solid. Evaporation of fraction B afforded **184** (10 mg, 2%) a yellow solid.

Data of **182**: R_f = 0.62 (SiO_2; EtOAc/CH_2Cl_2 1:9); m.p. 67–70 °C; ^{1}H NMR (400 MHz, $CDCl_3$): δ = 1.13 (t, *J* = 7.1 Hz, 3 H; H_3C(3',8' or 11')), 1.27 (overlapping t, *J* = 7.1 Hz, 3 H; H_3C(5')), 1.29 (overlapping t, *J* = 7.1 Hz, 3 H; H_3C(3',8' or 11')), 1.33 (t, *J* = 7.1 Hz, 3 H; H_3C(3',8' or 11')), 3.07 (s, 6 H, $N(CH_3)_2$), 4.00 (m, 2 H; H_2C(4')), 4.02 (overlapping q, *J* = 7.1 Hz, 2 H; H_2C(2',7' or 10')), 4.26 (q, *J* = 7.1 Hz, 2 H; H_2C(2',7' or 10')), 4.34 (q, *J* = 7.1 Hz, 2 H; H_2C(2',7' or 10')), 6.63 (d, *J* = 9.1 Hz, 2 H; H–C(2,6)), 7.88 (d, *J* = 9.1 Hz, 2 H; H–C(3,5)), 7.99 ppm (s, 1 H; H–C(8)); ^{13}C NMR (100 MHz, $CDCl_3$): δ = 14.21 (1 C, H_3C(3',8' or 11')), 14.27 (2 overlapping C, H_3C(3',8' or 11')), 15.00 (1 C, H_3C(5')), 40.15 (2 C, $N(CH_3)_2$), 60.53 (1 C, H_2C(2',7' or 10')), 60.96 (1 C, H_2C(2',7' or 10')), 62.17 (1 C, H_2C(2',7' or 10')), 66.22 (1 C, H_2C(4')), 108.28 (1 C, C(11)), 110.90 (2 C, HC(2,6)), 124.66 (1 C, C(4)), 131.56 (2 C, HC(3,5)), 134.44 (1 C, C(9)), 137.10 (1 C, HC(8)), 154.12 (1 C, C(1)), 164.15 (1 C,

C(1',6' or 9')), 164.91 (1 C, C(1',6' or 9')), 165.12 (1 C, C(1',6' or 9')), 165.20 (1 C, C(10)), 186.81 ppm (1 C, C(7)); IR (ATR): $\tilde{\nu}$ = 2982 (w), 1725 (m), 1652 (w), 1591 (s), 1547 (w), 1444 (w), 1375 (m), 1319 (w), 1265 (m), 1326 (m), 1188 (m), 1092 (m), 1026 (w), 944 (w), 870 (w), 822 cm^{-1} (w); UV/Vis ($CHCl_3$): λ_{max} (ε) = 401 (11100 $M^{-1}cm^{-1}$); HR-ESI-MS *m/z* (%): 462.2118 (100, $[M + H]^+$, calcd for $C_{24}H_{32}NO_8$: 462.2122).

Data of **184**: R_f = 0.56 (SiO_2; EtOAc/CH_2Cl_2 1:9); m.p. 71–72 °C; ^{1}H NMR (400 MHz, $CDCl_3$): δ = 1.25 (overlapping t, J = 7.1 Hz, 3 H; $H_3C(11')$), 1.27 (overlapping t, J = 7.1 Hz, 6 H; $H_3C(5',8')$), 1.45 (t, J = 7.1 Hz, 3 H; $H_3C(2')$), 2.99 (s, 6 H, $N(CH_3)_2$), 4.15–4.25 (m, 6 H; $H_2C(4',7',10')$), 4.40 (q, J = 7.1, 2 H; $H_2C(1')$), 5.60 (s, 1 H; H–C(8)), 6.68 (d, J = 9.0 Hz, 2 H; H–C(2,6)), 7.42 ppm (d, J = 9.0 Hz, 2 H; H–C(3,5)); ^{13}C NMR (100 MHz, $CDCl_3$): δ = 14.19 (2 C, $H_3C(5',8')$), 14.28 (1 C, $H_3C(11')$), 15.00 (1 C, $H_3C(2')$), 40.40 (2 C, $N(CH_3)_2$), 56.08 (1 C, C(9)), 60.11 (1 C, $H_2C(10')$), 61.92 (2 C, $H_2C(4',7')$), 65.43 (1 C, $H_2C(1')$), 82.55 (1 C, C(10)), 95.45 (1 C, HC(8)), 111.89 (2 C, HC(2,6)), 119.48 (1 C, C(4)), 125.96 (2 C, HC(3,5)), 147.70 (1 C, C(7)), 151.25 (1 C, C(1)), 159.71 (1 C, C(11)), 166.46 (1 C, C(9')), 170.48 ppm (2 C, C(3',6')); IR (ATR): $\tilde{\nu}$ = 2982 (w), 1730 (s), 1689 (m), 1609 (s), 1525 (m), 1445 (w), 1366 (m), 1283 (m), 1196 (s), 1081 (s), 1040 (s), 946 (w), 864 (w), 821 (w), 644 cm^{-1} (w); UV/Vis ($CHCl_3$): λ_{max} (ε) = 315 (13000 $M^{-1}cm^{-1}$); HR-ESI-MS *m/z* (%): 462.2116 (100, $[M + H]^+$, calcd for $C_{24}H_{32}NO_8$: 462.2122).

Bis(cyanomethyl) Malonate (S1)

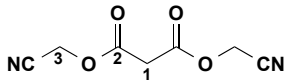

Malonic acid (2.0 g, 19.22 mmol) in chloroacetonitrile (6.4 mL) at 0 °C was treated with Et_3N (5.6 mL, 40.36 mmol), warmed slowly to 23 °C, and stirred for 16 h. The mixture was diluted with water (100 mL), extracted with CH_2Cl_2 (100 mL), and the separated organic phase dried ($MgSO_4$), filtered, and evaporated to give **S1** (2.06 g, 59%) as a clear colorless oil. R_f = 0.42 (SiO_2; EtOAc/cyclohexane 1:1); ^{1}H NMR (400 MHz, $CDCl_3$): δ = 3.61 (s, 2 H; $H_2C(1)$), 4.82 ppm (s, 4 H; $H_2C(3)$); ^{13}C NMR (100 MHz, $CDCl_3$): δ = 39.94 (1 C, $H_2C(1)$), 49.48 (2 C, $H_2C(3)$), 113.58 (2 C, CN), 163.99 ppm (2 C, C(2)); IR (ATR): $\tilde{\nu}$ = 2959 (w), 1750 (s), 1428 (w), 1374 (w),

1332 (w), 1268 (w), 1136 (s), 1041 (m), 1017 (w), 912 (m), 730 (s), 649 cm^{-1} (w); HR-ESI-MS *m*/*z* (%): 200.0666 (100, $[M+NH_4]^+$, calcd for $C_7H_{10}N_3O_4$: 200.0666).

1,1-Bis(cyanomethyl) 2,2-Diethyl ethene-1,1,2,2-tetracarboxylate (185)

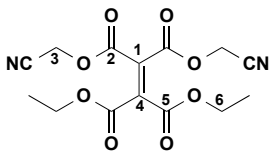

A solution of diethyl 2-oxomalonate (956 mg, 5.49 mmol) and malonate **S1** (250 mg, 1.37 mmol) in toluene (7 mL) was treated with acetic acid (59 μL, 1.03 mmol) and β-alanine (15 mg, 0.16 mmol) and heated at reflux under Dean-Stark conditions for 24 h. Evaporation and flash column chromatography (SiO_2; EtOAc/cyclohexane 3:7) gave **185** (203 mg, 44%) as a white solid. R_f = 0.55 (SiO_2; EtOAc/cyclohexane 1:1); m.p. 80–81 °C; ^{1}H NMR (400 MHz, $CDCl_3$): δ = 1.35 (t, J = 7.1 Hz, 6 H; $H_3C(7)$), 4.37 (q, J = 7.1 Hz, 4 H; $H_2C(6)$), 4.90 ppm (s, 4 H; $H_2C(3)$); ^{13}C NMR (100 MHz, $CDCl_3$): δ = 13.92 (2 C, $H_3C(7)$), 50.12 (2 C, $H_2C(3)$), 63.64 (2 C, $H_2C(6)$), 113.08 (2 C, CN), 130.70 (1 C, C(1)), 139.83 (1 C, C(4)), 160.26 (2 C, C(5)), 161.34 ppm (2 C, C(2)); IR (ATR): $\tilde{\nu}$ = 3003 (w), 1748 (s), 1726 (s), 1659 (w), 1472 (w), 1447 (w), 1420 (w), 1365 (w), 1295 (w), 1260 (s), 1225 (s), 1172 (w), 1128 (m), 1110 (w), 1098 (w), 1047 (m), 1030 (s), 1010 (s), 967 (w), 956 (w), 933 (w), 908 (w), 862 (w), 844 (w), 822 (w), 790 (w), 778 (w), 764 (m), 732 cm^{-1} (w); HR-ESI-MS *m*/*z* (%): 356.1083 (100, $[M + NH_4]^+$, calcd for $C_{14}H_{18}N_3O_8$: 356.1088).

3-(Cyanomethyl) 4,4-Diethyl 2-(cyanomethoxy)-6-[4-(dimethylamino)phenyl]-4*H*-pyran-3,4,4-tricarboxylate (186), **4,4-Diethyl 1,1-Bis(2,2,2-Cyanomethyl) 2-[4-(dimethylamino)phenyl]buta-1,3-diene-1,1,4,4-tetracarboxylate (187)** and **(*E*)-1,1-Bis(Cyanomethyl) 3-Ethyl 5-[4-(dimethylamino)phenyl]-2-ethoxy-5-oxopenta-1,3-diene-1,1,3-tricarboxylate (188)**

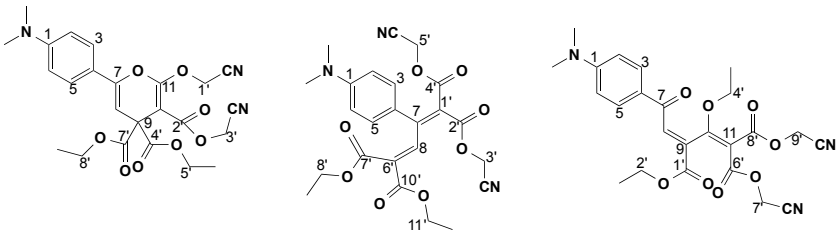

A solution of alkyne **102** (63 mg, 0.43 mmol) in $(CH_2Cl)_2$ (4.3 mL) was treated with alkene **185** (146 mg, 0.43 mmol) and stirred for 36 h at reflux. Evaporation and flash column chromatography (SiO_2; EtOAc/cyclohexane 1:4 v/v) afforded two fractions, A and B. Evaporation of fraction B afforded compound **188** (33 mg, 16%) as a red sticky oil. Fraction A (R_f = 0.44 (SiO_2; EtOAc/cyclohexane 3:7)) was resubjected to flash column chromatography (SiO_2; EtOAc/CH_2Cl_2 1:9 v/v) to afford two fractions, C and D. Evaporation of fraction C gave **187** (80 mg, 38%) as a red sticky oil. Evaporation of fraction D gave **186** (24 mg, 11%) as a yellow solid.

Data of **186**: R_f = 0.41 (SiO_2; EtOAc/CH_2Cl_2 1:9); m.p. 98–102 °C; ^{1}H NMR (400 MHz, $CDCl_3$): δ = 1.30 (t, J = 7.1 Hz, 6 H; H_3C(6',9')), 3.01 (s, 6 H, $N(CH_3)_2$), 4.26 (q, J = 7.1 Hz, 4 H; H_2C(5',8')), 4.78 (s, 2 H; H_2C(3')), 4.96 (s, 2 H; H_2C(1')), 5.65 (s, 1 H, H–C(8)), 6.70 (d, J = 9.0 Hz, 2 H; H–C(2,6)), 7.45 ppm (d, J = 9.0 Hz, 2 H; H–C(3,5)); ^{13}C NMR (100 MHz, $CDCl_3$): δ = 14.13 (2 C, H_3C(6',9')), 40.29 (2 C, $N(CH_3)_2$), 48.42 (1 C, H_2C(3')), 53.01 (1 C, H_2C(1')), 55.84 (1 C, C(9)), 62.66 (2 C, H_2C(5',8')), 83.38 (1 C, C(10)), 95.39 (1 C, HC(8)), 111.88 (2 C, HC(2,6)), 114.20 (1 C, CN), 114.59 (1 C, CN), 117.90 (1 C, C(4)), 126.25 (2 C, HC(3,5)), 148.20 (1 C, C(7)), 151.57 (1 C, C(1)), 158.66 (1 C, C(2')), 163.79 (1 C, C(11)), 169.39 ppm (2 C, C(4',7')); IR (ATR): $\tilde{\nu}$ = 2983 (w), 1735 (s), 1687 (m), 1608 (s), 1526 (m), 1444 (w), 1366 (m), 1223 (s), 1196 (s), 1170 (m), 1076 (s), 1041 (s), 946 (w), 911 (w), 861 (w), 819 (w), 774 (w), 731 (w), 648 (w), 622 cm^{-1} (w); UV/Vis ($CHCl_3$): λ_{max} (ε) = 322 (17200), 284 (14100 M^{-1}cm^{-1}); HR-MALDI-MS (DCTB) m/z (%): 484.1715 (5, $[M + H]^+$, calcd for $C_{24}H_{26}N_3O_8$: 484.1714), 443.1449 (100, $[M - CH_2CN]^+$).

Data of **187**: R_f = 0.59 (SiO_2; EtOAc/CH_2Cl_2 1:9); ^{1}H NMR (400 MHz, $CDCl_3$): δ = 1.12 (t, J = 7.1 Hz, 3 H; H_3C(9')), 1.33 (t, J = 7.1 Hz, 3 H; H_3C(12')), 3.02 (s, 6 H, $N(CH_3)_2$), 3.89 (q, J = 7.1 Hz, 2 H; H_2C(8')), 4.31 (q, J = 7.1 Hz, 2 H; H_2C(11')), 4.71 (s, 2 H; H_2C(5')), 4.83 (s, 2 H; H_2C(3')), 6.63 (d, J = 9.0 Hz, 2 H; H–C(2,6)), 7.17 (d, J = 9.0 Hz, 2 H; H–C(3,5)), 7.90 ppm (s, 1 H; H–C(8)); ^{13}C NMR (100 MHz, $CDCl_3$): δ = 13.83 (1 C, H_3C(9')), 14.15 (1 C, H_3C(12')), 40.06 (2 C,

$N(CH_3)_2$), 49.02 (1 C, $H_2C(5')$), 49.12 (1 C, $H_2C(3')$), 61.82 (1 C, $H_2C(8')$), 62.19 (1 C, $H_2C(11')$), 111.63 (2 C, HC(2,6)), 113.71 (1 C, CN), 113.98 (1 C, CN), 118.06 (1 C, C(1')), 121.51 (1 C, C(4)), 131.18 (2 C, HC(3,5)), 132.02 (1 C, C(6')), 142.63 (1 C, HC(8)), 152.47 (1 C, C(1)), 156.37 (1 C, C(7)), 161.70 (1 C, C(2')), 163.11 (1 C, C(10')), 164.07 (1 C, C(7')), 164.72 ppm (1 C, C(4')); IR (ATR): $\tilde{\nu}$ = 2984 (w), 1720 (s), 1604 (m), 1558 (w), 1524 (m), 1445 (w), 1368 (m), 1320 (w), 1292 (w), 1252 (s), 1204 (m), 1171 (s), 1137 (w), 1094 (s), 1068 (s), 1013 (w), 945 (w), 913 (w), 862 (w), 820 (w), 730 (w), 648 cm^{-1} (w); UV/Vis ($CHCl_3$): λ_{max} (ε) = 434 (10700), 294 (14000 $M^{-1}cm^{-1}$); HR-MALDI-MS (DCTB) *m/z* (%): 483.1636 (100, $[M]^+$, calcd for $C_{24}H_{25}N_3O_8$: 483.1636).

Data of **188**: R_f = 0.31 (SiO_2; EtOAc/cyclohexane 1:1); ^1H NMR (400 MHz, $CDCl_3$): δ = 1.35(0) (overlapping t, *J* = 7.1 Hz, 3 H; $H_3C(3'$ or $5')$), 1.35(3) (overlapping t, *J* = 7.1 Hz, 3 H; $H_3C(3'$ or $5')$), 3.09 (s, 6 H, $N(CH_3)_2$), 4.12 (m, 2 H, $H_2C(4')$), 4.37 (q, *J* = 7.1 Hz, 2 H; $H_2C(2')$), 4.58 (s, 2 H, $H_2C(7'$ or $9')$), 4.84 (s, 2 H, $H_2C(7'$ or $9')$), 6.66 (d, *J* = 9.2 Hz, 2 H; H–C(2,6)), 7.88 (d, *J* = 9.2 Hz, 2 H; H–C(3,5)), 8.12 ppm (s, 1 H; H–C(8)); ^{13}C NMR (100 MHz, $CDCl_3$): δ = 14.23 (1 C, $H_3C(3')$), 14.80 (1 C, $H_3C(5')$), 40.15 (2 C, $N(CH_3)_2$), 48.34 (1 C, $H_2C(7'$ or $9')$), 48.74 (1 C, $H_2C(7'$ or $9')$), 62.69 (1 C, $H_2C(2')$), 67.54 (1 C, $H_2C(4')$), 102.14 (1 C, C(11)), 111.08 (2 C, HC(2,6)), 114.23 (1 C, CN), 114.37 (1 C, CN), 124.14 (1 C, C(4)), 131.64 (2 C, HC(3,5)), 133.60 (1 C, C(9)), 137.67 (1 C, HC(8)), 154.42 (1 C, C(1)), 162.73 (1 C, C(6' or 8')), 162.83 (1 C, C(6' or 8')), 163.09 (1 C, C(1')), 172.32 (1 C, C(10)), 185.52 ppm (1 C, C(7)); IR (ATR): $\tilde{\nu}$ = 2986 (w), 1721 (m), 1649 (w), 1581 (s), 1543 (m), 1485 (w), 1437 (w), 1377 (m), 1320 (w), 1261 (s), 1236 (m), 1172 (s), 1069 (s), 1014 (m), 966 (w), 943 (w), 912 (w), 870 (w), 823 (w), 777 (w), 734 (w), 704 (w), 657 (w), 612 cm^{-1} (w); UV/Vis ($CHCl_3$): λ_{max} (ε) = 420 (10100), 265 (15500 $M^{-1}cm^{-1}$); HR-ESI-MS *m/z* (%): 484.1712 (100, $[M + H]^+$, calcd for $C_{24}H_{26}N_3O_8$: 484.1714).

1,1-Diethyl 2,2-Bis(2,2,2-trifluoroethyl)-ethene-1,1,2,2-tetracarboxylate (189)

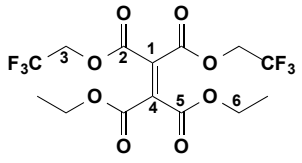

A solution of diethyl 2-oxomalonate (430 mg, 2.47 mmol) and bis(2,2,2-trifluoroethyl) malonate (662 mg, 662 mmol) in toluene (12 mL) was treated with acetic acid (106 μL, 1.85 mmol) and β-alanine (26 mg, 0.30 mmol) and heated at reflux under Dean-Stark conditions for 24 h. Evaporation and flash column chromatography (SiO_2; EtOAc/cyclohexane 3:7) gave **189** (293 mg, 28%) as a clear colorless oil. R_f = 0.52 (SiO_2; EtOAc/cyclohexane 3:7); ^{1}H NMR (400 MHz, $CDCl_3$): δ = 1.33 (t, J = 7.1 Hz, 6 H; $H_3C(7)$), 4.35 (q, J = 7.1 Hz, 4 H; $H_2C(6)$), 4.61 ppm (q, J = 8.2 Hz, 4 H; $H_2C(3)$); ^{13}C NMR (100 MHz, $CDCl_3$): δ = 13.87 (2 C, $H_3C(7)$), 62.03 (q, J = 37.8 Hz, 2 C, $H_2C(3)$), 63.37 (2 C, $H_2C(6)$), 122.4 (q, J = 277.1 Hz, 2 C, F_3C), 131.64 (1 C, C(1)), 138.98 (1 C, C(4)), 160.39 (2 C, C(2)), 161.56 ppm (2 C, C(5)); ^{19}F NMR (377 MHz, $CDCl_3$): δ = –73.65 (t, J = 8.2 Hz, 6 F; CF_3); IR (ATR): $\tilde{\nu}$ = 2987 (w), 1735 (m), 1449 (w), 1413 (w), 1370 (w), 1280 (m), 1222 (s), 1161 (s), 1103 (w), 1052 (m), 1015 (w), 981 (w), 911 (w), 862 (w), 767 (w), 732 (w), 649 cm^{-1} (w); HR-ESI-MS m/z (%): 442.0927 (100, $[M + NH_4]^+$, calcd for $C_{14}H_{18}F_6NO_8$: 442.0931).

4,4-Diethyl 3-(2,2,2-Trifluoroethyl) 6-[4-(dimethylamino)phenyl]-2-(2,2,2-trifluoroethoxy)-4*H*-pyran-3,4,4-tricarboxylate (190), **4,4-Diethyl 1,1-Bis(2,2,2-trifluoroethyl)2-[4-(Dimethylamino)phenyl]buta-1,3-diene-1,1,4,4 tetracarboxylate (191)** and **(*E*)-3-Ethyl 1,1-Bis(2,2,2-trifluoroethyl) 5-[4-(dimethylamino)phenyl]-2-ethoxy-5-oxopenta-1,3-diene-1,1,3-tricarboxylate (192).**

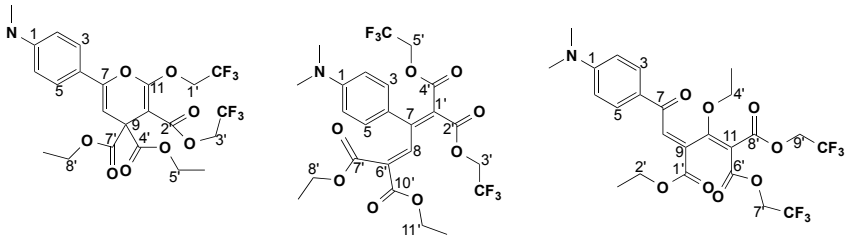

A solution of alkyne **102** (24 mg, 0.165 mmol) in $(CH_2Cl)_2$ (1.7mL) was treated with alkene **189** (70 mg, 0.165 mmol) and stirred for 36 h at reflux. Evaporation and flash column chromatography (SiO_2; EtOAc/cyclohexane 3:7 v/v) afforded two fractions, A and B. Evaporation of fraction B gave compound **192** (24 mg, 25%) as an orange oil. Fraction A (R_f = 0.42 (SiO_2; EtOAc/cyclohexane 3:7)) was resubjected to flash column chromatography (SiO_2; EtOAc/CH_2Cl_2 1:9 v/v) to

afford two fractions, C and D. Evaporation of fraction C gave **191** (36 mg, 38%) as a red sticky oil. Evaporation of fraction D gave **190** (22 mg, 23%) as an orange solid.

Data of **190**: R_f = 0.42 (SiO_2; EtOAc/cyclohexane 3:7); m.p. 112–114 °C; ^{1}H NMR (400 MHz, $CDCl_3$): δ = 1.28 (t, J = 7.1 Hz, 6 H; H_3C(6',9')), 3.01 (s, 6 H, $N(CH_3)_2$), 4.24 (q, J = 7.1 Hz, 4 H; H_2C(5',8')), 4.52 (q, J = 8.5 Hz, 2 H; H_2C(3')), 4.64 (q, J = 7.9 Hz, 2 H; H_2C(1')), 5.64 (s, 1 H, H–C(8)), 6.69 (d, J = 9.0 Hz, 2 H; H–C(2,6)), 7.38 ppm (d, J = 9.0 Hz, 2 H; H–C(3,5)); ^{13}C NMR (100 MHz, $CDCl_3$): δ = 14.06 (2 C, H_3C(6',9')), 40.34 (2 C, $N(CH_3)_2$), 55.93 (1 C, C(9)), 60.68 (1 C, J = 36.7 Hz, H_2C(3')), 62.44 (2 C, H_2C(5',8')), 64.95 (1 C, J = 37.3 Hz, H_2C(1')), 83.43 (1 C, C(10)), 95.53 (1 C, HC(8)), 111.88 (2 C, HC(2,6)), 118.34 (1 C, C(4)), 122.56 (q, J = 276.0 Hz; 1 C, F_3C(on C1')), 123.26 (q, J = 276.0 Hz; 1 C, F_3C(on C3')), 126.06 (2 C, HC(3,5)), 147.91 (1 C, C(7)), 151.48 (1 C, C(1)), 158.47 (1 C, C(11)), 164.28 (1 C, C(2')), 169.62 ppm (2 C, C(4',7')); ^{19}F NMR (377 MHz, $CDCl_3$): δ = –73.67 (td, J = 8.5, 2.0 Hz; 3 F, CF_3(on 3')), –74.10 (td, J = 7.9, 2.0 Hz, 3 F; CF_3(on 1')); IR (ATR): $\tilde{\nu}$ = 3090 (w), 2922 (w), 1728 (s), 1681 (w), 1609 (m), 1531 (w), 1450 (w), 1414 (w), 1358 (w), 1326 (w), 1283 (m), 1239 (m), 1203 (m), 1153 (s), 1110 (m), 1094 (s), 1051 (m), 1033 (s), 981 (w), 963 (w), 947 (w), 859 (w), 846 (w), 817 (w), 793 (w), 775 (w), 754 (w), 687 (w), 658 (w), 647 (w), 622 cm^{-1} (w); UV/Vis ($CHCl_3$): λ_{max} (ε) = 318 (19600), 282 (14400 $M^{-1}cm^{-1}$); HR-MALDI-MS (DCTB) m/z (%): 569.1478 (100, $[M]^+$, calcd for $C_{24}H_{25}F_6NO_8$: 569.1479).

Data of **191**: R_f = 0.42 (SiO_2; EtOAc/cyclohexane 3:7); ^{1}H NMR (400 MHz, $CDCl_3$): δ = 1.11 (t, J = 7.1 Hz, 3 H; H_3C(9')), 1.32 (t, J = 7.1 Hz, 3 H; H_3C(12')), 3.00 (s, 6 H, $N(CH_3)_2$), 3.87 (q, J = 7.1 Hz, 2 H; H_2C(8')), 4.30 (q, J = 7.1 Hz, 2 H; H_2C(11')), 4.45 (q, J = 8.5 Hz, 2 H; H_2C(3' or 5')), 4.56 (q, J = 8.5 Hz, 2 H; H_2C(3' or 5')), 6.59 (d, J = 9.0 Hz, 2 H; H–C(2,6)), 7.16 (d, J = 9.0 Hz, 2 H; H–C(3,5)), 7.91 ppm (s, 1 H; H–C(8)); ^{13}C NMR (100 MHz, $CDCl_3$): δ = 13.77 (1 C, H_3C(9')), 14.18 (1 C, H_3C(12')), 40.14 (2 C, $N(CH_3)_2$), 61.16 (1 C, J = 37.0 Hz, H_2C(3' or 5')), 61.22 (1 C, J = 37.0 Hz, H_2C(3' or 5')), 61.81 (1 C, H_2C(8')), 62.13 (1 C, H_2C(11')), 111.45 (2 C, HC(2,6)), 120.13 (1 C, C(1')), 121.91 (1 C, C(4)), 122.78 (q, J = 276.0 Hz; 1 C, F_3C(on C3' or C5')), 122.88 (q, J = 276.0 Hz; 1 C, F_3C(on C3' or C5')), 131.03 (2 C, HC(3,5)), 131.78 (1 C, C(6')), 142.84 (1 C, HC(8)), 152.23 (1 C, C(1)), 155.03 (1 C, C(7)), 161.77 (1 C, C(2' or 4')), 163.27 (1 C, C(10')), 164.20 (1 C, C(7')), 164.65 ppm (1 C, C(2' or 4')); ^{19}F NMR (377 MHz, $CDCl_3$): δ = –73.43 (t, J = 8.5 Hz; 3 F, CF_3(on

3' or 5')), –73.67 (t, J = 8.5 Hz; 3 F, CF_3(on 3' or 5')); IR (ATR): $\tilde{\nu}$ = 2983 (w), 1726 (m), 1606 (w), 1566 (w), 1525 (w), 1447 (w), 1412 (w), 1370 (w), 1281 (m), 1252 (m), 1159 (s), 1100 (m), 1072 (m), 976 (w), 863 (w), 819 (w), 648 cm^{-1} (w); UV/Vis ($CHCl_3$): λ_{max} (ε) = 421 (9800), 289 (14300 $M^{-1}cm^{-1}$); HR-MALDI-MS (DCTB) *m/z* (%): 569.1478 (100, $[M]^+$, calcd for $C_{24}H_{25}F_6NO_8$: 569.1479).

Data of **192**: R_f = 0.27 (SiO_2; EtOAc/cyclohexane 3:7); ^{1}H NMR (400 MHz, $CDCl_3$): δ = 1.32 (overlapping t, J = 7.2 Hz, 3 H; H_3C(3' or 5')), 1.33 (overlapping t, J = 7.2 Hz, 3 H; H_3C(3' or 5')), 3.09 (s, 6 H, $N(CH_3)_2$), 4.11 (m, 2 H, H_2C(4')), 4.35 (m, 4 H; H_2C(2',7' or 9')), 4.58 (q, J = 8.5 Hz, 2 H, H_2C(7' or 9')), 6.65 (d, J = 9.2 Hz, 2 H; H–C(2,6)), 7.87 (d, J = 9.2 Hz, 2 H; H–C(3,5)), 8.10 ppm (s, 1 H; H–C(8)); ^{13}C NMR (100 MHz, $CDCl_3$): δ = 14.14 (1 C, H_3C(3')), 14.77 (1 C, H_3C(5')), 40.16 (2 C, $N(CH_3)_2$), 60.23 (1 C, J = 36.7 Hz, H_2C(7' or 9')), 60.73 (1 C, J = 36.7 Hz, H_2C(7' or 9')), 62.55 (1 C, H_2C(2')), 67.23 (1 C, H_2C(4')), 103.60 (1 C, C(11)), 110.99 (2 C, HC(2,6)), 122.94 (q, J = 276.0 Hz; 1 C, F_3C(on C7' or C9')), 123.11 (q, J = 276.0 Hz; 1 C, F_3C(on C7' or C9')), 124.33 (1 C, C(4)), 131.62 (2 C, HC(3,5)), 133.75 (1 C, C(9)), 137.64 (1 C, HC(8)), 154.35 (1 C, C(1)), 162.82 (1 C, C(6' or 8')), 162.97 (1 C, C(6' or 8')), 163.35 (1 C, C(1')), 170.73 (1 C, C(10)), 185.85 ppm (1 C, C(7)); ^{19}F NMR (377 MHz, $CDCl_3$): δ = –73.48 (t, J = 8.5 Hz; 3 F, CF_3(on 3' or 5')), –73.74 (t, J = 8.5 Hz; 3 F, CF_3(on 3' or 5')); IR (ATR): $\tilde{\nu}$ = 2984 (w), 1725 (m), 1653 (w), 1586 (s), 1546 (w), 1438 (w), 1411 (w), 1377 (m), 1259 (s), 1157 (s), 1091 (s), 1028 (m), 989 (w), 976 (m), 944 (w), 871 (w), 823 (w), 779 (w), 705 (w), 648 cm^{-1} (w); UV/Vis ($CHCl_3$): λ_{max} (ε) = 414 (11200), 260 (17100 $M^{-1}cm^{-1}$); HR-MALDI-MS (DCTB) *m/z* (%): 569.1478 (100, $[M]^+$, calcd for $C_{24}H_{25}F_6NO_8$: 569.1479).

Ethyl 3,4-Dicyano-5,6-bis [4-(dimethylamino)phenyl]-2-ethoxy-4*H*-pyran-4-carboxylate (193) and **(2*Z*,4*Z*)-Diethyl 2,5-Dicyano-3,4-bis[4-(dimethylamino)phenyl] hexa-2,4-dienedioate (194)**

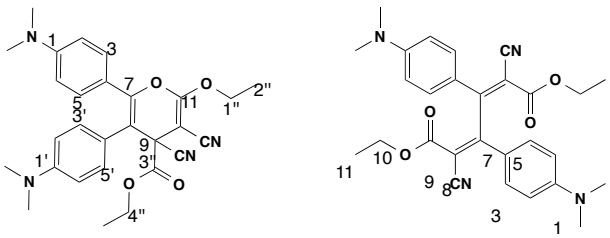

A solution of alkyne **132** (50 mg, 0.189 mmol) in MeCN (2 ml) was treated with alkene **164** (42 mg, 0.189 mmol) and stirred for 2 h at 25 °C. Evaporation and column chromatography (SiO_2; EtOAc/cyclohexane 1:4) afforded two fractions, A and B. Evaporation of A afforded (±)-**193** (12 mg, 13%) as a orange solid. Evaporation of fraction B gave **194** (64 mg, 70%) a red solid.

Data of (±)-**193**: R_f = 0.45 (SiO_2; EtOAc/cyclohexane 4:6); m.p. 130–131 °C; ^{1}H NMR (400 MHz, CD_2Cl_2): δ = 1.19 (t, J = 7.1 Hz, 3 H; OCH_2CH_3), 1.46 (t, J = 7.1 Hz, 3 H; $CO_2CH_2CH_3$), 2.92 (s, 6 H, NMe_2), 2.94 (s, 6 H, NMe_2), 4.18 (q, J = 6.9 Hz, 2 H; OCH_2CH_3), 4.45 (q, J = 6.9 Hz, 2 H; $CO_2CH_2CH_3$), 6.49 (d, J = 8 Hz, 2 H; H–C(2', 6')), 6.63 ppm (d, J = 8 Hz, 2 H; H–C(3', 5')), 7.08 ppm (d, J = 8 Hz, 4 H; H–C(2', 3', 5', 6')); ^{13}C NMR (101 MHz, CD_2Cl_2): δ = 14.26 (1 C, OCH_2CH_3), 15.14 (1 C, $CO_2CH_2CH_3$), 40.31 (1 C, NMe_2), 40.53 (1 C, NMe_2), 52.19 (1 C, C(3)), 61.51 (1 C, C(2)), 64.51 (1 C, OCH_2CH_3), 66.97 (1 C, $CO_2CH_2CH_3$), 106.27 (1 C, C(5)), 111.38 (2 C, C(2', 6')), 112.57 (2 C, C(3',5')), 115.14 (1 C, CN), 117.26 (1 C, CN), 118.77 (1 C, C(7, 7')), 121.11 (C, C(1')), 130.35 (2 C, 2 C(2', 6')), 131.78 (2 C, C(2', 6')), 147.86 (1 C, C(1')), 150.95 (1 C, C(4)), 151.26 (2 C, C(4')), 163.64 (1 C, $CO_2CH_2CH_3$), 166.74 (1 C(2)) ppm; IR (ATR): $\tilde{\nu}$ = 2984 (w), 2346 (w), 1739 (s), 1631 (w), 1606 (m), 1522 (m), 1445 (w), 1366 (w), 1295 (w), 1216 (s), 1196 (s), 1171 (w), 1138 (w), 1097 (m), 1201 (m), 944 (w), 913 (w), 855 (w), 816 (m), 729 (w), 647 (w), 625 cm^{-1} (w); UV/Vis ($CHCl_3$): λ_{max} (ε) = 273 nm (17500 M^{-1}cm^{-1}); HR-MALDI-MS (DCTB) m/z (%): 486.2260 (100, $[M]^+$) calcd for $C_{28}H_{30}N_4O_4$: 486.2262).

Data for **194**: R_f = 0.38 (SiO_2; EtOAc/cyclohexane 4:6); m.p. 134–135 °C; ^{1}H NMR (400 MHz, $CDCl_3$): δ = 1.21 (t, J = 7.1 Hz, 3 H; $CO_2CH_2CH_3$), 3.05 (s, 6 H, NMe_2), 4.08–4.15 (m, 2 H; $CO_2CH_2CH_3$), 6.64 (d, J = 8 Hz, 2 H; H–C(3',5')), 7.69 ppm (d, J = 8 Hz, 2 H; H–C(2',6')); ^{13}C NMR (101 MHz, $CDCl_3$): δ = 14.16 (2 C, $CO_2CH_2CH_3$), 40.08 (2 C, $NMe)_2$), 61.95 (2 C, $CO_2CH_2CH_3$), 97.45 (2 C, (C(1)), 111.23 (2 C, C(3', 5')), 118.29 and 121.76 (2 C, 2 CN), 132.44 55 (2 C, C(2', 6')), 152.79 (2 C, 2 C(4')), 162.31 (2 C, 2 $CO_2CH_2CH_3$)), 167.55 (2 C, (C(2)) ppm; IR (ATR): $\tilde{\nu}$ = 2982 (w), 1725 (m), 1652 (w), 1591 (s), 1547 (w), 1444 (w), 1375 (m), 1319 (w), 1265 (m), 1326 (m), 1188 (m), 1092 (m), 1026 (w), 944 (w), 870 (w), 822 cm^{-1}; UV/Vis ($CHCl_3$): λ_{max} (ε) = 449 (20700), 324 nm (18000 M^{-1}cm^{-1}); HR-MALDI-MS (DCTB) m/z (%): 486.2262 (100, $[M]^+$) calcd for $C_{28}H_{30}N_4O_4$: 486.2262).

Diethyl 2-{3,3-Dicyano-1,2-bis[4-(dimethylamino)phenyl]allylidene}malonate (195) and **(*Z*)-Ethyl 2-[2,2-Dicyano-1-ethoxyvinyl]-3,4-bis[4-(dimethylamino)phenyl]-4-oxobut-2-enoate (196)**

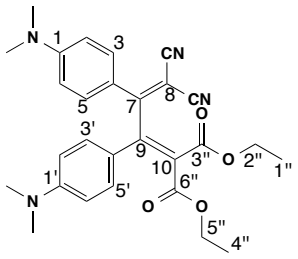

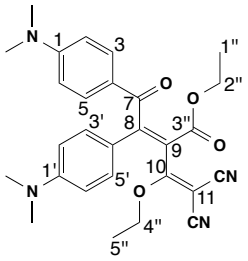

A solution of alkyne **132** (100 mg, 0.378 mmol) in MeCN (2 ml) was treated with alkene **164** (84 mg, 0.378 mmol) and stirred for 2 h at 25 °C. Evaporation and column chromatography (SiO_2; EtOAc/cyclohexane 1:4) afforded two fractions, A and B. Evaporation of A afforded **195** (156 mg, 85%) as a rede solid. Evaporation of fraction B provided **196** (2 mg, 1%) as a red solid.

Data of **195**: R_f = 0.45 (SiO_2; EtOAc/cyclohexane 4:6); m.p. 130–131 °C; ^{1}H NMR (400 MHz, $CDCl_3$): δ = 1.17 (t, J = 7.1 Hz, 3 H, $CO_2CH_2CH_3$), 1.34 (t, J = 7.1 Hz, 3 H; $CO_2CH_2CH_3$), 2.98 (s, 6 H, NMe_2), 3.08 (s, 6 H, NMe_2), 4.09 (q, J = 7.1 Hz, 2 H, $CO_2CH_2CH_3$), 4.24 (q, J = 7.1 Hz, 2 H, $CO_2CH_2CH_3$), 6.58 (d, J = 8 Hz, 2 H; H–C(3',5')), 6.66 ppm (d, J = 8 Hz, 2 H; H–C(3',5')), 7.21 ppm (d, J = 8 Hz, 2 H; H–C(2',6')), 7.87 ppm (d, J = 8 Hz, 2 H; H–C(2',6')); ^{13}C NMR (101 MHz, $CDCl_3$): δ = 14.00 (1 C, $CO_2CH_2CH_3$), 14.08 (1 C, $CO_2CH_2CH_3$), 40.11 (4 C, NMe_2), 61.71 (1 C, $CO_2CH_2CH_3$), 61.83 (1 C, $CO_2CH_2CH_3$), 74.65 (1 C, C(1)), 111.54 (2 C, C(3',5')), 111.68 (2 C, C(3',5')), 114.47 (1 C, CN), 115.75 (1 C, CN), 120.33 (1 C, C(1')), 122.57 (1 C, C(1')), 125.45 (1 C, C(3)), 130.43 (2 C, C(2',6')), 132.52 (2 C, C(2',6')), 151.26 (1 C, C(4)), 151.76 (1 C, (C(4')), 153.49 (1 C, (C(4')), 163.30 (1 C, $CO_2CH_2CH_3$), 166.49 (1 C, C(2)), 171.11 ppm (1 C, (C(5)). IR (ATR): $\tilde{\nu}$ = 2990 (w), 2321(w), 1728 (s), 1602 (w), 1621 (m), 1501 (m), 1458 (w), 1364 (w), 1274 (w), 1218 (s), 1198 (s), 1161 (w), 1128 (w), 1090 (m), 1198 (m), 921 (w), 900 (w), 824 (w), 816 (m), 729 (w), 647 (w), 625 cm^{-1} (w); UV/Vis ($CHCl_3$): λ_{max} (ε) = 450

(26600), 360 nm (18600 $M^{-1}cm^{-1}$); HR-MALDI-MS (DCTB) *m/z* (%): 486.2261 (100, $[M]^+$) calcd for $C_{28}H_{30}N_4O_4$: 486.2262.

Data of **196**: R_f = 0.42 (SiO_2; EtOAc/cyclohexane 4:6); m.p. 130–131 °C; ^1H NMR (400 MHz, $CDCl_3$): δ = 1.12 (t, *J* = 7.1 Hz, 3 H; $CO_2CH_2CH_3$), 1.34 (t, *J* = 7.1 Hz, 3 H; $CO_2CH_2CH_3$), 3.01 (s, 6 H, NMe_2), 3.03 (s, 6 H, NMe_2), 4.14 (q, *J* = 7.1 Hz, 2 H, $CO_2CH_2CH_3$), 4.25–4.31 (m, 2 H; $CO_2CH_2CH_3$), 6.59 (d, *J* = 8 Hz, 2 H; H–C(3',5')), 6.64 ppm (d, *J* = 8 Hz, 2 H; H–C(3',5')), 7.29 ppm (d, *J* = 8 Hz, 2 H; H–C(2',6')), 7.89 ppm (d, *J* = 8 Hz, 2 H; H–C(2',6')); ^{13}C NMR (101 MHz, $CDCl_3$): δ = 13.82 (1 C, $CO_2CH_2CH_3$), 14.78 (1 C, $CO_2CH_2CH_3$), 39.89 (1 C, NMe_2), 40.02 (1 C, NMe_2), 62.11 (1 C, $CO_2CH_2CH_3$), 68.67 (1 C, (C(4)), 69.37(1 C, $CO_2CH_2CH_3$), 111.01 (2 C, C(3',5')), 111.76 (2 C, C(3',5')), 111.90 (2 C, C(2',6')), 113.48 (C, C(1')), 113.61 (2 C, C(1')), 119.16 and 123.89 (2 C, 2 CN), 130.39 (2 C, C(2',6')), 131.49 (1 C, C(1)), 152.15 (1 C, C(4')), 153.76 (1 C, C(4')), 161.83 (1 C, C(2)), 162.37 (1 C, $CO_2CH_2CH_3$), 182.97 (1 C, $CO_2CH_2CH_3$), 192.48. ppm (1 C, C(3)); IR (ATR): $\tilde{\nu}$ = 2984 (w), 2346 (w), 1739 (s), 1631 (w), 1606 (m), 1522 (m), 1445 (w), 1366 (w), 1295 (w), 1216 (s), 1196 (s), 1171 (w), 1138 (w), 1097 (m), 1201 (m), 944 (w), 913 (w), 855 (w), 816 (m), 729 (w), 647 (w), 625 cm^{-1} (w); UV/Vis ($CHCl_3$): λ_{max} (ε) = 424 (18000), 348 nm (24000 $M^{-1}cm^{-1}$); HR-MALDI-MS (DCTB) *m/z* (%): 486.2261 (100, $[M]^+$) calcd for $C_{28}H_{30}N_4O_4$: 486.2262.

Diethyl2-(3,3-Dicyano-2-(4-(dimethylamino)phenyl)-1-phenylallylidene)malonate (198)

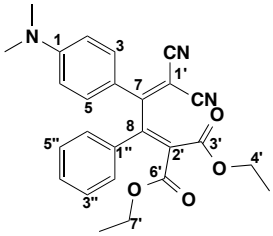

A solution of alkyne **197** (200 mg, 0.90 mmol) in MeCN (9 mL) was treated with alkene **162** (201 mg, 0.90 mmol) and stirred for 16 h at 82 °C. Evaporation and flash column chromatography (SiO_2; EtOAc/cyclohexane 3:7) gave **198** (382 mg, 95%) as a red solid. R_f = 0.57 (SiO_2; EtOAc/cyclohexane 1:1); m.p. 131–132 °C; ^1H NMR (400 MHz, $CDCl_3$): δ = 1.06 (t, *J* = 7.1 Hz, 3 H; $H_3C(5')$), 1.20 (t, *J* = 7.1 Hz, 3 H; $H_3C(8')$), 3.10 (s, 6 H, $N(CH_3)_2$), 4.14 (overlapping q, *J* = 7.1 Hz, 2 H;

$H_2C(4')$), 4.18 (overlapping q, J = 7.1 Hz, 2 H; $H_2C(7')$), 6.68 (d, J = 9.3 Hz, 2 H; H–C(2,6)), 7.33 (m, 5 H, H–C(2''–6'')), 7.86 ppm (d, J = 9.3 Hz, 2 H; H–C(3,5)); ^{13}C NMR (100 MHz, $CDCl_3$): δ = 13.78 (1 C, $H_3C(5')$), 13.96 (1 C, $H_3C(8')$), 40.12 (2 C, $N(CH_3)_2$), 62.05 (1 C, $H_2C(4')$), 62.23 (1 C, $H_2C(7')$), 74.43 (1 C, C(1')), 111.65 (2 C, HC(2,6)), 114.44 (1 C, CN), 115.35 (1 C, CN), 118.97 (1 C, C(4)), 128.43 (2 C, HC(3'',5'')), 128.87 (2 C, HC(2'',6'')), 130.39 (1 C, HC(4'')), 130.60 (1 C, C(2')), 132.52 (2 C, HC(3,5)), 135.48 (1 C, C(1'')), 150.12 (1 C, C(8)), 153.69 (1 C, C(1)), 162.70 (1 C, C(6')), 165.05 (1 C, C(3')), 169.49 ppm (1 C, C(7)); IR (ATR): $\tilde{\nu}$ = 2983 (w), 2215 (m), 1723 (m), 1601 (s), 1543 (w), 1489 (s), 1439 (m), 1378 (s), 1335 (m), 1287 (m), 1244 (s), 1207 (s), 1170 (s), 1097 (m), 1078 (w), 1056 (m), 1015 (w), 944 (w), 862 (w), 820 (w), 734 (m), 697 (m), 647 (w), 630 cm^{-1} (w); UV/Vis ($CHCl_3$): λ_{max} (ε) = 448 (31800), 305 (15300 M^{-1}cm^{-1}); HR-MALDI-MS (DCTB) m/z (%): 443.1840 (100, $[M]^+$, calcd for $C_{26}H_{25}N_3O_4$: 443.1840).

Diethyl 2-(2-Ferrocenyl-3,3-dicyanoallylidene)malonate (200)

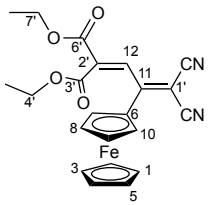

A solution of ethynylferrocene (**199**) (195 mg, 0.93 mmol) in MeCN (10 mL) was treated with alkene **162** (206 mg, 0.93 mmol) and stirred for 5 h at 82 °C. Evaporation and flash column chromatography (SiO_2; EtOAc/cyclohexane 3:7) delivered **200** (313 mg, 78 %) as a blue solid. R_f = 0.37 (SiO_2; EtOAc/cyclohexane 3:7); m.p. 76–78 °C; ^{1}H NMR (400 MHz, $CDCl_3$): δ = 1.19 (t, J = 7.1 Hz, 3 H; $H_3C(5')$), 1.36 (t, J = 7.1 Hz, 3 H; $H_3C(8')$), 4.15 (q, J = 7.1 Hz, 2 H; $H_2C(4')$), 4.33 (s, 5 H, H–C(1–5)), 4.35 (q, J = 7.1 Hz, 2 H; $H_2C(7')$), 4.82 (m, 2 H; H–C(8,9)), 4.99 (d, J = 2.0 Hz, 2 H; H–C(7,10)), 7.56 ppm (s, 1 H; H–C(8)); ^{13}C NMR (100 MHz, $CDCl_3$): δ = 13.93 (1 C, $H_3C(5')$), 14.15 (1 C, $H_3C(8')$), 62.34 (1 C, $H_2C(4')$), 62.73 (1 C, $H_2C(7')$), 71.17 (2 C, HC(7,10)), 71.78 (5 C, HC(1–5)), 74.59 (1 C, C(6)), 74.98 (2 C, HC(8,9)), 75.77 (1 C, C(1')), 113.60 (1 C, CN), 114.49 (1 C, CN), 133.67 (1 C, C(2')), 138.57 (1 C, HC(12)), 162.60 (1 C, C(6')), 162.66 (1 C, C(3')), 170.92 ppm (1 C, C(11)); IR (ATR): $\tilde{\nu}$ = 2987 (w), 2903 (w), 2223 (m), 1833 (w), 1770 (w), 1717 (s), 1532 (s), 1477 (w), 1448 (m), 1413 (w), 1376 (m), 1346 (w), 1332 (w), 1294 (w), 1254 (s), 1226 (s), 1175 (w), 1132 (w), 1108 (w), 1096 (w), 1062 (s), 1003 (m), 943

(w), 903 (w), 862 (w), 940 (w), 807 (w), 753 (w), 736 (w), 697 (w), 640 (w), 606 cm^{-1} (w); UV/Vis ($CHCl_3$): λ_{max} (ε) = 565 (2200), 332 (10600 $M^{-1}cm^{-1}$); HR-MALDI-MS (DCTB) *m/z* (%): 432.0767 (100, $[M]^+$, calcd for $C_{22}H_{20}FeN_2O_4$: 432.0767).

Diethyl 2-[2-(4-Aminophenyl)-3,3-dicyanoallylidene]malonate (202)

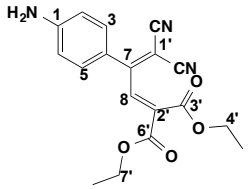

A solution of 4-ethynylaniline (**201**) (159 mg, 1.35 mmol) in MeCN (7 mL) was treated with alkene **162** (300 mg, 1.35 mmol) and stirred for 48 h at 25 °C. Evaporation and flash column chromatography (SiO_2; EtOAc/cyclohexane 1:1 v/v) gave **202** (330 mg, 72%) as a deep red solid. R_f = 0.34 (SiO_2; EtOAc/cyclohexane 1:1); m.p. 93–95 °C; ^{1}H NMR (400 MHz, $CDCl_3$): δ = 1.11 (t, *J* = 7.1 Hz, 3 H; $H_3C(5')$), 1.33 (t, *J* = 7.1 Hz, 3 H; $H_3C(8')$), 3.86 (q, *J* = 7.1 Hz, 2 H; $H_2C(4')$), 4.32 (q, *J* = 7.1 Hz, 2 H; $H_2C(7')$), 4.42 (br s, 2 H, NH_2), 6.64 (d, *J* = 8.8 Hz, 2 H; H–C(2,6)), 7.44 (d, *J* = 8.8 Hz, 2 H; H–C(3,5)), 7.73 ppm (s, 1 H; H–C(8)); ^{13}C NMR (100 MHz, $CDCl_3$): δ = 13.80 (1 C, $H_3C(5')$), 14.11 (1 C, $H_3C(8')$), 62.21 (1 C, $H_2C(4')$), 62.79 (1 C, $H_2C(7')$), 80.06 (1 C, C(1')), 113.15 (1 C, CN), 113.97 (1 C, CN), 114.19 (2 C, HC(2,6)), 121.25 (1 C, C(4)), 132.31 (2 C, HC(3,5)), 136.94 (1 C, C(2')), 138.53 (1 C, HC(8)), 151.98 (1 C, C(1)), 162.45 (1 C, C(6')), 163.02 (1 C, C(3')), 165.92 ppm (1 C, C(7)); IR (ATR): $\tilde{\nu}$ = 3475 (w), 3375 (w), 3236 (w), 2983 (w), 2926 (w), 2219 (w), 1723 (s), 1627 (m), 1602 (s), 1497 (s), 1446 (w), 1373 (w), 1328 (m), 1253 (s), 1222 (m), 1182 (s), 1065 (m), 1015 (w), 926 (w), 861 (w), 834 (w), 726 cm^{-1} (w); UV/Vis ($CHCl_3$): λ_{max} (ε) = 413 (12400), 286 (16400 $M^{-1}cm^{-1}$); HR-MALDI-MS (DCTB) *m/z* (%): 362.1111 (100, $[M + Na]^+$), 339.1215 (4, $[M + H]^+$), 367.1527, (11, $[M]^+$, calcd for $C_{18}H_{17}N_3O_4$: 339.1214).

Diethyl 2-(3,3-Dicyano-2-phenylallylidene)malonate (203)

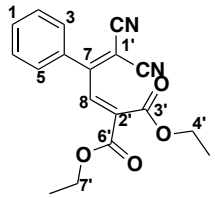

A solution of aniline **202** (80 mg, 0.236 mmol) in THF (2.4 mL) was treated with *tert*-butyl nitrite (56 μL, 0.471 mmol) and stirred under nitrogen for 1 h at 60 °C. Evaporation and flash column chromatography (SiO_2; EtOAc/cyclohexane 3:7 v/v) gave **203** (32 mg, 42%) as a pale yellow oil. R_f = 0.38 (SiO_2; EtOAc/cyclohexane 3:7); ^{1}H NMR (400 MHz, $CDCl_3$): δ = 1.07 (t, J = 7.2 Hz, 3 H; $H_3C(5')$), 1.33 (t, J = 7.1 Hz, 3 H; $H_3C(8')$), 3.63 (q, J = 7.2 Hz, 2 H; $H_2C(4')$), 4.33 (q, J = 7.1 Hz, 2 H; $H_2C(7')$), 7.44-7.51 (complex m, 4 H; H–C(2,3,5,6)), 7.56 (m, 1 H; H–C(1)), 7.81 ppm (s, 1 H; H–C(8)); ^{13}C NMR (100 MHz, $CDCl_3$): δ = 13.71 (1 C, $H_3C(5')$), 14.11 (1 C, $H_3C(8')$), 62.26 (1 C, $H_2C(4')$), 63.02 (1 C, $H_2C(7')$), 88.80 (1 C, C(1')), 111.64 (1 C, CN), 112.30 (1 C, CN), 129.03 (2 C, HC(2,6 or 3,5)), 129.52 (2 C, HC(2,6 or 3,5)), 132.07 (1 C, C(2')), 132.70 (1 C, HC(1)), 136.00 (1 C, HC(8)), 138.37 (1 C, C(4)), 162.33 (1 C, C(6')), 162.77 (1 C, C(3')), 167.09 ppm (1 C, C(7)); IR (ATR): $\tilde{\nu}$ = 2987 (w), 2902 (w), 2220 (m), 1723 (s), 1611 (w), 1578 (s), 1467 (w), 1445 (w), 1394 (m), 1368 (s), 1346 (s), 1296 (m), 1249 (s), 1225 (s), 1164 (s), 1095 (m), 1062 (s), 1015 (m), 940 (w), 921 (w), 860 (w), 825 (w), 793 (w), 770 (w), 733 (w), 698 (w), 971 (w), 639 (w), 616 cm^{-1} (w); UV/Vis ($CHCl_3$): λ_{max} (ε) = 291 (11300 M^{-1}cm^{-1}); HR-MALDI-MS (3-HPA) *m/z* (%): 347.1003 (100, [M + Na]$^+$, calcd for $C_{18}H_{16}N_2NaO_4$: 347.1002).

Diethyl 2-[3,3-Dicyano-2-(4-nitrophenyl)allylidene]malonate (204)

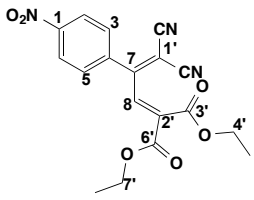

A solution of aniline **202** (80 mg, 0.236 mmol) in $CHCl_3$ (2.4 mL) at reflux was treated with *m*CPBA (163 mg, 0.943 mmol) and heating continued for 2 h. The cooled mixture was diluted with $NaHCO_3$ (10 mL of a sat. aq solution) and the

separated organic phase dried ($MgSO_4$), filtered, evaporated and subjected to flash column chromatography (SiO_2; EtOAc/cyclohexane 3:7 v/v) to give **204** (65 mg, 75%) as a pale yellow oil. R_f = 0.54 (SiO_2; EtOAc/cyclohexane 3:7); ^{1}H NMR (400 MHz, $CDCl_3$): δ = 1.10 (t, J = 7.1 Hz, 3 H; $H_3C(5')$), 1.33 (t, J = 7.1 Hz, 3 H; $H_3C(8')$), 3.68 (q, J = 7.1 Hz, 2 H; $H_2C(4')$), 4.34 (q, J = 7.1 Hz, 2 H; $H_2C(7')$), 7.63 (d, J = 8.8 Hz, 2 H; H–C(3,5)), 7.81 (s, 1 H; H–C(8)) 8.34 ppm (d, J = 8.8 Hz, 2 H; H–C(2,6)); ^{13}C NMR (100 MHz, $CDCl_3$): δ = 13.75 (1 C, $H_3C(5')$), 14.10 (1 C, $H_3C(8')$), 62.59 (1 C, $H_2C(4')$), 63.33 (1 C, $H_2C(7')$), 91.51 (1 C, C(1')), 110.77 (1 C, CN), 111.44 (1 C, CN), 124.06 (2 C, HC(2,6)), 130.69 (2 C, HC(3,5)), 134.55 (1 C, HC(8)), 137.62 (1 C, C(4)), 139.01 (1 C, C(2')), 149.81 (1 C, C(1)), 161.96 (1 C, C(6')), 162.57 (1 C, C(3')), 164.59 ppm (1 C, C(7)); IR (ATR): $\tilde{\nu}$ = 2986 (w), 2231 (w), 1724 (s), 1602 (w), 1524 (s), 1466 (w), 1446 (w), 1349 (s), 1248 (s), 1223 (s), 1094 (m), 1063 (m), 1013 (m), 925 (w), 857 (m), 845 (m), 795 (w), 757 (w), 734 (w), 701 (w), 613 cm^{-1} (w); UV/Vis ($CHCl_3$): λ_{max} (ε) = 311 (15800), 270 (16300 M^{-1}cm^{-1}); HR-MALDI-MS (3-HPA) m/z (%): 392.0853 (100, [M + Na]$^+$), 370.1035 (45, [M + H]$^+$, calcd for $C_{18}H_{16}N_3O_6$: 370.1034).

Diethyl 2-[3,3-Dicyano-2-(4-iodophenyl)allylidene]malonate (205)

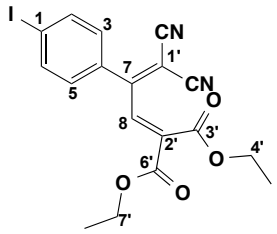

A solution of aniline **202** (92 mg, 0.271 mmol) in MeCN (1.4 mL) was added to a solution of *tert*-butyl nitrite (49 μL, 0.407 mmol) and iodine (206 mg, 0.813 mmol) in MeCN (2.7 mL) under nitrogen. The resulting mixture was stirred for 3 h at 25 °C, diluted with $Na_2S_2O_3$ (15 mL of a 1 M aq. solution) and extracted with CH_2Cl_2 (3 × 15 mL). The combined organic phases were dried ($MgSO_4$), filtered, evaporated and columned (SiO_2; EtOAc/cyclohexane elution 3:7 v/v) to give **205** (96 mg, 79%) as pale yellow crystals. R_f = 0.58 (SiO_2; EtOAc/cyclohexane 3:7); m.p. 92–93 °C; ^{1}H NMR (400 MHz, $CDCl_3$): δ = 1.10 (t, J = 7.2 Hz, 3 H; $H_3C(5')$), 1.32 (t, J = 7.1 Hz, 3 H; $H_3C(8')$), 3.70 (q, J = 7.2 Hz, 2 H; $H_2C(4')$), 4.32 (q, J = 7.1 Hz, 2 H; $H_2C(7')$), 7.16 (d, J = 8.6 Hz, 2 H; H–C(3,5)), 7.76 (s, 1 H; H–C(8)) 7.83 ppm (d, J = 8.6 Hz, 2

H; H–C(2,6)); ^{13}C NMR (100 MHz, $CDCl_3$): δ = 13.71 (1 C, $H_3C(5')$), 14.05 (1 C, $H_3C(8')$), 62.42 (1 C, $H_2C(4')$), 63.05 (1 C, $H_2C(7')$), 88.89 (1 C, C(1')), 99.99 (1 C, C(1)), 111.38 (1 C, CN), 112.05 (1 C, CN), 130.73 (2 C, HC(3,5)), 131.30 (1 C, C(4)), 135.50 (1 C, HC(8)), 138.27 (2 C, HC(2,6)), 138.54 (1 C, C(2')), 162.11 (1 C, C(6')), 162.68 (1 C, C(3')), 165.96 ppm (1 C, C(7)); IR (ATR): $\tilde{\nu}$ = 2999 (w), 2229 (w), 1725 (s), 1696 (s), 1618 (w), 1583 (w), 1552 (w), 1531 (w), 1483 (w), 1469 (w), 1444 (w), 1385 (m), 1366 (w), 1333 (w), 1245 (s), 1191 (w), 1155 (w), 1117 (w), 1094 (m), 1058 (s), 1009 (s), 962 (w), 925 (w), 862 (m), 841 (w), 829 (m), 811 (w), 765 (w), 696 (w), 686 (w), 613 cm^{-1} (w); UV/Vis ($CHCl_3$): λ_{max} (ε) = 354 (8900), 293 (12700 $M^{-1}cm^{-1}$); HR-MALDI-MS (3-HPA) *m/z* (%): 472.9969 (100, $[M + Na]^+$, calcd for $C_{18}H_{15}IN_2NaO_4$: 472.9969).

Diethyl2-{3,3-Dicyano-2-[4'-(dimethylamino)-[1,1'-biphenyl]-4yl]allylidene} malonate (206)

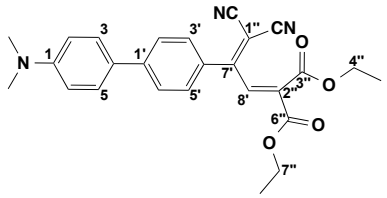

Iodide **205** (30 mg, 0.067 mmol), (4-(dimethylamino)phenyl)boronic acid (13 mg, 0.080 mmol), Cs_2CO_3 (87 mg, 0.268 mmol) and $[Pd(PPh_3)_4]$ (8 mg, 0.007 mmol) were dried under vacuum and purged with argon. Toluene (1.4 mL) that had been degassed by bubbling argon for 30 min was added and the reaction stirred at 50 °C for 16 h. The cooled reaction mixture was diluted with water (10 mL) and the separated aqueous phase extracted with EtOAc (3 x 10 mL). The combined organic phases were dried ($MgSO_4$), filtered, evaporated, and subjected to flash column chromatography (SiO_2; EtOAc/cyclohexane 1:7 v/v) to afford **206** (21 mg, 72%) as a red solid. R_f = 0.43 (SiO_2; EtOAc/cyclohexane 3:7); m.p. 52 °C; ^{1}H NMR (400 MHz, $CDCl_3$): δ = 1.06 (t, *J* = 7.2 Hz, 3 H; $H_3C(5'')$), 1.34 (t, *J* = 7.1 Hz, 3 H; $H_3C(8'')$), 3.03 (s, 6 H, $N(CH_3)_2$), 3.70 (q, *J* = 7.2 Hz, 2 H; $H_2C(4'')$), 4.34 (q, *J* = 7.1 Hz, 2 H; $H_2C(7'')$), 6.79 (d, *J* = 8.9 Hz, 2 H; H–C(2,6)), 7.52–7.56 (m, 4 H; H–C(3,5,3',5')), 7.66 (d, *J* = 8.5 Hz, 2 H; H–C(2',6')), 7.82 ppm (s, 1 H; H–C(8')); ^{13}C NMR (100 MHz, $CDCl_3$): δ = 13.77 (1 C, $H_3C(5'')$), 14.15 (1 C, $H_3C(8'')$), 40.46 (2 C,

$N(CH_3)_2$), 62.32 (1 C, $H_2C(4'')$), 62.94 (1 C, $H_2C(7'')$), 85.90 (1 C, C(1'')), 112.24 (1 C, CN), 112.68 (2 C, HC(2,6)), 112.94 (1 C, CN), 126.04 (2 C, HC(2',6')), 126.30 (1 C, C(4)), 128.01 (2 C, HC(3,5)), 129.29 (1 C, C(2'')), 130.32 (2 C, HC(3',5')), 137.13 (1 C, HC(8')), 137.99 (1 C, C(4')), 145.98 (1 C, C(1')), 150.98 (1 C, C(1)), 162.43 (1 C, C(6'')), 162.91 (1 C, C(3'')), 166.67 ppm (1 C, C(7')); IR (ATR): $\tilde{\nu}$ = 2923 (m), 2201 (m), 1723 (m), 1581 (s), 1536 (m), 1497 (w), 1444 (w), 1366 (s), 1346 (s), 1294 (m), 1250 (s), 1167 (s), 1063 (s), 1015 (m), 942 (m), 860 (w), 811 (m), 734 (w), 699 (w), 671 (w), 621 cm^{-1} (w); UV/Vis ($CHCl_3$): λ_{max} (ε) = 488 (7800), 327 (20400 $M^{-1}cm^{-1}$); HR-MALDI-MS (DCTB) *m/z* (%): 443.1839, (100, $[M]^+$, calcd for $C_{26}H_{25}N_3O_4$: 443.1840).

Diethyl 2-{3,3-Dicyano-2-[4-((4-(dimethylamino)phenyl)ethynyl)phenyl]allyl idene}malonate (207)

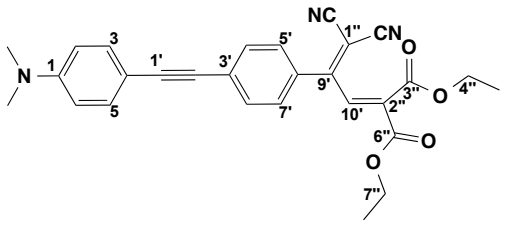

A solution of iodide **205** (40 mg, 0.088 mmol) and acetylene **102** (16 mg, 0.106 mmol) in THF (1.8 mL) was degassed with bubbling argon for 30 min, treated with $^{i}Pr_2NH$ (37 µL, 0.264 mmol), $[PdCl_2(PPh_3)_2]$ (6 mg, 0.009 mmol), and CuI (2 mg, 0.009 mmol), and stirred for 16 h at 24 °C. Evaporation and flash column chromatography (SiO_2; EtOAc/cyclohexane 3:7 v/v) afforded **207** (32 mg, 78 %) as a red solid. R_f = 0.36 (SiO_2; EtOAc/cyclohexane 3:7); m.p. 84 °C; ^{1}H NMR (400 MHz, $CDCl_3$): δ = 1.10 (t, *J* = 7.1 Hz, 3 H; $H_3C(5'')$), 1.34 (t, *J* = 7.1 Hz, 3 H; $H_3C(8'')$), 3.02 (s, 6 H, $N(CH_3)_2$), 3.72 (q, *J* = 7.1 Hz, 2 H; $H_2C(4'')$), 4.34 (q, *J* = 7.1 Hz, 2 H; $H_2C(7'')$), 6.67 (d, *J* = 9.0 Hz, 2 H; H–C(2,6)), 7.42 (d, *J* = 9.0 Hz, 2 H; H–C(3,5)), 7.44 (d, *J* = 8.7 Hz, 2 H; H–C(5',7')), 7.55 (d, *J* = 8.7 Hz, 2 H; H–C(4',8')), 7.80 ppm (s, 1 H; H–C(10')); ^{13}C NMR (100 MHz, $CDCl_3$): δ = 13.79 (1 C, $H_3C(5'')$), 14.13 (1 C, $H_3C(8'')$), 40.28 (2 C, $N(CH_3)_2$), 62.43 (1 C, $H_2C(4'')$), 63.01 (1 C, $H_2C(7'')$), 86.98 (1 C, C(2')), 87.35 (1 C, C(1'')), 96.13 (1 C, C(1')), 108.86 (1 C, C(4)), 111.88 (2 C, HC(2,6)), 111.91 (1 C, CN), 112.50 (1 C, CN), 129.60 (2 C, HC(5',7')), 129.62 (1 C, C(3')), 130.35 (1 C, C(2'')), 131.42 (2 C, HC(4',8')), 133.29 (2 C, HC(3,5)), 136.40 (1

C, HC(10')), 138.28 (1 C, C(6')), 150.75 (1 C, C(1)), 162.33 (1 C, C(6")), 162.79 (1 C, C(3")), 166.24 ppm (1 C, C(9')); IR (ATR): $\tilde{\nu}$ = 2987 (m), 2922 (m), 2201 (s), 1727 (s), 1578 (s), 1526 (m), 1485 (w), 1444 (w), 1366 (s), 1347 (s), 1254 (s), 1166 (s), 1136 (s), 1092 (s), 1063 (s), 1016 (w), 942 (w), 886 (w), 860 (w), 839 (w), 823 (w), 810 (w), 794 (w), 734 (w), 699 (w), 671 (w), 639 (w), 612 cm^{-1} (w); UV/Vis ($CHCl_3$): λ_{max} (ε) = 487 (10100), 348 (28300 $M^{-1}cm^{-1}$); HR-MALDI-MS (DCTB) *m/z* (%): 467.1839 (100, $[M]^+$, calcd for $C_{28}H_{25}N_3O_4$: 467.1840).

Diethyl 2-{3,3-Dicyano-2-[4-(1,1,4,4-tetracyano-3-(4-(dimethylamino)phenyl) buta-1,3-dien-2-yl)phenyl]allylidene}malonate (208)

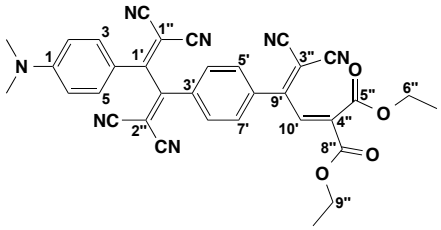

A solution of alkyne **207** (20 mg, 0.0428 mmol) in MeCN (0.5 mL) was treated with TCNE (**1**) (5.5 mg, 0.0428 mmol) and stirred for 1 h at 24 °C. Evaporation and flash column chromatography (SiO_2; EtOAc/cyclohexane 1:1 v/v) afforded **208** (23 mg, 89 %) as a black metallic solid. R_f = 0.45 (SiO_2; EtOAc/cyclohexane 1:1); m.p. 107–108 °C; ^{1}H NMR (400 MHz, $CDCl_3$): δ = 1.11 (t, *J* = 7.1 Hz, 3 H; H_3C(7")), 1.33 (t, *J* = 7.1 Hz, 3 H; H_3C(10")), 3.20 (s, 6 H, $N(CH_3)_2$), 3.74 (q, *J* = 7.1 Hz, 2 H; H_2C(6")), 4.34 (q, *J* = 7.1 Hz, 2 H; H_2C(9")), 6.77 (d, *J* = 9.4 Hz, 2 H; H–C(2,6)), 7.61 (d, *J* = 8.8 Hz, 2 H; H–C(4',8')), 7.76 (s, 1 H; H–C(10')), 7.78–7.81 ppm (m, 4 H, H–C(3,5,5',7')); ^{13}C NMR (100 MHz, $CDCl_3$): δ = 13.85 (1 C, H_3C(7")), 14.09 (1 C, H_3C(10")), 40.41 (2 C, $N(CH_3)_2$), 62.88 (1 C, H_2C(6")), 63.23 (1 C, H_2C(9")), 73.95 (1 C, C(1")), 89.94 (1 C, C(2")), 90.57 (1 C, C(3")), 110.84 (1 C, CN), 110.99 (1 C, CN), 111.49 (1 C, CN), 111.63 (1 C, CN), 112.72 (2 C, HC(2,6)), 113.60 (1 C, CN), 114.12 (1 C, CN), 117.31 (1 C, C(4)), 129.66 (2 C, HC(5',7')), 130.53 (2 C, HC(4',8')), 132.60 (2 C, HC(3,5)), 135.03 (1 C, HC(10')), 135.08 (1 C, C(3')), 136.75 (1 C, C(6')), 138.88 (1 C, (C4")), 154.82 (1 C, C(1)), 161.85 (1 C, C(9')), 162.03 (1 C, C(8")), 162.56 (1 C, C(5")), 164.85 (1 C, C(2')), 167.33 ppm (1 C, C(1')); IR (ATR): $\tilde{\nu}$ = 2987 (w), 2902 (w), 2201 (m), 1724 (m), 1605 (w), 1578 (s), 1485 (w), 1442 (w), 1369 (s), 1345 (s), 1296 (m), 1251 (s),

1168 (s), 1064 (s), 1015 (w), 941 (w), 886 (w), 860 (w), 823 (m), 793 (w), 734 (w), 699 (w), 671 (w), 615 cm^{-1} (w); UV/Vis ($CHCl_3$): λ_{max} (ε) = 466 (29700), 306 (20600 $M^{-1}cm^{-1}$); HR-MALDI-MS (DCTB) *m/z* (%): 595.1963 (100, $[M]^+$, calcd for $C_{34}H_{25}N_7O_4$: 595.1963).

Diethyl 2-{3,3-Dicyano-2-[4-(1,1-dicyano-3-(4-(dicyanomethylene)cyclohexa-2,5-dien-1-ylidene)-3-(4-(dimethylamino)phenyl)prop-1-en-2-yl)phenyl]allylidene} malonate (209)

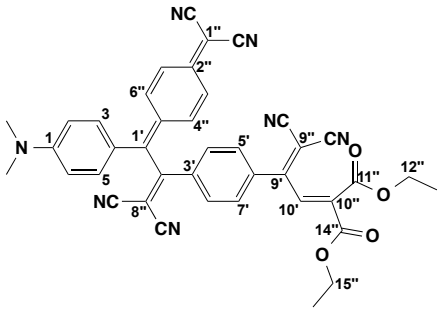

A solution of alkyne **207** (20 mg, 0.0428 mmol) in MeCN (0.5 mL) was treated with TCNQ (8.7 mg, 0.0428 mmol) and stirred for 1 h at 24 °C. Evaporation and flash column chromatography (SiO_2; EtOAc/cyclohexane 1:1 v/v) afforded **209** (24 mg, 84 %) as a black metallic solid. R_f = 0.34 (SiO_2; EtOAc/cyclohexane 1:1); m.p. 127–129 °C; ^1H NMR (400 MHz, $CDCl_3$): δ = 1.03 (t, *J* = 7.1 Hz, 3 H; $H_3C(13'')$), 1.33 (t, *J* = 7.1 Hz, 3 H; $H_3C(16'')$), 3.13 (s, 6 H, $N(CH_3)_2$), 3.49 (q, *J* = 7.1 Hz, 2 H; $H_2C(12'')$), 4.33 (q, *J* = 7.1 Hz, 2 H; $H_2C(15'')$), 6.71 (d, *J* = 9.2 Hz, 2 H; H–C(2,6)), 6.98 (dd, *J* = 9.6, 2.0 Hz, 1 H; H–C(2'' or 6'')), 7.23 (overlapping d, *J* = 9.5 Hz, 2 H; H–C(3,5)), 7.23 (overlapping dd, *J* = 9.6, 2.0 Hz, 1 H; H–C(3'' or 5'')), 7.30 (dd, *J* = 9.6, 2.0 Hz, 1 H; H–C(3'' or 5'')), 7.47 (dd, *J* = 9.6, 2.0 Hz, 1 H; H–C(2'' or 6'')), 7.54 (d, *J* = 8.8 Hz, 2 H; H–C(4',8')), 7.71 (d, *J* = 8.8 Hz, 2 H; H–C(4',8')), 7.74 ppm (s, 1 H; H–C(10')); ^{13}C NMR (100 MHz, $CDCl_3$): δ = 13.82 (1 C, $H_3C(13'')$), 14.11 (1 C, $H_3C(16'')$), 40.33 (2 C, $N(CH_3)_2$), 62.36 (1 C, $H_2C(12'')$), 63.29 (1 C, $H_2C(15'')$), 74.43 (1 C, C(7'')), 89.94 (1 C, C(9'')), 90.45 (1 C, C(8'')), 110.99 (1 C, CN), 111.62 (1 C, CN), 111.80 (1 C, CN), 112.45 (1 C, CN), 112.77 (2 C, HC(2,6)), 114.45 (1 C, CN), 114.57 (1 C, CN), 122.93 (1 C, C(4)), 125.73 (1 C, HC(3'' or 5'')), 126.00 (1 C, HC(3'' or 5'')), 129.88 (2 C, HC(5',7')), 130.39 (2 C, HC(4',8')), 132.47 (1 C, C(1')), 133.84 (1 C, HC(2'' or 6'')), 134.42 (2 C, HC(3,5)), 134.99 (1 C, HC(10')),

135.66 (1 C, HC(2'' or 6'')), 135.94 (1 C, C(6')), 138.28 (1 C, C(3')), 138.59 (1 C, (C10'')), 150.05 (1 C, C(9')), 153.05 (1 C, C(1)), 153.87 (1 C, C(C4'')), 161.99 (1 C, C(14'')), 162.49 (1 C, C(11'')), 164.86 (1 C, C(1')), 170.64 ppm (1 C, C(2')); IR (ATR): $\tilde{\nu}$ = 2987 (w), 2922 (w), 2200 (s), 1724 (m), 1610 (w), 1577 (s), 1445 (w), 1394 (w), 1366 (s), 1345 (s), 1295 (w), 1251 (m), 1163 (s), 1064 (s), 1016 (w), 941 (w), 920 (w), 884 (w), 825 (w), 793 (w), 734 (w), 698 (w), 970 (w), 638 (w), 615 cm^{-1} (w); UV/Vis ($CHCl_3$): λ_{max} (ε) = 672 (23600), 339 (28300 $M^{-1}cm^{-1}$); HR-MALDI-MS (DCTB) *m/z* (%): 671.2274 (100, $[M]^+$, calcd for $C_{40}H_{29}N_7O_4$: 671.2276).

Dimethyl 2-{3,3-Dicyano-2-[4-(dimethylamino)phenyl]allylidene}malonate (210)

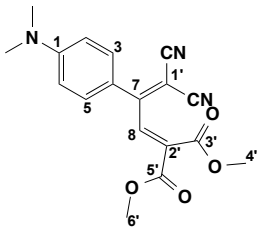

A solution of ethyl ester **163** (500 mg, 1.36 mmol) in MeOH (14 mL) was treated with a few drops of conc. H_2SO_4 and heated at reflux for 48 h. The mixture was quenched with Et_3N (1 mL), evaporated, and subjected to flash column chromatography (SiO_2; EtOAc/cyclohexane 1:1 v/v) to give **210** (286 mg, 62%) as a red solid. R_f = 0.19 (SiO_2; EtOAc/cyclohexane 3:7); m.p. 84 °C; ^{1}H NMR (400 MHz, $CDCl_3$): δ = 3.10 (s, 6 H, $N(CH_3)_2$), 3.43 (s, 3 H; $H_2C(4')$), 3.88 (s, 3 H; $H_2C(6')$), 6.66 (d, J = 9.2 Hz, 2 H; H–C(2,6)), 7.54 (d, J = 9.2 Hz, 2 H; H–C(3,5)), 7.80 ppm (s, 1 H; H–C(8)); ^{13}C NMR (100 MHz, $CDCl_3$): δ = 40.17 (2 C, $N(CH_3)_2$), 52.81 (1 C, $H_3C(4')$), 53.46 (1 C, $H_3C(6')$), 77.38 (1 C, C(1')), 111.37 (2 C, HC(2,6)), 113.72 (1 C, CN), 114.59 (1 C, CN), 119.09 (1 C, C(4)), 132.12 (2 C, HC(3,5)), 135.91 (1 C, C(2')), 140.22 (1 C, HC(8)), 153.76 (1 C, C(1)), 162.89 (1 C, C(5')), 163.49 (1 C, C(3')), 164.93 ppm (1 C, C(7)); IR (ATR): $\tilde{\nu}$ = 2954 (w), 2216 (m), 1727 (s), 1601 (s), 1541 (w), 1494 (s), 1436 (s), 1378 (s), 1335 (m), 1294 (w), 1259 (s), 1209 (s), 1189 (s), 1173 (s), 1067 (m), 978 (w), 944 (w), 923 (w), 809 (w), 766 (w), 731 (w), 630 cm^{-1} (w); UV/Vis ($CHCl_3$): λ_{max} (ε) = 456 (18200), 306 (16100 $M^{-1}cm^{-1}$); HR-MALDI-MS (DCTB) *m/z* (%): 339.1213 (100, $[M]^+$, calcd for $C_{18}H_{17}N_3O_4$: 339.1214).

(±)-Diethyl 2-{[6-Amino-5-cyano-4-(4-(dimethylamino)phenyl)-3-methyl-2,4-dihydro pyrano[2,3-*c*]pyrazol-4-yl]methylene}malonate (211)

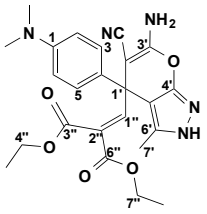

A solution of **163** (100 mg, 0.27 mmol) and 3-methyl-1*H*-pyrazol-5(4*H*)-one (**212**) (29 mg, 0.30 mmol) in 1:1 EtOH/1,4-dioxane (1 mL) in a microwave vial was degassed by bubbling argon for 30 min. *N*,*N*-diisopropylethylamine (474 μL, 2.72 mmol) was added and the mixture heated by microwave irradiation at 65 °C for 3.5 h. The mixture was diluted with water (20 mL) and extracted with EtOAc (3 x 20 mL). The combined organic phases were dried ($MgSO_4$), filtered, evaporated, and subjected to flash column chromatography (SiO_2; EtOAc/cyclohexane 1:1 v/v) then recrystallized from CH_2Cl_2 and cyclohexane (1:1) to give (±)-**211** (66 mg, 38%) as pale yellow crystals. R_f = 0.14 (SiO_2; EtOAc/cyclohexane 1:1); m.p. 110 °C (decomp.); ^{1}H NMR (300 MHz, $CDCl_3$): δ = 1.26 (overlapping t, J = 7.1 Hz, 3 H; H_3C(5'' or 8'')), 1.27 (overlapping t, J = 7.1 Hz, 3 H; H_3C(5'' or 8'')), 2.03 (s, 3 H; H_3C(7')), 2.98 (s, 6 H, $N(CH_3)_2$), 4.26 (m, 4 H; H_2C(4'',7'')), 5.29 (s, 2 H; H_2N), 5.75 (s, 1 H; H–C(1''), 6.72 (d, J = 8.8 Hz, 2 H; H–C(2,6)), 7.34 (d, J = 8.8 Hz, 2 H; H–C(3,5)), 8.94 ppm (s, 1 H; HN); ^{13}C NMR (100 MHz, CD_2Cl_2): δ = 14.05 (1 C, H_3C(5'' or 8'')), 14.15 (1 C, H_3C(5'' or 8'')), 15.98 (1 C, H_3C(7')), 40.70 (2 C, $N(CH_3)_2$), 58.94 (1 C, C(2')), 60.72 (1 C, C(1')), 62.99 (1 C, H_2C(4'' or 7'')), 63.48 (1 C, H_2C(4'' or 7'')), 81.14 (1 C, C(5')), 108.28 (1 C, HC(1'')), 112.31 (2 C, HC(2,6)), 117.91 (1 C, CN), 125.76 (1 C, C(4)), 128.62 (2 C, HC(3,5)), 138.53 (1 C, C(2'')), 151.58 (1 C, C(1)), 154.13 (1 C, C(4')), 157.66 (1 C, C(6')), 166.76 (1 C, C(3'' or 6'')), 167.50 (1 C, C(3'' or 6'')), 175.15 ppm (1 C, C(3')); IR (ATR): $\tilde{\nu}$ = 2987 (m), 2202 (m), 1724 (s), 1607 (m), 1578 (s), 1523 (m), 1443 (m), 1367 (s), 1250 (s), 1168 (s), 1065 (s), 942 (w), 824 (w), 736 (w), 671 cm^{-1} (w); HR-ESI-MS *m*/*z* (%): 466.2082 (100, $[M + H]^+$, calcd for $C_{24}H_{28}N_5O_5$: 466.2085).

Diethyl 2-{4-Cyano-5-(dimethylamino)-3-[4-(dimethylamino)phenyl]-1*H*-pyrrol-2-yl}malonate (213)

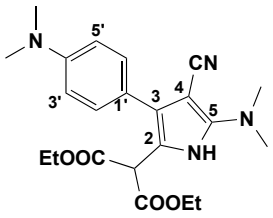

A mixture of **163** (560 mg, 1.53 mmol) and a 2.0 M THF solution of dimethylamine (1.52 mL, 3.05 mmol) in THF (15 mL) was subjected to General Procedure G and crystallized in EtOAc/cyclohexane 3:7 to give **213** (512 mg, 82%) as colorless crystals. R_f = 0.19 (SiO_2; EtOAc/cyclohexane 3:7); m.p. 155–156 °C; ^{1}H NMR (400 MHz, $CDCl_3$): δ = 1.28 (t, J = 7.1 Hz, 6 H; OCH_2CH_3), 2.97 (s, 6 H; Me_2N–C(4')), 3.11 (s, 6 H; Me_2N–C(5)), 4.17–4.27 (m, 4 H; OCH_2CH_3), 4.73 (s, 1 H; H–C–C(2)), 6.78 (d, J = 8.8 Hz, 2 H; H–C(3',5')), 7.32 (d, J = 8.8 Hz, 2 H; H–C(2',6')), 8.25 ppm (br. s, 1 H; NH); ^{13}C NMR (100 MHz, $CDCl_3$): δ = 14.14 (2 C; OCH_2CH_3), 40.60 (2 C; Me_2N–C(5)), 40.63 (2 C; Me_2N–C(4')), 48.79 (1 C, CH–C(2)), 62.43 (2 C; OCH_2CH_3), 73.24 (1 C, C(4)), 110.47 (1 C, C(2)), 112.66 (2 C, HC(3',5')), 119.39 (1 C, CN), 120.21 (1 C, C(1')), 126.41 (1 C, C(3)), 129.96 (2 C, HC(2',6')), 149.57 (1 C, C(5)), 149.93 (1 C, C(4')), 167.99 ppm (2 C, C=O); UV/Vis ($CHCl_3$): λ_{max} (ε) = 280 (19800 $M^{-1}cm^{-1}$); IR (ATR): $\tilde{\nu}$ = 3232 (w), 3179 (w), 2987 (w), 2901 (w), 2194 (m), 1738 (s), 1717 (m), 1601 (w), 1579 (m), 1522 (w), 1463 (w), 1407 (w), 1367 (w), 1348 (w), 1288 (w), 1247 (m), 1212 (m), 1160 (w), 1137 (w), 1066 (w), 1028 (s), 964 (w), 944 (w), 862 (w), 827 (w), 807 (w), 731 (w), 700 (w), 660 (w), 623 cm^{-1} (w); HR-ESI-MS m/z (%): 413.2177 (100, $[M + H]^+$, calcd for $C_{22}H_{29}N_4O_4$: 413.2183).

Diethyl 2-{4-Cyano-3-[4-(dimethylamino)phenyl]-5-(piperidin-1-yl)-1*H*-pyrrol-2-yl}malonate (214)

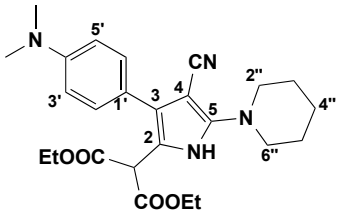

A mixture of **163** (50 mg, 0.14 mmol) and piperidine (28 μL, 0.28 mmol) in THF (1.4 mL) was subjected to General Procedure G. Flash column chromatography (SiO_2; EtOAc/cyclohexane 3:7) gave **214** (48 mg, 76%) as a pale yellow oil. R_f = 0.19 (SiO_2; EtOAc/cyclohexane 3:7); ^{1}H NMR (400 MHz, $CDCl_3$): δ = 1.28 (t, J = 7.1 Hz, 6 H; OCH_2CH_3), 1.58–1.62 (m, 2 H; H_2C(4")), 1.68–1.74 (m, 4 H; H_2C(3",5")), 2.97 (s, 6 H; Me_2N–C(4')), 3.35–3.38 (m, 4 H; H_2C(2",6")), 4.17–4.26 (m, 4 H; OCH_2CH_3), 4.74 (s, 1 H; H–C–C(2)), 6.78 (d, J = 8.8 Hz, 2 H; H–C(3',5')), 7.31 (d, J = 8.8 Hz, 2 H; H–C(2',6')), 8.44 ppm (br. s, 1 H; NH); ^{13}C NMR (100 MHz, $CDCl_3$): δ = 14.13 (2 C; OCH_2CH_3), 23.97 (1 C, H_2C(4")), 25.52 (2 C, H_2C(3",5")), 40.62 and 40.63 (2 C; Me_2N–C(4')), 48.77 (1 C, CH–C(2)), 50.18 (2 C, H_2C(2",6")), 62.44 (2 C; OCH_2CH_3), 76.03 (1 C, C(4)), 111.06 (1 C, C(2)), 112.67 (2 C, HC(3',5')), 118.74 (1 C, CN), 120.14 (1 C, C(1')), 126.18 (1 C, C(3)), 129.96 (2 C, HC(3',5')), 149.75 (1 C, C(4')), 149.92 (1 C, C(5)), 167.92 ppm (2 C, C=O); IR (ATR): $\tilde{\nu}$ = 3337 (w), 2927 (m), 2851 (w), 2201 (m), 1732 (s), 1616 (w), 1556 (s), 1520 (w), 1451 (m), 1366 (w), 1302 (w), 1223 (w), 1196 (m), 1023 (w), 943 (w), 922 (w), 858 (w), 921 cm^{-1} (w); HR-MALDI-MS (DCTB) *m/z* (%): 452.2419 (56, $[M]^+$, calcd for $C_{25}H_{32}N_4O_4$: 452.2419), 451.2340 (100, $[M - H]^+$).

Diethyl 2-{5-[Butyl(methyl)amino]-4-cyano-3-[4-(dimethylamino)phenyl]-1*H*-pyrrol-2-yl)malonate (215)

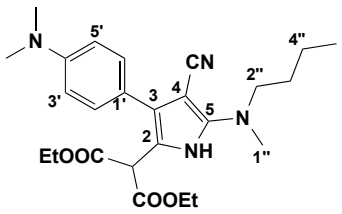

A mixture of **163** (51 mg, 0.14 mmol) and *N*-methylbutylamine (33 μL, 0.28 mmol) in THF (1.4 mL) was subjected to General Procedure G. Flash column

chromatography (SiO_2; EtOAc/cyclohexane 3:7) gave **215** (50 mg, 79%) as a pale yellow oil. R_f = 0.19 (SiO_2; EtOAc/cyclohexane 3:7); ^{1}H NMR (400 MHz, $CDCl_3$): δ = 0.97 (t, J = 7.3 Hz, 3 H; $H_3C(5'')$), 1.28 (t, J = 7.1 Hz, 6 H; OCH_2CH_3), 1.37–1.43 (m, 2 H; $H_2C(4'')$), 1.61–1.68 (m, 2 H; $H_2C(3'')$), 2.97 (s, 6 H; Me_2N–C(4')), 3.09 (s, 3 H; $H_3C(1'')$), 3.40 (t, J = 7.5 Hz, 2 H; $H_2C(2'')$), 4.17–4.26 (m, 4 H; $CO_2CH_2CH_3$), 4.73 (s, 1 H; H–C–C(2)), 6.78 (d, J = 8.8 Hz, 2 H; H–C(3',5')), 7.32 (d, J = 8.8 Hz, 2 H; H–C(2',6')), 8.21 ppm (br. s, 1 H; NH); ^{13}C NMR (100 MHz, $CDCl_3$): δ = 14.06 (1 C, $H_3C(5'')$), 14.11 (2 C; OCH_2CH_3), 20.04 (1 C, $H_2C(4'')$), 29.81 (1 C, $H_2C(3'')$), 29.81 (1 C, $H_3C(1'')$), 40.61 (2 C; Me_2N–C(4')), 48.81 (1 C, CH–C(2)), 52.94 (1 C, $H_2C(2'')$), 62.37 (2 C; OCH_2CH_3), 72.48 (1 C, C(4)), 111.17 (1 C, C(2)), 112.64 (2 C, HC(3',5')), 119.42 (1 C, CN), 120.31 (1 C, C(1')), 126.22 (1 C, C(3)), 129.95 (2 C, HC(3',5')), 148.88 (1 C, C(5)), 149.88 (1 C, C(4')), 167.98 ppm (2 C, C=O); IR (ATR): $\tilde{\nu}$ = 3350 (w), 2926 (m), 2852 (w), 2195 (m), 1730 (s), 1616 (w), 1578 (s), 1520 (m), 1460 (m), 1411 (w), 1366 (m), 1309 (m), 1225 (m), 1195 (m), 1145 (m), 1094 (w), 1031 (m), 944 (w), 927 (w), 861 (w), 820 (m), 742 (w), 701 (w), 618 cm^{-1} (w); HR-ESI-MS m/z (%): 455.2650 (100, $[M + H]^+$, calcd for $C_{25}H_{35}N_4O_4$: 455.2653).

Diethyl 2-{4-Cyano-5-[dihexylamino]-3-[4-(dimethylamino)phenyl]-1*H*-pyrrol-2-yl}malonate (216)

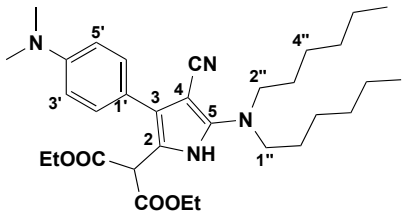

A mixture of **163** (87 mg, 0.24 mmol) and dihexylamine (110 μL, 0.47 mmol) in THF (2.4 mL) was subjected to General Procedure A, however time was extended to 1 h. Flash column chromatography (SiO_2; EtOAc/cyclohexane 3:7) gave **216** (88 mg, 67%) as a pale yellow oil. R_f = 0.41 (SiO_2; EtOAc/cyclohexane 3:7); ^{1}H NMR (400 MHz, $CDCl_3$): δ = 0.85–0.94 (m, 6 H; $H_3C(6'')$, 1.28 (t, J = 7.1 Hz, 6 H; OCH_2CH_3), 1.30–1.40 (m, 12 H; $H_2C(3'',4'',5'')$), 1.65 (qd, J = 7.5, 3.5 Hz, 4 H; $H_2C(2'')$), 2.97 (s, 6 H; Me_2N–C(4')), 3.23–3.56 (m, 4 H; $H_2C(1'')$), 4.17–4.26 (m, 4 H: $CO_2CH_2CH_3$), 4.72 (s, 1 H: H–C–C(2)), 6.78 (d, J = 8.8 Hz, 2 H; H–C(3',5')), 7.32 (d, J = 8.8 Hz, 2 H; H–C(2',6')), 8.20 ppm (br. s, 1 H; NH); ^{13}C NMR (100 MHz, $CDCl_3$): δ = 14.12 (2 C, $H_3C(6'')$), 14.14 (2 C; OCH_2CH_3), 22.73 (2 C, $H_2C(5'')$), 26.53 (2 C,

$H_2C(4'')$), 28.33 (2 C, $H_2C(3'')$), 31.77 (2 C, $H_3C(2'')$), 40.64 (2 C; *Me*$_2$N–C(4')), 48.84 (1 C, *C*H–C(2)), 51.32 (2 C, $H_2C(1'')$), 62.35 (2 C; O*C*H_2CH$_3$), 72.41 (1 C, C(4)), 110.04 (1 C, C(2)), 112.65 (2 C, HC(3',5')), 119.36 (1 C, CN), 120.42 (1 C, C(1')), 126.04 (1 C, C(3)), 129.99 (2 C, HC(3',5')), 148.00 (1 C, C(5)), 149.86 (1 C, C(4')), 167.97 ppm (2 C, C=O); IR (ATR): $\tilde{\nu}$ = 3445 (w), 2929 (m), 2857 (m), 2194 (m), 1732 (s), 1616 (m), 1576 (s), 1521 (m), 1462 (m), 1367 (m), 1309 (m), 1225 (m), 1146 (m), 1030 (m), 945 (w), 862 (w), 820 (m), 727 (w), 618 cm^{-1} (w); HR-ESI-MS *m*/*z* (%): 553.3742 (100, $[M + H]^+$, calcd for $C_{32}H_{49}N_4O_4$: 553.3748).

Diethyl 2-{5-Amino-4-cyano-3-[4-(dimethylamino)phenyl]-1*H*-pyrrol-2-yl}malonate (217)

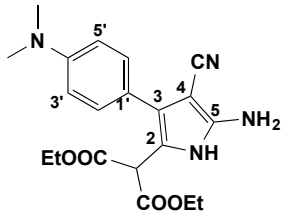

A mixture of **163** (42 mg, 0.11 mmol) in 2.0 M solution of NH_3 in isopropanol (1.1 mL) was subjected to General Procedure G, however time was extended to 1 h. Flash column chromatography (SiO_2; EtOAc/cyclohexane 1:1) gave **217** (24 mg, 53%) as a brown solid. R_f = 0.10 (SiO_2; EtOAc/cyclohexane 1:1); m.p. 194–195 °C; ^{1}H NMR (400 MHz, CD_3OD): δ = 1.30 (t, *J* = 7.1 Hz, 6 H; OCH$_2$C*H*$_3$), 2.98 (s, 6 H; Me$_2$N–C(4')), 4.22 (q, *J* = 7.1 Hz, 4 H; OC*H*$_2$CH$_3$), 4.68 (s, 1 H; H–C–C(2)), 6.82 (d, *J* = 8.8 Hz, 2 H; H–C(3',5')), 7.24 ppm (d, *J* = 8.8 Hz, 2 H; H–C(2',6')), NH and NH_2 signals not observed; ^{13}C NMR (100 MHz, CD_3OD): δ = 14.36 (2 C; OCH$_2$*C*H$_3$), 40.75 (2 C; *Me*$_2$N–C(5)), 51.36 (1 C, *C*H–C(2)), 62.82 (2 C; O*C*H_2CH$_3$), 73.54 (1 C, C(4)), 109.48 (1 C, C(2)), 113.85 (2 C, HC(3',5')), 118.87 (1 C, CN), 120.64 (1 C, C(1')), 126.74 (1 C, C(3)), 129.72 (2 C, HC(2',6')), 149.69 (1 C, C(5)), 151.53 (1 C, C(4')), 169.93 ppm (2 C, C=O); IR (ATR): $\tilde{\nu}$ = 3336 (m), 2982 (m), 2199 (m), 1731 (s), 1614 (s), 1571 (s), 1516 (s), 1356 (m), 1225 (s), 821 cm^{-1} (w); HR-ESI-MS *m*/*z* (%): 385.1868 (100, $[M + H]^+$, calcd for $C_{20}H_{25}N_4O_4$: 385.1870).

Diethyl 2-{5-Amino-4-cyano-1-cyclopentyl-3-[4-(dimethylamino)phenyl]-1*H*-pyrrol-2-yl}malonate (218)

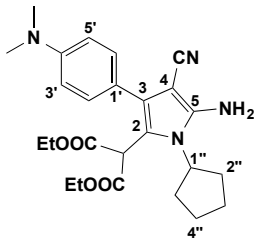

A mixture of **163** (50 mg, 0.14 mmol) and cyclopentylamine (27 μL, 0.27 mmol) in THF (1.4 mL) was subjected to General Procedure G. Flash column chromatography (SiO_2; EtOAc/cyclohexane 3:7) gave **218** (50 mg, 81%) as a white solid. R_f = 0.24 (SiO_2; EtOAc/cyclohexane 3:7); m.p. 172–174 °C; ^{1}H NMR (400 MHz, $CDCl_3$): δ = 1.28 (t, J = 7.1 Hz, 6 H; OCH_2CH_3), 1.65–1.71 (m, 2 H; H_{ax}–C(3",4")), 1.84–1.89 (m, 2 H; H_{eq}–C(3",4")), 1.98–2.15 (m, 4 H; H_2C(2",5")), 2.97 (s, 6 H; Me_2N–C(4')), 3.97 (br. s, 2 H; NH), 4.16–4.28 (m, 4 H: $CO_2CH_2CH_3$), 4.61 (p, J = 9.1 Hz, 1 H; H–C(1")), 4.93 (s, 1 H: H–C–C(2)), 6.76 (d, J = 8.8 Hz, 2 H; H–C(3',5')), 7.25 ppm (d, J = 8.8 Hz, 2 H; H–C(2',6')); ^{13}C NMR (100 MHz, $CDCl_3$): δ = 14.25 (2 C; OCH_2CH_3), 25.62 (2 C, H_2C(3",4")), 29.52 (2 C, H_2C(2",5")), 40.64 (2 C; Me_2N–C(4')), 49.48 (1 C, CH–C(2)), 58.09 (1 C, H_2C(1")), 62.23 (2 C; OCH_2CH_3), 77.63 (1 C, C(4)), 112.66 (2 C, HC(3',5')), 115.43 (1 C, C(2)), 117.44 (1 C, CN), 120.79 (1 C, C(1')), 125.24 (1 C, C(3)), 130.20 (2 C, HC(3',5')), 145.22 (1 C, C(5)), 149.94 (1 C, C(4')), 168.21 ppm (2 C, C=O); IR (ATR): $\tilde{\nu}$ = 3409 (w), 3325 (w), 3238 (w), 2970 (m), 2930 (m), 2206 (m), 1728 (s), 1642 (m), 1614 (m), 1556 (m), 1518 (m), 1491 (m), 1461 (m), 1404 (w), 1364 (m), 1308 (m), 1247 (m), 1194 (m), 1173 (m), 1146 (s), 1090 (m), 1059 (m), 1019 (m), 947 (m), 899 (w), 857 (w), 818 (m), 741 (m), 700 (w), 680 (w), 641 (w), 621 cm^{-1} (w); HR-ESI-MS m/z (%): 453.2500 (100, $[M + H]^+$, calcd for $C_{25}H_{33}N_4O_4$: 453.2496).

Diethyl 2-{5-Amino-4-cyano-1-cyclopropyl-3-[4-(dimethylamino)phenyl]-1*H*-pyrrol-2-yl}malonate (219)

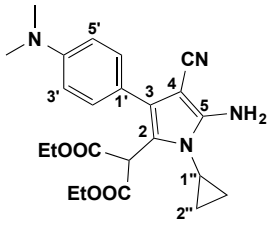

A mixture of **163** (50 mg, 0.14 mmol) and cyclopropylamine (19 μL, 0.27 mmol) in THF (1.4 mL) was subjected to General Procedure G. Flash column chromatography (SiO_2; EtOAc/cyclohexane 3:7) gave **219** (41 mg, 69%) as a light brown solid. R_f = 0.26 (SiO_2; EtOAc/cyclohexane 3:7); m.p. 164–166 °C; ^{1}H NMR (400 MHz, $CDCl_3$): δ = 0.99–1.04 (m, 2 H; H_{ax}–C(2'')), 1.06–1.10 (m, 2 H; H_{eq}–C(2'')), 1.21 (t, J = 7.1 Hz, 6 H; OCH_2CH_3), 2.86–2.92 (m, 1 H; H–C(1'')), 2.94 (s, 6 H; Me_2N–C(4')), 4.09–4.28 (m, 4 H: $CO_2CH_2CH_3$), 4.35 (br. s, 2 H; NH), 4.94 (s, 1 H: H–C–C(2)), 6.71 (d, J = 8.8 Hz, 2 H; H–C(3',5')), 7.27 ppm (d, J = 8.8 Hz, 2 H; H–C(2',6')); ^{13}C NMR (100 MHz, $CDCl_3$): δ = 7.32 (2 C; C(2'')), 14.01 (2 C; OCH_2CH_3), 25.14 (1 C; C(1")), 40.67 (2 C; Me_2N–C(4')), 50.22 (1 C, CH–C(2)), 62.05 (2 C; OCH_2CH_3), 74.31 (1 C, C(4)), 112.43 (2 C, HC(3',5')), 114.45 (1 C, C(2)), 117.45 (1 C, CN), 120.65 (1 C, C(1')), 125.36 (1 C, C(3)), 130.11 (2 C, HC(3',5')), 147.82 (1 C, C(5)), 150.06 (1 C, C(4')), 168.08 ppm (2 C, C=O); IR (ATR): $\tilde{\nu}$ = 3313 (w), 2981 (w), 2205 (w), 1733 (s), 1615 (m), 1554 (s), 1521 (m), 1451 (m), 1366 (m), 1198 (m), 1031 (w), 945 (w), 823 cm^{-1} (w); HR-ESI-MS m/z (%): 425.2484 (100, $[M + H]^+$, calcd for $C_{25}H_{33}N_4O_4$: 425.2184).

Diethyl 2-{5-Amino-1-butyl-4-cyano-3-[4-(dimethylamino)phenyl]-1*H*-pyrrol-2-yl}malonate (220)

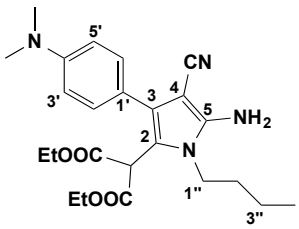

A mixture of **163** (50 mg, 0.14 mmol) and *N*-butylamine (27 μL, 0.27 mmol) in THF (1.4 mL) was subjected to General Procedure G. Flash column

chromatography (SiO_2; EtOAc/cyclohexane 3:7) gave **220** (45 mg, 73%) as a light brown solid. R_f = 0.31 (SiO_2; EtOAc/cyclohexane 3:7); m.p. 170–172 °C; ^{1}H NMR (400 MHz, $CDCl_3$): δ = 0.94 (t, J = 7.1 Hz, 3 H; H–C(4'')), 1.26 (t, J = 7.1 Hz, 6 H; OCH_2CH_3), 1.35 (s, J = 7.1 Hz, 2 H; H–C(3'')), 1.60 (q, J = 7.1 Hz, 2 H; H–C(2''), 2.96 (s, 6 H; Me_2N–C(4')), 3.78–3.82 (m, 2 H: H–C(1'')), 4.03 (br. s, 2 H; NH), 4.09–4.28 (m, 4 H: $CO_2CH_2CH_3$), 4.90 (s, 1 H: H–C–C(2)), 6.76 (d, J = 8.8 Hz, 2 H; H–C(3',5')), 7.29 ppm (d, J = 8.8 Hz, 2 H; H–C(2',6')); ^{13}C NMR (100 MHz, $CDCl_3$): δ = 13.71 (1 C; C(4'')), 14.01 (2 C; OCH_2CH_3), 20.16 (1 C, C(3'')), 30.97 (1 C, C(2'')), 40.51 (2 C; Me_2N–C(4')), 44.67 (1 C, C(1'')), 49.33 (1 C, CH–C(2)), 62.07 (2 C; OCH_2CH_3), 76.19 (1 C, C(4)), 112.50 (2 C, HC(2',6')), 113.92 (1 C, C(2)), 117.42 (1 C, CN), 120.64 (1 C, C(1')), 125.52 (1 C, C(3)), 130.05 (2 C, HC(3',5')), 145.53 (1 C, C(5)), 149.83 (1 C, C(4')), 167.93 ppm (2 C, C=O); IR (ATR): $\tilde{\nu}$ = 3413 (w), 3319 (w), 3241 (w), 2971 (m), 2930 (m), 2201 (m), 1731 (s), 1640 (m), 1615 (m), 1554 (m), 1516 (m), 1487 (m), 1463 (m), 1402 (w), 1364 (m), 1307 (m), 1249 (m), 1192 (m), 1178 (m), 1141 (s), 1091 (m), 1059 (m), 1015 (m), 944 (m), 899 (w), 847 (w), 821 (m), 740 (m), 700 (w), 680 (w), 649 (w), 619 cm^{-1} (w); HR-ESI-MS m/z (%): 441.2495 (100, $[M + H]^+$, calcd for $C_{25}H_{33}N_4O_4$: 441.2496).

Diethyl 2-{5-Amino-4-cyano-3-[4-(dimethylamino)phenyl]thiophen-2-yl}malonate (221)

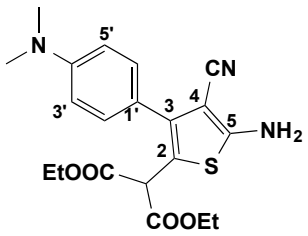

A mixture of **163** (200 mg, 0.054 mmol) and DABCO (61 mg, 0.54 mmol) in THF (5.4 mL) was treated with $Na_2S{\bullet}9H_2O$ (261 mg, 1.09 mmol) and heated at 65 °C for 20 min. The reaction was quenched with a saturated aqueous NH_4Cl solution (40 mL). The aqueous layer was extracted with CH_2Cl_2 (3 x 20 ml), dried ($MgSO_4$), filtered and concentrated. Flash column chromatography (SiO_2; EtOAc/cyclohexane 1:9) gave **221** (160 mg, 76%) as colorless crystals. R_f = 0.35 (SiO_2; EtOAc/cyclohexane 1:1); m.p. 192–193 °C; ^{1}H NMR (400 MHz, $CDCl_3$): δ = 1.27 (t, J = 7.1 Hz, 6 H; OCH_2CH_3), 3.00 (s, 6 H; Me_2N–C(4')), 4.17–4.26 (m, 4 H;

OCH_2CH$_3$), 4.84 (br. s, 2 H; NH$_2$), 4.88 (s, 1 H; H–C–C(2)), 6.76 (d, J = 8.8 Hz, 2 H; H–C(3',5')), 7.24 ppm (d, J = 8.8 Hz, 2 H; H–C(2',6')); ^{13}C NMR (100 MHz, CDCl$_3$): δ = 14.14 (2 C; OCH$_2$*C*H$_3$), 40.47 (2 C; *Me*$_2$N–C(5)), 51.39 (1 C, *C*H–C(2)), 62.40 (2 C; O*C*H$_2$CH$_3$), 90.22 (1 C, C(4)), 112.36 (2 C, HC(3',5')), 112.63 (1 C, C(2)), 115.79 (1 C, CN), 120.49 (1 C, C(1')), 130.11 (2 C, HC(2',6')), 140.60 (1 C, C(3)), 150.52 (1 C, C(4')), 162.45 (1 C, C(5)), 169.93 ppm (2 C, C=O); IR (ATR): $\tilde{\nu}$ = 3427 (m), 3327 (m), 3224 (m), 2981 (m), 2206 (m), 1729 (m), 1610 (s), 1520 (s), 1445 (m), 1393 (m), 1366 (m), 1302 (m), 1197 (m), 1173 (m), 1140 (m), 1095 (w), 1063 (w), 1023 (m), 946 (w), 918 (w), 860 (w), 827 (m), 732 cm^{-1} (w); HR-ESI-MS *m*/*z* (%): 401.1404 (100, [M + H]$^+$, calcd for $C_{20}H_{23}N_3O_4S$: 401.1404).

Diethyl 2-{4-Cyano-3-[4-(dimethylamino)phenyl]-5-morpholino-1*H*-pyrrol-2-yl}malonate (222)

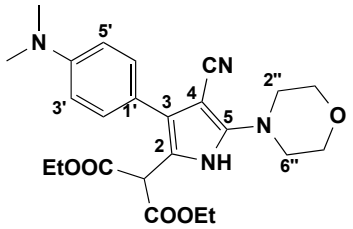

A mixture of **163** (50 mg, 0.14 mmol) and morpholine (24 μL, 0.28 mmol) in THF (1.4 mL) was subjected to General Procedure G under argon. Flash column chromatography (SiO$_2$; EtOAc/cyclohexane 3:7) gave **222** (31 mg, 39%) as a yellow solid. R_f = 0.38 (SiO$_2$; EtOAc/cyclohexane 3:7); m.p. 129–130 °C; ^{1}H NMR (400 MHz, CDCl$_3$): δ = 1.28 (t, J = 7.1 Hz, 6 H; OCH$_2$C*H*$_3$), 2.98 (s, 6 H; Me$_2$N–C(4')), 3.38–3.40 (m, 4 H; H$_2$C(2'',6'')), 3.82–3.85 (m, 4 H; H$_2$C(3'',5'')), 4.17–4.27 (m, 4 H; OCH_2CH$_3$), 4.75 (s, 1 H; H–C–C(2)), 6.78 (d, J = 8.8 Hz, 2 H; H–C(3',5')), 7.31 (d, J = 8.8 Hz, 2 H; H–C(2',6')), 8.58 ppm (br. s, 1 H; NH); ^{13}C NMR (100 MHz, CDCl$_3$): δ = 14.13 (2 C; OCH$_2$*C*H$_3$), 40.60 (2 C; *Me*$_2$N–C(4')), 48.69 (1 C, *C*H–C(2)), 49.01 (2 C, H$_2$C(2'',6'')), 62.56 (2 C; O*C*H$_2$CH$_3$), 66.43 (2 C, H$_2$C(3'',5'')), 76.84 (1 C, C(4)), 111.71 (1 C, C(2)), 112.65 (2 C, HC(3',5')), 118.24 (1 C, CN), 119.73 (1 C, C(1')), 126.40 (1 C, C(3)), 129.95 (2 C, HC(3',5')), 148.66 (1 C, C(4')), 150.02 (1 C, C(5)), 167.89 ppm (2 C, C=O); IR (ATR): $\tilde{\nu}$ = 3334 (w), 2979 (w), 2856 (w), 2203 (m), 1731 (s), 1616 (m), 1557 (s), 1520 (m), 1450 (m), 1366 (m), 1308 (m), 1243 (m), 1198 (s), 1149 (s), 1118 (s), 1067 (w), 1031 (m), 944 (m), 923 (m), 882 (w), 863 (w),

823 (m), 736 (w), 618 cm^{-1} (w); HR-MALDI-MS (DCTB) *m/z* (%): 455.2289 (100, $[M + H]^+$, calcd for $C_{24}H_{31}N_4O_5$: 455.2289).

Diethyl 2-{1-[*tert*-Butoxycarbonyl]-4-cyano-3-[4-(dimethylamino)phenyl]-5-morpholino-1*H*-pyrrol-2-yl}malonate (223)

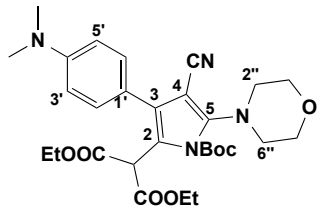

A mixture of **163** (50 mg, 0.14 mmol) and morpholine (24 μL, 0.28 mmol) in THF (1.4 mL) was subjected to General Procedure G. The resulting mixture was treated with Boc_2O (71 mg, 0.38 mmol), Et_3N (41 μL, 0.38 mmol), and DMAP (cat.) and stirred at 65 ºC with microwave irradiation for 1 h. Concentration and flash column chromatography (SiO_2; EtOAc/cyclohexane 3:7) gave **223** (46 mg, 56%) as a pale yellow oil. R_f = 0.60 (SiO_2; EtOAc/cyclohexane 3:7); ^{1}H NMR (400 MHz, $CDCl_3$): δ = 1.28 (t, J = 7.1 Hz, 6 H; OCH_2CH_3), 1.60 (s, 9 H; $C(CH_3)_3$), 2.98 (s, 6 H; Me_2N–C(4')), 3.33–3.35 (m, 4 H; H_2C(2'',6'')), 3.79–3.82 (m, 4 H; H_2C(3'',5'')), 4.06–4.23 (m, 4 H; OCH_2CH_3), 4.86 (s, 1 H; H–C–C(2)), 6.74 (d, J = 8.8 Hz, 2 H; H–C(3',5')), 7.27 ppm (d, J = 8.8 Hz, 2 H; H–C(2',6')); ^{13}C NMR (100 MHz, $CDCl_3$): δ = 14.16 (2 C; OCH_2CH_3), 27.92 (3 C, $C(CH_3)_3$), 40.52 (2 C; Me_2N–C(4')), 49.80 (1 C, CH–C(2)), 52.00 (2 C, H_2C(2'',6'')), 61.98 (2 C; OCH_2CH_3), 67.25 (2 C, H_2C(3'',5'')), 86.49 (1 C, $C(CH_3)_3$), 87.43 (1 C, C(4)), 112.45 (2 C, HC(3',5')), 116.14 (1 C, C(2)), 117.39 (1 C, C(1')), 118.69 (1 C, CN), 128.25 (1 C, C(3)), 130.42 (2 C, HC(3',5')), 148.95 (1 C, C(4')), 149.08 (1 C, N–C=O), 150.40 (1 C, C(5)), 167.25 ppm (2 C, C=O); IR (ATR): $\tilde{\nu}$ = 2981 (w), 1750 (s), 1533 (w), 1261 (m), 1143, 921 cm^{-1} (w); HR-MALDI-MS (DCTB) *m/z* (%): 555.2813 (100, $[M + H]^+$, calcd for $C_{29}H_{39}N_4O_7$: 555.2813).

Diethyl 2-{1-[*tert*-Butoxycarbonyl]-4-cyano-3-[4-(dimethylamino)phenyl]-5-[1*H*-imidazol-1-yl]-1*H*-pyrrol-2-yl}malonate (224)

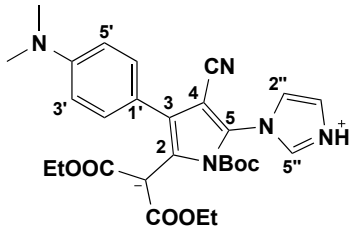

A mixture of **163** (50 mg, 0.14 mmol) and imidazole (19 mg, 0.28 mmol) in THF (1.4 mL) was subjected to General Procedure G. The resulting mixture was treated with Boc_2O (71 mg, 0.38 mmol), Et_3N (41 μL, 0.38 mmol), and DMAP (cat.) and stirred at 65 ºC with microwave irradiation for 1 h. Concentration and flash column chromatography (SiO_2; EtOAc/cyclohexane 3:7) gave **224** (55 mg, 73%) as a pale yellow solid. This species exists as a zwitterionic species with H–C–C(2) protonating the imidazole. R_f = 0.13 (SiO_2; EtOAc/cyclohexane 1:1); m.p. 172–173 °C; ^{1}H NMR (400 MHz, $CDCl_3$): δ = 1.21 (t, J = 7.1 Hz, 6 H; OCH_2CH_3), 1.51 (s, 9 H; $C(CH_3)_3$), 2.95 (s, 6 H; Me_2N–C(4')), 4.16–4.27 (m, 4 H; OCH_2CH_3), 6.56 (d, J = 9.0 Hz, 2 H; H–C(3',5')), 6.83 (t, J = 1.3 Hz, 1 H; H–C(2")), 7.06–7.08 (m, 3 H; H–C(2',6',5")), 7.29 (t, J = 1.3 Hz, 1 H; H–C(3")), 7.54 ppm (br. s, 1 H; NH(H–C–C(2) protonating imidazole); ^{13}C NMR (100 MHz, $CDCl_3$): δ = 14.03 (2 C; OCH_2CH_3), 28.07 (3 C, $C(CH_3)_3$), 40.13 (2 C; Me_2N–C(4')), 63.15 (2 C; OCH_2CH_3), 71.21 (1 C, C(4)), 83.71 (3 C, $C(CH_3)_3$), 96.23 (1 C, C–C(2)), 111.88 (2 C, HC(3',5')), 114.24 (1 C, C(2)), 116.16 (1 C, CN), 119.34 ((1 C, HC(2")),), 121.00 (1 C, C(1')), 129.10 (2 C, HC(3',5')), 129.54 (1 C, HC(5")), 138.59 (1 C, C(3)), 139.36 (1 C, HC(3")), 150.48 (1 C, C(5)), 151.05 (1 C, C(4')), 152.60 (1 C, N–C=O)), 162.73 ppm (2 C, C=O); IR (ATR): $\tilde{\nu}$ = 2982 (w), 2932 (w), 2214 (w), 1778 (m), 1727 (s), 1598 (s), 1526 (m), 1483 (m), 1367 (m), 1235 (s), 1202 (s), 1145 (s), 1049 (s), 945 (w), 912 (w), 855 (m), 819 (m), 794 (m), 769 (m), 732 (s), 681 (m), 669 (w), 656 (m), 644 (w), 632 (w), 622 (m), 609 (m), 603 cm^{-1} (w); HR-MALDI-MS (DCTB) m/z (%): 536.2524 (100, [M + H]$^+$, calcd for $C_{28}H_{34}N_5O_6$: 536.2504).

Tetraethyl 2,2'-(Piperazine-1,4-diylbis{4-cyano-3-[4-(dimethylamino)phenyl]-1*H*-pyrrole-5,2-diyl})dimalonate (225)

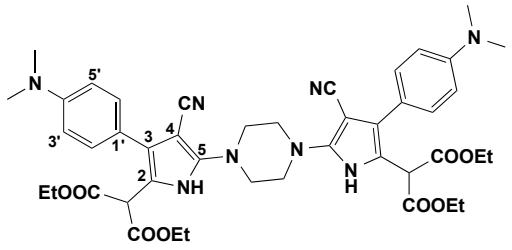

A mixture of **163** (50 mg, 0.14 mmol) and piperazine (6 mg, 0.07 mmol) in THF (1.4 mL) was subjected to General Procedure G. Flash column chromatography (SiO_2; EtOAc/cyclohexane 3:7) gave **225** (60 mg, 54%) as a black solid. R_f = 0.40 (SiO_2; EtOAc/cyclohexane 1:1); m.p. 208 °C; ^{1}H NMR (400 MHz, $CDCl_3$): δ = 1.29 (t, J = 7.1 Hz, 12 H; OCH_2CH_3), 2.97 (s, 12 H; Me_2N–C(4')), 3.55 (s, 8 H; H_2C(piperazine)), 4.19–4.28 (m, 8 H; OCH_2CH_3), 4.76 (s, 2 H; H–C–C(2)), 6.79 (d, J = 8.8 Hz, 4 H; H–C(3',5')), 7.31 (d, J = 8.8 Hz, 4 H; H–C(2',6')), 8.63 ppm (br. s, 2 H; NH); ^{13}C NMR (100 MHz, $CDCl_3$): δ = 14.18 (4 C; OCH_2CH_3), 40.63 (4 C; Me_2N–C(4')), 48.79 (2 C, CH–C(2)), 49.02 (4 C, H_2C(piperazine)), 62.63 (4 C; OCH_2CH_3), 78.03 (1 C, C(4)), 112.166 (2 C, C(2)), 112.70 (4 C, HC(3',5')), 117.96 (2 C, CN), 119.72 (2 C, C(1')), 126.45 (2 C, C(3)), 129.98 (2 C, HC(3',5')), 148.16 (2 C, C(4')), 150.06 (2 C, C(5)), 167.79 ppm (4 C, C=O); IR (ATR): $\tilde{\nu}$ = 3313 (w), 2981 (w), 2205 (w), 1733 (s), 1615 (m), 1554 (s), 1521 (m), 1451 (m), 1366 (m), 1198 (m), 1031 (w), 945 (w), 823 cm^{-1} (w); HR-MALDI-MS (DCTB) m/z (%): 820.3903 (100, $[M]^+$, calcd for $C_{44}H_{52}N_8O_8$: 820.3908).

Diethyl 2-{4-Cyano-5-[1,3-dimethoxy-1,3-dioxopropan-2-yl]-3-[4-(dimethylamino)phenyl]-1*H*-pyrrol-2-yl}malonate (226)

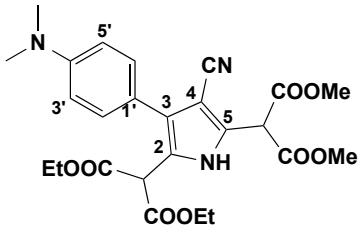

A mixture of **163** (50 mg, 0.14 mmol), dimethyl malonate (31 μL, 0.27 mmol), and K_2CO_3 (19 mg, 0.14 mmol) in THF (1.4 mL) was subjected to General Procedure B for 17 h. Flash column chromatography (SiO_2; EtOAc/cyclohexane 3:7)

gave **226** (32 mg, 62%) as a brown oil. R_f = 0.45 (SiO_2; EtOAc/cyclohexane 1:1); ^{1}H NMR (400 MHz, $CDCl_3$): δ = 1.33 (t, J = 7.1 Hz, 6 H; OCH_2CH_3), 2.98 (s, 6 H; Me_2N–C(4')), 3.78 (s, 6 H; OCH_3), 4.25–4.34 (m, 4 H; OCH_2CH_3), 4.88 (s, 1 H; H–C–C(2)), 5.01 (s, 1 H; H–C–C(5)), 6.79 (d, J = 8.8 Hz, 2 H; H–C(3',5')), 7.29 (d, J = 8.8 Hz, 2 H; H–C(2',6')), 10.20 ppm (br. s, 1 H; NH); ^{13}C NMR (100 MHz, $CDCl_3$): δ = 14.09 (2 C; OCH_2CH_3), 40.56 (2 C; Me_2N–C(5)), 48.74 (1 C, CH–C(2)), 49.96 (1 C, CH–C(5)), 53.52 (2 C; OCH_3), 63.01 (2 C; OCH_2CH_3), 94.22 (1 C, C(4)), 112.74 (2 C, HC(3',5')), 115.72 (1 C, C(2)), 119.17 (1 C, CN), 119.53 (1 C, C(1')), 127.44 (1 C, C(3)), 129.92 (2 C, HC(2',6')), 130.43 (1 C, C(5)), 150.17 (1 C, C(4')), 166.10 (2 C; C(5)–C–C=O), 167.52 ppm (2 C, C(2)–C–C=O); IR (ATR): $\tilde{\nu}$ = 3382 (w), 2927 (w), 2851 (w), 2222 (w), 1733 (s), 1614 (m), 1538 (w), 1511 (w), 1435 (w), 1366 (w), 1196 (s), 1147 (s), 1096 (w), 1064 (w), 1021 (m), 981 (w), 945 (w), 904 (w), 860 (w), 82 (w), 760 (w), 640 cm^{-1} (w); HR-ESI-MS m/z (%): 500.2023 (100, $[M + H]^+$, calcd for $C_{25}H_{30}N_3O_8$: 500.2027).

Diethyl 2-[3-(4-Aminophenyl)-4-cyano-5-(dimethylamino)-1*H*-pyrrol-2-yl]malonate (227)

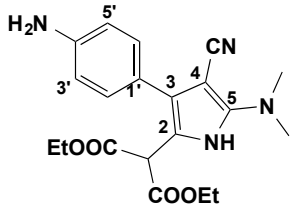

A mixture of **202** (75 mg, 0.20 mmol) and a 2.0 M THF solution of dimethylamine (195 μL, 0.39 mmol) in THF (2.0 mL) was subjected to General Procedure G. Flash column chromatography (SiO_2; EtOAc/cyclohexane 3:7) gave **227** (61 mg, 81%) as a white solid. R_f = 0.27 (SiO_2; EtOAc/cyclohexane 1:1); m.p. 121–122 °C; ^{1}H NMR (400 MHz, $CDCl_3$): δ = 1.27 (t, J = 7.1 Hz, 6 H; OCH_2CH_3), 3.08 (s, 6 H; Me_2N–C(5)), 3.75 (br. s, 2 H; NH_2), 4.14–4.28 (m, 4 H; OCH_2CH_3), 4.69 (s, 1 H; H–C–C(2)), 6.71 (d, J = 8.8 Hz, 2 H; H–C(3',5')), 7.21 (d, J = 8.8 Hz, 2 H; H–C(2',6')), 8.20 ppm (br. s, 1 H; NH); ^{13}C NMR (100 MHz, $CDCl_3$): δ = 14.06 (2 C; OCH_2CH_3), 40.51 (2 C; Me_2N–C(5)), 48.72 (1 C, CH–C(2)), 62.41 (2 C; OCH_2CH_3), 73.05 (1 C, C(4)), 110.59 (1 C, C(2)), 115.26 (2 C, HC(3',5')), 119.29 (1 C, CN), 122.27 (1 C, C(1')), 126.26 (1 C, C(3)), 130.18 (2 C, HC(2',6')), 145.99 (1 C, C(4')), 149.55 (1 C, C(5)), 167.88 ppm (2 C, C=O); IR (ATR): $\tilde{\nu}$ = 3440 (w), 3365 (w), 2982 (w), 2196

(m), 1728 (s), 1583 (s), 1517 (m), 1464 (m), 1407 (w), 1368 (w), 1296 (m), 1227 (m), 1180 (m), 1159 (m), 1931 (m), 960 (w), 911 (w), 837 (w), 731 (w), 641 cm^{-1} (w); HR-ESI-MS *m*/*z* (%): 385.1868 (100, $[M + H]^+$, calcd for $C_{20}H_{25}N_4O_4$: 385.1870).

Diethyl 2-[4-Cyano-5-(dimethylamino)-3-phenyl-1*H*-pyrrol-2-yl]malonate (228)

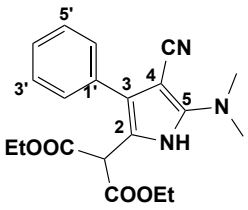

Method A: A mixture of **203** (20 mg, 0.06 mmol) and a 2.0 M THF solution of dimethylamine (124 μL, 0.12 mmol) in THF (0.6 mL) was subjected to General Procedure G. Flash column chromatography (SiO_2; EtOAc/cyclohexane 3:7) gave **228** (20 mg, 88%) as a yellow oil.

Method B: A mixture of **252** (40 mg, 0.12 mmol) and a 2.0 M THF solution of dimethylamine (248 μL, 0.24 mmol) in THF (1.2 mL) was subjected to General Procedure G, however time was increased to 45 min. Flash column chromatography (SiO_2; EtOAc/cyclohexane 3:7) gave **228** (20 mg, 45%) as a yellow oil.

Both Methods A and B gave spectroscopically identical material. $R_f = 0.16$ (SiO_2; EtOAc/cyclohexane 3:7); ^{1}H NMR (400 MHz, $CDCl_3$): δ = 1.28 (t, J = 7.1 Hz, 6 H; OCH_2CH_3), 3.13 (s, 6 H; Me_2N–C(5)), 4.16–4.29 (m, 4 H; OCH_2CH_3), 4.71 (s, 1 H; H–C–C(2)), 7.31–7.35 (m, 1 H; H–C(4')), 7.39–7.44 (m, 4 H; H–C(2',3',5',6')), 8.37 ppm (br. s, 1 H; NH); ^{13}C NMR (100 MHz, $CDCl_3$): δ = 14.12 (2 C; OCH_2CH_3), 40.58 (2 C; Me_2N–C(5)), 48.69 (1 C, CH–C(2)), 62.58 (2 C; OCH_2CH_3), 73.04 (1 C, C(4)), 111.29 (1 C, C(2)), 119.03 (1 C, CN), 126.11 (1 C, C(3)), 127.53 (1 C, HC(4')), 128.76 (2 C, HC(2',6' or 3',5')), 129.26 (2 C, HC(2',6' or 3',5')), 132.34 (1 C, C(1')), 149.76 (1 C, C(5)), 167.80 ppm (2 C, C=O); IR (ATR): $\tilde{\nu}$ = 3326 (br. w), 2983 (w), 2198 (m), 1730 (s), 1575 (s), 1465 (m), 1443 (m), 1423 (w), 1406 (w), 1368 (w), 1229 (s), 1181 (s), 1095 (m), 1071 (m), 1028 (m), 959 (w), 942 (w), 860 (w), 781 (w), 732 (w), 701 (m), 624 cm^{-1} (w); HR-ESI-MS *m*/*z* (%): 370.1761 (100, $[M + H]^+$, calcd for $C_{20}H_{24}N_3O_4$: 370.161).

Diethyl 2-[4-Cyano-5-(dimethylamino)-3-(4-nitrophenyl)-1*H*-pyrrol-2-yl]malonate (229)

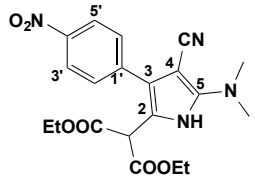

A mixture of **204** (80 mg, 0.22 mmol) and a 2.0 M THF solution of dimethylamine (216 μL, 0.43 mmol) in THF (2.1 mL) was subjected to General Procedure G. Flash column chromatography (SiO_2; EtOAc/cyclohexane 3:7) gave **229** (84 mg, 94%) as an orange solid. R_f = 0.11 (SiO_2; EtOAc/cyclohexane 1:1); m.p. 168–178 °C; ^{1}H NMR (400 MHz, $CDCl_3$): δ = 1.29 (t, J = 7.1 Hz, 6 H; OCH_2CH_3), 3.15 (s, 6 H; Me_2N–C(5)), 4.19–4.30 (m, 4 H; OCH_2CH_3), 4.63 (s, 1 H; H–C–C(2)), 7.61 (d, J = 8.9 Hz, 2 H; H–C(3',5')), 8.29 (d, J = 8.9 Hz, 2 H; H–C(2',6')), 8.55 ppm (br. s, 1 H; NH); ^{13}C NMR (100 MHz, $CDCl_3$): δ = 14.13 (2 C; OCH_2CH_3), 40.48 (2 C; Me_2N–C(5)), 48.58 (1 C, CH–C(2)), 62.93 (2 C; OCH_2CH_3), 72.30 (1 C, C(4)), 112.71 (1 C, C(2)), 118.53 (1 C, CN), 123.93 (1 C, C(3)), 124.16 (2 C, HC(2',6')), 129.82 (2 C, HC(3',5')), 139.26 (1 C, C(4')), 147.04 (1 C, C(1')), 150.07 (1 C, C(5)), 167.33 ppm (2 C, C=O); IR (ATR): $\tilde{\nu}$ = 3330 (w), 2981 (w), 2197 (m), 1744 (m), 1712 (s), 1592 (s), 1519 (s), 1463 (m), 1367 (w), 1338 (m), 1300 (m), 1151 (m), 1067 (m), 1024 (m), 962 (w), 933 (w), 862 (m), 743 (w), 707 (w), 622 cm^{-1} (w); HR-ESI-MS *m/z* (%): 415.1608 (100, $[M + H]^+$, calcd for $C_{20}H_{23}N_4O_6$: 415.1612).

Diethyl 2-[4-Cyano-5-(dimethylamino)-3-(4-iodophenyl)-1*H*-pyrrol-2-yl]malonate (230)

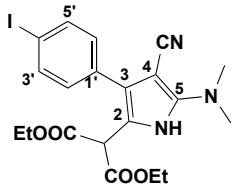

A mixture of **205** (100 mg, 0.22 mmol) and a 2.0 M THF solution of dimethylamine (222 μL, 0.44 mmol) in THF (2.2 mL) was subjected to General Procedure G. Flash column chromatography (SiO_2; EtOAc/cyclohexane 3:7) gave **230** (100 mg, 91%) as a brown solid. R_f = 0.60 (SiO_2; EtOAc/cyclohexane 1:1); m.p. 177–178 °C; ^{1}H NMR (400 MHz, $CDCl_3$): δ = 1.26 (t, J = 7.1 Hz, 6 H; OCH_2CH_3),

3.10 (s, 6 H; Me_2N–C(5)), 4.09–4.28 (m, 4 H; OCH_2CH$_3$), 4.62 (s, 1 H; H–C–C(2)), 7.18 (d, J = 8.4 Hz, 2 H; H–C(3',5')), 7.73 (d, J = 8.4 Hz, 2 H; H–C(2',6')), 8.43 ppm (br. s, 1 H; NH); ^{13}C NMR (100 MHz, $CDCl_3$): δ = 14.04 (2 C; OCH$_2$*C*H$_3$), 40.44 (2 C; *Me*$_2$N–C(5)), 48.56 (1 C, *C*H–C(2)), 62.59 (2 C; O*C*H$_2$CH$_3$), 72.43 (1 C, C(4)), 93.24 (1 C, C(4')), 111.47 (1 C, C(2)), 118.78 (1 C, CN), 124.86 (1 C, C(3)), 130.99 (2 C, HC(3',5')), 131.82 (1 C, C(1')), 137.82 (2 C, HC(2',6')), 149.75 (1 C, C(5)), 167.48 ppm (2 C, C=O); IR (ATR): $\tilde{\nu}$ = 3347 (br. w), 2982 (w), 2196 (m), 1727 (s), 1580 (s), 1464 (m), 1442 (m), 1398 (w), 1368 (w), 1297 (m), 1229 (m), 1175 (m), 1147 (s), 1105 (m), 1063 (w), 1026 (s), 966 (w), 910 (m), 872 (w), 821 (m), 728 (s), 647 (w), 619 cm^{-1} (w); HR-ESI-MS *m*/*z* (%): 496.0727 (100, [*M* + H]$^+$, calcd for $C_{20}H_{23}IN_3O_4$: 496.0728).

Diethyl 2-[4-Cyano-5-(dimethylamino)-3-(ferrocenyl)-1*H*-pyrrol-2-yl]malonate (231)

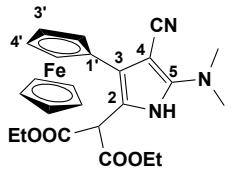

A mixture of **200** (45 mg, 0.10 mmol) and a 2.0 M THF solution of dimethylamine (104 μL, 0.21 mmol) in THF (1.0 mL) was subjected to General Procedure A. Flash column chromatography (SiO_2; EtOAc/cyclohexane 3:7) gave **231** (33 mg, 66%) as a yellow oil. R_f = 0.14 (SiO_2; EtOAc/cyclohexane 3:7); ^{1}H NMR (400 MHz, $CDCl_3$): δ = 1.31 (t, J = 7.1 Hz, 6 H; OCH$_2$C*H*$_3$), 3.11 (s, 6 H; Me_2N–C(5)), 4.19 (s, 5 H; (Fe(C_5H_5)), 4.22–4.29 (m, 6 H; H–C(2',5'), OC*H*$_2$CH$_3$), 4.64 (m, 2 H, H–C(3',4')), 5.18 (s, 1 H; H–C–C(2)), 8.28 ppm (br. s, 1 H; NH); ^{13}C NMR (100 MHz, $CDCl_3$): δ = 14.18 (2 C; OCH$_2$*C*H$_3$), 40.58 (2 C; *Me*$_2$N–C(5)), 48.86 (1 C, *C*H–C(2)), 62.57 (2 C; O*C*H$_2$CH$_3$), 67.72 (2 C, HC(3',4')), 68.31 (2 C, HC(2',5')), 69.65 (5 C, Fe(C_5H_5)), 73.00 (1 C, C(4)), 78.17 (1 C, C(1')), 110.86 (1 C, C(2)), 119.78 (1 C, CN), 121.73 (1 C, C(3)), 150.01 (1 C, C(5)), 167.74 ppm (2 C, C=O); IR (ATR): $\tilde{\nu}$ = 3250 (br. w), 2981 (w), 2198 (m), 1733 (s), 1591 (s), 1463 (m), 1368 (w), 1296 (m), 1029 (w), 960 (w), 881 (w), 863 (w), 833 (w), 736 (w), 675 (w), 644 (w), 632 (w), 617 cm^{-1} (w); HR-ESI-MS *m*/*z* (%): 478.1418 (100, [*M* + H]$^+$, calcd for $C_{24}H_{28}FeN_3O_4$: 478.1424).

(±)-Ethyl 2-Cyano-2-{4-cyano-5-[dimethylamino]-3-[4-(dimethylamino) phenyl]-1*H*-pyrrol-2-yl}acetate (±-232)

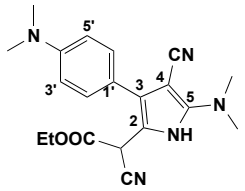

A mixture of *cis*-**160** (45 mg, 0.14 mmol) and a 2.0 M THF solution of dimethylamine (140 μL, 0.28 mmol) in THF (1.4 mL) was subjected to General Procedure G. Flash column chromatography (SiO_2; EtOAc/cyclohexane 3:7) gave (±)-**232** (27 mg, 52%) as a yellow solid. The same procedure was followed with *trans*-**161** to also give (±)-**232** (24 mg, 47%) as a yellow solid. The products from both reactions were identical in all respects. R_f = 0.46 (SiO_2; EtOAc/cyclohexane 1:1); slow decomp. at 25 °C; ^{1}H NMR (400 MHz, $CDCl_3$): δ = 1.33 (t, J = 7.1 Hz, 3 H; OCH_2CH_3), 2.99 (s, 6 H; Me_2N–C(4')), 3.13 (s, 6 H; Me_2N–C(5)), 4.27–4.3 (m, 2 H; OCH_2CH_3), 4.85 (s, 1 H; H–C–C(2)), 6.78 (d, J = 8.8 Hz, 2 H; H–C(3',5')), 7.25 (d, J = 8.8 Hz, 2 H; H–C(2',6')), 7.97 ppm (br. s, 1 H; NH); ^{13}C NMR (100 MHz, $CDCl_3$): δ = 14.09 (1 C; OCH_2CH_3), 34.95 (1 C, CH–C(2)), 40.53 (2 C; Me_2N–C(5)), 40.56 (2 C; Me_2N–C(4')), 63.92 (1 C; OCH_2CH_3), 73.55 (1 C, C(4)), 106.45 (1 C, C(2)), 112.72 (2 C, HC(3',5')), 114.85 (1 C, C(3)), 118.68 (1 C, CN), 118.92 (1 C, CN), 128.08 (1 C, C(1')), 129.82 (2 C, HC(2',6')), 150.04 (1 C, C(5)), 150.30 (1 C, C(4')), 164.81 ppm (1 C, C=O); IR (ATR): $\tilde{\nu}$ = 3336 (m), 2925 (m), 2854 (m), 2206 (m), 1730 (m), 1600 (s), 1514 (s), 1488 (s), 1464 (m), 1363 (s), 1264 (s), 1171 (s), 1118 (m), 1061 (m), 1018 (s), 973 (w), 940 (m), 908 (m), 822 (m), 729 (s), 668 (w), 646 cm^{-1} (w); HR-ESI-MS *m*/*z* (%): 364.1767 (100, $[M - H]^+$, calcd for $C_{20}H_{22}N_5O_2$: 364.1773).

Diethyl 2-{5-[Dimethylamino]-3-[4-(dimethylamino)phenyl]-4-[ethoxy carbonyl]-1*H*-pyrrol-2-yl}malonate (233)

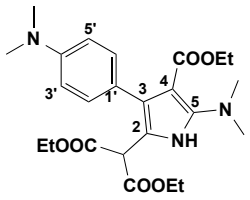

A mixture of **170** (40 mg, 0.10 mmol) and a 2.0 M THF solution of dimethylamine (96 μL, 0.19 mmol) in THF (1.0 mL) was subjected to General Procedure H for 17 h. Flash column chromatography (SiO_2; EtOAc/cyclohexane 3:7) gave **233** (32 mg, 73%) as a red solid. R_f = 0.54 (SiO_2; EtOAc/cyclohexane 1:1); m.p. 129–130 °C; ^{1}H NMR (400 MHz, $CDCl_3$): δ = 0.99 (t, J = 7.1 Hz, 3 H; C(4)–$CO_2CH_2CH_3$), 1.25 (t, J = 7.1 Hz, 6 H; OCH_2CH_3), 2.96 (s, 6 H; Me_2N–C(4')), 2.97 (s, 6 H; Me_2N–C(5)), 4.02 (q, J = 7.1 Hz, 2 H; C(4)–$CO_2CH_2CH_3$), 4.12–4.25 (m, 4 H; OCH_2CH_3), 4.58 (s, 1 H; H–C–C(2)), 6.72 (d, J = 8.8 Hz, 2 H; H–C(3',5')), 7.13 (d, J = 8.8 Hz, 2 H; H–C(2',6')), 8.56 ppm (br. s, 1 H; NH); ^{13}C NMR (100 MHz, $CDCl_3$): δ = 14.14 (2 C; OCH_2CH_3), 14.17 (1 C; C(4)–$CO_2CH_2CH_3$), 40.92 (2 C; Me_2N–C(5)), 42.75 (2 C; Me_2N–C(4')), 48.85 (1 C, CH–C(2)), 59.04 (1 C; C(4)–$CO_2CH_2CH_3$), 62.18 (2 C; OCH_2CH_3), 99.18 (1 C, C(4)), 111.97 (2 C, HC(3',5')), 112.55 (1 C, C(2)), 123.41 (1 C, C(1')), 126.17 (1 C, C(3)), 131.26 (2 C, HC(2',6')), 148.30 (1 C, C(5)), 149.53 (1 C, C(4')), 164.82 (1 C; C(4)–C=O), 167.99 ppm (2 C, C=O); IR (ATR): $\tilde{\nu}$ = 3350 (br. w), 2980 (w), 1730 (s), 1867 (m), 1596 (m), 1554 (m), 1520 (m), 1446 (m), 1366 (m), 1303 (m), 1195 (s), 1172 (s), 1082 (s), 1025 (m), 944 (w), 821 (w), 640 cm^{-1} (w); HR-ESI-MS m/z (%): 460.2440 (100, $[M + H]^+$, calcd for $C_{24}H_{34}N_3O_6$: 460.2442).

Dimethyl 2-{4-Cyano-5-[dimethylamino]-3-[4-(dimethylamino)phenyl]-1*H*-pyrrol-2-yl)malonate (234)

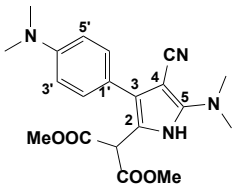

A mixture of **210** (40 mg, 0.12 mmol) and a 2.0 M THF solution of dimethylamine (118 μL, 0.24 mmol) in THF (1.2 mL) was subjected to General

Procedure G. Flash column chromatography (SiO_2; EtOAc/cyclohexane 3:7) gave **234** (34 mg, 75%) as a yellow solid. R_f = 0.33 (SiO_2; EtOAc/cyclohexane 1:1); m.p. 138–140 °C; ^{1}H NMR (400 MHz, $CDCl_3$): δ = 2.97 (s, 6 H; Me_2N–C(4')), 3.11 (s, 6 H; Me_2N–C(5)), 3.77 (s, 6 H; OCH_3), 4.79 (s, 1 H; H–C–C(2)), 6.78 (d, J = 8.8 Hz, 2 H; H–C(3',5')), 7.29 (d, J = 8.8 Hz, 2 H; H–C(2',6')), 8.19 ppm (br. s, 1 H; NH); ^{13}C NMR (100 MHz, $CDCl_3$): δ = 40.58 (2 C; *Me*$_2$N–C(5)), 40.60 (2 C; *Me*$_2$N–C(4')), 48.40 (1 C, *C*H–C(2)), 53.30 (2 C; OCH_3), 73.21 (1 C, C(4)), 110.13 (1 C, C(2)), 112.69 (2 C, HC(3',5')), 119.28 (1 C, CN), 120.02 (1 C, C(1')), 126.61 (1 C, C(3)), 129.89 (2 C, HC(2',6')), 149.63 (1 C, C(5)), 149.97 (1 C, C(4')), 168.39 ppm (2 C, C=O); IR (ATR): $\tilde{\nu}$ = 3232 (w), 3179 (w), 2987 (w), 2901 (w), 2194 (m), 1738 (s), 1717 (m), 1601 (w), 1579 (m), 1522 (w), 1463 (w), 1407 (w), 1367 (w), 1348 (w), 1288 (w), 1247 (m), 1212 (m), 1160 (w), 1137 (w), 1066 (w), 1028 (s), 964 (w), 944 (w), 862 (w), 827 (w), 807 (w), 731 (w), 700 (w), 660 (w), 623 cm^{-1} (w); HR-ESI-MS *m*/*z* (%): 385.1865 (100, $[M + H]^+$, calcd for $C_{20}H_{25}N_4O_4$: 385.1870).

(±)-Ethyl (3*R*,4*S*,*Z*)-2-(1-Cyano-2-ethoxy-2-oxoethylidene)-5-(dimethyl amino)-3-(4-(dimethylamino)phenyl)-3,4-dihydro-2*H*-pyrrole-4-carboxylate (±-235)

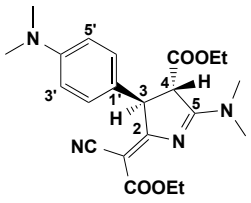

A mixture of **166** (100 mg, 0.27 mmol) and a 2.0 M THF solution of dimethylamine (272 μL, 0.54 mmol) in THF (2.7 mL) was subjected to General Procedure G. Flash column chromatography (SiO_2; EtOAc/cyclohexane 3:7) gave (±)-**235** (91 mg, 82%) as a white solid. The same procedure was followed with **167** to also give (±)-**235** (100 mg, 90%) as a white solid. The products from both reactions were identical in all respects. R_f = 0.15 (SiO_2; EtOAc/cyclohexane 1:1); m.p. 188–189 °C; ^{1}H NMR (400 MHz, $CDCl_3$): δ = 1.18 (t, J = 7.2 Hz, 3 H; C(2)=C–$COCH_2CH_3$), 1.30 (t, J = 7.1 Hz, 3 H; C(4)–$CO_2CH_2CH_3$), 2.91 (s, 6 H; Me_2N–C(4')), 3.10 (s, 3 H; Me_2N–C(5)), 3.42 (s, 3 H; Me_2N–C(5)), 3.72 (d, J = 1.5 Hz, 1 H; H–C(4)), 3.99–4.11 (m, 2 H; C(2)=$CCO_2CH_2CH_3$), 4.24 (q, J = 7.1 Hz, 2 H; C(4)–$CO_2CH_2CH_3$), 5.15 (d, J = 1.5 Hz, 1 H; H–C(3)), 6.62 (d, J = 8.8 Hz, 2 H; H–

C(3',5')), 6.97 ppm (d, J = 8.8 Hz, 2 H; H–C(2',6')); ^{13}C NMR (100 MHz, $CDCl_3$): δ = 14.24 (1 C; C(2)=C–$COCH_2CH_3$), 14.35 (1 C; C(4)–$CO_2CH_2CH_3$), 40.02 (1 C; Me_2N–C(5)), 40.23 (1 C; Me_2N–C(5)), 40.61 (2 C; Me_2N–C(4')), 55.34 (1 C, HC(3)), 59.34 (1 C, HC(4)), 60.44 (1 C; C(2)=C$CO_2CH_2CH_3$), 62.49 (1 C; C(4)–$CO_2CH_2CH_3$), 84.14 (1 C, C(2)=C), 112.75 (2 C, HC(3',5')), 118.07 (1 C, CN), 127.48 (2 C, HC(2',6')), 128.33 (1 C, C(1')), 149.82 (1 C, C(4')), 164.37 (1 C; C(2)=C–C=O), 168.00 (1 C, C(4)–C=O), 175.42 (1 C, C(5)), 187.77 ppm (1 C, C(2)); IR (ATR): $\tilde{\nu}$ = 2989 (w), 2208 (w), 1726 (m), 1698 (m), 1646 (w), 1614 (w), 1515 (s), 1472 (w), 1419 (s), 1398 (m), 1365 (w), 1334 (s), 1262 (s), 1229 (s), 1208 (m), 1169 (w), 1119 (m), 1101 (s), 1035 (m), 971 (w), 950 (w), 894 (m), 984 (w), 845 (w), 817 (w), 805 (w), 771 (w), 632 cm^{-1} (w); HR-ESI-MS m/z (%): 413.2183 (100, $[M + H]^+$, calcd for $C_{22}H_{29}N_4O_4$: 413.2183).

Diethyl 2-[4-Cyano-5-(dimethylamino)-3-(4-methoxyphenyl)-1*H*-pyrrol-2-yl]malonate (236)

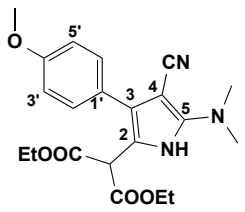

A mixture of **257** (90 mg, 0.25 mmol) and a 2.0 M THF solution of dimethylamine (253 μL, 0.51 mmol) in THF (2.5 mL) was subjected to General Procedure G. Flash column chromatography (SiO_2; EtOAc/cyclohexane 3:7) gave **236** (69 mg, 68%) as a yellow solid. R_f = 0.60 (SiO_2; EtOAc/cyclohexane 1:1); m.p. 108–110 °C; ^{1}H NMR (400 MHz, $CDCl_3$): δ = 1.28 (t, J = 7.1 Hz, 6 H; OCH_2CH_3), 3.12 (s, 6 H; Me_2N–C(5)), 3.83 (s, 3 H; OMe), 4.17–4.27 (m, 4 H; OCH_2CH_3), 4.68 (s, 1 H; H–C–C(2)), 6.96 (d, J = 8.8 Hz, 2 H; H–C(3',5')), 7.35 (d, J = 8.8 Hz, 2 H; H–C(2',6')), 8.30 ppm (br. s, 1 H; NH); ^{13}C NMR (100 MHz, $CDCl_3$): δ = 14.14 (2 C; OCH_2CH_3), 40.59 (2 C; Me_2N–C(5)), 48.72 (1 C, CH–C(2)), 55.43 (1 C, MeO), 62.55 (2 C; OCH_2CH_3), 73.19 (1 C, C(4)), 110.95 (1 C, C(2)), 114.27 (2 C, HC(3',5')), 119.19 (1 C, CN), 124.70 (1 C, C(1')), 125.87 (1 C, C(3)), 130.43 (2 C, HC(2',6')), 149.63 (1 C, C(5)), 159.16 (1 C, C(4')), 167.87 ppm (2 C, C=O); IR (ATR): $\tilde{\nu}$ = 3329 (br. w), 2982 (w), 2197 (m), 1731 (s), 1582 (s), 1513 (m), 1463 (m), 1420 (w), 1368 (w), 1289 (m),

1246 (s), 1177 (s), 1149 (m), 1113 (w), 1032 (m), 960 (w), 933 (w), 840 (w), 796 (w), 730 cm^{-1} (w); HR-ESI-MS *m/z* (%): 400.1867 (100, $[M + H]^+$, calcd for $C_{21}H_{26}N_3O_5$: 400.1867).

Diethyl 2-[4-Cyano-5-(dimethylamino)-3-octyl-1*H*-pyrrol-2-yl]malonate (237)

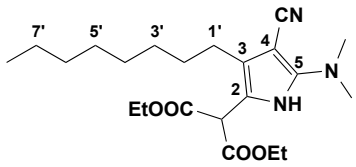

A mixture of **272** (100 mg, 0.28 mmol) and a 2.0 M THF solution of dimethylamine (277 μL, 0.55 mmol) in THF (2.8 mL) was subjected to General Procedure G. Flash column chromatography (SiO_2; EtOAc/cyclohexane 3:7) gave **237** (85 mg, 75%) as a clear, colorless oil. R_f = 0.59 (SiO_2; EtOAc/cyclohexane 1:1); ^{1}H NMR (400 MHz, $CDCl_3$): δ = 0.85-0.88 (m, 3 H; $H_3C(8')$), 1.25–1.32 (m, 16 H; OCH_2CH_3,$H_2C(3',4',5',6',7')$), 1.50–1.57 (m, 2 H; $H_2C(2')$), 2.39–2.42 (m, 2 H; $H_2C(1')$), 3.05 (s, 6 H; Me_2N–C(5)), 4.16–4.26 (m, 4 H; OCH_2CH_3), 4.59 (s, 1 H; H–C–C(2)), 8.15 ppm (br. s, 1 H; NH); ^{13}C NMR (100 MHz, $CDCl_3$): δ = 14.12 (2 C; OCH_2CH_3), 14.23 (1 C, $H_3C(8')$), 22.80 (1 C, $H_2C(7')$), 25.00 (1 C, $H_2C(6')$), 29.43 (1 C, $H_2C(5')$), 29.55 (1 C, $H_2C(4')$), 29.58 (1 C, $H_2C(3')$), 30.67 (1 C, $H_2C(2')$), 32.01 (1 C, $H_2C(1')$), 40.50 (2 C; Me_2N–C(5)), 48.37 (1 C, CH–C(2)), 62.42 (2 C; OCH_2CH_3), 73.01 (1 C, C(4)), 110.33 (1 C, C(2)), 119.14 (1 C, CN), 125.12 (1 C, C(3)), 149.21 (1 C, C(5)), 167.73 ppm (2 C, C=O); IR (ATR): $\tilde{\nu}$ = 3337 (br. w), 2927 (m), 2856 (w), 2197 (m), 1733 (s), 1582 (m), 1466 (m), 1368 (w), 1212 (m), 1144 (m), 1095 (w), 1027 (m), 932 (w), 915 (w), 860 (w), 732 (m), 647 cm^{-1} (w); HR-MALDI-MS (3-HPA) *m/z* (%): 406.2700 (100, $[M + H]^+$, calcd for $C_{22}H_{35}N_3O_4$: 406.2700).

Diethyl 2-(5-Amino-4-cyano-3-phenylthiophen-2-yl)malonate (238)

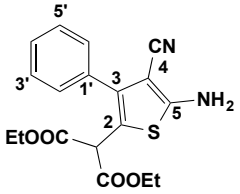

A mixture of **252** (32 mg, 0.10 mmol) and DABCO (11 mg, 0.10 mmol) in THF (1 mL) was treated with $Na_2S{\cdot}9H_2O$ (24 mg, 0.10 mmol) and heated at 65 °C for 20 min. The reaction was quenched with a saturated aqueous NH_4Cl solution (40

mL). The aqueous layer was extracted with CH_2Cl_2 (3 x 20 ml), dried ($MgSO_4$), filtered, and concentrated. Flash column chromatography (SiO_2; EtOAc/cyclohexane 1:9) gave **238** (160 mg, 71%) as a yellow solid. R_f = 0.39 (SiO_2; EtOAc/cyclohexane 1:1); m.p. 112–114 °C; ^{1}H NMR (400 MHz, $CDCl_3$): δ = 1.26 (t, J = 7.1 Hz, 6 H; OCH_2CH_3), 4.15–4.28 (m, 4 H; OCH_2CH_3), 4.79 (s, 1 H; H–C–C(2)), 4.88 (br. s, 2 H; NH_2), 7.34–7.49 ppm (m, *5* H; H–C(2', 3', 4',5',6',)); ^{13}C NMR (100 MHz, $CDCl_3$): δ = 14.12 (2 C; OCH_2CH_3), 51.32 (1 C, CH–C(2)), 62.53 (2 C; OCH_2CH_3), 89.98 (1 C, C(4)), 114.02 (1 C, CN), 115.32 (1 C, C(5)), 128.81 (1 C, C(4')), 128.98 (2 C, HC(2',6')), 129.34 (2 C, HC(3',5')), 132.95 (1 C, C(3)), 140.11 (1 C, C(2)), 162.79 (1 C, C(1')), 167.44 ppm (2 C, C=O); IR (ATR): $\tilde{\nu}$ = 2986 (w), 2228 (m), 1736 (m), 1667 (m), 1627 (w), 1596 (w), 1563 (s), 1449 (w), 1406 (w), 1382 (w), 1352 (w), 1320 (w), 1295 (w), 1249 (s), 1225 (s), 1182 (w), 1091 (w), 1007 (m), 912 (w), 868 (w), 580 (w), 768 (w), 730 (w), 689 (w), 647 (w), 610 cm^{-1} (w); HR-ESI-MS *m/z* (%): 376.1326 (100, $[M + NH_4]^+$, calcd for $C_{18}H_{21}N_3O_4S$: 376.1326).

Ethyl 2-{4-Cyano-5-[dimethylamino]-3-[4-(dimethylamino)phenyl]-1*H*-pyrrol-2-yl}acetate (239)

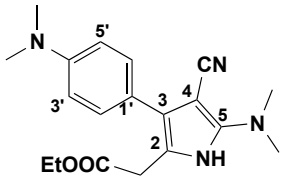

A mixture of **213** (30 mg, 0.07 mmol), LiCl (6 mg, 0.14 mmol) and H_2O (3 μL, 0.14 mmol) in Me_2SO (0.7 mL) was heated at 160 ºC under N_2 for 2 h. Flash column chromatography (SiO_2; EtOAc/cyclohexane 3:7) gave **239** (19 mg, 82%) as a colorless oil. R_f = 0.29 (SiO_2; EtOAc/cyclohexane 1:1); ^{1}H NMR (300 MHz, $CDCl_3$): δ = 1.28 (t, J = 7.1 Hz, 3 H; OCH_2CH_3), 2.97 (s, 6 H; Me_2N–C(4')), 3.08 (s, 6 H; Me_2N–C(5)), 3.59 (s, 2 H; H_2C–C(2)), 4.18 (q, J = 7.1 Hz, 2 H; OCH_2CH_3), 6.78 (d, J = 8.8 Hz, 2 H; H–C(3',5')), 7.26 (d, J = 8.8 Hz, 2 H; H–C(2',6')), 8.31 ppm (br. s, 1 H; NH); ^{13}C NMR (100 MHz, $CDCl_3$): δ = 14.29 (1 C; OCH_2CH_3), 31.27 (1 C, H_2C–C(2)), 40.72 (2 C; Me_2N–C(4')), 40.82 (2 C; Me_2N–C(5)), 61.53 (1 C; OCH_2CH_3), 72.97 (1 C, C(4)), 112.00 (1 C, C(2)), 112.74 (2 C, HC(3',5')), 119.61 (1 C, CN), 120.94 (1 C, C(1')), 123.98 (1 C, C(3)), 129.82 (2 C, HC(2',6')), 149.26 (1 C, C(5)), 149.72 (1 C, C(4')), 171.76 ppm (1 C, C=O); IR (ATR): $\tilde{\nu}$ = 3278 (br. w), 2804 (w), 2192 (s), 1731 (s), 1586 (s), 1523 (s), 1445 (w), 1411 (w), 1345 (m), 1271 (w), 1197

(m), 1166 (m), 1034 (w), 945 (w), 878 (w), 829 (w), 790 (w), 746 (w), 638 cm^{-1} (w); HR-MALDI-MS (DCTB) *m/z* (%): 357.1921 (100, $[M + OH]^+$), 339.1815 (23, $[M + OH]^+$), calcd for $C_{19}H_{23}N_4O_2$: 339.1816).

Diethyl 6-Cyano-5-[dimethylamino]-7-[4-(dimethylamino)phenyl]-2,3-dihydro-1*H*-pyrrolizine-1,1-dicarboxylate (240)

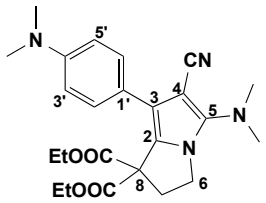

A mixture of **213** (40 mg, 0.10 mmol), 1,2-dibromoethane (16 μL, 0.19 mmol), and K_2CO_3 (27 mg, 0.19 mmol) in DMF (1 mL) was heated at 80 ºC under N_2 for 12 h. Flash column chromatography (SiO_2; EtOAc/cyclohexane 3:7) gave **240** (36 mg, 85%) as a pale yellow oil. R_f = 0.46 (SiO_2; EtOAc/cyclohexane 1:1); ^{1}H NMR (400 MHz, $CDCl_3$): δ = 1.08 (t, J = 7.1 Hz, 6 H; OCH_2CH_3), 2.93 (s, 6 H; Me_2N–C(4')), 2.96 (s, 6 H; Me_2N–C(5)), 3.06 (dd, J = 7.1, 6.4 Hz, 2 H; $H_2C(7)$), 3.88 (dd, J = 7.1, 6.4 Hz, 2 H; $H_2C(6)$), 3.96–4.14 (m, 4 H; OCH_2CH_3), 6.70 (d, J = 8.9 Hz, 2 H; H–C(3',5')), 7.39 ppm (d, J = 8.9 Hz, 2 H; H–C(2',6')); ^{13}C NMR (100 MHz, $CDCl_3$): δ = 13.80 (2 C; OCH_2CH_3), 39.12 (1 C, $H_2C(7)$), 40.83 (2 C; Me_2N–C(4')), 42.84 (2 C; Me_2N–C(5)), 43.77 (1 C, $H_2C(6)$), 59.32 (1 C, C(8)), 62.32 (2 C; OCH_2CH_3), 82.61 (1 C, C(4)), 112.45 (2 C, HC(3',5')), 118.30 (1 C, CN), 121.27 (1 C, C(2)), 121.49 (1 C, C(1')), 123.03 (1 C, C(3)), 129.55 (2 C, HC(2',6')), 146.18 (1 C, C(5)), 149.79 (1 C, C(4')), 169.24 ppm (2 C, C=O); IR (ATR): $\tilde{\nu}$ = 2981 (w), 2802 (w), 2203 (m), 1727 (s), 1615 (m), 1517 (m), 1446 (m), 1427 (m), 1366 (m), 1263 (m), 1218 (m), 1194 (m), 1141 (m), 1097 (m), 1059 (m), 1035 (m), 1017 (m), 944 (m), 912 (m), 859 (w), 823 (m), 768 (w), 728 (s), 647 cm^{-1} (w); HR-MALDI-MS (DCTB) *m/z* (%): 438.2262 (100, $[M]^+$, calcd for $C_{24}H_{30}N_4O_4$: 438.2262).

Diethyl 2-{4-Cyano-5-[dimethylamino]-3-[4-(phenylethynyl)phenyl]-1*H*-pyrrol-2-yl)malonate (241)

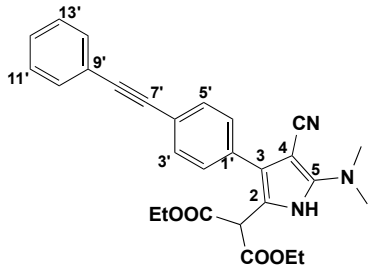

A solution of **230** (70 mg, 0.14 mmol) in 1:1 THF and diisopropylamine (1.4 mL) was degassed with bubbling argon for 30 min, treated with phenylacetylene (31 μL, 0.28 mmol), [$PdCl_2(PPh_3)_2$] (19 mg, 0.03 mmol), and CuI (5 mg, 0.03 mmol), and stirred for 1 h at 24 ºC. Evaporation and flash column chromatography (SiO_2; EtOAc/cyclohexane 3:7) gave **241** (34 mg, 52%) as a yellow oil. R_f = 0.70 (SiO_2; EtOAc/cyclohexane 1:1); ^{1}H NMR (400 MHz, $CDCl_3$): δ = 1.28 (t, J = 7.1 Hz, 6 H; OCH_2CH_3), 3.13 (s, 6 H; Me_2N–C(5)), 4.18–4.28 (m, 4 H; OCH_2CH_3), 4.70 (s, 1 H; H–C–C(2)), 7.32–7.38 (m, 3 H; H–C(11',12',13')), 7.43 (d, J = 8.5 Hz, 2 H; H–C(4',6')), 7.53–7.55 (m, 2 H; H–C(10',14')), 7.59 (d, J = 8.5 Hz, 2 H; H–C(3',5')), 8.44 ppm (br. s, 1 H; NH); ^{13}C NMR (100 MHz, $CDCl_3$): δ = 14.09 (2 C; OCH_2CH_3), 40.51 (2 C; Me_2N–C(5)), 48.66 (1 C, CH–C(2)), 62.64 (2 C; OCH_2CH_3), 72.66 (1 C, C(4)), 89.39 (1 C, C(7' or 8')), 90.07 (1 C, C(7' or 8')), 111.62 (1 C, C(2)), 118.88 (1 C, CN), 122.38 (1 C, C(1')), 123.41 (1 C, C(9')), 125.41 (1 C, C(3)), 128.35 (1 C, HC(12'), 128.44 (2 C, HC(11',13'), 128.73 (1 C, C(4')), 129.12 (2 C, HC(2',6'), 131.72 (2 C, HC(10',14'), 131.98 (2 C, HC(3',5'), 149.85 (1 C, C(5)), 167.64 ppm (2 C, C=O); IR (ATR): $\tilde{\nu}$ = 3278 (br. w), 2982 (w), 2198 (m), 1732 (s), 1594 (s), 1512 (w), 1463 (m), 1443 (m), 1368 (w), 1297 (m), 1229 (m), 1229 (m), 1178 (m), 1149 (m), 1095 (w), 1070 (w), 1031 (m), 961 (w), 850 (w), 757 (m), 732 (w), 691 cm^{-1} (w); HR-MALDI-MS (DCTB) m/z (%): 469.1997 (30, $[M]^+$, calcd for $C_{28}H_{27}N_3O_4$: 469.1996), 468.1917 (100, $[M - H]^+$).

Diethyl 2-{4-Cyano-3-[4-(dimethylamino)phenyl]-5-morpholino-2*H*-pyrrol-2-ylidene}malonate (248)

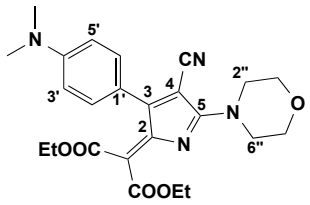

A mixture of **222** (51 mg, 0.14 mmol) and morpholine (24 μL, 0.28 mmol) in THF (1.4 mL) was subjected to General Procedure A. Flash column chromatography (SiO_2; EtOAc/cyclohexane 3:7) then exposure to air gave **248** (25 mg, 39%) as a yellow solid. R_f = 0.43 (SiO_2; EtOAc/cyclohexane 1:1); m.p. 67–68 °C; ^{1}H NMR (400 MHz, CD_2Cl_2): δ = 1.08 (t, J = 7.1 Hz, 3 H; *trans*-OCH_2CH_3), 1.30 (t, J = 7.1 Hz, 3 H; *cis*-OCH_2CH_3), 3.11 (s, 6 H; Me_2N–C(4')), 3.14–3.20 (m, 2 H; H_{ax}–C(2",6")), 3.26–3.32 (m, 2 H; H_{eq}–C(2",6")), 3.61–3.73 (m, 4 H; H_2C(3",5")), 3.92 (q, J = 7.1 Hz, 2 H; *trans*-OCH_2CH_3), 4.24 (q, J = 7.1 Hz, 2 H; *cis*-OCH_2CH_3), 6.71 (d, J = 9.4 Hz, 2 H; H–C(3',5')), 7.79 ppm (d, J = 9.4 Hz, 2 H; H–C(2',6')); ^{13}C NMR (100 MHz, CD_2Cl_2): δ = 14.32 (1 C; *trans*-OCH_2CH_3), 14.55 (1 C; *cis*-OCH_2CH_3), 40.45 (2 C; Me_2N–C(4')), 51.18 (2 C, H_2C(2",6")), 61.02 (1 C; *trans*-OCH_2CH_3), 61.76 (1 C; *cis*-OCH_2CH_3), 66.22 (2 C, H_2C(3",5")), 75.46 (1 C, C(4)), 102.45 (1 C, *C*–C(2)), 112.01 (2 C, HC(3',5')), 115.29 (1 C, CN), 115.92 (1 C, C(2)), 120.01, (1 C, C(1')), 133.11 (2 C, HC(3',5')), 154.56 (1 C, C(4')), 159.14 (1 C, C(5)), 166.16 (1 C, *trans*-C=O), 166.6 (1 C, *cis*-C=O), 166.99 ppm (1 C, C(3)); IR (ATR): $\tilde{\nu}$ = 2927 (w), 2215 (m), 1687 (m), 1604 (s), 1541 (m), 1497 (s), 1440 (m), 1381 (m), 1334 (m), 1291 (m), 1210 (s), 1174 (s), 1118 (m), 1092 (m), 1061 (m), 1032 (w), 822 (w), 734 cm^{-1} (w); HR-MALDI-MS (DCTB) *m*/*z* (%): 452.2054 (100, $[M]^+$, calcd for $C_{24}H_{28}N_4O_5$: 452.2054).

5-[Dimethylamino]-3-[4-(dimethylamino)phenyl]-2-oxo-2*H*-pyrrole-4-carbo nitrile (249)

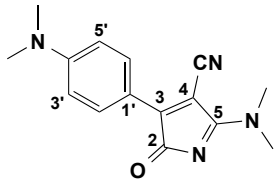

A mixture of **213** (450 mg, 1.09 mmol) in dichloromethane (10 mL) was treated with PCC (705 mg, 3.27 mmol), stirred for 30 min, diluted with a saturated aqueous solution of $NaHCO_3$ (20 mL), and the separated aqueous phase extracted with dichloromethane (3 x 20 mL). The combined organic phases were dried ($MgSO_4$), filtered, and concentrated. Flash column chromatography (SiO_2; MeOH/dichloromethane 1:9) gave **249** (123 mg, 42%) as a purple solid. R_f = 0.58 (SiO_2; MeOH/dichloromethane 1:9); m.p. 255–256 °C; ^{1}H NMR (400 MHz, $CDCl_3$): δ = 3.13 (s, 6 H; Me_2N–C(4')), 3.46 (s, 3 H; MeN–C(5)), 3.65 (s, 3 H; MeN–C(5)), 6.72 (d, J = 9.3 Hz, 2 H; H–C(3',5')), 8.47 ppm (d, J = 9.3 Hz, 2 H; H–C(2',6')); ^{13}C NMR (100 MHz, $CDCl_3$): δ = 39.55 (1 C; *Me*N–C(5)), 40.17 (2 C; *Me*$_2$N–C(4')), 42.20 (1 C; *Me*N–C(5)), 94.40 (1 C, C(4)), 111.92 (2 C, HC(3',5')), 117.04 (1 C, C(1')), 117.93 (1 C, CN), 133.77 (2 C, HC(3',5')), 153.67 (1 C, C(4')), 156.09 (1 C, C(3)), 173.42 (1 C, C(5)), 181.14 ppm (1 C, C(2)); IR (ATR): $\tilde{\nu}$ = 2925 (w), 2200 (w), 1698 (w), 1598 (s), 1567 (m), 1519 (m), 1442 (w), 1364 (s), 1299 (w), 1267 (m), 1210 (m), 1168 (m), 1120 (w), 1059 (w), 929 (w), 821 (w), 791 (w), 750 (w), 721 (w), 631 cm^{-1} (w); UV/Vis ($CHCl_3$): λ_{max} (ε) = 545 (18700), 430 (5600), 406 (8100), 388 (7900), 285 (9500 M^{-1}cm^{-1}); HR-MALDI-MS (3-HPA) *m/z* (%): 269.1397 (100, $[M + H]^+$, calcd for $C_{15}H_{17}N_4O$: 269.1397); C 67.05, H 6.01, N 20.63, calcd for $C_{15}H_{16}N_4O$: C 67.15, H 6.01, N 20.88.

5-[Dimethylamino]-3-[4-(dimethylamino)phenyl]-2-oxo-2*H*-pyrrole-4-carbonitrile 2,2,2-Trifluoroacetate (250)

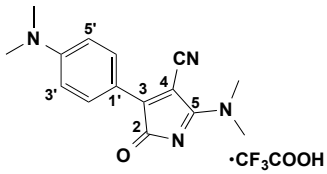

A mixture of **249** (50 mg, 0.19 mmol) in dichloromethane (5 mL) was treated with trifluoroacetic acid (17 μL, 0.22 mmol) and the solvent removed to give **250** (71 mg, 100%) as a blue solid. m.p. 130–131 °C; ^{1}H NMR (400 MHz, $CDCl_3$): δ = 3.32 (s, 6 H; Me_2N–C(4')), 3.62 (br. s, 3 H; MeN–C(5)), 3.83 (br. s, 3 H; MeN–C(5)), 6.84 (d, J = 7.7 Hz, 2 H; H–C(3',5')), 8.62 ppm (d, J = 7.7 Hz, 2 H; H–C(2',6')); ^{13}C NMR (100 MHz, $CDCl_3$): δ = 40.94 (2 C; *Me*$_2$N–C(4')), 42.04 (1 C; *Me*N–C(5)), 45.02 (1 C; *Me*N–C(5)), 84.77 (1 C, C(4)), 113.96 (2 C, HC(3',5')), 117.54 (1 C, C(1')), 115.96 (1 C, CN), 135.68 (2 C, HC(3',5')), 147.35 (1 C, C(3 or 5)), 156.31 (1 C, C(4')), 161.91 (1 C, C(3 or 5)), 166.89 ppm (1 C, C(2)), (CF_3COO^- peaks not observed); ^{19}F NMR (376 MHz, $CDCl_3$): δ = –75.87 ppm (s); IR (ATR): $\tilde{\nu}$ = 2917 (w), 2849 (w), 2204 (w), 1740 (m), 1663 (m), 1605 (s), 1561 (w), 1519 (m), 1505 (w), 1470 (w), 1390 (s), 1359 (s), 1302 (w), 1131 (br. s), 981 (m), 937 (w), 924 (w), 836 (m), 815 (s), 797 (m), 745 (w), 716 (m), 707 (m), 624 cm^{-1} (w); UV/Vis ($CHCl_3$): λ_{max} (ε) = 638 (40500), 599 (32500), 299 (10000 M^{-1}cm^{-1}); HR-MALDI-MS (DCTB) *m*/*z* (%): 269.1397 (100, [M – CF_3COO^-]$^+$, calcd for $C_{15}H_{17}N_4O$: 269.1397).

Ethyl 2-(2,2-Dicyano-1-ethoxyvinyl)-4-oxo-4-phenylbut-2-enoate (252)

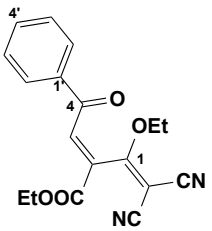

A solution of phenylacetylene (**251**) (50 mg, 0.5 mmol) in $(CH_2Cl)_2$ (10 mL) was treated with alkene **162** (110 mg, 0.5 mmol) and stirred for 58 h at reflux. Evaporation and flash column chromatography (SiO_2; EtOAc/cyclohexane 3:7 v/v) gave **252** (101 mg, 62%) as a pale yellow solid. R_f = 0.27 (SiO_2; EtOAc/cyclohexane 3:7); m.p. 100–102 °C; ^{1}H NMR (400 MHz, $CDCl_3$): δ = 1.40 (t, J = 7.1 Hz, 3 H;

$CO_2CH_2CH_3$), 1.49 (t, J = 7.1 Hz, 3 H; OCH_2CH_3), 4.31 (q, J = 7.1 Hz, 2 H; $CO_2CH_2CH_3$), 4.43 (q, J = 7.1 Hz, 2 H; OCH_2CH_3), 7.54–7.58 (m, 2 H; H–C(3',5')), 7.69 (tt, J = 8.0, 1.3 Hz, 1 H; H–C(4')), 7.98–8.10 (m, 2 H; H–C(2',6')) 8.30 ppm (s, 1 H; H–C(3)); ^{13}C NMR (100 MHz, $CDCl_3$): δ = 14.24 (1 C, $CO_2CH_2CH_3$), 14.82 (1 C, OCH_2CH_3), 63.78 (1 C, $CO_2CH_2CH_3$), 66.70 (1 C, C=$C(CN)_2$), 70.59 (1 C, OCH_2CH_3), 110.11 and 112.59 (2 C, 2 CN), 129.34 (2 C, C(2',6')), 129.42 (2 C, C(3',5')), 133.24 (1 C, C(1')), 135.10 (1 C, C(2)), 135.38 (1 C, C(4')), 142.01 (1 C, C(3)), 161.31 (1 C, CO_2), 180.49 (1 C, C(4)=O), 188.52 ppm (1 C, C(1)); IR (ATR): $\tilde{\nu}$ = 2986 (w), 2228 (m), 1736 (m), 1667 (m), 1627 (w), 1596 (w), 1563 (s), 1449 (w), 1406 (w), 1382 (w), 1352 (w), 1320 (w), 1295 (w), 1249 (s), 1225 (s), 1182 (w), 1091 (w), 1007 (m), 912 (w), 868 (w), 580 (w), 768 (w), 730 (w), 689 (w), 647 (w), 610 cm^{-1} (w); UV/Vis ($CHCl_3$): λ_{max} (ε) = 340 (8000), 261 nm (15900 $M^{-1}cm^{-1}$); HR-ESI-MS m/z (%): 342.1454 (100, $[M + NH_4]^+$ calcd for $C_{18}H_{20}N_3O_4$: 342.1448).

2-Phenylbuta-1,3-diene-1,1,4,4-tetracarbonitrile (253)[175]

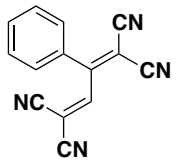

A solution of phenylacetylene (**251**) (50 mg, 0.5 mmol) in $(CH_2Cl)_2$ (5 mL) was treated with alkene **90** (110 mg, 0.5 mmol) and stirred for 58 h at reflux. Evaporation and flash column chromatography (SiO_2; EtOAc/cyclohexane 3:7 v/v) gave **253** (100 mg, 10%) as a pale red solid. Analytical data matched those of the literature.[175]

Ethyl 2-(2,2-Dicyano-1-ethoxyvinyl)-4-(naphthalen-1-yl)-4-oxobut-2-enoate (255)

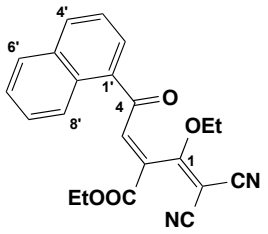

A solution of 1-ethynylnaphthalene (76 mg, 0.5 mmol) in $(CH_2Cl)_2$ (5 mL) was treated with alkene **162** (110 mg, 0.5 mmol) and stirred for 56 h at reflux. Evaporation and flash column chromatography (SiO_2; EtOAc/cyclohexane 1:1 v/v) gave **255** (125 mg, 67%) as a yellow solid. R_f = 0.18 (SiO_2; EtOAc/cyclohexane 3:7); m.p. 112–114 °C; ^{1}H NMR (400 MHz, $CDCl_3$): δ = 1.41 (t, J = 7.1 Hz, 3 H; $CO_2CH_2CH_3$), 1.53 (t, J = 7.1 Hz, 3 H; OCH_2CH_3), 4.36–4.47 (m, 4 H; 2 OCH_2CH_3); 7.58–7.64 (m, 2 H; H–C(7',8')), 7.69–7.73 (m, 1 H; H–C(3')), 7.94 (m, 1 H; H–C(6')), 8.09 (d, J = 8 Hz, 1 H; H–C(2')), 8.15 (d, J = 8.0 Hz, 1 H; H–C(4')), 8.31 (s, 1 H; H–C(3)), 8.84 ppm (d, J = 8.0 Hz, 1 H; H–C(9')); ^{13}C NMR (100 MHz, $CDCl_3$): δ = 14.27 (1 C, $CO_2CH_2CH_3$), 14.88 (1 C, OCH_2CH_3), 63.73 (1 C, $CO_2CH_2CH_3$), 66.72 (1 C, $C=C(CN)_2$), 70.62 (1 C, OCH_2CH_3), 110.87 and 112.81 (2 C, 2 CN), 124.64 (1 C, C(9')), 125.58 (1 C, C(7')), 127.38 (1 C, C(3')), 129.08 (1 C, C(10')), 129.59 (1 C, C(2')), 130.21 (1 C, C(6 ')), 130.54 (1 C, C(8')), 131.83 (1 C, C(5')), 132.57 (1 C, C(3)), 134.15 (1 C, C(4')), 136.14 (1 C, C(1')), 145.05 (1 C, C(2)), 161.47 (1 C, CO_2), 180.69 (1 C, C(4)=O), 190.61 ppm (1 C, C(1)); IR (ATR): $\tilde{\nu}$ = 2988 (w), 2227 (m), 1725 (s), 1661 (m), 1598 (s), 1563 (s), 1511 (w), 1424 (w), 1380 (w), 1349 (w), 1310 (w), 1295 (w), 1253 (s), 1224 (s), 1176 (s), 1092 (w), 1010 (s), 869 (w), 845 (s), 817 (w), 773 (w), 756 (w), 718 (w), 685 (w), 634 cm^{-1} (w); UV/Vis ($CHCl_3$): λ_{max} (ε) = 338 (7900), 260 nm (16800 м$^{-1}$см$^{-1}$); HR-ESI-MS m/z (%):392.1601 (100, [M + NH_4]$^+$ calcd for $C_{22}H_{22}N_3O_4^+$: 392.1605).

Ethyl 4-[(1,1'-Biphenyl)-4-yl]-2-(2,2-dicyano-1-ethoxyvinyl)-4-oxobut-2-enoate (256)

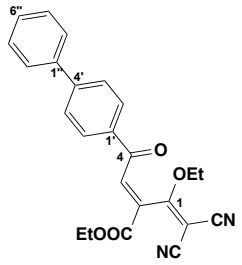

A solution of 4-ethynyl-1,1'-biphenyl (89 mg, 0.5 mmol) in $(CH_2Cl)_2$ (5 mL) was treated with alkene **162** (110 mg, 0.5 mmol) and stirred for 56 h at reflux. Evaporation and flash column chromatography (SiO_2; EtOAc/cyclohexane 1:1 v/v) gave **256** (146 mg, 73%) as a yellow solid. R_f = 0.26 (SiO_2; EtOAc/cyclohexane 3:7); m.p. 115–118 °C; ^{1}H NMR (400 MHz, CD_2Cl_2): δ = 1.40 (t, J = 7.1 Hz, 3 H; $CO_2CH_2CH_3$), 1.49 (t, J = 8.0 Hz, 3 H; OCH_2CH_3), 4.32 (q, J = 8.0 Hz, 2 H; $CO_2CH_2CH_3$), 4.43 (q, J = 8.0, 4.0 Hz, 2 H; OCH_2CH_3), 7.42–7.46 (m, 1 H; H–C(6'')), 7.46–7.49 (d, J = 8.0 Hz, 2 H; H–C(3'',5'')), 7.69 (d, J = 8.0 Hz, 2 H; H–C(2'',6'')), 7.82 (d, J = 8.0 Hz, 2 H; H–C(3',5')), 8.11 (d, J = 8.0 Hz, 2 H; H–C(2',6')), 8.38 (s, 1 H; H–C(3)); ^{13}C NMR (100 MHz, CD_2Cl_2): δ = 14.44 (1 C, $CO_2CH_2CH_3$), 15.08 (1 C, OCH_2CH_3), 64.24 (1 C, $CO_2CH_2CH_3$), 66.85 (1 C, $C{=}C(CN)_2$), 71.21 (1 C, OCH_2CH_3), 111.41 and 113.07 (2 C, 2 CN), 127.90 (2 C, C(3',5')), 128.31 (2 C, C(3'',5'')), 129.34 (1 C, C(6'')), 129.62 (2 C, C(2',6')), 130.36 (2 C, C(2'',6'')), 133.62 (1 C, C(1'')), 134.43 (1 C, C(1')), 139.80 (1 C, C(6)'), 142.15 (1 C, C(3)), 148.31 (1 C, C(2)), 161.81 (1 C, CO_2), 181.34 (1 C, C(4)=O), 188.32 ppm (1 C, C(1)); IR (ATR): $\tilde{\nu}$ = 2985 (w), 2228 (m), 1732 (m), 1667 (m), 1625 (w), 1596 (w), 1563 (s), 1449 (w), 1406 (w), 1382 (w), 1352 (w), 1320 (w), 1295 (w), 1249 (s), 1225 (s), 1181 (w), 1091 (w), 1007 (m), 912 (w), 868 (w), 580 (w), 768 (w), 732 (w), 689 (w), 647 (w), 632 cm^{-1} (w); UV/Vis ($CHCl_3$): λ_{max} (ε) = 342 (8100), 260 nm (16200 м$^{-1}$cm^{-1}); HR-ESI-MS m/z (%): 423.1313 (100, [M + Na]$^+$ calcd for $C_{24}H_{20}N_2NaO_4^+$: 423.1315).

Ethyl 2-(2,2-Dicyano-1-ethoxyvinyl)-4-(4-methoxyphenyl)-4-oxobut-2-enoate (257)

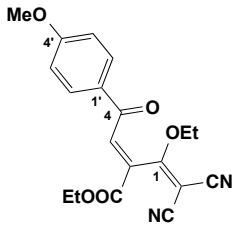

A solution of 4-ethynylanisole (65 mg, 0.5 mmol) in $(CH_2Cl)_2$ (5 mL) was treated with alkene **162** (110 mg, 0.5 mmol) and stirred for 56 h at reflux. Evaporation and flash column chromatography (SiO_2; EtOAc/cyclohexane 1:1 v/v) gave **257** (132 mg, 75%) as a yellow solid. R_f = 0.12 (SiO_2; EtOAc/cyclohexane 3:7); m.p. 96–98 °C; ^{1}H NMR (400 MHz, $CDCl_3$): δ = 1.40 (t, J = 7.1 Hz, 3 H; $CO_2CH_2CH_3$), 1.48 (t, J = 7.1 Hz, 3 H; OCH_2CH_3), 3.91 (s, 3 H, OMe), 4.29 (q, J = 7.1 Hz, 2 H; $CO_2CH_2CH_3$), 4.42 (q, J = 7.1 Hz, 2 H; OCH_2CH_3), 7.01 (d, J = 9.0 Hz, 2 H; H–C(3',5')), 7.98 (d, J = 9.0 Hz, 2 H; H–C(2',6')), 8.29 ppm (s, 1 H; H–C(3)); ^{13}C NMR (100 MHz, $CDCl_3$): δ = 14.24 (1 C, $CO_2CH_2CH_3$), 14.80 (1 C, OCH_2CH_3), 55.87 (1 C, OMe), 63.64 (1 C, $CO_2CH_2CH_3$), 66.53 (1 C, $C=C(CN)_2$)), 70.51 (1 C, OCH_2CH_3), 110.97 and 112.70 (2 C, 2 CN), 114.73 (2 C, C(3',5')), 128.30 (1 C, C(1')), 131.96 (2 C, C(2',6')), 132.48 (1 C, C(2)), 142.57 (1 C, C(3)), 161.45 (1 C, C(4')), 165.44 (1 C, CO_2), 180.91 (1 C, C(4)=O), 186.48 ppm (1 C, C(1)); IR (ATR): $\tilde{\nu}$ = 2988 (w), 2227 (m), 1725 (s), 1661 (m), 1598 (s), 1563 (s), 1511 (w), 1424 (w), 1380 (w), 1349 (w), 1310 (w), 1295 (w), 1253 (s), 1224 (s), 1176 (s), 1092 (w), 1010 (s), 869 (w), 845 (s), 817 (w), 773 (w), 756 (w), 718 (w), 685 (w), 634 cm^{-1} (w); UV/Vis ($CHCl_3$): λ_{max} (ε) = 339 nm (8700 M^{-1}cm^{-1}); HR-MALDI-MS (DCTB) m/z (%): 354.1216 (100, $[M + Na]^+$), 355.1289 (20, $[M + H]^+$), 354.1210, (70, $[M]^+$, calcd for $C_{19}H_{18}N_2O_5$: 354.1210).

Ethyl 2-(2,2-Dicyano-1-ethoxyvinyl)-4-(1*H*-indol-5-yl)-4-oxobut-2-enoate (258)

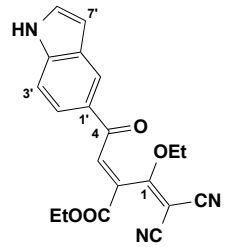

A solution of 5-ethynyl-1*H*-indole (72 mg, 0.5 mmol) in $(CH_2Cl)_2$ (5 mL) was treated with alkene **162** (110 mg, 0.5 mmol) and stirred for 56 h at reflux. Evaporation and flash column chromatography (SiO_2; EtOAc/cyclohexane 1:1 v/v) gave **258** (147 mg, 81%) as a yellow solid. R_f = 0.19 (SiO_2; EtOAc/cyclohexane 3:7); m.p. 115–120 °C; ^{1}H NMR (400 MHz, CD_2Cl_2): δ = 1.40 (t, J = 7.1 Hz, 3 H; $CO_2CH_2CH_3$), 1.47 (t, J = 8 Hz, 3 H; OCH_2CH_3), 4.32 (q, J = 8 Hz, 2 H; $CO_2CH_2CH_3$), 4.46 (q, J = 8 Hz, 2 H; OCH_2CH_3), 6.74–6.75 (m, 1 H; H–C(7')), 7.37–7.38 (m, 1 H; H–C(6')), 7.54 (d, J = 8 Hz, 1 H; H–C(3')), 7.89 (dd, J = 8 Hz, 1 Hz, 1 H; H–C(2')), 8.39–8.40 (m, 1 H; H–C(9')), 8.49 (s, 1 H; H–C(3)), 8.46–8.73 ppm (br, 1 H); m.p. 120–122 °C; ^{13}C NMR (100 MHz, CD_2Cl_2): δ =14.46 (1 C, $CO_2CH_2CH_3$), 15.06 (1 C, OCH_2CH_3), 64.05 (1 C, $CO_2CH_2CH_3$), 66.60 (1 C, C=$C(CN)_2$)), 71.07 (1 C, OCH_2CH_3), 105.18 (1 C, C(7')), 111.61 (1 C, CN) , 112.56 (1 C, C(3')), 113.18 (1 C, CN), 122.23 (1 C, C(2')), 125.11 (1 C, C(9')), 127.29 (1 C, C(6')), 128.33 (1 C, C(8')), 128.61 (1 C, C(1')), 132.50 (1 C, C(3)), 140.07 (1 C, C(4')), 143.37 (1 C, C(2)), 162.07 (1 C, CO_2), 182.01 (1 C, C(4)=O), 188.16 ppm (1 C, C(1)); IR (ATR): $\tilde{\nu}$ = 3100 (s), 2988 (w), 2227 (m), 1725 (s), 1661 (m), 1598 (s), 1563 (s), 1511 (w), 1424 (w), 1380 (w), 1349 (w), 1310 (w), 1295 (w), 1253 (s), 1224 (s), 1176 (s), 1092 (w), 1010 (s), 869 (w), 845 (s), 817 (w), 773 (w), 756 (w), 718 (w), 685 (w), 634 cm^{-1} (w); UV/Vis ($CHCl_3$): λ_{max} (ε) = 346 nm (8900 M^{-1}cm^{-1}); HR-ESI-MS m/z (%): 386.1111 (100, $[M + Na]^+$ calcd for $C_{20}H_{17}N_3NaO_4^+$: 386.1111).

Ethyl 4-(Benzofuran-5-yl)-2-(2,2-dicyano-1-ethoxyvinyl)-4-oxobut-2-enoate (259)

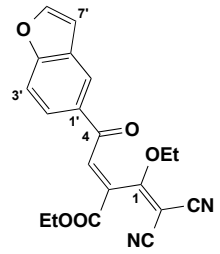

A solution of 5-ethynylbenzofuran (71 mg, 0.5 mmol) in $(CH_2Cl)_2$ (5 mL) was treated with alkene **162** (110 mg, 0.5 mmol) and stirred for 56 h at reflux. Evaporation and flash column chromatography (SiO_2; EtOAc/cyclohexane 1:1 v/v) gave **259** (144 mg, 79%) as a yellow solid. R_f = 0.21 (SiO_2; EtOAc/cyclohexane 3:7); m.p. 118–120 °C; ^{1}H NMR (400 MHz, CD_2Cl_2): δ = 1.44 (t, J = 7.1 Hz, 3 H; $CO_2CH_2CH_3$), 1.52 (t, J = 8 Hz, 3 H; OCH_2CH_3), 4.36 (q, J = 8 H, 2 H; $CO_2CH_2CH_3$), 4.47 (q, J = 8 Hz, 2 H; OCH_2CH_3), 6.99–7.00 (dd, J = 8, 1 Hz, 1 H; H–C(7')), 7.70 (d, J = 8 Hz, 1 H; H–C(6')), 7.83 (d, J = 8 Hz, 1 H; H–C(3')), 8.06 (d,d, J = 8, 1 Hz, 1 H; H–C(2')), 8.39 (d, J = 1 Hz, 1 H; H–C(9')), 8.47 (s, 1 H, H–C(4)) ; ^{13}C NMR (100 MHz, CD_2Cl_2): 14.44 (1 C, $CO_2CH_2CH_3$), 15.07 (1 C, OCH_2CH_3), 64.21 (1 C, $CO_2CH_2CH_3$), 66.84 (1 C, C=$C(CN)_2$), 71.21 (1 C, OCH_2CH_3), 107.92 (1 C, C(7')), 111.42 (1 C, CN), 112.92 (1 C, C(3')), 113.08 (1 C, CN), 124.57 (1 C, C(2')), 126.25 (1 C, C(9')), 128.76 (1 C, C(6')), 131.32 (1 C, C(8')), 133.30 (1 C, C(4')), 142.74 (1 C, C(1')), 147.90 (1 C, C(3)), 159.10 (1 C, C(2)), 161.85 (1 C, CO_2), 181.39 (1 C, C(4)=O), 188.32 ppm (1 C, C(1)); IR (ATR): $\tilde{\nu}$ = 2988 (w), 2227 (m), 1725 (s), 1661 (m), 1598 (s), 1563 (s), 1511 (w), 1424 (w), 1380 (w), 1349 (w), 1310 (w), 1295 (w), 1253 (s), 1224 (s), 1176 (s), 1092 (w), 1010 (s), 869 (w), 845 (s), 817 (w), 773 (w), 756 (w), 718 (w), 685 (w), 634 cm^{-1} (w); UV/Vis ($CHCl_3$): λ_{max} (ε) = 343 nm (8800 M^{-1} cm^{-1}); HR-ESI-MS m/z (%): 387.0950 (100, $[M + Na]^+$ calcd for $C_{20}H_{16}N_2NaO_5^+$: 387.0951).

Ethyl 2-(2,2-Dicyano-1-ethoxyvinyl)-4-oxo-4-(thioen-3-yl)but-2-enoate (260)

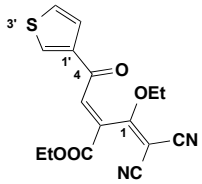

A solution of 3-ethynylthiophene (54 mg, 0.5 mmol) in $(CH_2Cl)_2$ (5 mL) was treated with alkene **162** (110 mg, 0.5 mmol) and stirred for 56 h at reflux. Evaporation and flash column chromatography (SiO_2; EtOAc/cyclohexane 1:1 v/v) gave **260** (120 mg, 73%) as a yellow solid. $R_f = 0.21$ (SiO_2; EtOAc/cyclohexane 3:7); m.p. 94–96 °C; ^{1}H NMR (400 MHz, $CDCl_3$): δ = 1.39 (t, J = 7.1 Hz, 3 H; $CO_2CH_2CH_3$), 1.47 (t, J = 8.0 Hz, 3 H; OCH_2CH_3), 4.26 (q, J = 8.0.0 H, 2 H; $CO_2CH_2CH_3$), 4.42 (q, J = 8.0 Hz, 2 H; OCH_2CH_3), 7.42–7.44 (d,d J = 8.0, 1.0 Hz, 1 H; H–C(5')), 7.62 (d,d, J = 8, 1 Hz, 1 H; H–C(4')), 8.13 (s, 1 H; H–C(3)), 8.28–8.30 ppm (m, 1 H; H–C(2')); ^{13}C NMR (100 MHz, $CDCl_3$): δ = 14.11 (1 C, $CO_2CH_2CH_3$), 14.70 (1 C, OCH_2CH_3), 63.68 (1 C, $CO_2CH_2CH_3$), 66.40 (1 C, $C{=}C(CN)_2$), 70.38 (1 C, OCH_2CH_3), 110.80 and 112.54 (2 C, 2 CN), 126.91 (1 C, C(4')), 127.96 (1 C, C(5')), 132.98 (1 C, C(3)), 135.99 (1 C, C(2')), 140.59 (1 C, C(1')), 141.13 (1 C, C(2)), 161.21 (1 C, CO_2), 180.46 (1 C, C(4)=O), 181.17 (1 C, C(1)) ppm; IR (ATR): $\tilde{\nu}$ = 2986 (w), 2229 (w), 1731 (m), 1668 (m), 1596 (w), 1560 (m), 1449 (w), 1377 (w), 1329 (m), 1234 (s), 1186 (m), 1096 (w), 1059 (w), 1001 (w), 974 (w), 910 (w), 849 (w), 799 (w), 714 (m), 688 (w), 646 cm^{-1} (w); UV/Vis ($CHCl_3$): λ_{max} (ε) = 329 nm (7700 M^{-1}cm^{-1}); HR-ESI-MS m/z (%):353.0563 (100, $[M + Na]^+$ calcd for $C_{16}H_{14}N_2NaO_4S^+$: 353.0566).

Ethyl 2-(2,2-Dicyano-1-ethoxyvinyl)-4-oxo-4-(thiophen-2-yl)but-2-enoate (261)

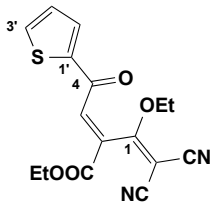

A solution of 2-ethynylthiophene (54 mg, 0.50 mmol) in $(CH_2Cl)_2$ (5 mL) was treated with alkene **162** (110 mg, 0.50 mmol) and stirred for 56 h at reflux.

Evaporation and flash column chromatography (SiO_2; EtOAc/cyclohexane 1:1 v/v) gave **261** (129 mg, 78%) as a yellow liquid. R_f = 0.21 (SiO_2; EtOAc/cyclohexane 3:7); ^{1}H NMR (400 MHz, $CDCl_3$): δ = 1.39 (t, J = 7.1 Hz, 3 H; $CO_2CH_2CH_3$), 1.45 (t, J = 8.0 Hz, 3 H; OCH_2CH_3), 4.25 (q, J = 8.0 H, 2 H; $CO_2CH_2CH_3$), 4.42 (q, J = 8.0 Hz, 2 H; OCH_2CH_3), 7.27–7.29 (d,d J = 8.0, 1.0 Hz, 1 H; H–C(4')), 7.91–7.93 (d,d, J = 8.0, 1.0 Hz, 1 H; H–C(5')), 7.96–7.97 ppm(m, 1 H; H–C(3')), 8.17 (s, 1 H; H–C(3)); ^{13}C NMR (100 MHz, $CDCl_3$): δ = 14.41 (1 C, $CO_2CH_2CH_3$), 15.07 (1 C, OCH_2CH_3), 64.30 (1 C, $CO_2CH_2CH_3$), 66.75 (1 C, C=$C(CN)_2$), 71.11 (1 C, OCH_2CH_3), 111.45 and 113.01 (2 C, 2 CN), 129.75 (1 C, C(4')), 133.62 (1 C, C(5')), 135.74 (1 C, C(3')), 138.41 (1 C, C(3)), 140.35 (1 C, C(1')), 143.50 (1 C, C(2)), 161.73 (1 C, CO_2), 180.13 (1 C, C(4)=O), 181.11 (1 C, C(1)) ppm; IR (ATR): $\tilde{\nu}$ = 2984 (w), 2225 (w), 1729 (m), 1669 (m), 1598 (w), 1561 (m), 1449 (w), 1372 (w), 1331(m), 1231 (s), 1179 (m), 1084 (w), 1056 (w), 1000 (w), 972 (w), 915(w), 848 (w), 798 (w), 711 (m), 697 (w), 640 cm^{-1} (w); UV/Vis ($CHCl_3$): λ_{max} (ε) = 325 nm (7600 $M^{-1}cm^{-1}$); HR-ESI-MS m/z (%):353.0563 (100, $[M + Na]^+$ calcd for $C_{16}H_{14}N_2NaO_4S^+$: 353.0566).

Ethyl 2-(2,2-Dicyano-1-ethoxyvinyl)-4-oxo-4-(*p*-tolyl)but-2-enoate (262)

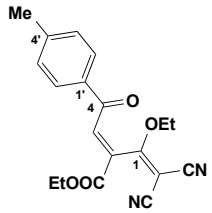

A solution of 1-ethynyl-4-methylbenzene (58 mg, 0.5 mmol) in $(CH_2Cl)_2$ (5 mL) was treated with alkene **162** (110 mg, 0.5 mmol) and stirred for 56 h at reflux. Evaporation and flash column chromatography (SiO_2; EtOAc/cyclohexane 1:1 v/v) gave **262** (123 mg, 73%) as a yellow solid. R_f = 0.20 (SiO_2; EtOAc/cyclohexane 3:7); m.p. 102–104 °C; ^{1}H NMR (400 MHz, $CDCl_3$): δ = 1.40 (t, J = 7.1 Hz, 3 H; $CO_2CH_2CH_3$), 1.48 (t, J = 8.1 Hz, 3 H; OCH_2CH_3), 2.46 (s, 3 H), 4.30 (q, J = 8.1 H, 2 H; $CO_2CH_2CH_3$), 4.42 (q, J = 8.1 Hz, 2 H; $CO_2CH_2CH_3$), 7.35 (d, J = 8.1 Hz, 2 H, H–C(3',5')), 7.89 (d, J = 8.1 Hz, 2 H, H–C(2',6')), 8.29 (s, 1 H; H–C(3)); ^{13}C NMR (100 MHz, $CDCl_3$): δ = 14.25 (1 C, $CO_2CH_2CH_3$), 14.82 (1 C, OCH_2CH_3), 22.13 (1 C, CH_3), 63.71 (1 C, $CO_2CH_2CH_3$), 66.66 (1 C, C=$C(CN)_2$), 70.55 (1 C, $CO_2CH_2CH_3$),

110.92 and 112.63 (2 C, 2 CN), 129.51 (2 C, C(3',5')), 130.14 (2 C, C(2',6')), 132.72 (1 C, C(1')), 132.84 (1 C, C(2)), 142.42 (1 C, C(3)), 146.88 (1 C, C(4')), 161.40 (1 C, CO_2), 180.68 (1 C, C(4)=O), 187.96 ppm (1 C, C(1)); IR (ATR): $\tilde{\nu}$ = 2986 (w), 2228 (m), 1736 (m), 1667 (m), 1627 (w), 1596 (w), 1563 (s), 1449 (w), 1406 (w), 1382 (w), 1352 (w), 1320 (w), 1295 (w), 1249 (s), 1225 (s), 1182 (w), 1091 (w), 1007 (m), 912 (w), 868 (w), 580 (w), 768 (w), 730 (w), 689 (w), 647 (w), 610 cm^{-1} (w); UV/Vis ($CHCl_3$): λ_{max} (ε) = 339 (8300), 260 nm (16200 $M^{-1}cm^{-1}$); HR-ESI-MS *m/z* (%): 356.1604 (100, $[M + NH_4]^+$ calcd for $C_{19}H_{22}N_3O_4^+$: 356.1605).

Ethyl 2-(2,2-dicyano-1-ethoxyvinyl)-4-oxo-4-(*m*-tolyl)but-2-enoate (263)

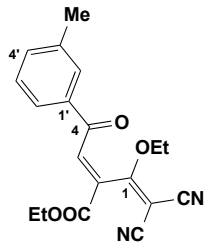

A solution of 1-ethynyl-3-methylbenzene (58 mg, 0.5 mmol) in $(CH_2Cl)_2$ (5 mL) was treated with alkene **162** (110 mg, 0.5 mmol) and stirred for 56 h at reflux. Evaporation and flash column chromatography (SiO_2; EtOAc/cyclohexane 1:1 v/v) gave **263** (127 mg, 75%) as a yellow liquid. R_f = 0.20 (SiO_2; EtOAc/cyclohexane 3:7); ^{1}H NMR (400 MHz, CD_2Cl_2): δ = 1.39 (t, *J* = 7.1 Hz, 3 H; $CO_2CH_2CH_3$), 1.47 (t, *J* = 8.0 Hz, 3 H; OCH_2CH_3), 2.45 (s, 3 H), 4.30 (q, *J* = 8.0 Hz, 2 H; $CO_2CH_2CH_3$), 4.42 (q, *J* = 8 Hz, 2 H; OCH_2CH_3), 7.44–7.48 (m, 2 H; H–C(2',4')), 7.53–7.55 (m, 1 H; H–C(3')), 7.81–7.85 (m, 1 H, H–C(6')), 8.33 ppm (s, 1 H; H–C(3)); ^{13}C NMR (100 MHz, CD_2Cl_2): δ = 14.42 (1 C, $CO_2CH_2CH_3$), 15.05 (1 C, OCH_2CH_3), 21.59 (1 C, CH_3), 64.21 (1 C, $CO_2CH_2CH_3$), 66.82 (1 C, $C=C(CN)_2$), 71.16 (1 C, OCH_2CH_3), 111.40 and 113.02 (2 C, 2 CN), 126.96 (1 C, C(6')), 129.61 (1 C, C(5')), 130.11 (1 C, C(2')), 133.43 (1 C, C(3)), 135.70 (1 C, C(4')), 136.55 (1 C, C(3')), 140.03 (1 C, C(1')), 142.35 (1 C, C(2)), 161.80 (1 C, CO_2), 181.30 (1 C, C(4)=O), 189.03 ppm (1 C, C(1)); IR (ATR): $\tilde{\nu}$ = 2988 (w), 2227 (m), 1725 (s), 1661 (m), 1598 (s), 1563 (s), 1511 (w), 1424 (w), 1380 (w), 1349 (w), 1310 (w), 1295 (w), 1253 (s), 1224 (s), 1176 (s), 1092 (w), 1010 (s), 869 (w), 845 (s), 817 (w), 773 (w), 756 (w), 718 (w), 685 (w),

634 cm^{-1} (w); UV/Vis ($CHCl_3$): λ_{max} (ε) = 341 (8100), 258 nm (16100 $M^{-1}cm^{-1}$); HR-ESI-MS *m/z* (%): 356.1604 (100, $[M + NH_4]^+$ calcd for $C_{19}H_{22}N_3O_4^+$: 356.1605).

Ethyl 4-(4-Chlorophenyl)-2-(2,2-dicyano-1-ethoxyvinyl)-4-oxobut-2-enoate (264)

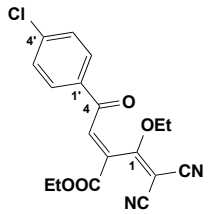

A solution of 1-chloro-4-ethynylbenzene (68 mg, 0.50 mmol) in $(CH_2Cl)_2$ (5 mL) was treated with alkene **162** (110 mg, 0.50 mmol) and stirred for 56 h at reflux. Evaporation and flash column chromatography (SiO_2; EtOAc/cyclohexane 1:1 v/v) gave **264** (129 mg, 72%) as a yellow solid. R_f = 0.21 (SiO_2; EtOAc/cyclohexane 3:7); m.p. 108–110 °C; ^{1}H NMR (400 MHz, CD_2Cl_2): δ = 1.43 (t, J = 7.1 Hz, 3 H; $CO_2CH_2CH_3$), 1.51 (t, J = 8.0 Hz, 3 H; OCH_2CH_3), 4.34 (q, J = 8.0 H, 2 H; $CO_2CH_2CH_3$), 4.46 (q, J = 8.0 Hz, 2 H; OCH_2CH_3), 7.61 (d, J = 8.0 Hz, 2 H; H–C(3',5')), 8.02 (d, J = 8.0 Hz, 2 H; H–C(2',6')), 8.33 (s, 1 H; H–C(3)); ^{13}C NMR (100 MHz, CD_2Cl_2): 14.42 (1 C, $CO_2CH_2CH_3$), 15.07 (1 C, OCH_2CH_3), 64.34 (1 C, $CO_2CH_2CH_3$), 67.00 (1 C, $C{=}C(CN)_2$), 71.29 (1 C, OCH_2CH_3), 111.29 and 113.00 (2 C, 2 CN), 130.18 (2 C, C(3',5')), 131.13 (2 C, C(2',6')), 134.07 (1 C, C(1')), 134.08 (1 C, C(2)), 141.67 (1 C, C(3)), 142.36 (1 C, C(4')), 161.66 (1 C, CO_2), 180.93 (1 C, C(4)=O), 187.90 ppm (1 C, C(1)); IR (ATR): $\tilde{\nu}$ = 2927 (m), 2856 (m), 2229 (m), 1737 (m), 1701 (m), 1565 (s), 1465 (w), 1381 (m), 1349 (m), 1240 (s), 1097 (w), 1016 (m), 853 (s), 614 (w) cm^{-1}; UV/Vis ($CHCl_3$): λ_{max} (ε) = 325 nm (7600 $M^{-1}cm^{-1}$); HR-ESI-MS: *m/z* (%) 376.1058 (100, $[M + NH_4]^+$ calcd for $C_{18}H_{19}ClN_3O_4^+$: 376.1059).

Ethyl 2-(2,2-Dicyano-1-ethoxyvinyl)-4-oxo-4-(4-(trifluoromethyl)phenyl)but-2-enoate (265)

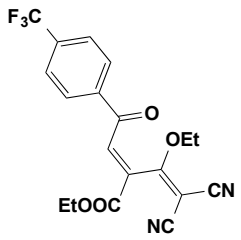

A solution of 1-ethynyl-4-(trifluoromethyl)benzene (85 mg, 0.5 mmol) in $(CH_2Cl)_2$ (5 mL) was treated with alkene **162** (110 mg, 0.5 mmol) and stirred for 56 h at reflux. Evaporation and flash column chromatography (SiO_2; EtOAc/cyclohexane 1:1 v/v) gave **265** (120 mg, 61%) as a yellow oil. R_f = 0.20 (SiO_2; EtOAc/cyclohexane 3:7); ^{1}H NMR (400 MHz, CD_2Cl_2): δ = 1.39 (t, J = 7.1 Hz, 3 H; $CO_2CH_2CH_3$), 1.47 (t, J = 8.1 Hz, 3 H; OCH_2CH_3), 4.41 (q, J = 8.1 H, 2 H; $CO_2CH_2CH_3$), 4.43 (q, J = 8 Hz, 2 H; OCH_2CH_3), 7.26 (m, 2 H; H–C(3',5')), 8.07 (m, 2 H; H–C(2',6')), 8.30 ppm (s, 1 H; H–C(3)); ^{13}C NMR (100 MHz, CD_2Cl_2): δ = 14.42 (1 C, $CO_2CH_2CH_3$), 15.07 (1 C, OCH_2CH_3), 30.26 (1 C, $CO_2CH_2CH_3$), 64.31 (1 C, $O_2CH_2CH_3$), 68.24 (1 C, C=C(CN)$_2$), 71.27 (1 C, OCH_2CH_3), 98.57 (q, J = 32.9 Hz, 1 C), 111.32 and 113.01 (2 C, 2 CN), 117.10 (d, J = 2.6 Hz, 1 C), 132.26 (2 C, C(3',5')), 132.73 (1 C, C(2)), 133.86 (1 C, C(3)), 141.91 (2 C, C(2',6') 161.69 (1 C, CO_2), 181.04 (1 C, C(4)=O), 187.45 ppm (1 C, C(1)); ^{19}F NMR (377 MHz, $CDCl_3$): δ = –73.65 (t, J = 8.2 Hz, 3 F; CF_3); IR (ATR): $\tilde{\nu}$ = 2988 (w), 2227 (m), 1725 (s), 1661 (m), 1598 (s), 1563 (s), 1511 (w), 1424 (w), 1380 (w), 1349 (w), 1310 (w), 1295 (w), 1253 (s), 1224 (s), 1176 (s), 1092 (w), 1010 (s), 869 (w), 845 (s), 817 (w), 773 (w), 756 (w), 718 (w), 685 (w), 634 cm^{-1} (w); UV/Vis ($CHCl_3$): λ_{max} (ε) = 329nm (7900 M^{-1}cm^{-1}); HR-ESI-MS m/z (%): 410.1325 (100, [M + NH_4]$^+$ calcd for $C_{19}H_{19}F_3N_3O_4^+$: 410.1322).

Ethyl 4-(4-Acetylphenyl)-2-(2,2-dicyano-1-ethoxyvinyl)-4-oxobut-2-enoate (266)

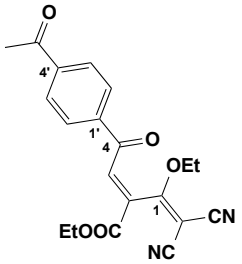

A solution of 1-(4-ethynylphenyl)ethanone (72 mg, 0.5 mmol) in $(CH_2Cl)_2$ (5 mL) was treated with alkene **162** (110 mg, 0.5 mmol) and stirred for 56 h at reflux. Evaporation and flash column chromatography (SiO_2; EtOAc/cyclohexane 1:1 v/v) gave **266** (82 mg, 45%) as a yellow solid. R_f = 0.21 (SiO_2; EtOAc/cyclohexane 3:7); m.p. 104–106 °C; ^{1}H NMR (400 MHz, CD_2Cl_2): δ = 1.40 (t, J = 7.1 Hz, 3 H; $CO_2CH_2CH_3$), 1.48 (t, J = 8.0 Hz, 3 H; OCH_2CH_3), 2.65 (s, 3 H), 4.30 (q, J = 8.0 Hz, 2 H; $CO_2CH_2CH_3$), 4.44 (q, J = 8.0 Hz, 2 H; OCH_2CH_3), 8.11 (s, 4 H), 8.34 (s, 1 H; H–C(3)); ^{13}C NMR (100 MHz, CD_2Cl_2): δ =13.85 (1 C, $CO_2CH_2CH_3$), 14.51 (1 C, OCH_2CH_3), 26.82 (1 C, *Me*–C=O), 63.82 (1 C, $CO_2CH_2CH_3$), 66.43 (1 C, C=$C(CN)_2$), 70.78 (1 C, OCH_2CH_3), 110.69 and 112.41 (2 C, 2 CN), 128.81 (2 C, C(3',5')), 129.36 (2 C, C(2',6')), 133.71 (1 C, C(2)), 137.88 (1 C, C(1')), 141.02 (1 C, C(3)), 141.60 (1 C, C(4')), 161.04 (1 C, CO_2), 180.27 (1 C, C(4)=O), 188.14 (1 C, C(1)=O), 196.98 ppm (1 C, Me–*C*=O); IR (ATR): $\tilde{\nu}$ = 2988 (w), 2227 (m), 1725 (s), 1661 (m), 1598 (s), 1563 (s), 1511 (w), 1424 (w), 1380 (w), 1349 (w), 1310 (w), 1295 (w), 1253 (s), 1224 (s), 1176 (s), 1092 (w), 1010 (s), 869 (w), 845 (s), 817 (w), 773 (w), 756 (w), 718 (w), 685 (w), 634 cm^{-1} (w); UV/Vis ($CHCl_3$): λ_{max} (ε) = 335 nm (8200 $M^{-1}cm^{-1}$); HR-ESI-MS *m*/*z* (%): 384.1553 (100, $[M + NH_4]^+$ calcd for $C_{20}H_{22}N_3O_5^+$: 384.1554).

Ethyl 4-[*N*-Benzyl-4-(methylphenyl)sulfonamide]-2-(2,2-dicyano-1-ethoxyvinyl)-4-oxobut-2-enoate (268)

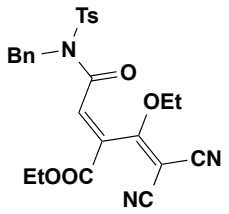

A solution of *N*-benzyl-*N*-ethynyl-4-methylaniline[237] (200 mg, 0.7 mmol) in $(CH_2Cl)_2$ (7 mL) was treated with alkene **162** (156 mg, 0.7 mmol) and stirred for 16 h at reflux. Evaporation and flash column chromatography (SiO_2; EtOAc/cyclohexane 3:7 v/v) gave **268** (300 mg, 84%) as a white solid. R_f = 0.24 (SiO_2; EtOAc/cyclohexane 3:7); m.p. 106–109 °C; ^{1}H NMR (400 MHz, $CDCl_3$): δ = 1.33 and 1.35 (2 t, J = 7.1 Hz, 6 H; 2 OCH_2CH_3), 2.46 (s, 3 H, CH_3), 4.10 (q, J = 7.1 Hz, 2 H; $CO_2CH_2CH_3$), 4.33 (q, J = 7.1 Hz, 2 H; OCH_2CH_3), 5.03 (s, 2 H; CH_2), 7.36 (m, 7 H; H–C(2',2'',3',4',5',6',6'')), 7.80 ppm (m, 3 H; H–C(4,3'',5'')); ^{13}C NMR (100 MHz, $CDCl_3$): δ = 14.08 (1 C, $CO_2CH_2CH_3$), 14.63 (1 C, OCH_2CH_3), 21.85 (1 C, CH_3), 50.41 (1 C, CH_2), 63.71 (1 C, $CO_2CH_2CH_3$), 66.54 (1 C, C=$C(CN)_2$), 70.67 (1 C, OCH_2CH_3), 110.48 and 112.54 (2 C, 2 CN), 127.66 (2 C, C(3',5')), 128.36 (1 C, C(4')), 128.40 (2 C, C(3'',5'')), 129.07 (2 C, C(2',6')), 130.13 (2 C, C(2'',6'')), 133.41 (1 C, C(1')), 134.82 (1 C, C(1'')), 135.32 (1 C, C(4'')), 139.44 (1 C, C(2)), 146.47 (1 C, C(3)), 160.69 (1 C, C=O), 162.88 (1 C, C(4)=O), 179.48 ppm (1 C, C(1)); IR (ATR): $\tilde{\nu}$ = 2981 (w), 2229 (w), 1715 (m), 1687 (m), 1596 (w), 1571 (m), 1496 (w), 1454 (w), 1441 (w), 1384 (w), 1363 (s), 1333 (w), 1298 (m), 1262 (m), 1214 (m), 1188 (w), 1171 (s), 1129 (w), 1087 (m), 1019 (m), 957 (w), 922 (w), 887 (w), 865 (w), 845 (w), 819 (w), 505 (w), 778 (w), 738 (s), 717 (w), 704 (w), 692 (w), 652 (w), 611 cm^{-1} (w); UV/Vis ($CHCl_3$): λ_{max} (ε) = 259 nm (16600 M^{-1}cm^{-1}); HR-ESI-MS *m*/*z* (%): 525.1799 (100, $[M + NH_4]^+$), calcd for $C_{26}H_{29}N_4O_6S^+$: 525.1802).

(*R*,*E*)-Ethyl 4-(4-Benzyl-2-oxooxazolidin-3-yl)-2-(2,2-dicyano-1-ethoxyvinyl)-4-oxobut-2-enoate ((*R*)-269)

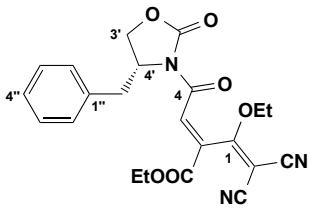

A solution of (*S*)-4-benzyl-3-ethynyloxazolidin-2-one[238] (100 mg, 0.5 mmol) in $(CH_2Cl)_2$ (5 mL) was treated with alkene **162** (110 mg, 0.5 mmol) and stirred for 56 h at reflux. Evaporation and flash column chromatography (SiO_2; EtOAc/cyclohexane 1:1 v/v) gave (*R*)-**269** (177 mg, 84%) as a white foaming solid. R_f = 0.23 (SiO_2; EtOAc/cyclohexane 4:6); m.p. 120–123 °C; $[\alpha]_D^{20}$ = –68°(c =1.0 in $CHCl_3$); ^{1}H NMR (400 MHz, CD_2Cl_2): δ = 1.37 (t, *J* = 7.1 Hz, 3 H; $CO_2CH_2CH_3$), 1.46 (t, *J* = 7.1 Hz, 3 H; OCH_2CH_3), 2.90 (dd, *J* = 8.0, 1.0 Hz, 1 H; C–H(3')), 3.31 (dd, *J* = 8.0, 1.0 Hz, 1 H; C–H(3')), 4.23–4.25 (m, 2 H), 4.33–4.44 (m, 3 H), 4.74–4.80 (m, 1 H; C–H(4')), 7.23–7.24 (m, 2 H), 7.28–7.39 (m, 3 H), 8.40 ppm (s, 1 H; H–C(3)); ^{13}C NMR (100 MHz, CD_2Cl_2): δ = 14.38 (1 C, $CO_2CH_2CH_3$), 15.10 (1 C, OCH_2CH_3), 37.93 (1 C, CH_2–Ph), 55.68 (1 C, C(4')), 64.31(1 C, $CO_2CH_2CH_3$), 67.38 (1 C, C(1)), 67.86 (1 C, OCH_2CH_3), 71.25 (1 C, C(3')), 111.40 and 112.89 (2 C, 2 CN), 128.07 (1 C, C(4'')), 129.59 (2 C, C(2',6')), 130.01(2 C, C(2',6')), 133.81(1 C, C(1'')), 135.19 (1 C, C(2)), 138.31 (1 C, C(3)), 153.36 (1 C, C=O), 161.51 (1 C, C=O), 162.46 (1 C, C(4)=O), 180.42 (1 C, C(1)) ppm; IR (ATR): $\tilde{\nu}$ = 2979 (w), 2220 (w), 1718 (m), 1682 (m), 1599 (w), 1561 (m), 1484 (w), 1453 (w), 1448 (w), 1380 (w), 1360 (s), 1336 (w), 1290 (m), 1259 (m), 1219 (m), 1188 (w), 1169 (s), 1121 (w), 1082 (m), 1010 (m), 958 (w), 920 (w), 889 (w), 860(w), 840 (w), 810 (w), 500 (w), 770 (w), 730 (s), 712 (w), 700 (w), 692 (w), 659 (w), 609 cm^{-1} (w); UV/Vis ($CHCl_3$): λ_{max} (ε) = 254 (15900 M^{-1}cm^{-1}); HR-ESI-MS *m*/*z* (%): 441.1768 (100, $[M + NH_4]^+$), calcd for $C_{22}H_{25}N_4O_6^+$: 441.1769).

Ethyl 4-(Benzylthio)-2-(2,2-dicyano-1-ethoxyvinyl)-4-oxobut-2-enoate (270)

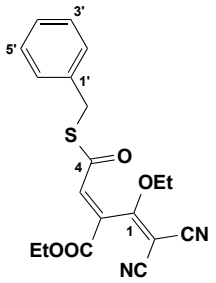

A solution of benzyl ethynyl thioether[239] (54 mg, 0.50 mmol) in $(CH_2Cl)_2$ (5 mL) was treated with alkene **162** (110 mg, 0.50 mmol) and stirred for 56 h at reflux. Evaporation and flash column chromatography (SiO_2; EtOAc/cyclohexane 1:1 v/v) gave **270** (138 mg, 75%) as a yellow solid. R_f = 0.21 (SiO_2; EtOAc/cyclohexane 3:7); m.p. 98–102 °C; ^{1}H NMR (400 MHz, CD_2Cl_2): δ = 1.35 (t, J = 7.1 Hz, 3 H; $CO_2CH_2CH_3$), 1.40 (t, J = 8.0 Hz, 3 H; OCH_2CH_3), 4.16 (q, J = 8 H, 2 H; $CO_2CH_2CH_3$), 4.32 (s, 2 H; CH_2), 4.37 (q, J = 8.0 Hz, 2 H; OCH_2CH_3), 7.24–7.37 (m, 5 H; H–C(2',3',4',5',6')), 7.43 ppm (s, 1 H; H–C(3)); ^{13}C NMR (100 MHz, CD_2Cl_2): δ = 13.78 (1 C, $CO_2CH_2CH_3$), 14.50 (1 C, OCH_2CH_3), 34.41 (1 C, CH_2), 63.80 (1 C, $CO_2CH_2CH_3$), 66.91 (1 C, C=C(CN)$_2$), 70.52 (1 C, OCH_2CH_3), 110.77 and 112.14 (2 C, 2 CN), 127.84 (1 C, C(4')), 128.80 (2 C, C(2',6')), 128.93 (2 C, C(3',5')), 129.71 (1 C, C(1')), 135.85 (1 C, C(3)), 140.64 (1 C, C(2)), 160.91 (1 C, CO_2), 179.38 (1 C, C(4)=O), 186.80 (1 C, C(1)) ppm; IR (ATR): $\tilde{\nu}$ = 2988 (w), 2227 (m), 1725 (s), 1661 (m), 1598 (s), 1563 (s), 1511 (w), 1424 (w), 1380 (w), 1349 (w), 1310 (w), 1295 (w), 1253 (s), 1224 (s), 1176 (s), 1092 (w), 1010 (s), 869 (w), 845 (s), 817 (w), 773 (w), 756 (w), 718 (w), 685 (w), 634 cm^{-1} (w); UV/Vis ($CHCl_3$): λ_{max} (ε) = 256 (15700 M^{-1}cm^{-1}); HR-ESI-MS: m/z (%)388.1326 (100, [M + NH_4]$^+$ calcd for $C_{19}H_{22}N_3O_4S^+$: 388.1326).

Ethyl 4-Cyclopropyl-2-(2,2-dicyano-1-ethoxyvinyl)-4-oxobut-2-enoate (271)

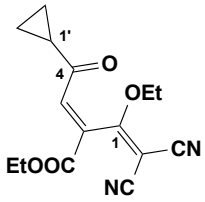

A solution of ethynylcyclopropane (33 mg, 0.5 mmol) in $(CH_2Cl)_2$ (5 mL) was treated with alkene **162** (110 mg, 0.5 mmol) and stirred for 56 h at reflux. Evaporation and flash column chromatography (SiO_2; EtOAc/cyclohexane 3:7 v/v) gave **271** (102 mg, 71%) as a clear colorless oil. R_f = 0.39 (SiO_2; EtOAc/cyclohexane 3:7); ^{1}H NMR (400 MHz, $CDCl_3$): δ = 1.17–1.23 (m, 2 H; 2 H–C(2',3')), 1.27–1.31 (m, 2 H; 2 H–C(2',3')), 1.37 (t, J = 8.0 Hz, 3 H; $CO_2CH_2CH_3$), 1.42 (t, J = 8.0 Hz, 3 H; OCH_2CH_3), 2.19–2.25 (m, 1 H; H–C(1')), 4.17 (q, J = 8.0 H, 2 H; $CO_2CH_2CH_3$), 4.39 (q, J = 8.0 Hz, 2 H; OCH_2CH_3), 7.68 ppm (s, 1 H; ; H–C(3)); ^{13}C NMR (100 MHz, $CDCl_3$): δ = 14.24 (2 C, C(2',3')), 14.80 (1 C, $CO_2CH_2CH_3$)), 22.78 (1 C, $CO_2CH_2CH_3$)), 63.69 (1 C, OCH_2CH_3), 66.57 (1 C, C=C(CN)$_2$), 66.52 (1 C, C(1')), 70.37 (1 C, $CO_2CH_2CH_3$), 110.91 and 112.68 (2 C, 2 CN), 130.68 (1 C, C(2)), 142.72 (1 C, C(3)), 161.40 (1 C, CO_2), 180.53 (1 C, C(4)=O), 198.89 ppm (1 C, C(1)); IR (ATR): $\tilde{\nu}$ = 2921 (m), 2852 (m), 2218 (m), 1732 (m), 1706 (m), 1559 (s), 1461 (w), 1382 (m), 1348 (m), 1237 (s), 1085 (w), 1021(m), 850 cm^{-1} (w); UV/Vis ($CHCl_3$): λ_{max} (ε) = 331 nm (5900 M^{-1}cm^{-1}); HR-ESI-MS m/z (%): 306.1445 (100, [M + NH_4]$^+$ calcd for $C_{15}H_{20}N_3O_4^+$: 306.1448).

Ethyl 2-(2,2-Dicyano-1-ethoxyvinyl)-4-oxododec-2-enoate (272)

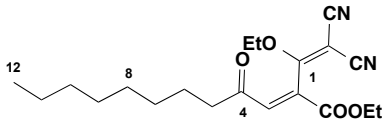

A solution of 1-decyne (71 mg, 0.51 mmol) in $(CH_2Cl)_2$ (5.1 mL) was treated with alkene **162** (114 mg, 0.51 mmol) and stirred for 58 h at reflux. Evaporation and flash column chromatography (SiO_2; EtOAc/cyclohexane 3:7 v/v) gave **272** (88 mg, 49%) as a clear colorless oil. R_f = 0.41 (SiO_2; EtOAc/cyclohexane 3:7); ^{1}H NMR (400 MHz, $CDCl_3$): δ = 0.87 (br. t, J = 8.0 Hz, 3 H; H–C(12)), 1.26–1.35 (m, 10 H; H_2C(7,8,9,10,11)), 1.37 (t, J = 7.1 Hz, 3 H; $CO_2CH_2CH_3$), 1.44 (t, J = 7.1 Hz, 3 H;

OCH_2CH_3), 1.66 (q, J = 7.3 Hz, 2 H, $H_2C(6)$), 2.71 (t, J = 7.3 Hz, 2 H, $H_2C(5)$), 4.19 (q, J = 7.1 Hz, 2 H; $CO_2CH_2CH_3$), 4.38 (q, J = 7.1 Hz, 2 H; OCH_2CH_3), 7.53 ppm (s, 1 H; H–C(3)); ^{13}C NMR (100 MHz, $CDCl_3$): δ = 14.21 (1 C, $H_3C(12)$), 14.24 (1 C, $CO_2CH_2CH_3$)), 14.82 (1 C, OCH_2CH_3)), 22.78 (1 C, $H_2C(11)$), 23.41 (1 C, $H_2C(6)$), 29.12 and 29.20 and 29.40 and 31.92 (4 C, C(7,8,9,10)), 43.71 (1 C, C(5)), 63.74 (1 C, $CO_2CH_2CH_3$), 66.48 (1 C, C=$C(CN)_2$), 70.42 (1 C, OCH_2CH_3)), 110.84 and 112.72 (2 C, CN), 131.36 (1 C, C(2)), 142.43 (1 C, C(3)), 161.32 (1 C, CO_2), 180.49 (1 C, C(4)=O), 199.14 ppm (1 C, C(1)); IR (ATR): $\tilde{\nu}$ = 2927 (m), 2856 (m), 2229 (m), 1737 (m), 1701 (m), 1565 (s), 1465 (w), 1381 (m), 1349 (m), 1240 (s), 1097 (w), 1016 (m), 853 cm^{-1} (w); UV/Vis ($CHCl_3$): λ_{max} (ε) = 330 nm (6100 M^{-1}cm^{-1}); HR-MALDI-MS (DCTB) m/z (%): 383.1941 (100, $[M + Na]^+$ calcd for $C_{20}H_{28}N_2NaO_4$: 383.1946).

Ethyl 2-(2,2-Dicyano-1-ethoxyvinyl)-3-methyl-4-oxo-4-phenylbut-2-enoate (276)

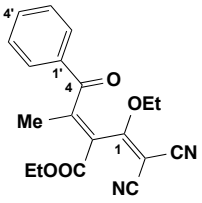

A solution of 1-phenyl-1-propyne (63 mg, 0.54 mmol) in $(CH_2Cl)_2$ (5.4 mL) was treated with alkene **162** (120 mg, 0.54 mmol) and stirred for 58 h at reflux. Evaporation and flash column chromatography (SiO_2; EtOAc/cyclohexane 3:7 v/v) gave **276** (100 mg, 55%) as a pale yellow oil. R_f = 0.37 (SiO_2; EtOAc/cyclohexane 3:7); ^{1}H NMR (400 MHz, $CDCl_3$): δ = 1.38 (t, J = 7.1 Hz, 3 H; $CO_2CH_2CH_3$), 1.40 (t, J = 7.1 Hz, 3 H; OCH_2CH_3), 2.59 (s, 3 H, *Me*–C(3)), 4.37 and 4.38 (2 q, J = 7.1 Hz, 4 H; 2 OCH_2CH_3), 7.53–7.58 (m, 2 H; H–C(3',5')), 7.68 (tt, J = 8.0, 1.3 Hz, 1 H; H–C(5')), 7.89–7.92 ppm (m, 2 H; H–C(2',6')); ^{13}C NMR (100 MHz, $CDCl_3$): δ = 14.30 (1 C, $CO_2CH_2CH_3$)), 14.64 (1 C, OCH_2CH_3), 19.30 (1 C, CH_3), 62.73 (1 C, $CO_2CH_2CH_3$), 63.09 (1 C, C=$C(CN)_2$), 70.56 (1 C, OCH_2CH_3), 110.95 and 113.02 (2 C, 2 CN), 122.93 (1 C, C(2)), 129.28 (2 C, C(3',5')), 130.23 (2 C, C(2',6')), 132.66 (1 C, C(1')), 135.33 (1 C, C(4')), 161.30 (1 C, C(3)), 161.65 (1 C, CO_2), 180.95 (1 C, C(4)=O), 195.41 ppm (1 C, C(1)); IR (ATR): $\tilde{\nu}$ = 2986 (w), 2229 (w), 1731 (m), 1668 (m), 1596 (w), 1560 (m), 1449 (w), 1377 (w), 1329 (m), 1234 (s), 1186 (m), 1096 (w), 1059 (w), 1001 (w), 974 (w), 910 (w), 849 (w), 799 (w), 714 (m), 688 (w),

646 cm^{-1} (w); UV/Vis ($CHCl_3$): λ_{max} (ε) = 338 (8400), 257 nm (16200 $M^{-1}cm^{-1}$); HR-ESI-MS *m/z* (%): 356.1605 (100, $[M + NH_4]^+$ calcd for $C_{19}H_{22}N_3O_4^+$: 356.1605).

Ethyl 3-Benzoyl-2-(2,2-Dicyano-1-ethoxyvinyl)pent-2-enoate (274)

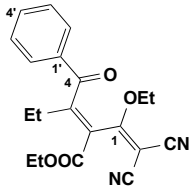

A solution of but-1-yn-1-ylbenzene (65 mg, 0.50 mmol) in $(CH_2Cl)_2$ (5 mL) was treated with alkene **162** (110 mg, 0.50 mmol) and stirred for 58 h at reflux. Evaporation and flash column chromatography (SiO_2; EtOAc/cyclohexane 3:7 v/v) gave **274** (95 mg, 52%) as a pale yellow oil. R_f = 0.37 (SiO_2; EtOAc/cyclohexane 3:7); ^{1}H NMR (400 MHz, $CDCl_3$): δ = 1.13 (t, *J* = 7.1 Hz, 3 H; CH_2CH_3), 1.36 (t, *J* = 7.1 Hz, 3 H; $CO_2CH_2CH_3$), 1.39 (t, *J* = 7.1 Hz, 3 H; OCH_2CH_3), 3.09 (q, *J* = 7.1 Hz, 2 H; CH_2CH_3), 4.34 and 4.36 (q, *J* = 7.1 Hz, 4 H; 2 OCH_2CH_3), 7.54–7.58 (m, 2 H; H–C(3',5')), 7.68–7.72 (m, 1 H; H–C(5')), 7.91–7.93 ppm (m, 2 H; H–C(2',6')); ^{13}C NMR (100 MHz, $CDCl_3$): δ =12.75 (1 C, $CO_2CH_2CH_3$)), 14.43 (1 C, CH_2CH_3)), 14.85 (1 C, CH_2CH_3)), 26.17 (1 C, OCH_2CH_3)), 63.21 (1 C, $CO_2CH_2CH_3$), 68.61 (1 C, $C=C(CN)_2$), 70.94 (1 C, OCH_2CH_3), 111.37 and 113.35 (2 C, 2 CN), 122.52 (1 C, C(2)), 129.56 (2 C, C(3',5')), 130.42 (2 C, C(2',6')), 133.90 (1 C, C(1')), 135.53 (1 C, C(4')), 161.94 (1 C, C(3)), 166.81 (1 C, CO_2), 181.11 (1 C, C(4)=O), 195.68 (1 C, C(1)) ppm; IR (ATR): $\tilde{\nu}$ = 2982 (w), 2225 (w), 1730 (m), 1669 (m), 1601 (w), 1559 (m), 1453 (w), 1375(w), 1328 (m), 1229 (s), 1178 (m), 1089(w), 1042(w), 990 (w), 970 (w), 915 (w), 848 (w), 803 (w), 712 (m), 686 (w), 651 cm^{-1} (w); UV/Vis ($CHCl_3$): λ_{max} (ε) = 341 (8400), 256 nm (16100 $M^{-1}cm^{-1}$); HR-ESI-MS *m/z* (%):370.1760 (100, $[M + NH_4]^+$ calcd for $C_{20}H_{24}N_3O_4^+$: 370.1761).

8.3. X-ray Crystallographic Data

8.3.1. Crystal Data

Crystals of compounds **33a**, **109, 131, 133a, 133b, 134a, 150a, 150b, 151b, 156b, 157a, 157b, 159, 160, 163,** (±)-**165, 169, 170, 171, 175,** (±)-**193, 196, 213, 221, 227, 229, 255, 258, 262** and **269** were measured on a Bruker/Nonius Kappa APEX-II diffractometer. Crystals were measured on a Bruker APEX-II Duo diffractometer. In both cases, sealed-tube graphite-monochromated MoKα radiation (λ = 0.71073 Å) was used and the samples kept at 100 K during data collection (Oxford Cryosystems Cryostream 700). Using OLEX2,[239] the structures were solved with the XT[239] structure solution program and refined with the XL[240] refinement package. All hydrogen atoms were constrained to ideal geometries and refined with fixed isotropic displacement parameters (in terms of a riding model). CCDC (980629 (**33a**)), (980623 (**109**)), (1058921 (**131**)), (1058926 (**133a**)), (1058925 (**133b**)), (1061800 (**134a**), (1058929 (**150a**), (1058920 (**150b**)), (1058927 (**151b**)), (1058928 (**156b**)), (1058924 (**157a**)), (1058922 (**157b**)), ((1419181 (**159**)), (1419175 (**160**)), (1419182 (**163**)), (1419178 ((±)-**165**)), (1419180 (**169**)), (1419176 (**170**)), (1419179 (**171**)), (1419177 (**175**)), (1419173 ((±)-**193**)), and (1419174 ((**196**)), (1431910 (**213**)), (1431911 (**221**)), (1431912 (**227**)), (1431913 (**229**)), (1429488 (**255**)), (1429491 (**258**)), (1429490 (**262**)), and (1429492 (**269**)) contain the supplementary crystallographic data for this paper. These data can be obtained free of charge from The Cambridge Crystallographic Data Centre, 12 Union Road, Cambridge CB2 1EZ, UK (fax: +44(1223)-336-033; e-mail: deposit@ccdc.cam.ac.uk), or *via* www.ccdc.cam.ac.uk/getstructures.

Crystal Data for 33a. Crystal data at 100 K for $C_{58}Cl_6H_{74}$, M = 983.87 g mol^{-1}, monoclinic, space group $P2_1$, a = 13.6232(16) Å, b = 16.196(2) Å, c = 27.716(4) Å, β = 104.031(2)°, V = 5932.9(13) Å^3, Z = 4, D_c = 1.101 g/cm^3, μ(CuKα) = 0.322 mm^{-1}. Crystals (linear dimensions approx. 0.24 mm x 0.19 mm x 0.08 mm) were grown from slow evaporation of *n*hexane/chloroform 9:1 at 0 °C. Number of measured and unique reflections 42312 and 26598, respectively (R_{int} = 0.0386). Final R_1 = 0.0562, wR_2 = 0.1151 for 26598 independent reflections with $I >$

$2\sigma(I)$, 1308 parameters and $3.762 < 2\theta < 55.306°$ (corresponding R values based on all 42314 reflections are 0.0841 and 0.1284, respectively)

Crystal Data for 109. Crystal data at 100 K for $C_{56}H_{74}$, M = 747.15 g mol^{-1}, monoclinic, space group $P2_1$, a = 12.923(3) Å, b = 9.8532(17) Å, c = 21.529(4) (19) Å, β = 107.183(3)°, V = 2619.0(8) Å^3, Z = 2, D_c = 0.947 g/cm^3, μ(CuKα) = 0.053 mm^{-1}. Crystals (linear dimensions approx. 0.29 mm x 0.12 mm x 0.01 mm) were grown from slow evaporation of *n*hexane/chloroform 9:1 at 0 °C. Number of measured and unique reflections 17639 and 7517, respectively (R_{int} = 0.0465). Final R_1 = 0.0448, wR_2 = 0.0866 for 7517 independent reflections with $I > 2\sigma(I)$, 529 parameters and $3.298 < 2\theta < 52.774°$ (corresponding R values based on all 17639 reflections are 0.0763

Crystal Data for 131. Crystal data at 100 K for $C_{33}H_{28}ClN_4O_2$, M = 548.04 g mol^{-1}, monoclinic, space group P-1, a = 8.0970(8) Å, b = 12.2435(12), c = 14.9160(15) Å, β = 105.026(6)°, V = 1367.3(2) Å^3, Z = 2, D_c = 1.331 g/cm^3, μ(CuKα) = 0.178 mm^{-1}. Crystals (linear dimensions approx. 0.040 mm x 0.100 mm x 0.160 mm) were grown from slow evaporation of pentane/chloroform at 25 °C. Number of measured and unique reflections 21148 and 6245, respectively (R_{int} = 0.0369). Final R_1 = 0.0514, wR_2 = 0.1255 for 6245 independent reflections with $I > 2\sigma(I)$, 473 parameters and $1.74 < 2\theta < 27.58°$ (corresponding R values based on all 21148 reflections are 0.0921 and 0.1397, respectively)

Crystal Data for 133a. Crystal data at 100 K for $C_{31}H_{26}Cl_2N_4O_2$, M = 557.46 g mol^{-1}, monoclinic, space group C2/c, a = 33.090(2) Å, b = 11.5983(9), c = 30.487(2) Å, β = 94.617(2)°, V = 11662.6(15) Å^3, Z = 6, D_c = 1.270 g/cm^3, μ(CuKα) = 0.257 mm^{-1}. Crystals (linear dimensions approx. 0.4 mm x 0.14 mm x 0.11 mm) were grown from slow evaporation of pentane/DCM at 25 °C. Number of measured and unique reflections 48896 and 13278, respectively (R_{int} = 0.0384). Final R_1 = 0.0814, wR_2 = 0.1594 for 13278 independent reflections with $I > 2\sigma(I)$, 710 parameters and $3.722 < 2\theta < 54.998°$ (corresponding R values based on all 48896 reflections are 0.0814 and 0.1594, respectively).

Crystal Data for 133b. Crystal data at 100 K for $C_{60}H_{48}N_8O_4$, M = 945.06 g mol^{-1}, monoclinic, space group P-1, a = 10.7919(11) Å, b = 14.9371(16) Å, c =

17.309(2) Å, β = 92.220(5)°, V = 2411(5) Å^3, Z = 2, D_c = 1.302 g/cm^3, μ(CuKα) = 0.084 mm^{-1}. Crystals (linear dimensions approx. 0.080 mm x 0.120 mm x 0.200 mm) were grown from slow evaporation of pentane/DCM at 25 °C. Number of measured and unique reflections 21235 and 10593, respectively (R_{int} = 0.0820). Final R_1 = 0.0839, wR_2 = 0.1406 for 10593 independent reflections with $I > 2\sigma(I)$, 658 parameters and 2.14 < 2θ < 27.44° (corresponding R values based on all 21235 reflections are 0.2118 and 0.1843, respectively).

Crystal Data for 134a. Crystal data at 100 K for $C_{21}H_{14}N_2O_3$, M = 342.34 g mol^{-1}, monoclinic, space group $Pbca$, a = 7.6196(6) Å, b = 20.278(4) Å, c = 21.360(5) Å, β = 90 °, V = 3300.2(12) Å^3, Z = 8, D_c = 1.378 g/cm^3, μ(CuKα) = 0.094 mm^{-1}. Crystal were grown from slow evaporation of pentane/DCM at 25 °C. Number of measured and unique reflections 24266 and 3806, respectively (R_{int} = 0.0605). Final R_1 = 0.00422, wR_2 = 0.1131 for 3806 independent reflections with $I > 2\sigma(I)$, 236 parameters and 3.814 < 2θ < 55.138° (corresponding R values based on all 24266 reflections are 0.0678 and 0.1340, respectively).

Crystal Data for 134a. Crystal data at 100 K for $C_{28}H_{18}N_4O_4$, M = 474.46 g mol^{-1}, monoclinic, space group $P2_1/c$, a = 8.3939(3) Å, b = 22.8222(8) Å, c = 14.0623(4) Å, β = 119.661(2)°, V = 2340.89(14) Å^3, Z = 4, D_c = 1.346 g/cm^3, μ(CuKα) = 0.093 mm^{-1}. Crystals (linear dimensions approx. 0.24 mm x 0.2 mm x 0.11 mm) were grown from slow evaporation of pentane/DCM at 25 °C. Number of measured and unique reflections 21467 and 5378, respectively (R_{int} = 0.0320). Final R_1 = 0.0375, wR_2 = 0.0850 for 5378 independent reflections with $I > 2\sigma(I)$, 327 parameters and 3.57 < 2θ < 55.102° (corresponding R values based on all 21467 reflections are 0.0498 and 0.0914, respectively).

Crystal Data for 150a. Crystal data at 100 K for $C_{29}H_{18}N_4O_2$, M = 454.47 g mol^{-1}, triclinic, space group P-1, a = 13.1134(11) Å, b = 13.5996(10) Å, c = 14.3738(11) Å, β = 97.269(3)°, V = 2226.1(3) Å^3, Z = 4, D_c = 1.356 g/cm^3, μ(CuKα) = 0.088 mm^{-1}. Crystals (linear dimensions approx. 0.32 mm x 0.12 mm x 0.1 mm) were grown from slow evaporation of pentane/DCM at 25 °C. Number of measured and unique reflections 36512 and 9263, respectively (R_{int} = 0.0426). Final R_1 = 0.0500, wR_2 = 0.1087 for 9263 independent reflections with $I > 2\sigma(I)$, 635

parameters and $3.472 < 2\theta < 55.2°$ (corresponding R values based on all 36512 reflections are 0.0776 and 0.1204, respectively).

Crystal Data for 150b. Crystal data at 100 K for $C_{59}H_{38}Cl_2N_8O_4$, M = 993.87 g mol^{-1}, monoclinic, space group $C2/c$, a = 13.519(4) Å, b = 27.436(7) Å, c = 13.378(3) Å, β = 109.555(4)°, V = 4676(2) Å^3, Z = 4, D_c = 1.412 g/cm^3, μ(CuKα) = 0.201 mm^{-1}. Crystals (linear dimensions approx. 0.11 mm x 0.06 mm x 0.01 mm) were grown from slow evaporation of pentane/DCM at 25 °C. Number of measured and unique reflections 10064 and 2480, respectively (R_{int} = 0.1378). Final R_1 = 0.0682, wR_2 = 0.1578 for 2480 independent reflections with $I > 2\sigma(I)$, 336 parameters and $4.388 < 2\theta < 41.818°$ (corresponding R values based on all 10064 reflections are 0.1422 and 0.1934, respectively).

Crystal Data for 151b. Crystal data at 100 K for $C_{31}H_{23}N_3O_4$, M = 501.52 g mol^{-1}, monoclinic, space group $P2_1/c$, a = 7.3361(5) Å, b = 20.6719(14) Å, c = 17.8180(10) Å, β = 113.602(3)°, V = 2476.1(3) Å^3, Z = 4, D_c = 1.345 g/cm^3, μ(CuKα) = 0.090 mm^{-1}. Crystals (linear dimensions approx. 0.21 mm x 0.16 mm x 0.05 mm) were grown from slow evaporation of pentane/DCM at 25 °C. Number of measured and unique reflections 45502 and 5722, respectively (R_{int} = 0.0532). Final R_1 = 0.0421, wR_2 = 0.0966 for 5722 independent reflections with $I > 2\sigma(I)$, 346 parameters and $3.178 < 2\theta < 55.23°$ (corresponding R values based on all 45502 reflections are 0.0618 and 0.1057, respectively).

Crystal Data for 156b. Crystal data at 100 K for $C_{50}H_{32}N_4O_2$, M = 720.79 g mol^{-1}, triclinic, space group P-1, a = 11.0042(6) Å, b = 11.3825(6) Å, c = 15.6022(9) Å, β = 92.362(3)°, V = 2476.1(3) Å^3, Z = 4, D_c = 1.259 g/cm^3, μ(CuKα) = 0.612 mm^{-1}. Crystals (linear dimensions approx. 0.16 mm x 0.04 mm x 0.005 mm) were grown from slow evaporation of pentane/DCM at 25 °C. Number of measured and unique reflections 15783 and 6054, respectively (R_{int} = 0.0280). Final R_1 = 0.0280, wR_2 = 0.0966 for 6054 independent reflections with $I > 2\sigma(I)$, 505 parameters and $5.674 < 2\theta < 126.028°$ (corresponding R values based on all 15783 reflections are 0.0393 and 0.0901, respectively).

Crystal Data for 157a. Crystal data at 100 K for $C_{23}H_{14}N_4O_2$, M = 378.38 g mol^{-1}, monoclinic, space group $P2_1/c$, a = 9.4734(5) Å, b = 17.9231(9) Å, c =

11.6853(5) Å, β = 111.712(2)°, V = 1843.32(16) Å^3, Z = 4, D_c = 1.363 g/cm^3, μ(CuKα) = 0.090 mm^{-1}. Crystals linear dimensions approx. 0.4 mm x 0.26 mm x 0.16 mm) were grown from slow evaporation of pentane/DCM at 25 °C. Number of measured and unique reflections 27200 and 4192, respectively (R_{int} = 0.0368). Final R_1 = 0.0372, wR_2 = 0.0907 for 4192 independent reflections with $I > 2\sigma(I)$, 264 parameters and 4.628 < 2θ < 55.16° (corresponding R values based on all 27200 reflections are 0.0464 and 0.0965, respectively).

Crystal Data for 157b. Crystal data at 100 K for $C_{23}H_{14}N_4O_2$, M = 378.38 g mol^{-1}, monoclinic, space group $P2_1/c$, a = 7.3541(6) Å, b = 24.756(2) Å, c = 11.1721(8) Å, β = 113.219(5)°, V = 1869.2(3) Å^3, Z = 4, D_c = 1.345 g/cm^3, μ(CuKα) = 0.089 mm^{-1}. Crystals (linear dimensions approx. 0.4 mm x 0.26 mm x 0.16 mm) were grown from slow evaporation of pentane/DCM at 25 °C. Number of measured and unique reflections 25076 and 4315, respectively (R_{int} = 0.0392). Final R_1 = 0.0462, wR_2 = 0.1067 for 4315 independent reflections with $I > 2\sigma(I)$, 264 parameters and 3.29 < 2θ < 55.05° (corresponding R values based on all 25076 reflections are 0.0762 and 0.1224, respectively).

Crystal Data for 159. Crystal data at 100 K for $C_{18}H_{16}N_4O_2$, M = 320.35 g mol^{-1}, monoclinic, space group $P2_1$/c, a = 7.5360(3) Å, b = 27.7123(11) Å, c = 7.9319(3) Å, β = 91.601(2)°, V = 1655.85(11) Å^3, Z = 4, D_c = 1.285 g/cm^3, μ(CuKα) = 0.707 mm^{-1}. Clear dark red plates (linear dimensions approx. 0.2 mm x 0.14 mm x 0.01 mm) were grown from slow evaporation of hexane/CH_2Cl_2 solution at 25 °C. Number of measured and unique reflections 11551 and 2922 respectively (R_{int} = 0.0411). Final R_1 = 0.0380, wR_2 = 0.0989 for 2922 independent reflections with $I > 2\sigma(I)$, 244 parameters and 11.608 < 2θ < 135.092° (corresponding R values based on all 11551 reflections are 0.0441 and 0.1042, respectively).

Crystal Data for 160. Crystal data at 100 K for $C_{18}H_{16}N_4O_2$, M = 320.35 g mol^{-1}, orthorhombic, space group Pbca, a = 18.2514(14) Å, b = 8.6194(6) Å, c = 20.6536(16) Å, V = 3249.1(4) Å^3, Z = 8, D_c = 1.310 g/cm^3, μ(MoKα) = 0.089 mm^{-1}. Black needles (linear dimensions approx. 0.32 mm x 0.14 mm x 0.1 mm) were grown from slow evaporation of diethyl ether/pentane at 25 °C. Number of measured and unique reflections 46470 and 3753 respectively (R_{int} = 0.0568). Final R_1 = 0.0381,

wR_2 = 0.0877 for 3753 independent reflections with $I > 2\sigma(I)$, 220 parameters and 4.464 < 2θ < 55.168° (corresponding R values based on all 46470 reflections are 0.0575 and 0.0990, respectively).

Crystal Data for 163. Crystal data at 100 K for $C_{20}H_{21}N_3O_4$, M = 367.40 g mol^{-1}, triclinic, space group $P\bar{1}$, a = 7.1137(14) Å, b = 11.174(3) Å, c = 13.276(3) Å, α = 104.444(9)°, β = 95.541(8)°, γ = 105.628(9)°, V = 968.9(4) Å^3, Z = 2, D_c = 1.259 g/cm^3, μ(MoKα) = 0.089 mm^{-1}. Clear brownish red plates (linear dimensions approx. 0.26 mm x 0.22 mm x 0.06 mm) were grown from slow evaporation of hexane/CH_2Cl_2 solution at 25 °C. Number of measured and unique reflections 16697 and 4496 respectively (R_{int} = 0.0408). Final R_1 = 0.0429, wR_2 = 0.0890 for 4496 independent reflections with $I > 2\sigma(I)$, 248 parameters and 4.32 < 2θ < 55.532° (corresponding R values based on all 16697 reflections are 0.0702 and 0.1015, respectively).

Crystal Data for (±)-165. Crystal data at 100 K for $C_{20}H_{21}N_3O_4$, M = 367.40 g mol^{-1}, monoclinic, space group $P2_1/c$, a = 9.470(1) Å, b = 18.274(3) Å, c = 11.007(1) Å, β = 95.809(5)°, V = 1894.9(5) Å^3, Z = 4, D_c = 1.288 g/cm^3, μ(MoKα) = 0.091 mm^{-1}. Clear colorless needles (linear dimensions approx. 0.27 mm x 0.12 mm x 0.04 mm) were grown from slow evaporation of cyclohexane at 25 °C. Number of measured and unique reflections 20236 and 4362 respectively (R_{int} = 0.0461). Final R_1 = 0.0471, wR_2 = 0.1003 for 4362 independent reflections with $I > 2\sigma(I)$, 248 parameters and 4.324 < 2θ < 55.202° (corresponding R values based on all 20236 reflections are 0.0880 and 0.1165, respectively).

Crystal Data for 169. Crystal data at 100 K for $C_{22}H_{26}N_2O_6$, M = 414.45 g mol^{-1}, triclinic, space group $P\bar{1}$, a = 9.8154(6) Å, b = 10.3762(6) Å, c = 11.1204(6) Å, α = 80.806(2)°, β = 87.501(2)°, γ = 68.040(1)°, V = 1036.75(10) Å^3, Z = 2, D_c = 1.328 g/cm^3, μ(MoKα) = 0.097 mm^{-1}. Clear light yellow plates (linear dimensions approx. 0.2 mm x 0.13 mm x 0.04 mm) were grown from slow evaporation of cyclohexane at 25 °C. Number of measured and unique reflections 27249 and 4777 respectively (R_{int} = 0.0303). Final R_1 = 0.0339, wR_2 = 0.0832 for 4777 independent reflections with $I > 2\sigma(I)$, 287 parameters and 3.71 < 2θ < 55.042° (corresponding R values based on all 27249 reflections are 0.0436 and 0.0883,

respectively). One terminal methyl group of a COOEt ligand (C12 in Figure S9) is disordered over two positions (60:40 ratio).

Crystal Data for 170. Crystal data at 173 K for $C_{22}H_{26}N_2O_6$, M = 414.45 g mol^{-1}, triclinic, space group $P\bar{1}$, a = 7.0036(8) Å, b = 11.1692(14) Å, c = 14.5159(19) Å, α = 86.765(4)°, β = 88.293(4)°, γ = 77.786(4)°, V = 1107.8(2) Å^3, Z = 2, D_c = 1.242 g/cm^3, μ(MoKα) = 0.091 mm^{-1}. Clear orange blocks (linear dimensions approx. 0.35 mm x 0.29 mm x 0.16 mm) were grown from slow evaporation of hexane/CH_2Cl_2 at 25 °C. Number of measured and unique reflections 18393 and 5084 respectively (R_{int} = 0.0375). Final R_1 = 0.0484, wR_2 = 0.1140 for 5084 independent reflections with $I > 2\sigma(I)$, 276 parameters and 4.558 < 2θ < 55.026° (corresponding R values based on all 18393 reflections are 0.0789 and 0.1282, respectively). Below 150 K, the crystals undergo a phase transition which destroys them, hence the measurement was carried out at 173 K.

Crystal Data for 171. Crystal data at 100 K for $C_{22}H_{26}N_2O_6$, M = 414.45 g mol^{-1}, monoclinic, space group $P2_1/c$ a = 14.0585(8) Å, b = 12.3850(6) Å, c = 14.7990(8) Å, β = 121.324(4)°, V = 2201.1(2) Å^3, Z = 4, D_c = 1.251 g/cm^3, μ(MoKα) = 0.091 mm^{-1}. Clear orange plates (linear dimensions approx. 0.20 mm x 0.15 mm x 0.03 mm) were grown from slow evaporation of cyclohexane at 25 °C. Number of measured and unique reflections 23112 and 5051 respectively (R_{int} = 0.0549). Final R_1 = 0.0466, wR_2 = 0.0977 for 5051 independent reflections with $I > 2\sigma(I)$, 287 parameters and 4.604 < 2θ < 55.028° (corresponding R values based on all 23112 reflections are 0.0903 and 0.1144, respectively). One terminal methyl group of a COOEt ligand (C15 in Figure S13) is disordered over two positions (90:10 ratio).

Crystal Data for 175. Crystal data at 100 K for $C_{21}H_{24}N_2O_6$, M = 400.42 g mol^{-1}, monoclinic, space group $P2_1/c$, a = 10.2914(4) Å, b = 19.0858(7) Å, c = 13.2267(5) Å, β = 126.722(2)°, V = 2082.40(14) Å^3, Z = 4, D_c = 1.277 g/cm^3, μ(CuKα) = 0.782 mm^{-1}. Clear yellow plates (linear dimensions approx. 0.16 mm x 0.12 mm x 0.02 mm) were grown from slow evaporation of cyclohexane at 25 °C. Number of measured and unique reflections 14049 and 3618 respectively (R_{int} = 0.0355). Final R_1 = 0.0353, wR_2 = 0.0855 for 3618 independent reflections with $I > 2\sigma(I)$, 267 parameters and 9.266 < 2θ < 133.3° (corresponding R values based on all

14049 reflections are 0.0408 and 0.0894, respectively). The crystals diffracted very weakly, with some reflections already disappearing below the noise level approaching the standard resolution.

Crystal Data for (±)-193. Crystal data at 200 K for $C_{28}H_{30}N_4O_4$, M = 486.56 g mol^{-1}, triclinic, space group $P\bar{1}$, a = 13.3591(11) Å, b = 14.1483(11) Å, c = 15.5163(12) Å, α = 75.212(2)°, β = 73.446(2)°, γ = 68.270(2)°, V = 2574.2(4) Å^3, Z = 4, D_c = 1.255 g/cm^3, μ(CuKα) = 0.085 mm^{-1}. Clear colorless planks (linear dimensions approx. 0.12 mm x 0.05 mm x 0.03 mm) were crystallized by co-evaporation from Pentane/DCM 9:1 at 25 °C. Number of measured and unique reflections 22548 and 7392 respectively (R_{int} = 0.0447). Final R_1 = 0.0458, wR_2 = 0.0967 for 7392 independent reflections with $I > 2\sigma(I)$, 681 parameters and 3.144 < 2θ < 46.512° (corresponding R values based on all 22548 reflections are 0.0901 and 0.1134, respectively). The crystals undergo a destructive phase transition between 200 K and 150 K, and were accordingly measured at 200 K. At this temperature, the crystals diffracted very weakly, with the data not quite reaching the standard resolution (sin(θ)/λ = 0.556). The asymmetric unit contains both enantiomers. One terminal methyl group of a COOEt ligand of the *S* enantiomer (C28A (right)) is disordered over two positions (80:20 ratio).

Crystal Data for 196. Crystal data at 100 K for $C_{28}H_{30}N_4O_4 \cdot CH_2Cl_2$, M = 486.56 g mol^{-1}, triclinic, space group $P\bar{1}$, a = 10.5466(10) Å, b = 11.5371(13) Å, c = 13.1838(13) Å, α = 102.174(4)°, β = 108.408(3)°, γ = 95.016(4)°, V = 1467.2(3) Å^3, Z = 2, D_c = 1.101 g/cm^3, μ(MoKα) = 0.075 mm^{-1}. Clear orange plates (linear dimensions approx. 0.18 mm x 0.10 mm x 0.04 mm) were crystallized by co-evaporation from Pentane/DCM 9:1 at 25 °C. Number of measured and unique reflections 19936 and 6780 respectively (R_{int} = 0.0353). Final R_1 = 0.0495, wR_2 = 0.1309 for 6780 independent reflections with $I > 2\sigma(I)$, 331 parameters and 3.364 < 2θ < 55.284° (corresponding R values based on all 19936 reflections are 0.0716 and 0.1396, respectively). The unit cell additionally contains a dichloromethane molecule, which could clearly be identified but not modeled due to severe disorder. The solvent was removed from the data using the inbuilt masking procedure in Olex2, leaving a void in the affected position. The procedure was documented in the submitted cif file to allow reconstruction of the original data.

Crystal Data for 213. Crystal data at 100 K for $C_{22}H_{28}N_4O_4$, M = 412.48 g mol^{-1}, monoclinic, space group $P2_1/c$, a = 15.0264(17) Å, b = 19.058(2) Å, c = 15.9395(19) Å, β = 112.057(3)°, V = 4230.5(9) Å^3, Z = 8, D_c = 1.295 g/cm^3, μ(CuKα) = 0.091 mm^{-1}. Clear light red blocks (linear dimensions approx. 0.16 mm x 0.11 mm x 0.07 mm) were grown from slow evaporation of cyclohexane/ethyl acetate solution at 25 °C. Number of measured and unique reflections 70222 and 9755, respectively (R_{int} = 0.0490). Final R_1 = 0.0479, wR_2 = 0.1115 for 9755 independent reflections with $I > 2\sigma(I)$, 559 parameters and 2.924 < 2θ < 55.34° (corresponding R values based on all 70222 reflections are 0.0762 and 0.1261, respectively).

Crystal Data for 221. Crystal data at 100 K for $C_{20}H_{23}N_3O_4S$, M = 401.47 g mol^{-1}, monoclinic, space group $P2_1$, a = 8.5140(3) Å, b = 22.5000(7) Å, c = 11.0395(4) Å, β = 107.1540(10)°, V = 2020.71(12) Å^3, Z = 4, D_c = 1.320 g/cm^3, μ(CuKα) = 0.191 mm^{-1}. Clear dark yellow blocks (linear dimensions approx. 0.32 mm x 0.21 mm x 0.1 mm) were grown from slow evaporation of hexane/ethyl acetate solution at 25 °C. Number of measured and unique reflections 16283 and 9026, respectively (R_{int} = 0.0223). Final R_1 = 0.0328, wR_2 = 0.791 for 9026 independent reflections with $I > 2\sigma(I)$, 526 parameters and 3.62 < 2θ < 55.044° (corresponding R values based on all 16283 reflections are 0.0370 and 0.0812, respectively).

Crystal Data for 227. Crystal data at 100 K for $C_{20}H_{24}N_4O_4$, M = 384.43 g mol^{-1}, triclinic, space group $P\bar{1}$, a = 7.83118(6) Å, b = 10.2287(9) Å, c = 13.5191(12) Å, β = 106.051(3)°, V = 969.70(14) Å^3, Z = 2, D_c = 1.317 g/cm^3, μ(CuKα) = 0.094 mm^{-1}. Clear colorless blocks (linear dimensions approx. 0.32 mm x 0.16 mm x 0.11 mm) were grown from slow evaporation of hexane/ethyl acetate solution at 25 °C. Number of measured and unique reflections 11055 and 4491, respectively (R_{int} = 0.0267). Final R_1 = 0.0400, wR_2 = 0.0969 for 4491 independent reflections with $I > 2\sigma(I)$, 269 parameters and 4.274 < 2θ < 55.354° (corresponding R values based on all 11055 reflections are 0.0526 and 0.1044, respectively).

Crystal Data for 229. Crystal data at 100 K for $C_{20}H_{22}N_4O_6$, M = 414.41 g mol^{-1}, monoclinic, space group $P2_1/c$, a = 9.5426(6) Å, b = 13.1663(9) Å, c = 16.2954(10) Å, β = 101.215(2)°, V = 2008.3(2) Å^3, Z = 4, D_c = 1.371 g/cm^3, μ(CuKα) = 0.103 mm^{-1}. Clear orange blocks (linear dimensions approx. 0.22 mm x

0.2 mm x 0.12 mm) were grown from slow evaporation of cyclohexane/ethyl acetate solution at 25 °C. Number of measured and unique reflections 17387 and 4603, respectively (R_{int} = 0.0528). Final R_1 = 0.0478, wR_2 = 0.1049 for 4603 independent reflections with $I > 2\sigma(I)$, 307 parameters and $4.352 < 2\theta < 54.968°$ (corresponding R values based on all 17387 reflections are 0.0789 and 0.1195, respectively).

Crystal Data for 255. Crystal data at 100 K for $C_{22}H_{18}N_2O_4$, M = 374.38 g mol^{-1}, monoclinic, space group *C*c, a = 18.610(3) Å, b = 13.797(3) Å, c = 7.7321(12) Å, β = 104.984(6)°, V = 1917.8(6) Å^3, Z = 4, D_c = 1.297 g/cm^3, μ(CuKα) = 0.090 mm^{-1}. Clear orange blocks (linear dimensions approx. 0.24 mm x 0.05 mm x 0.03 mm) were grown from slow evaporation of cyclohexane/ethyl acetate solution at 25 °C. Number of measured and unique reflections 7243 and 3812, respectively (R_{int} = 0.0528). Final R_1 = 0.0552, wR_2 = 0.0943 for 3812 independent reflections with $I > 2\sigma(I)$, 255 parameters and $5.906 < 2\theta < 55.19°$ (corresponding R values based on all 7243 reflections are 0.0995 and 0.1089, respectively).

Crystal Data for 258. Crystal data at 100 K for $C_{20}H_{17}N_3O_4$, M = 363.36 g mol^{-1}, orthorhombic, space group Pbca, a = 7.7159(6) Å, b = 12.5831(9) Å, c = 37.373(3) Å, β = 90°, V = 3628.6(5) Å^3, Z = 4, D_c = 1.330 g/cm^3, μ(CuKα) = 0.095 mm^{-1}. Clear yellow pale blocks (linear dimensions approx. 0.21 mm x 0.19 mm x 0.04 mm) were grown from slow evaporation of pentane/CH_2Cl_2 solution at 25 °C. Number of measured and unique reflections 34462 and 4161, respectively (R_{int} = 0.0478). Final R_1 = 0.0470, wR_2 = 0.1007 for 4161 independent reflections with $I > 2\sigma(I)$, 249 parameters and $5.712 < 2\theta < 55.14°$ (corresponding R values based on all 4161 reflections are 0.0601 and 0.1058, respectively).

Crystal Data for 262. Crystal data at 100 K for $C_{19}H_{18}N_2O_4$, M = 338.35 g mol^{-1}, triclinic, space group P-1, a = 7.1902(4) Å, b = 9.9128(6) Å, c = 13.7914(7) Å, α = 110.135(2) β = 95.686(2)°, γ = 102.891(2), V = 882.88(9) Å^3, Z = 2, D_c = 1.273 g/cm^3, μ(CuKα) = 0.090 mm^{-1}. Clear light yellow blocks (linear dimensions approx. 0.30 mm x 0.20 mm x 0.06 mm) were grown from slow evaporation of pentane/CH_2Cl_2 solution at 25 °C. Number of measured and unique reflections 15513 and 4088, respectively (R_{int} = 0.0271). Final R_1 = 0.0376, wR_2 = 0.0883 for 4088 independent reflections with $I > 2\sigma(I)$, 229 parameters and $3.206 < 2\theta < 55.2°$

(corresponding R values based on all 4088 reflections are 0.0511 and 0.0971, respectively).

Crystal Data for 269. Crystal data at 100 K for $C_{26}H_{25}N_3O_6S$, M = 507.55 g mol^{-1}, triclinic, space group P-1, a = 10.1160(4) Å, b = 11.5544(4) Å, c = 11.7110(4) Å, α = 87.1294(9)° β = 78.5789(8)°, γ = 71.8413(8), V = 1274.81(8) Å^3, Z = 2, D_c = 1.322 g/cm^3, μ(CuKα) = 0.173 mm^{-1}. clear colorless irregular blocks (linear dimensions approx. 0.37 mm x 0.25 mm x 0.12 mm) were grown from slow evaporation of pentane/CH_2Cl_2 solution at 25 °C. Number of measured and unique reflections 29782 and 7766, respectively (R_{int} = 0.0183). Final R_1 = 0.0312, wR_2 = 0.0845 for 7766 independent reflections with $I > 2\sigma(I)$, 328 parameters and 3.548 < 2θ < 61.126° (corresponding R values based on all 4088 reflections are 0.0358 and 0.0882, respectively).

8.3.2. ORTEP Representation

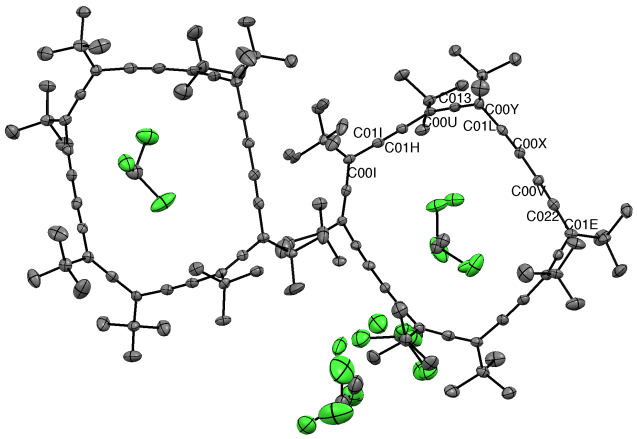

Figure 61. ORTEP representation of the molecular structure of $(P)_4$-(–)-**33a** (100 K, crystallized from *n*hexane/chloroform 9:1). Thermal ellipsoids are shown at the 50% probability level. Hydrogens are omitted for clarity. Selected bond lengths [Å] and bond angles [°]: C001–C01I 1.434(7), C01I–C01H 1.200(7), C01H–C00U 1.434(7), C00U–C013 1.312(7), C013–C01L 1.314(7), C01L–C00Y 1.438(7), C00Y–C00X

1.192(7), C00X–C00V 1.385(7), C00V–C022 1.194(7), C022–C01E 1.440(7); C01H–C00U-C013 118.8(5), C013–C01L–C00Y 117.3(5).

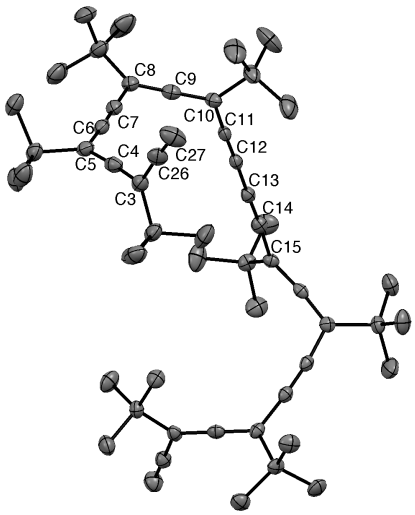

Figure 62. ORTEP representation of the molecular structure of $(P)_4$-(+)-**109** (100 K, crystallized from *n*hexane/chloroform 9:1). Thermal ellipsoids are shown at the 50% probability level. Hydrogens are omitted for clarity. Selected bond lengths [Å] and bond angles [°]: C3–C4 1.314(4), C4–C5 1.317(4), C5–C6 1.437(4), C6–C7 1.201(4), C7–C8 1.436(4), C8–C9 1.316(4), C9–C10 1.318(4), C10–C11 1.438(4), C11–C12 1.203(4), C12–C13 1.380(4), C13–C14 1.204(4), C14–C15 1.432(4), C3–C26 1.443(4), C26–C27 1.179(4); C3–C4-C5 176.1(3), C4–C5–C6 120.0(3), C7–C8–C9 117.9(3), C9–C10–C11 120.1(3), C10–C11–C12 176.9(3).

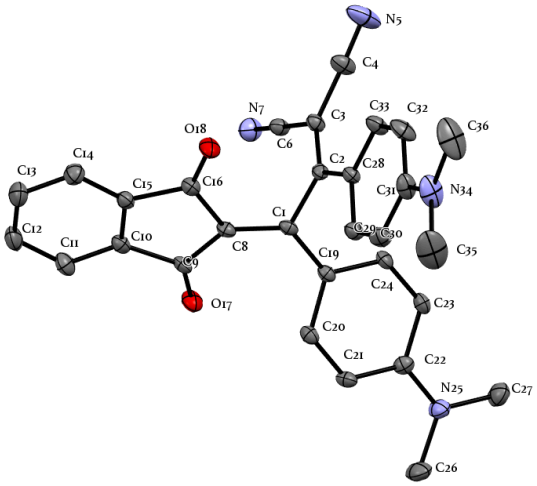

Figure 63. ORTEP representation of the molecular structure of **133a** (100 K, crystallized by co-evaporation from Pentane/DCM 9:1). Thermal ellipsoids are shown at the 50% probability level. Hydrogens are omitted for clarity. Selected bond lengths [Å] and bond angles [°]: C1-C8 1.380(3), C8-C9 1.480(3), C9-C10 1.497(3), C10-C11 1.388(3), C11-C12 1.390(3), C12-C13 1.395(3), C19-C24 1.416(2), C22-C23 1.423(3), C23-C24 1.371(3), C8-C1-C2-C3 -76.6(2), C19-C1-C2-C3 101.5(2), C19-C1-C2-C28 -78.2(2).

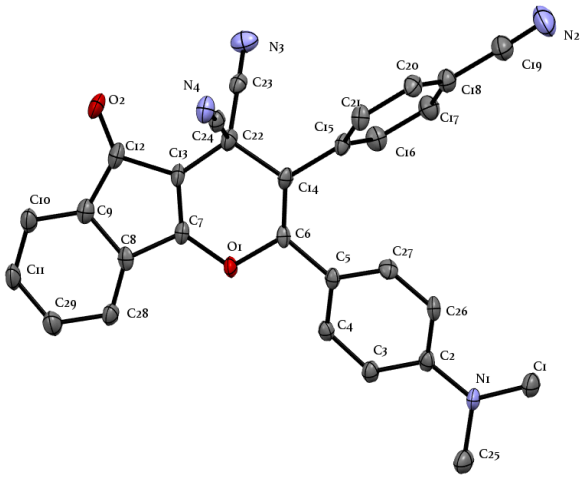

Figure 64. ORTEP representation of the molecular structure of **150a** (100 K, crystallized by co-evaporation from Pentane/DCM 9:1). Thermal ellipsoids are shown at the 50% probability level. Hydrogens are omitted for clarity. Selected bond lengths [Å] and bond angles [°]: C35-C36 1.445(3), C36-C37 1.511(3), C36-C58 1.511(3), C37-C49 1.345(3), C37-C38 1.488(3), C49-C37-C38-C48 111.5(2), C49-C37-C38-C39 -66.0(3).

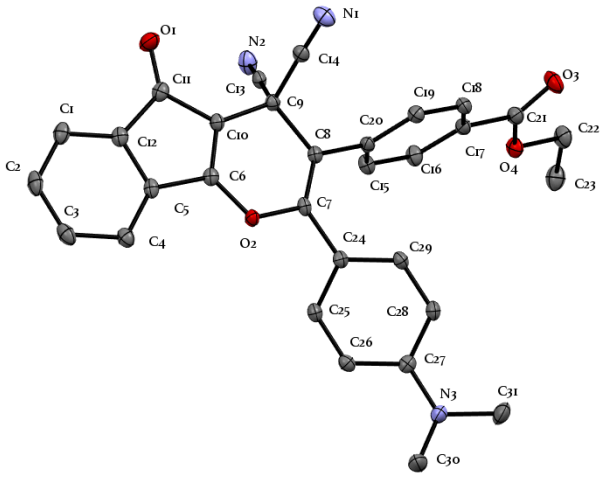

Figure 65: ORTEP representation of the molecular structure of **151b** (100 K, crystallized by co-evaporation from Pentane/DCM 9:1). Thermal ellipsoids are shown at the 50% probability level. Hydrogens are omitted for clarity. Selected bond lengths [Å] and bond angles [°]: C1-C2 1.403(2), C2-C3 1.382(2), C3-C4 1.407(2), C4-C5 1.373(2), C5-C6 1.4682(18), C7-C8 1.3504(19), C8-C9 1.5474(19), C9-C10 1.4995(19), C7-C24 1.4697(19), C24-C25 1.4037(19), C25-C26 1.377(2), C26-C27 1.4085(19), O2-C7-C8-C20 -172.18(14), C7-O2-C6-C10 -10.0(2).

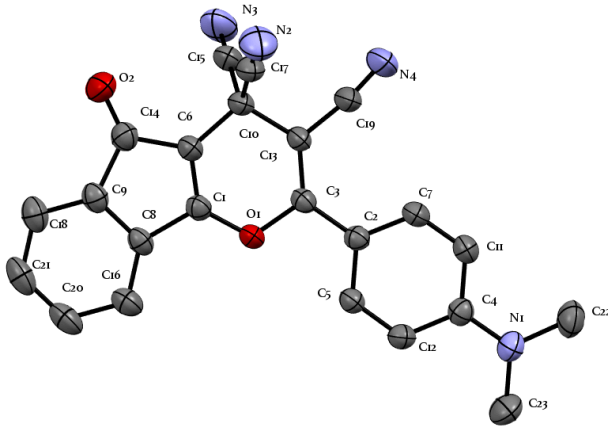

Figure 66. ORTEP representation of the molecular structure of **157b** (100 K, crystallized by co-evaporation from Pentane/DCM 9:1). Thermal ellipsoids are shown at the 50% probability level. Hydrogens are omitted for clarity. Selected bond lengths [Å] and bond angles [°]: C4-C11 1.408(2), C7-C11 1.359(2), C2-C7 1.402(2), C2-C3 1.445(2), C3-C13 1.362(2), C10-C13 1.534(2), C9-C18 1.376(2), C18-C21 1.396(3), C7-C2-C3-C13 10.8(3), O1-C1-C6-C10 3.2(3), O1-C1-C6-C14 178.80(14).

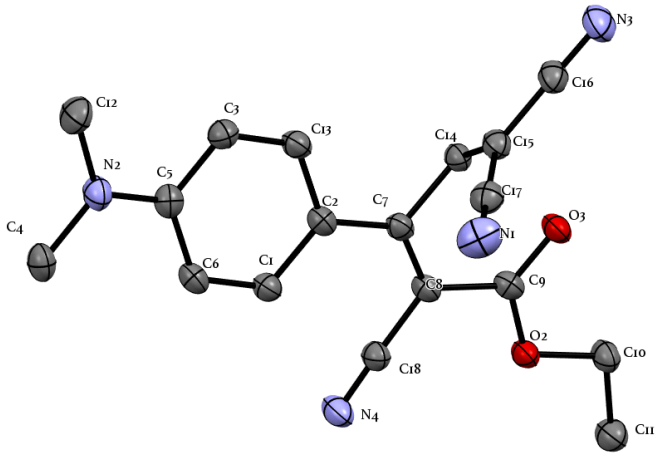

Figure 67. ORTEP plot of **159**, arbitrary numbering, H-atoms omitted for clarity. Atomic displacement parameters at 100 K are drawn at 50% probability level. Selected bond lengths (Å), angles (°), and torsional angles (°): C5–C3 1.412(2), C5–C6 1.419(2), C3–C13 1.371(2), C6–C1 1.370(2), C13–C2 1.414(2), C1–C2 1.410(2), C7–C8 1.377(2), C14–C15 1.340(2), C8–C18 1.430(2), C8–C9 1.482(2), C18-C8-C9 115.3(1), C17-C15-C16 116.8(1), C1-C2-C7-C8 16.1(2) C1-C2-C7-C14 –164.6(1), C15-C14-C7-C8 –110.4(1), C2-C7-C14-C15 70.2(2).

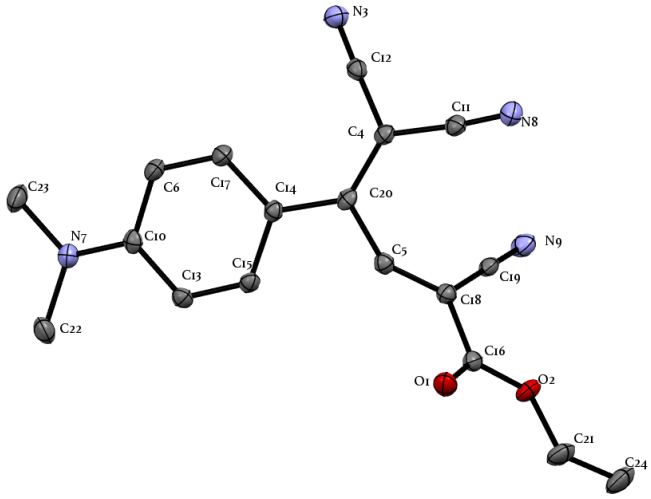

Figure 68. ORTEP plot of **160**, arbitrary numbering, H-atoms omitted for clarity. Atomic displacement parameters at 100 K are drawn at 50% probability level. Selected bond lengths (Å), angles (°), and torsional angles (°): C10–C13 1.414(2), C10–C6 1.416(2), C6–C17 1.369(2), C13–C15 1.366(2), C15–C14 1.407(2), C17–C14 1.412(2), C20–C4 1.375(2), C5–C18 1.3332(2), C12-C4-C11 113.0(1), C17-C14-C20-C4 –16.9(2), C17-C14-C20-C5 162.0(1), C4-C20-C5-C18 –58.5(2).

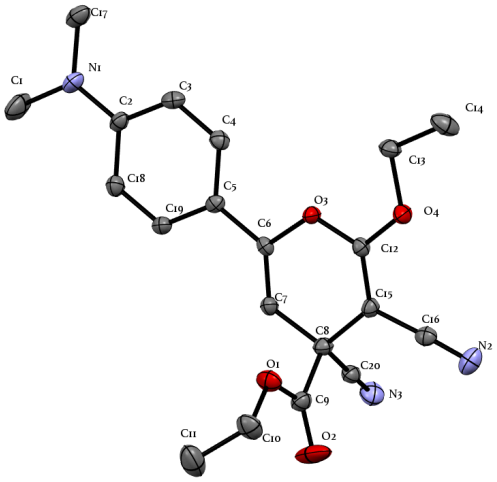

Figure 69. ORTEP plot of (±)-**159**, arbitrary numbering, H-atoms omitted for clarity. Atomic displacement parameters at 100 K are drawn at 50% probability level. Selected bond lengths (Å), angles (°), and torsional angles (°): C2–C3 1.408(2), C2–C18 1.404(2), C18–C19 1.375(2), C3–C4 1.376(2), C4–C5 1.392(2), C19–C5 1.391(2), C6–C7 1.318(2), C12–C15 1.343(2), O4–C12 1.313(2), C15–C16 1.420(2), C9-C8-C20 106.4(1), C6-O3-C12 118.7(1), C4-C5-C6-O3 6.1(2) C4-C5-C6-C7 –173.0(2).

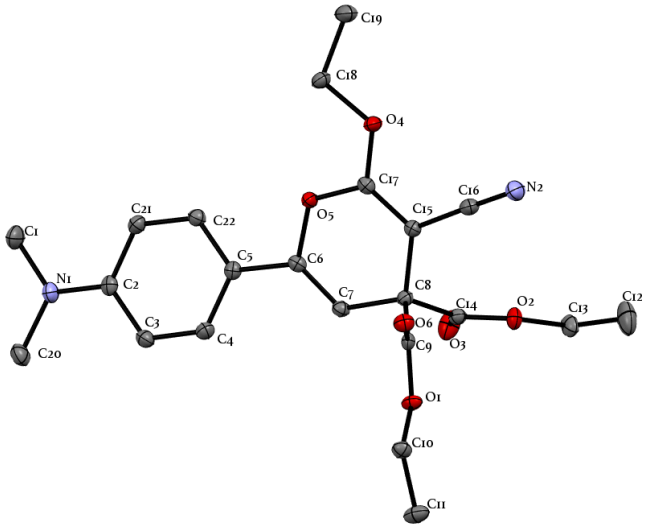

Figure 70. ORTEP plot of **169**, arbitrary numbering, H-atoms omitted for clarity. Atomic displacement parameters at 100 K are drawn at 50% probability level. Selected bond lengths (Å), angles (°), and torsional angles (°): C2–C3 1.416(1), C2–C21 1.413(2), C21–C22 1.381(2), C3–C4 1.378(2), C4–C5 1.402(2), C22–C5 1.398(1), C6–C18 1.328(1), C15–C17 1.353(1), O4–C17 1.323(2), C15–C16 1.425(2), C9-C8-C14 110.51(9), C6-O5-C17 118.63(9), C8-C7-C6-C18 –23.7(2) C22-C5-C6-O5 13.9(1), C22-C5-C6-C7 –165.2(1).

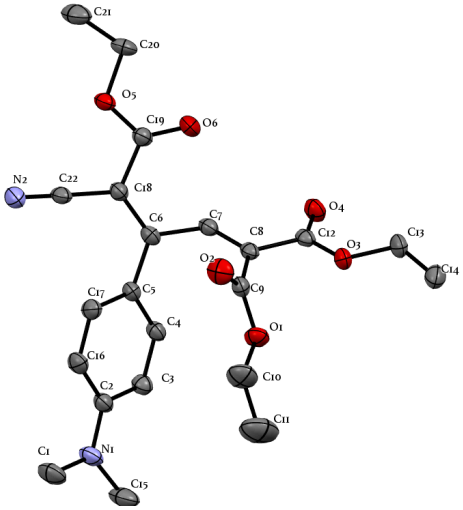

Figure 71. ORTEP plot of **170**, arbitrary numbering, H-atoms omitted for clarity. Atomic displacement parameters at 100 K are drawn at 50% probability level. Selected bond lengths (Å), angles (°), and torsional angles (°): C2–C3 1.408(2), C2–C16 1.405(2), C16–C17 1.375(2), C3–C4 1.375(2), C4–C5 1.401(2), C17–C5 1.399(2), C6–C18 1.363(2), C7–C8 1.328(2), C18–C22 1.431(2), C18–C19 1.486(2), C8–C9 1.499(2), C8–C12 1.491(2), C22-C18-C19 116.0(1), C9-C8-C12 120.6(1), C17-C5-C6-C18 –33.2(2) C17-C5-C6-C7 146.0(2), C5-C6-C7-C8 –52.6(2).

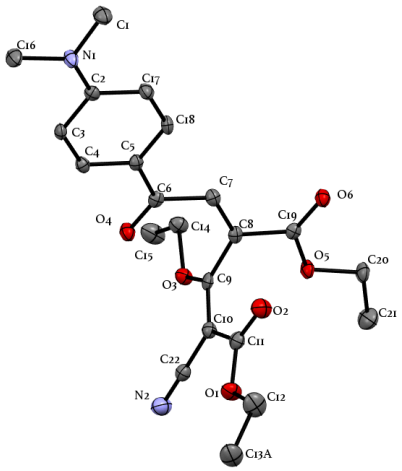

Figure 71. ORTEP plot of **171**, arbitrary numbering, H-atoms omitted for clarity. Atomic displacement parameters at 100 K are drawn at 50% probability level. Selected bond lengths (Å), angles (°), and torsional angles (°): C2–C3 1.418(2), C2–C17 1.414(3), C17–C18 1.374(2), C3–C4 1.370(2), C4–C5 1.404(3), C18–C5 1.401(2), C7–C8 1.332(2), C9–C10 1.356(3), O3–C9 1.333(2), O9–C8 1.501(2), C10–C11 1.466(3), C10–C22 1.433(2), C7-C8-C19 119.2(2), O3-C9-C10 117.0(2), C22-C10-C11 119.3(2), C18-C5-C6-C7 –0.2(3), C7-C8-C9-C10 –100.0(2).

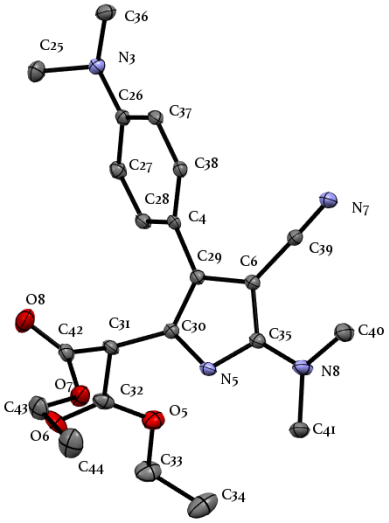

Figure 72. ORTEP plot of **213**, arbitrary numbering, H-atoms omitted for clarity. Atomic displacement parameters at 100 K are drawn at 50% probability level. Selected bond lengths (Å), angles (°), and torsional angles (°):C26–C37 1.400(2), C37–C38 1.383(2), C27–C28 1.387(2), C28–C4 1.399(2), C4–C38 1.400(2), C4–C29 1.474(2), N5–C30 1.394(2), C29–C30 1.366(2), C6–C29 1.448(2), C6–C35 1.398(2), C35–N5 1.365(2), C35–N8 1.379(2), C6–C39 1.417(2), C29-C30-C31 108.7(1), C35-N8-C41 113.1(1), C30-C29-C4-C28 130.3(2).

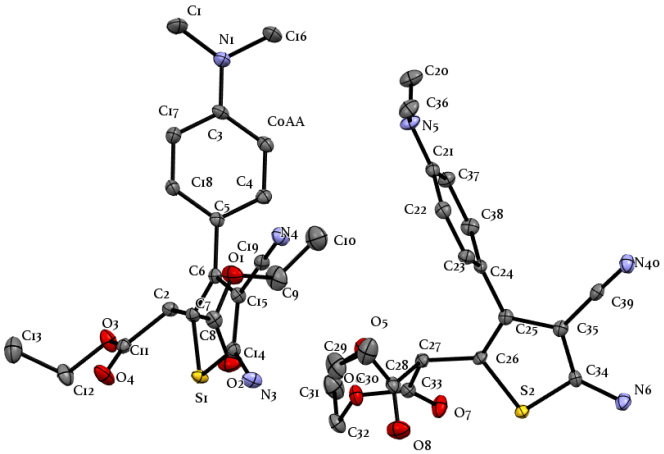

Figure 73. ORTEP plot of **221**, arbitrary numbering, H-atoms omitted for clarity. Atomic displacement parameters at 100 K are drawn at 50% probability level. Selected bond lengths (Å), angles (°), and torsional angles (°): C20–C17 1.411(4), C20–C3 1.401(4), C3–C4 1.388(3), C17–C18 1.382(3), C18–C5 1.389(4), C5–C4 1.403(4), C5–C6 1.482(3), S1–C7 1.750(2), C7–C6 1.358(3), C6–C15 1.444(4), C15–C14 1.390(3), C14–S1 1.729(3), C14–N3 1.356(4), C15–C19 1.418(3), C7–C2 1.505(4), C8-C2-C11 108.6(2), C7-C6-C5-C4 –105.0(3).

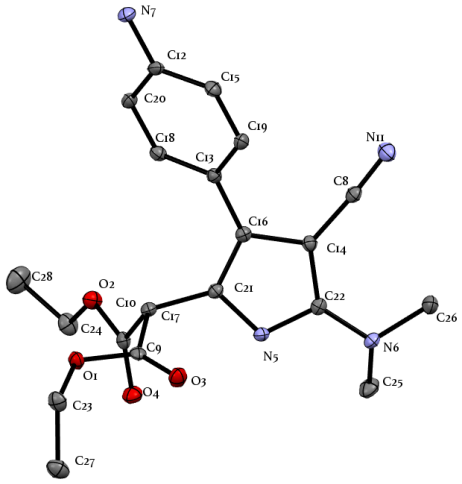

Figure 74. ORTEP plot of **227**, arbitrary numbering, H-atoms omitted for clarity. Atomic displacement parameters at 100 K are drawn at 50% probability level. Selected bond lengths (Å), angles (°), and torsional angles (°): C12–C20 1.380(2), C12–C15 1.385(3), C15–C19 1.382(3), C18–C20 1.388(3), C13–C18 1.399(3), C13–C19 1.395(2), C13–C16 1.473(3), N5–C21 1.384(2), C16–C21 1.360(2), C13–C16 1.451(3), C14–C22 1.392(2), C22–N5 1.369(2), C22–N8 1.365(2), C17–C21 1.497(2), C22-N8-C25 116.2(2), C21-C16-C13-C19 145.0(2).

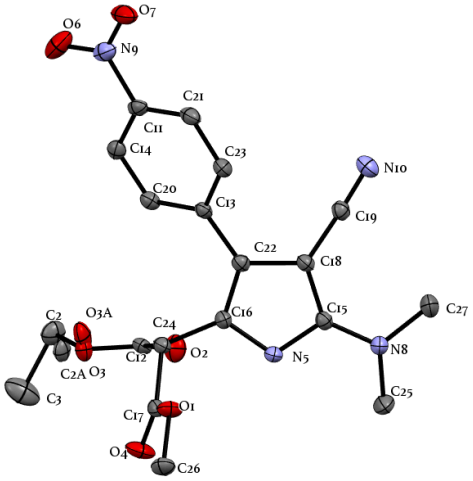

Figure 75. ORTEP plot of **229**, arbitrary numbering, H-atoms omitted for clarity. Atomic displacement parameters at 100 K are drawn at 50% probability level. Selected bond lengths (Å), angles (°), and torsional angles (°): C11–C14 1.380(2), C11–C21 1.385(3), C21–C23 1.382(3), C14–C20 1.388(3), C20–C13 1.399(3), C23–C13 1.395(2), C13–C22 1.473(3), N5–C16 1.384(2), C16–C22 1.360(2), C22–C18 1.451(3), C18–C15 1.392(2), C15–N5 1.369(2), C15–N8 1.365(2), C16–C24 1.497(2), C25-N8-C27 116.2(2), C12-C24-C27 108.5(1), C16-C22-C13-C23 145.0(2).

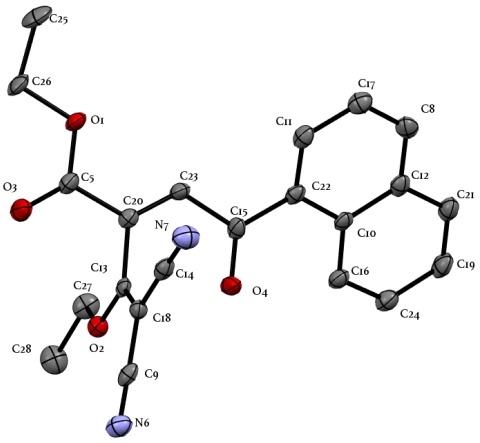

Figure 76. ORTEP representation of the molecular structure of **255** (100 K, crystallized from pentane/DCM 9:1). Thermal ellipsoids are shown at the 50% probability level. Hydrogens are omitted for clarity. Selected bond lengths [Å] and bond torsions [°]: C5–C20 1.502(6), C13–C18 1.360(6), C18–C20 1.504(6), C20–C23 1.341(6), C10–C14 1.4925(15), C14–C15 1.3593(17), C13–C18–C20–C23 92.6(5).

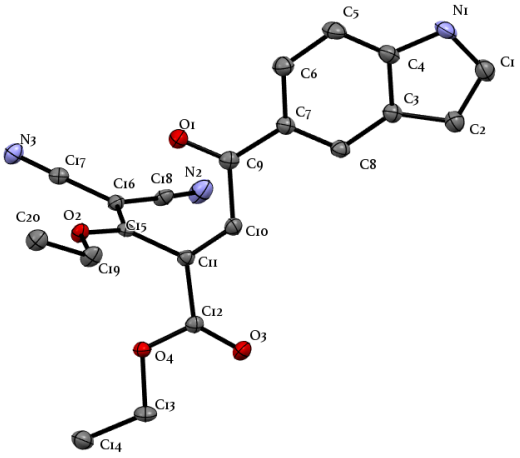

Figure 77. ORTEP representation of the molecular structure of **258** (100 K, crystallized from pentane/DCM 9:1). Thermal ellipsoids are shown at the 50% probability level. Hydrogens are omitted for clarity. Selected bond lengths [Å] and bond torsions [°]: C10–C11 1.334(2), C11–C15 1.498(2), C15–C16 1.365(2), C10–C11–C15–C16 84.7(2).

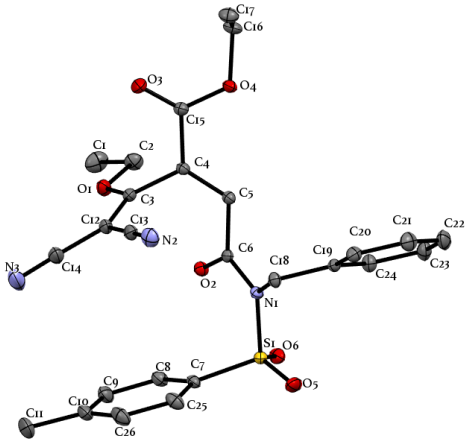

Figure 78. ORTEP representation of the molecular structure of **269** (100 K, crystallized from pentane/DCM 9:1). Thermal ellipsoids are shown at the 50% probability level. Hydrogens are omitted for clarity. Selected bond lengths [Å] and bond torsions [°]: C3–C4 1.4909(12), C4–C5 1.3347(12), C5–C6 1.4977(11), C12–C3–C4–C5 71.92(11).

Chapter 9

References

9. References

[1] T. N. Hoheisel, S. Schrettl, R. Szilluweit, H. Frauenrath, *Angew. Chem.* **2010**, *122*, 6644–6664; *Angew. Chem. Int. Ed.* **2010**, *49*, 6496–6515. Nanostructured Carbonaceous Materials from Molecular Precursors.

[2] A. Hirsch, *Nat Mater.* **2010**, *9*, 868–871. The era of carbon allotropes.

[3] J. Liu, J. W. Y. Lam, B. Z. Tang, *Chem. Rev.* **2009**, *109,* 5799–5867. Acetylenic Polymers: Syntheses, Structures, and Functions.

[4] U. H. F. Bunz, Y. Rubin, Y. Tobe, *Chem. Soc. Rev.* **1999**, *28*, 107–109. Polyethynylated cyclic π-systems: scaffoldings for novel two and three-dimensional carbon networks.

[5] G. P. Moss, P. A. S. Smith, D. Tavernier, *Pure Appl. Chem*. **1995**, *67*, 1307–1375. Glossary of Class Names of Organic Compounds and Reactivity Intermediates Based on Structure.

[6] J. H. van't Hoff, *La Chimie Dans L'espace*, Bazemdijk, Rotterdam, **1875**.

[7] P. Maitland, W. H. Mills, *Nature* **1935**, *135*, 994. Experimental Demonstration of the Allene Asymmetry.

[8] W. R. Roth, G. Ruf, P. W. Ford, *Chem. Ber*. **1974**, *107*, 48–52. Rotational Barrier in 1,2-Dienes - Resonance Energy of Allylic Radical.

[9] *Allenes in Organic Synthesis*, (Eds.: H. F. Schuster, G. M. Coppola), Wiley-Interscience, New York, **1984**.

[10] *Modern Allene Chemistry*, (Eds.: N. Krause, A. S. K. Hashmi), Wiley-VCH, Weinheim, **2004**.

[11] S. C. Yu, S. M. Ma, *Chem. Commun.* **2011**, *47*, 5384–5418. How Easy Are the Syntheses of Allenes?

[12] S. M. Ma, *Chem. Rev*. **2005**, *105*, 2829–2871. Some Typical Advances in

the Synthetic Applications of Allenes.

[13] A. Hoffmann-Röder, N. Krause, *Angew. Chem.* **2004**, *116*, 1216–1236; *Angew. Chem. Int. Ed*. **2004**, *43*, 1196–1216. Synthesis and Properties of Allenic Natural Products and Pharmaceuticals.

[14] X. T. Pu, X. B. Qi, J. M. Ready, *J. Am. Chem. Soc*. **2009**, *131*, 10364–10365. Allenes in Asymmetric Catalysis: Asymmetric Ring Opening of meso-Epoxides Catalyzed by Allene-Containing Phosphine Oxides.

[15] F. Cai, X. Pu, X. Qi, V. Lynch, A. Radha, J. M. Ready*, J. Am. Chem. Soc.* **2011**, *113*, 12066–18069. Chiral Allene-Containing Phosphines in Asymmetric Catalysis.

[16] M. Alcarazo, C. W. Lehmann, A. Anoop, W. Thiel, A. Fürstner, *Nat. Chem.* **2009**, *1*, 295–301. Coordination Chemistry at Carbon.

[17] M. Melaimi, M. Soleilhavoup, G. Bertrand, *Angew. Chem*. **2010**, *122*, 8992–9032; *Angew. Chem. Int. Ed.* **2010**, *49*, 8810–8849. Stable Cyclic Carbenes and Related Species Beyond Diaminocarbenes.

[18] M. Alcarazo, *Dalton Trans*. **2011**, *40*, 1839–1845. On the Metallic Nature of Carbon in Allenes and Heterocumulenes.

[19] B. S. Burton, H. von Pechmann, *Ber. Dtsch. Chem. Ges.* **1887**, *20*, 145–149**.** Ueber die Einwirkung von Chlorphosphor auf Acetondicarbonsäureäther.

[20] E. R. H. Jones, G. H. Mansfield, M. L. H. Whiting, *J. Chem. Soc*. **1954**, 3208–3212. Researches on acetylenic compounds. Part XLVII. The prototropic rearrangements of some acetylenic dicarboxylic acids.

[21] C. J. Elsevier, P. J. Vermeer, *J. Org. Chem.* **1989**, *54*, 3726–3730. Synthesis and stereochemistry of allenes. Part 3. Highly stereoselective synthesis of chiral alkyl allenes by organocopper(I)-induced anti 1,3-substitution of chiral propynyl esters.

[22] O. W. Gooding, C. C. Beard, D. Y. Jackson, D. L. Wren, G. F. Cooper, *J. Org. Chem.* **1991**, *56*, 1083–1088. Enantioselective Formation of Functionalized 1,3-Disubstituted Allenes: Synthesis of α–Allenic ω-Carbomethoxy Alcohols of High Optical Purity.

[23] K. Zab, H. Kruth, C. Tschierske, *J. Chem. Soc., Chem. Commun*. **1996**, 977–978. Liquid-crystalline allene derivatives.

[24] K. M. Brummond, A. D. Kerekes, H. Wan, *J. Org. Chem.* **2002**, *67*, 5156–5163. Chiral Nonracemic α-Alkylidene and *α*-Silylidene Cyclopentenones from Chiral Allenes Using an Intramolecular Allenic Pauson−Khand-Type Cycloaddition.

[25] C. Zelder, N. Krause, Eur. *J. Org. Chem*. **2004**, 3968–3971. Enantioselective Synthesis and Circular Dichroism of Endocyclic Allenes.

[26] M. Yoshida, T. Gotou, M. Ihara, *Tetrahedron Lett*. **2004**, *45*, 5573–5575. Palladium-Catalyzed Direct Coupling Reaction of Propargylic Alcohols with Arylboronic Acids.

[27] M. Yoshida, H. Ueda, M. Ihara, *Tetrahedron Lett*. **2005**, *46*, 6705–6708. Palladium-Catalyzed Coupling Reaction of Propargylic Oxiranes with Arylboronic Acids in Aqueous Media.

[28] R. Riveiros, D. Rodriguez, J. P. Sestelo, L. A. Sarandeses, *Org. Lett*. **2006**, *8*, 1403–1406. Palladium-Catalyzed Cross-Coupling Reaction of Triorganoindium Reagents with Propargylic Esters.

[29] X. Pu, J. M. Ready, *J. Am. Chem. Soc.* **2008**, *13*0, 10874–10875. Direct and Stereospecific Synthesis of Allenes via Reduction of Propargylic Alcohols with $Cp_2Zr(H)Cl$.

[30] M. A. Schade, S. Yamada, P. Knochel, *Chem. Eur. J.* **2011**, *17*, 4232–4237. Synthesis of Polyfunctional Allenes by Successive Copper-Mediated Substitutions.

[31] H. Li, D. Grassi, L. Guénée, T. Bürgi, A. Alexakis, *Chem. Eur. J.* **2014**, *20*, 16694–16706. Copper-Catalyzed Propargylic Substitution of Dichloro Substrates: Enantioselective Synthesis of Trisubstituted Allenes and Formation of Propargylic Quaternary Stereogenic Centers.

[32] R. C. Livingston, L. R. Cox, V. Gramlich, F. Diederich, *Angew. Chem*. **2011**, *113*, 2396–2399; *Angew. Chem. Int. Ed*. **2011**, *40*, 2334–2337. 1,3-Diethynylallenes: New Modules for Three-Dimensional Acetylenic Scaffolding

[33] R. Livingston, L. R. Cox, S. Odermatt, F. Diederich, *Helv. Chim. Acta* **2002**, *85*, 3052–3077. 1,3-Diethynylallenes: Carbon-Rich Modules for Three-Dimensional Acetylenic Scaffolding.

[34] M. K. J. ter Wiel, S. Odermatt, P. Schanen, P. Seiler, F. Diederich, *Eur. J. Org. Chem.* **2007**, 3449–3462. 1,3-Diethynylallenes: Stable Monomers, Length-Defined Oligomers, Asymmetric Synthesis, and Optical Resolution.

[35] J. L. Alonso-Gómez, P. Schanen, P. Rivera-Fuentes, P. Seiler, F. Diederich, *Chem. Eur. J.* **2008**, *14*, 10564–10568. 1,3-Diethynylallenes (DEAs): Enantioselective Synthesis, Absolute Configuration, and Chiral Induction in 1,1,4,4-Tetracyanobuta-1,3-Dienes (TCBDs).

[36] P. Rivera-Fuentes, F. Diederich, *Angew. Chem*. **2012**, *124*, 2872–2882; *Angew. Chem. Int. Ed*. **2012**, *51*, 2818–2828. Allenes in Molecular Materials.

[37] *Cumulenes and Allenes, Science of Synthesis, Vol. 44* (Ed.: N. Krause) Thieme: Stuttgart, Germany, **2007**.

[38] *Modern Allene Chemistry, Vol. 2* (Eds.: N. Krause, A. S. K. Hashmi), Wiley-VCH: Weinheim, Germany, **2008**.

[39] F. Diederich, *Cyclophanes, Monographs in Supramolecular Chemistry*, Vol. 2 (Ed.: J. F. Stoddart), Royal Society of Chemistry, Cambridge, **1991**.

[40] F.Vögtle, *Cyclophane Chemistry*, Wiley, New York, **1993**.

[41] H. Hopf, R. Gleiter, *Modern Cyclophane Chemistry,* Wiley-VCH,

Chichester, **2004**.

[42] J. Bodwell, T. Sato, *Angew. Chem*. **2002**, *114*, 4175–4177; *Angew. Chem. Int. Ed.* **2002**, *41*, 4003–4005. "Polyunsaturated" Cyclophanes.

[43] A. Urbano, *Angew. Chem*. **2003**, *115*, 4116–4119; *Angew. Chem. Int. Ed*. **2003**, *42*, 3986–3989. Recent Developments in the Synthesis of Helicene-Like Molecules.

[44] M. M. Haley, J. J. Pak, S. C. Brand, *Top. Curr. Chem*. **1999**, *201*, 81–130. Macrocyclic Oligo (phenylacetylenes) and Oligo(phenyldiacetylenes).

[45] U. H. Bunz, Y. Rubin, Y. Tobe, *Chem. Soc. Rev.* **1999**, *28*, 107–119. Polyethynylated cyclic π-systems: scaffoldings for novel two and three-dimensional carbon networks.

[46] C. Grave, A. D. Schlüter, *Eur. J. Org. Chem.* **2002**, 3075–3098. Shape-Persistent, Nano-Sized Macrocycles.

[47] D. Zhao, J. S. Moore, *Chem. Commun.* **2003**, 807–818. Shape-persistent arylene ethynylene macrocycles: syntheses and supramolecular chemistry.

[48] J. A. Marsden, G. J. Palmer, M. M. Haley, *Eur. J. Org. Chem*. **2003**, 2355–2369. Synthetic Strategies for Dehydrobenzo[*n*]annulenes.

[49] S. Höger, *Chem. Eur. J.* **2004**, *10*, 1320–1329. Shape-Persistent Macrocycles: From Molecules to Materials.

[50] S. Thorand, F. Vögtle, N. Krause, *Angew. Chem*. **1999**, 111, 3929–3931; *Angew. Chem. Int. Ed*. **1999**, *38*, 3721–3723. Synthesis of the First [3_4]Allenophane: 1,3,10,12,19,21,28,30-Octamethyl[3.3.3.3]paracyclophan-1,2,10,11,19,20,28,29-octaene.

[51] M. D. Clay, A. G. Fallis, *Angew. Chem*. **2005**, *117*, 4107–4110; *Angew. Chem. Int. Ed*. **2005**, *44*, 4039–4042. Acetylenic Allenophanes: An Asymmetric Synthesis of a Bis(alleno)-bis(butadiynyl)-meta-cyclophane.

[52] M. Leclère, A. G. Fallis, *Angew. Chem*. **2008**, *120*, 578–582; *Angew. Chem. Int. Ed.* **2008**, *47*, 568–572. Asymmetric Allenophanes: Synthesis of a Tris-*meta* allenophane and Tetrakis-*meta*-allenophane by Sequential Cross-Coupling.

[53] S. Odermatt, J. L. Alonso-Gómez, P. Seiler, M. M. Cid, F. Diederich, *Angew. Chem*. **2005**, *117*, 5203–5207; *Angew. Chem. Int. Ed.* **2005**, *44*, 5074–5078. Shape-Persistent Chiral Alleno-Acetylenic Macrocycles and Cyclophanes by Acetylenic Scaffolding with 1,3-Diethynylallenes.

[54] M. W. Klett, R. P. Johnson, *J. Am. Chem. Soc*. **1985**, *107*, 3963–3971. Cumulene Photochemistry - Photorearrangements of Tetraphenyl and Triphenyl-C_3 Isomers.

[55] M. Hasegawa, Y. Sone, S. Iwata, H. Matsuzawa, Y. Mazaki, *Org. Lett*. **2011**, *13*, 4688–4691. Tetrathiafulvalenylallene: A New Class of Donor Molecules Having Strong Chiroptical Properties in Neutral and Doped States.

[56] J. L. Alonso-Gómez, A. Navarro-Vázquez, M. M. Cid, *Chem. Eur. J.* **2009**, *15*, 6495–6503. Chiral (2,5)Pyrido[7$_4$]Allenoacetylenic Cyclophanes: Synthesis and Characterization.

[57] J. L. Alonso-Gómez, P. Rivera-Fuentes, N. Harada, N. Berova, F. Diederich, *Angew. Chem*. **2009**, *121*, 5653–5656; *Angew. Chem. Int. Ed*. **2009**, *48*, 5545–5548. An Enantiomerically Pure Alleno-Acetylenic Macrocycle: Synthesis and Rationalization of Its Outstanding Chiroptical Response.

[58] P. Rivera-Fuentes, J. L. Alonso-Gómez, A. G. Petrovic, P. Seiler, F. Santoro, N. Harada, N. Berova, H. S. Rzepa, F. Diederich, *Chem. Eur. J.* **2010**, *16*, 9796–9807. Enantiomerically Pure Alleno-Acetylenic Macrocycles: Synthesis, Solid-State Structures, Chiroptical Properties, and Electron Localization Function Analysis.

[59] P. Rivera-Fuentes, B. Nieto-Ortega, W. B. Schweizer, J. T. López Navarrete, J. Casado, F. Diederich, *Chem. Eur. J.* **2011**, *17*, 3876–3885. Enantiopure, Monodisperse Alleno-Acetylenic Cyclooligomers: Effect of Symmetry and Conformational Flexibility on the Chiroptical Properties of Carbon-Rich Compounds.

[60] M. D. Tzirakis, N. Marion, W. B. Schweizer, F. Diederich, *Chem. Commun*. **2013**, *49*, 7605–7607. A shape-persistent alleno-acetylenic macrocycle with a modifiable periphery: synthesis, chiroptical properties and H-bond-driven self-assembly into a homochiral columnar structure.

[61] M. D. Tzirakis, M. N. Alberti, H. Weissman, B. Rybtchinski, F. Diederich, *Chem. Eur. J*. **2014**, *20*, 16070–16073. Enantiopure Laterally Functionalized Alleno-Acetylenic Macrocycles: Synthesis, Chiroptical Properties, and Self-Assembly in Aqueous Media.

[62] S. Castro-Fernández, I. R. Lahoz, A. L. Llamas-Saiz, J. L. Alonso-Gómez, M. M. Cid, A. Navarro-Vázquez, *Org. Lett*. **2014**, *16*, 1136−1139. Preparation and Characterization of a Halogen-Bonded Shape-Persistent Chiral Alleno-acetylenic Inclusion Complex.

[63] P. Metrangolo, Y. Carcenac, M. Lahtinen, T. Pilati, K. Rissanen, A. Vij, G. Resnati, *Science* **2009**, *323*, 1461–1464. Nonporous Organic Solids Capable of Dynamically Resolving Mixtures of Diiodoperfluoroalkanes.

[64] Farina, A.; Meille, S. V.; Messina, M. T.; Metrangolo, P.; Resnati, G.; Vecchio, G. *Angew. Chem.* **1999**, *111*, 2585–2588; *Angew. Chem. Int. Ed.* **1999**, *38*, 2433–2436. Resolution of Racemic 1,2-Dibromohexafluoropropane through Halogen-Bonded Supramolecular Helices.

[65] S. Míguel-Lago, A. L. Llamas-Saiz, M. M. Cid, J. L. Alonso-Gómez, *Chem. Eur. J.* **2015**, *21*, 18085–18088. A Covalent Organic Helical Cagewith Remarkable Chiroptical Amplification.

[66] S. H. Gellman, *Acc. Chem. Res.* **1998**, *31*, 173–180. Foldamers: A Manifesto.

[67] D. J. Hill, M. J. Mio, R. B. Prince, T. S. Hughes, J. S. Moore, *Chem. Rev*. **2001**, *101*, 3893–4011. A Field Guide to Foldamers.

[68] M. M. Green, J. W. Park, T. Sato, A. Teramoto, S. Lifson, R. L. B. Selinger, J. V. Selinger, *Angew. Chem*. **1999**, *111*, 3328–3345; *Angew. Chem. Int. Ed*.

1999, *38*, 3138–3154. The Macromolecular Route to Chiral Amplification.

[69] K. Maeda, E. Yashima, *Top. Curr. Chem*. **2006**, *265*, 47–88. Dynamic Helical Structures: Detection and Amplification of Chirality.

[70] M. Fujiki, *Top. Curr. Chem*. **2008**, *284*, 119–186. Helix Generation, Amplification, Switching, and Memory of Chromophoric Polymers.

[71] T. Bai, S. M. Ma, G. C. Jia, Coord. *Chem. Rev.* **2009**, *253*, 423–448. Insertion Reactions of Allenes with Transition Metal Complexes.

[72] K. Osakada, D. Takeuchi, *Adv. Polym. Sci*. **2004**, *171*, 137–194. Coordination Polymerization of Dienes, Allenes, and Methylenecycloalkanes.

[73] M. Kijima, K. Hiroki, H. Shirakawa, *Macromol. Rapid Commun*. **2002**, *23*, 901–904. The First Conjugated Allene Polymer.

[74] K. Hiroki, M. Kijima, *Chem. Lett*. **2005**, *34*, 942–943. Synthesis and Properties of Conjugated Copolymer Having Alternate Structure of Diphenylanthracene and Allene.

[75] P. Rivera-Fuentes, J. L. Alonso-Gómez, A. G. Petrovic, F. Santoro, N. Harada, N. Berova, F. Diederich, *Angew. Chem*. **2010**, *122*, 2296–2300; *Angew. Chem. Int. Ed*. **2010**, *49*, 2247–2250. Amplification of Chirality in Monodisperse, Enantiopure Alleno-Acetylenic Oligomers.

[76] I.-E. S. Müller, B. Bernet, C. Dengiz, W. B. Schweizer, F. Diederich, *Eur. J. Org. Chem.* **2014**, 941–953. Towards Stapling of Helical Alleno-Acetylene Oligomers-Synthesis of An Enantiopure Bis(ethynylvinylidene)-Substituted Cyclohexadeca-1,3,9,11-tetrayne.

[77] C. M. Reisinger, P. Rivera-Fuentes, S. Lampart, W. B. Schweizer, F. Diederich, *Chem. Eur. J.* **2011**, *17*, 12906–12911. Cascade Pericyclic Reactions of Alleno-Acetylenes: Facile Access to Highly Substituted Cyclobutene, Dendralene, Pentalene, and Indene Skeletons.

[78] S. J. Wezenberg, F. Ferroni, S. Pieraccini, W. B. Schweizer, A. Ferrarini, G. P. Spada, F. Diederich, *Chem. Commun*. **2013**, *3*, 22845–22848. Effective cholesteric liquid crystal inducers based on axially chiral alleno-acetylenes.

[79] M. D. Tzirakis, J.-P. Gisselbrecht, C. Boudon, F. Diederich, *Tetrahedron* **2014**, *70*, 6193–6202. Alleno-acetyllenic scaffolding for the construction of axially chiral C_{60} dimers.

[80] O. Gidron, M.-O. Ebert, N. Trapp, F. Diederich, *Angew. Chem*. **2014**, *126*, 13833–13837; *Angew. Chem. Int. Ed*. **2014**, *53*, 13614–13614. Chiroptical Detection of Nonchromophoric, Achiral Guests by Enantiopure Alleno-Acetylenic Helicages.

[81] O. Gidron, M. Jirásek, N. Trapp, M.-O. Ebert, X. Zhang, F. Diederich, *J. Am. Chem. Soc.* **2015**, *137*, 12502–12505.

[82] H. Shirakawa, E. J. Louis, A. G. MacDiarmid, C. K. Chiang, A. J. Heeger, *Chem. Commun.* **1977**, 578–580. Synthesis of Electrically Conducting Organic Polymers: Halogen Derivatives of Polyacetylene, $(CH)_x$.

[83] O. N. Witt, *Ber. Dtsch. Chem. Ges.* **1876**, *9*, 522–527. Zur Kenntniss des Baues und der Bildung Färbender Kohlenstoffverbindungen.

[84] R. Gompper, H.-U. Wagner, *Angew. Chem.* **1988**, *100*, 1492–1511; *Angew. Chem. Int. Ed.* **1988**, *27*, 1437–1455. Donor–Acceptor-Substituted Cyclic π-Electron Systems–Probes for Theories and Building Blocks for New Materials.

[85] Y. Ohmori, *Laser Photonics Rev*. **2009**, *4*, 300–310. Development of Organic Light-Emitting Diodes for Electro-Optical Integrated Devices.

[86] L. Duan, J. Qiao, Y. Sun, Y. Qiu, *Adv. Mater.* **2011**, *23*, 1137–1144. Strategies to Design Bipolar Small Molecules for OLEDs: Donor-Acceptor Structure and Non-Donor-Acceptor Structure.

[87] G. Horowitz, *Adv. Mater.* **1998**, *10*, 365–377. Organic Field-Effect Transistors.

[88] C. D Dimitrakopoulos, P. R. L. Malenfant, *Adv. Mater.* **2002**, *14*, 99–117. Organic Thin Film Transistors for Large Area Electronics.

[89] O. Knopfmacher, M. L. Hammock, A. L. Appleton, G. Schwartz, J. Mei, T. Lei, J. Pei, Z. Bao, *Nat. Commun.* **2014**, *5*, 2954. Highly Stable Organic Polymer Field-Effect Transistor Sensor for Selective Detection in the Marine Environment.

[90] A. Hagfeldt, G. Boschloo, L. Sun, L. Kloo, H. Pettersson, *Chem. Rev.* **2010**, *110*, 6595–6663. Dye-Sensitized Solar Cells.

[91] Y. Wu, W. Zhu, *Chem. Soc. Rev.* **2013**, *42*, 2039–2058. Organic sensitizers from D-π-A to D-A-π-A: effect of the internal electron-withdrawing units on molecular absorption, energy levels and photovoltaic performances.

[92] T.-D. Kim, K.-S. Lee, *Macromol. Rapid. Commun.* **2015**, *36*, 943–958. D-π-A Conjugated Molecules for Optoelectronic Applications.

[93] S. R. Marder, L.-T. Cheng, B. G. Tiemann, A. C. Friedli, M. Blanchard-Desce, J. W. Perry, J. Skindhøj, *Science* **1994**, *263*, 511–514. Large First Hyperpolarizabilities in Push–Pull Polyenes by Tuning of the Bond Length Alternation and Aromaticity.

[94] R. R. Tykwinski, U. Gubler, R. E. Martin, F. Diederich, C. Bosshard, P. Günter, *J. Phys. Chem., B* **1998**, *102*, 4451–4465. Structure-Property Relationships in Third-Order Nonlinear Optical Chromophores.

[95] J. C. May, I. Biaggio, F. Bures, F. Diederich, *Appl. Phys. Lett.* **2007**, *90*, 251106. Extended Conjugation and Donor-Acceptor Substitution to Improve the Third-Order Optical Nonlinearity of Small Molecules.

[96] B. Breiten, I. Biaggio, F. Diederich, *Chimia* **2010**, *64*, 409–413. Nonplanar Push–Pull Chromophores for Opto-Electronic Applications.

[97] A. D. McNaught, A. Wilkinson, *IUPAC Compendium of Chemical Terminology: The Gold Book*. 2nd ed. Blackwell Scientific Publications, Oxford, **2012**.

[98] S. R. Forrest, M. E. Thompson (Guest Editors), *Chem. Rev.* **2007**, *107*,

923–1386. Special Issue on Organic Electronics and Opto-Electronics.

[99] J. Roncali, P. Leriche, A. Cravino, *Adv. Mater.* **2007**, *19*, 2045–2060. From One-to Three-Dimensional Organic Semiconductors: In Search of the Organic Silicon?

[100] M. Irfan, K. D. Belfield, A. Saeed, *RSC Adv.* **2015,** *5*, 48760–48768. Carbazole/fluorene based conjugated small molecules: synthesis and comparative studies on the optical, thermal and electrochemical properties

[101] M. Kivala, F. Diederich, *Acc. Chem. Res.* **2009**, *42*, 235–248. Acetylene-Derived Strong Organic Acceptors for Planar and Nonplanar Push–Pull Chromophores.

[102] S.-i. Kato, F. Diederich, *Chem. Commun.* **2010**, *46*, 1994–2006. Non-planar Push–Pull Chromophores.

[103] M. T. Beels, M. S. Fleischman, I. Biaggio, B. Breiten, M. Jordan, F. Diederich, *Opt. Mater. Express* **2012**, *2*, 294–303. Compact TCBD based molecules and supramolecular assemblies for third-order nonlinear optics.

[104] S. Barlow, S. R. Marder in *Functional Organic Materials*, (Eds.: T. J. J. Müller, U. H. F. Bunz), Wiley-VCH, Weinheim, **2007**.

[105] S. Biswas, O. Shalev, M. Shtein, *Annu. Rev. Chem. Biomol. Eng.* **2013**, *4*, 289–317. Thin-film growth and patterning techniques for small molecular organic compounds used in optoelectronic device applications.

[106] B. Esembeson, M. L. Scimeca, T. Michinobu, F. Diederich, I. Biaggio, *Adv. Mater.* **2008**, *20*, 4584–4587. A High-Optical Quality Supramolecular Assembly for Third-Order Integrated Nonlinear Optics.

[107] H. C. Kolb, M. G. Finn, K. B. Sharpless, *Angew. Chem.* **2001**, *113*, 2056–2075; *Angew. Chem. Int. Ed.* **2001**, *40*, 2004–2021. Click Chemistry: Diverse Chemical Function from a Few Good Reactions.

[108] M. I. Bruce, J. R. Rodgers, M. R. Snow, A. G. Swincer, *J. Chem. Soc., Chem. Commun.* **1981**, 271–272. Cyclopentadienyl-Ruthenium and -Osmium Chemistry. Cleavage of Tetracyanoethylene under Mild Conditions: X-Ray Crystal Structures of [Ru{η^3-C(CN)$_2$CPhC=C(CN)$_2$}(PPh$_3$)(η-C$_5$H$_5$)] and [Ru{C[=C(CN)$_2$]CPh=C(CN)$_2$}-(CNBu^t)(PPh$_3$) (η-C$_5$H$_5$)].

[109] C. Cai, I. Liakatas, M.-S. Wong, M. Bösch, C. Bosshard, P. Günter, S. Concilio, N. Tirelli, U. W. Suter, *Org. Lett.* **1999**, *1*, 1847–1849. Donor–Acceptor-Substituted Phenylethenyl Bithiophenes: Highly Efficient and Stable Nonlinear Optical Chromophores.

[110] Y. Morioka, N. Yoshizawa, J.-i. Nishida, Y. Yamashita, *Chem. Lett.* **2004**, *33*, 1190–1191. Novel Donor-π-Acceptor Compounds Containing 1,3-Dithiol-2-ylidene and Tetracyanobutadiene Units.

[111] T. Mochida, S. Yamazaki, *J. Chem. Soc., Dalton Trans.* **2002**, 3559–3564. Mono- and Diferrocenyl Complexes with Electron-Accepting Moieties Formed by the Reaction of Ferrocenylalkynes with Tetra-Cyanoethylene.

[112] M. I. Bruce, B. D. Kelly, B. W. Skelton, A. H. White, *J. Organomet. Chem.* **2000**, *604*, 150–156. Syntheses and Reactions of Ruthenium Complexes Containing C$_6$ and C$_8$ Chains.

[113] K. Onitsuka, N. Ose, F. Ozawa, S. Takahashi, *J. Organomet. Chem.* **1999**, *578*, 169–177. Reactions of Acetylene-Bridged Diplatinum Complexes with Tetracyanoethylene.

[114] T. Michinobu, J. C. May, J. H. Lim, C. Boudon, J.-P. Gisselbrecht, P. Seiler, M. Gross, I. Biaggio, F. Diederich, *Chem. Commun.* **2005**, 737–739. A new class of organic donor-acceptor molecules with large third-order optical nonlinearities.

[115] C. Koos, P. Vorreau, T. Vallaitis, P. Dumon, W. Bogaerts, R. Baets, B. Esembeson, I. Biaggio, T. Michinobu, F. Diederich, W. Freude, J. Leuthold, *Nat. Photonics* **2009**, *3*, 216–219. All-optical high-speed signal processing with silicon–organic hybrid slot waveguides.

[116] J. Covey, A. D. Finke, X. Xu, W. Wu, Y. Wang, F. Diederich, R. T. Chen, *Opt. Express*, **2014**, *22*, 24530–24544. All-optical switching with 1-ps response time in a DDMEBT enabled silicon grating coupler/resonator hybrid device.

[117] T. Michinobu, C. Boudon, J.-P. Gisselbrecht, P. Seiler, B. Frank, N. N. P. Moonen, M. Gross, F. Diederich, *Chem. Eur. J.* **2006**, *12*, 1889–1905. Donor-Substituted 1,1,4,4-Tetracyanobutadienes (TCBDs): New Chromophores with Efficient Intramolecular Charge-Transfer Interactions by Atom-Economic Synthesis.

[118] M. Kivala, C. Boudon, J.-P. Gisselbrecht, P. Seiler, M. Gross, F. Diederich, *Angew. Chem.* **2007**, *119*, 6473–6477; *Angew. Chem. Int. Ed*. **2007**, *46*, 6357–6360. Charge-Transfer Chromophores by Cycloaddition–Retroelectrocyclization: Multivalent Systems and Cascade Reactions.

[119] B. B. Frank, B. C. Blanco, S. Jakob, F. Ferroni, S. Pieraccini, A. Ferrarini, C. Boudon, J.-P. Gisselbrecht, P. Seiler, G. P. Spada, F. Diederich, *Chem. Eur. J.* **2009**, *15*, 9005–9016. *N*-Arylated 3,5-Dihydro-4*H*-dinaphtho[2,1-c:1',2'-e]azepines: Axially Chiral Donors with High Helical Twisting Powers for Nonplanar Push–Pull Chromophores.

[120] M. Štefko, M. D. Tzirakis, B. Breiten, M.-O. Ebert, O. Dumele, W. B. Schweizer, J.-P. Gisselbrecht, C. Boudon, M. T. Beels, I. Biaggio, F. Diederich, *Chem. Eur. J.* **2013**, *19*, 12693–12704. Donor–Acceptor (D–A)-Substituted Polyyne Chromophores: Modulation of Their Optoelectronic Properties by Varying the Length of the Acetylene Spacer.

[121] F. Tancini, F. Monti, K. Howes, A. Belbakra, A. Listorti, W. B. Schweizer, P. Reutenauer, J. L. Alonso-Gómez, C. Chiorboli, L. M. Urner, J.-P. Gisselbrecht, C. Boudon, N. Armaroli, F. Diederich, *Chem. Eur. J.* **2014**, *20*, 202–216. Cyanobuta-1,3-dienes as Novel Electron Acceptors for Photoactive Multicomponent Systems.

[122] L. M. Urner, M. Sekita, N. Trapp, W. B. Schweizer, M. Wörle, J.-P. Gisselbrecht. C. Boudon, D. M. Guldi, F. Diederich, *Eur. J. Org. Chem.* **2015**, 91–108. Systematic Variation of Cyanobuta-1,3-dienes and Expanded

Tetracyanoquinodimethane Analogues as Electron Acceptors in Photoactive, Rigid Porphyrin Conjugates.

[123] M. Chiu, B. H. Tchitchanov, D. Zimmerli, I. A. Sanhueza, F. Schoenebeck, N. Trapp, W. B. Schweizer, F. Diederich, *Angew. Chem.* **2015**, *127*, 356–361; *Angew. Chem. Int. Ed*. **2015**, *54*, 349–354. Strain-Accelerated Formation of Chiral, Optically Active Buta-1,3-dienes.

[124] C. Dengiz, B. Breiten, J.-P. Gisselbrecht, C. Boudon, N. Trapp, W. B. Schweizer, F. Diederich, *J. Org. Chem.* **2015**, *80*, 882–896. Synthesis and Optoelectronic Properties of Janus-Dendrimer-Type Multivalent Donor–Acceptor Systems.

[125] P. Gawel, C. Dengiz, A. D. Finke, N. Trapp, C. Boudon, J.-P. Gisselbrecht, F. Diederich, *Angew. Chem.* **2014**, *126*, 4430–4434; *Angew. Chem. Int. Ed.* **2014**, *53*, 4341–4345. Synthesis of Cyano-Substituted Diaryltetracenes from Tetraaryl[3]cumulenes.

[126] E. A. Margulies, Y.-L. Wu, P. Gawel, S. A. Miller, L. E. Shoer, R. D. Schaller, F. Diederich, M. R. Wasielewski, *Angew. Chem.* **2015**, *127*, 8803–8807; *Angew. Chem. Int. Ed.* **2015**, *54*, 8679–8683. Sub-Picosecond Singlet Exciton Fission in Cyano-SubstitutedDiaryltetracenes.

[127] M. Kivala, C. Boudon, J.-P. Gisselbrecht, P. Seiler, M. Gross, F. Diederich, *Chem. Commun.* **2007**, 4731–4733. A novel reaction of 7,7,8,8-tetracyanoquinodimethane (TCNQ): charge transfer chromophores by [2 + 2] cycloaddition with alkynes.

[128] P. Reutenauer, M. Kivala, P. D. Jarowski, C. Boudon, J.-P. Gisselbrecht, M. Gross, F. Diederich, *Chem. Commun.* **2007**, 4898–4900. New strong organic acceptors by cycloaddition of TCNE and TCNQ to donor-substituted cyanoalkynes.

[129] M. Kivala, C. Boudon, J.-P. Gisselbrecht, B. Enko, P. Seiler, I. B. Müller, N. Langer, P. D. Jarowski, G. Gescheidt, F. Diederich, *Chem. Eur. J.* **2009**, *15*, 4111–4123. Organic Super-Acceptors with Efficient Intramolecular

Charge-Transfer Interactions by [2+2] Cycloadditions of TCNE, TCNQ, and F4-TCNQ to Donor-Substituted Cyanoalkynes.

[130] H. Masai, K. Sonogashira, N. Hagihara, *J. Organomet. Chem.* **1972**, *34*, 397–404. The charge-transfer interaction of 7,7,8,8-tetracyanoquinodimethane with trans-bis(trialkylphosphine)-dialkynylplatinum(II) and related complexes.

[131] K. Onuma, Y. Kai, N. Yasuoka, N. Kasai, *Bull. Chem. Soc. Jpn.* **1975**, *48*, 1696–1700. The Crystal and Molecular Structure of trans-Bis(trimethylphosphine)propynyl-1-(4′-dicyanomethylene-cyclohexa-2′-5′-dien-1-ylidenl-3,3-dicyano-2-methyl-prop-2-en-1-ylplatinum, a Reaction Product of trans-Bis(trimethylphosphine)bis(propynyl)platinum and 7,7,8,8-Tetracyanoquinodimethane.

[132] S. Hünig, E. Herberth, *Chem. Rev*. **2004**, *104*, 5535–5564. *N,N'*-Dicyanoquinone Diimides (DCNQIs): Versatile Acceptors for Organic Conductors.

[133] M. Chiu, B. Jaun, M. T. R. Beels, I. Biaggio, J.-P. Gisselbrecht, C. Boudon, W. B. Schweizer, M. Kivala, F. Diederich, *Org. Lett.* **2012**, *14*, 54–57. *N,N′*-Dicyanoquinone Diimide-Derived Donor–Acceptor Chromophores: Conformational Analysis and Optoelectronic Properties.

[134] G. Jayamurugan, J.-P. Gisselbrecht, C. Boudon, F. Schoenebeck, W. B. Schweizer, B. Bernet, F. Diederich, *Chem. Commun.* **2011**, *47*, 4520–4522. Expanding the chemical space for push–pull chromophores by non-concerted [2+2] and [4+2] cycloadditions: access to a highly functionalised 6,6-dicyanopentafulvene with an intense, low-energy charge-transfer band.

[135] G. Jayamurugan, O. Dumele, J.-P. Gisselbrecht, C. Boudon, W. B. Schweizer, B. Bernet, F. Diederich, *J. Am. Chem. Soc.* **2013**, *135*, 3599–3606. Expanding the Chemical Structure Space of Opto-Electronic Molecular Materials: Unprecedented Push−Pull Chromophores by Reaction of a Donor-Substituted Tetracyanofulvene with Electron-Rich Alkynes.

[136] A. D. Finke, O. Dumele, M. Zalibera, D. Confortin, P. Cias, G. Jayamurugan, J.-P. Gisselbrecht, C. Boudon, W. B. Schweizer, G. Gescheidt, F. Diederich, *J. Am. Chem. Soc.* **2012**, *134*, 18139–18146. 6,6-Dicyanopentafulvenes: Electronic Structure and Regioselectivity in [2 + 2] Cycloaddition−Retroelectrocyclization Reactions.

[137] E. J. Donckele, O. Gidron, N. Trapp, F. Diederich, *Chem. Eur. J.* **2014**, *20*, 9558–9566. Outstanding Chiroptical Properties: A Signature of Enantiomerically Pure Alleno-Acetylenic Macrocycles and Monodisperse Acyclic Oligomers.

[138] T. Imahori, C. Hori, Y. Kondo, *Adv. Synth. Catal.* **2004**, *346*, 1090–1092. Functionalization of Alkynes Catalyzed by t-Bu-P4 Base.

[139] R. Rossi, A. Carpita, C. Bigelli, *Tetrahedron Lett.* **1985**, *26*, 523–526. A palladium-promoted route to 3-alkyl-4-(1-alkynyl)-hexa-1,5-dyn-3-enes and/or 1,3-diynes.

[140] G. Snatzke, *Angew. Chem.* **1979**, *91*, 380–393; *Angew. Chem. Int. Ed.* **1979**, *18*, 363–377. Circular Dichroism and Absolute Conformation: Application of Qualitative MO Theory to Chiroptical Phenomena.

[141] S. F. Mason, *Molecular Optical Activity & the Chiral Discrimination*, Cambridge University Press, Cambridge, **1982**, pp. 47–50.

[142] A. D. Becke, *J. Chem. Phys.* **1993**, *98*, 5648–5652. Density-functional thermochemistry. III. The role of exact exchange.

[143] V. Barone, M. Cossi, *J. Phys. Chem. A* **1998**, *102*, 1995–2001. Quantum Calculation of Molecular Energies and Energy Gradients in Solution by a Conductor Solvent Mode.

[144] R. E. Stratmann, G. E. Scuseria, M. J. Frisch, *J. Chem. Phys.* **1998**, *109*, 8218–8224. An efficient implementation of time-dependent density-functional theory for the calculation of excitation energies of large molecules.

[145] T. Yanai, D. P. Tew, N. C. Handy, *Chem. Phys. Lett.* **2004**, *393*, 51–57. A new hybrid exchange–correlation functional using the Coulomb-attenuating method (CAM-B3LYP).

[146] S. Grimme, S. Ehrlich, L. Goerigk, *J. Comp. Chem*. **2011**, *32*, 1456–1465. Effect of the damping function in dispersion corrected density functional theory.

[147] M. J. Frisch, G. W. Trucks, H. B. Schlegel, G. E. Scuseria, M. A. Robb, J. R. Cheeseman, G. Scalmani, V. Barone, B. Mennucci, G. A. Petersson, H. Nakatsuji, M. Caricato, X. Li, H. P. Hratchian, A. F. Izmaylov, J. Bloino, G. Zheng, J. L. Sonnenberg, M. Hada, M. Ehara, K. Toyota, R. Fukuda, J. Hasegawa, M. Ishida, T. Nakajima, Y. Honda, O. Kitao, H. Nakai, T. Vreven, J. A. Montgomery, Jr., J. E. Peralta, F. Ogliaro, M. Bearpark, J. J. Heyd, E. Brothers, K. N. Kudin, V. N. Staroverov, R. Kobayashi, J. Normand, K. Raghavachari, A. Rendell, J. C. Burant, S. S. Iyengar, J. Tomasi, M. Cossi, N. Rega, J. M. Millam, M. Klene, J. E. Knox, J. B. Cross, V. Bakken, C. Adamo, J. Jaramillo, R. Gomperts, R. E. Stratmann, O. Yazyev, A. J. Austin, R. Cammi, C. Pomelli, J. W. Ochterski, R. L. Martin, K. Morokuma, V. G. Zakrzewski, G. A. Voth, P. Salvador, J. J. Dannenberg, S. Dapprich, A. D. Daniels, Ö. Farkas, J. B. Foresman, J. V. Ortiz, J. Cioslowski, and D. J. Fox, *Gaussian 09*, Revision A.1, Gaussian, Inc., Wallingford CT, **2009**.

[148] E. J. Donckele, A. D. Finke, L. Ruhlmann, C. Boudon, N. Trapp, F. Diederich, *Org. Lett.* **2015**, *17*, 3506–3509. The [2 + 2] Cycloaddition–Retroelectrocyclization and [4 + 2] Hetero-Diels–Alder Reactions of 2-(Dicyanomethylene)indan-1,3-dione with Electron-Rich Alkynes: Influence of Lewis Acids on Reactivity.

[149] H. Junek, H. Sterk, *Tetrahedron Lett.* **1968**, 4309–4310. Synthesen mit Nitrilen, 19.mitt.: die Partielle Retro-Michael-Addition von Tetracyanäthylen an Indandion-1,3.

[150] M. R. Bryce, S. R. Davies, M. Hasan, G. J. Ashwell, M. Szablewski, M. G. B. Drew, R. Short, M. B. J. Hursthouse, *Chem. Soc., Perkin Trans*. *2*, **1989**, 1 285–1292. Preparation and magnetic properties of a range of metal and organic

cation salts of 2,3-dicyano-1,4-naphthoquinone (DCNQ). X-Ray crystal structure of (methyltriphenylphosphonium)$_1$(DCNQ)$_1$(H2O)$_1$ and 2-dicyanomethylene-indan-1,3-dione (DCID). The rearrangement of DCID to DCNQ.

[151] G. Jayamurugan, A. D. Finke, J.-P. Gisselbrecht, C. Boudon, W. Schweizer, B. F. Diederich, F. *J. Org. Chem*. **2014**, *79*, 426–431. One-Pot Access to Push–Pull Oligoenes by Sequential [2 + 2] Cycloaddition–Retroelectrocyclization Reactions.

[152] W. L. Mock, R. M. Nugent, *J. Am. Chem. Soc.* **1975**, *97*, 6521–6526. Geometry of the adducts of 2,4-hexadienes with N-sulfinylarylsulfonamides. Stereospecific but nonconcerted Diels-Alder reaction.

[153] D. A. Evans, J. S. Johnson, E. J. Olhava, *J. Am. Chem. Soc.* **2000***, 122,* 1635–1649. Enantioselective Synthesis of Dihydropyrans. Catalysis of Hetero Diels−Alder Reactions by Bis(oxazoline) Copper(II) Complexes.

[154] R. R. R. Taylor, R. A. Batey, *J. Org. Chem*. **2013**, *78*, 1404–1420. A Hetero Diels–Alder Approach to the Synthesis of Chromans (3,4-Dihydrobenzopyrans) Using Oxonium Ion Chemistry: The Oxa-Povarov Reaction.

[155] S. Hatakeyama, N. Ochi, H. Numata, S. Takano, *J. Chem. Soc., Chem. Commun*. **1988**, 1202–1204. A new route to substituted 3-methoxycarbonyldihydropyrans; enantioselective synthesis of (–)-methyl elenolate.

[156] G. R. Green, J. M. Evans, A. K. Vong, In *Comprehensive Heterocyclic Chemistry II*; A. R. Katritzky, C. W. Rees, E. F. V. Scriven (Eds.); Pergamon Press: Oxford, **1995**; vol. 5, pp 469–490.

[157] R. R. Kumar, S. Perumal, J. C. Menéndez, P. Yogeeswari, D. Sriram, *Bioorg. Med. Chem*. **2011**, *19*, 3444–3450. Antimycobacterial activity of novel 1,2,4-oxadiazole-pyranopyridine/chromene hybrids generated by chemoselective 1,3-dipolar cycloadditions of nitrile oxides.

[158] B. Valeur, *Molecular Fluorescence Principles and Applications*, Wiley-VCH: Weinheim, **2002**.

[159] N. Martínez de Baroja, J. Garín J. Orduna, R. Andreu, M. J. Blesa, B. Villacampa, R. Alicante, S. Franco, *J. Org. Chem.* **2012,** *77*, 4634–4644. Synthesis, Characterization, and Optical Properties of 4*H*-Pyran-4-ylidene Donor-Based Chromophores: The Relevance of the Location of a Thiophene Ring in the Spacer.

[160] Z. Guo, W. H. Zhu, H. Tian, *Chem. Commun.* **2012**, *48*, 6073–6084. Dicyanomethylene-4*H*-pyran chromophores for OLED emitters, logic gates and optical chemosensors.

[161] A. Shaabani, A. H. Rezayan, A. Sarvary, A. Rahmati, H. R. Khavasi, *Catal. Commun.* **2008**, *9*, 1082–1086. Pyridine catalyzed reaction of tetracyanoethylene and activated 1,3-dicarbonyl CH-acid compounds: A rapid and efficient synthesis of pyran annulated heterocyclic systems.

[162] P. Li, L.-L. Luo, X.-S Li, J.-W. Xie, *Tetrahedron* **2010**, *66*, 7590–7594. A Simple Method for the Synthesis of Functionalized 6-Aryl-6*H*-dibenzo[*b,d*]pyran Derivatives from 3-Nitro-2*H*-chromenes.

[163] W.-B. Chen, Z.-J; Wu, Q.-L. Pei, L.-F. Cun, X.-M. Zhang, W.-C. Yuan, *Org. Lett.* **2010**, *12*, 3132–3135. Highly Enantioselective Construction of Spiro[4*H*-pyran-3,3'-oxindoles] Through a Domino Knoevenagel/Michael/Cyclization Sequence Catalyzed by Cupreine.

[164] S. Banerjee, A. Horn, H. Khatri, G. Sereda, *Tetrahedron Lett.* **2011**, *52*, 1878–1881. A green one-pot multicomponent synthesis of 4*H*-pyrans and polysubstituted aniline derivatives of biological, pharmacological, and optical applications using silica nanoparticles as reusable catalyst.

[165] D. Ma, Y. Qiu, J. Dai, C. Fu, S. Ma, *Org. Lett.* **2014**, *16*, 4742–4745. *N*-Heterocyclic Carbene-Promoted Annulation Reaction of Allenals with Chalcones: Synthesis of Polysubstituted Pyranyl Aldehydes.

[166] Y. Gu, F. Li, P. Hu, D. Liao, Y. Tong, *Org. Lett.* **2015**, *17*, 1106–1109. Highly Enantioselective [4 + 2] Cycloaddition of Allenoates and 2-Olefinic Benzofuran-3-ones.

[167] W. Srisiri, A. B. Padias, H. K., Jr. Hall, *J. Org. Chem.* **1994**, *59*, 5424–5435. Influence of Lewis Acids on the Cycloaddition Reactions of Cyano- and Carbomethoxy-Substituted Olefins.

[168] J. Pommerehne, H. Vestweber, W. Guss, R. F. Mahrt, H. Bässler, M. Porsch, Daub, *J. Adv. Mater.* **1995**, *7*, 551–554. Efficient two layer leds on a polymer blend basis.

[169] B. W. D. D'Andrade, S. Datta, S. R. Forrest, P. Djurovich, E. Polikarpov, M. E. Thompson, *Org. Electron.* **2005**, *6*, 11–20. Relationship between the ionization and oxidation potentials of molecular organic semiconductors.

[170] W. Yue, S.-L. Suraru, D. Bialas, M. Müller, F. Würthner, F. *Angew. Chem.* **2014**. *126,* 6273–6276*; Angew. Chem. Int. Ed.* **2014**, *53*, 6159–6162. Synthesis and Properties of a New Class of Fully Conjugated Azahexacene Analogues.

[171] T. A. Reekie, E. J. Donckele, L. Ruhlmann, C. Boudon, N. Trapp, F. Diederich, *Eur. J. Org. Chem.* **2015**, 7264–7275. Ester-Substituted Electron-Poor Alkenes for the Cycloaddition–Retroelectrocyclization (CA–RE) and Related Reactions.

[172] C. Hansch, A. Leo, R. W. Taft, *Chem. Rev.* **1991**, *91*, 165–195. A Survey of Hammett Substituent Constants and Resonance and Field Parameters.

[173] P. Schiess, H. L. Chia, *Helv. Chim. Acta* **1970**, *53*, 485–495. Valenzisomerisierung von cis-Dienonen I. 2-Vinyl-3,4,5,6-tetrahydrobenzaldehyd; Pyrolyse. von 6-Oxabicyclo [3,1,0] hex-2-en [1].

[174] F.-G. Klärner, D. Schröer, *Angew. Chem.* **1987***, 99,* 1295–1297*; Angew. Chem. Int. Ed. Engl.* **1987**, *26*, 1294–1295. 1,5-EIectrocyclization in Homofuran, Homopyrrole, and Homothiophene.

[175] A. R. Lacy, A. Vogt, C. Boudon, J.-P. Gisselbrecht, W. B. Schweizer, F. Diederich, *Eur. J. Org. Chem.* **2013**, 869–879. Post-Cycloaddition–Retroelectrocyclization Transformations of Polycyanobutadienes.

[176] M. C. Witschel, M. Rottmann, A. Schwab, U. Leartsakulpanich, P. Chitnumsub, M. Seet, S. Tonazzi, G. Schwertz, F. Stelzer, T. Mietzner, C. McNamara, F. Thater, C. Freymond, A. Jaruwat, C. Pinthong, P. Riangrungroj, M. Oufir, M. Hamburger, P. Mäser, L. M. Sanz-Alonso, S. Charman, S. Wittlin, Y. Yuthavong, P. Chaiyen, F. Diederich, *J. Med. Chem.* **2015**, *58*, 3117–3130. Inhibitors of Plasmodial Serine Hydroxymethyltransferase (SHMT): Cocrystal Structures of Pyrazolopyrans with Potent Blood- and Liver-Stage Activities.

[177] M. Witschel, M. Rottmann, M. Kaiser, R. Brun, *PLoS Neglected Trop. Dis.* **2012**, *6*, e1805. Agrochemicals against malaria, sleeping sickness, Leishmaniasis and Chagas disease.

[178] M. Witschel, F. Stelzer, J. Hutzler, T. Qu, K. Mietzner, K. Kreuz, K. Grossmann, R. Aponte, H. W. Höffken, F. Carlo, T. Ehrhardt, A. Simon, R. L. Parra, PCT Int. Appl. WO 2013182472 A1, **2013**. Pyrazolopyrans having herbicidal and pharmaceutical properties.

[179] M. De Rosa, R. P. Issac, M. Marquez, M. Orozco, F. J. Luque, M. D. Timken, *J. Chem. Soc., Perkin Trans. 2* **1999**, 1433–1437. 2-Aminopyrrole and simple 1-substituted 2-aminopyrroles: preparation and ab initio study on the effect of solvent on the amino–imino tautomeric equilibrium.

[180] M. T. Cocco, C. Congiu, V. Onnis, *Bioorg. Med. Chem.* **2003**, *11*, 495–503. Synthesis and In Vitro Antitumoral Activity of New *N*-Phenyl-3-pyrrolecarbothioamides.

[181] V. Onnis, A. De Logu, M. T. Cocco, R. Fadda, R. Meleddu, C. Congiu, *Eur. J. Med. Chem.* **2009**, *44*, 1288–1295. Antimicrobial studies of some novel quinazolinones fused with [1,2,4]-triazole, [1,2,4]-triazine and [1,2,4,5]-tetrazine rings.

[182] M. B. Wallace, M. E. Adams, T. Kanouni, C. D. Mol, D. R. Dougan, V. A. Feher, S. M. O'Connell, L. Shi, P. Halkowycz, Q. Dong, *Bioorg. Med. Chem. Lett.* **2010**, *20*, 4156–4158. Structure-Based Design and Synthesis of Pyrrole Derivatives as MEK Inhibitors.

[183] E. J. Donckele, T. A. Reekie, G. Maneti, S. Püntener, N. Trapp, D. Diederich, *Org. Lett.* **2016**, *18,* 2252–2255. A Three-Step Synthesis of Tetrasubstituted NH-Pyrroles.

[184] D. L. Boger, C. W. Boyce, M. A. Labrili, C. A. Sehon, Q. Jin, *J. Am. Chem. Soc.* **1999**, *121*, 54–62. Total Syntheses of Ningalin A, Lamellarin O, Lukianol A, and Permethyl Storniamide A Utilizing Heterocyclic Azadiene Diels−Alder Reactions.

[185] P. A. Jacobi, L. D. Coutts, J. Guo, S. I. Hauck, S. H. Leung, *J. Org. Chem.* **2000**, *65*, 205–213. New Strategies for the Synthesis of Biologically Important Tetrapyrroles. The "B,C + D +A" Approach to Linear Tetrapyrroles.

[186] G. R. Martinez, D. R. Hirschfeld, P. J. Maloney, D. S. Yang, R. P. Rosenkranz, K. A. M. Walker, *J. Med. Chem.* **1989**, *32*, 890–897. [(1H-imidazol-1-yl)methyl]- and [(3-pyridinyl)methyl]pyrroles as Thromboxane Synthetase Inhibitors.

[187] I. K. Khanna, R. M. Weier, Y. Yu, P. W. Collins, J. M. Miyashiro, C. M.; Koboldt, A. W. Veenhuizen, J. L. Currie, K. Seibert, P. C. Isakson, *J. Med. Chem.* **1997**, *40*, 1619–1633. 1,2-Diarylpyrroles as Potent and Selective Inhibitors of Cyclooxygenase-2.

[191] L. Knorr, *Ber. Dtsch. Chem. Ges.* **1884**, *17*, 1635–1642. Synthese von Pyrrolderivaten.

[192] C. Paal, *Ber. Dtsch. Chem. Ges.* **1885**, *18*, 367–371. Synthese von Thiophen- und Pyrrolderivaten.

[193] A. Hantzsch, *Ber. Dtsch. Chem. Ges.* **1890**, *23*, 1474–1476. Neue Bildungsweise von Pyrrolderivaten.

[194] V. Nair, A. U. Vinod, C. Rajesh, *J. Org. Chem.* **2001**, *66*, 4427–4429. A Novel Synthesis of 2-Aminopyrroles Using a Three-Component Reaction.

[195] L. V. Frolova, N. M. Evdokimov, K. Hayden, I. Malik, S. Rogelj, A. Kornienko, I. V. Magedov, *Org. Lett.* **2011**, *13*, 1118–1121. One-Pot Multicomponent

Synthesis of Diversely Substituted 2-Aminopyrroles. A Short General Synthesis of Rigidins A, B, C, and D.

[196] X. Wang, X.-P. Xu, S.-Y. Wang, W. Zhou, S.-J. Ji, *Org. Lett.* **2013**, *15*, 4246–4249. Highly Efficient Chemoselective Synthesis of Polysubstituted Pyrroles via Isocyanide-Based Multicomponent Domino Reaction.

[197] M. Egi, K. Azechi, S. Akai, *Org. Lett.* **2009**, *11*, 5002–5005. Cationic Gold(I)-Mediated Intramolecular Cyclization of 3-Alkyne-1,2-diols and 1-Amino-3-alkyn-2-ols: A Practical Route to Furans and Pyrroles.

[198] A. V. Kel'in, A. W. Sromek, V. Gevorgyan, *J. Am. Chem. Soc.* **2001**, *123*, 2074–2075. A Novel Cu-Assisted Cycloisomerization of Alkynyl Imines: Efficient Synthesis of Pyrroles and Pyrrole-Containing Heterocycles.

[199] B. Gabriele, G. Salerno, A. Fazio, *J. Org. Chem.* **2003**, *68*, 7853–7861. General and Regioselective Synthesis of Substituted Pyrroles by Metal-Catalyzed or Spontaneous Cycloisomerization of (Z)-(2-En-4-ynyl)amines.

[200] D. J. Gorin, N. R. Davis, F. D. Toste, *J. Am. Chem. Soc.* **2005**, *127*, 11260–11261. Gold(I)-Catalyzed Intramolecular Acetylenic Schmidt Reaction.

[201] M. R. Rivero, S. L. Buchwald, *Org. Lett.* **2007**, *9*, 973–976. Copper-Catalyzed Vinylation of Hydrazides. A Regioselective Entry to Highly Substituted Pyrroles.

[202] X.-Y. Xiao, A.-H. Zhou, C. Shu, F. Pan, T. Li, L.-W. Ye, *Chem. Asian J.* **2015**, *10*, 1854–1858. Atom-Economic Synthesis of Fully Substituted 2-Aminopyrroles via Gold-Catalyzed Formal [3+2] Cycloaddition between Ynamides and Isoxazoles.

[203] E. Marchand, G. Morel, S. Sinbandhit, *Eur. J. Org. Chem.* **1999**, 1729–1738. A New Access to 2-(Alkylamino)- and 2-(Arylamino)pyrroles by Addition of Isocyanides to Protonated 1-Azabutadienes.

[204] X. Qi, H. Xiang, Q. He, C. Yang, *Org. Lett.* **2014**, *16*, 4186–4189. Facile Synthesis of 1-Substituted 2-Amino-3-cyanopyrroles: New Synthetic Precursors for 5,6-Unsubstituted Pyrrolo[2,3-*d*]pyrimidines

[205] V. Estévez, M. Villacampa, J. C. Menéndez, *Chem. Soc. Rev.* **2010**, *39*, 4402–4421. Multicomponent reactions for the synthesis of pyrroles.

[206] V. Estévez, M. Villacampa, J. C. Menéndez, *Chem. Soc. Rev.* **2014**, *43*, 4633–4657. Recent advances in the synthesis of pyrroles by multicomponent reactions.

[207] K. Gewald, K. *Chem. Ber*. **1965**, *98*, 3571–3577. Heterocyclen aus CH-aciden Nitrilen, VII. 2-Amino-thiophene aus *α*-Oxo-mercaptanen und methylenaktiven Nitrilen.

[208] K. Gewald, E. Schinke, H. Böttcher, *Chem. Ber.* **1966**, *99*, 94–100. Heterocyclen aus CH-aciden Nitrilen, VIII. 2-Amino-thiophene aus methylenaktiven Nitrilen, Carbonylverbindungen und Schwefel.

[209] A. P. Krapcho, J. F. Weimaster, J. M. Eldridge, E. G. E. Jahngen, A. J. Lovey, W. P. Stephens, *J. Org. Chem.* **1978**, *43*, 138−147. Synthetic Applications and Mechanism Studies of the Decarbalkoxylations of Geminal Diesters and Related Systems Effected in Dimethyl Sulfoxide by Water and/or by Water with Added Salts.

[210] E. J. Donckele, T. A. Reekie, N. Trapp, F. Diederich, *Eur. J. Org. Chem*. **2016**, 7264–7275. Penta-2,4-dien-1-ones by Formal [3+2] Cycloaddition–Rearrangement of Electron-Deficient Diethyl 2-(Dicyanomethylene)malonate with Alkynes.

[211] Synthetic Applications of 1,3-Dipolar Cycloaddition Chemistry Toward Heterocycles and Natural Products (Eds.: A. Padwa, W. H. Pearson,), Wiley, New York, **2002**.

[212] R. Criegee, *Angew. Chem.* **1975**, *87*, 765–771; *Angew. Chem. Int. Ed.* **1975**, *11*, 745–752. Mechanism of Ozonolysis.

[213] R. Huisgen, *Angew. Chem.* **1963**, *75*, 604–637; *Angew. Chem. Int. Ed*. **1963**, 2, 565–598. 1,3-Dipolar Cycloadditions. Past and Future.

[214] R. Huisgen, G. Szeimies, L. Möbius, *Chem. Ber.* **1967**, *100*, 2494–2507. 1.3-Dipolare Cycloadditionen, XXXII. Kinetik der Additionen organischer Azide an CC-Mehrfachbindungen.

[215] A. Quilico, G. Stagno D'Alcontres, P. Grünanger, *Nature*, **1950**, *166*, 226–227. A New Reaction of Ethylenic Double Bonds.

[216] R. Huisgen, W. Scheer, G. Szeimies, H. Huber, *Tetrahedron Lett.* **1966**, *7*, 397–404. 1.3-Cycloadditionen von Azomethin-Yliden aus Aziridin-Carbonestern.

[217] R. Huisgen, W. Scheer, H. Huber, *J. Am. Chem. Soc.* **1967**, *89*, 1753–1755. Stereospecific Conversion of cis-trans Isomeric Aziridines to Open-Chain Azomethine Ylides.

[218] B. M. Trost, *Science*, **1991**, *254*, 1471–1477. The atom economy--a search for synthetic efficiency.

[219] M. Betou, N. Kerisit, E. Meledje, Y. R. Leroux, C. Katan, J.-F. Halet, J.-C. Guillemin, Y. Trolez, *Chem. Eur. J.* **2014**, *20*, 9553–9557. High-Yield Formation of Substituted Tetracyanobutadienes from Reaction of Ynamides with Tetracyanoethylene.

[220] P. Ballester, J. de Mendoza, *Supramolecular Chemistry: Strategies for Macrocycle Synthesis* (Eds. F. Diederich, *Modern* P. J. Stang, R. R. Tykwinski), Wiley-VCH, Weinheim, **2008**, pp 69–107.

[221] *Synthetic Applications of 1,3-Dipolar Cycloaddition Chemistry Toward Heterocycles and Natural Products* (Eds. A. Padwa, W. H. Pearson), Wiley, New York, **2002**.

[222] R. R. Kumar, S. Perumal, P. Senthilkumar, P. Yogeeswarim D. Sriram, *Bioorg. Med. Chem. Lett.* **2007**, *17*, 6459–6462. An atom efficient, solvent-free,

green synthesis and antimycobacterial evaluation of 2-amino-6-methyl-4-aryl-8-[(*E*)-arylmethylidene]-5,6,7,8-tetrahydro-4*H*-pyrano[3,2-*c*]pyridine-3-carbonitriles.

[223] R. R. Kumar, S. Perumal, P. Menendez, P. Yogeeswari, D. Sriram, *Bioorg. Med. Chem. Lett.* **2011**, *19*, 3444–3450. Antimycobacterial Activity of Novel 1,2,4- Oxadiazole-Pyranopyridine/Chromene Hybrids Generated by Chemoselective 1,3-Dipolar Cycloadditions of Nitrile Oxides.

[224] S. D. Roughley, A. M. Jordan, *J. Med. Chem.* **2011**, *54*, 3451−3479. The Medicinal Chemist's Toolbox: An Analysis of Reactions Used in the Pursuit of Drug Candidates.

[225] D. G. Stark, T. J. C. O'Riordan, A. D. Smith, *Org. Lett.* **2014**, *16*, 6496−6499. Synthesis of Di-, Tri-, and Tetrasubstituted Pyridines from (Phenylthio)carboxylic Acids and 2-[Aryl(tosylimino)methyl]acrylates.

[226] J. A. Varela, C. Saa, *Chem. Rev.* **2003**, *103*, 3787−3802. Construction of Pyridine Rings by Metal-Mediated [2 + 2 + 2] Cycloaddition.

[227] J. M. Neely, T. Rovis, *Org. Chem. Front.* **2014**, *1*, 1010−1015. Pyridine synthesis by [4 + 2] cycloadditions of 1-azadienes: hetero-Diels Alder and transition metal-catalysed approaches.

[228] Jiang, Y.; Park, C.-M.; Loh, T. P. *Org. Lett*. **2014**, *16*, 3432−3435. Transition-Metal-Free Synthesis of Substituted Pyridines via Ring Expansion of 2-Allyl-2H-azirines.

[228] Jiang, Y.; Park, C.-M.; Loh, T. P. *Org. Lett*. **2014**, *16*, 3432−3435. Transition-Metal-Free Synthesis of Substituted Pyridines via Ring Expansion of 2-Allyl-2H-azirines.

[229] K. Watanabe, Y. Andou, Y.Shirai, H. Nishida, *Chem. Lett*. **2010**, *7*, 698–699. Racemization-free Monomer: α-Hydroxyisobutyric Acid from Bio-based Lactic Acid.

[230] F. Miege, B. M. Trost, *J. Am. Chem. Soc.* **2014**, *136*, 3016–3019. Development of ProPhenol Ligands for the Diastereo- and Enantioselective Synthesis of *β*-Hydroxy-*α*-amino Esters.

[231] A. E. Stiegman E. Graham, K. J. Perry, L. R. Khundkar, L.-T. Cheng, J. W. Perry, *J. Am. Chem. Soc.* **1991**, 113, 7658–7666. The Electronic Structure and Second-Order Nonlinear Optical Properties of Donor-Acceptor Acetylenes: A Detailed Investigation of Structure-Property Relationships.

[232] D. Sun, S. V. Rosokha, J. K. Kochi, *Angew. Chem.* **2005**, *117*, 5263–5266; *Angew. Chem., Int. Ed*. **2005**, *44*, 5133–5136. Through-Space (Cofacial) *π*-Delocalization among Multiple Aromatic Centers: Toroidal Conjugation in Hexaphenylbenzene-like Radical Cations.

[233] B. Liu, L. Jun, H.-Q. Wang, Y.-D. Zhao, Z.-L. Hang, *J. Mol. Struct*. **2007**, *833*, 82–87. Synthesis and spectroscopic properties of symmetrically substituted two-photon absorbing molecules with rigid elongated *π*-conjugation.

[234] P. Reutenauer, E. Buhler, P. J. Boul, S. J. Candau, J.-M. Lehn, *Chem. Eur. J.* **2009**, *15*, 1893–1900. Room Temperature Dynamic Polymers Based on Diels–Alder Chemistry.

[235] H. K. Hall, Jr., R. C. Sentman, *J. Org. Chem.* **1982**, *47*, 4572–4577. Dimethyl 1,1-dicyanoethene-2,2-dicarboxylate, a New Electrophilic Olefin.

[236] C. J. Ireland, K. Jones, J. S. Pizey, S. Johnson, *Synth. Commun.* **1976**, *6*, 185–191. Tetra-Substituted Ethylenes.

[237] M. O. Frederick, J. A. Mulder, M. R. Tracey, R. P. Hsung, J. Huang, K. C. M. Kurtz, L. Shen, C. J. Douglas, *J. Am. Chem. Soc*. **2003**, *125*, 2368–2369. A Copper-Catalyzed C−N Bond Formation Involving sp-Hybridized Carbons. A Direct Entry to Chiral Ynamides via N-Alkynylation of Amides.

[238] E. Block, C. Guo, M. Thiruvazhi, P. J. Toscano, *J. Am. Chem. Soc.* **1994**, *116*, 9403–9404. Total Synthesis of Thiarubrine B [3-(3-Buten-1-ynyl)-6-(1,3-pentadiynyl)-1,2-dithiin], the Antibiotic Principle of Giant Ragweed (Ambrosia trifida).

[239] O. V. Dolomanov, L. J. Bourhis, R. J. Gildea, J. A. K. Howard, H. Puschmann, *J. Appl. Cryst.* **2009**, *42*, 339–341. OLEX2: a complete structure solution, refinement and analysis program.

[240] G. M. Sheldrick, *Acta Cryst.* **2008**, *A64*, 112–122. A short history of SHELX.

Chapter 10

Appendix

10. Appendix

10.1. NMR Spectra

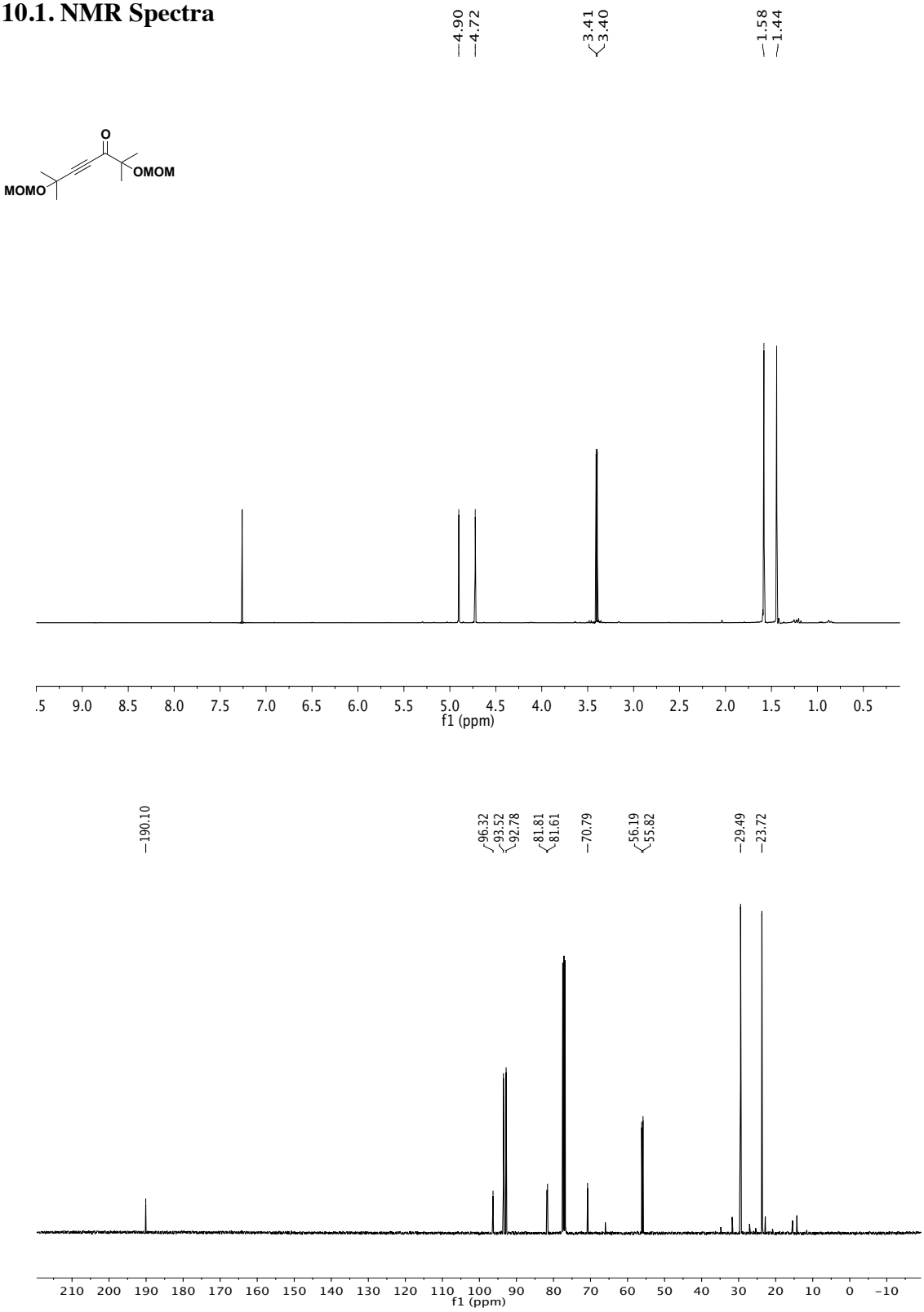

Figure 79. ^{1}H NMR (top) and ^{13}C NMR (bottom) spectra of compound **118** in $CDCl_3$.

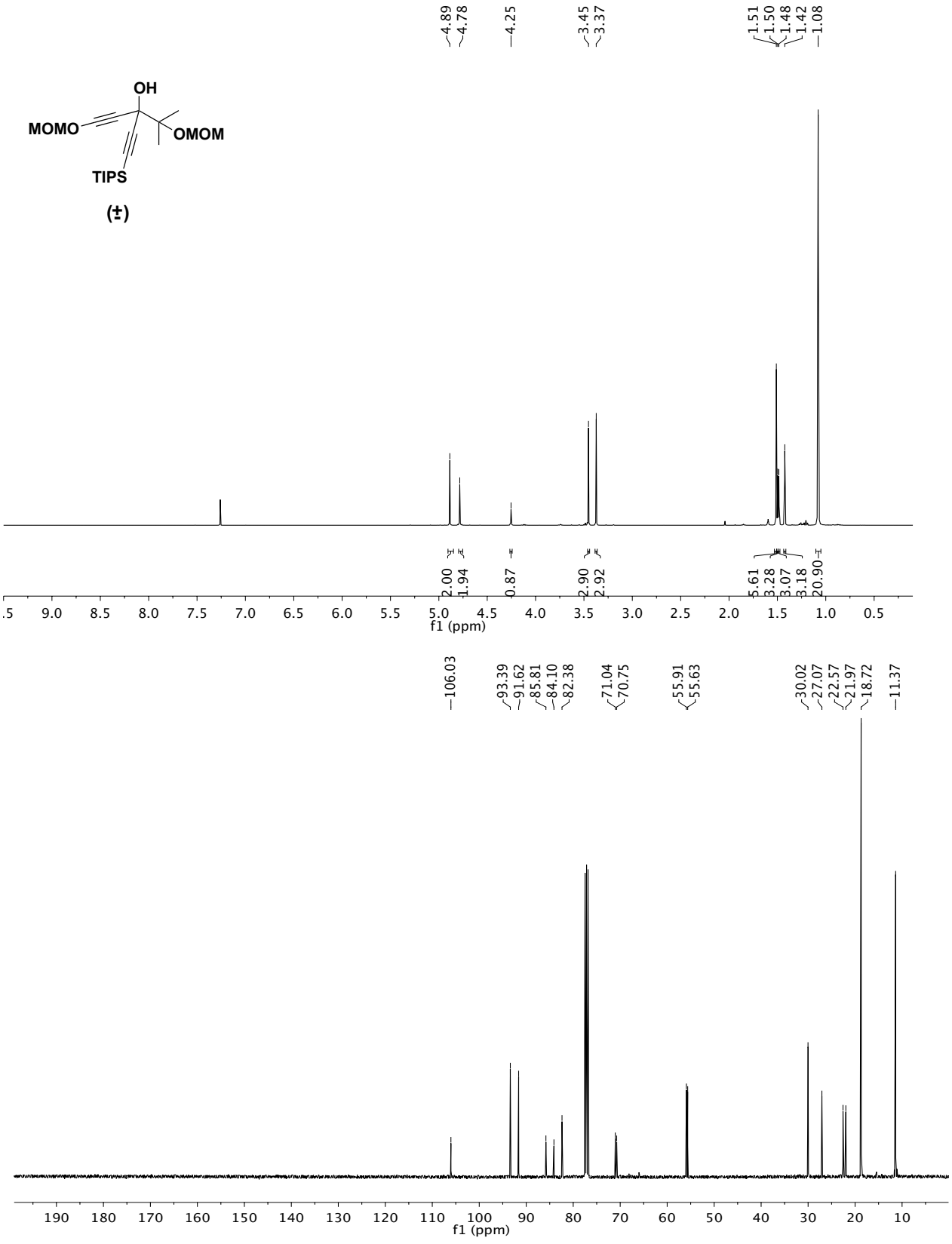

Figure 80. ^{1}H NMR (top) and ^{13}C NMR (bottom) spectra of compound **119** in $CDCl_3$.

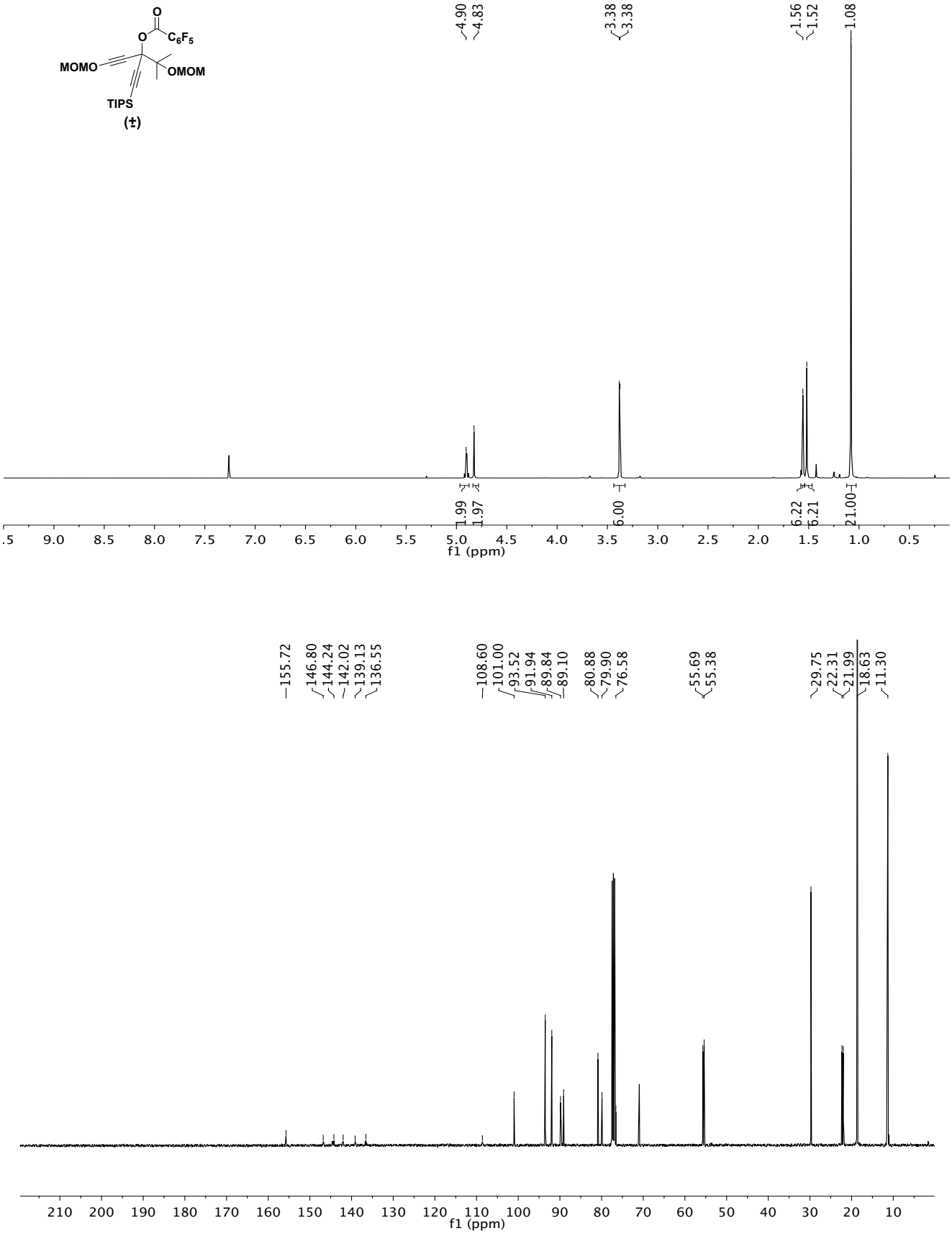

Figure 81. ^{1}H NMR (top) and ^{13}C NMR (bottom) spectra of compound **120** in $CDCl_3$.

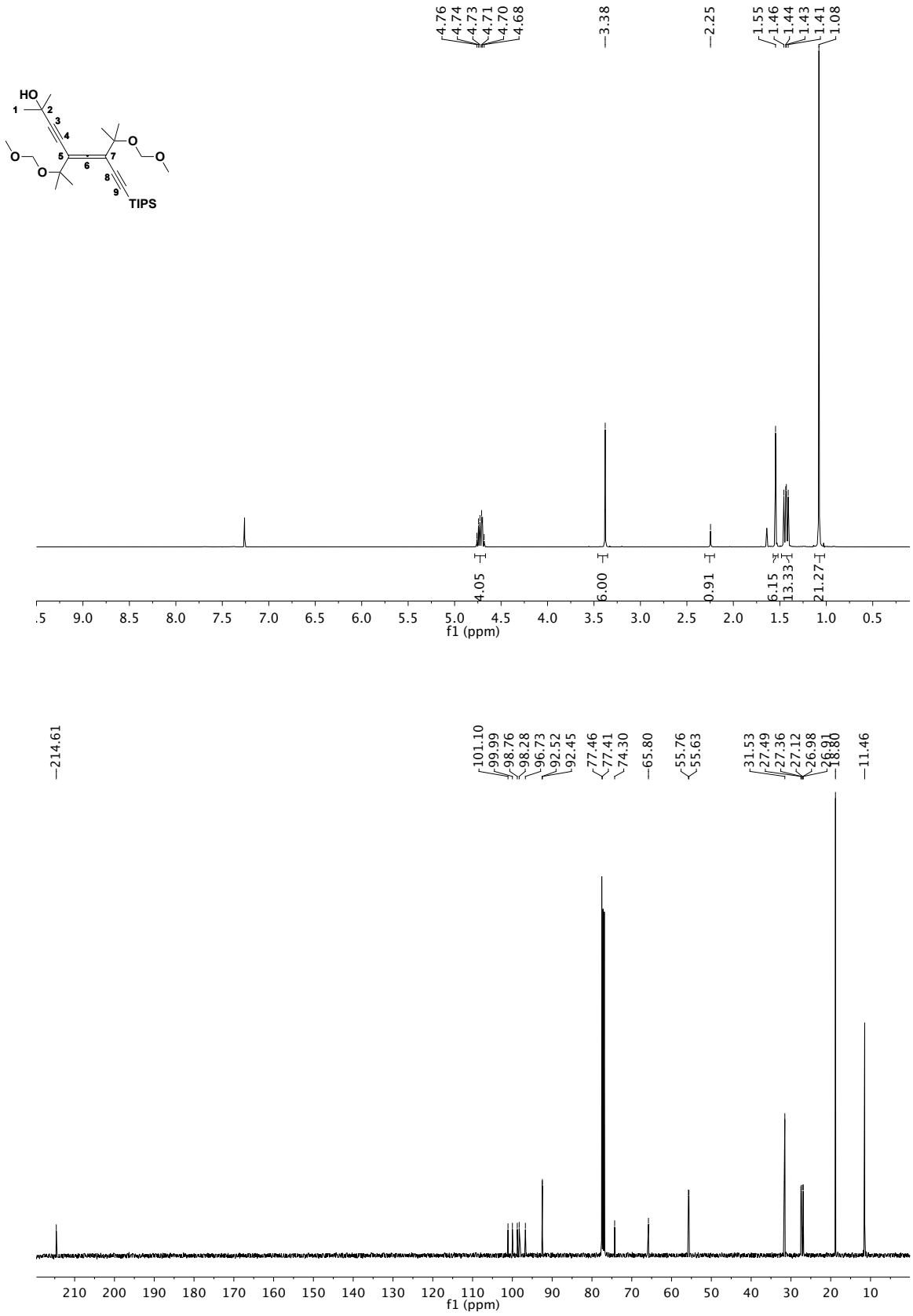

Figure 82. ^{1}H NMR (top) and ^{13}C NMR (bottom) spectra of compound **121** in $CDCl_3$.

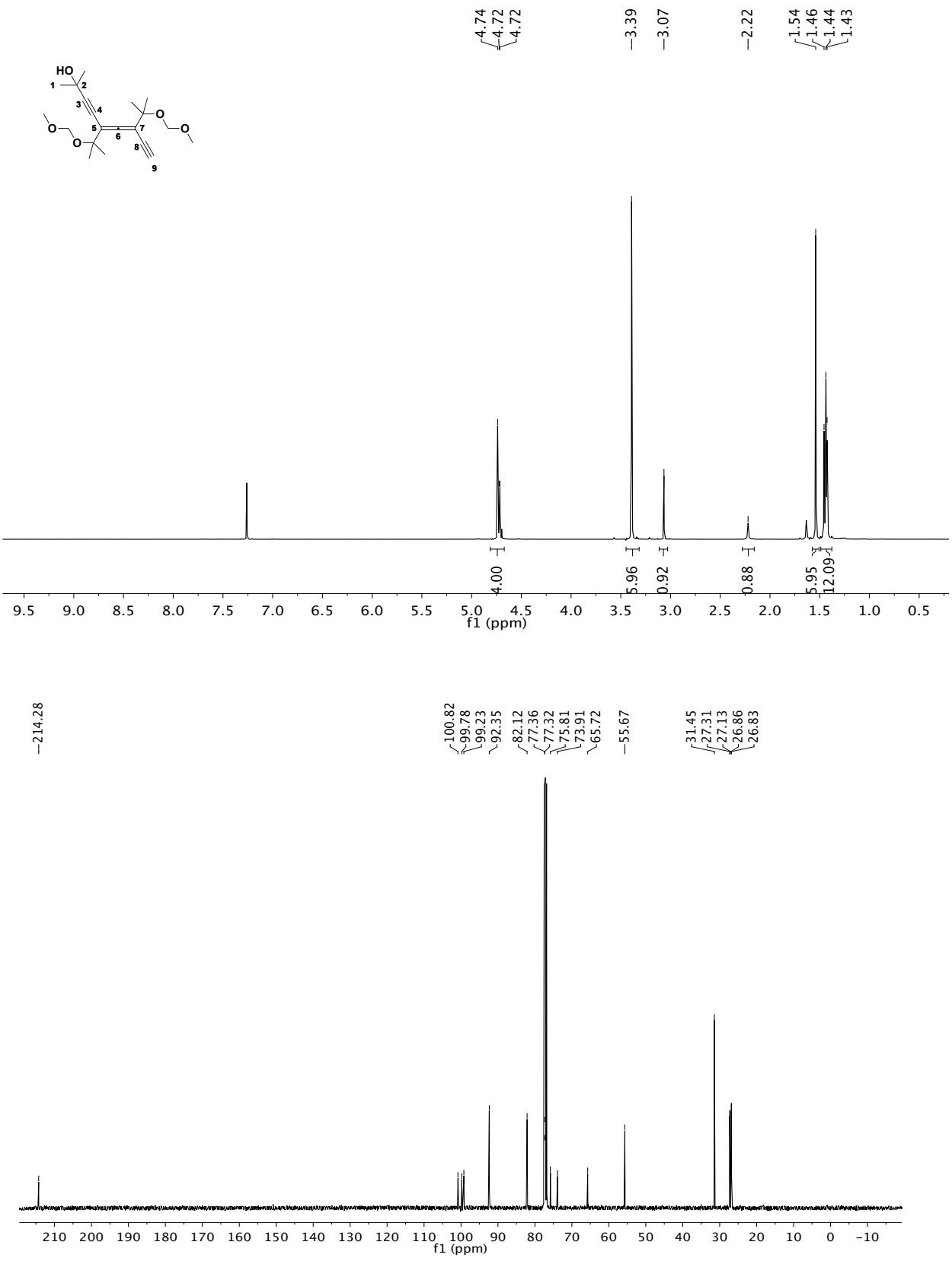

Figure 83. ^{1}H NMR (top) and ^{13}C NMR (bottom) spectra of compound **114** in $CDCl_3$.

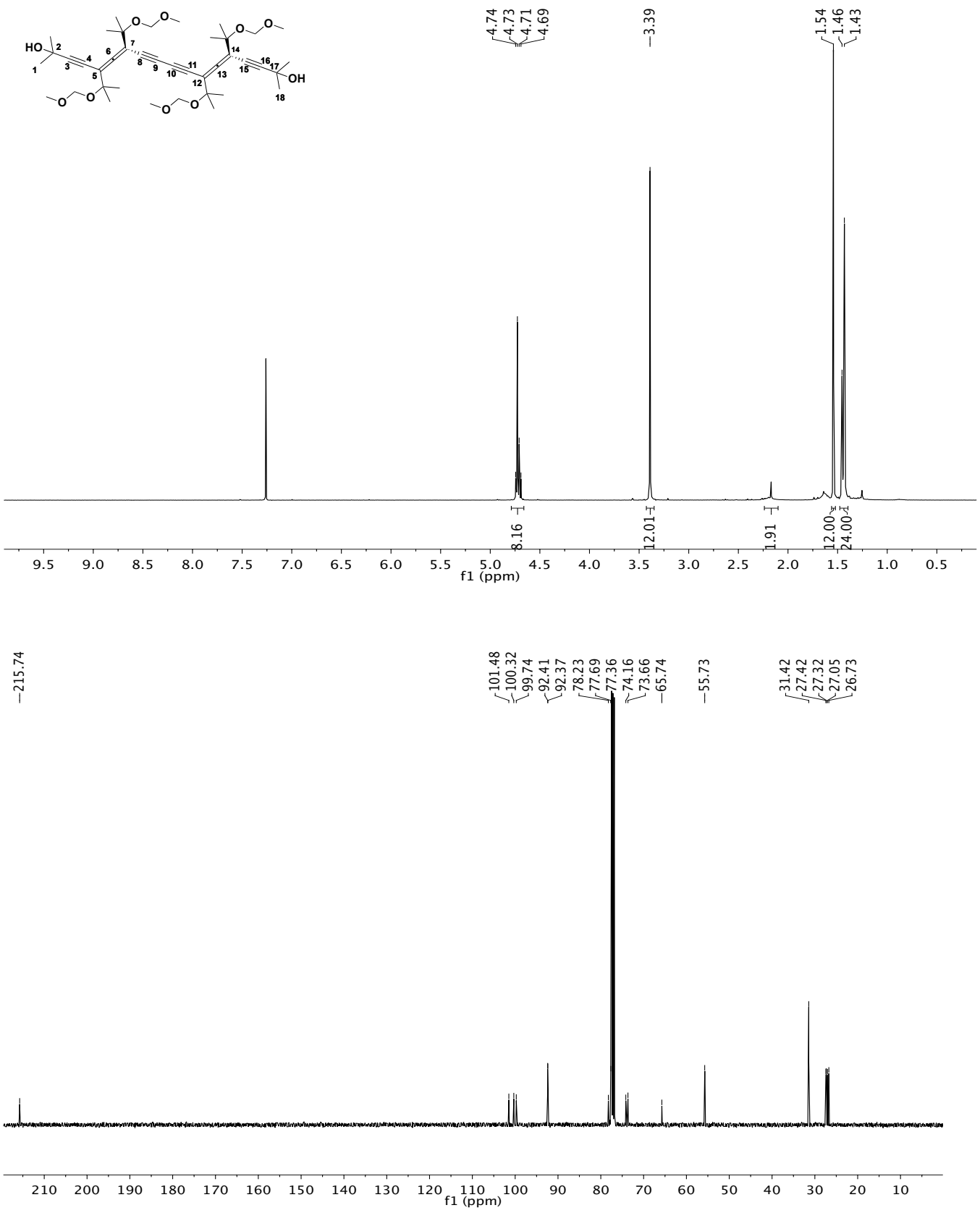

Figure 84. ^{1}H NMR (top) and ^{13}C NMR (bottom) spectra of compound **122** in $CDCl_3$.

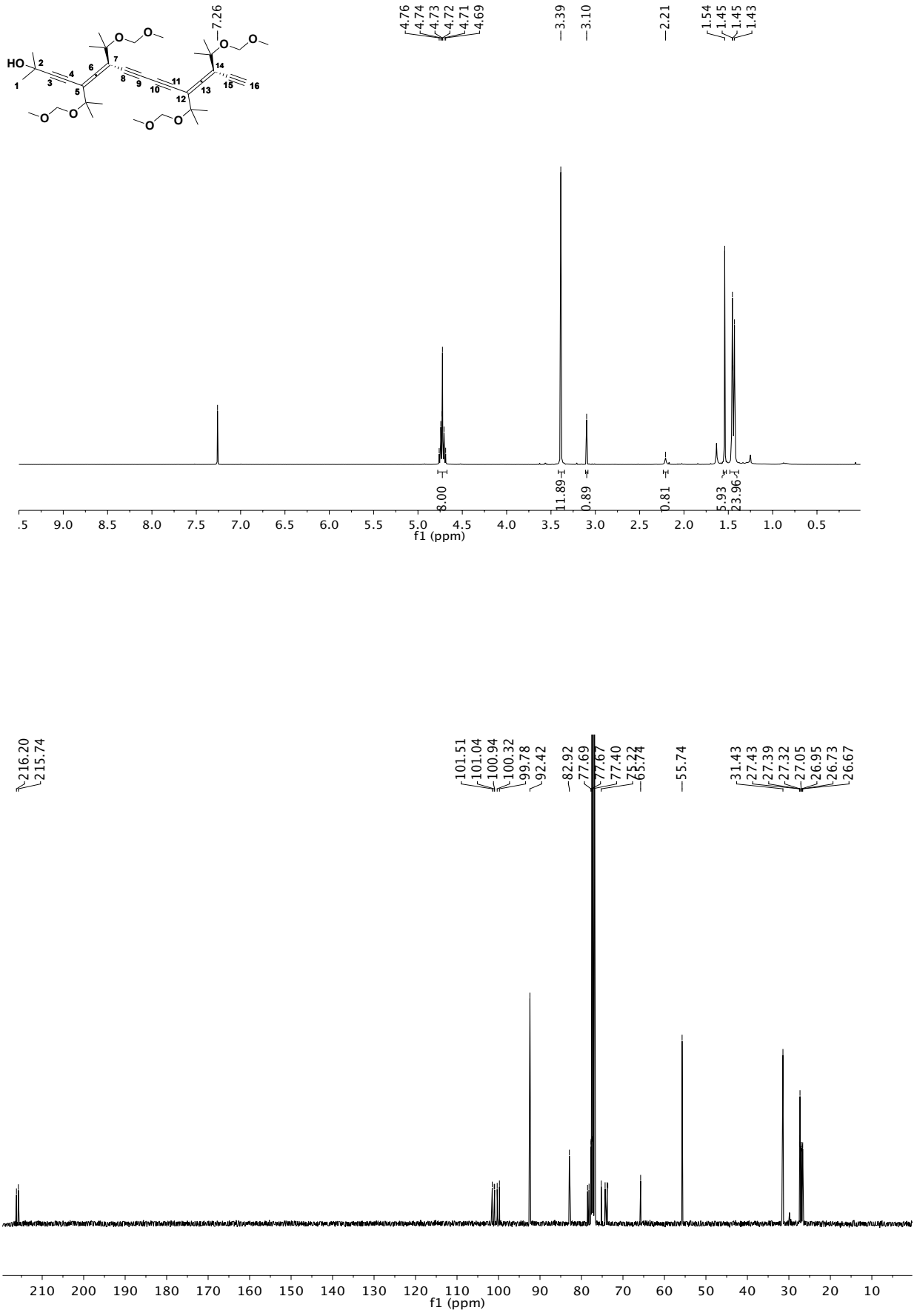

Figure 85. ^{1}H NMR (top) and ^{13}C NMR (bottom) spectra of compound **123** in $CDCl_3$.

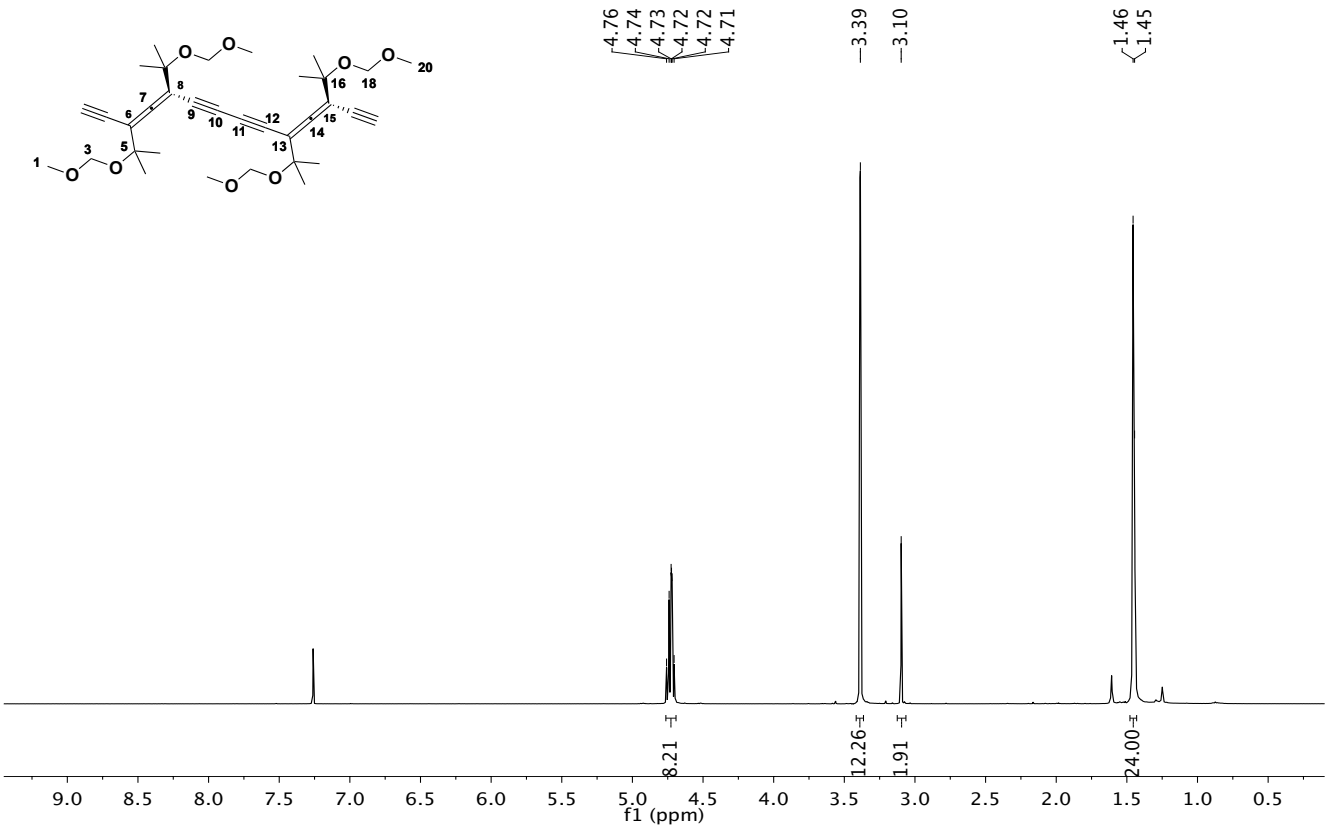
4.76
4.74
4.73
4.72
4.72
4.71
3.39
3.10
1.46
1.45
8.21
12.26
1.91
24.00
f1 (ppm)

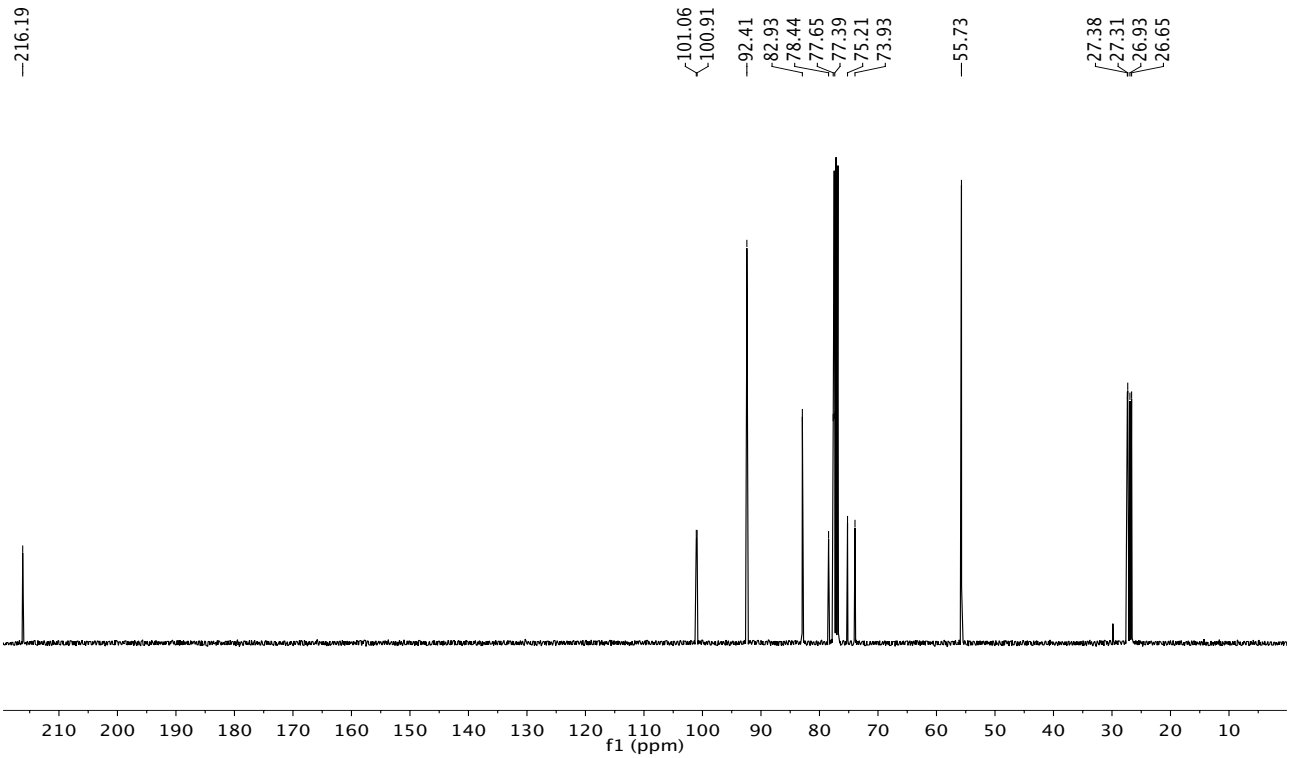
216.19
101.06
100.91
92.41
82.93
78.44
77.65
77.39
75.21
73.93
55.73
27.38
27.31
26.93
26.65
f1 (ppm)

Figure 86. ^{1}H NMR (top) and ^{13}C NMR (bottom) spectra of compound **124** $CDCl_3$.

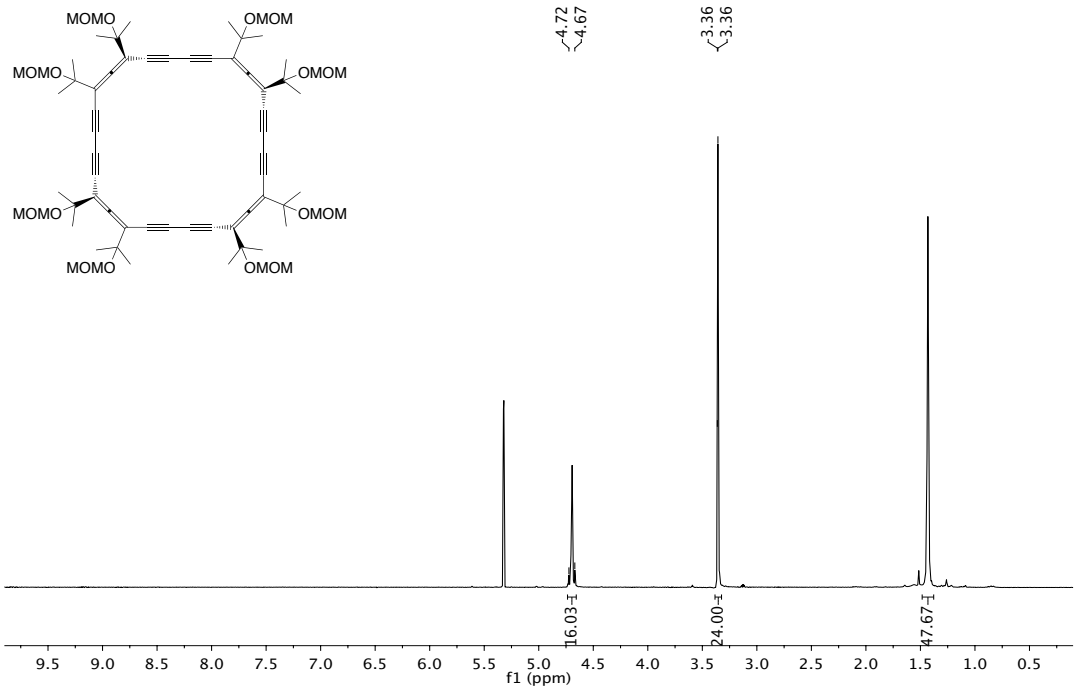

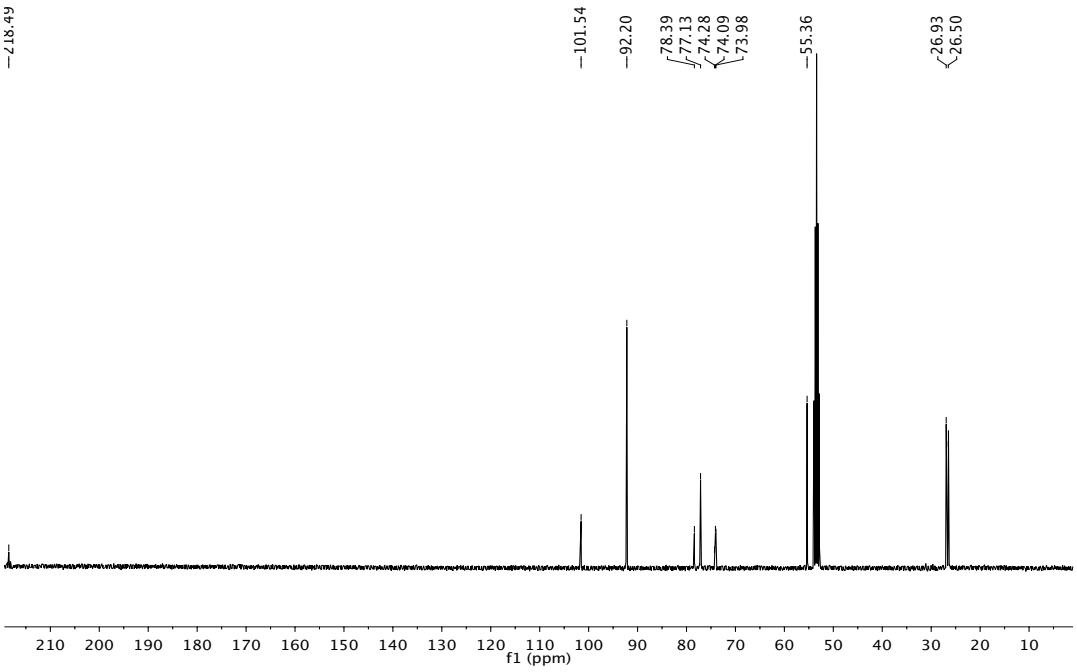

Figure 87. ^{1}H NMR (top) and ^{13}C NMR (bottom) spectra of compound **125** in CD_2Cl_2.

10.2. Electrochemistry of Reaction Products

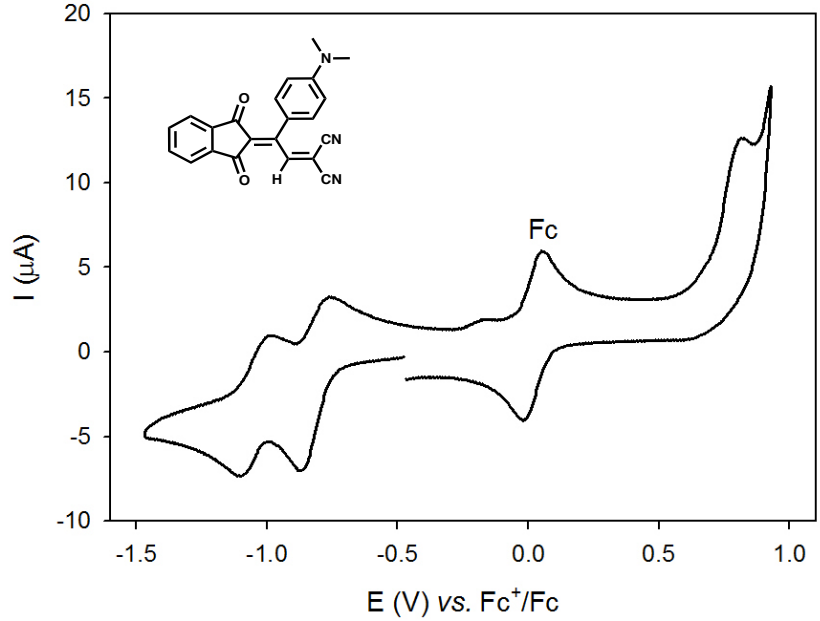

Figure 88. Cyclic voltammetry of **130** in CH_2Cl_2 + 0.1 M nBu$_4$NPF$_6$ in the presence of ferrocene on a glassy carbon working electrode at a scan rate of 0.1 Vs^{-1} (298 K).

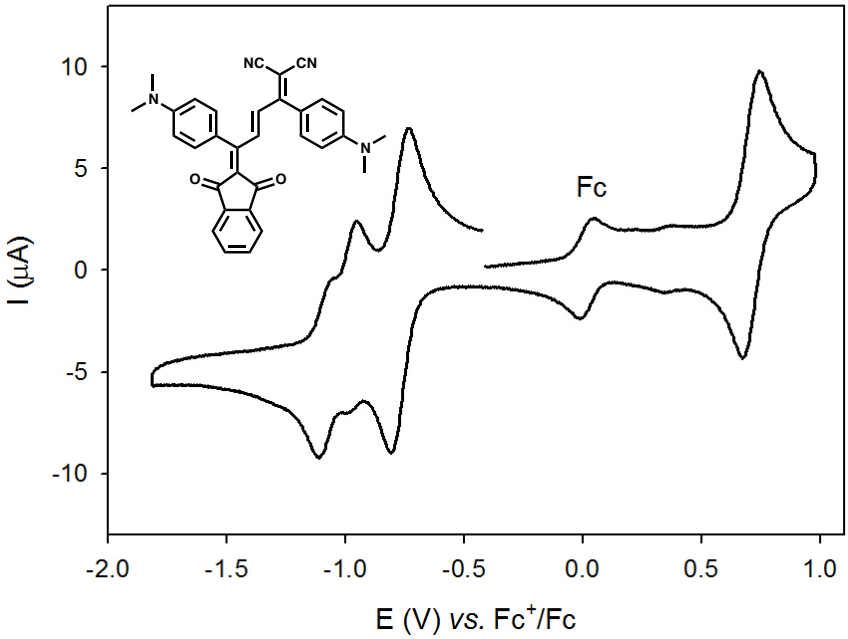

Figure 89. Cyclic voltammetry of **131** in CH_2Cl_2 + 0.1 M nBu$_4$NPF$_6$ in the presence of ferrocene on a glassy carbon working electrode at a scan rate of 0.1 Vs^{-1} (298 K).

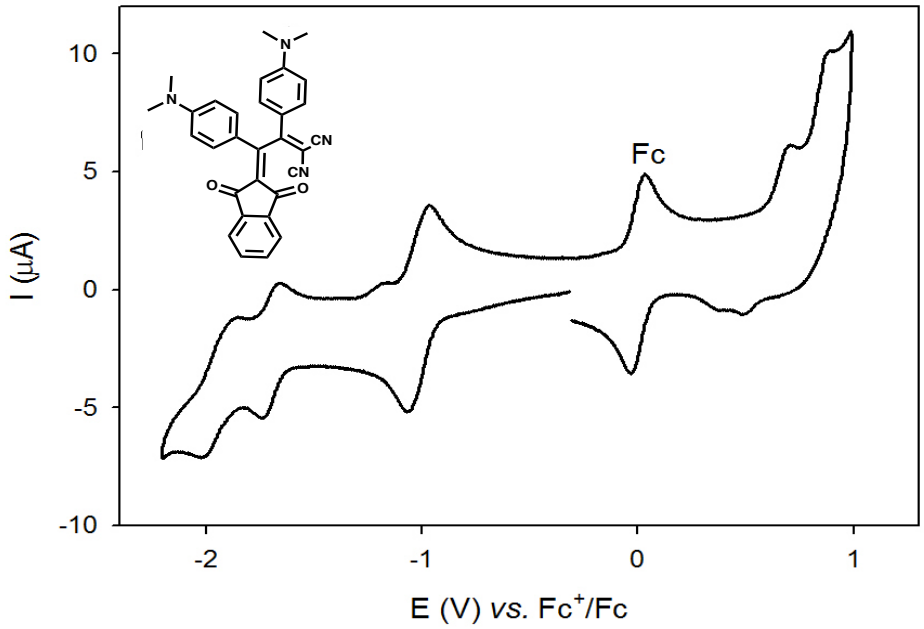

Figure 90. Cyclic voltammetry of **133a** in CH_2Cl_2 + 0.1 M nBu_4NPF_6 in the presence of ferrocene on a glassy carbon working electrode at a scan rate of 0.1 Vs^{-1} (298 K).

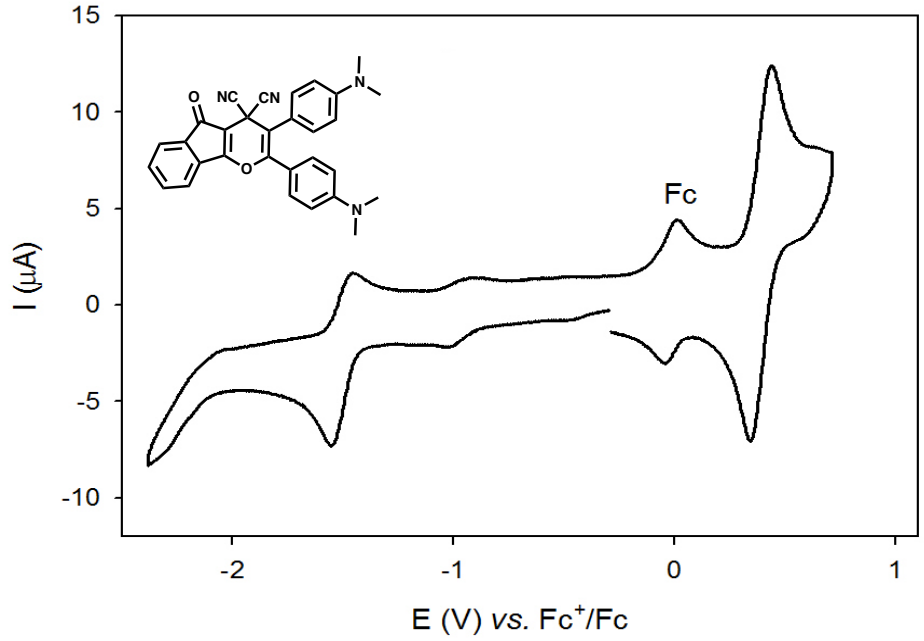

Figure 91. Cyclic voltammetry of **133b** in CH_2Cl_2 + 0.1 M nBu_4NPF_6 in the presence of ferrocene on a glassy carbon working electrode at a scan rate of 0.1 Vs^{-1} (298 K).

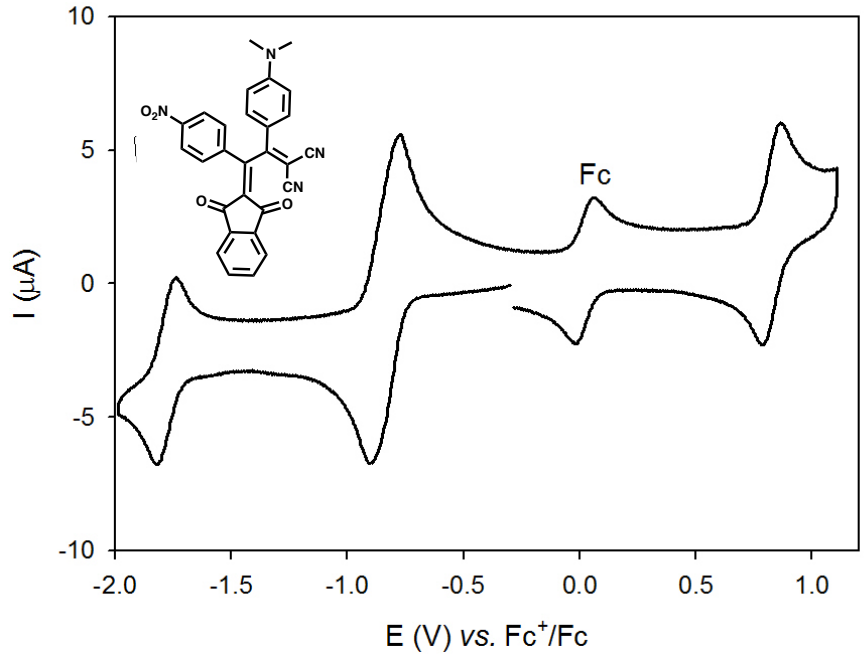

Figure 92. Cyclic voltammetry of **149a** in CH_2Cl_2 + 0.1 M nBu$_4$NPF$_6$ in the presence of ferrocene on a glassy carbon working electrode at a scan rate of 0.1 Vs^{-1} (298 K).

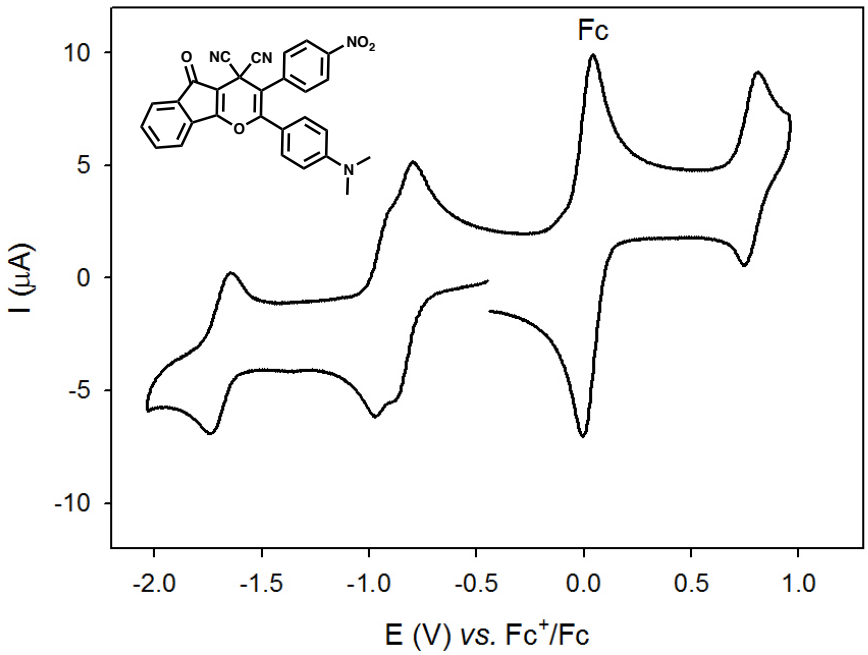

Figure 93. Cyclic voltammetry of **149b** in CH_2Cl_2 + 0.1 M nBu$_4$NPF$_6$ in the presence of ferrocene on a glassy carbon working electrode at a scan rate of 0.1 Vs^{-1} (298 K).

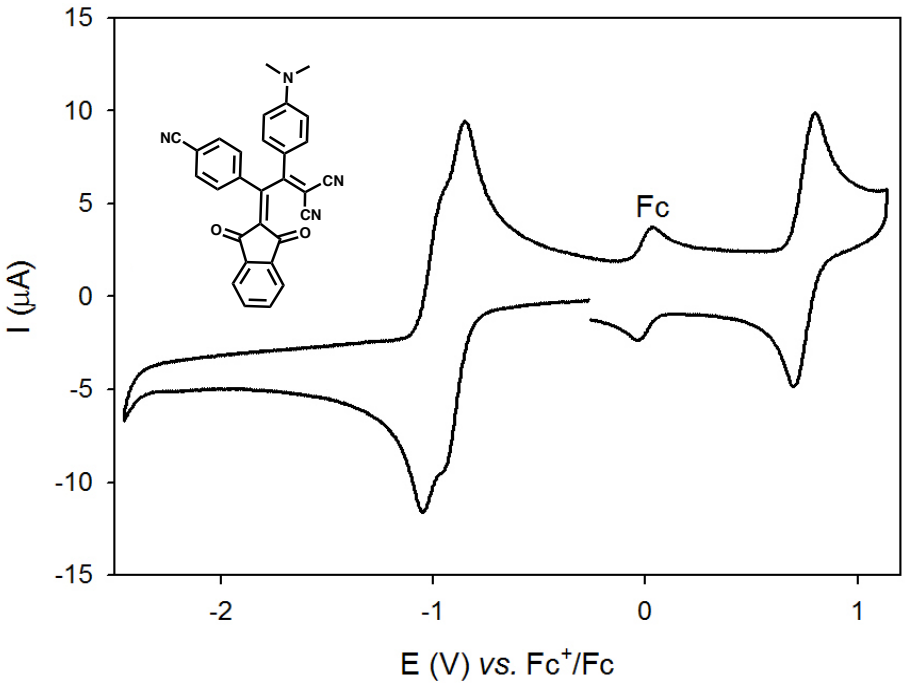

Figure 94. Cyclic voltammetry of **150a** in CH_2Cl_2 + 0.1 M nBu_4NPF_6 in the presence of ferrocene on a glassy carbon working electrode at a scan rate of 0.1 Vs^{-1} (298 K).

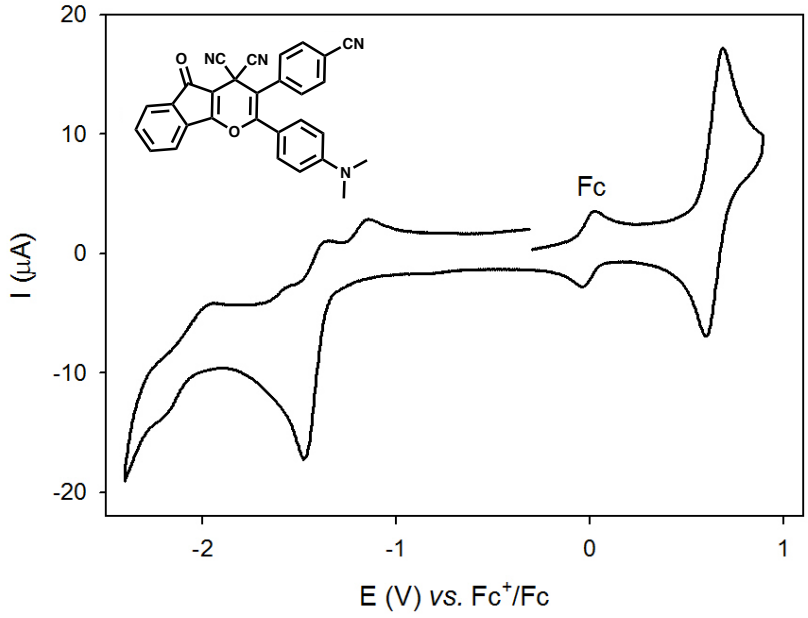

Figure 95. Cyclic voltammetry of **150b** in CH_2Cl_2 + 0.1 M nBu_4NPF_6 in the presence of ferrocene on a glassy carbon working electrode at a scan rate of 0.1 Vs^{-1} (298 K).

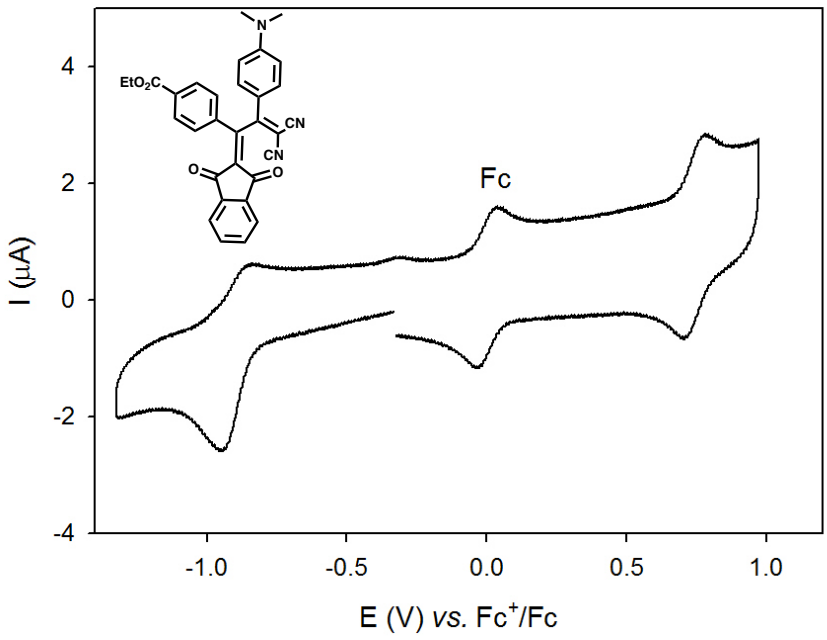

Figure 96. Cyclic voltammetry of **151a** in CH_2Cl_2 + 0.1 M nBu_4NPF_6 in the presence of ferrocene on a glassy carbon working electrode at a scan rate of 0.1 Vs^{-1} (298 K).

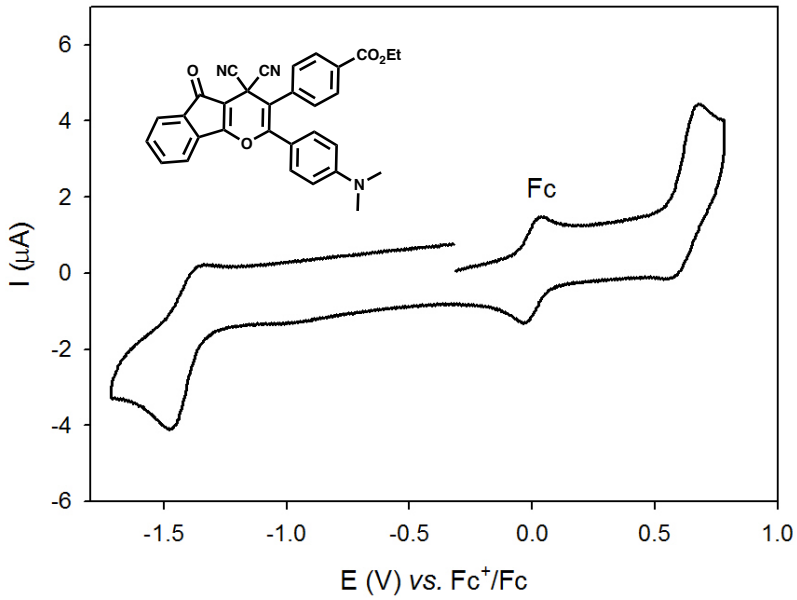

Figure 97. Cyclic voltammetry of **151b** in CH_2Cl_2 + 0.1 M nBu_4NPF_6 in the presence of ferrocene on a glassy carbon working electrode at a scan rate of 0.1 Vs^{-1} (298 K).

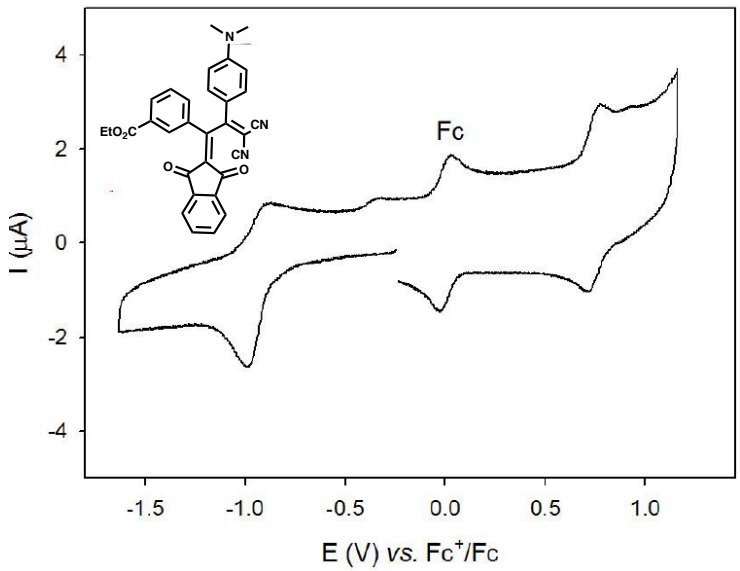

Figure 98. Cyclic voltammetry of **152a** in CH_2Cl_2 + 0.1 M nBu_4NPF_6 in the presence of ferrocene on a glassy carbon working electrode at a scan rate of 0.1 Vs^{-1} (298 K).

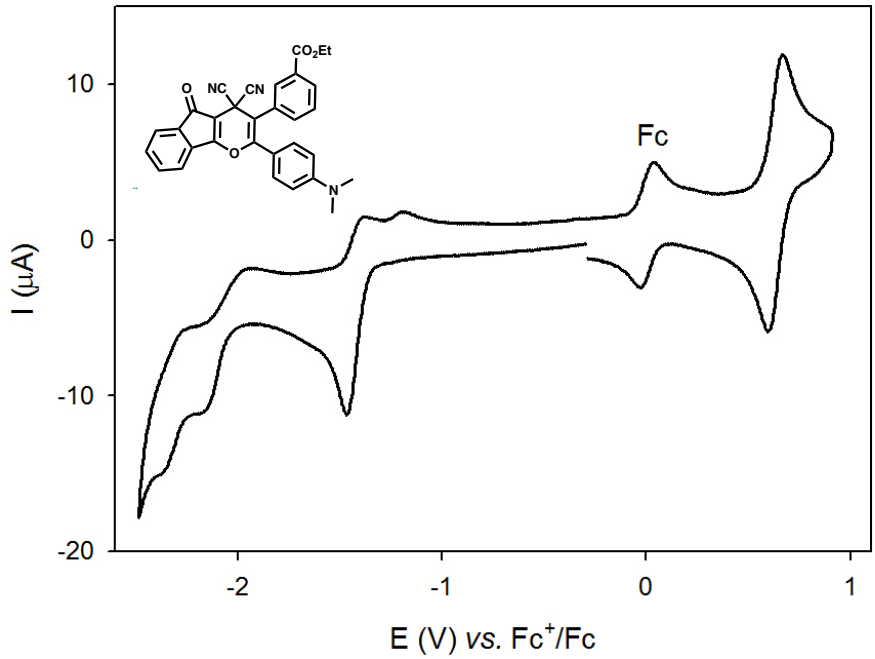

Figure 99. Cyclic voltammetry of **152b** in CH_2Cl_2 + 0.1M nBu_4NPF_6 in the presence of ferrocene on a glassy carbon working electrode at a scan rate of 0.1 Vs^{-1} (298 K).

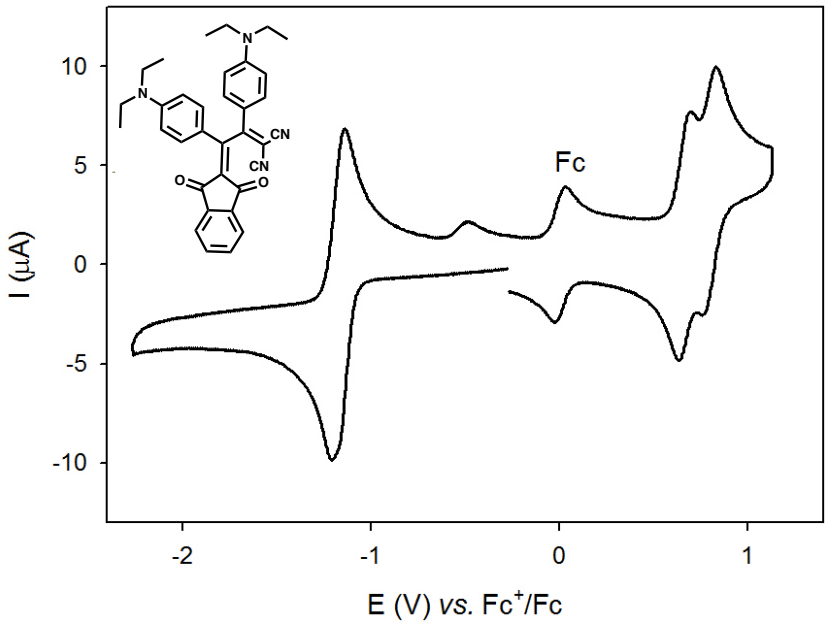

Figure 100. Cyclic voltammetry of **153a** in CH_2Cl_2 + 0.1M nBu_4NPF_6 in the presence of ferrocene on a glassy carbon working electrode at a scan rate of 0.1 Vs^{-1} (298 K).

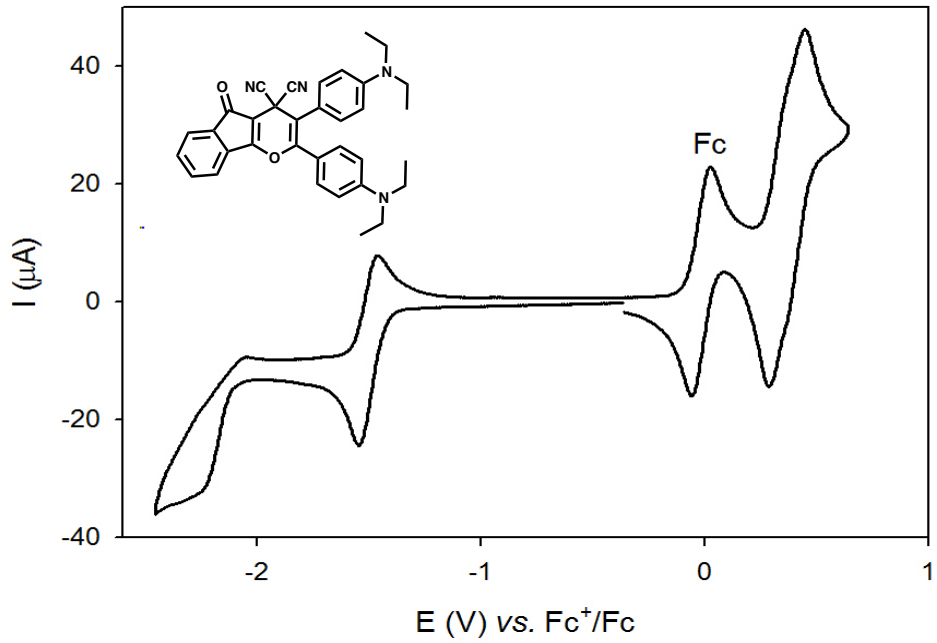

Figure 101. Cyclic voltammetry of **153b** in CH_2Cl_2 + 0.1M nBu_4NPF_6 in the presence of ferrocene on a glassy carbon working electrode at a scan rate of 0.1 Vs^{-1} (298 K).

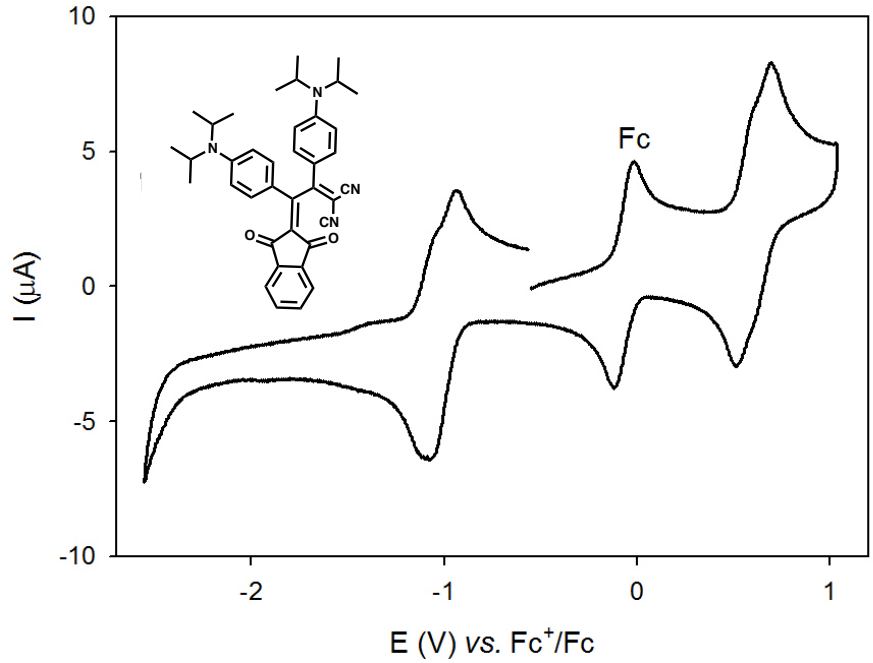

Figure 102. Cyclic voltammetry of **154a** in CH_2Cl_2 + 0.1 M nBu_4NPF_6 in the presence of ferrocene on a glassy carbon working electrode at a scan rate of 0.1 Vs^{-1} (298 K).

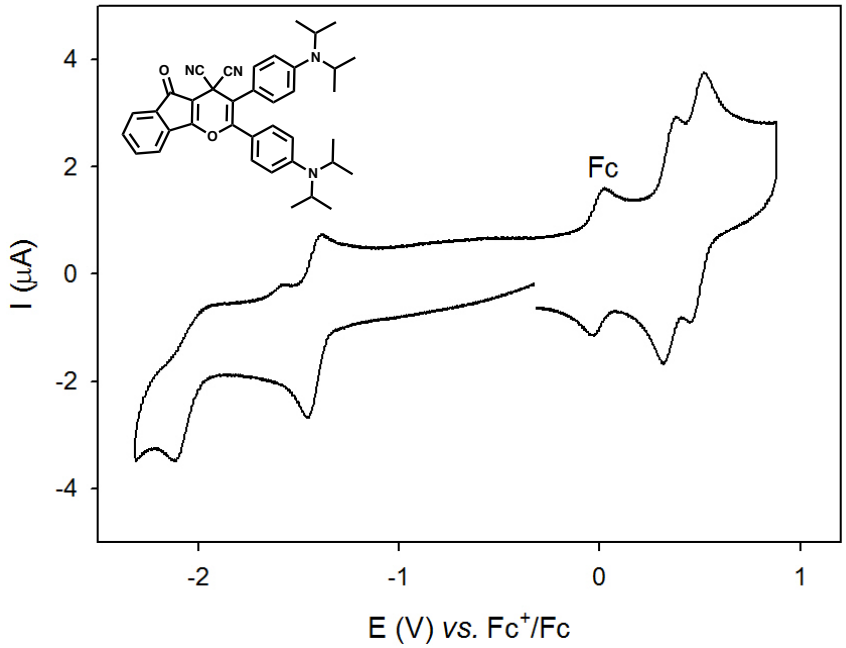

Figure 103. Cyclic voltammetry of **154b** in CH_2Cl_2 + 0.1 M nBu_4NPF_6 in the presence of ferrocene on a glassy carbon working electrode at a scan rate of 0.1 Vs^{-1} (298 K).

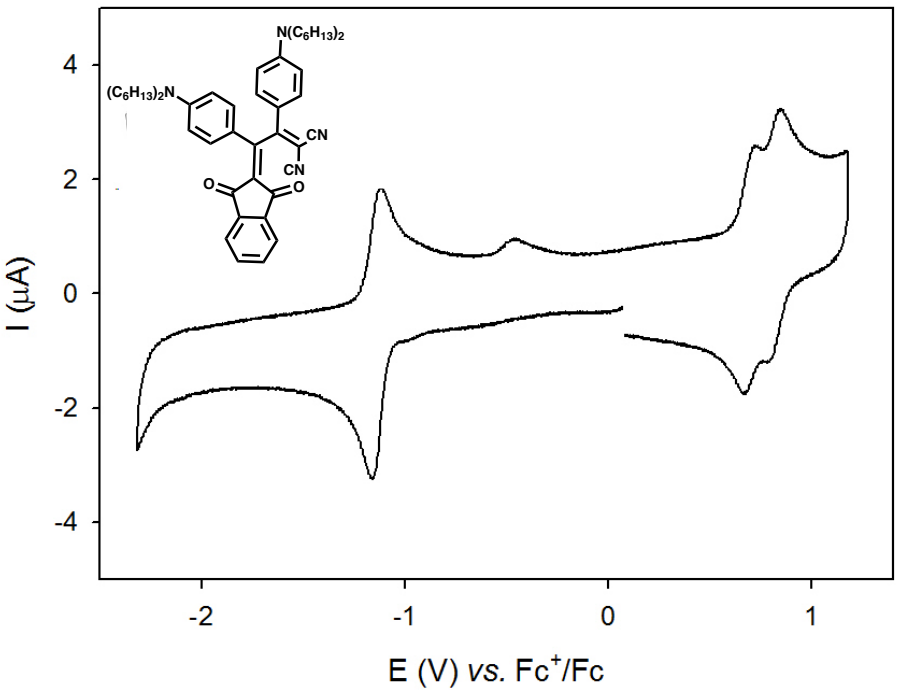

Figure 104. Cyclic voltammetry of **155a** in CH_2Cl_2 + 0.1 M nBu$_4$NPF$_6$ without ferrocene on a glassy carbon working electrode at a scan rate of 0.1 Vs^{-1} (298 K).

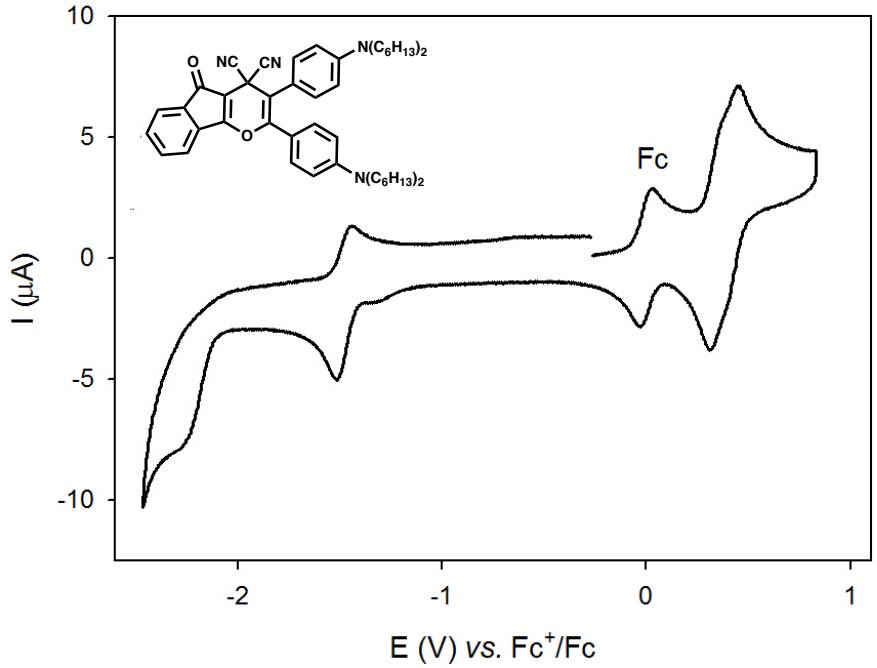

Figure 105. Cyclic voltammetry of **155b** in CH_2Cl_2 + 0.1 M nBu$_4$NPF$_6$ in the presence of ferrocene on a glassy carbon working electrode at a scan rate of 0.1 Vs^{-1} (298 K).

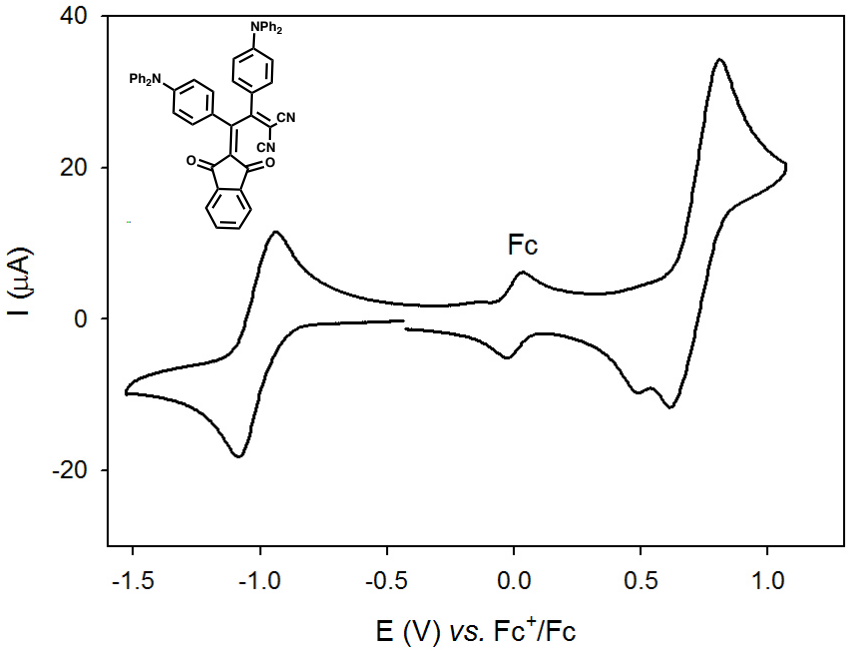

Figure 106. Cyclic voltammetry of **156a** in CH_2Cl_2 + 0.1 M nBu_4NPF_6 in the presence of ferrocene on a glassy carbon working electrode at a scan rate of 0.1 Vs^{-1} (298 K).

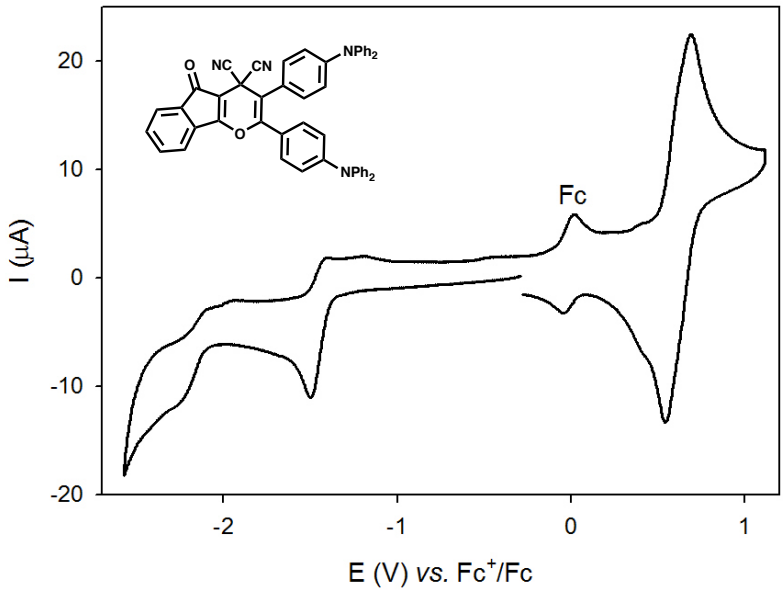

Figure 107. Cyclic voltammetry of **156b** in CH_2Cl_2 + 0.1 M nBu_4NPF_6 in the presence of ferrocene on a glassy carbon working electrode at a scan rate of 0.1 Vs^{-1} (298 K).

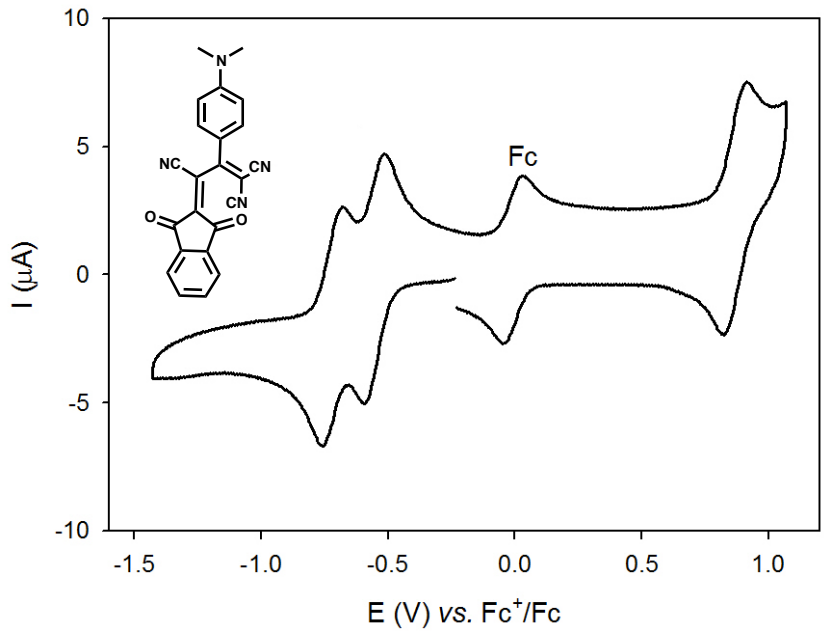

Figure 108. Cyclic voltammetry of **157a** in CH_2Cl_2 + 0.1M nBu_4NPF_6 in the presence of ferrocene on a glassy carbon working electrode at a scan rate of 0.1 Vs^{-1} (298 K).

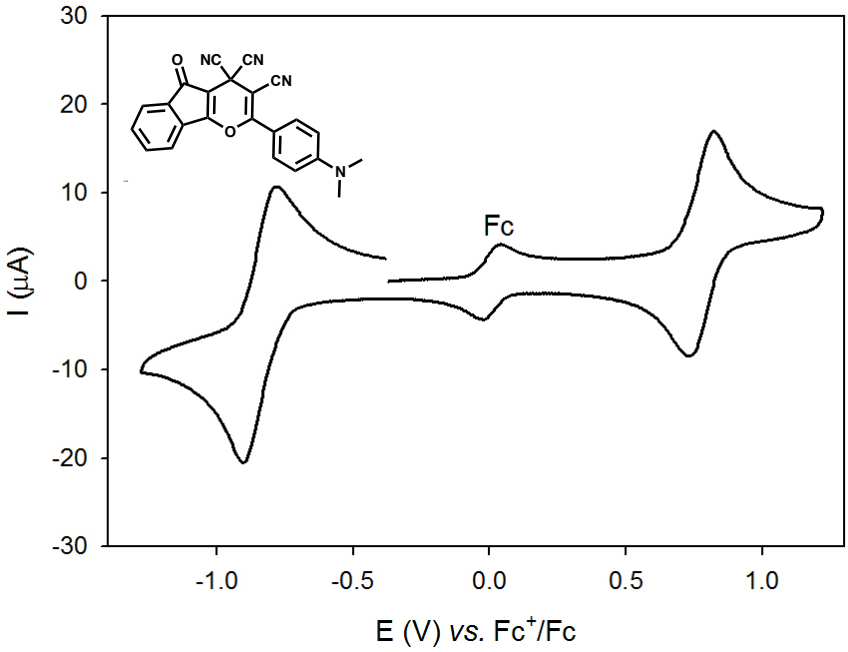

Figure 109. Cyclic voltammetry of **157b** in CH_2Cl_2 + 0.1 M nBu_4NPF_6 in the presence of ferrocene on a glassy carbon working electrode at a scan rate of 0.1 Vs^{-1} (298 K).

Table 10. Supplementary Cyclic voltammetry and rotating disk voltammetry data recorded in CH_2Cl_2 0.1 M nBu_4NPF_6 of products from Chapter 4.

Species	Cyclic voltammetry[a]			Rotating disk voltammetry	
	E° [V][b]	ΔEp [mV][c]	Ep [V][d]	$E_{1/2}$ [V]	Slope [mV][e]
(±)-**165**	+0.58	130		+0.63 (1e⁻)	95
173 and **174**	+0.72	120		+0.83 (1e⁻)	110
	+0.54	60		+0.56 (1e⁻)	70
	–1.28	130		–1.38 (1e⁻)	130
	–1.42	130		–1.66 (1e⁻)	120
175			+0.86	+0.83 (1e⁻)	
			–1.52	+1.53 (1e⁻)	
182			+0.78	+0.41 (1e⁻)	90
	+0.50	80		+0.59 (1e⁻)	60
			–1.62	–1.38 (1e⁻)	60
				–1.64 (1e⁻)	140
184	+0.78	90		+0.78 (1e⁻)	75
			–1.62	–1.62 (2e⁻)	120
186	+0.52	70		+0.53 (1e⁻)	60
188	+0.79	90		+0.80 (1e⁻)	70
			–1.47	–1.52 (2e⁻)	120
190	+0.51	65		+0.51 (1e⁻)	60
192	+0.78	75		+0.77 (1e⁻)	75
	–1.45	140		–1.46 (2e⁻)	80
(±)-**193**	+0.36	79		+0.37 (2e⁻)	70
194	+0.76	60		+0.79 (1e⁻)	60
	+0.66	60		+0.66 (1e⁻)	60
	–1.35	170		–1.43 (2e⁻)	140
195	+0.81	57		+0.83 (1e⁻)	55
	+0.68	54		+0.69 (1e⁻)	55
	–1.46	167		–1.50 (2e⁻)	130
196	+0.81	100		+0.84 (1e⁻)	80
	+0.64	85		+0.66 (1e⁻)	60
	–1.41	190		–1.53 (2e⁻)	150
198	+0.79	100		+0.82 (1e⁻)	60
	–1.32	95		–1.40 (2e⁻)	70
200	+0.40	65		+0.41 (1e⁻)	60
	–1.17	65		–1.17 (1e⁻)	60
	–1.38	70		–1.38 (1e⁻)	70
202			+0.95	–0.93 (1e⁻)	70
	–1.10	98		–1.15 (1e⁻)	70
	–1.38	111		–1.47 (1e⁻)	90
206	+0.45	61		+0.46 (1e⁻)	55
	–1.00	72		–0.99 (1e⁻)	70
	–1.31	93		–1.34 (1e⁻)	110
207			+0.48	+0.45 (1e⁻)	70
	–1.00	75		–0.99 (1e⁻)	70
	–1.31	89		–1.27 (1e⁻)	145
210	+0.80	100		+0.80 (1e⁻)	80
	–1.12	100		–1.12 (1e⁻)	70
	–1.34	95		–1.42 (1e⁻)	75

a) Scan rate, v = 0.1 V s^{-1}. b) $E^o = (E_{pc} + E_{pa})/2$, where E_{pc} and E_{pa} correspond to the cathodic and anodic peak potentials, respectively. c) $E_p = E_{pa} - E_{pc}$. d) E_p = irreversible peak potential. e)

Logarithmic analysis of the wave obtained by plotting E versus Log[I/(I_{lim}–I)]; I_{lim} is the limiting current and I the current.

Table 11. Supplementary Cyclic voltammetry and rotating disk voltammetry data recorded in CH_2Cl_2 0.1 M nBu$_4$NPF$_6$ of electron deficient alkenes.

Species	Cyclic voltammetry[a]			Rotating disk voltammetry	
	E° [V][b]	ΔEp [mV][c]	Ep [V][d]	$E_{1/2}$ [V]	Slope [mV][e]
67 (TCNE)[114]	–0.32	f)	–1.35	f) f)	f) f)
158	–0.44 –1.28	55 120		–0.47 (1e$^-$) –1.40 (1e$^-$)	80 85
162	–0.81 –1.34	70 175		–0.77 (1e$^-$) –1.40 (1e$^-$)	60 110
164	–0.66 –1.27	85 180		–0.71 (1e$^-$) –1.44 (1e$^-$)	70 100
168	–1.10 –1.37	90 165		–1.10 (1e$^-$) –1.45 (1e$^-$)	75 120
181	–1.44	250		–1.57 (2e$^-$)	130
185	–1.13	180		–1.24 (2e$^-$)	200

a) Scan rate, v = 0.1 V s^{-1}. b) E^o = (E_{pc} + E_{pa})/2, where E_{pc} and E_{pa} correspond to the cathodic and anodic peak potentials, respectively. c) E_p = E_{pa} – E_{pc}. d) E_p = irreversible peak potential. e) Logarithmic analysis of the wave obtained by plotting E versus Log[I/(I_{lim}–I)]; I_{lim} is the limiting current and I the current. f) Data not reported.

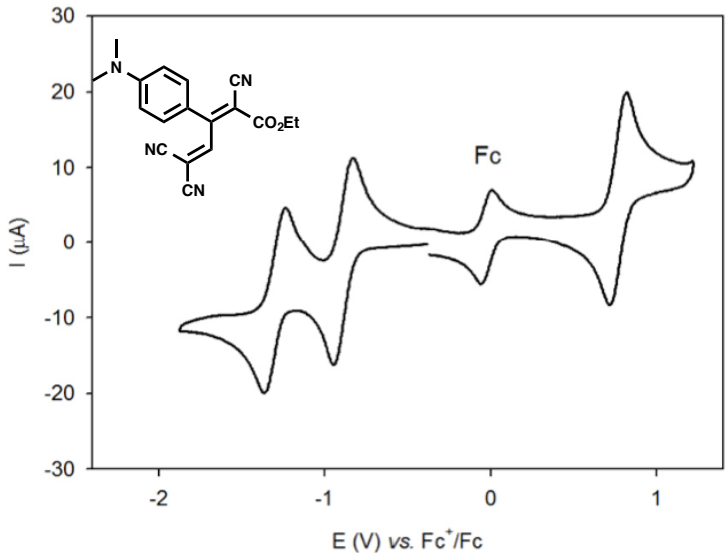

Figure 110. Cyclic voltammetry of **159** in CH_2Cl_2 + 0.1 M nBu$_4$NPF$_6$ in the presence of ferrocene on a glassy carbon working electrode at a scan rate of 0.1 Vs^{-1} (298 K).

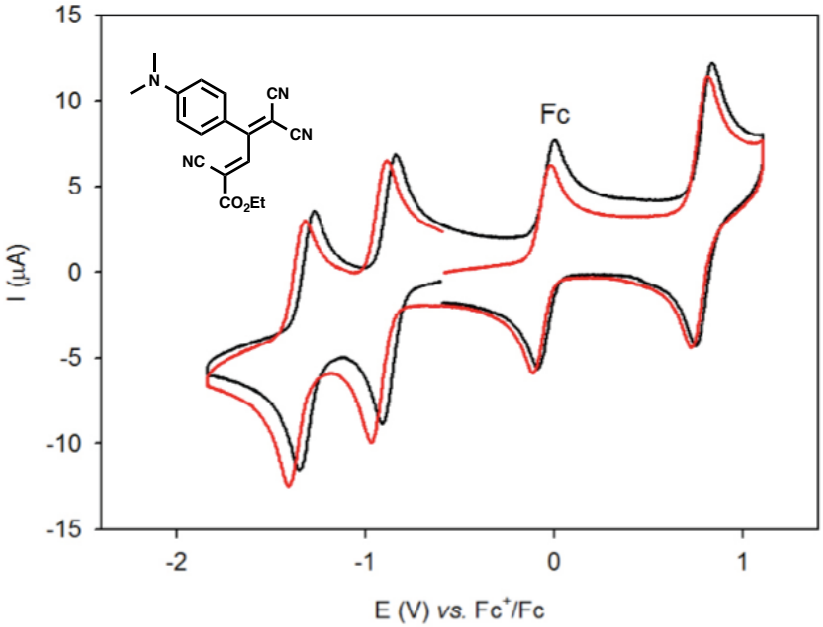

Figure 111. Cyclic voltammetry of **160** in CH_2Cl_2 + 0.1 M nBu$_4$NPF$_6$ in the presence of ferrocene on a glassy carbon working electrode at a scan rate of 0.1 Vs^{-1} (298 K).

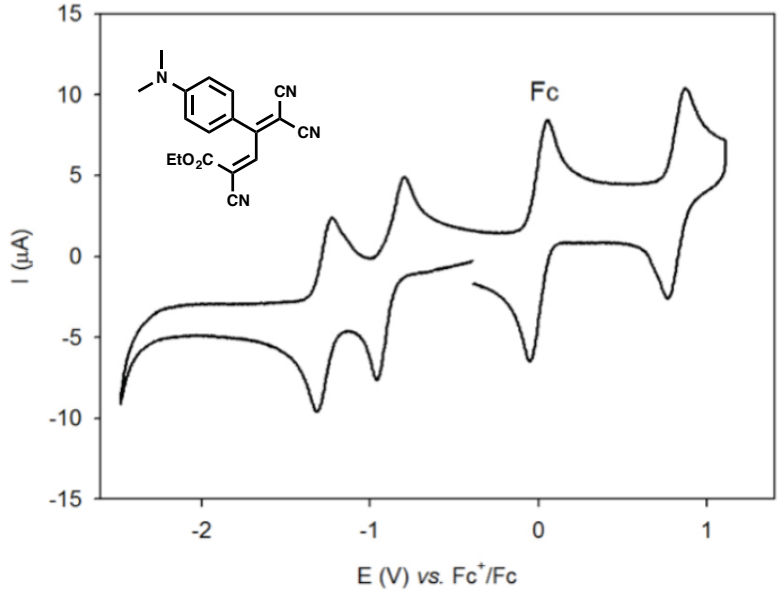

Figure 112. Cyclic voltammetry of **161** in CH_2Cl_2 + 0.1 M nBu$_4$NPF$_6$ in the presence of ferrocene on a glassy carbon working electrode at a scan rate of 0.1 Vs^{-1} (298 K).

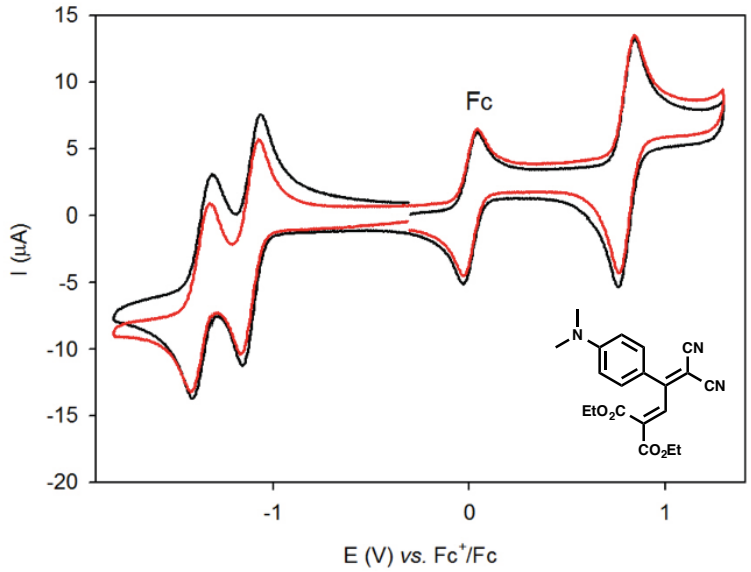

Figure 113. Cyclic voltammetry of **163** in CH_2Cl_2 + 0.1 M nBu$_4$NPF$_6$ in the presence of ferrocene on a glassy carbon working electrode at a scan rate of 0.1 Vs^{-1} (298 K).

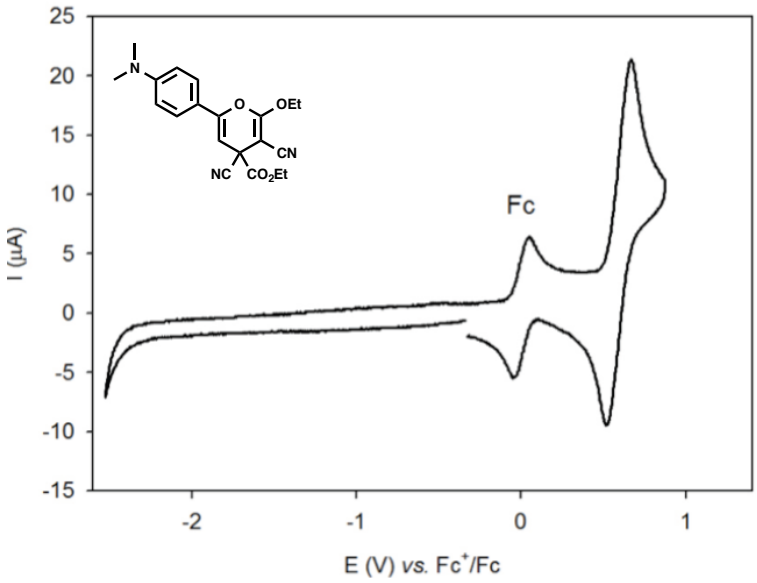

Figure 114. Cyclic voltammetry of (±)-**165** in CH_2Cl_2 + 0.1 M nBu$_4$NPF$_6$ in the presence of ferrocene on a glassy carbon working electrode at a scan rate of 0.1 Vs^{-1} (298 K).

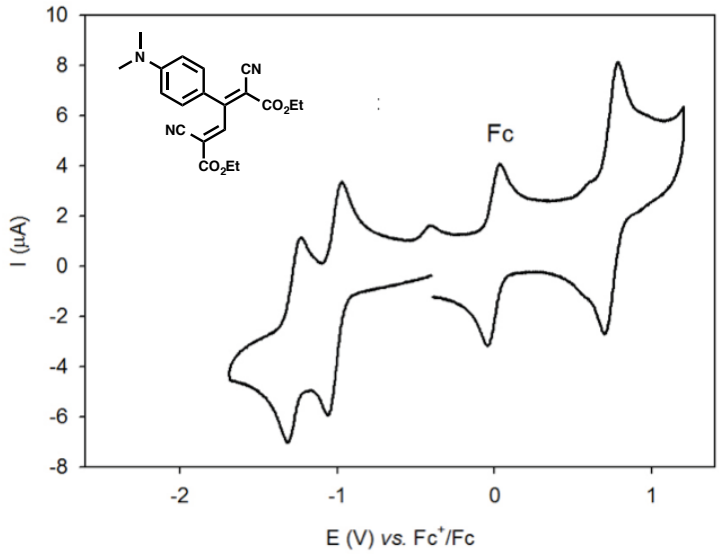

Figure 115. Cyclic voltammetry of **166** in CH_2Cl_2 + 0.1 M nBu_4NPF_6 in the presence of ferrocene on a glassy carbon working electrode at a scan rate of 0.1 Vs^{-1} (298 K).

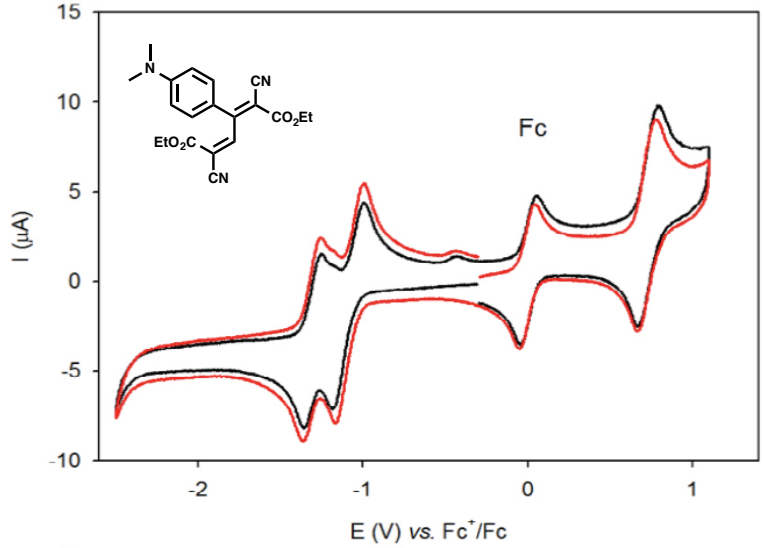

Figure 116. Cyclic voltammetry of **167** in CH_2Cl_2 + 0.1 M nBu_4NPF_6 in the presence of ferrocene on a glassy carbon working electrode at a scan rate of 0.1 Vs^{-1} (298 K).

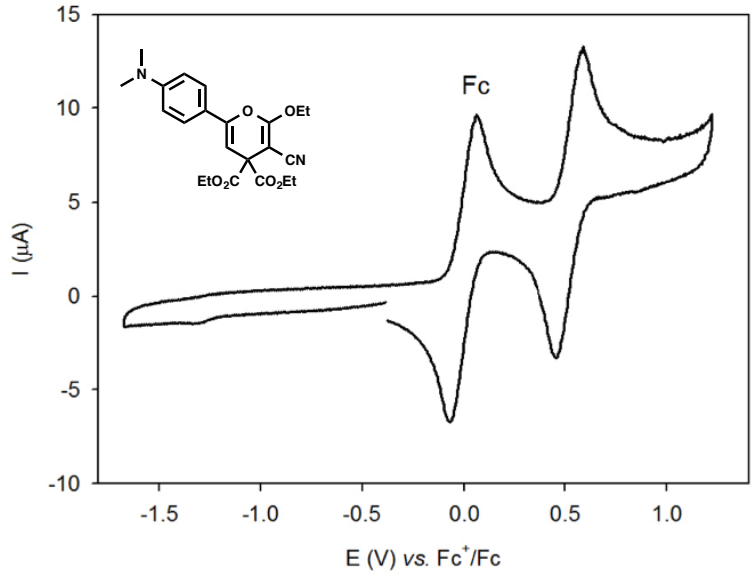

Figure 117. Cyclic voltammetry of **169** in CH_2Cl_2 + 0.1 M nBu$_4$NPF$_6$ in the presence of ferrocene on a glassy carbon working electrode at a scan rate of 0.1 Vs^{-1} (298 K).

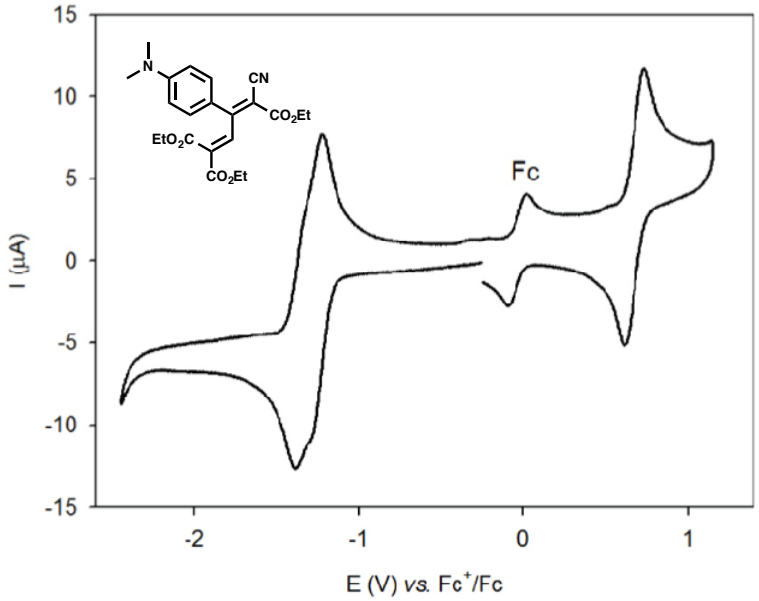

Figure 118. Cyclic voltammetry of **170** in CH_2Cl_2 + 0.1 M nBu$_4$NPF$_6$ in the presence of ferrocene on a glassy carbon working electrode at a scan rate of 0.1 Vs^{-1} (298 K).

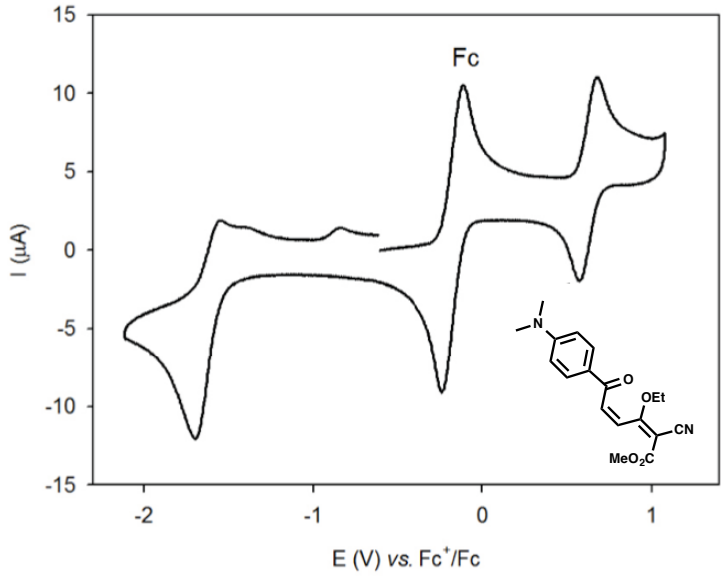

Figure 119. Cyclic voltammetry of **171** in CH_2Cl_2 + 0.1 M nBu_4NPF_6 in the presence of ferrocene on a glassy carbon working electrode at a scan rate of 0.1 Vs^{-1} (298 K).

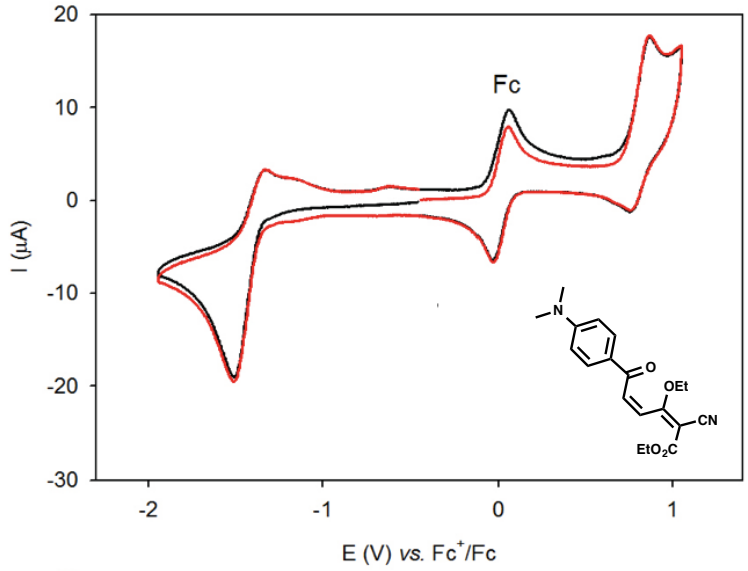

Figure 120. Cyclic voltammetry of **175** in CH_2Cl_2 + 0.1 M nBu_4NPF_6 in the presence of ferrocene on a glassy carbon working electrode at a scan rate of 0.1 Vs^{-1} (298 K).

10.3. Solvatochronism

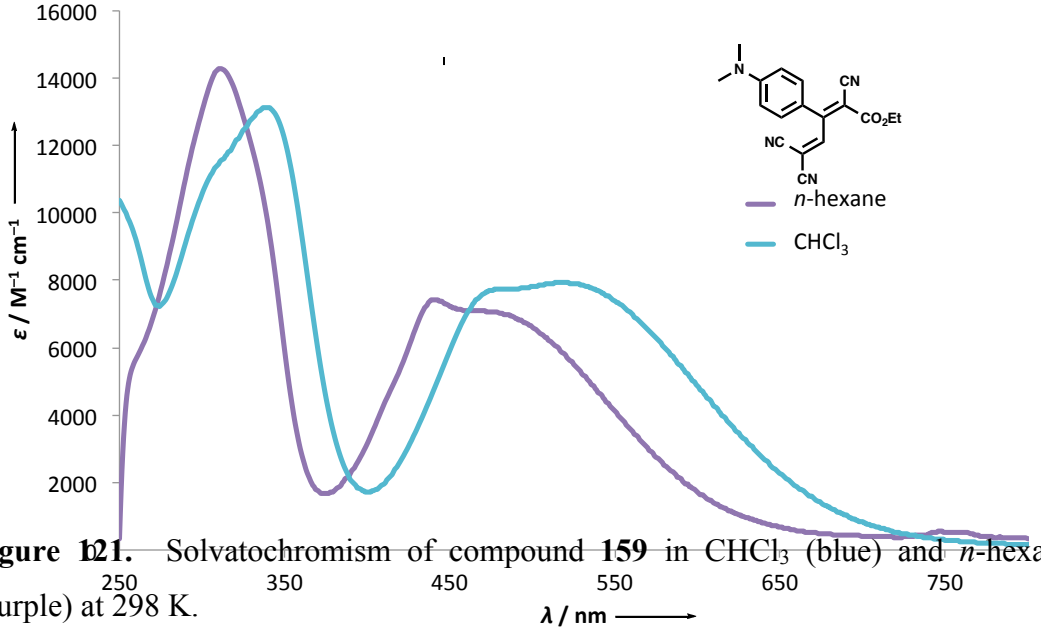

Figure 121. Solvatochromism of compound **159** in $CHCl_3$ (blue) and *n*-hexane (purple) at 298 K.

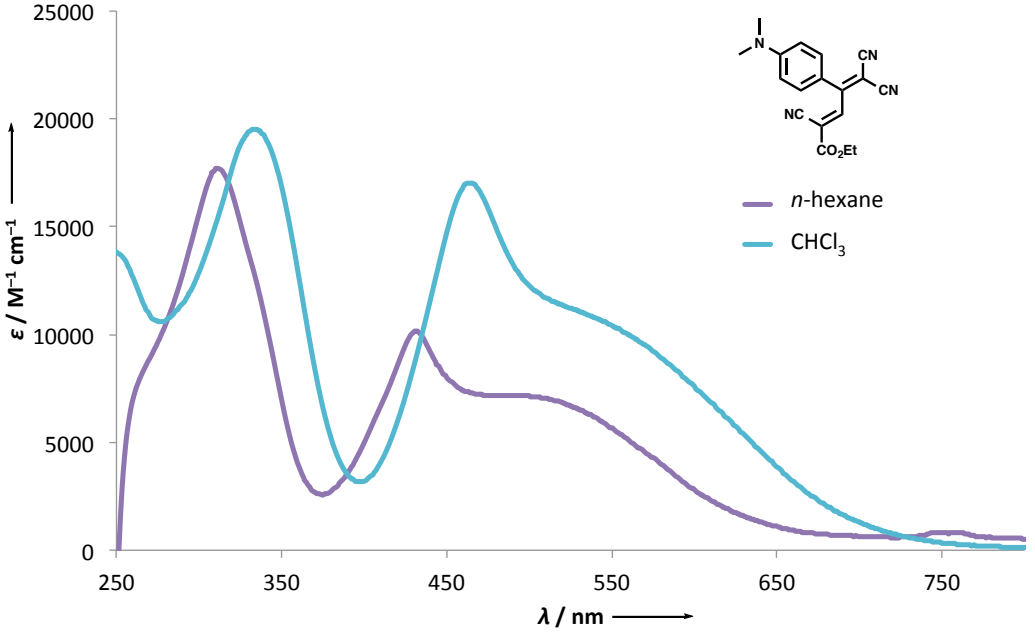

Figure 122. Solvatochromism of compound **160** in $CHCl_3$ (blue) and *n*-hexane (purple) at 298 K.

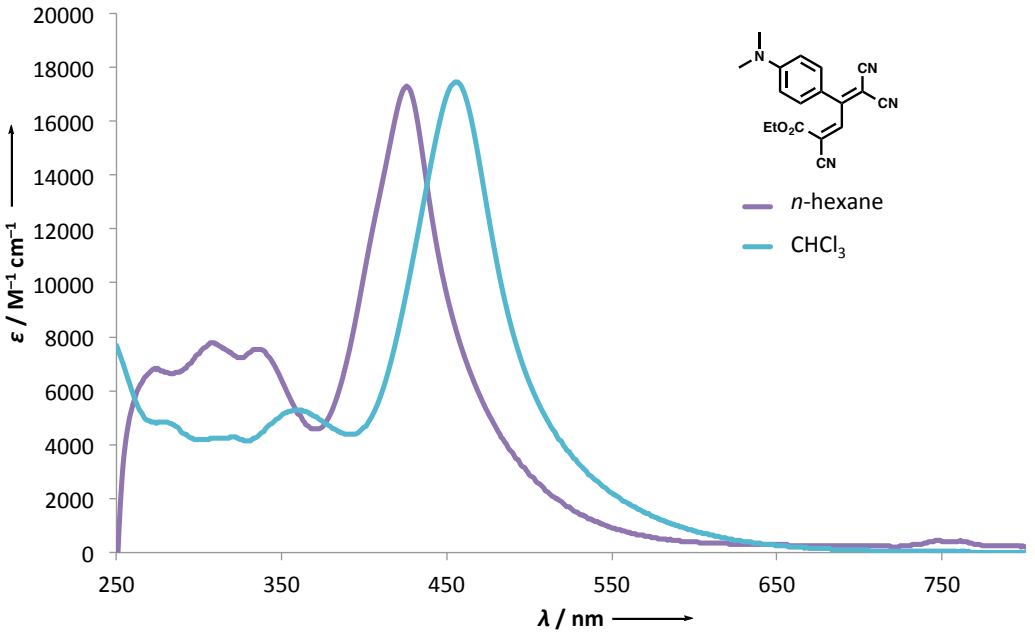

Figure 123. Solvatochromism of compound **162** in $CHCl_3$ (blue) and *n*-hexane (purple) at 298 K.

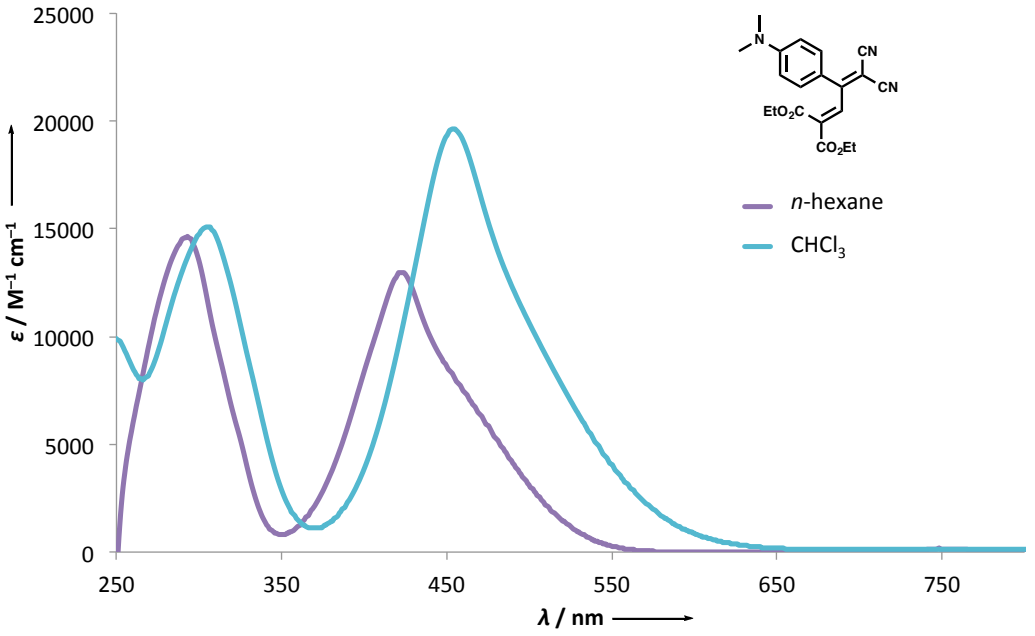

Figure 124. Solvatochromism of compound **163** in $CHCl_3$ (blue) and *n*-hexane (purple) at 298 K.

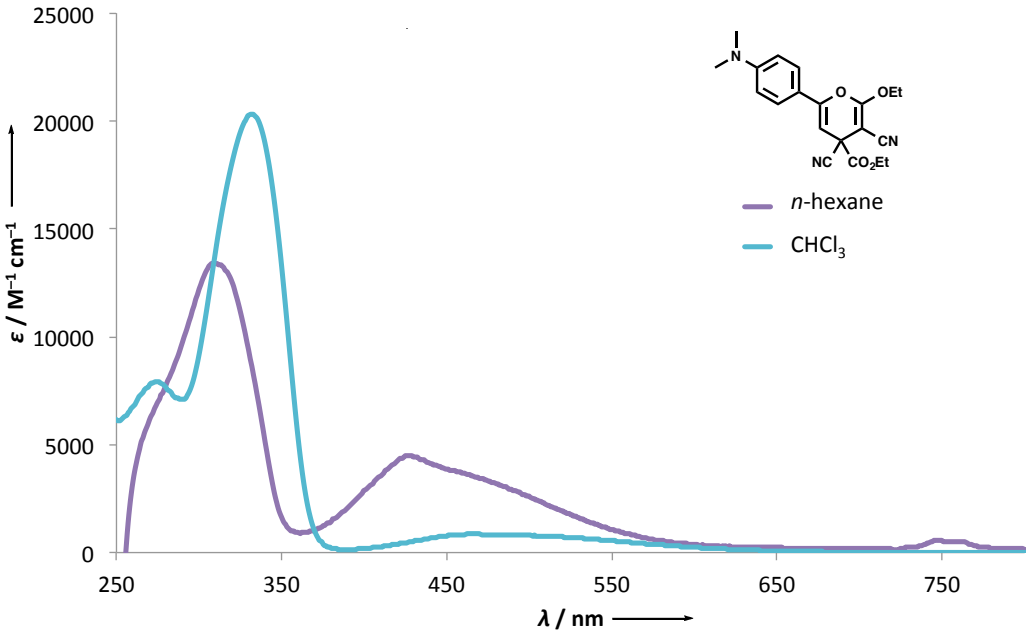

Figure 125. Solvatochromism of compound (±)-**165** in $CHCl_3$ (blue) and *n*-hexane (purple) at 298 K.

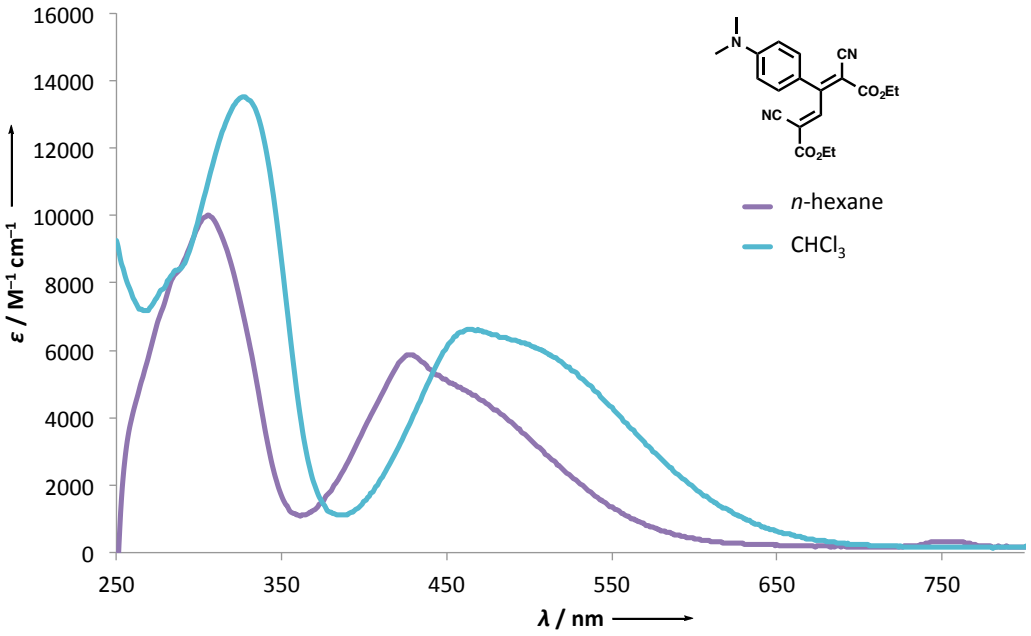

Figure 126. Solvatochromism of compound **166** in $CHCl_3$ (blue) and *n*-hexane (purple) at 298 K.

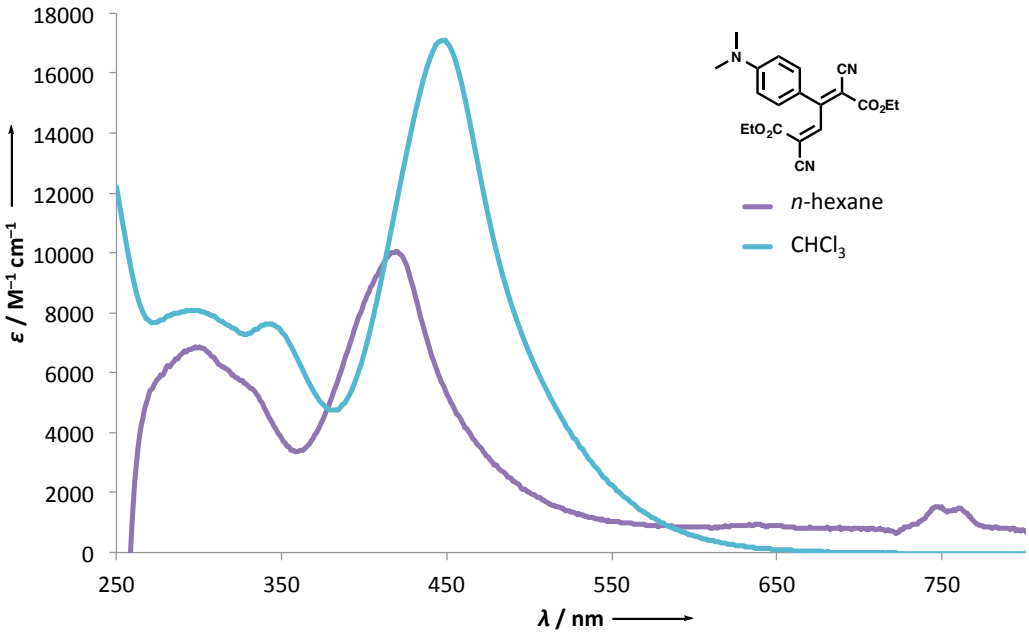

Figure 127. Solvatochromism of compound **167** in $CHCl_3$ (blue) and *n*-hexane (purple) at 298 K.

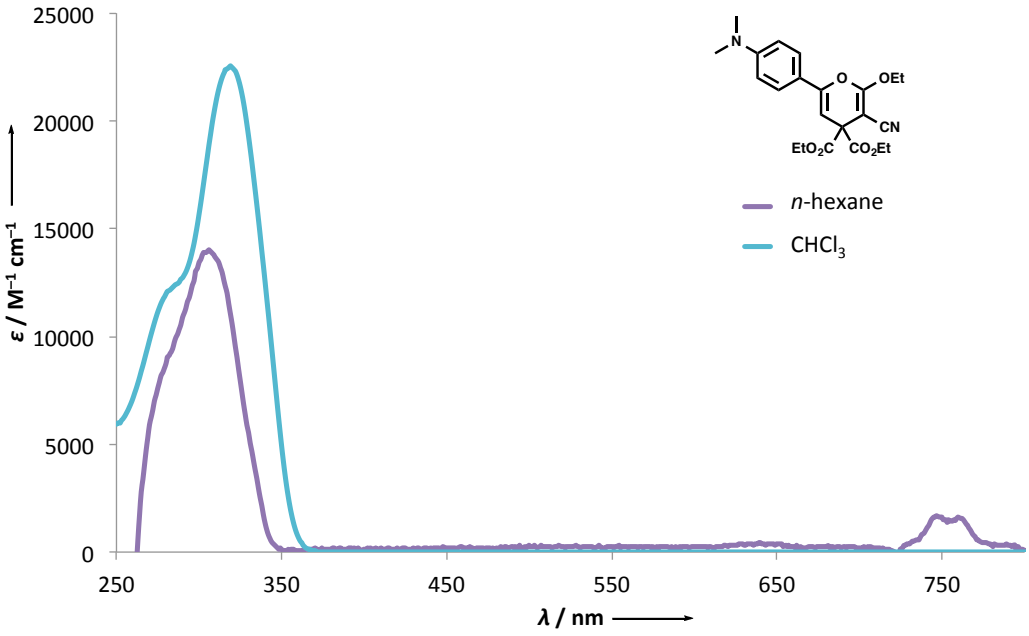

Figure 128. Solvatochromism of compound **169** in $CHCl_3$ (blue) and *n*-hexane (purple) at 298 K.

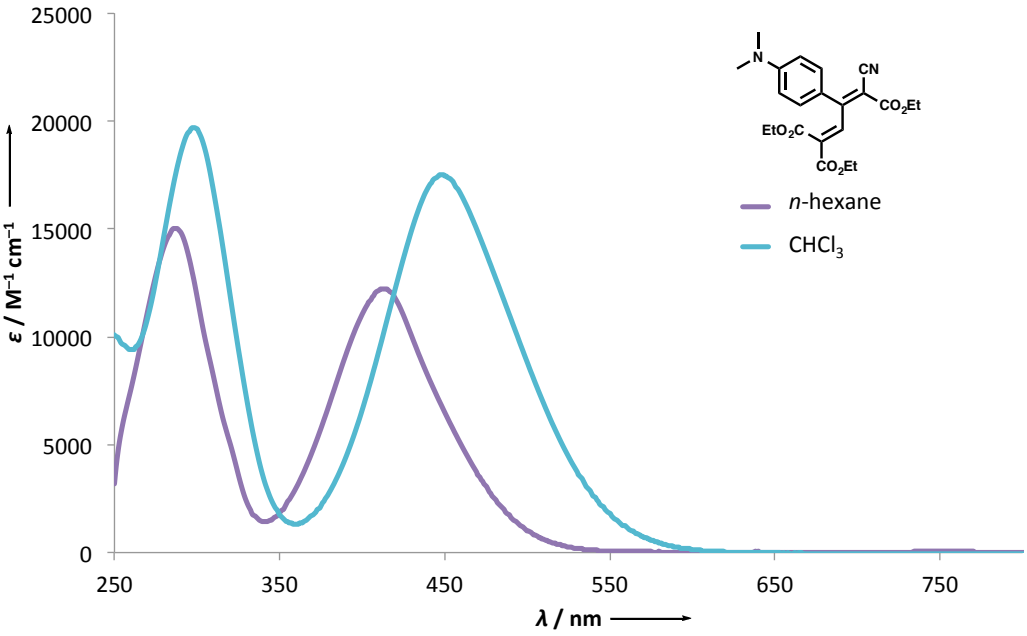

Figure 129. Solvatochromism of compound **21** in $CHCl_3$ (blue) and *n*-hexane (purple) at 298 K.

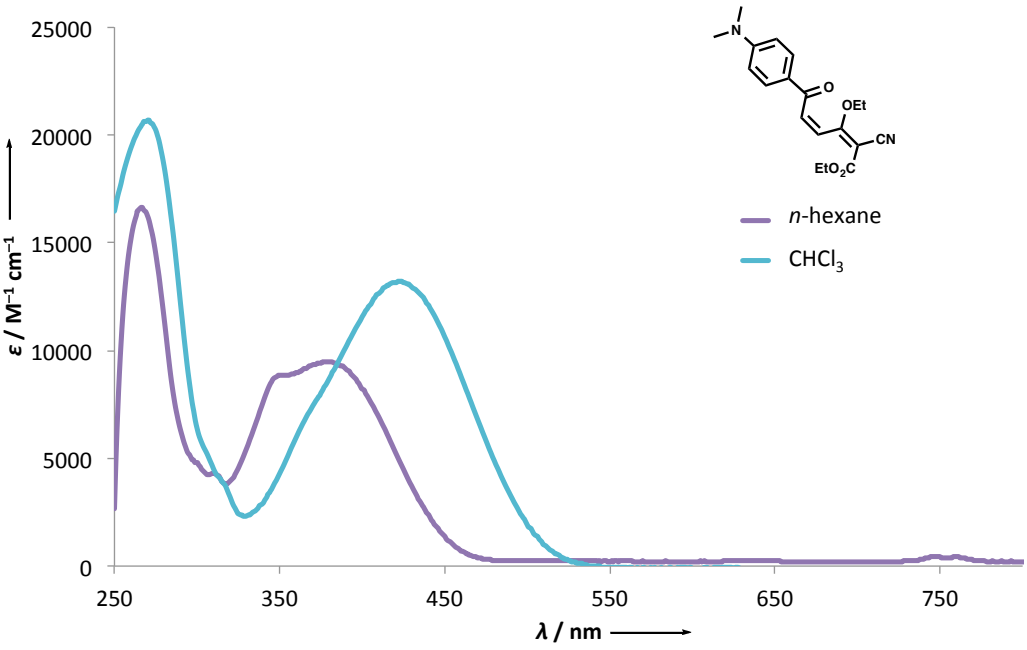

Figure 130. Solvatochromism of compound **175** in $CHCl_3$ (blue) and *n*-hexane (purple) at 298 K.

Curriculum Vitae

Etienne Donckele
Date of birth: 31.07.1988
Place of Birth: Mantes-la-jolie
Citizenship: French

Education

Feb. 2013 – Sept. 2016	**Ph.D. in Chemistry**, ETH Zürich, Switzerland Advisor: Prof. Dr. François Diederich
Sept. 2011 – Jul. 2012	**M.Sc. in Molecular and Biological Chemistry**, EPFL, Switzerland
Sept. 2010 – Jul. 2011	**Bsc. in Chemistry and Cancer biology**, Harvard Extension School, USA
Sept. 2008 – Jun. 2011	**"Diplome d'ingénieur" in Chemistry and Chemical Engineering**, CPE Lyon, France
Sept. 2006 – Jun. 2008	**Higher National Diploma in Chemistry**, IUT Rouen, France

Professional Experience

Jul. 2012 – Dec. 2012	**Master Thesis**, Stanford University, United States of America Advisor: Prof. Dr. Barry M. Trost
Oct. 2011 – May 2012	**Master Semester Project**, EPFL, Switzerland Advisor: Prof. Dr. Jérome Waser
Jul. 2010 – Jul. 2011	**One Year Placement**, Broad Institute of MIT and Harvard, United States of America Advisor: Dr. Lisa Marcaurelle and Eric Jacobsen
Feb. 2009 – Apr. 2008	**Bachelor Thesis**, Université du Québec à Montréal (UQAM), Canada Advisor: Prof. Dr. Daniel Chapdelaine

Zürich, September 2016 Etienne Donckele